Satya P. Gupta *Editor*

Hydroxamic Acids

A Unique Family of Chemicals with
Multiple Biological Activities

Springer

Hydroxamic Acids

Satya P. Gupta

Editor

Hydroxamic Acids

A Unique Family of Chemicals with
Multiple Biological Activities

Springer

Editor
Satya P. Gupta
Department of Pharmaceutical Technology
Meerut Institute of Engineering and Technology
Meerut
India

Preface

Hydroxamic acids, which can be represented by a general formula RCONR′OH, where R, R′ may be aryl or substituted aryl moiety, constitute a very unique family of chemicals that possess a wide spectrum of biological activities. They act as selective inhibitors of many enzymes, such as matrix metalloproteinases (MMPs), peroxidases, hydrolases, ureases, lipoxygenases, cyclooxygenases, histone deacetylase and peptide deformylases, and consequently possess hypotensive, anti-cancer, anti-malarial, anti-tuberculosis and anti-fungal properties. Their CONHOH moiety has been identified as a key functional group to develop potential therapeutic agents targeting cardiovascular diseases, HIV, Alzheimer's disease, allergic diseases, metal poisoning and iron overload. Hydroxamic acids are also used industrially as anti-oxidants, inhibitors of corrosion, for the extraction of toxic elements, as a means of flotation of minerals and even for their ability to serve as redox switches for electronic devices. They can also act as nitric oxide donors. This versatility of hydroxamic acids depends on their ability to act as a bidentate ligand to chelate with metal ions such as Fe^{2+} and Zn^{2+} at the active site of the enzymes. Their hydroxamic acid moiety, CONHOH, is not only a strong metal-binding group but also possesses multiple sites for potential hydrogen bond interactions with the enzymes. Thus, the metal-chelating property and multiple hydrogen-bond formation ability of hydroxamic acids have made them an intriguing family of compounds with a wide spectrum of therapeutic roles. One of the first therapeutic roles of hydroxamic acids was associated with their use as siderophores, a class of low molecular weight iron-sequestering agents. Siderophores have vast therapeutic potential to deal with iron overload in transfusion-dependent patients, such as those suffering from thalassemia. Because of these enormous therapeutic applications, the hydroxamic acids have greatly drawn the attention of both theoretical and experimental chemists to make studies on them for the design and development of drugs against a number of diseases. This book therefore presents some very interesting chapters on them, written by experts, covering their various chemical and pharmaceutical aspects.

The book contains 11 chapters in total. Since the multi-faceted activity of hydroxamic acids depends on the chemical aspects of these compounds, the very first chapter written by Gupta and Anjana describes in detail The Chemistry of Hydroxamic Acids covering their synthesis, structure, chelating, hydrogen-bonding

and nitric oxide releasing properties, and general mechanism of inhibition of various enzymes. The second chapter written by Kakkar on Theoretical Studies on Hydroxamic Acids further adds to their chemistry, discussing their conformation, tautomerism, metal ion selectivity, and complexation.

Among the various enzymes which have been found to be inhibited by hydroxamic acids, the carbonic anhydrases (CAs), MMPs and histone deacetylases (HDACs) have been most widely studied. Therefore, the three consecutive Chaps. 3–5, namely Hydroxamic Acids as Carbonic Anhydrase Inhibitors by Supuran, Structure–Activity Relationships of Hydroxamic Acids as Matrix Metalloproteinase Inhibitors by Patil and Gupta and Hydroxamic Acids as Histone Deacetylase Inhibitors by Thaler et al. describe vividly the different types of hydroxamic acids inhibiting these enzymes and their structure–activity relationships. However, no less important have been hydroxamic acids acting as inhibitors of ribonucleotide reductase, as the inhibitors of this enzyme have been developed as potent anticancer agents. Therefore, Chap. 6 Hydroxamic Acids as Ribonucleotide Reductase Inhibitors written by Basu and Sinha presents a few kinds of hydroxamates that inhibit carbonucleotide reductase, their mode of action, and progress in computer-aided SAR studies on them leading to the development of anticancer drugs.

Inhibitors of MMPs, HDACs, and ribonucleotide reductase have been developed as potent anticancer drugs. Therefore, a discussion of the inhibitors of these enzymes that belong particularly to hydroxamic acid class and have been evaluated against cancers have been nicely presented by Gupta et al. in Chap. 7 entitled as Hydroxamic Acid Derivatives as Anticancer Agents. These authors also discuss in this chapter the future prospects of design of potent anticancer agents based on hydroxamic acids.

Since HDAC inhibitors have been most attractive as anticancer agents, detailed quantitative structure–activity relationship (QSAR) studies have also been made on them in order to find the physicochemical and structural properties of the compounds governing their activity, so that the design of potent anticancer drugs may be rationalized. Hadjipavlau-Litina and Pontiki, therefore, presented in Chap. 8 entitled as Quantitative Structure-Activity Relatioship Studies on Hydroxamic Acids Acting as Histone Deacetylase Inhibitors a detailed account of QSAR studies on hydroxamic acids acting as HDAC inhibitors. All 2D and 3D QSAR studies pointed out that anticancer activity of these compounds are basically controlled by their hydrophobic and streric properties.

The activity of the enzyme urease, which is produced in the body by a bacterium called *Helicobacter pylori* (*H. pylori*), plays a critical role in the pathogenesis of several diseases, such as urinary tract infections, urolithiasis, pyelonephritis, hepatic encephalopathy, hepatic coma, cancer, etc. Therefore, the inhibitors of urease have been greatly studied and hydroxamic acids have occupied the foremost position among the urease inhibitors. Thus Chap. 9 Hydroxamic Acids as Inhibitors of Urease in the Treatment of *Helocobacter pylori* Infections written by Muri and Barros gives a detailed account of hydroxamic acids acting as urease inhibitors and of their structure–activity relationships. The chapter also

describes the new technologies for the delivery of effective urease inhibitors in the body.

Hydroxamic acid derivatives have recently been recommended for the therapeutic treatment of several diseases, such as hypertension, cancer, as well as inflammations and infectious diseases, due to their ability to chelate metals, especially in metalloenzymes. In Chap. 10 entitled as Therapeutic Potential of Hydroxamic Acids for Microbial Diseases, Rodrigues et al. therefore present the potential use of hydroxamates and their derivatives for the treatment and control of such diseases, along with a general overview of their structure, synthesis and inhibition mechanism. Application of hydroxamic acids as chelating mineral collectors for ore beneficiation is a unique area of their use and has attracted the attention of limited workers in this unique area. Therefore, a review of the use of alkyl and aryl hydroxamic acids in mineral processing is finally presented by Natarajan in Chap. 11 entitled as Hydroxamic Acids as Chelating Mineral Collectors. In this chapter, basic information on mineral flotation chemistry is provided for the non-expert.

Thus an attempt has been made to cover all aspects of hydroxamic acids, a unique class of chemicals having multiple biological activities. Articles covered in this book are not only of interest to those working in this area but also to general readers. As an editor of this book, I have greatly enjoyed reading all the chapters and also hope the readers will do so. I greatly acknowledge the interest and zeal of all the authors for contributing such interesting and useful chapters.

Meerut (U.P), India   Satya P. Gupta

Contents

The Chemistry of Hydroxamic Acids

Satya P. Gupta and Anjana Sharma

Abstract This chapter presents the chemical structure of hydroxamic acids, the routes of their synthesis, and their chemical properties. A discussion is presented as to how their metal chelating and hydrogen bonding properties make them a class of compounds that may have multiple biological activities. A brief description of all important enzymes that can be inhibited by hydroxamic acids is also presented. The most important enzymes that are inhibited by hydroxamic acids are matrix metalloproteinases, TNF-α converting enzyme, angiotensin-converting enzyme, lipoxygenase, LTA4 hydrolase, urease, peptide deformylase, histone deacetylase, UDP-3-O-[R-3-hydroxymyristoyl]-GlcNAc deacetylase, procollagen C-proteinase, aggrecanase, and carbonic anhydrase. Thus the hydroxamic acid moiety plays an important role as a pharmacophore to develop drugs against a variety of diseases, such as cancer, cardiovascular diseases, HIV, Alzheimer's, malaria, allergic diseases, tuberculosis, metal poisoning, iron overload, etc. Besides, hydroxamic acid moiety has also been exploited to develop potential insecticides, antimicrobials, antioxidants, anti-corrosive agents, siderophores, and as a means of flotations of minerals. It is also discussed that hydroxamic acids are also effective nitric oxide (NO) donors, because of which they produce hypotensive effects.

S. P. Gupta (✉)
Department of Applied Sciences, Meerut Institute of Engineering and Technology,
Meerut 250005, India
e-mail: spgbits@gmail.com

A. Sharma
Department of Pharmaceutical Technology, Meerut Institute of Engineering
and Technology, Meerut 250005, India

Abbreviations

ACE	Angiotensin-converting enzyme
CA	Carbonic anhydrase
ECM	Extracellular matrix
HAT	Histone acetylase
HDAC	Histone deacetylase
Hedta	*N*-(hydroxyethyl)-ethylenediamine-triacetic acid
HP	*Helicobacter pylori*
HPETEA	5-Hydroperoxy-6, 8, 11, 14-eicosatetraenoic acid
LO	Lipoxygenase
LTs	Leukotrienes
MMPs	Matrix metalloproteinases
MTs	Membrane types
NO	Nitric oxide
PCP	Procollagen C-proteinase
PDF	Peptide deformylase
RA	Rheumatoid arthritis
Ru-NO	Ruthenium nitrosyls
TACE	TNF-α converting enzyme
TIMMPs	Tissue inhibitors of matrix metalloproteinases
TNF-α	Tumor necrosis factor-α

Contents

1 Introduction

Hydroxamic acids, that can be represented by a general formula RCONR′OH, where R, R′ may be an aryl or substituted aryl moiety, refer to a class of organic acids, which are much weaker than structurally related carboxylic acids (Marmion et al. 2004). Hydroxamic acids have been known since 1869 with the discovery of oxalohydroxamic acid by Lossen (1869). However, the real momentum on studies on the synthesis and structures of hydroxamic acids and their biological activities was gained after 1980. These weak acids constitute one of the most important families of organic bioligands; and one of the first physiological roles of these compounds was associated with their use as siderophores, a class of low molecular weight iron-sequestering agents. Siderophores and their analogs have vast therapeutic potential, e.g., trishydroxamate siderophore desferrioxamine B (Desferal, **1**) is effectively used to deal with iron overload in transfusion-dependent patients such as those suffering from thalassemia.
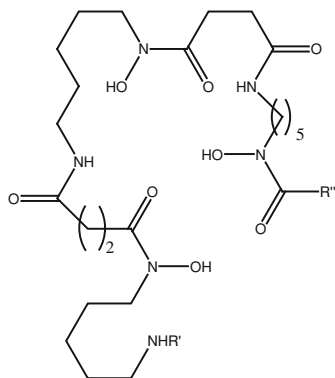
1

   Besides being used as siderophores, hydroxamic acids play a number of other biological and pharmacological roles, e.g., they act as potent and selective inhibitors of a large number of enzymes, such as matrix metalloproteinases (Muri et al. 2002; Steward and Thomas 2000; Botos et al. 1996; Sani et al. 2004; Tegoni et al. 2004), peroxidases (Indiani et al. 2003; O′Brien et al. 2000; Tsukamoto et al. 1999), hydrolases (Brown et al. 2004a, b), ureases (Amtul et al. 2002; Benini et al. 2000; Brown et al. 1998; Arnold et al. 1998), lipoxygenases (Muri et al. 2002), cyclooxygenases (Dooley et al. 2003; Connolly et al. 1999), histone deacetylases (Marks et al. 2000; Johnstone 2002; Jung 2001; Kelly et al. 2002), peptide deformylases (Chen et al. 2004), etc. The detailed role of hydroxamic acid derivatives as enzyme inhibitors has been well described by Muri et al. (2002) and Lou and Kang (2003). Besides acting as enzyme inhibitors, hydroxamic acids have also been reported to act as hypotensive (Zamora et al. 1995), anticancer (Steward et al.

2000; Bouchain and Delorme 2003; Steward 1999; Brammar et al. 2000; Holms et al. 2001), antimalarial (Mishra et al. 2003; Apfel et al. 2000; Holland et al. 1998; Tsafack et al. 1995; Golenser et al. 1995), anti-tuberculosis and anti-fungal agents (Miller 1989). Additionally, they have been also found to possess the potency against HIV, Alzheimer's disease, and cardiovascular disorders (El Yazal and Pang 1999, 2000). Now, our interest lies in the discussion of the synthesis, structure, and physicochemical properties of such a group of chemicals that possesses a wide spectrum of biological properties.

2 Synthesis and Structure

Hydroxamic acids are generally the products of hydroxylamine (NH_2OH) and carboxylic acids (RCOOH). When an acyl group replaces one of the nitrogen-bound hydrogens in the hydroxylamine molecule, a monohydroxamic acid, RCONHOH, is formed. This occurs when an O/N-protected hydroxylamine molecule is allowed to react with an activated acyl group as shown below:

$$RCOX + NH_2OH \rightarrow RCONHOH + HX \tag{1}$$

Devocelle et al. (2003), however, reported a convenient two-step procedure for the parallel synthesis of low molecular weight hydroxamic acids from carboxylic acids and hydroxylamine with the use of polymer supported 1-hydroxybenzotri-azole (Fig. 1) (Marmion et al. 2004). A simple one pot method for the synthesis of
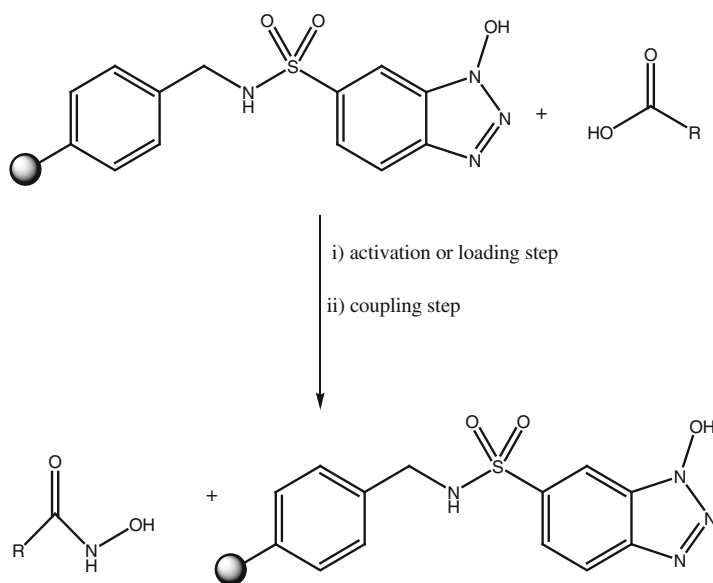
Fig. 1 The route of polymer supported synthesis of hydroxamic acids

hydroxamic acids in high yields has also been described by Giacomelli et al. (2003). The recent development of more efficient methods for the synthesis of hydroxamic acids can be found in a review by Yang and Lou (2003).

The monohydroxamic acid has been found to exist in two tautomeric forms as:

Keto form   Enol form
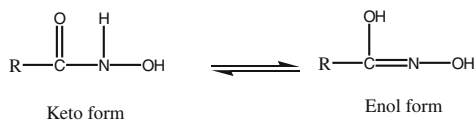
and both forms exhibit the geometrical isomerism as

Z-keto   E-keto

Z-enol   E-enol
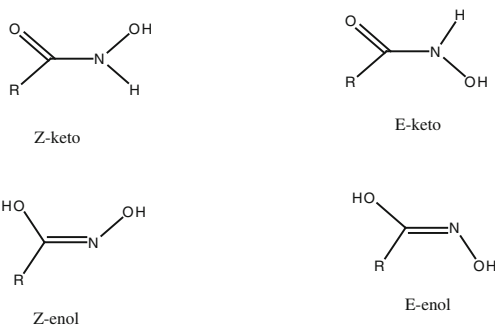
These structures of monohydroxamic acids have been related to the derivatives which contain the system

or
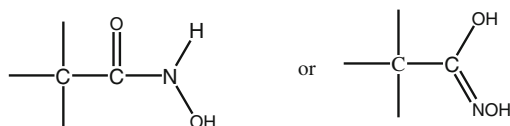
resembling the structure of hydroxyureas or carbamyl hydroxamic acids as shown below

or

Hydroxyureas   Carbamylhydroxamicacids
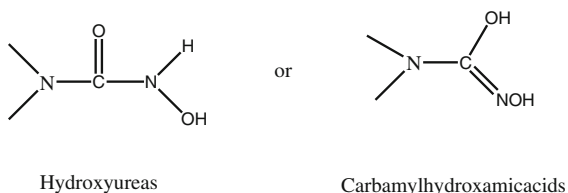
In aqueous solution, the monohydroxamic acids behave as weak acids; for example, the ionization constant of acetohydroxamic acid is 2.8×10^{-8}.

3 The Chelating and Hydrogen Bonding Properties of Hydroxamic Acids

It is well established that several biomedical applications of hydroxamic acids arise as a result of their strong chelating and H-bond forming abilities. They can also act as monodentate and as well as a bidentate ligand through their deprotonated hydroxamate moiety and carbonyl oxygen atom as represented by Fig. 2. As discussed by Scolnick et al. (1997), a hydroxamic acid can also act as a monodentate ligand through its nitrogen atom (Fig. 3).

As apparent in Fig. 2, a hydroxamate can form a stable five-membered chelate and, as can be seen in Fig. 4, its chelating behavior can be enriched by incorporating secondary coordinating groups at adjacent sites in the molecule. Figure 4 shows the formation of a dinuclear complex of Cu (II) with an α-aminohydroxamate with two modes of hydroxamate coordination, O, O- and as well as N, N-coordination, each giving a five-membered ring (Kurzak et al. 1986, 1987).

When β-aminohydroxamic acids form complexes, their N,N-coordination gives a six-membered ring, while O,O-coordination gives only a five-membered ring as shown in Fig. 5 for the complex of Cu (II) with a β-alaninehydroxamic acid (Kurzak et al. 1991).

The ability of the H-bond formation of hydroxamic acids plays no less important role than their chelating ability in their biomedical applications. As shown in Fig. 3, a hydroxamic acid can form H-bonds through its OH group, NH group, and carbonyl oxygen. OH and NH groups can act both as H-bond donor and H-bond acceptor and the carbonyl oxygen as an H-bond acceptor. Thus depending

Fig. 2 Representation of a monodentate (**a**) and a bidentate (**b**) complexation of a hydroxamate
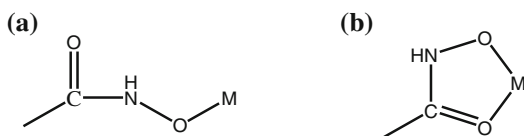
Fig. 3 Monodentate N-bonded complex formation of a hydroxamate with carbonic anhydrase enzyme
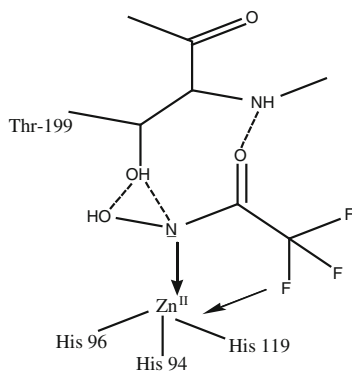
Fig. 4 A Cu (II) complex of amino acid exhibiting two modes of hydroxamate coordination: O, O- and N, N-coordination
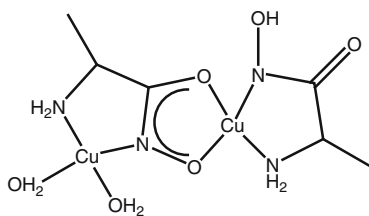
Fig. 5 The structure of a complex of Cu (II) formed with a β-alaninehydroxamic acid showing the formation of six-membered ring with N, N-coordination and a five-membered ring with O, O-coordination of the hydroxamate
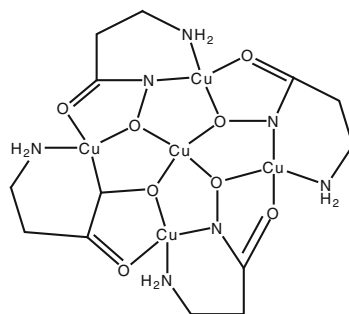
upon number of sites available in receptor, hydroxamic acids can form 3–5 hydrogen bonds, strengthening drug–receptor interactions.

4 Nitric Oxide Releasing Property

While most of the medicinal properties of hydroxamic acids depend on their ability to inhibit many enzymes because of their chelating and hydrogen bonding properties, there is one pathophysiological role of these acids which depends on their ability to release nitric oxide (NO). There are numerous pathological conditions where NO plays an important role (Adams et al. 1999; Stuehr 1999; Saavedra and Keefer 2000; Kumar et al. 2013). NO is of critical importance as a mediator of vasodilation in blood vessels. It also acts on cardiac muscle to decrease contractility and heart rate and thus saves from coronary artery disease. Marmion et al. (2000) have shown that hydroxamic acids are effective NO donors and they readily transfer NO to ruthenium (III) to form highly stable ruthenium nitrosyls, Ru–NO, which cause vascular relaxation of rat aorta by NO-mediated activation of the Fe(II) heme-containing enzyme, guanylate cyclase. In this respect, benzohydroxamic acid ($C_6H_5CONHOH$) has been found to be the best NO-releasing agent. Acetohydroxamic acid and salicylhydroxamic acid, however, also act as good NO-releasing agents. Hydroxamic acids react with [Ru(Hedta)Cl]$^-$ (Hedta: *N*-(hydroxyethyl)-ethylenediamine-triacetic acid) in aqueous solution at room temperature to produce the ruthenium nitrosyl complex, [Ru(edta)(NO)Cl]$^{2-}$.

5 Inhibition of Enzymes

The enormous biological and pharmacological applications of hydroxamic acids can be attributed to their ability to inhibit a large number of enzymes whose over-activations are responsible for variety of diseases. Some of the important enzymes that have been targeted by hydroxamic acids to develop variety of drugs are discussed below with respect to their biological roles and the diseases caused by their over-activation.

5.1 Matrix Metalloproteinases

Matrix metalloproteinases (MMPs) are a class of zinc-containing enzymes that degrade and remodel essentially all the components of extracellular matrix (ECM), such as membrane collagens, aggrecan, fibronectin, and laminin (Brinckerhoff and Matrician 2002; Burzlaff 2006; Gupta 2007; Sternlicht and Werb 2001; Verma and Hansh 2007; Yadav et al. 2011; Whittaker et al. 1999; Verma 2012). To date at least 26 MMPs are known, which have been classified into six groups based on their structural homology and substrate specificity: collagenases (MMP-1, -8, -13, and -18), gelatinases (MMP-2 and -9), stromelysins (MMP-3, -10, and -11), matrilysins (MMP-7, and -26), membrane types (MTs) (MMP-14, -15, -16, -17, -24, and -25), and others (MMP-12, -19, -20, -21, -22, -23, -27, and -29) (Yadav et al. 2011; Overall and Lopez-Otin 2002; Supuran and Scozzafava 2002; Verma and Hansch 2007; Visse and Nagase 2003; Whittakar et al. 1999; Verma 2012). MMPs are involved in a variety of physiological processes that require degradation of connective tissues, such as tissue remodeling or repair, bone remodeling, cervical dilation, embryonic development, wound healing, etc. However, over-activation of these MMPs results in an imbalance between them and their endogenous regulators called tissue inhibitors of matrix metalloproteinases (TIMMPs) that can lead to wide array of disease processes such as tumor metastasis (Heath and Grochow 2000; Skiles et al. 2000), rheumatoid arthritis (Eliott and Cawston 2001), osteoarthritis (Leff 1999; Shlopov 1997), periodontal disease (Overall et al. 1987), multiple sclerosis (Yong et al. 1998), congestive heart failure (Li and Feldman 2001), etc. The development of MMP inhibitors as potential therapeutic agents for the treatment of cancer and rheumatoid arthritis has recently been an area of intense interest among medicinal chemists (Whittaker et al. 1999; Skotnicki et al. 1999).

5.2 Tumor Necrosis Factor-α Converting Enzyme

TNF-α converting enzyme (TACE) is an another member of the family of zinc-containing metalloproteinases, which cleaves a membrane bound protein

(pro-TNF-α), releasing to the circulation a 17 kDa proinflammatory and immunomodulatory cytokine, TNF-α (Black et al. 1997; Moss et al. 2001). The release of this cytokine in blood circulation may lead to inflammatory diseases, such as rheumatoid arthritis (RA), multiple sclerosis, and Crohn's disease (Vassali 1992). Therefore, there has been a great deal of interest in design and development of TACE inhibitors in order to suppress the amount of circulating TNF-α (Nelson and Zask 1999; Newton and Decicco 1999).

5.3 Angiotensin-Converting Enzyme

Angiotensin-converting enzyme (ACE) is a part of renin–angiotensin system, where it is used to convert a decapeptide, angiotensin I (AI), to an octapeptide, angiotensin II (AII), which stimulates G-protein coupled angiotensin II (type I) receptors causing a potent vasoconstriction. Inhibition of ACE decreases the level of AII in the body leading to a decrease in the blood pressure. ACE has been extensively exploited as the target for designing the anti-hypertensive agents. The design and development of its inhibitors have been extensively presented in some reviews (Hooper 1996; Whittaker et al. 1999).

5.4 Lipoxygenase

The enzyme 5-lipoxygenase (5-LO) is involved in the biosynthetic pathway of leukotrienes (LTs) where it converts arachidonic acid to 5-hydroperoxy-6, 8, 11, 14-eicosatetraenoic acid (5-HPETEA) leading to LTs. These oxygenated eicosanoids are implicated in inflammatory and allergic reactions (Rokach 1989), in which LTC_4, LTD_4, and LTE_4 are potent bronchoconstrictors and are involved in bronchial asthma, inflammation, tissue injury, liver diseases, and shock. LTs may also lead to arthritis and psoriasis. Therefore, 5-LO inhibition represents potential approach for designing drugs against these diseases (Summers et al. 1990).

5.5 Leukotriene A_4 Hydrolase

Leukotriene A_4 (LTA_4) hydrolase belongs to the family of zinc-containing enzymes that catalyzes the hydrolytic conversion of LTA_4 to LTB_4 in the metabolic pathway of arachidonic acid. LTB_4 is potent chemotactic factor and plays an important role in the inflammatory response by stimulating the adhesion of circulating neutrophils to the vascular endothelium and directing their migration toward the inflammation sites. Thus, the inhibition LTA_4 hydrolase has drawn

great attention of chemists for designing effective anti-inflammatory agents (Hogg et al. 1995, 1998; Ollman et al. 1995).

5.6 Urease

Urease is an enzyme that is produced by a bacterium called *Helicobacter pylori* (HP). This enzyme catalyzes the hydrolysis of urea to ammonia and carbamic acid resulting finally into carbon dioxide and ammonia. This ammonia elevates the level of pH in the stomach and breaks the gastric mucosa (Sidebotham et al. 1991) and ammonia itself inhibits the consumption of oxygen and reduces the production of ATP in gastric mucous cells or in mitochondria (Tsujii et al. 1992). Thus, urease activity plays a critical role in the pathogenesis of several diseases, such as urinary tract infections, urolithiasis, pyelonephritis, hepatic encephalopathy, hepatic coma, cancer, etc. The presence of urease in the body results from HP infections. The urease activity in the soil leads to significant environmental and economic problems by releasing large amount of ammonia into the atmosphere during nitrogen fertilization with urea. This release of ammonia induces plant damage by ammonia toxicity and increase in the pH of the soil.

5.7 Peptide Deformylase

Peptide deformylase (PDF) is an essential enzyme in both gram-positive and gram-negative bacteria, where it helps the synthesis of protein for the bacteria. In eubacteria, the protein synthesis is initiated with *N*-formyl methionine, and the newly synthesized polypeptide is converted to mature protein by first removing *N*-formyl group by PDF and then methionine by methionine amino peptidase. Thus, PDF is a potentially attractive target for antibacterial drug design. The activity of PDF may also lead to bacterial infections. The fact that PDF is metalloproteinase of which there is no analogous human MMP makes the enzyme an especially attractive target for antibacterial drug discovery (Hackbarth et al. 2002).

5.8 Histone Deacetylase

Histone acetylases (HATs) and histone deacetylases (HDACs) are a group of enzymes that catalyze acetylation and deacetylation of lysine residues in the *N*-terminal tails of core histones. HDACs catalyze the removal of acetyl groups for the ε-amino groups of lysine residues clustered near the amino terminus of nucleosomal histones. The cell-cycle progression and differentiation depends on the activity of HDACs and the deregulation of their activity is associated with

several cancers (Kouzarides 1999), and therefore HDAC inhibitors are thought to have great potential to be developed as new anticancer drugs (Marks et al. 2001). Some of them have already been found to act as potential anticancer drugs in vivo, and currently are in clinical trials in cancer patients. To date, at least 11 different isoforms of HDAC have been recognized (Gray and Ekstrom 2001) and many of them have been exploited to develop the drugs for the treatment of cell proliferative diseases (Marks et al. 2000; Johnstone 2002; Jung 2001; Kelly et al. 2002).

5.9 UDP-3-O-[R-3-Hydroxymyristoyl]-GlcNAc Deacetylase

This enzyme is involved in the second step of lipid A biosynthesis, and therefore is a good target for development of novel antibiotics (Onishi et al. 1996).

5.10 Procollagen C-Proteinase

The enzyme Procollagen C-Proteinase (PCP) is involved in the production of collagen, but its overactivity leads to excessive production of collagen which can lead to many fibrotic diseases, including arthritis and adult respiratory distress syndrome. Therefore, the inhibition of this enzyme may lead to develop drugs for the treatment of these inflammatory conditions.

5.11 Aggrecanase

Aggrecanase is supposed to play an important role in the catabolism of aggrecanase in human arthritic diseases (Arner et al. 1999), and therefore its selective inhibitors are thought to be useful in the prevention of joint destruction.

5.12 Carbonic Anhydrase

The ubiquitous enzyme carbonic anhydrase (CA) is a well characterized metalloenzyme, containing one zinc ion (Zn^{2+}) per polypeptide chain. Its main physiological function is to catalyze the reversible hydration of carbon dioxide to bicarbonate ion as shown below:

$$CO_2 + H_2O \rightleftharpoons HCO_3^- + H^+$$
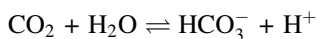
This interconversion of carbon dioxide and bicarbonate in animals leads to maintain acid–base balance in blood and other tissues, and to help transport carbon dioxide out of tissues. By producing protons and bicarbonate ions, CA plays a key role in the regulation of pH and fluid balance in different parts of our body. In our stomach lining, it plays a role in secreting acid, while the same enzyme helps to make pancreatic juices alkaline and our saliva neutral. The transport of the protons and bicarbonate ions produced in our kidney and eyes influence the water content of the cells at these locations. In higher vertebrates, including humans, a number of isozymes of CA have been investigated (Supuran et al. 2004), which perform different functions at their specific locations, and their absence or malfunction can lead to diseased states, ranging from the loss of acid production in the stomach to kidney failure. Thus the study of their inhibition has been found to be of great value to develop the drugs acting as antiglaucoma agents, diuretics, antiepileptics, and in the management of mountain sickness, gastric and duodenal ulcers, neurological disorders, or osteoporosis (Supuran and Scozzafava 2000; Supuran et al. 2004).

6 General Mechanism of Inhibition

Since, as already discussed, hydroxamates act as bidentate ligands and are able to form the hydrogen bonds, they can act as powerful inhibitors of any enzyme that contains metal ion and residues able to act as hydrogen-bond donors or acceptors. Almost all the enzymes discussed above, except a few, contain Zn^{2+} ion, and hence are easily coordinated with any hydroxamic acid derivative. In most of the zinc-containing enzymes, hydroxamates bind bidentately to their catalytic Zn^{2+} ion to create a distorted trigonal bipyramidal geometry around the Zn^{2+} as shown in

Fig. 6 A schematic diagram showing the interaction of a hydroxamate with a representative zinc-containing enzyme (matrilysin) and conserved water molecule. Adapted with permission from Browner et al. (1995). Copyright 1995 American Chemical Society
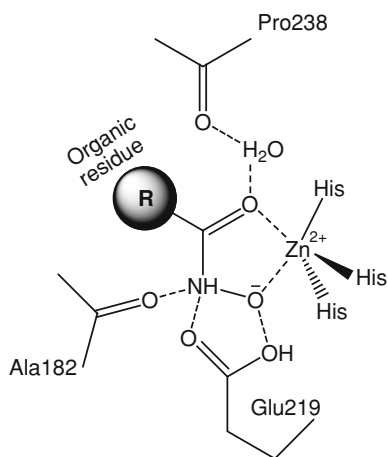
Fig. 6, representing a schematic diagram for the interactions of a hydroxamate with matrilysin, as an example (Browner et al. 1995). Figure 6 also shows that in addition to the chelation, the hydroxamate anion (RCONH–O$^-$) of the inhibitor can also form a short but strong H-bond with the neighboring carboxylate moiety of Glu 219 and its –NH-moiety an H-bond with the neighboring carbonyl oxygen of Ala182. Additionally, the van der Waals and hydrophobic interactions are also possible that can stabilize the inhibitor–enzyme complex. Figure 6 also shows that the inhibitor also interacts with the conserved water molecule.

7 Conclusion

Hydroxamic acids possess multiple biological activities due to their ability to chelate the metal ions bidentately and form strong hydrogen bonds. Because of their these properties, they interact with a variety of metal-containing enzymes, such as matrix metalloproteinases, TNF-α converting enzyme, angiotensin-converting enzyme, lipoxygenase, LTA4 hydrolase, urease, peptide deformylase, histone deacetylase, UDP-3-O-[R-3-hydroxymyristoyl]-GlcNAc deacetylase, pro-collagen C-proteinase, aggrecanase, carbonic anhydrase, etc. By targeting these enzymes, hydroxamic acids have been developed as drugs against variety of diseases, such as cancer, cardiovascular diseases, HIV, Alzheimer's, malaria, allergic diseases, hypertension, tuberculosis, glaucoma, ulcers, metal poisoning, iron overload, etc. Besides, they have also been developed as insecticides, antimicrobials, antioxidants, anti-corrosive agents, siderophores, and as a means of flotations of minerals. Hydroxamic acids are also effective NO donors and they readily transfer NO to ruthenium (III) to form highly stable ruthenium nitrosyls, Ru–NO, which cause vascular relaxation of rat aorta by NO-mediated activation of the Fe(II) heme-containing enzyme, guanylate cyclase. Thus, hydroxamic acids constitute an important class of chemicals of immense therapeutic importance.

References

Adams DR, Brochwicz-Lewinski M, Butler AR (1999) Nitric oxide: physiological roles, biosynthesis and medical uses. Fortschr Chem Org Naturst 76:1–211

Amtul Z, Rahman AU, Siddiqui RA, Choudhry MI (2002) Chemistry and mechanism of urease. Curr Med Chem 9:1323–1348

Apfel CM, Banner DW, Bur D et al (2000) Hydroxamic acid derivatives as potent peptide deformylase inhibitors and antibacterial agents. J Med Chem 43:2324–2331

Arner EC, Pratta MA, Decicco CP et al (1999) Aggrecanase. A target for the design of inhibitors of cartilage degradation. Ann N Y Acad Sci 878:92–107

Arnold M, Brown DA, Deeg O et al (1998) Hydroxamate-bridged dinuclear nickel complexes as models for urease inhibition. Inorg Chem 37:2920–2925

Benini S, Rypniewski WR, Wilson KS et al (2000) The complex of *Bacillus pasteurii* urease with acetohydroxamate anion from X-ray data at 1.55 Å resolution. J Biol Inorg Chem 5:110–118

Black RA, Rauch CT, Kozlosky CJ et al (1997) A metalloproteinase disintegrin that releases tumour-necrosis factor-alpha from cells. Nature 385:729–733

Botos I, Scapozza L, Zhang D, Liotta LA, Meyer EF (1996) Batimastat, a potent matrix mettaloproteinase inhibitor, exhibits an unexpected mode of binding. Proc Natl Acad Sci USA 93:2749–2754

Bouchain G, Delorme D (2003) Novel hydroxamate and anilide derivatives as potent histone deacetylase inhibitors: synthesis and antiproliferative evaluation. Curr Med Chem 10:2359–2372

Brammer R, Buckels J, Bramhall S (2000) Advances in non-operative therapy in pancreatic cancer. Int J Clin Pract 54:373–381

Brinckerhoff CE, Matrisian LM (2002) Matrix metalloproteinases: a tail of frog that became a prince. Nat Rev Mol Cell Biol 3:207–214

Brown DA, Cuffe LP, Fitzpatrick NJ et al (1998) Novel elimination of hydroxylamine and formation of a nickel tetramer on reactions of glutarodihydroxamic acid with model dinickel hydrolases. Chem Commun 2433–2434

Brown DA, Cuffe LP, Fitzpatrick NJ, Ryan AT (2004a) A DFT study of model complexes of zinc hydrolases and their inhibition by hydroxamic acids. Inorg Chem 43:297–302

Brown DA, Glass WK, Fitzpatrick NJ et al (2004b) Structural variations in dinuclear model hydrolases and hydroxamate inhibitor models: synthetic, spectroscopic and structural studies. Inorg Chim Acta 357:1411–1436

Browner MF, Smith WW, Castelhano AL (1995) Matrilysin-inhibitor complex: common among metalloproteases. Biochemistry 34:6602–6610

Burzlaff N (2006) Model complexes for zinc containing enzymes. In: Douglas B, McDaniel DH, Alexander JJ (eds) Concepts and models in bioinorganic chemistry, vol 17. Wiley, New York, pp 397–429

Chen D, Hackbarth C, Ni ZJ et al (2004) Peptide deformylase inhibitors as antibacterial agents: Identification of VRC3375, a proline-3-alkylsuccinyl hydroxamate derivative, by using an integrated combinatorial and medicinal chemistry approach. Antimicrob Agents Chemother 48:250–261

Connolly PJ, Wetter SK, Beers KN et al (1999) N-Hydroxyurea and hydroxamic acid inhibitors of cyclooxygenase and 5-lipoxygenase. Bioorg Med Chem 9:979–984

Devocelle M, McLoughlin BM, Sharkey CT et al (2003) A convenient parallel synthesis of low molecular weight hydroxamic acids using polymer-supported 1-hydroxybenzotriazole. Org Biomol Chem 1:850–853

Dooley CM, Devocelle M, Mcloughlin B et al (2003) A novel family of hydroxamate-based acylating inhibitors of cyclooxygenase. Mol Pharmacol 63:450–455

El Yazal J, Pang YP (1999) Novel stable configurations and tautomers of the neutral and deprotonated hydroxamic acids predicted from high-level ab initio calculations. J Phys Chem A 103:8346–8350

El Yazal J, Pang YP (2000) Proton dissociation energies of zinc-coordinated hydroxamic acids and their relative affinities for zinc: insights into design of zinc proteinase inhibitors. J Phys Chem B 104:6499–6504

Eliott S, Cawston T (2001) The clinical potential of matrix metalloproteinase inhibitors in the rheumatic disorders. Drugs Aging 18:87–99

Giacomelli G, Porcheddu A, Salaris M (2003) Simple one-flask method for the preparation of hydroxamic acid. Org Lett 5:2715–2717

Golenser J, Tsafack A, Amichai Y et al (1995) Antimalarial action of hydroxamate-based iron chelators and potentiation of desferrioxamine action by reversed siderophores. Antimicrob Agents Chemother 39:61–65

Gray GG, Ekstrom TJ (2001) The human histone deacetylase family. Exp Cell Res 262:75–82

Gupta SP (2007) Quantitative structure-activity relationship studies on zinc-containing metalloproteinase inhibitors. Chem Rev 107:3042–3087

Hackbarth CJ, Chen DZ, Lewis JG et al (2002) *N*-alkyl urea hydroxamic acids as a new class of peptide deformylase inhibitors with antibacterial activity. Antimicrob Agents Chemother 46:2752–2764

Heath EI, Grochow LB (2000) Clinical potential of matrix metalloprotease inhibitors in cancer therapy. Drugs 59:1043–1055

Hogg JH, Ollman IR, Wetterholm A et al (1995) Amino hydroxamic acids as potent inhibitors of leukotriene A4 hydrolase. Bioorg Med Chem 3:1405–1415

Hogg JH, Ollman IR, Wetterholm A et al (1998) Probing the activities and mechanisms of leukotriene A4 hydrolase with synthetic inhibitors. Chem Eur J 4:1698–1713

Holland KP, Elford HL, Bracchi V (1998) Antimalarial activities of polyhydroxyphenyl and hydroxamic acid derivatives. Antimicrob Agents Chemother 42:2456–2458

Holms J, Mast K, Marcotte P et al (2001) Discovery of selective hydroxamic acid inhibitors of tumor necrosis factor-α converting enzyme. Bioorg Med Chem Lett 11:2907–2970

Hooper NM (1996) Zinc metalloproteases in health and disease. Taylor & Francis, London

Indiani C, Santoni E, Becucci M et al (2003) New Insight into the peroxidase-hydroxamic acid interaction revealed by the combination of spectroscopic and crystallographic studies. Biochemistry 42:14066–14074

Johnstone RW (2002) Histone-deacetylase inhibitors: novel drugs for the treatment of cancer. Nat Rev Drug Discov 1:287–299

Jung M (2001) Inhibitors of histone deacetylase as new anticancer agents. Curr Med Chem 8:1505–1511

Kelly WK, O'Connor OA, Marks PA (2002) Histone deacetylase inhibitors: from target to clinical trials. Exp Opin Invest Drugs 11:1695–1713

Kouzarides T (1999) Histone acetylases and deacetylases in cell proliferation. Curr Opin Genet Dev 9:40–48

Kumar H, Gupta S P, Siddiqui A, Kumar V (2013) Advances in design and development of inhibitors of nitric oxide synthases. Curr Enzyme Inhib 9:117–141

Kurzak B, Farkas E, Glowiak T (1991) X-Ray and potentiometric studies on a pentanuclear copper(II) complex with β-alaninehydroxamic acid. J Chem Soc Dalton Trans 163–167

Kurzak B, Kurzak K, Jezierska J (1986) Solution properties of Cu(II)-L-α-alaninehydroxamic acid. Inorg Chim Acta 125:77–82

Kurzak B, Kurzak K, Jezierska J (1987) Solution properties of Cu(II) L-α-leucinehydroxamic acid. Inorg Chim Acta 130:189–193

Leff RL (1999) Clinical trials of stromelysin inhibitor. Osteoarthritis, matrix metalloproteinase inhibition, cartilage loss, surrogate markers, and clinical implications. Ann N Y Acad Sci 878:201–207

Li YY, Feldman AM (2001) Matrix metalloproteinases in the progression of heart failure: potential therapeutic implications. Drugs 61:1239–1252

Lossen H (1869) Synthesis of oxahydroxamic acid. Liebigs Ann Chem 150:314–316

Lou B, Yang K (2003) Molecular diversity of hydroxamic acids: Part II. Potential therapeutic applications. Mini Rev Med Chem 3:609–620

Marks PA, Richon VM, Breslow A et al (2001) Histone deacetylase inhibitors as new cancer drugs. Curr Opin Oncol 13:477–483

Marks PA, Richon VM, Rifkind RA (2000) Histone deacetylase inhibitors: inducers of differentiation or apoptosis of transformed cells. J Natl Cancer Inst 92:1210–1216

Marmion CJ, Griffith D, Nolan KB (2004) Hydroxamic acids - an intriguing family of bioligands and enzyme inhibitors. Eur J Inorg Chem 15:3003–3016

Miller MJ (1989) Synthesis and therapeutic potential of hydroxamic base siderophores and analogues. Chem Rev 89:1563–1569

Mishra RC, Tripathi R, Katiyar D et al (2003) Synthesis of new glycosylated β-amino hydroxamates class of antimalarials. Bioorg Med Chem 11:5363–5374

Moss ML, White JM, Lambert MH et al (2001) TACE and other ADAM proteases as targets for drug discovery. Drug Discov Today 6:417–426

Muri EM, Nieto MJ, Sindelar RD et al (2002) Hydroxamic acids as pharmacological agents. Curr Med Chem 9:1631–1653

Nelson FC, Zask A (1999) The therapeutic potential of small molecule TACE inhibitors. Expert Opin Invest Drugs 8:383–392

Newton RC, Decicco CP (1999) Therapeutic potential and strategies for inhibiting tumor necrosis factor-alpha. J Med Chem 42:2295–2314

O'Brien EC, Farkas E, Gil MJ et al (2000) Metal complexes of salicylhydroxamic acid (H2Sha), anthranilic hydroxamic acid and benzohydroxamic acid. Crystal and molecular structure of [Cu (phen) 2(Cl)]Cl x H2Sha, a model for a peroxidase-inhibitor complex. J Inorg Biochem 79:47–51

Ollmann IR, Hogg JH, Munoz B et al (1995) Investigation of the inhibition of leukotriene A4 hydrolase. Bioorg Med Chem 3:969–995

Onishi HR, Pelak BA, Gerckens LS et al (1996) Antibacterial agents that inhibit lipid A biosynthesis. Science 274:980–982

Overall CM, Lopez-Otin C (2002) Strategies for MMP inhibition in cancer: innovations for the post trial era. Nat Rev Cancer 2:657–672

Overall CM, Wiebkin OW, Thonard JC (1987) Demonstration of tissue collagenase activity in vivo and its relationship to inflammation severity in human gingiva. J Periodontal Res 22:81–88

Rokach J (1989) Bioactive Molecules Vol 11: Leukotrienes and lipoxygenases: chemical, biological, and clinical aspects. Elsevier, Amsterdam

Saavedra J, Keefer LK (2000) NO better pharmaceuticals. Chem Br 36:30–33

Sani M, Belotti D, Giavazzi R et al (2004) Synthesis and evaluation of stereopure α-trifluoromethyl-malic hydroxamates as inhibitors of matrix metalloproteinases. Tetrahedron Lett 45:1611–1615

Scolnick LR, Clements AM, Liao JC et al (1997) Novel binding mode of hydroxamate inhibitors to human carbonic anhydrase II. J Am Chem Soc 119:850–851

Shlopov BV, Lie WR, Mainardi CL et al (1997) Osteoarthritic lesions: involvement of three different collagenases. Arthritis Rheum 40:2065–2074

Sidebotham RL, Batten JJ, Karim QN et al (1991) Breakdown of gastric mucus in presence of *Helicobacter pylori*. J Clin Pathol 44:52–57

Skiles JW, Monovich LG, Jeng AY (2000) Matrix metalloproteinase inhibitors for treatment of cancer. Ann Rep Med Chem 35:167–176

Skotnicki JS, Zask A, Nelson FC (1999) Design and synthetic considerations of matrix metalloproteinase inhibitors. Ann N Y Acad Sci 878:61–72

Sternlicht M, Werb Z (2001) How matrix metalloproteinases regulate cell behavior. Annu Rev Cell Dev Biol 17:463–516

Steward WP (1999) Marimastat (BB2516): current status of development. Cancer Chemother Pharmacol 43(Suppl):S56–S60

Steward WP, Thomas AL (2000) Marimastat: the clinical development of a matrix metalloproteinase inhibitor. Expert Opin Investig Drugs 9:2913–2922

Stuehr DJ (1999) Mammalian nitric oxide synthases. Biochim Biophys Acta (BBA). Bioenerg 1411:217–230

Summers JB, Kim KH, Mazdiyasni H et al (1990) Hydroxamic acid inhibitors of 5-lipoxygenase: quantitative structure-activity relationships. J Med Chem 33:992–998

Supuran CT, Scozzafava A (2000) Carbonic anhydrase inhibitors and their therapeutic potential. Expert Opin Ther Pat 10:575–600

Supuran CT, Scozzafaca A (2002) Matrix Metalloproteinases. In: Smith HJ, Simons C (eds) Proteinase and peptidase inhibition: recent potential targets for drug development. Taylor and Francis, London, pp 35–61

Supuran CT, Scozzafava A, Conway J (eds) (2004) Carbonic anhydrase: its inhibitors and activators. CRC Press, Boca Raton

Tegoni M, Dallavalle F, Santos A (2004) Succinylhydroxamic derivatives of α-amino acids as MMP inhibitors. Study of complex-formation equilibria with Cu^{2+}, Ni^{2+} and Zn^{2+}. J Inorg Biochem 98:209–218

Tsafack A, Golenser J, Libman J et al (1995) Mode of action of iron (III) chelators as antimalarials. III. Overadditive effects in the combined action of hydroxamate-based agents on in vitro growth of Plasmodium falciparum. Mol Pharmacol 47:403–409

Tsujii M, Kawano S, Tsuji S et al (1992) Mechanism of gastric mucosal damage induced by ammonia. Gastroenterology 102:1881–1888

Tsukamoto K, Itakura H, Sato K et al (1999) Binding of salicylhydroxamic acid and several aromatic donor molecules to *arthromyces ramosus* peroxidase investigated by X-Ray crystallography, optical difference spectroscopy, NMR relaxation, molecular dynamics, and Kinetic. Biochemistry 38:12558–12568

Vassali P (1992) The pathophysiology of tumor necrosis factors. Annu Rev Immunol 10:411–452

Verma RP (2012) Hydroxamic acids as matrix metalloproteinase inhibitors In: Gupta SP (ed) Matrix metalloproteinase inhibitors: specificity of binding and structure-activity relationships. Springer, Basel AG, pp 137–176

Verma RP, Hansch C (2007) Matrix metalloproteinases (MMPs): chemical-biological functions and (Q)SARs. Biorg Med Chem 15:2223–2268

Visse R, Nagase H (2003) Matrix metalloproteinases and tissue inhibitors of metalloproteinases: structure, function, and biochemistry. Circ Res 92:827–839

Whittaker M, Flyod CD, Brown P et al (1999) Design and therapeutic application of matrix metalloproteinase inhibitors. Chem Rev 99:2735–2776

Yadav MR, Murumkar PR, Zambre VP (2011) Advances in studies on collagenase inhibitors. In: Gupta SP (ed) Matrix metalloproteinase inhibitors: specificity of binding and structure activity relationships. Springer, Basel AG, pp 83–135

Yong VW, Krekoski CA, Forsyth PA et al (1998) Matrix metalloproteinases and diseases of the CNS. Trends Neurosci 21:75–80

Zamora R, Grzesiok A, Weber H et al (1995) Oxidative release of nitric oxide accounts for guanylyl cyclase stimulating, vasodilator and anti-platelet activity of Piloty's acid: a comparison with Angeli's salt. Biochem J 312:333–339

Theoretical Studies on Hydroxamic Acids

Rita Kakkar

Abstract Hydroxamic acids find many applications in chemistry and biology and have been the subject of many experimental investigations. Theoretical studies are not as frequent. However, the smallest homolog, formohydroxamic acid (FHA), has been studied at various levels, including high-level ab initio and density functional with large basis sets. All studies indicate that it exists as the Z-amide tautomer and deprotonation occurs from the nitrogen. Many combined experimental and theoretical studies confirm these conclusions. The interaction of formohydroxamic acid with solvent molecules and its adducts with various compounds have also been theoretically investigated. The higher homologs have not been studied as much. Acetohydroxamic acid, also known as Lithostat, has also been investigated at various levels of theory and experiment. Interest in this compound arises from the fact that it is a known inhibitor of urease. Other investigated hydroxamic acids include benzohydroxamic acid, whose conformational properties have also been investigated. Because of their association with inhibition of the urease enzyme and matrix metalloproteinases, as well as their application as siderophores, the complexation chemistry of hydroxamic acids is very important. However, very few theoretical studies aimed at deciphering the complexation of hydroxamic acids have appeared in the literature. Studies on metal ion selectivity of hydroxamic acids reveal that the affinity toward Ni(II), the metal ion present in urease, is due to its electrophilic nature. However, several QSAR and docking studies have appeared in the literature relating to applications of hydroxamic acids as inhibitors.

Keywords DFT · Conformation · Tautomerism · Metal ion selectivity · Complexation · Urease inhibition

R. Kakkar (✉)
Department of Chemistry, University of Delhi, Delhi 110007, India
e-mail: rkakkar@chemistry.du.ac.in

Abbreviations

|	
AHA	Acetohydroxamic acid
AIMD	Ab initio molecular dynamics
BHA	Benzohydroxamic acid
BPU	*Bacillus pasteurii*
DFT	Density functional theory
FHA	Formohydroxamic acid
GGA	Generalized gradient approximation
HDAC	Histone deacetylase
HOMO	Highest occupied molecular orbital
HP	*Helicobacter pylori*
HSAB	Hard and soft (Lewis) acids and bases
IW	Irving-Williams
KAU	*Klebsiella aerogenes*
KCX	Lysine NZ-carboxylic acid
LDA	Local density approximation
LUMO	Lowest unoccupied molecular orbital
MD	Molecular dynamics
MMP	Matrix metalloproteinase
NBPT	N-(n-Butyl) thiophosphoric triamide
OXHA	Oxalodihydroxamic acid
PBE	Perdew-Burke-Ernzerhof
PDF	Peptide deformylase
QSAR	Quantitative structure activity relationships
SHA	Salicylhydroxamic acid

Contents

1 Introduction

According to the IUPAC Gold Book (McNaught and Wilkinson 1997), hydroxamic acids are "Compounds, RC(=O)NHOH, derived from oxoacids $R_kE(=O)_l(OH)_m$ ($l \neq 0$) by replacing –OH by –NHOH, and hydrocarbyl derivatives thereof. Specific examples are preferably named as *N*-hydroxy amides". They contain the oxime (–N–OH) and the carbonyl (C=O) groups and have the following structure:
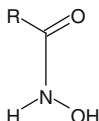
Hydroxamic acids are hydrophilic organic compounds that can exhibit keto-iminol tautomerism, and both tautomers may exist as **Z** (*zusammen*) or **E** (*entgegen*) diastereomers. They are much weaker acids than the structurally related carboxylic acids RC(=O)OH, and produce hydroxamate ions. The deprotonation could be either from the nitrogen or the oxygen, making them N-acids or O-acids. The hydroxamic acid grouping imparts chelating properties to these acids and their *N*-substituted derivatives, which serve as bidentate di-oxygen ligands toward many metal ions such as Fe(III) and Cu(II). The complexes are highly colored and are useful for the spectrophotometric (Agrawal and Patel 1980) and gravimetric (Agrawal and Roshania 1980) analysis of the metal ions.

Hydroxamate ions are best known as iron chelators (Miller 1989). Some hydroxamates are siderophores, which are compounds produced by microorganisms for the abstraction of iron from iron-deficient environments (Kehl 1982; Raymond et al. 1984; Weinberg 1989). Hydroxamate siderophores have been studied extensively due to their role as Fe(III)-specific sequestering agents, and potential pharmacological applications connected either with the microbial Fe(III) transport role or with the in vivo decontamination of Fe(III)-overload patients. Though the relationship between the biological effects and the strong chelating ability of hydroxamic acids is well established, very little is known about the metal complexes formed with natural cyclic monohydroxamic acids (Hiriart et al. 1985; Tipton and Buell 1970). This is due to the decomposition of these compounds in solution and precipitation in the presence of metal ions such as Cu(II).

Hydroxamic acids have particular affinities for 'hard' cations such as Fe(III), Np(IV), and Pu(IV) (Baroncelli and Grossi 1965; Barocas et al. 1966; Desaraju and Winston 1986; Taylor et al. 1998) with which they form five-membered chelate rings. The strong complexation of hydroxamic acids with plutonium has been used for the elimination of actinides and other hazardous metal ions from radioactive wastewater streams and for the recovery of plutonium and its extraction. They can also reduce a range of metal ions, such as Np(VI), which is very rapidly reduced to Np(V) (Colston et al. 2000).

On acid hydrolysis of free hydroxamic acids, hydroxylamine and the parent carboxylic acid are formed (Ghosh 1997). Metal ions bound to hydroxamates also hydrolyze, and complexes of Pu(IV) with formohydroxamic and acetohydroxamic acids (AHA) are slowly reduced to free Pu(III) ions (Todd and Wigelund 2006).

The chelating ability of hydroxamic acids has been used to link pharmaceutically useful ions such as radioactive or paramagnetic ions to monoclonal antibodies that direct the ion to a desired target tissue for tumor or tissue imaging or therapy purposes.

The use of hydroxamate coordination polymers as molecular magnets (Kahn 2000) has also been explored (Milios et al. 2002). Due to all these applications, the coordination chemistry of hydroxamates has evoked much interest (Brown et al. 2001; Gaynor et al. 2001; Marmion et al. 2004).

A variety of hydroxamic acid derivatives have recently been touted for their potential use as inhibitors of hypertension, tumor growth, inflammation, infectious agents, asthma, arthritis, and more. Other biological applications include inhibition of enzymes such as prostaglandin H synthase, peroxidases, ureases, and matrix metalloproteinases (MMPs) which degrade the barriers holding cells in place and are involved in tumor growth. Investigations of DNA cleavage by hydroxamic acids in the presence of metal ions (Chittari et al. 1998; Hashimoto and Nakamura 1995, 1996; Hashimoto et al. 1992, 1966, 1997, 1998; Joshi and Ganesh 1992, 1994a, b) have yielded promising results.

A recent theoretical study has been carried out on a new application of hydroxamic acids, as collectors for selective flotation of diaspore over aluminosilicates. Jiang et al. (2012) carried out a Density Functional Theory (DFT) study of the effect of carboxyl hydroxamic acids on the flotation behavior of diaspore and aluminosilicate minerals. Gece and Bilgiç (2010) studied the corrosion inhibition characteristics of two hydroxamic acids, i.e. oxalyldihydroxamic acid and pimeloyl-1,5-di-hydroxamic acid, on carbon steel using DFT. The authors related the inhibition efficiency to quantum chemical parameters such as E_{HOMO}, E_{LUMO}, calculated using B3LYP/6-31+G**, in order to elucidate the inhibition mechanism of these compounds. They found the inhibition to be due to the **E** isomer.

However, in spite of their various applications, very little was known about their structures for more than even 100 years after they were first reported by Lossen (1869). In the absence of spectral data, it was difficult to assign the correct structure from the various possible isomeric and tautomeric structures, and rotamers thereof in solution (Brown et al. 1982, 1991, 1996) and no experimental gas phase data concerning their structures were available. Added to that is the fact

that the various structures are close in energy, and accurate computational methods were not available at that time to distinguish between the structures. It could also not be established whether they are O-acids or N-acids, i.e., whether deprotonation takes place from –OH or –NH.

However, the correct assignment of their structures is extremely important because most of the applications of hydroxamic acids arise from their chelating ability, for which the correct orientation of the chelating atoms is essential. Theoretical methods can help provide information about the ground state conformation, and, if it is not the right conformation for chelation, the energy required to attain the required conformation.

It is no surprise, therefore, that a number of experimental and theoretical studies directed toward the elucidation of the structures and properties of hydroxamic acids have appeared in the literature. This article reviews the present-day knowledge of simple hydroxamic acids and their properties obtained from theoretical studies. The article is organized as follows: the simplest hydroxamic acid, formohydroxamic acid (FHA) has been the subject of various theoretical studies, ranging from semiempirical to ab initio and density functional. The former were found to be inaccurate for predicting the relative energies of tautomers, and so the literature concerning this acid from ab initio and density functional studies is first reviewed. This is followed by a description of the higher analogs and some simple aromatic acids. Literature pertaining to their complexation behavior is next reviewed, followed by theoretical studies on their biological activities.

2 Formohydroxamic Acid

The simplest hydroxamic acid, FHA, has been the subject of various experimental and theoretical investigations in the vapor and solution phases (Bagno et al. 1994; Bauer and Exner 1974; Blom and Günthard 1981; Bordwell et al. 1990; Bracher and Small 1970; Brown et al. 1991, 1996, 1998; Decouzon et al. 1990; Exner 1964; Fishbein and Carbone 1965; Fitzpatrick and Mageswaran 1989; García et al. 2000; Guo and Ho 1999; Larsen 1988; Lipczyñska-Kochany and Iwamura 1982; Mora-Diez et al. 2006; Remko and Šefčíková 2000; Remko 2002; Remko et al. 1993; Sałdyka and Mielke 2002, 2003a; Sant'Anna 2001; Turi et al. 1992; Ventura et al. 1993; Wang and Houk 1988; Wiberg and Laidig 1988; Wu and Ho 1998; Yazal and Pang 1999; Yen et al. 2000). In view of the diverse results obtained from previous calculations and experimental observations, Kakkar et al. (2003) carried out a systematic study of the structures of some primary and secondary hydroxamic acids: –RCONR'OH; R = H, CH_3, C_2H_5; R' = CH_3 (formo-, aceto-, propano-, and N-methylacetohydroxamic acids). They determined the relative acidities and stable configurations and tautomers of the neutral and deprotonated hydroxamic acids, which can serve as model hydroxamic acids used in cancer drug design, since these acids contain the smallest unit C=O…NH that can bind to the DNA helix.
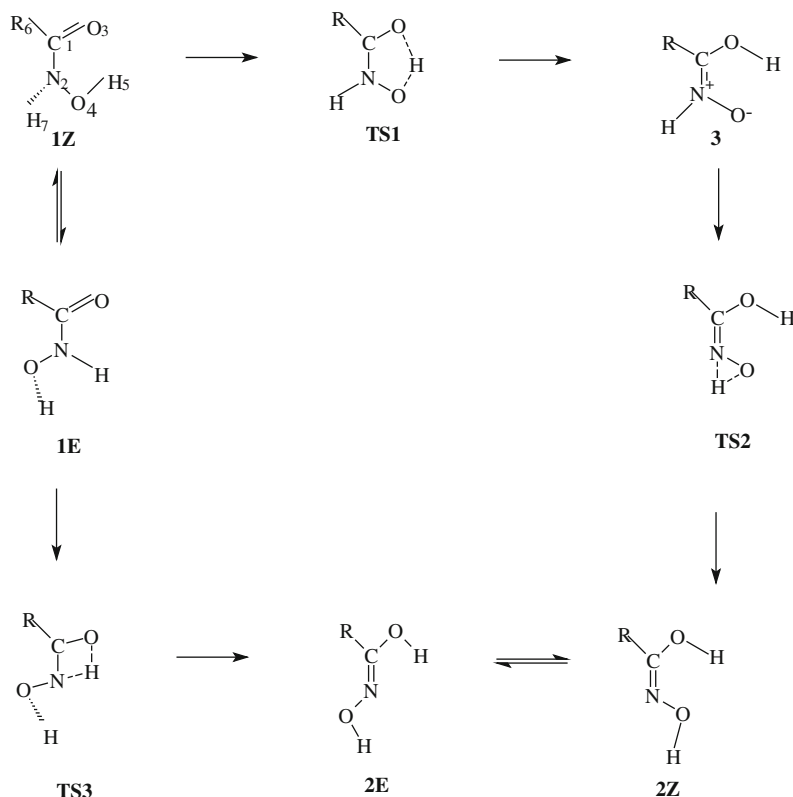
Fig. 1 The tautomeric forms of hydroxamic acids (R = H, CH_3, C_2H_5) and the transition states interconnecting them

All the systems may exist in three tautomeric forms, viz. two rotamers of the keto form (**1E**, **1Z**), two rotamers of the iminol form (**2E**, **2Z**), and one zwitterionic iminol form, **3**. The various forms and their interconversions are depicted in Fig. 1 (Wu and Ho 1998).

2.1 Relative Energies

FHA, being the smallest member of the family, has been studied at various levels of theory. Bauer and Exner (1974) reported that the keto forms, **1E** and **1Z** (Fig. 1), are favored over the iminol forms, **2E** and **2Z**. Low-level ab initio calculations suggested that the **1E** tautomer exists preferentially in the gas phase, but inclusion of correlation energy shifted the preference to **1Z** (Turi et al. 1992; Wu and Ho 1998). This conclusion was confirmed by Remko et al. (1993). The order of gas phase stability, as determined by Wu and Ho (1998) by ab initio theoretical

calculation, is **1Z > 2Z > 1E > 2E**. However, experimental studies on the structure of FHA using X-ray (Larsen 1988) and ^{17}O NMR (Lipczyñska-Kochany and Iwamura 1982) indicated that the most stable structure is **1E** in its crystals and **1Z** in solution.

DFT calculations at the B3LYP/6-311++G**//B3LYP/6-31G* level (Kakkar et al. 2003) place the order of gas phase stabilities as **1Z > 1E > 2Z > 2E > 3**. Again, the keto tautomers were found to be preferred over the iminol ones, but the order of stabilities of the two rotamers of the keto form was found to be different from that reported by Wu and Ho (1998). The finding that **1Z** is more stable than **1E** agrees with the expectation based on stabilization of **1Z** due to intramolecular hydrogen bonding (see Fig. 1), and the smaller value of the dipole moment of **1Z** (3.00 D compared to 3.37 D of **1E**), which also agrees with the finding (Wang and Houk 1988; Wiberg and Laidig 1988) that the rotamer with the smaller dipole moment is always more stable in vacuum. However, the difference in energy between the **1Z** and **1E** rotamers is very small, and we may conclude that **1Z** and **1E** coexist in the gas phase, as found experimentally from IR spectra (Sałdyka and Mielke 2003a). At 298.15 K and 1 atm pressure, the Gibbs energy difference between the **1Z** and **1E** forms was found to be only 0.6 kcal mol^{-1} (Kakkar et al. 2003), which implies that **1Z** is present to the extent of ∼75 %. However, none of the two semiempirical methods, AM1 and PM3, were able to give the correct order of stabilities. The two keto forms (**1Z** and **1E**) were found to be nonplanar, whereas the two iminol forms, **2E** and **2Z**, are nearly planar. Since the crystal data pertain to the **1E** form (Larsen 1988), the calculated optimized geometries for **1E** were compared with the experimental ones, and the agreement was found to be within 2 %, validating the DFT method.

These predictions were confirmed by later theoretical and experimental studies. Sałdyka and Mielke (2007) investigated the keto-iminol tautomerism of AHA and FHA isolated in argon matrixes by full Xe arc irradiation. For FHA, the relative abundances of **1Z**, **2Z**, and **1E** were found to be 94.3, 2.5, and 3.1 %, respectively, in agreement with their MP2/6-311++G(2d,2p) predicted values (85, 3.99, 11, and 0.0062 %) based on calculated ΔE_{ZPE} energies 1.43, 1.25, and 5.29 kcal mol^{-1} of **2Z**, **1E**, and **2E** relative to **1Z**.

2.2 Intramolecular Proton Transfer

The potential energy profiles for the intramolecular proton transfer of FHA tautomers (Fig. 1) have also been investigated at the G2 (Wu and Ho 1998) and DFT (Kakkar et al. 2003) levels. The energies of the transition states reflect their different respective ring strains, and the energy order is **TS2 > TS3 > TS1**, since the three transition states involve three, four, and five membered rings, respectively. Wu and Ho (1998) discussed in detail the transformation from the keto form (**1Z**) to the enol form (**2Z**). They concluded that, of the two possible pathways for the transformation (**2Z**, see Fig. 1), the first pathway, that is, **1Z → 3 → 2Z**,

involves the highly strained three-centered transition state (**TS2**) and does not seem likely. The second pathway, **1Z → 1E → 2E → 2Z**, involves the relatively less strained four-center-like transition state, **TS3**, and should be thus preferred. However, they did not take into account the substantial rotational barrier from **2E** to **2Z**. At the B3LYP/6-311++G**//B3LYP/6-31G* level (Kakkar et al. 2003), the barrier is 45.2 kcal mol^{-1}, which is much higher than the general rotational barrier for C–N bonds, in the range 10–15 kcal mol^{-1} (Blom and Günthard 1981). This is to be expected, since in this case the rotation is about the C=N double bond. In fact, the transition state has a higher energy (51.0 kcal mol^{-1}) than either **TS1** or **TS3**. It is therefore quite likely that the **2E** tautomer formed initially does not undergo subsequent isomerization to the more stable rotamer, **2Z**. The calculated rotational barrier separating **1Z** and **1E** is, however, much smaller (17.3 kcal mol^{-1}). The path for the transformation of **1E** to **2E** via the transition state **TS3** was found to have an activation energy of 43.4 kcal mol^{-1}, as compared with the calculated G2 (Wu and Ho 1998) barrier of 42.4 kcal mol^{-1}. Both theoretical results are in close agreement. Thus, DFT calculations, which can be performed at a fraction of the cost of the high level G2 calculations, perform as well. The overall activation energies for the two pathways are 53.5 and 51.0 kcal mol^{-1}, respectively, and the latter is only slightly preferred.

B3LYP/6-311++G* calculations on the tautomerism in some hydroxamic acids in the gas phase, in solvent, and in the presence of 1–3 water molecules (Tavakol 2009) also revealed the greater stability of the **1Z** tautomer. The calculations showed that the energy barrier of gas phase tautomerism is very high, but the presence of water molecules decreases the barrier.

Besides intramolecular hydrogen bonding that stabilizes the **1Z** tautomer, intermolecular hydrogen bonding with solvent molecules has also been theoretically investigated.

2.3 Intermolecular Hydrogen Bonding

Of the monohydrates of the **1Z** and **1E** forms of FHA, shown below, **1Z·H₂O** was found to be more stable than **1E·H₂O** by 2.5 kcal mol^{-1} (Kakkar et al. 2003). Thus, **1Z** becomes more strongly favored in aqueous solution.

1Z.H₂O   **1E.H₂O**
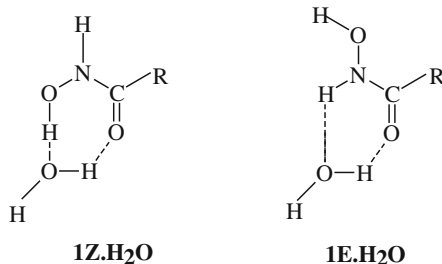
The reaction enthalpy for the process

$$1Z \ + \ H_2O \rightarrow 1Z \cdot H_2O$$
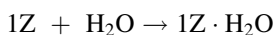
was found to be -8.3 kcal mol^{-1} and that for

$$1E \ + \ H_2O \rightarrow 1E \cdot H_2O$$
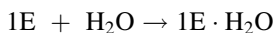
as -6.3 kcal mol^{-1}. Thus, hydrogen bonding with water stabilizes **1Z** to a greater extent than **1E**. Kaur and Kohli (2008) investigated the intra- and intermolecular hydrogen bonding in FHA at the MP2/6-31+G* level. They reported that intramolecular hydrogen bonding exists only in the **1Z** isomer, though there are multiple hydrogen bond donor and acceptor groups present in the other isomers. Adduct formation with a water molecule results in intermolecular hydrogen bonding, which is stronger than the intramolecular hydrogen bonding. However, their results are at variance with the experimental observation (García et al. 2003, 2005) that complexation with free hydroxamic acids is slower than that with the anions, indicating that the intramolecular hydrogen bond is hard to break, and blocks the reaction site. NMR studies have also shown lack of exchange of this proton.

Senthilkumar and Kolandaivel (2006) applied ab initio and DFT methods to study the hydrogen bonding in the complexes formed between FHA and water molecules. They found that FHA has the **1Z** form in all the complexes. ^{1}H and ^{13}C NMR, combined with B3LYP/6-311++G(d,p) chemical shifts in DMSO solution, revealed that 2-(hydroxyimino)propanohydroxamic acid forms hydrogen bonds with solvent molecules in solution (Kaczor and Proniewicz 2005), but exists as dimers in the solid state.

Sałdyka and Mielke (2005a) studied the complexes of FHA with water and ammonia using FTIR matrix isolation spectroscopy and MP2/6-311++G(2d,2p) calculations. Their analysis of the experimental spectra of the FHA/H$_2$O(NH$_3$)/Ar matrixes indicated formation of strongly hydrogen-bonded complexes in which the NH group of FHA acts as a proton donor toward the oxygen atom of water or the nitrogen atom of ammonia. Though theoretical calculations indicate that the most stable complexes are the cyclic structures in which the water or ammonia molecules are inserted within the intramolecular hydrogen bond of the FHA molecule and act as proton donors for the CO group and proton acceptors for the OH group of FHA, these were not observed in the matrixes, which indicates high energy barrier for their formation.

Sałdyka and Mielke (2004a, b) recorded the argon matrix infrared spectra of the complexes formed between FHA and nitrogen/carbon monoxide. In the case of nitrogen, two isomeric complexes with the nitrogen atom attached to the NH or OH group of FHA were found. Theoretical vibrational frequencies at the MP2/6-311++G(2d,2p) level were found to be in good agreement with the experimental data. Three isomeric complexes were formed with carbon monoxide: in two of the complexes, the carbon atom of carbon monoxide interacts with the NH or OH group of FHA and, in the third, the oxygen of carbon monoxide interacts with –NH

of FHA. Again, the observed vibrational frequencies were found to be in good agreement with the calculated B3LYP/6-311++G(2d,2p) values.

Kaur and Kohli (2012) investigated the hydrogen-bonding abilities of a few amino acid side chains through aggregation of methylamine, methanol, and acetic acid with formo- and thioformohydroxamic acids using MP2/6-31+G* calculations.

Denis and Ventura (2001) carried out a density functional study of the neutral and ionic chelates of boric acid with FHA. The calculated IR spectrum for the bis(hydroxamate) boron chelate was found to be in excellent agreement with the experimental spectrum.

The structures and gas phase metal affinities of FHA derivatives were studied using B3LYP/6-311+G(d,p) and CPCM solvations (Šille et al. 2010). The stability order of the alkali metal ion complexes ($Li^+ > Na^+ > K^+$) was found to be as expected on the basis of the ionic radii of the alkali metal ions.

2.4 Aqueous Phase Calculations

The calculated Gibbs energies of **1E**, **2Z**, and **2E** in aqueous solution relative to **1Z** (Kakkar et al. 2003) were found to be 7.5, 5.0, and 7.2 kcal mol^{-1} at 298.15 K and 1 atm. Thus, the **1Z** form becomes more emphatically favored in aqueous solution, in agreement with experiment (Lipczyñska-Kochany and Iwamura 1982), and the iminol forms also become apparent (stability order: **1Z** > **2Z** > **2E** > **1E**).

Aqueous solvation reduces the C–N bond length considerably, and there is a concomitant increase in the carbonyl bond length, signifying that delocalization of electrons takes place from the carbonyl bond to the carbon–nitrogen bond. The N–C and C=O stretching frequencies increase by 39 cm^{-1} and decrease by 174 cm^{-1}, respectively. The carbonyl oxygen is also involved in intermolecular hydrogen bonding with water molecules. The variation in the C–N, O–N, and O–C bond lengths in the isolated, complexed with one water molecule and in bulk water environments for the two rotamers is interesting. Solvation in **1Z** considerably reduces the C–N and O–N bond lengths, but lengthens the C–O bond only slightly. This shows that the intramolecular hydrogen bond remains intact in aqueous solution, in agreement with experimental observations (García et al. 2003, 2005). For **1E**, however, it is the C–O bond that shows the largest increase. In both cases, while the other two bonds show a constant increase or decrease in going from the isolated molecule to a complex with a single water molecule and then to bulk water, the O–N bond is shortest in the single water molecule complex, accounting for the destabilization.

2.5 Anions

Since the **1Z** form seems to be the favored one in the gas phase and in aqueous solution, dissociation could occur either from the NO–H group leading to the anion **1a**, both *cis* and *trans* forms of which are possible (Fig. 2), making FHA an

Fig. 2 Possible anion structures

1a cis   **1a** trans

1b   **1c**
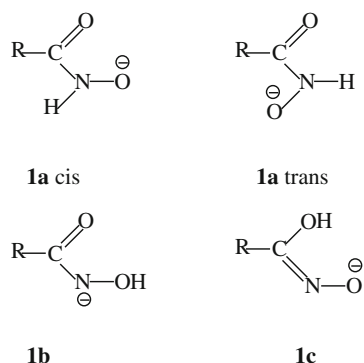
O-acid. However, if the N–H proton were to dissociate, it would be an N-acid, leading to the anion **1b**. In addition, there is a possibility of dissociation from the NO–H group of the almost equally stable **1E**, leading to structure **1c**, and making FHA an O-acid (see Fig. 2).

The **1b** anion was found (Kakkar et al. 2003) to be the most stable, followed by **1a-*cis***, **1a-*trans*,** and **1c** in that order. The finding that **1b** is more stable than the other anions agrees with other high-level ab initio (Ventura et al. 1993; Bagno et al. 1994) calculations. The greater stability of **1b** over **1a-*cis***, both of which are derived from **1Z**, can be easily explained. In the former, an electron resonance involving the N–C=O bonds is possible, which should stabilize the two unshared electron pairs on the nitrogen atom. That this occurs is confirmed by the following: The C–N bond length in **1b** reduces to 1.318 Å from 1.361 Å in **1Z**, and its vibrational frequency also increases by 56 cm^{-1}. Similarly, the carbonyl bond length increases to 1.276 Å compared to 1.225 Å in **1Z**. Its vibrational frequency also reduces by 96 cm^{-1}. This implies that a resonance exists between the keto and iminol forms, as shown below:

1b

keto   iminol
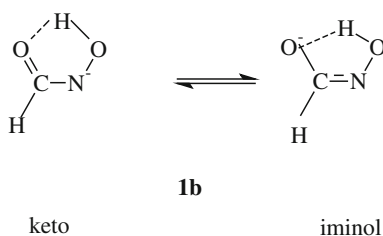
IR studies (Exner 1964) also show a red shift in the carbonyl frequency, indicating that it is in resonance with the nitrogen lone pairs. From the calculated partial atomic charges on the various atoms in **1Z** and **1b**, it is seen that the largest increase in negative charge occurs at the carbonyl oxygen, followed by the change at the nitrogen on formation of the anion **1b** from **1Z**. This again supports the concept of resonance in the anion, as the deprotonated FHA may be considered as the nitrogen-deprotonated keto form, or, alternatively, the *C*-hydroxy oxygen-deprotonated iminol form.

In contrast, if the proton dissociates from the oxygen atom to form **1a-*cis***, no such electron resonance is possible, which can stabilize the anion, but the originally existing intramolecular hydrogen bonding also disappears, increasing the instability of the resultant anion. The greater stability of **1b** implies that FHA is an N-acid in the gas phase, and this is in accord with most experimental and theoretical conclusions (Remko et al. 1993; Wu and Ho 1998). The calculated gas phase basicity for the formohydroxate ion is 347.2 kcal mol^{-1}. However, it may be mentioned that, as the three forms **1Z**, **1E**, and **2Z** are in equilibrium in the gas phase, it may also be considered as an O-acid as a result of deprotonation from the oxygen of the **2Z** form. This is supported by the structure of the anion, which is a resonance hybrid of the two forms.

Wu and Ho (1998) also argued for N-acid behavior of hydroxamic acids thus: since structure **1Z** is the most stable conformation of FHA in the aqueous phase, its acidity would depend on which hydrogen atom (attached to the N atom or the O atom) can be dissociated easily. Since the barrier to the transformation **1Z → 3** is smaller than that for the intramolecular proton transfer (**1Z → 1E → 2E → 2Z**), the former reaction takes place faster and the proton on O_4 (H_5) is not available for dissociation, as it remains between the two oxygens, O_4 and O_3. The **1Z** to **2Z** transformation, which involves the transfer of the proton (H_7) attached to N_2, however, is more difficult and thus this proton is relatively easy to dissociate.

Leung (2006) applied ab initio molecular dynamics (AIMD) to study the hydration structures and electronic properties of the formohydroxamate anion in water. It was found that, in the O-deprotonated anions, the negative charge is concentrated on the oxime oxygen, while in the N-deprotonated case, it is partially delocalized between the nitrogen and the adjoining oxime oxygen atom.

Senthilnithy et al. (2006) carried out ab initio calculations on isomers of *N*-phenylbenzohydroxamic acid derivatives and their deprotonation process. They found that the acid dissociation constants obtained using CBS-QB3 gas phase energies and HF/6-31+G(d)/CPCM hydration energies closely agree with the experimental values, provided that the most stable isomer for the molecule and the anion in water are taken as the Z-isomer. Senthilnithy et al. (2008) treated the first hydration shell of the O-deprotonated and N-deprotonated anions explicitly using HF/6-31+G(d), and the rest of the solvent as a continuous dielectric using CPCM, and found that the O–H bond dissociation is favored in aqueous medium. They supported their cluster calculations with a molecular dynamics (MD) simulation. Dissanayake and Senthilnithy (2009) presented a thermodynamic cycle to calculate pK_a values of hydroxamic acids, including the gas phase N–H deprotonation of the hydroxamic acid, the solvent phase transformation of the N-ion to the O-ion and the solvation of the hydroxamic acid molecule and the O-ion in water. Kaur et al. (2009) also calculated the pK_a values for deprotonation from formo- and thioformohydroxamic acids and concluded that these are N-acids.

The photodecomposition of FHA yielding the hydrogen-bonded complexes HNCO–H_2O and NH_2OH–CO has been studied both experimentally and theoretically (Sałdyka and Mielke 2003b). B3LYP/6-311++G(2d,2p) calculations provided support for the proposed structures.

3 Higher Homologs

3.1 Aceto- and Propanohydroxamic Acids

The next two higher homologs of FHA are aceto- and propanohydroxamic acids. The former (AHA) is also known as Lithostat, a drug used to cure kidney ailments, although it has several side effects, such as hemolytic anemia, blood clotting, and headaches. Fishbein and Carbone (1965) first reported its function as an inhibitor of the enzyme urease.

A similar trend in energy is observed in the case of these two molecules (Kakkar et al. 2003), with the energy gap between the **1E** and **1Z** forms becoming smaller with each substitution, until for propanohydroxamic acid, the **1E** form becomes favored over **1Z**. X-ray crystallographic analysis of AHA revealed the stable structure to be the **1Z** form in the solid state (Bracher and Small 1970). The greater stability of the **1E** form for propanohydroxamic acid in the gas phase seems contrary to the fact that an intramolecular hydrogen bond in the **1Z** form is disabled in **1E**. However, the small differences in energy suggest that both aceto- and propanohydroxamic acids exist in the **1Z** and **1E** forms that are in equilibrium in the gas phase. This prediction is consistent with previous ab initio calculations (Yazal and Pang 1999). Mora-Diez et al. (2006) also reported the greater stability of the **1Z** form based on their MP2(FC)/AUG-cc-pVDZ level calculations.

Sałdyka and Mielke (2007) reported that the relative abundances of the **1Z**, **2Z**, and **1E** isomeric structures in the AHA/Ar matrixes, obtained by deposition of the vapor over solid AHA sample heated to 301 K, are 95.1, 3.7, and 1.2 %, respectively. The results of their calculations at the MP2/6-311++G(2d,2p) agreed with the experimentally determined order of stability of the AHA isomers.

As far as the activation barriers are concerned, for the pathway from **1Z** to **2E** involving **TS3,** the overall barriers are 43.4, 40.8, and 39.0 kcal mol^{-1}, respectively, for formo-, aceto-, and propanohydroxamic acids (Kakkar et al. 2003). The barriers decrease slightly with every methyl substitution.

Theoretical and experimental studies of the solvent effect on the protonation of AHA have been carried out (García et al. 2000; Munoz-Caro et al. 2000). Mora-Diez et al. (2006) calculated the structures of the aggregates of the neutral and anionic forms of AHA with a water molecule at the MP2(FC)/AUG-cc-pVDZ level of theory, in order to evaluate the effect of intermolecular hydrogen bond formation on the deprotonation processes of AHA. They reported that the intra-molecular hydrogen bonding is preserved in the **1Z·H$_2$O** aggregate, as found for FHA (Kakkar et al. 2003), but the **1E·H$_2$O** system represents the most stable aggregate.

The observation that **1b** is the most stable form of the anion (Kakkar et al. 2003) agrees well with high-level ab initio and density functional calculations (Yazal and Pang 1999). Decouzon et al. (1990) measured gas phase acidities of AHA as well as those of its N-methyl and O-methyl derivatives, concluding that it behaves essentially as an N-acid in the gas phase, with a gas phase basicity of the

N-anion equal to 339.1 ± 2 kcal mol^{-1}. The theoretically calculated value of 337.1 kcal mol^{-1} (Kakkar et al. 2003) agrees well with this value. For propanohydroxamic acid, the calculated value is 335.3 kcal mol^{-1}. Other authors (Bordwell et al. 1990; Ventura et al. 1993; Bagno et al. 1994; Mora-Diez et al. 2006; Vrcek et al. 2008) also confirmed N-acid behavior for hydroxamic acids in gas phase and in DMSO solution. Kaczor and Proniewicz (2004) carried out DFT (6-311++G(d,p)) calculations of NMR spectra in DMSO solution for FHA and oxalodihydroxamic (OXHA) acid aggregates with two DMSO molecules via hydrogen bonding between the labile protons of the acids and the oxygens of the solvent molecules. They found excellent correlation between the calculated and observed NMR spectra. Again, the **Z** forms were found to be more stable, with OXHA existing exclusively in this form.

Ab initio molecular orbital calculations with 4-31G//4-31**G,** 6-3lG*//4-31G, and 6-31+G//4-31G basis sets were used to examine the structure, relative energy, protonation, and deprotonation of a series of seven hydroxamic acids in the gas phase (Yamin et al. 1996). The results showed that the most probable protonation site is the carbonyl oxygen atom, while deprotonation proceeds by loss of the NH hydrogen. MP2(FC)/AUG-cc-pVDZ calculations and NMR, spectrophotometric, and potentiometric measurements of the isomers of AHA and their deprotonation processes (Senent et al. 2003) gave essentially the same results: the **1Z** conformer is most stable in the gas phase and deprotonation occurs from the nitrogen in aqueous solution. García et al. (2000) carried out an experimental and theoretical study at the B3LYP/cc-pVDZ level on the solvent effect on protonation of AHA. They also found that the carbonyl is the most active site for protonation.

Sałdyka and Mielke (2005b) studied the dimerization of the keto tautomer of AHA using FTIR matrix isolation spectroscopy and B3LYP/6-31+G(d,p) calculations. Analysis of the AHA/Ar matrix spectra indicated formation of two dimers in which the intramolecular hydrogen bonds within the two interacting AHA molecules are retained.

Binary AHA…HX complexes of AHA with hydrogen halides, HX (X = F, Cl, Br) were investigated using the second order perturbation theory (Joshi and Gejji 2005). In the case of the complex with hydrogen fluoride, the latter acts as both a proton-donor to the carbonyl oxygen and as a proton-acceptor from the hydroxyl group. In the case of the chloro- and bromo-substituted derivatives, however, hydrogen-bonded interactions exist with the carbonyl oxygen and the methyl protons of AHA.

3.2 N-Methylacetohydroxamic Acid

In contrast to the situation for the above acids, in *N*-substituted derivatives, there is no possibility of the enol form as the nitrogen lacks a hydrogen atom for transfer to the carbonyl oxygen. In this case, too, it was found (Kakkar et al. 2003) that, like propanohydroxamic acid, the **1Z** form is less stable than **1E** by 0.8 kcal mol^{-1}.

However, the small difference suggests that both forms are in equilibrium in the gas phase. For the anion, it is found that the **1a-*trans*** form is more stable than **1a-*cis*** by 10.9 kcal mol^{-1}. This agrees with the prediction of previous ab initio calculations (Yazal and Pang 1999). The gas phase basicity of the anion (343.4 kcal mol^{-1}) agrees with the experimental value (Decouzon et al. 1990) of 346.9 ± 2 kcal mol^{-1}.
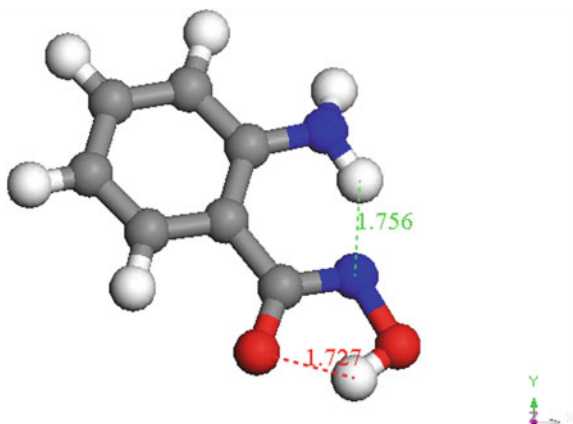
3.3 Arylhydroxamic Acids

Aromatic hydroxamic acids have also been extensively studied. García et al. (2005) carried out a theoretical and experimental study on the conformations, protonation sites, and metal complexation of benzohydroxamic acid (BHA). Their calculations at the RHF/cc-pVDZ level, refined by the B3LYP/AUG-cc-pVDZ method, indicated that, in the gas phase, **1Z** is the most stable structure of both neutral and deprotonated BHA. In acetone solution at −80 °C, the E/Z ratio was estimated as 3. They also experimentally observed the formation of E–E, Z–Z, and E–Z dimers, which dissociate in aqueous solution. The theoretical results showed that, as in AHA, intramolecular hydrogen bonding is strong. This agrees with the experimental observation in the dynamic ^{1}H NMR spectrum of BHA (García et al. 2005) in acetone solution (with residual water) that the coalescence temperature between the two proton singlets of the **E** isomer increases from −10 to 5 °C when the proportion of residual water of the solvent is increased by 30 %. This indicates that water hinders the interchange between the two protons of the E–NHOH group, probably due to hydrogen bond formation. The authors (García et al. 2003, 2005) also observed that the rate of complexation of Ni(II) with **1Z** hydroxamic acids is slower than that with the corresponding anions. This indicates that in aqueous solution, intramolecular hydrogen bonding is stronger than the intermolecular hydrogen bonding with water molecules, and this blocks the reaction site, slowing down the rate of complexation. Recently, the structure of BHA was investigated at the B3LYP, MP2, and MP4(SDQ) levels of theory and compared to the corresponding structures of formyl analogs (Al-Saadi 2012). All levels of theory predicted the molecule to exist predominantly in a near-planar structure adopting a *cis* conformation where the hydroxyl group eclipses the carbonyl bond.

For salicylhydroxamic acid (SHA) and *p*-hydroxybenzohydroxamic acid, García et al. (2007) found evidence for extended aggregation. B3LYP/AUG-cc-pVDZ level calculations showed that the most stable gas phase conformer is **1Z**, a structure with all three phenolate, carboxylate, and hydroxamate oxygen atoms in the *cis* position. The most stable monoanion is the N-deprotonated **1Z**.

For the three isomeric aminophenylhydroxamic acids, too, the **1Z** keto form was found to be the most stable (Kakkar et al. 2006a) in each case. Among the three isomers, 2-aminophenylhydroxamic acid was found to be the most stable, despite the two hydrogens in close proximity in the former. Hyperconjugative interactions with nitrogen and intramolecular hydrogen bonding reduce the

carbonyl bond order in the **Z** isomers of the acids. In the anions formed by
deprotonation of –OH, only the hyperconjugative interactions operate, but these
too reduce the carbonyl bond order to ~ 1.6.

All three acids are stabilized by intramolecular hydrogen bonding and the
Z forms are more stable than their **E** counterparts by several kcal mol^{-1}, unlike the
case of the simple hydroxamic acids. Besides, the **E** forms are nonplanar and do
not represent energy minima in the case of 2-aminophenylhydroxamic acid, which
possesses a small imaginary vibrational frequency (155 cm^{-1}) and the 4-amino-
phenyl isomer, for which the imaginary frequency is 45 cm^{-1}. In this case, too, the
acids are N-acids, as the **b** anion is more stable than **a** in all cases. The difference
in energies between the two anions is highest for the anion of 2-amin-
ophenylhydroxamic acid (19.5 kcal mol^{-1}), as there is extensive hydrogen
bonding in the **b** anion in this case (see Fig. 3). This partly explains why this
isomer has a tendency to form complexes by deprotonation from both nitrogen and
oxygen, while the other acids undergo deprotonation at oxygen only on complex
formation.

4 Metal Ion Chelation

By far, the most important application of hydroxamic acids is as metal ion che-
lators. The coordination chemistry of hydroxamic acids has been reviewed (Codd
2008), laying emphasis on the expansive role of hydroxamic acids in chemical
biology.

Metal-hydroxamate complexes exhibit structural diversity (Dessi et al. 1992;
Farkas et al. 1998a, b, 2000; Gaynor et al. 2001; Kurzak et al. 1992; Marmion et al.
2000; Milios et al. 2002). Hydroxamate ions have two oxygen atoms and may
bond to the metal ion in two different ways: monodentate or bidentate

configurations. Besides, they may also coordinate through the nitrogen atom and one oxygen atom. However, the bulk of experimental data favor the bidentate mode using two oxygen atoms. An X-ray diffraction study of the Fe(III) complex showed that the chelation involves the oxygen belonging to the carbonyl and NHOH groups (Lindner and Göttlicher 1969). Investigations on the complex formation with simple primary hydroxamic acid ligands in aqueous solution demonstrated clearly that, depending on the pH, two (O,O) binding modes of the ligands are accessible to metal ions like Cu(II) and V(IV) (Dessi et al. 1992; Farkas et al. 1998a). The more common hydroxamato (1-) type mode arises from the first deprotonation step and involves the coordination of the NHO^- moiety. The hydroximato (2-) form of the ligand is produced by further metal-induced deprotonation of the NHO^- at high pH. The coordination of the nitrogen atom of the hydroxamic moiety was never found in metal complexes formed by simple hydroxamic acids. Hydroxamic acids have been found to bind in other coordination modes as well (Milios et al. 2002).

However, in order to chelate to metal ions, the acid should adopt the required *cis* (**Z**) conformation. The reaction scheme shown in Fig. 1 entails rotations about the C–N bond for the interconversion between the two pairs of rotational isomers **1Z**, **1E** and **2Z**, **2E**. While the latter barrier is quite high, the smaller barrier to the CN rotation from **1Z** to **1E** plays an important role in metal ion chelation. The effects of this barrier are also reflected in kinetic parameters obtained from the sequestration of iron by hydroxamic acids from the polynuclear iron complex, $[Fe_{11}O_6(OH)_6(O_2CPh)_{15}]$. The substituents at nitrogen and carbon can modify the *cis/trans* (**Z/E**) ratio, as was found for a series of monohydroxamic acids (Brown et al. 1991, 1996). As the required conformation for the formation of a normal (O,O) chelate is *cis*, correlation between the **Z/E** ratio and the stability of the chelate (both thermodynamic and kinetic), can be expected.

4.1 Barriers to Rotation

For FHA, the calculated (Kakkar et al. 2003) rotational barriers at the DFT level in the gas phase and in aqueous solution are, respectively, 17.9 and 20.2 kcal mol^{-1}, respectively. For AHA, the gas phase barrier is calculated as 16.7 kcal mol^{-1}. Thus, the rotational barriers increase on aqueous solvation. Although the MP2/6-311G** calculations (Brown et al. 1998) predict otherwise, the rotational barriers decrease with increasing methyl substitution for the gas phase. Part of the discrepancy between the DFT results and those of Brown et al. (1998) could be due to underestimation of the stability of the **Z** form in their calculations, because of non-inclusion of diffuse functions that could lead to an incorrect description of hydrogen bonding effects. For *N*-methyl acetohydroxamic acid, the calculated rotational barrier from the more stable **1E** form is 16.6 kcal mol^{-1}, as compared with a value of 16.0 kcal mol^{-1} from MP2/6-311G** calculations (Brown et al.

1998). Niño et al. (2000) compared their MP2(FC)/cc-pVDZ and B3LYP/cc-pVDZ results for barriers to nitrogen inversion and methyl rotation in AHA, and found large differences in the two results.

4.2 Choice of an Appropriate Methodology

Hydroxamic acids are known to inhibit urease, a nickel-containing metalloenzyme. Three factors determine the specificity of a given metal-binding site for a particular transition metal ion (Bertini et al. 1995; Rulísék and Vondrášek 1998): the coordination geometry, the size of the preformed cavity in more complex ligands, and the affinity of functional groups participating in metal–ligand bonds for a specific transition metal ion. The third factor, and probably the most difficult one to address, is the different affinities of a particular ligand for different transition metal ions, which is often based on qualitative or semi-quantitative theories or principles such as the hard and soft acids and bases (HSAB) principle of Parr and Pearson (1983) and Pearson (1963) and the Irving-Williams (IW) series of stability constants (Sigel and McCormick 1970; Martin 1987). Nevertheless, a quantitative evaluation of the affinity is feasible only with accurate quantum chemical calculations on model systems, which is why a reliable computational scheme for the calculation of transition metal complexes containing metal–ligand bonds with ionic character is desired.

However, due to several reasons, there are very few quantum mechanical calculations on the electronic effects in the interaction of metal ions with biological systems. The first reason is the large number of electrons and spin states that must be considered for transition metal ions owing to their partially filled d orbitals, which makes it difficult to assign the ground spin state. Unrestricted calculations, which take up twice as much time as the restricted calculations, need to be performed on these systems in order to identify the ground state. Often the basis sets for these metal ions are also unavailable. The SCF convergence is also slow, owing to the mixing of the d orbitals with the s orbitals. Moreover, Jahn-Teller distortions remove symmetries, making the calculations even more computationally expensive. Nevertheless, advances in computational methodologies have now made it possible to perform accurate DFT calculations at modest cost and with reasonable accuracy, which sometimes even surpasses experimental determinations. In particular, Generalized Gradient Approximation (GGA) combines accuracy with reasonable computational cost.

Hydroxamic acids, particularly AHA, are known inhibitors of the urease enzyme. They block the Ni(II) ion of the enzyme by binding selectivity to it. The particular affinity of hydroxamic acids for Ni(II) was investigated (Kakkar et al. 2006b). In this study, the authors compared the complexation behavior of selected hydroxamic acids toward eight divalent ions, including Pd(II), Cd(II), Hg(II), Mn(II), Co(II), Ni(II), Cu(II), and Zn(II). All these metal ions are important constituents of metalloproteins and are also major pollutants of the environment,

and hence a scheme for their removal from the environment is essential. Several binding modes were considered in the work.

However, as very few theoretical studies on the complexation behavior of hydroxamic acids were available at that time, the authors (Kakkar et al. 2006a) first tested their methodology against the Cu(II) complexes of the three isomeric aminophenylhydroxamic acids, since their crystal data are available (Gaynor et al. 2001). They tested two LDA functionals and eight GGA functionals, employing numerical basis sets of double-ξ quality plus polarization functions (DNP) to describe the valence orbitals.

Although hydroxamate ions usually bind to metal ions through the two oxygen atoms (i.e., as (O,O)-bidentate chelating agents), other binding modes are also possible, and this range can be greatly increased if the hydroxamate ligand contains secondary binding groups, resulting in many diverse and intriguing structures (Milios et al. 2002). This was found in the complexes formed between the isomeric aminophenylhydroxamic acids (AphaH$_2$) and CuSO$_4 \cdot$5H$_2$O (Gaynor et al. 2001). While 4-aminophenylhydroxamic acid (4-AphaH$_2$) gives the simple square planar complex Cu(4-AphaH)$_2 \cdot$2H$_2$O, 2-aminophenylhydroxamic acid (2-AphaH$_2$) gives a fused 'dimeric' metallocrown of the formula [Cu$_5$(2-Apha)$_4$(μ-SO$_4$)$\cdot$(H$_2$O)$_2$]$_2$, in which the metal ions display extensive magnetic coupling (with potential applications in the field of magnetoelectronics). The complex has a 'clam-like' structure, in which (2-Apha^{2-}) is doubly deprotonated 2-aminophenylhydroxamic acid. The coordination is through deprotonated nitrogen and it contains bridging hydroximate (-2) functions, combined with the $\{O, \mu_2\text{-}O'\}$ chelating/bridging mode. 3-aminophenylhydroxamic acid (3-AphaH$_2$) gives a trinuclear helical polymer of formula [Cu$_3$(3-AphaH)$_4$SO$_4\cdot$(H$_2$O)]$_n\cdot$8H$_2$O, which has a supramolecular structure with large open cavities, which can be useful in trapping guest molecules.

The ability to accurately describe the three structurally diverse complexes by different pseudopotentials was discussed by the authors (Kakkar et al. 2006a). The following conclusions were drawn: both the LDA geometries, particularly VWN, are in good agreement with experiment, but the gradient-corrected DFT methods tend to exaggerate the Cu–O$_1$ bond length when compared with the experimental (Gaynor et al. 2001) value. On the other hand, LDA-VWN overbinds the Cu–O$_4$ bond, yielding a bond length that is too short by 0.034 Å. Some of the GGA functionals, namely BOP, RPBE, and HCTH, are particularly bad when it comes to predicting Cu–O bond lengths. The only GGA functional that gives good agreement with experiment is PBE (Perdew et al. 1996), for which the error is only 1.6 % in relation to experiment, in spite of the fact that the latter refer to the solid state, which is subject to deformation because of solid state effects. In particular, this is the only method that produces equal Cu–O$_1$ and Cu–O$_2$ bond lengths (see Fig. 4) for the two rings, in agreement with experiment. All other methods predict asymmetry in the two rings. In most cases, the overall errors are smaller for bond angles than for bond distances.

The authors proceeded with the GGA-PBE method on the complexes. The 2-aminophenylhydroxamic acid isomer was found to be the most stable of the three, but the complexation energy values indicate slightly greater stability of

**Fig. 4** Structure of the Cu(II) complex of 4-aminophenylhydroxamic acid
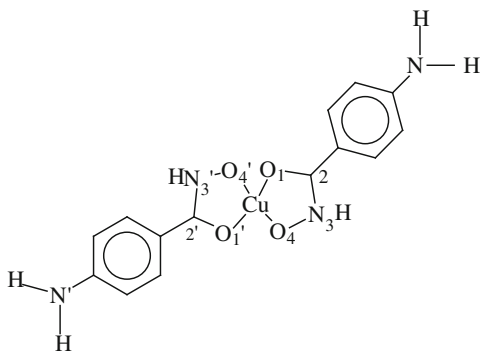
the 4-aminophenylhydroxamic acid complex. In each complex, both five-membered Cu-hydroxamate rings were found to be planar, causing delocalization of electrons in the $O_1C_2N_3$ moiety. The C_2C_6 bond is essentially single, permitting the phenyl ring to rotate about this bond. The phenyl rings are twisted with respect to the hydroxamate grouping by $\sim 20°$ in each case.

The group charge of the hydroxamate ligand changes from a value of -1.0 in the free state to ~ -0.3 in the three complexes, signifying electron transfer from the ligand to Cu(II) and coordination bond formation. The complexes were found to have sizable covalent character, each Cu–O bond having a covalent bond order slightly higher than 0.5.

Kakkar et al. (2006a) also observed that Mulliken charges are unreliable, as they are basis-size dependent. Plots of the electrostatic potential maps for the three complexes are shown in Fig. 5. These maps give an idea about the range of electron density around the complex. For 2- and 3-aminophenylhydroxamate complexes, the 0.016 au (10 kcal mol^{-1}) isoelectronic contour is plotted. However, for the 4-aminophenylhydroxamate complex, the potential extends only between -5.1×10^{-4} and 2.9×10^{-7} au, and hence the 1×10^{-10} au contour is plotted.

The three maps demonstrate the differences in the electronic behavior of the three complexes. The 2- and 3-aminophenylhydroxamate complexes exhibit similar contours. However, the map for the 4-aminophenylhydroxamate complex

Fig. 5 Isopotential maps for the Cu(II) complex of 2- and 3-aminophenylhydroxamic acid (Isovalue = 0.016 au), and 4-aminophenylhydroxamic acid (Isovalue = 1×10^{-10} au)
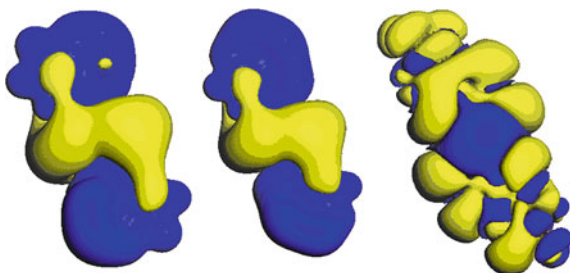
bears no resemblance to that of the other two. The smaller extent of the potential in the case of the 4-aminophenylhydroxamate complex may explain its reluctance to polymerize.

4.3 Metal Ion Selectivity

Having shown that the GGA-PBE functional combined with the DZP basis set gives a satisfactory description of the bonding in the Cu(II) aminophenylhydroxamic acid complexes, Kakkar et al. (2006b) proceeded with DFT calculations on a number of square planar hydroxamate chelates of several divalent metal ions in order to determine their respective affinities for hydroxamic acid ligands. Except Mn(II), which prefers the quartet spin state, the metal ions were seen to prefer the low-spin state. Though the favored geometry is square planar, the Zn(II) complex is considerably distorted (Fig. 6).

The calculated binding mode (–NOH deprotonated) was found to be in agreement with experiment. The complexation energies follow the order Cd(II) < Mn(II) < Hg(II) < Zn(II) < Pd(II) < Co(II) < Cu(II) < Ni(II), which is almost the IW series, with two notable exceptions, Pd(II) and Ni(II), both of which are d^8 ions. The authors explained the lesser stability of Pd(II) complexes than that predicted from the IW series on the basis of the HSAB principle. The hydroxamate ligand contains negatively charged carboxylate-like oxygens, and is hence hard, and should not prefer the soft metal ions, Cd(II), Hg(II), and Pd(II). In fact, palladium shows a preference for the hydroximate binding mode (Hall et al. 2002). The other exception is Ni(II), for which the binding energy was found to be the largest. This was explained on the basis of higher covalent character in the Ni(II) complex.

Extensive calculations showed that, although the interactions are mainly dominated by electrostatic forces, there is a covalent contribution as well that introduces subtle variations in binding affinities of various metal ions. Thus, although a reasonable correlation was found between the complexation energies and reciprocals of the ionic radii of the metal ions, deviations were attributed to some covalent character of the metal–ligand bonds, which modify a ligand's affinity for a metal ion and introduce subtle variations that are ultimately responsible for their biological action. A linear relationship between the partial charge on the metal ion and the LUMO energy showed that metal ions with lower lying vacant orbitals are able to form covalent coordination with the FHA ligand. The covalent bond order of the metal–ligand bonds is quite high. The affinity of the formohydroxamate ion for Ni(II) is satisfactorily explained on the basis of larger charge transfer from the ligand, and is reflected in the Ni(II) ligand bond orders, which are close to unity. The authors (Kakkar et al. 2006b) discussed the bonding characteristics of the investigated complexes, as well as the optimum size of the metal binding site. Some other hydroxamic acids were also investigated in the
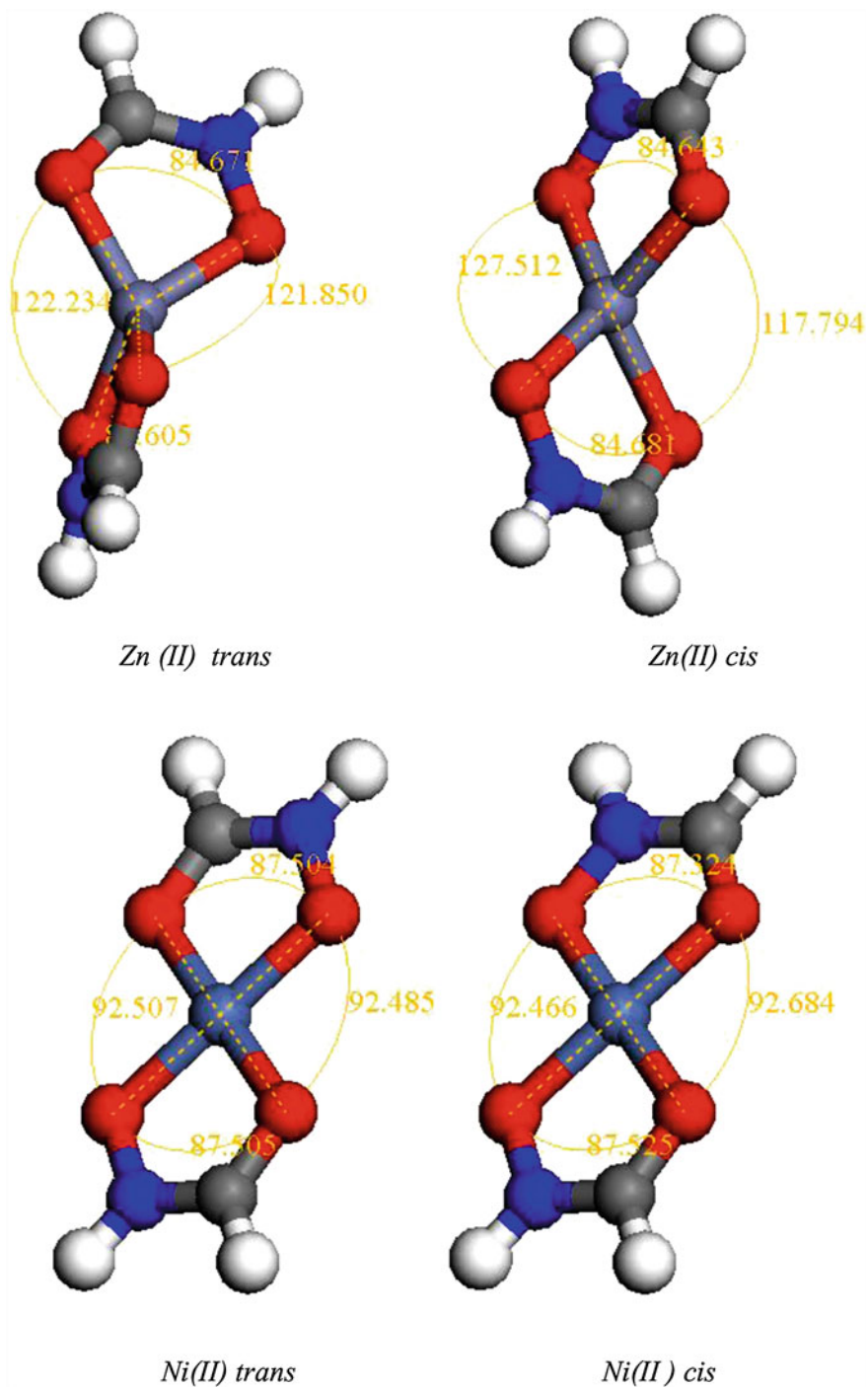
Fig. 6 Optimized structures of the *cis* and *trans* forms of the formohydroxamate complexes of Zn(II) and Ni(II). Color code: H-white, C-grey, N-blue, O-red. The top ring contains the M–O_2–C–N–O_1–(M = Zn, Ni) five-membered ring. The corresponding atoms of the lower ring are numbered with a prime

Fig. 7 Plot of the HOMOs for **a** formohydroxamate anion, and the *trans* formohydroxamate complexes of **b** Ni(II), and **c** Zn(II)
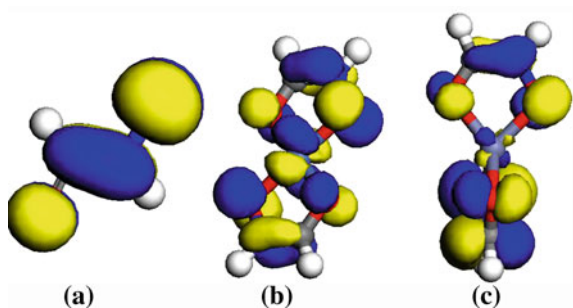
work. For hydroximate complexes and complexes with other hydroxamic acids, the Ni(II) complex was again found to be the most stable.

The plots of the highest occupied molecular orbitals of the ligand, the Ni(II) complex and the Zn(II) complex (Fig. 7) show that the ligand orbitals are retained in the HOMO of the complexes, but, in the case of Ni(II), the metal *d* orbital also becomes a part of the HOMO, showing an interaction between the Ni(II) *d* orbitals and the ligand. There is no participation of the metal orbitals for the Zn(II) complex.

The authors (Kakkar et al. 2006b) applied the knowledge gained about coordination bonding to investigate the metalloprotein urease and its inhibition by AHA.

5 Urease Inhibition

The interactions of transition metal ions with biomolecules (metalloproteins, peptides, DNA, RNA molecules, etc.) represent one of the fundamental aspects exploited by living organisms in performing their essential tasks. The role of transition metal ions in the structure and function of these systems is immense, though often unknown at the atomic or electronic level. One of the most important properties of bioinorganic systems is the relationship between molecular structure and energetics. Molecular structures can be efficiently studied by atomic resolution experimental techniques, but they do not provide any energy values. Thus, it is very tempting to complement bioinorganic experiments with energy evaluations, which can be presently achieved by state-of-the-art quantum mechanical calculations.

The metalloenzyme urease holds a very important place in the history of enzymology (Lippard 1995). Sumner (1926) crystallized the enzyme, but only some 50 years later was urease found to contain Ni(II) (Dixon et al. 1975) a transition metal previously recorded as an oddity with respect to biological activity. Urease catalyzes the hydrolysis of urea to ammonia and carbamate according to the equation

$$CO(NH_2)_2 + H_2O \rightarrow H_2NCOO^- + NH_4^+$$
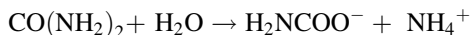
in plants, algae, fungi, and several microorganisms (Ciurli et al. 1999). The carbamate produced simultaneously decomposes, at the physiological pH, to give a second molecule of ammonia and bicarbonate, according to the equation

$$H_2NCOO^- + H_2O \rightarrow HCO_3^- + NH_3$$
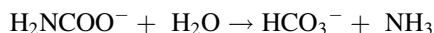
The hydrolysis of urea is difficult; the uncatalyzed reaction has never been observed (Blakeley et al. 1982). The stability of urea is attributed to its resonance energy (30–40 kcal mol^{-1}) (Wheland 1955). The enzyme converts urea into products at a rate 10^{14} times faster than the spontaneous decomposition rate (Blakeley et al. 1982).

Crystal structures of urease from three different microorganisms, *Klebsiella aerogenes* (KAU), *Bacillus pasteurii* (BPU), and *Helicobacter pylori* (HP), have been reported, providing a detailed picture of the active site (Jabri et al. 1995; Benini et al. 1999; Pearson et al. 2000; Ha et al. 2001). Hydroxamic acids are an important family of urease inhibitors. The most studied derivative is AHA, shown to behave as a slow-binding inhibitor (Dixon et al. 1975; Ciurli et al. 1999). The structure of the AHA-inhibited C319A mutant of KAU has been reported (Koga et al. 1998). The structure of the AHA-inhibited BPU has also been solved at 1.55 Å resolution (Benini et al. 2000). Manunza et al. (1999) performed MD calculations on the active site of urease from KAU and its adducts with urea, hydroxamic acid and N-(n-butyl)-phosphoric triamide (NBPT).

The quantum mechanical approach was used to model urease and its inhibition by AHA (Kakkar et al. 2006b) using the GGA-PBE DFT functional. For each of the ureases from two different microorganisms, KAU and HP, for which crystal structures have been determined (Jabri et al. 1995; Pearson et al. 2000; Ha et al. 2001), calculations were carried out for the uninhibited urease and its AHA inhibited structure. The urease from BPU has a similar structure to that from KAU, and was hence omitted from the analysis.

As the structures are too large for DFT calculations to be performed on the entire system, the active site consisting of the two nickel atoms and the ligands bound to them were modeled only, resulting in structures still having a formidable number of around 320 atoms.

5.1 Klebsiella Aerogenes Urease

The active site for in the native urease consists of two nickel atoms, complexed with *His* 133, *His* 135, *His* 245, *His* 271, KCX 216, *Asp* 359, and HOH 500–502. When complexed with AHA, the active site again consists of the two nickel atoms, *His* 133, *His* 135, *His* 245, *His* 271, KCX 216, and *Asp* 345, but HOH 500–502 are replaced by AHA, HAE 558, which bridges the two nickel atoms.

The final structures, labeled *A* (native) and *E* (complexed with AHA) are depicted in Fig. 8. In *A*, it can be seen that one Ni(II) atom is complexed with KCX via Ox1, *His* 246 via ND1, HOH 500 and 501 via their oxygens and *His* 272 via NE2. Likewise, the second nickel atom is also pentacoordinate, being linked to *His* 134 and *His* 136 via NE2, KCX via Ox2, *Asp* via OD1, and HOH 500 and 502 via their oxygens. HOH 500 serves as a bridging group, and is present as the hydroxyl ion. The Ni…Ni distance is long (3.743 Å) because of the bridge. The overall charge on this fragment is +1.0.

In *E*, on the other hand, one of the nickels (Ni(1)) is four coordinate. Hydroxamate is a bidenate ligand and binds to the two nickel atoms. Thus, Ni(2) coordinates to KCX via its oxygen Ox2, *His* 133, and *His* 135 via their nitrogens NE2, *Asp* 345 via OD1, and HAE via O1. Ni(1) is coordinated to *His* 245 via its nitrogen ND1, *His* 271 via its nitrogen NE2, KCX via Ox1, and HAE via O2. The overall charge on the fragment is +1.0. The Ni…Ni distance decreases slightly to 3.699 Å as a result of the hydroxamate bridging.

The electrophilic nature of the two nickels is obvious from the drastic decrease in positive charge from +2.0 each to ∼0.2. Contrary to expectations, the bridging OH group is positively charged and cannot behave as a nucleophile, as envisaged by most proposed reaction mechanisms for urease action. In fact, it is the free oxygen of the aspartate residue that has the maximum negative charge, and which probably behaves as a nucleophile to extract a proton from urea, causing it to decompose to ammonia and a bound cyanate (Barrios and Lippard 2000). Such a mechanism is in accord with the experimental observation of a rate of urea hydrolysis independent of pH, since this confirms that an internal atom is involved in the proton extraction. The electrostatic potential map for *A*, shown in Fig. 9, also shows a negative potential only near the aspartate oxygen.

For the acetohydroxamate-complexed urease, too, there is a negative potential only near the aspartate oxygen (Fig. 9). This complex is further stabilized by hydrogen bonding between the aspartate oxygen and the NH proton of
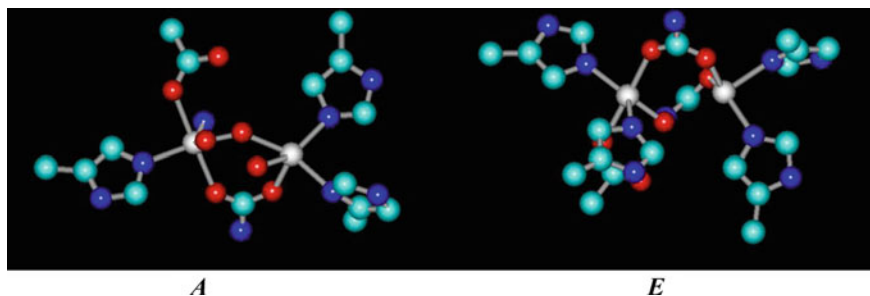
Fig. 8 Final structures of the native *A* and complexed with acetohydroxamic acid *E* taken for the study. Color code: carbons-cyan, nitrogens-blue, oxygens-red, nickels-white. Hydrogens have been omitted for clarity
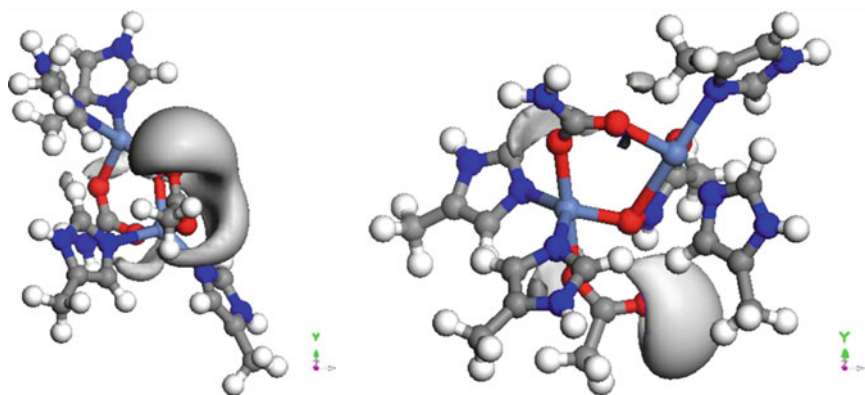
Fig. 9 Isopotential maps of *A* and *E*

acetohydroxamate. Further, there is an overall slight positive charge (0.151) on the bound hydroxamate moiety. This is smaller than the positive charge on the OH moiety (0.538) it replaces, and is also reflected in an increase in the positive charge of the two nickels in the AHA-bound complex.

5.2 Helicobacter Pylori Urease

The active site for the native urease consists of two nickel atoms, complexed with *His* 136, *His* 138, *His* 248, *His* 274, KCX 219, *Asp* 362, and HOH 572. For the AHA-bound complex, the active site again consists of the two nickel atoms, *His* 136, *His* 138, *His* 248, *His* 274, KCX 219, and *Asp* 362, but HOH 572 is replaced by AHA, which bridges the two nickel atoms.
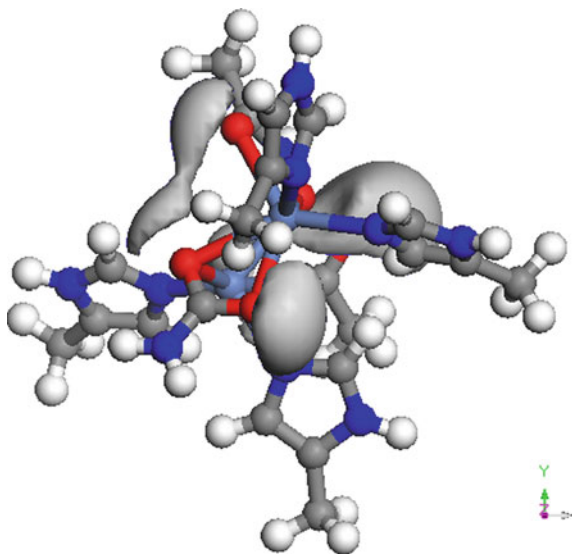
The final structures of *Z* (native) and *Y* (complexed with AHA) are depicted in Fig. 10. In *Z*, it can be seen that one Ni(II) atom is complexed with KCX via Ox2,
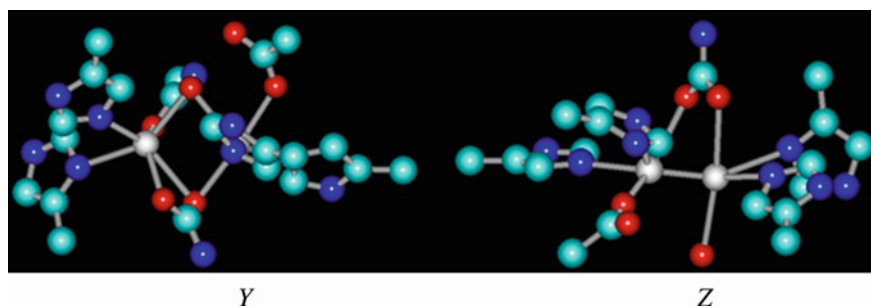
Fig. 10 Final structures of the *Y* and *Z* fragments taken for the study. Color code: carbons-cyan, nitrogens-blue, oxygens-red, nickel-white. Hydrogens have been omitted for clarity

the other Ni, *His* 274 via NE2, water via its oxygen and *His* 248 via ND1. Likewise, the second nickel atom is also pentacoordinate, being linked to *His* 136 and *His* 138 via NE2, KCX via Ox2, *Asp* via OD1, and the other nickel atom. The overall charge on this moiety is +2. The Ni…Ni distance is short (2.128 Å). The overall charge on this fragment is +2.0.

In *Y*, on the other hand, one of the nickels (Ni(2)) is hexacoordinate. Hydroxamate is a bidendate ligand and binds to the two nickel atoms. The octahedral coordination comes from the fact that in this case, there is coordination of this nickel atom with both the oxygens of KCX. Thus, Ni(2) coordinates to KCX via both oxygens Ox1 and Ox2, *His* 248 via ND1, *His* 274 via NE2, and HAE via O1 and O2. Ni(1) is coordinated to both *His* 136 and *His* 138 via their nitrogens NE2, KCX via its Ox2, *Asp* 362 via OD2, and HAE via O1. The overall charge on the fragment is +1.0. The Ni…Ni distance increases to 3.125 Å as a result of the hydroxamate bridging.

The nickels, especially Ni(1), in this case have higher positive charges (~ 0.5). The electrostatic potential map for *Y*, shown in Fig. 11, also shows a negative potential only near the aspartate oxygen, although the negative charge on the aspartate oxygens is slightly smaller in this case.

6 Other Biological Applications

Hydroxamic acids exhibit a wide variety of biological activities (Kehl 1982). This has resulted in investigations on their role in biology, besides urease inhibition. Most of these studies have been directed at AHA. For instance, its interaction with

the vanadate ion has been studied both experimentally and theoretically (Duarte et al. 1998; Santos et al. 2003). Vanadate is a phosphate analog and can act as both an inhibitor of phosphate-metabolizing enzymes as well as an activator. It was found in these studies that AHA plays a role in the V(IV)/V(V) redox reaction.

Hydroxamic acids have also been investigated as siderophores (Santos et al. 1998; Edwards et al. 2005; Domagal-Goldman et al. 2009). In this connection, experimental and DFT studies have been performed (Edwards et al. 2005; Domagal-Goldman et al. 2009) on complexes of Fe(III) with desferrioxamine B (DFO-B), the most extensively studied siderophore with respect to mineral dissolution. DFO-B is a linear trihydroxamic acid composed of 1,5-diaminopentane and succinic acid residues.

Besides inhibition of urease, hydroxamic acids also inhibit a large number of other enzymes. Quantitative Structure Activity Relationship (QSAR) studies, MD, quantum mechanical, and docking studies directed toward the development of hydroxamic acid inhibitors for histone deacetylases (HDACs) (Dallavalle et al. 2009; Guo et al. 2005; Ragno et al. 2008), lipoxygenase (Hadjipavlou-Litina and Pontiki 2002), peptide deformylase (PDF) (Wang et al. 2006, 2008), MMPs (Hu and Shelver 2003; Kumar and Gupta 2003; Tuccinardi et al. 2006), and collagenase (Kumar and Gupta 2003) have been reported.

7 Conclusions

Hydroxamic acids find a number of applications in chemistry, biology, and geochemistry due to their roles as chelating agents, inhibitors of various enzymes, nitric oxide donors, siderophores, and many others. A large number of experimental and theoretical studies have been directed at understanding their unique chemistry. Theoretical studies have mostly focused on elucidation of the ground state structures and acidities. In particular, the smallest homolog, FHA, because of its small size, has been the subject of several theoretical studies ranging from semiempirical to high level ab initio and density functional. It is now well-established that this acid prefers the Z keto structure, in which there is strong intramolecular hydrogen bonding, and proton dissociation takes place from the nitrogen. It is also established that protonation of FHA occurs at the carbonyl oxygen. In solution, hydroxamic acids form intermolecular hydrogen bonds with the solvent, but the solvent is not able to dislodge the strong intramolecular hydrogen bonds. Hence, deprotonation from –OH is difficult, and this is reflected in the slower rate of complexion with metal ions.

It is heartening to note that the theoretical calculations complement experimental determinations. In fact, much of the literature concerns combined experimental and theoretical studies, and both are in accord with each other. This goes a long way in affirming belief in state-of-the-art theoretical calculations, which have now become possible, for small to medium-sized molecules, at least.

In spite of the fact that most of the applications of hydroxamic acids arise from their chelating abilities, very few theoretical studies have been reported, probably because of the difficulties in accurately modeling transition metal complexes. It is to be hoped that, with further increase in computational power and accurate basis sets for transition metals, we shall come close to completely deciphering metalloenzyme action. Some of the results obtained so far have shown that the hydroxamic acids are selective toward Ni(II) because of its electrophilicity and consequent covalent bond formation with the hydroxamate ligand, which uses the (O,O) coordination mode in its complexes. One of the most important applications of hydroxamic acids is as inhibitors of urease. Examination of the structures of urease from two organisms, KAU and HP, and their AHA complexes reveals that the Ni(II) ions are highly electrophilic and attract charge density from the bonded ligands. Most mechanisms hitherto proposed in the literature for urease action (Barrios and Lippard 2000) invoke a nucleophilic attack by the bridging OH on the electron deficient carbon of urea. Alternate mechanisms for urease action and inhibition (Milios et al. 2002) involve the extraction of a proton from the urea NH_2 group or the hydroxamic acid by the bridging hydroxyl. However, theoretical studies emphatically rule out the involvement of the bridging OH on two counts. The first is the positive charge on this group due to its proximity to two highly electrophilic Ni(II) ions and the other is the absence of this bridge in the urease from HP. Rather, the involvement of the oxygen of the aspartate ion, which is negatively charged, was proposed (Kakkar et al. 2006b). The formation of a hydrogen bond between the oxygen and the NH of AHA confirms its role in the binding. We feel that this examination of the urease active site should pave the way for the design of more efficient urease inhibitors.

References

Agrawal YK, Patel SA (1980) Hydroxamic acids: reagents for the solvent extraction and spectrophotometric determination of metals. Rev Anal Chem 4:237–238

Agrawal YK, Roshania RD (1980) Non-aqueous titrimetric determination of N-p-chlorophenylbenzohydroxamic acids: visual and potentiometric titration in dimethylformamide. Bull Soc Chim Belg 89:175–179

Al-Saadi AA (2012) Conformational analysis and vibrational assignments of benzohydroxamic acid and benzohydrazide. J Mol Struct 1023:115–122

Bagno A, Comuzzi C, Scorrano G (1994) Site of ionization of hydroxamic acids probed by heteronuclear NMR relaxation rate and NOE measurements. An experimental and theoretical study. J Am Chem Soc 116:916–924

Barocas A, Baroncelli F, Biondi GB, Grossi G (1966) The complexing power of hydroxamic acids and its effects on behaviour of organic extractants in the reprocessing of irradiated fuels II. J Inorg Nucl Chem 28:2961–2967

Baroncelli F, Grossi G (1965) The complexing power of hydroxamic acids and its effects on behaviour oforganic extractants in the reprocessing of irradiated fuels I. J Inorg Nucl Chem 27:1085–1092

Barrios AM, Lippard SJ (2000) Interaction of urea with a hydroxide-bridged dinuclear nickel center: an alternative model for the mechanism of urease. J Am Chem Soc 122:9172–9177

Bauer L, Exner O (1974) The chemistry of hydroxamic acids and *N*-hydroxyimides. Angew Chem Int Ed Engl 13:376–384

Benini S, Rypniewski WR, Wilson KS, Miletti S, Ciurli S, Mangani S (1999) A new proposal for urease mechanism based on the crystal structures of the native and inhibited enzyme from *Bacillus pasteurii*: why urea hydrolysis costs two nickels. Struct Fold Des 7:205–216

Benini S, Rypniewski WR, Wilson KS, Miletti S, Ciurli S, Mangani S (2000) The complex of *Bacillus pasteurii* urease with acetohydroxamate anion from X-ray data at 1.55 Å resolution. J Biol Inorg Chem 5:110–118

Bertini I, Briganti F, Scozzafava A (1995) In: Berthon G (ed) Handbook of metal–ligand interactions in biological fluids. Marcell-Dekker, New York, pp 81–91

Blakeley RL, Treston A, Andrews RK, Zerner B (1982) Nickel(II) promoted ethanolysis and hydrolysis N-(2-pyridylmethyl)urea. A model for urease. J Am Chem Soc 104:612–614

Blom CE, Günthard HH (1981) Rotational isomerism in methyl formate and methyl acetate; a low-temperature matrix infrared study using thermal molecular beams. Chem Phys Lett 84:267–271

Bordwell FG, Fried HE, Hughes DL, Lynch T-Y, Satish AV, Whang YE (1990) Acidities of carboxamides, hydroxamic acids, carbohydrazides, benzenesulfonamides, and benzenesulfonohydrazides in DMSO solution. J Org Chem 55:3330–3336

Bracher BH, Small RWH (1970) The crystal structure of acetohydroxamic acid hemihydrate. Acta Crystallogr B 26:1705–1709

Brown DA, Roche AL, Pakkanen TA, Pakkanen TT, Smolander K (1982) The X-ray crystal structure of bis(glycinohydroxamato)nickel(II). A novel co-ordination of nickel by a hydroxamic acid via the nitrogen atom of the NHOH group. J Chem Soc, Chem Commun 676–677

Brown DA, Glass WK, Mageswaran R, Ali Mohammed S (1991) ^{1}H and ^{13}C NMR studies of isomerism in hydroxamic acids. Magn Res Chem 29:40–45

Brown DA, Coogan RA, Fitzpatrick NJ, Glass WK, Abukshima DE, Shiels L, Ahlgrén M, Smolander K, Pakkanen TT, Pakkanen TA, Peräkylä M (1996) Conformational behaviour of hydroxamic acids: ab initio and structural studies. J Chem Soc, Perkin Trans 2:2673–2679

Brown DA, Cuffe L, Fitzpatrick NJ, Glass WK, Herlihy K (1998) COST D8 & ESF workshop on biological and medicinal aspects of metal speciation, JATE, Szeged, Hungary, 23–25 Aug 1998

Brown DA, Errington W, Glass WK, Haase W, Kemp TJ, Nimir H, Ostrovsky SM, Werner R (2001) Magnetic, spectroscopic, and structural studies of dicobalt hydroxamates and model hydrolases. Inorg Chem 40:5962–5971

Chittari P, Jadhav VR, Ganesh KN, Rajappa S (1998) Synthesis and metal complexation of chiral 3-mono-2-hydroxypyrrlopyrazine-1,4-diones or 3,3,-bis-allyl-2-hydroxy-pyrollopyrazine-1,4-diones. J Chem Soc, Perkin Trans I 1319–1324

Ciurli S, Benini S, Rypniewski WR, Wilson KS, Miletti S, Mangani S (1999) Structural properties of the nickel ions in urease: novel insights into the catalytic and inhibition mechanisms. Coord Chem Rev 190:331–355

Codd R (2008) Traversing the coordination chemistry and chemical biology of hydroxamic acids. Coord Chem Rev 252:1387–1408

Colston BJ, Choppin GR, Taylor RJ (2000) A preliminary study of the reduction of Np(VI) by formohydroxamic acid using stopped-flow near-infrared spectrophotometry. Radiochim Acta 88:329–334

Dallavalle S, Cincinelli R, Nannei R, Merlini L, Morini G, Penco S, Pisano C, Vesci L, Barbarino M, Zuco V, Cesare MD, Zunino F (2009) Design, synthesis, and evaluation of biphenyl-4-yl-acrylohydroxamic acid derivatives as histone deacetylase (HDAC) inhibitors. Eur J Med Chem 44:1900–1912

Decouzon M, Exner O, Gal J-F, Maria P-C (1990) The gas-phase acidity and the acidic site of acetohydroxamic acid: an FT-ICR study. J Org Chem 55:3980–3981

Denis P, Ventura ON (2001) Hydroxamic chelates of boric acid, a density functional study. J Mol Struct (Theochem) 537:173–180

Desaraju P, Winston A (1986) Synthesis and iron complexation studies of bis-hydroxamic acids. J Coord Chem 14:241–248

Dessi A, Micera G, Sanna D, Erre LS (1992) Vanadium(IV) and oxovanadium(IV) complexes of hydroxamic acids and related ligands. J Inorg Biochem 48:279–287

Dissanayake DP, Senthilnithy R (2009) Thermodynamic cycle for the calculation of ab initio pK_a values for hydroxamic acids. J Mol Struct (Theochem) 910:93–98

Dixon NE, Gazzola C, Watters JJ, Blakeley RL, Zerner B (1975) Jack bean urease (EC 3.5.1.5). A metalloenzyme. A simple biological role for nickel? J Am Chem Soc 97:4131–4133

Domagal-Goldman SD, Paul KW, Sparks DL, Kubicki JD (2009) Quantum chemical study of the Fe(III)-desferrioxamine B siderophore complex—electronic structure, vibrational frequencies, and equilibrium Fe-isotope fractionation. Geochim Cosmochim Acta 73:1–12

Duarte HA, Paniago EB, Carvalho S, De Almeida WB (1998) Interaction of N-hydroxyacetamide with vanadate: a density functional study. J Inorg Biochem 72:71–77

Edwards DC, Nielson SB, Jarzęcki AA, Spiro TG, Mynen SCB (2005) Experimental and theoretical vibrational spectroscopy studies of acetohydroxamic acid and desferrioxamine B in aqueous solution: effects of pH and iron complexation. Geochim Cosmochim Acta 69:3237–3248

Exner O (1964) Acyl derivatives of hydroxylamine. IX. A spectroscopic study of tautomerism of sulfohydroxamic acids. Collect Czech Chem Commun 29:1337–1343

Farkas E, Kozma E, Pethö M, Herlihy KM, Micera G (1998a) Equilibrium studies on copper(II)- and iron(III)-monohydroxamates. Polyhedron 17:3331–3342

Farkas E, Megyeri K, Somsák L, Kováks L (1998b) Interaction between Mo(VI) and siderophore models in aqueous solution. J Inorg Biochem 70:41–47

Farkas E, Enyedy ÉA, Micera G, Garribba E (2000) Coordination modes of hydroxamic acids in copper(II), nickel(II) and zinc(II) mixed-ligand complexes in aqueous solution. Polyhedron 19:1727–1736

Fishbein WN, Carbone PP (1965) Urease catalysis: II. Inhibition of the enzyme by hydroxyurea, hydroxylamine, and acetohydroxamic acid. J Biol Chem 240:2407–2414

Fitzpatrick NJ, Mageswaran R (1989) Theoretical study of hydroxamic acids. Polyhedron 8:2255–2263

García B, Ibeas S, Leal JM, Senent ML, Niño A, Muñoz-Caro C (2000) Theoretical and experimental study of the acetohydroxamic acid protonation: the solvent effect. Chem Eur J 6:2644–2652

García B, Ibeas S, Muñoz A, Leal JM, Ghinami C, Secco F, Venturini M (2003) NMR studies of phenylbenzohydroxamic acid and kinetics of complex formation with Nickel(II). Inorg Chem 42:5434–5441

García B, Ibeas S, Leal JM, Secco F, Venturini M, Senent ML, Niño A, Muñoz C (2005) Conformations, protonation sites, and metal complexation of benzohydroxamic acid. A theoretical and experimental study. Inorg Chem 44:2908–2919

García B, Secco F, Ibeas S, Muñoz A, Hoyuelos FJ, Leal JM, Senent ML, Venturini M (2007) Structural NMR and ab initio study of salicylhydroxamic and p-hydroxybenzohydroxamic acids: evidence for an extended aggregation. J Org Chem 72:7832–7840

Gaynor D, Starikova ZA, Haase W, Nolan KB (2001) Copper(II) complexes of isomeric aminophenylhydroxamic acids. A novel 'clam-like' dimeric metallacrown and polymeric helical structure containing interlinked unique copper(II) sites. J Chem Soc, Dalton Trans 1578–1581

Gece G, Bilgiç S (2010) A theoretical study of some hydroxamic acids as corrosion inhibitors for carbon steel. Corros Sci 52:3304–3308

Ghosh KK (1997) Kinetic and mechanistic aspects of acid catalysed hydrolysis of hydroxamic acids. Indian J Chem 36B:1089–1102

Guo J-X, Ho J-J (1999) Ab initio study of substitution effect and catalytic effect of intramolecular hydrogen transfer of N-substituted formamides. J Phys Chem A 103:6433–6441

Guo Y, Xiao J, Guo Z, Chu F, Cheng Y, Wu S (2005) Exploration of a binding mode of indole amide analogues as potent histone deacetylase inhibitors and 3D-QSAR analyses. Bioorg Med Chem 13:5424–5434

Ha N-C, Oh S-T, Sung JY, Cha KA, Lee MH, Oh B-H (2001) Supramolecular assembly and acid resistance of *Helicobacter pylori* urease. Nat Struct Biol 8:505–509

Hadjipavlou-Litina D, Pontiki E (2002) Quantitative–structure activity relationships on lipoxygenase inhibitors. IEJMD 1:134–141

Hashimoto S, Nakamura Y (1995) Nuclease activity of a hydroxamic acid derivative in the presence of various metal ions. J Chem Soc, Chem Commun 1413–1414

Hashimoto S, Nakamura Y (1996) Characterization of lanthanide-mediated DNA cleavage by intercalator-linked hydroxamic acids: comparison with transition systems. J Chem Soc, Perkin Trans 1 2623–2628

Hashimoto S, Ito S, Nakamura Y (1966) Nucleic acids sys series, vol 35. Oxford University Press, New York

Hashimoto S, Yamashita R, Nakamura Y (1992) DNA strand scissions by hydroxamic acids-copper(II) ion under aerobic conditions. Chem Lett 1639–1642

Hashimoto S, Itai K, Takeuchi Y, Nakamura Y (1997) Synthesis of bisnetropsin-linked hydroxamic acids and their DNA cleavage study in the presence of transition or lanthanide metal ions. Heterocyclic Commun 3:307–315

Hashimoto S, Yamamoto K, Yamada T, Nakamura Y (1998) Synthesis of bis(N-methylpyrrole oligopeptide-linked hydroxamic acids) and effective DNA cleavage by their vanadyl complexes. Heterocycles 48:939–947

Hall MD, Failes TW, Hibbs DE, Hambley TW (2002) Investigation of palladium(II) and platinum(II) complexes with salicylhydroxamic acid—structural and quantum mechanical studies. Inorg Chem 41:1223–1228

Hiriart MV, Corcuera LJ, Andrade C, Crivelli I (1985) Copper(II) complexes of a hydroxamic acid from maize. Phytochemistry 24:919–1922

Hu X, Shelver WH (2003) Docking studies of matrix metalloproteinase inhibitors: zinc parameter optimization to improve the binding free energy prediction. J Mol Graph Model 22:115–126

Jabri E, Carr MB, Hausinger RP, Karplus PA (1995) The crystal structure of urease from *Klebsiella aerogenes*. Science 268:998–1004

Jiang Y, Pan Y, Chen D, Wang F, Yan L, Li G, Xue Y (2012) A theoretical study of the effect of carboxyl hydroxamic acid on the flotation behaviour of diapore and aluminosilicate minerals. Clays Clay Miner 60:52–62

Joshi RR, Ganesh KN (1992) Chemical cleavage of plasmid DNA by Cu(II), Ni(II) and Co(III) desferal complexes. Biochem Biophys Res Commun 182:588–592

Joshi RR, Ganesh KN (1994a) Duplex and triplex directed DNA cleavage by oligonucleotide-Cu(II)/Co(II) metallodesferal conjugates. Biochim Biophys Acta 1201:454–460

Joshi RR, Ganesh KN (1994b) Metallodesferals as a new class of DNA cleavers: specificity, mechanism and targeting of DNA scission reactions. Proc-Indian Acad Sci, Chem Sci 106:1089–1108

Joshi KA, Gejji SP (2005) Electronic structure and vibrational analysis of AHA…HX complexes. Chem Phys Lett 415:110–114

Kaczor A, Proniewicz LM (2004) The structural study of acetohydroxamic and oxalodihydr-oxamic acids in DMSO solution based on the DFT calculations of NMR spectra. J Mol Struct 704:189–196

Kaczor A, Proniewicz LM (2005) Molecular structure of 2-(hydroxyimino)propanohydroxamic acid in solid state and DMSO solution. Spectrochim Acta, Part A 62:1023–1031

Kahn O (2000) Chemistry and physics of supramolecular materials. Acc Chem Res 33:647–657

Kakkar R, Grover R, Chadha P (2003) Conformational behavior of some hydroxamic acids. Org Biomol Chem 1:2200–2206

Kakkar R, Grover R, Gahlot P (2006a) Density functional study of the properties of isomeric aminophenylhydroxamic acids and their Cu(II) complexes. Polyhedron 25:759–766

Kakkar R, Grover R, Gahlot P (2006b) Metal ion selectivity of hydroxamates: a density functional study. J Mol Struct (Theochem) 767:175–184

Kaur D, Kohli R (2008) Intra and intermolecular hydrogen bonding in formohydroxamic acid. Int J Quantum Chem 108:119–134

Kaur D, Kohli R (2012) Understanding hydrogen bonding of hydroxamic acids with some amino acid side chain model molecules. Struct Chem 23:161–173

Kaur D, Kohli R, Kaur RP (2009) The role of isomerism and medium effects on stability of anions of formo and thioformohydroxamic acid. J Mol Struct (Theochem) 911:30–39

Kehl H (ed) (1982) Chemistry and biology of hydroxamic acids. Karger, New York

Koga T, Furutachi H, Nakamura T, Fukita N, Ohba M, Takahashi K, Okawa H (1998) Dinuclear nickel(II) complexes of phenol-based "end-off" compartmental ligands and their urea adducts relevant to the urease active site. Inorg Chem 37:989–996

Kumar D, Gupta SP (2003) A quantitative structure–activity relationship study on some matrix metalloproteinase and collagenase inhibitors. Bioorg Med Chem 11:421–426

Kurzak B, Kozlowski H, Farkas E (1992) Hydroxamic and amino hydroxamic acids and their complexes with metal ions. Coord Chem Rev 114:169–200

Larsen IK (1988) Structural characteristics of the hydroxamic acid group. Crystal structure of formohydroxamic acid. Acta Crystallogr B 44:527–533

Leung K (2006) Ab initio molecular dynamics study of the hydration of the formohydroxamate anion. Biophys Chem 124:222–228

Lindner HJ, Göttlicher S (1969) Die kristall- und molekülstruktur des eisen(III)-benzhydroxamat-trihydrates. Acta Crystallogr B 25:832–842

Lipczyñska-Kochany E, Iwamura H (1982) Oxygen-17 nuclear magnetic resonance studies. Pt. 10. Oxygen-17 nuclear magnetic resonance studies of the structures of benzohydroxamic acids and benzohydroxamate ions in solution. J Org Chem 47:5277–5282

Lippard SJ (1995) At last—the crystal structure of urease. Science 268:996–997

Lossen H (1869) Ueber die oxalohydroxamsäure. Justus Liebigs Ann Chem 150:314–320

Manunza B, Deiana S, Pintore M, Gessa C (1999) The binding mechanism of urea, hydroxamic acid and N-(N-butyl)-phosphoric triamide to the urease active site. A comparative molecular dynamics study. Soil Biol Biochem 31:789–796

Marmion CJ, Murphy T, Nolan KB, Docherty JR (2000) Hydroxamic acids are nitric oxide donors. Facile formation of ruthenium(II)-nitrosyls and NO-mediated activation of guanylate cyclase by hydroxamic acids. Chem Commun 13:1153–1154

Marmion CJ, Griffith D, Nolan KB (2004) Hydroxamic acids—an intriguing family of bioligands and enzyme inhibitors. Eur J Inorg Chem 15:3003–3016

Martin RB (1987) A stability ruler for metal ion complexes. J Chem Educ 64:402

McNaught AD, Wilkinson A (1997) IUPAC compendium of chemical terminology, 2nd edn (the "Gold Book"). Blackwell, Oxford

Milios CJ, Manessi-Zoupa E, Perlepes SP (2002) Modeling the coordination mode of hydroxamate inhibitors in urease: preparation, X-ray crystal structure and spectroscopic characterization of the dinuclear complex [Ni$_2$(O$_2$CMe)(LH)$_2$(tmen)$_2$](O$_2$CMe)·0.9H$_2$O·0.6EtOH (LH$_2$ = benzohydroxamic acid; tmen = N,N,N′,N′-tetramethylethyleneamine). Trans Met Chem 27:864–873

Miller MJ (1989) Synthesis and therapeutic potential of hydroxamic base siderophores and analogues. Chem Rev 89:1563–1579, and references therein

Mora-Diez N, Senent ML, García B (2006) Ab initio study of solvent effects on the acetohydroxamic acid deprotonation processes. Chem Phys 324:350–358

Munoz-Caro C, Nino A, Senent ML, Leal JM, Ibeas S (2000) Modeling of protonation processes in acetohydroxamic acid. J Org Chem 65:405–410

Niño A, Muñoz-Caro C, Senent ML (2000) Suitability of different levels of theory for modelling of hydroxamic acids. J Mol Struct (Theochem) 530:291–300

Parr RG, Pearson RG (1983) Absolute hardness: companion parameter to absolute electronegativity. J Am Chem Soc 105:7512–7516

Pearson RG (1963) Hard and soft acids and bases. J Am Chem Soc 85:3533–3539

Pearson MA, Park I-S, Schaller RA, Michel LO, Karplus PA, Hausinger RP (2000) Kinetic and structural characterization of urease active site variants. Biochemistry 39:8575–8584

Perdew JP, Burke K, Ernzerhof M (1996) Generalized gradient approximation made simple. Phys Rev Lett 77:3865–3868

Ragno R, Simeoni S, Rotili D, Caroli A, Botta G, Brosch G, Massa S, Mai A (2008) Class II-selective histone deacetylase inhibitors. Part 2: alignment-independent GRIND 3-D QSAR, homology and docking studies. Eur J Med Chem 43:621–632

Raymond KN, Müller G, Matzanke BF (1984) Complexation of iron by siderophores a review of their solution and structural chemistry and biological function. Top Curr Chem 123:49–102

Remko M (2002) The gas-phase acidities of substituted hydroxamic and silahydroxamic acids: a comparative ab initio study. J Phys Chem A 20:5005–5010

Remko M, Šefčíková J (2000) Structure, reactivity and vibrational spectra of formohydroxamic and silaformohydroxamic acids: a comparative ab initio study. J Mol Struct (Theochem) 528:287–296

Remko M, Mach P, Schleyer PVR, Exner O (1993) Ab initio study of formohydroxamic acid isomers, their anions and protonated forms. J Mol Struct (Theochem) 279:139–150

Rulíšek L, Vondrášek J (1998) Coordination geometries of selected transition metal ions (Co^{2+}, Ni^{2+}, Cu^{2+}, Zn^{2+}, Cd^{2+}, and Hg^{2+}) in metalloproteins. J Inorg Biochem 71:115–127

Saldyka M, Mielke Z (2002) Infrared matrix isolation studies and ab initio calculations of formhydroxamic acid. J Phys Chem A 106:3714–3721

Saldyka M, Mielke Z (2003a) Cis-trans isomerism of the keto tautomer of formohydroxamic acid. Chem Phys Lett 371:713–718

Saldyka M, Mielke Z (2003b) Photodecomposition of formohydroxamic acid. Matrix isolation FTIR and DFT studies. Phys Chem Chem Phys 5:4790–4797

Saldyka M, Mielke Z (2004a) The interaction of formohydroxamic acid with nitrogen: FTIR matrix isolation and ab initio studies. J Mol Struct 708:183–188

Saldyka M, Mielke Z (2004b) The interaction of formohydroxamic acid with carbon monoxide: FTIR matrix isolation and quantum chemistry studies. Chem Phys 300:209–216

Saldyka M, Mielke Z (2005a) Intra- and intermolecular hydrogen bonding in formohydroxamic acid complexes with water and ammonia: infrared matrix isolation and theoretical study. Chem Phys 308:59–68

Saldyka M, Mielke Z (2005b) Dimerization of the keto tautomer of acetohydroxamic acid—infrared matrix isolation and theoretical study. Spectrochim Acta, Part A 61:1491–1497

Saldyka M, Mielke Z (2007) Keto–iminol tautomerism in acetohydroxamic and formohydroxamic acids. Vib Spectrosc 45:46–54

Sant'Anna CMR (2001) A semiempirical study on hydroxamic acids: formohydroxamic acid and derivatives of the allelochemical dimboa. Quim Nova 24:583–587

Santos MA, Gaspar M, Gonçalves MLSS, Amorim MT (1998) Siderophore analogues. A new bis-(amine, amide, hydroxamate) ligand. Synthesis, solution chemistry, electrochemistry and molecular mechanics calculations for the iron complex. Inorg Chim Acta 278:51–60

Santos JM, Carvalho S, Paniago EB, Duarte HA (2003) Potentiometric, spectrophotometric and density functional study of the interaction of N-hydroxyacetamide with oxovanadium(IV): the influence of ligand to the V(IV)/V(V) oxi-reduction reaction. J Inorg Biochem 95:14–24

Senent ML, Niño A, Muñoz Caro C, Ibeas S, García B, Leal JM, Secco F, Venturini M (2003) Deprotonation sites of acetohydroxamic acid isomers. A theoretical and experimental study. J Org Chem 68:6535–6542

Senthilkumar L, Kolandaivel P (2006) Molecular interaction study of formohydroxamic acid (FHA) with water. J Mol Struct 791:149–157

Senthilnithy R, Gunawardhana HD, De Costa MDP, Dissanayake DP (2006) Absolute pK_a determination for N-phenylbenzohydroxamic acid derivatives. J Mol Struct (Theochem) 761:21–26

Senthilnithy R, Weerasinghe S, Dissanayake DP (2008) Stability of hydroxamate ions in aqueous medium. J Mol Struct (Theochem) 851:109–114

Sigel H, McCormick DB (1970) On the discriminating behavior of metal ions and ligands with regard to their biological significance. Acc Chem Res 3:201–208

Šille J, Garaj V, Ježko P, Remko M (2010) Gas phase and solution stability of complexes L…M, where M = Li$^+$, Na$^+$, K$^+$, Mg^{2+}, or Ca^{2+} and L = R-(CO)NHOH (R = H, NH$_2$, CH$_3$, CF$_3$, or phenyl). Acta Facultatis Pharmaceuticae Universitatis Comenianae Tomus L VII:1–18

Sumner JB (1926) The isolation and crystallization of the enzyme urease: preliminary paper. J Biol Chem 69:435–441

Tavakol H (2009) Computational study of simple and water-assisted tautomerism of hydroxamic acids. J Mol Struct (Theochem) 916:172–179

Taylor RJ, May I, Wallwork AL, Dennis IS, Hill NJ, Galkin BY, Zilberman BY, Fedorov YS (1998) The applications of formo- and aceto-hydroxamic acids in nuclear fuel reprocessing. J Alloy Compd 271–273:534–537

Tipton CL, Buell EL (1970) Ferric iron complexes of hydroxamic acids. Phytochemistry 9:1215–1217

Todd TA, Wigelund RA (2006) Advanced separation technologies for processing spent nuclear fuel and the potential benefits to a geologic repository. In: Lumetta GJ, Nash KL, Clark SB, Friese JI (eds) Separations for the nuclear fuel cycle in the 21st century. ACS symposium series, vol 933. ACS, Washington, pp 41–56

Tuccinardi T, Martinelli A, Nuti E, Carelli P, Balzano F, Uccello-Barretta G, Murphy G, Rossello A (2006) Amber force field implementation, molecular modelling study, synthesis and MMP-1/MMP-2 inhibition profile of (R)-and (S)-N-hydroxy-2-(N-isopropoxybiphenyl-4-ylsulfo-namido)-3-methylbutanamides. Bioorg Med Chem 14:4260–4276

Turi L, Dannenberg JJ, Rama J, Ventura ON (1992) Molecular orbital study of the structures of hydroxamic acids. J Phys Chem 96:3709–3712

Ventura ON, Rama JB, Turi L, Dannenberg JJ (1993) Acidity of hydroxamic acids: an ab initio and semiempirical study. J Am Chem Soc 115:5754–5761

Vrcek IV, Kos I, Weitner T, Birus M (2008) Acido-base behavior of hydroxamic acids: experimental and ab initio studies on hydroxyureas. J Phys Chem A 112:11756–11768

Wang X, Houk KN (1988) Theoretical elucidation of the origin of the anomalously high acidity of Meldrum's acid. J Am Chem Soc 110:1870–1872

Wang Q, Zhang D, Wang J, Cai Z, Xu W (2006) Docking studies of nickel-peptide deformylase (PDF) inhibitors: exploring the new binding pockets. Biophys Chem 122:43–49

Wang Q, Wang J, Cai Z, Xu W (2008) Prediction of the binding modes between BB-83698 and peptide deformylase from Bacillus stearothermophilus by docking and molecular dynamics simulation. Biophys Chem 134:178–184

Weinberg ED (1989) Quart Rev Biol 64:261–290

Wheland GW (1955) Resonance in organic chemistry. Wiley, New York

Wiberg KB, Laidig KE (1988) Acidity of (Z)- and (E)-methyl acetates: relationship to Meldrum's acid. J Am Chem Soc 110:1872–1874

Wu D-H, Ho J-J (1998) Ab initio study of intramolecular proton transfer in formohydroxamic acid. J Phys Chem A 102:3582–3586

Yamin LJ, Ponce CA, Estrada MR, Vert FT (1996) Protonation and deprotonation of hydroxamic acids. An MO ab initio study. J Mol Struct (Theochem) 360:109–117

Yazal JE, Pang Y-P (1999) Novel stable configurations and tautomers of the neutral and deprotonated hydroxamic acids predicted from high-level ab initio calculations. J Phys Chem A 103:8346–8350

Yen S-J, Lin C-Y, Ho J-J (2000) Ab initio study of proton transfer between protonated formohydroxamic acid and water molecules. J Phys Chem A 104:11771–11776

Hydroxamates as Carbonic Anhydrase Inhibitors

Claudiu T. Supuran

Abstract The 14 different mammalian carbonic anhydrase (CA, EC 4.2.1.1) isozymes as well as many such enzymes isolated up to now in other organisms, play important physiological functions such as pH regulation, signaling, biosynthetic reactions, electrolyte secretion, etc. Unsubstituted sulfonamides act as high affinity inhibitors for the first type of these enzymes, whereas hydroxamates were also shown to strongly inhibit many of them. The investigated hydroxamates as CA inhibitors (CAIs) include *N*-hydroxyurea, the aliphatic/aromatic hydroxamates of the type RCONHOH (R = Me, CF_3 and Ph), as well as sulfonylated amino acid hydroxamates of the type RSO_2NX-AA-CONHOH (X = H; benzyl; substituted benzyl; AA = amino acid moiety, such as those of Gly, Ala, Val, Leu). The most salient feature of the hydroxamates as CAIs regards their high versatility as zinc-binding groups (ZBGs). Indeed, depending on the nature of the R moiety of a hydroxamate of the type RCONHOH, the hydroxamate moiety can adopt different coordination modes to the catalytic zinc ion within the CA active site: monodentate through the deprotonated N atom; bidentate trough the NH and OH groups, or bidentate through the OH and O atoms (deprotonation at the OH moiety). These findings suggest that the enzyme-inhibitor interaction of the hydroxamate CAI class can be largely modulated by exploring different substitution patterns at the R group, thus providing interesting hints for the development of new CAIs of the non-sulfonamide type with pharmaceutical applications in the treatment of various diseases

Keywords Carbonic anhydrases · Carbonic anhydrase inhibitors · Hydroxamates · Hydroxyureas

C. T. Supuran (✉)
Dipartimento di Scienze Farmaceutiche, Università degli Studi di Firenze, Via Ugo Schiff 6, 50019 Sesto Fiorentino, Florence, Italy
e-mail: claudiu.supuran@unifi.it

Abbreviations

CA	Carbonic anhydrase
CAI	CA inhibitor
ChC	*Clostridium histolyticum* collagenase
MMPI	Matrix metalloproteinase inhibitor
MMP	Matrix metalloproteinase
ZBG	Zinc-binding group

Contents

1 Introduction on Carbonic Anhydrases

The ubiquitous enzyme carbonic anhydrase (CA, EC 4.2.1.1), is present in prokaryotes and eukaryotes as five genetically different families of enzymes, the α-CAs (mainly in vertebrates and in some green bacteria, fungi, and plants), β-CAs (mainly in bacteria, fungi, algae, and green plants), γ-CAs (in *Archaea* and mitochondria of plants) and the δ- and ζ-CA families, present in diatoms (Supuran 2008, 2010, 2011; Neri and Supuran 2011; Alterio et al. 2012). In higher vertebrates, 16 different CA isozymes were described up to now, which are involved in crucial physiological processes connected with respiration and transport of CO_2/bicarbonate between metabolizing tissues and the lungs, pH homeostasis, electrolyte secretion in a variety of tissues/organs, biosynthetic reactions, such as the lipogenesis, gluconeogenesis, and ureagenesis among others (Supuran 2008, 2010, 2011; Neri and Supuran 2011; Alterio et al. 2012). Some of these isozymes are cytosolic (such as CA I, CA II, CA III, CA VII, CA VIII, CA X, CA XI, and CA XIII), others are membrane-bound (CA IV, CA IX, CA XII, CA XIV, and XA XV), CA VA, and CA VB are present only in mitochondria, whereas CA VI is secreted in saliva; several isoforms are acatalytic (CA VIII, CA X, and CA XI) (Supuran 2008, 2010, 2011, 2012; Neri and Supuran 2011; Alterio et al. 2012).

In addition to the physiological reaction, the reversible hydration of carbon dioxide to bicarbonate, CAs also catalyze a variety of other reactions, such as the aldehyde hydration; the hydrolysis of carboxylic acid esters, as well as esters of sulfonic or phosphoric acids (Alterio et al. 2012; Supuran 2012). On the other

hand, CAs do not possess at all peptidase activity, which in turn is the only reaction catalyzed by the proteases of the matrix metalloproteinase (MMP) family with very great efficiency (Alterio et al. 2012). We mention this class of enzymes, the MMPs here, because the hydroxamates, compounds constituting the main topic of this chapter, are the most important class of MMP inhibitors (Nagase and Woessner 1999; Lovejoy et al. 1999; Borkakoti 2000; Borkakoti et al. 1994; Bottomley et al. 1998).

Specific inhibitors of both these types of zinc enzymes are well-known, and some of them were clinically used for more than 60 years (the sulfonamide CAIs) (Supuran 2008, 2010, 2011). Inhibition of CAs by aromatic/heterocyclic sulfonamides has been and it is successfully used in the treatment of a variety of diseases such as glaucoma, epilepsy, obesity, congestive heart failure, mountain sickness, gastric and duodenal ulcers, tumors, or as diuretic agents (Supuran 2008, 2010, 2011). MMPs on the other hand became targets for the drug design more recently, with several hydroxamate drugs in clinical use in the last decade (Whittaker et al. 1999; Supuran and Scozzafava 2002).

CAs and MMPs possess very similar metal coordination spheres within their catalytic sites, consisting of a Zn(II) ion coordinated by three histidines, with the fourth ligand being a water molecule/hydroxide ion, which is the nucleophile intervening in the catalytic cycle of both enzymes (Fig. 1) (Christianson and Ippolito 1991; Coleman 1998; Supuran and Winum 2009).

The main structural difference between these two types of enzymes regards the residues with which the zinc-bound water molecule/hydroxide ion interacts: in CAs, the non-protein zinc ligand forms a hydrogen bond with the hydroxyl moiety of Thr199 (hCA II numbering), which in turn is hydrogen-bonded to the carboxylate of Glu106, leading thus to a dramatic enhance of nucleophilicity of the water molecule/hydroxide ion (Scozzafava and Supuran 2000a; Supuran and Winum 2009). In the case of MMPs, the zinc-bound water molecule interacts with the carboxylate moiety of a conserved glutamate residue (Glu198 in MMP-8), probably forming two hydrogen bonds with it (Scozzafava and Supuran 2000a).
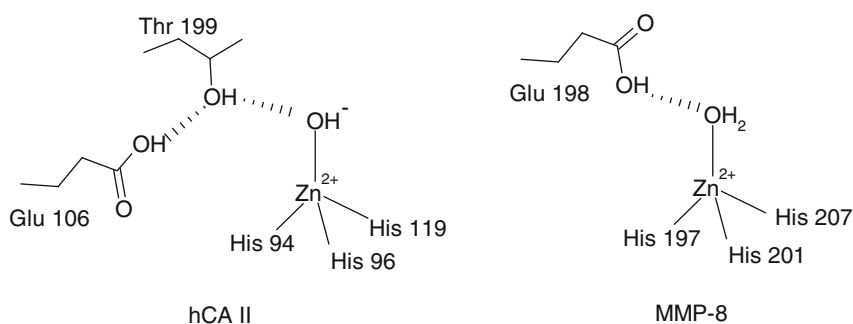

Fig. 1 Active site coordination of the Zn(II) ion in human CA isozyme II (hCA II) and human collagenase 2 (MMP-8). The non-protein zinc ligand of hCA II is a hydroxide ion (as shown above) or a water molecule, depending on the pH of the solution (Scozzafava and Supuran 2000a)

Thus, a very effective nucleophile is formed again, which will attack the amide scissile bond of the peptide substrate. The principal difference between the enzymatic mechanisms of CAs and MMPs consists in the fact that the nucleophilic adduct formed after the attack of the zinc-bound nucleophile to the substrate is the reaction product in the case of CAs (the bicarbonate ion), whereas the nucleophilic adduct is only a reaction intermediate in the case of the MMPs (Scozzafava and Supuran 2000a). This is also of crucial importance for the interaction of these enzymes with their inhibitors.

Inhibition of both CAs as well as MMPs is correlated with the coordination of the inhibitor molecule (in neutral or ionized state) to the catalytic metal ion, with or without substitution of the metal-bound water molecule (Supuran 2008; Scozzafava and Supuran 2000a). Thus, CA and MMP inhibitors (abbreviated as CAIs and MMPIs, respectively) must contain a zinc-binding group (ZBG) attached to a scaffold that will interact with other binding regions of the enzymes (Supuran and Winum 2009). In the case of CAIs, unsubstituted aromatic/heterocyclic sulfonamides as well as N-hydroxy-sulfonamides proved to be very effective inhibitors, with affinities in the low nanomolar range for isozymes such as CA I, CA II, CA IV, etc. These derivatives bind monodentately, as anions (RSO_2NH^-) to the Zn(II) ion within CA active site, interacting also with several other active site residues, by means of hydrogen bonds or hydrophobic interactions (Supuran 2008, 2010, 2011). It has been observed that CAIs possessing elongated molecules, able to interact with amino acid residues situated at the edge of the active site entrance (and obviously, with the zinc ion, as mentioned above), are among the most efficient ones (Scozzafava et al. 1999).

Depending on the ZBG contained in their molecule, MMPIs belong to several chemical classes, such as the carboxylates, the hydroxamates, the thiols, the phosphorus-based ligands, or the sulfodiimines, among others (Whittaker et al. 1999; Supuran and Scozzafava 2002). The strongest and most investigated class of MMPIs is constituted by the hydroxamates, as mentioned above (Whittaker et al. 1999; Supuran and Scozzafava 2002). The interaction of the catalytic domain of several MMPs with some inhibitors has been investigated by means of X-ray crystallography (Fig. 2) (Whittaker et al. 1999; Supuran and Scozzafava 2002).

Fig. 2 Schematic representation for the binding of a succinate hydroxamate inhibitor to MMP-7, as determined by X-ray crystallography. The Zn(II)-ligand and hydrogen bond interactions in the enzyme-inhibitor adduct are evidenced (Supuran and Scozzafava 2002)
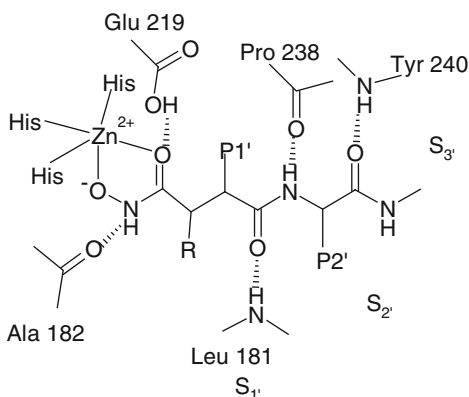
As seen in the above figure, hydroxamates bind bidentately to the catalytic Zn(II) ion of the MMP, which acquires a distorted trigonal bipyramidal geometry in this way (Whittaker et al. 1999; Supuran and Scozzafava 2002). The hydroxamate anion forms a short and strong hydrogen bond with the carboxylate moiety of Glu219, which is orientated toward the unprimed binding regions, whereas the NH hydroxamate participates in a hydrogen bond with the carbonyl oxygen of Ala182. Thus, several strong interactions are achieved at the zinc site, without any significant unfavorable contacts (Whittaker et al. 1999; Supuran and Scozzafava 2002). However, we will not insist on the MMP inhibition of the hydroxamates as this topic is treated in other chapters of the book.

However, investigating hydroxamates which act as strong MMPIs, also as CAIs, was quite logical considering the similar active site architecture of the two classes of such enzymes. Such studies started some years ago with the report of Christianson's group of the X-ray crystal structure of two aliphatic hydroxamates complexed to CA II (Scolnick et al. 1997). They were followed by the report of *N*-hydroxyurea (the simplest hydroxamate) as CAI against all the catalytically active mammalian isoforms (Supuran and Scozzafava 2003). The X-ray structure of this compound complexed to CA II has also been reported subsequently (Temperini et al. 2006). A rather large number of amino acid hydroxamates have been thereafter designed and investigated as CAIs (in addition to their MMP inhibition studies) (Scozzafava and Supuran 2000a, b, c), and more recently, aromatic hydroxamates have also been investigated as CAIs (Di Fiore et al. 2012).

2 *N*-Hydroxyurea as CA Inhibitor

The idea to investigate *N*-hydroxyurea as CAI started after the discovery that urea acts in such a way (Briganti et al. 1999). Indeed, our group discovered that cyanamide acts as a suicide inhibitor of CA, being transformed to urea (actually ureate) which thereafter coordinated to the Zn(II) from the CA active site. We thus investigated whether *N*-hydroxyurea, the simplest stable hydroxamate (H_2N-CO-NHOH) may inhibit CAs and discovered that it inhibits several mammalian CA isoforms with inhibition constants in the micromolar–submicromolar range (Supuran and Scozzafava 2003). Hydroxyurea acts as a weak, non-competitive inhibitor of both CA I and II isozymes, for their 4-nitrophenyl acetate esterase activity. The spectrum of the adduct of hydroxyurea with the Co(II)-substituted CA II was similar to the spectra of tetrahedral such adducts (e.g., with sulfamide, acetazolamide, or cyanamide), proving a direct interaction of the inhibitor molecule with the metal center of the enzyme, whose geometry remains tetrahedral. Based on the X-ray crystal structure of the adducts of hCA II with ureate and hydroxamate inhibitors, the hypothetical binding of hydroxyurea was proposed to be achieved in deprotonated state, with the nitrogen atom coordinated to Zn(II), and the OH group of the inhibitor making a hydrogen bond with Thr199. This binding was thereafter confirmed when the X-ray crystal structure of the adduct of

Fig. 3 Binding of
N-hydroxyurea (**a**), methyl
hydroxamate (**b**) and
trifluoromethyl hydroxamate
(**c**) to hCA II, as determined
by X-ray crystallography
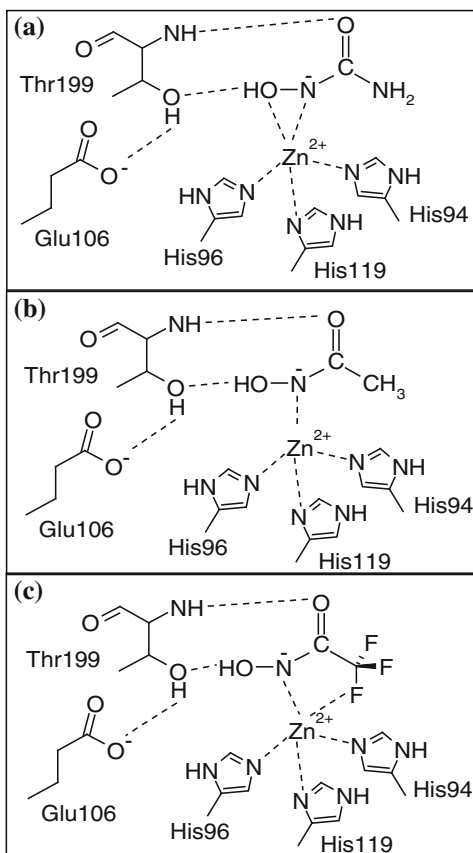
CA II complexed with *N*-hydroxyurea has been reported (Fig. 3a). The crystal-lographic structure of the human (h) hCA II/N-hydroxyurea adduct showed that this molecule binds to the Zn^{2+} ion of hCA II active site in a bidentate mode, by means of the oxygen and nitrogen atoms of the NHOH moiety. Additional hydrogen bonds involving the hydroxyl and the carbonyl moieties of the inhibitor and the enzyme residue Thr199 were also observed (Fig. 3a).[91] Worth noting is that the related acetohydroxamic and trifluoroacetohydroxamic acids, although containing the same hydroxamate functionality, were demonstrated to adopt a very different binding mode (see next section).

3 Aliphatic Hydroxamates

Christianson's group investigated two simple hydroxamates (methyl- and trifluo-romethyl hydroxamates) as CAIs, and reported the X-ray structure of such an adduct (hCA II–CF$_3$CONHOH) (Scolnick et al. 1997). The second compound

binds to hCA II with an affinity of 3.8 μM but its interaction with the Zn(II) ion of CA active site is very different from that of the classical sulfonamide inhibitors. Thus, the ionized nitrogen atom of the hydroxamate moiety of both compounds, was directly coordinated to Zn(II), whereas a fluorine atom of the trifluoromethyl moiety also participated in the interaction with the metal ion (Fig. 3b, c). In addition, hydrogen bonds between the hydroxamate OH and active site residue Thr199 were also evidenced, which further stabilize the E–I adduct (Fig. 3b, c).

It may be thus observed a highly versatile behavior of the hydroxamate ZBG in the three simple "aliphatic" CAIs investigated so far by means of X-ray crystallography.

4 Amino Acid Hydroxamates

Based on the data presented above for N-hydroxyurea and aliphatic hydroxamates acting as CAIs, a large series of sulfonylated amino acid hydroxamates were investigated as CAIs (Scozzafava and Supuran 2000a). The following types of compounds were included in the study: (i) sulfonylated amino acid hydroxamates possessing an unsubstituted RSO_2NH-amino acyl moiety. The amino acid hydroxamates included in the study were the Gly, Ala, Val, and Leu derivatives (Table 1); (ii) sulfonylated amino acid hydroxamates possessing a substituted RSO_2NX-amino acyl moiety, where X is generally a benzyl or a 2- or 4-substituted benzyl group (the same amino acid hydroxamates as above were included in the study, Table 1). For all these types of compounds, three different examples have been employed (R moieties) from the large series of available aliphatic, aromatic, and heterocyclic derivatives reported previously by our group. They included the perfluorobutyl, the pentafluorophenyl, and the 4-methoxyphenyl sulfonyl moieties, and were chosen in such a way as to include a very potent, a slightly weaker, and an even weaker MMPI. Anyhow, all these three groups incorporated in amino acid hydroxamates, generally led to potent MMPIs, with affinities (for the most active derivatives) in the (low) nanomolar range (5–15 nM) for the different MMPs as well as for the *Clostridium histolyticum* collagenase (ChC) (Van Wart and Steinbrink 1981; Scozzafava and Supuran 2000a).

The inhibition data with compounds **1–39**, presented in Table 1 led to the following observations: (i) sulfonyl amino acyl hydroxamates possessing moieties of the type RSO_2NH-amino acyl (such as **1–3**; **7–9**; **13–15; and 19–21**) generally acted as efficient CAIs, and were relatively weak MMP and ChC inhibitors. Thus, for CAs, these inhibitors generally showed affinities in the range of 7–50 nM (hCA I); 8–45 nM (hCA II); and 10–40 nM (bCA IV), whereas for the different MMPs investigated here and ChC, their affinities were in the range of 40–>200 nM. For the three types of investigated derivatives, the most active were the pentafluorophenylsulfonyl derivatives, followed by the corresponding perfluorobutyl ones, whereas the least active were the corresponding 4-methoxyphenyl-substituted compounds. For CA inhibition, best activity was observed for the Gly derivatives,
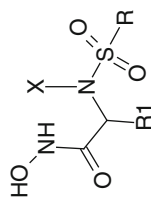
Table 1 Inhibition of MMPs, ChC and CAs with the hydroxamates **1–39**

No.	R1	X	R	K_i^a(nM)							
				MMP-1[b]	MMP-2[b]	MMP-8[b]	MMP-9[b]	ChC[c]	hCA I[d]	hCA II[d]	bCA IV[d]
1	H	H	$n\text{-}C_4F_9$	>200	75	130	125	80	18	15	16
2	H	H	C_6F_5	145	44	125	100	54	7	8	10
3	H	H	$4\text{-MeO-}C_6H_4$	>200	110	155	143	120	30	32	29
4	H	$C_6H_5CH_2$	$n\text{-}C_4F_9$	30	3.9	5.3	5	13	105	85	100
5	H	$C_6H_5CH_2$	C_6F_5	7	1.5	1.1	1.2	6	90	36	42
6	H	$C_6H_5CH_2$	$4\text{-MeO-}C_6H_4$	60	18	31	42	27	>200	120	145
7	Me	H	$n\text{-}C_4F_9$	>200	69	118	121	79	21	16	17
8	Me	H	C_6F_5	150	40	116	96	45	7	8	10
9	Me	H	$4\text{-MeO-}C_6H_4$	>200	87	125	137	130	32	35	30
10	Me	$C_6H_5CH_2$	$n\text{-}C_4F_9$	26	3.2	4.9	4.3	12	121	92	107
11	Me	$C_6H_5CH_2$	C_6F_5	7	0.9	1.1	1.4	6	84	38	43
12	Me	$C_6H_5CH_2$	$4\text{-MeO-}C_6H_4$	58	15	19	35	20	195	120	136
13	iPr	H	$n\text{-}C_4F_9$	>200	66	111	120	78	29	15	20
14	iPr	H	C_6F_5	139	41	104	89	40	8	11	13
15	iPr	H	$4\text{-MeO-}C_6H_4$	>200	82	126	126	103	33	39	38
16	iPr	$C_6H_5CH_2$	$n\text{-}C_4F_9$	21	2.4	4.2	4.3	10	140	108	124
17	iPr	$C_6H_5CH_2$	C_6F_5	7	0.8	1.0	1.2	5	88	45	48
18	iPr	$C_6H_5CH_2$	$4\text{-MeO-}C_6H_4$	43	11	13	27	17	>200	>200	185
19	iBu	H	$n\text{-}C_4F_9$	>200	62	108	36	69	36	18	30
20	iBu	H	C_6F_5	155	39	101	122	38	10	11	19
21	iBu	H	$4\text{-MeO-}C_6H_4$	>200	84	123	78	95	50	5	39

(continued)

Table 1 (continued)

No.	R1	R	X	MMP-1[b]	MMP-2[b]	MMP-8[b]	K^a(nM) MMP-9[b]	ChC[c]	hCA I[d]	hCA II[d]	bCA IV[d]
22	iBu	$n\text{-}C_4F_9$	$C_6H_5CH_2$	16	1.9	3.3	4.0	8	180	116	139
23	iBu	C_6F_5	$C_6H_5CH_2$	6	0.8	0.6	1.1	5	100	56	75
24	iBu	$4\text{-MeO-}C_6H_4$	$C_6H_5CH_2$	44	10	9	1.3	13	>200	>200	190
25	H	$n\text{-}C_4F_9$	$2\text{-}O_2NC_6H_4CH_2$	25	3.7	5.5	4.6	13	>200	100	120
26	H	C_6F_5	$2\text{-}O_2NC_6H_4CH_2$	6	1.4	1.0	1.3	6	127	74	49
27	H	$4\text{-MeO-}C_6H_4$	$2\text{-}O_2NC_6H_4CH_2$	54	15	27	39	24	>200	170	140
28	H	$n\text{-}C_4F_9$	$4\text{-}O_2NC_6H_4CH_2$	62	1.5	2.4	2.0	12	>200	118	136
29	H	C_6F_5	$4\text{-}O_2NC_6H_4CH_2$	3	0.7	0.1	0.6	5	150	107	130
30	H	$4\text{-MeO-}C_6H_4$	$4\text{-}O_2NC_6H_4CH_2$	28	18	21	31	20	>200	>200	>200
31	Me	$n\text{-}C_4F_9$	$2\text{-}O_2NC_6H_4CH_2$	24	2.9	5.1	4.4	10	>200	>200	>200
32	Me	C_6F_5	$2\text{-}O_2NC_6H_4CH_2$	7	0.8	1.1	1.0	5	>200	160	>200
33	Me	$4\text{-MeO-}C_6H_4$	$2\text{-}O_2NC_6H_4CH_2$	39	13	20	24	19	>200	>200	>200
34	Me	$n\text{-}C_4F_9$	$4\text{-}O_2NC_6H_4CH_2$	60	1.4	2.3	1.5	11	>200	>200	>200
35	Me	C_6F_5	$4\text{-}O_2NC_6H_4CH_2$	4	0.7	0.3	0.6	5	>200	>200	>200
36	Me	$4\text{-MeO-}C_6H_4$	$4\text{-}O_2NC_6H_4CH_2$	25	15	18	28	21	>200	>200	>200
37	Me	$n\text{-}C_4F_9$	$2\text{-ClC}_6H_4CH_2$	37	3.7	6.4	5.0	11	>200	>200	>200
38	Me	C_6F_5	$2\text{-ClC}_6H_4CH_2$	10	1.5	1.3	1.7	5	>200	>200	>200
39	Me	$4\text{-MeO-}C_6H_4$	$2\text{-ClC}_6H_4CH_2$	53	12	27	31	22	>200	>200	>200

[a] K_I-s values were obtained from Easson–Stedman plots using a linear regression program, from at least three different assays. Standard errors were of 5–10 % (Scozzafava and Supuran 2000a)

[b] With the thioester substrate Ac-ProLeuGly-S-LeuLeuGlyOEt, spectrophotometrically (Scozzafava and Supuran 2000a)

[c] With FALGPA as substrate, spectrophotometrically (Scozzafava and Supuran 2000a)

[d] With 4-NPA as substrate, by the esterase method, spectrophotometrically (Scozzafava and Supuran 2000a)

followed by the corresponding Ala derivatives, which in turn were more active than the corresponding Val and Leu derivatives. Just the opposite was generally true for MMP and ChC inhibition, with the bulkier Val and Leu derivatives generally more inhibitory than the corresponding Ala and Gly derivatives (Table 1); (ii) sulfonyl amino acyl hydroxamates possessing RSO_2N(benzyl/substituted benzyl)-amino acyl moieties (such as **10–12**; **16–18**; **22–241;** and **28–45**) were weak or very weak CA inhibitors, but showed excellent MMP and ChC inhibitory properties. Thus, these compounds were generally 4–8 times weaker CA inhibitors as compared to the corresponding unsubstituted compounds mentioned above, whereas their affinities for MMPs were very much enhanced as compared to those of the corresponding unsubstituted compounds. It was in fact reported that the benzyl moiety of this type of hydroxamate inhibitors fits well within the $S_{2'}$ site of the protease, contributing substantially to the formation of strong E–I adducts. Obviously the different MMPs possess quite diverse affinities for these derivatives, with important differences between the deep pocket (MMP-2; MMP-8; and MMP-9) and the short pocket enzymes (MMP-1). Thus, as already shown previously by us for some structurally related derivatives, the deep pocket enzymes MMP-2, MMP-8, and MMP-9 are much more susceptible to be inhibited by this class of hydroxamates (K_I-s in the range of 0.6–20 nM) than collagenase 1, MMP-1 (K_I-s in the range of 7–60 nM). Again the pentafluorophenylsulfonyl derivatives were the most active inhibitors, followed by the corresponding perfluorobutyl ones, whereas the least active were the corresponding 4-methoxyphenyl-substituted compounds. The Leu derivatives were generally more active than the corresponding Val derivatives, which in turn were more inhibitory than the Ala and Gly derivatives; (iii) further substitution (with nitro or chloro moieties, in position 2 or 4) of the $P_{2'}$ benzyl moiety, such as in compounds **25–39** lead to a slight enhancement of the MMP inhibitory properties, to an enhancement of the ChC inhibitory effects, and to a drastic reduction of the CA inhibitory properties of the corresponding compounds (Table 1) (Scozzafava and Supuran 2000a). A putative binding mode for these compounds to the CAs was also proposed and is shown in Fig. 4, but this binding mode has not yet been confirmed by means of X-ray crystallography. An interesting QSAR study of these compounds has also bee reported by Gupta et al. (2003).
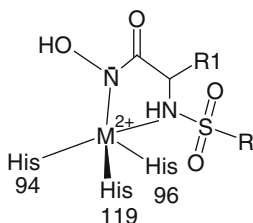
Fig. 4 Proposed binding of a sulfonylated amino acid hydroxamate (as monoanion) to the metal ion within the active site of CA (M = Zn(II) for the native enzyme or Co(II) for the cobalt-substituted one) (Scozzafava and Supuran 2000a)
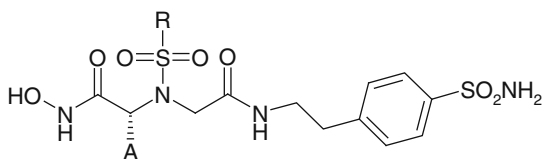
A = H, i-Pr

R = Ph, 4-MeO-C$_6$H$_4$, 4-PhO-C$_6$H$_4$

The data of Table 1 proved that potent CAIs can be obtained from the class of investigated sulfonylated amino acid hydroxamates (Scozzafava and Supuran 2000a). Although it was noted that in addition to MMPs, hydroxamates also inhibit other metalloproteinases, such as leucine aminopeptidase, neprilysin, thermolysis, and tumor necrosis factor-alpha among others (Supuran and Winum 2009), affinities as high as for the CAs (in the nanomolar range) were not evidenced up to now (Scozzafava and Supuran 2000a). Thus, such results are quite promising for the eventual design of novel types of potent CAIs, or of compounds with a dual activity, both as CAIs and MMPIs (Fig. 5). In fact, such derivatives were subsequently reported (Santos et al. 2007; Marques et al. 2008).

Compounds **40** reported using this dual drug approach (Santos et al. 2007; Marques et al. 2008) are iminodiacetic derivatives which possess the following derivatization type in their scaffolds: (i) one of the COOH moieties of the iminodiacetic moiety has been transformed to the hydroxamate ZBG; (ii) the other COOH moiety has been derivatized by transforming it to the amide, by reaction with 4-aminoethyl-benzenesulfonamide, a well-known CAI (Supuran 2008). This part of the molecule should interact only with the CAs, whereas the hydroxamate part may interact both with CAs as well as MMPs (Santos et al. 2007; Marques et al. 2008); (iii) the central imino moiety has been transformed to a secondary aromatic sulfonamide, and (iv) an isopropyl moiety may be present or absent on one of the CH$_2$ spacers coming from the iminodiacetic moiety.

Some of these compounds were low nanomolar CAIs and MMPs against several such enzymes (isoforms) involved in tumorigenesis (e.g., CA IX, CA XII, MMP-8, MMP-9, MMP-13, etc.) (Santos et al. 2007; Marques et al. 2008).

5 Aromatic Hydroxamates

The simple compound phenylhydroxamate, PhCONHOH **41**, has recently investigated by means of kinetic and X-ray crystallographic techniques, for its interaction with all mammalian CA isoforms, CA I–XIV (Di Fiore et al. 2012). Hydroxamate **41** inhibited all CA isoforms, with inhibition constants in the range of 0.94–179 μM, being thus less effective as CAI compared to the sulfonamides,

which usually are micro–nano molar CAIs (Supuran 2008). However, there were several notable features of the inhibition profile of compound **41**. Thus, the dominant, offtarget isoform hCA II was the least inhibited by **41** (K_I of 179 μM). The other highly abundant cytosolic isoform hCA I was also relatively resistant to inhibition by **41** (K_I of 83.1 μM). An interesting aspect of the hydroxamate **41** was that it strongly inhibited two transmembrane isoforms, hCA XII and XIV, with inhibition constants in the range of 0.94–9.51 K_I of 179 μM. As many trans-membrane isoforms are important drug targets for the development of antiglau-coma or anticancer therapies, this class of underexplored CAIs may constitute an interesting starting point for compounds with increased selectivities for such isoforms over the cytosolic, highly abundant offtarget ones hCA I and II. It should be also noted that many of the investigated CA isoforms (e.g., hCA III, IV, VA, VB, VI, VII, and XIII) were modestly inhibited by **41**, with K_Is in the range of 23.0–84.7 K_I of 179 μM. Hydroxamate **41** inhibited most efficiently hCA XIV (Di Fiore et al. 2012).

But the most interesting facts emerged when the X-ray crystal structure of **41** complexed to hCA II has been resolved (Di Fiore et al. 2012). The binding of the inhibitor molecule did not cause any significant change in the overall protein structure. Hydroxamate **41** binds to the hCA II active site with the CO and OH groups which simultaneously coordinate to the zinc ion to form an energetically favorable 5-membered chelate complex (Fig. 6a, b). The inhibitor binding was also stabilized by several other interactions with enzyme active site residues; in particular, the nitrogen atom forms a hydrogen bond with the Thr200OG1 atom (N- - -Thr200OG1 = 3.12 Å), whereas the phenyl ring, whose position is rather well superimposable to that of the phenyl ring in the hCA II/acetohydroxamic acid adduct (Fig. 6c), was involved in a number of van der Waals interactions with the side chains of residues Gln92, Val121, Phe131, Leu141, Val143, Leu198, and Thr200 (Fig. 6a). Although, several controversial data have been reported on the
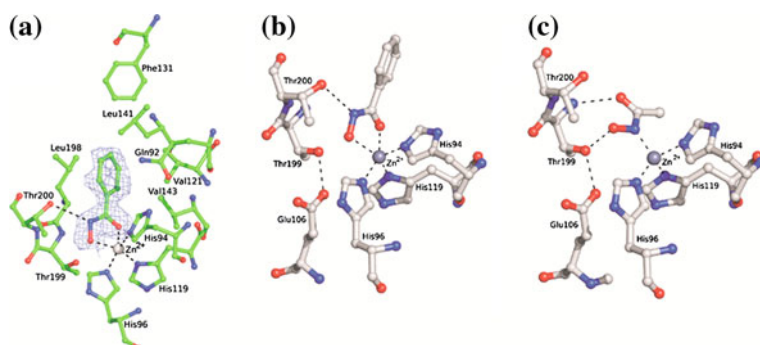
Fig. 6 (**a**) Active site region in the hCA II–**41** complex. The simulated annealing omit 2|Fo|-|Fc| electron density map inhibitor, contoured at 1.0 sigma, and associated to the inhibitor molecule is also shown. (**b**) Zn^{2+} coordination geometry of N-(Hydroxy)-benzamide **41**. (**c**) Zn^{2+} coordination geometry of acetohydroxamic acid (PDB code 1AM6) (Di Fiore et al. 2012)

putative deprotonation site of hydroxamates of type R-CONHOH, highlighting that the solvent and the environment can play a key role in favoring the *N*-deprotonation or the O-deprotonation, the observation that compound **41** coordinates to the catalytic zinc ion through its CO and OH groups suggests that in this case the O-deprotonated form is the most probable (Di Fiore et al. 2012). For this reason, the deprotonated oxygen atom cannot form a hydrogen bond with the Thr199OG1 atom, although being at a distance of only 2.74 Å from it. Indeed, the Thr199OG1 atom is known to be involve in the classical H-bond with Glu106[1,23] and thus it does not have further hydrogens to donate to the hydroxamate functionality (Fig. 6b). It is worth noting that the zinc ion coordination observed in the adduct here reported is identical to that described for the majority of the MMP/hydroxamate complexes so far structurally characterized (Whittaker et al. 1999), but is completely different from that observed in other CA/aliphatic hydroxamate adducts studied earlier (Scolnick et al. 1997) and discussed above. The observation that hydroxamate derivatives of type R-CONHOH can adopt such completely different coordination modes to the CA catalytic zinc ion, depending on the nature of the R substituent, strongly suggests that this ZBG is very versatile and can represent an interesting alternative to the classical sulfonamides for the development of more selective CAIs.

6 Conclusion

As MMPs, the main class of metalloenzymes interacting with the hydroxamates, CAs is also zinc enzymes possessing at the active center a Zn(II) ion coordinated by three His residues and a water molecule/hydroxide ion. The latter one is crucial for catalysis and is many times replaced by inhibitors binding to the metal center. The 14 different mammalian CAs as well as many such enzymes isolated up to now in other organisms, play important physiological functions such as pH regulation, signaling, biosynthetic reactions, electrolyte secretion, etc. Unsubstituted sulfonamides act as high affinity inhibitors for the first type of these enzymes, whereas hydroxamates were also shown to strongly inhibit some of them. The investigated hydroxamates as CA inhibitors include *N*-hydroxyurea, the aliphatic/aromatic hydroxamates of the type RCONHOH (R = Me, CF_3 and Ph), as well as sulfonylated amino acid hydroxamates of the type RSO_2NX-AA-CONHOH (X = H; benzyl; substituted benzyl; AA = amino acid moiety, such as those of Gly, Ala, Val, Leu). The most salient feature of the hydroxamates as CAIs regards their very high versatility as ZBGs. Indeed, depending on the nature of the R moiety of a hydroxamate of the type RCONHOH, this ZBG can adopt different coordination modes to the catalytic zinc ion within the CA active site: monodentate through the deprotonated N atom; bidentate trough the NH and OH atoms, or bidentate through the OH and O atoms (deprotonation at the OH moiety). These findings suggest that the enzyme-inhibitor interaction of the hydroxamate CAI class can be largely modulated by exploring different substitution patterns at the R

group, thus providing interesting hints for the development of new CAIs of the non-sulfonamide type with pharmaceutical applications in the treatment of various diseases.

References

Alterio V, Di Fiore A, D'Ambrosio K et al (2012) Multiple binding modes of inhibitors to carbonic anhydrases: how to design specific drugs targeting 15 different isoforms? Chem Rev 112:4421–4468

Borkakoti N (2000) Structural studies of matrix metalloproteinases. J Mol Med 78:261–268

Borkakoti N, Winkler FK, Williams DH et al (1994) Structure of the catalytic domain of human fibroblast collagenase complexed with an inhibitor. Nat Struct Biol 1:106–110

Bottomley KM, Johnson WH, Walter DS (1998) Matrix metalloproteinase inhibitors in arthritis. J Enz Inhib 13:79–102

Briganti F, Mangani S, Scozzafava A et al (1999) Carbonic anhydrase catalyzes cyanamide hydration to urea: is it mimicking the physiological reaction? J Biol Inorg Chem 4:528–536

Christianson DW, Ippolito JA (1991) Structure-function relationship between the carbonic anhydrases and the zinc proteases. In: Botrè F, Gros G, Storey BT (eds) Carbonic Anhydrase. VCH, New York, pp 95–110

Coleman JE (1998) Zinc enzymes. Curr Opin Chem Biol 2:222–234

Di Fiore A, Maresca A, Supuran CT, De Simone G (2012) Hydroxamate represents a versatile zinc binding group for the development of new carbonic anhydrase inhibitors. Chem Commun 48:8838–8840

Gupta SP, Maheswaran V, Pande V, Kumar D (2003) A comparative QSAR study on carbonic anhydrase and matrix metalloproteinase inhibition by sulfonylated amino acid hydroxamates. J Enzyme Inhib Med Chem 18:7–13

Lovejoy B, Welch AR, Carr S et al (1999) Crystal structures of MMP-1 and -13 reveal the structural basis for selectivity of collagenase inhibitors. Nat Struct Biol 6:217–221

Marques SM, Nuti E, Rossello A et al (2008) Dual inhibitors of matrix metalloproteinases and carbonic anhydrases: iminodiacetyl-based hydroxamate-benzenesulfonamide conjugates. J Med Chem 51:7968–7979

Nagase H, Woessner JF (1999) Matrix metalloproteinases. J Biol Chem 274:21491–21494

Neri D, Supuran CT (2011) Interfering with pH regulation in tumours as a therapeutic strategy. Nat Rev Drug Discov 10:767–777

Santos MA, Marques S, Vullo D et al (2007) Carbonic anhydrase inhibitors. Inhibition of cytosolic/tumor-associated isoforms I, II and IX with iminodiacetic carboxylates/hydroxamates also incorporating benzenesulfonamide moieties. Bioorg Med Chem Let 17:1538–1543

Scolnick LR, Clements AM, Liao J et al (1997) Novel binding mode of hydroxamate inhibitors to human carbonic anhydrase II. J Am Chem Soc 119:850–851

Scozzafava A, Menabuoni L, Mincione F et al (1999) Carbonic anhydrase inhibitors: synthesis of water-soluble, topically effective intraocular pressure lowering aromatic/heterocyclic sulfonamides containing cationic or anionic moieties: is the tail more important than the ring? J Med Chem 42:2641–2650

Scozzafava A, Supuran CT (2000a) Carbonic anhydrase and matrix metalloproteinase inhibitors. Sulfonylated amino acid hydroxamates with MMP inhibitory properties act as efficient inhibitors of carbonic anhydrase isozymes I, II and IV, and N-hydroxysulfonamides inhibit both these zinc enzymes. J Med Chem 43:3677–3687

Scozzafava A, Supuran CT (2000b) Protease inhibitors. Part 5. Alkyl/arylsulfonyl- and arylsulfonylureido-/arylureido-glycine hydroxamate inhibitors of *Clostridium histolyticum* collagenase. Eur J Med Chem 35:299–307

Scozzafava A, Supuran CT (2000c) Protease inhibitors. Part 9. Synthesis of *Clostridium histolyticum* collagenase inhibitors incorporating sulfonyl-L-alanine hydroxamate moieties. Bioorg Med Chem Lett 10:499–502

Scozzafava A, Supuran CT (2003) Hydroxyurea is a carbonic anhydrase inhibitor. Bioorg Med Chem 11:2241–2246

Supuran CT (2008) Carbonic anhydrases: novel therapeutic applications for inhibitors and activators. Nat Rev Drug Discov 7:168–181

Supuran CT (2010) Carbonic anhydrase inhibitors. Bioorg Med Chem Lett 20:3467–3474

Supuran CT (2011) Carbonic anhydrase inhibitors and activators for novel therapeutic applications. Future Med Chem 3:1165–1180

Supuran CT (2012) Structure-based drug discovery of carbonic anhydrase inhibitors. J Enzyme Inhib Med Chem 27:759–772

Supuran CT, Scozzafava A (2002) Matrix metalloproteinases (MMPs). In proteinase and peptidase inhibition: recent potential targets for drug development, Smith HJ, Simons C, Eds., Taylor & Francis, London, pp 35–61

Supuran CT, Winum JY (2009) Introduction to zinc enzymes as drug targets. In: Supuran CT, Winum JY (eds) Drug Design of Zinc-Enzyme Inhibitors: Functional, Structural, and Disease Applications. Wiley, Hoboken, pp 3–12

Temperini C, Innocenti A, Scozzafava A, Supuran CT (2006) N-Hydroxyurea—a versatile zinc binding function in the design of metalloenzyme inhibitors. Bioorg Med Chem Lett 16:4316–4320

Van Wart HE, Steinbrink DR (1981) A continuous spectrophotometric assay for *Clostridium histolyticum* collagenase. Anal Biochem 113:156–165

Whittaker M, Floyd CD, Brown P, Gearing AJH (1999) Design and therapeutic application of matrix metalloproteinase inhibitors. Chem Rev 99:2735–2776

Structure–Activity Relationship Studies of Hydroxamic Acids as Matrix Metalloproteinase Inhibitors

Vaishali M. Patil and Satya P. Gupta

Abstract The chapter specifically deals with the structure–activity relationship studies on various classes of hydroxamates acting as matrix metalloproteinase (MMP) inhibitors. Among all classes of MMP inhibitors, hydroxamates are important in that their zinc-binding group CONHOH makes them a bidentate ligand to act with any metal-containing enzyme. Most of the MMP inhibitors developed by pharmaceutical companies belong to this category of compounds. The position of hydroxamate nitrogen suggests that it is protonated and forms a hydrogen bond with carbonyl oxygen of the enzyme backbone. In addition to zinc-binding affinity, several other properties of the hydroxamic acids depending upon their structures control their MMP inhibition activity. Various categories of hydroxamates such as succinyl, malonic acid, sulfonamide-based, aryl acid-based, sulfone-based, N-benzoyl aminobutyric acids, aminoproline-based, aminopyrrolidine-based, and phosphonamide/phosphinamide-based hydroxamates have been found to act as MMP inhibitors. A detailed structure–activity relationship (SAR) study of all these categories of hydroxamates has been presented.

Abbreviations

MMP	Matrix metalloproteinase
MMPI	Matrix metalloproteinase inhibitor
QSAR	Quantitative structure–activity relationship

V. M. Patil
School of Pharmacy, Bharat Institute of Technology, Meerut 250103, India

S. P. Gupta (✉)
Meerut Institute of Engineering and Technology, Meerut 250005, India
e-mail: spgbits@gmail.com

SAR   Structure-activity relationship
TACE   TNF-α converting enzyme
TIMP   Tissue inhibitors of metalloproteinases
TNF   Tumor necrosis factor-α
ZBG   Zinc-binding group

Contents

1 Introduction

More than 100 years ago, Lossen discovered the first hydroxamic acid and in the present time it is one of the well-studied compounds having numerous applications. The pharmacological potential of hydroxamic acids in a variety of disease conditions, such as viral diseases (Torres 1995; Szekeres et al. 1997), malaria, Alzheimer's disease (Parvathy et al. 1998; El Yazal and Pang 2000), allergic diseases (Igeta et al. 2000; Valapour et al. 2002), tuberculosis (Miller 1989; Shingledecker et al. 2000), cancer, cardiovascular diseases (Jeng and Lombaert 1997), and metal poisoning (Domingo 1998; Weisburger and Weisburger 1973) is well reported. This diverse profile of hydroxamic acids can be attributed to their efficiency in blocking a variety of enzymes, viz., ureases (Zhang et al. 1999; Mishra et al. 2002), peroxidases (Tsukamoto et al. 1999), matrix metalloproteinases (MMPs) (Leung et al. 2000; Hidalgo and Eckhardt 2001), hydrolases (Brown et al. 2004a, b), lipoxygenases (Muri et al. 2002), cyclooxygenases (Dooley et al.

2003; Connolly et al. 1999), histone deacetylases (Marks et al. 2000; Johnstone 2002; Jung 2001; Kelly et al. 2002), peptide deformylases (Chen et al. 2004), etc. In the past decades, an extraordinary work has been carried out on their design, synthesis, and structure–activity relationships (SARs) which support their diverse therapeutic properties (Lipczynska-Kochany 1988). Here we focus on the SAR studies of several groups of hydroxamic acids/hydroxamates relevant to their biomedical applications as matrix metalloproteinase inhibitors (MMPIs).

2 Structural Features of MMPIs

MMPs belong to the family of proteolytic enzymes and regulate a plethora of physiological and pathological functions. Their complex role also contributes to unintended side effects during clinical trials. For more than three decades, MMPs have been heralded as promising targets for the treatment of different diseases as discussed before and scientists have been involved in finding potent inhibitors for them. The unique site specificity and selectivity of MMPIs for different MMP targets (Gupta and Patil 2012) have been the focus of recent research. Over activation of MMPs results in an imbalance between the activity of MMPs and tissue inhibitors of metalloproteinases (TIMPs) that can lead to a variety of pathological disorders (Aranapakam et al. 2003a, b; Venkatesan et al. 2004; Brown et al. 2004a). Although the role of each MMP is not known for certain, the study of their inhibition has evoked great interest. A variety of connective tissues and proinflammatory cells including fibroblasts, osteoblasts, endothelial cells, macrophages, neutrophils, and lymphocytes excrete these MMPs, of which most are expressed as inactive zymogens, that are subsequently processed by other proteolytic enzymes, e.g., serine proteases, furin, plasmin, and others, to generate the active forms. Under normal physiological conditions, the proteolytic activity of the MMPs is controlled at any of the following three known stages: transcription, activation of the zymogens, or inhibition by TIMPs. In pathological conditions, this equilibrium is shifted toward increased MMP activity leading to tissue degradation (Cheng et al. 2000; Kontogiorgis et al. 2005).

Since all MMPs belong to the family of zinc-containing enzymes, all contain, in common, a zinc atom (divalent cation Zn^{2+}), and through this metal atom they affect the amide bond hydrolysis. In the amide hydrolysis, this Zn^{2+} ion is generally tetrahedrally coordinated to three donor groups from the enzyme and a water molecule (Leung et al. 2000; Gupta 2007). Based on the conclusions drawn by various research groups, the basic structural features required for an effective MMPI are: (i) the presence of a functional group, such as a carboxylic group (COOH), hydroxamic group (CONHOH), and sulfhydryl group (SH), that may be able to chelate the active site Zn^{2+} ion of the enzyme (such a group is referred to as a zinc-binding group, ZBG), (ii) at least one functional group capable of hydrogen bonding with the enzyme backbone, and (iii) one or more side chains that can have effective van der Waals interactions with the enzyme subsites. Based on these

requirements, a large number of synthetic MMP inhibitors (MMPIs) have been reported by various research groups from industry and academia (Supuran and Scozzafava 2002).

Many of the MMPIs have been investigated by employing computational methods like substrate-based design (Johnson et al. 1987), structure-based design (Babine and Bender 1997), and combinatorial chemistry (Shuttleworth 1998; Whittakar 1998). In the development of synthetic MMPIs, substrate-based design has been the principal approach and three classes of compounds have been developed, viz, (a) compounds that have amino acid residues on both sides of ZBG, e.g., Pn– —P2–P1–ZBG–P1′–P2′——— –Pn′; (b) compounds that have amino acids residues on only right-hand side of the ZBG, e.g., ZBG–P1′–P2′——— –Pn′ and are called right-hand (RHS) inhibitors; and (c) compounds that have amino acids residues on only left-hand side of the ZBG, e.g., Pn– —P2–P1–ZBG and are called left-hand side (LHS) inhibitors (Here P's and P″'s refer to the standard nomenclature of amino acid residues as defined in peptide substrates) (Babine and Bender 1997).

3 Hydroxamates as MMPIs

Among all the classes of MMPIs, the hydroxamates, that contain hydroxamic acid group (CONHOH), have been more extensively studied. The synthetic MMPIs have been categorized in structure-based drug design into three classes, *i.e.,* compounds with amino acid residues on both sides of ZBG, compounds with amino acid residues on only the right-hand side of ZBG, and compounds with amino acid residues on only the left-hand sides of ZBG. Among all these three classes, the right-hand side inhibitors were mostly found to be more potent (Gupta 2007; Whittaker et al. 1999). Further, the hydroxamic acid-based MMPIs have been categorized based on their structural features as:

(1) Succinyl hydroxamates
(2) Malonic acid-based hydroxamates
(3) Sulfonamide-based hydroxamates
(4) Aryl acid-based hydroxamates
(5) Anthranilic acid-based hydroxamates

Hydroxamates are among one of the most explored zinc-binding compounds for the development of MMPIs, and most interestingly the first three MMPIs used to treat cardiovascular diseases are from the hydroxamate category (Whittaker et al. 1999). In 1978, Nishino and Power (1978) first introduced a hydroxamate as a ZBG for designing an inhibitor, thermolysin, which provided an encouragement to develop hydroxamate-containing MMPIs (Moore and Spilburg 1986a, b).

At Pfizer, Robinson et al. (2000) designed some nonpeptidic and sulfonamide hydroxamates with an objective to improve the selectivity and were successful in the development of pyrrolidinone-based hydroxamates, e.g., **a** (Fig. 1), having good
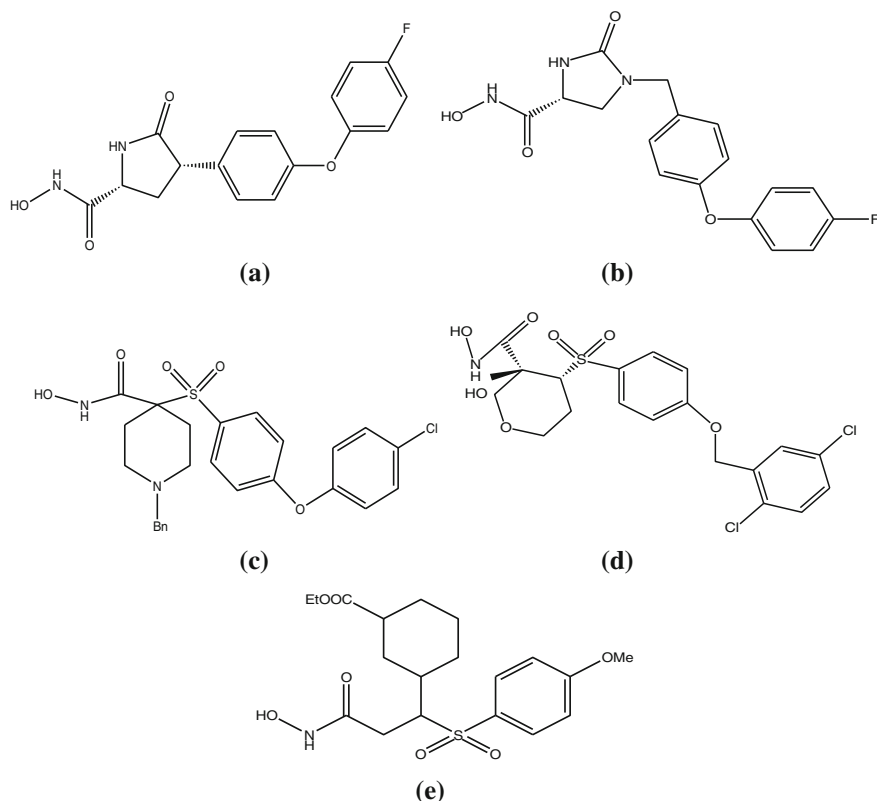
Fig. 1 Structures of some important hydroxamates developed at Pfizer

selectivity for MMP-1. Further structural modifications led to novel series of imi-dazolidine-based MMPIs, such as **b** (Fig. 1), as strong inhibitors of MMP-13 (Robinson et al. 2001). Simultaneously, compound **c** (Fig. 1) has been developed for the treatment of osteoarthritis (Aranapakam et al. 2003a, b) and SAR studies con-cluded a better potency of aromatic sulfonyl compounds than that of aliphatic/heteroaromatic sulfonyl derivatives. Some tetrahydopyran-centered sulfone hy-droxamates, such as **d** (Fig. 1),were developed as selective inhibitors of MMP-13 at Pfizer (Noe et al. 2004) and further structure optimization led to the development of **e** (Fig. 1) having sub-nanomolar potency against MMP-2 (Salvino et al. 2000).

4 Story of Some Clinical Success

The designing of earlier MMPIs was based on the knowledge of the amino acid sequence of collagen at the site of cleavage by MMP-1 (collagenase-1). Among the very first hydroxamates studied, batimastat (BB-94, **1**) and marimastat

(BB-2516, **2**) that were initially found to be clinically useful were the peptidic inhibitors. It was observed that for this type of inhibitors, the presence of a P1′ residue (α to the hydroxamate moiety) leads to a broad-spectrum activity against a variety of MMPs (Whittaker et al. 1999; Bottomley et al. 1998). However, both were withdrawn after clinical trials for cancer due to poor selectivity and poor bioavailability. These studies concluded that compounds which mimicked the sequences of the right-hand side of the cleavage site (primed sites P1′, P2′, P3′, etc.), with a hydroxamic acid moiety incorporated as the zinc-binding group, exhibited better inhibition (Yao et al. 2001).

1, BB-94 (Batimastat)   **2**, BB-2516 (Marimastat)
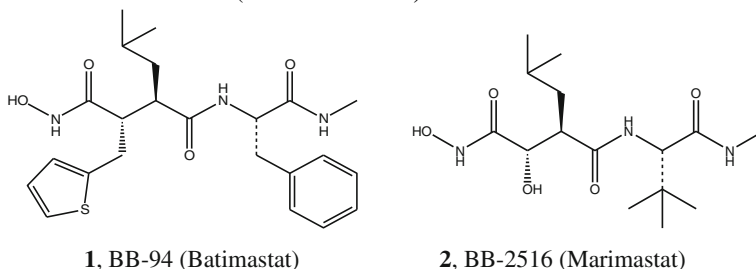
Among the non-peptide MMPIs, the sulfonamide hydroxamate derivatives CGS27023A (**3a**) and CGS25966 (**3b**) have entered clinical trials (Heath and Grochow 2000). In this case, NMR spectroscopy and the three-dimensional solution structure were used to define the mode of binding with MMP-3 (Zhang et al. 2000). The isopropyl and pyridylmethyl substituents were found to accommodate the hydrophobic S1 and S2′ subsites. Compound **4** from the similar chemical category was found an MMP-13 inhibitor at subnanomolar range (Kimura et al. 2001).

3a; Y=N, **3b**; Y=CH   **4**
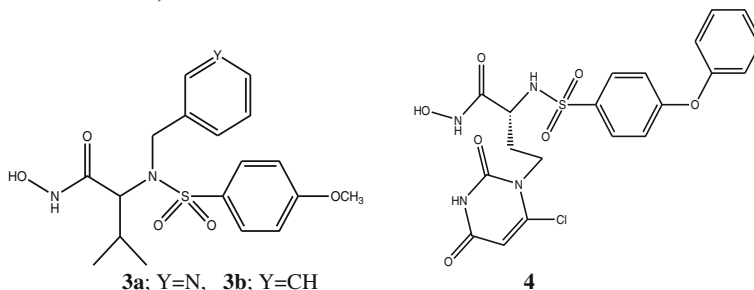
Some sulfone MMPIs (**5**, **6**) having hydroxamic acid moiety were found to have bidentate interactions with MMP-13 in the reported X-ray crystal structures. The selectivity of these compounds for MMP-13 was attributed to their affinity for the S1′ pocket. This class of inhibitors mimics a carbonyl interaction in peptide-based inhibitors and one of the oxygen of sulfone group serves as the hydrogen bond acceptor from the amide group of Leu185. However, of these two, **6** was withdrawn from Phase II clinical trials for osteoarthritis due to musculoskeletal side effects (Tu et al. 2008).

5   **6**
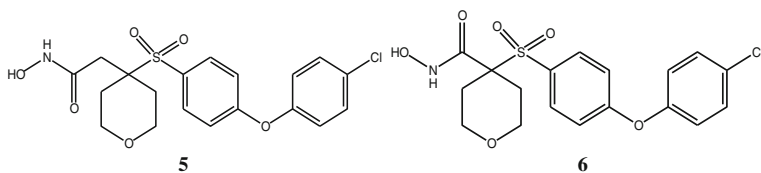
Simultaneously, a series of reverse hydroxamate peptides (**7–9**) were reported as broad-spectrum inhibitors of tumor necrosis factor-α (TNF-α) converting enzyme (TACE) and MMPs (Andrews et al. 2000). Compound **7** had IC_{50} values of 19, 20, 16, and 42 nM for MMP-1, -3, -9, and TACE inhibition, respectively, but failed to show any specificity for TACE against MMPs and this may be the reason behind their side effects such as tendonitis and musculoskeletal effects. Compound **9**, prepared in a combinatorial fashion, was found to inhibit MMP-3 and -13 ($IC_{50} > 100$ nM) as well as TACE and TNF-α ($IC_{50} < 100$ nM).

7   **8**

9
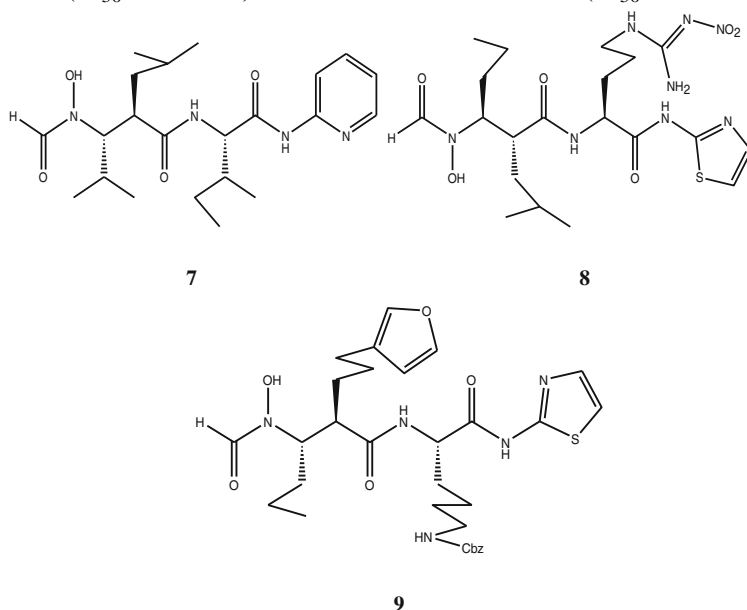
5 SAR Studies

5.1 Succinyl Hydroxamic Acid Derivatives

Succinyl hydroxamates have been found to be much stronger MMPIs than those belonging to other groups (Johnson et al. 1987) and thus they have been the most widely studied MMPIs until recently. Compounds **1** (batimastat) and **2** (marimastat) are a few of the potent MMPIs that belong to this category (Whittaker et al.

1999; Supuran and Scozzafava 2002; Levin et al. 2004). Both the compounds showed very good activities in several disease models and another compound (**10**) was found to be orally bioavailable. The bioavailability of **10** was attributed to the presence of a hydrophilic OH moiety at α-carbon, which could probably increase the water solubility of the compound (Levin et al. 2004). Some compounds were obtained by incorporating *cis*-(1*S*, 2*R*)-amino-2-indanol scaffold and optimized as potent, selective, and orally bioavailable inhibitor of
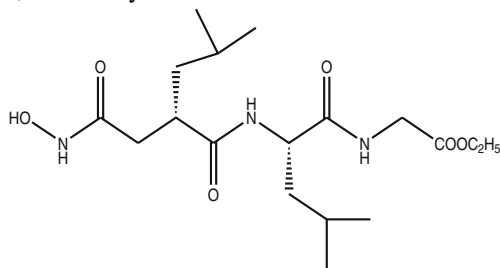
10

aggrecanase. A series of 13- and 14-membered macrocyclic amines, such as **11** and **12**, were developed by linking P1 and P2′ groups of succinic acid-based inhibitors. The selectivity profile of compound **12** against MMP-8 and -9 was attributed to the macrocyclic template and the long phenylpropyl P1 group accommodating in the deep S1 pocket.
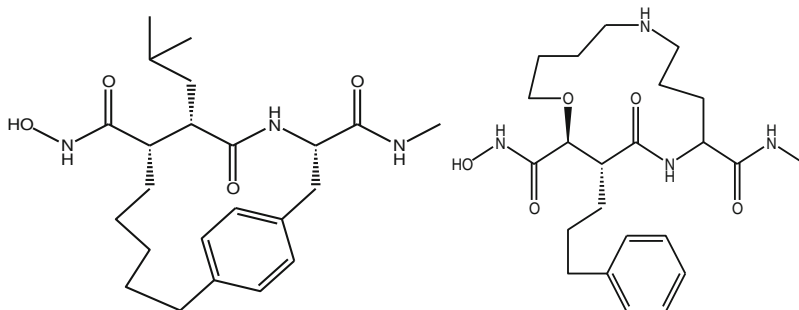
11   **12**

A large series of succinyl hydroxamates (**13**) having variations in P1′ and P3′ groups and P2′ as *t*-butyl group had been evaluated against MMP-2 and -3 (Fray et al. 2001; Fray and Dickinson 2001). The SAR conclusions drawn in the studies were that at P1′ position, the phenylpropyl substituent was conducive to MMP-2 and -3 inhibition and that the *o*-F and *o*-Me at phenyl ring showed remarkable improvement in MMP-3 selectivity as compared to larger groups like Et, OMe, and CF_3 which caused significant loss of activities. These authors concluded that the size of R_1- and R_2-substituents contributes toward MMP-2 selectivity. At R_2 position, the Me and *t*-Bu groups were well tolerated in comparison to the cycloalkyl group. It was also noted that chirality of R_2 plays an important role, i.e., *R*-enantiomer retains potency similar to Me analog against MMP-3 but leads to a loss of potency against MMP-2. Compound **14** was identified as a potent and

selective MMP-3 inhibitor having 303 times selectivity against MMP-2 (Fray and Dickinson 2001).

13   **14**
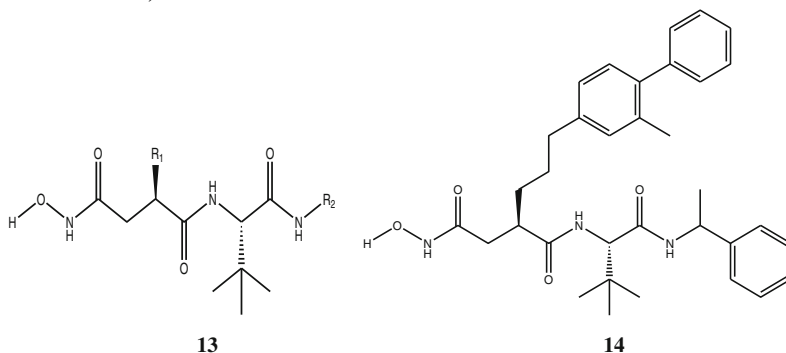
## 5.2 Malonic Acid-Based Hydroxamates

15
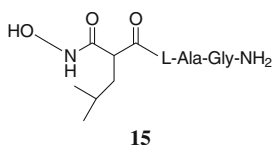
The malonic acid-based hydroxamates were observed to exhibit nonsubstrate-like binding, e.g., compound **15** binds with the Zn^{2+} of MMPs in the same manner as normal hydroxamates do, but its secondary binding is quite different. The C-terminal Ala-Gly-NH$_2$ moiety adopts a bent conformation that is inserted into the S1$'$ pocket. Thus, it exhibited nonsubstrate-like binding to the active site and consequently represented a new interesting lead for obtaining malonic acid-based MMP inhibitors (Roedern et al. 1998; Krumme et al. 1998). The SAR studies have shown hydrophobic interactions at S1 subsite of the substituents like isobutyl, (CH$_2$)$_2$Ph, CH$_2$Ph, or Ph. For S1$'$ subsite the OEt and N-morpholide were not favored while the C-terminal aromatic groups were found to improve inhibitory potency. There is further improvement in activity with NH-n-octyl substituent.

5.3 Sulfonamide-Based Hydroxamates

Sulfonamide-based hydroxamates, as represented by **16**, contain a sulfonamide moiety and involve hydrogen bonding as well as direct hydrophobic interaction with S1$'$ pocket to improve the enzyme-inhibitor binding. Some of these inhibitors (**3**, **4**) were reported to act as efficient MMPIs (Shuttleworth 1998; Whittaker et al. 1999; Supuran and Scozzafava 2002) and further change in their structural features

could lead to better inhibitors (Jeng et al. 1998; Whittaker et al. 1999; Hannessian et al. 1999).

16
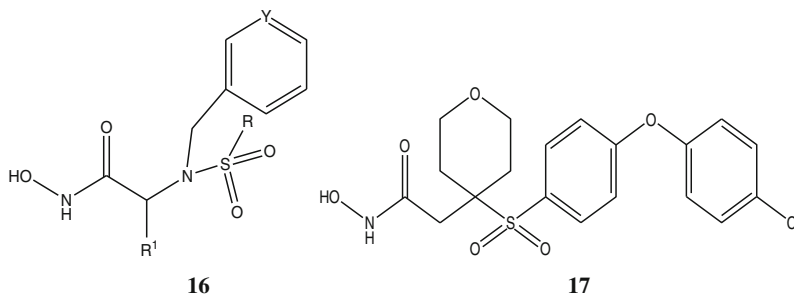
Y= H, Cl, NO$_2$; R = alkyl, aryl
R^1 = H (Gly derivatives), Me (Ala derivatives),
    i-Pr (Val derivatives), i-Bu (Leu derivatives)

17

While analogs of **16** were found to possess nanomolar potencies against MMP-1, -2, -8, and -9 (Supuran and Scozzafava 2002), **17** (a sulfone derivative) was observed to be very strong, highly selective, and orally bioavailable MMP inhibitor (Whittaker et al. 1999).

All the sulfonamide-based hydroxamates studied were derived from α-amino acids, with a single sp^3-hydridized carbon atom separating the sulfonamide nitrogen and the zinc chelating hydroxamic acid moiety. Assuming that an increase in this separation, with connecting atoms held rigidly, may lead to more potent compounds, Levin et al. (2001) attempted to design aryl acid-based sulfonamide hydroxamates as represented by an anthranilic acid-based scaffold (**18**). They prepared three regioisomeric (*ortho*, *meta*, and *para*) analogs of **18** with R^1 = CH$_2$Ph and R^2 = OCH$_3$. Of these, the *ortho* analog **19** was found to be the most potent inhibitor with an IC$_{50}$ value below 1 μM against MMP-1, -9, and -13.

18

19
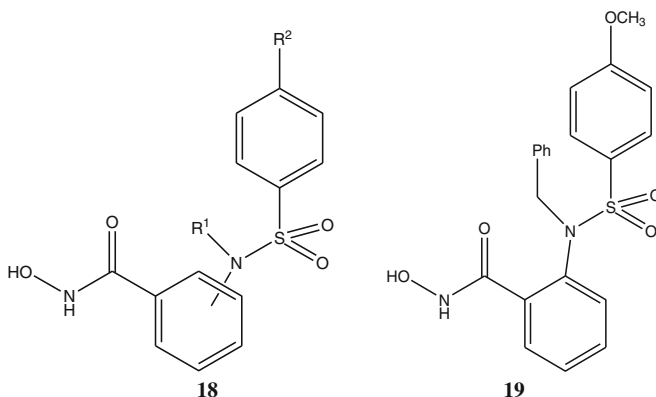
Similarly, a new class of *N*-substituted arylsulfonamido-based hydroxamic acid inhibitors was developed by Rossello et al. (2004) having at the sulfonamido

nitrogen either an oxyalkyl side chain (**20**) or simply an alkyl side chain (**21**), instead of simply hydrogen atom.

20   **21**
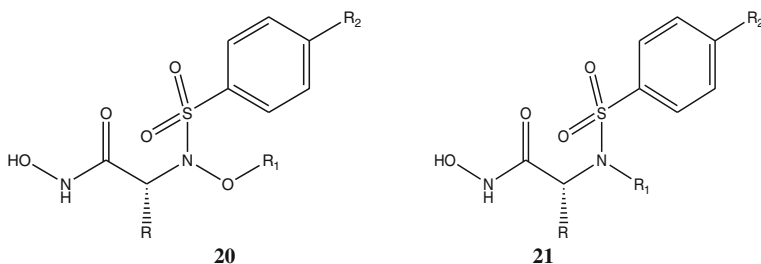
Compounds belonging to the series of **20** were found capable of blocking tumor cell invasion by potent and selective inhibition of MMP-2 and -9. Compound (**R**)-**22**, an analog of **20** with *R*-configuration at carbon α to hydroxamic group, showed a very good inhibitory activity profile toward MMP-2, -9, and -14 with IC$_{50}$ equal to 0.41, 16, and 7.7 nM, respectively (Rossello et al. 2005a).

(**R**)-**22**
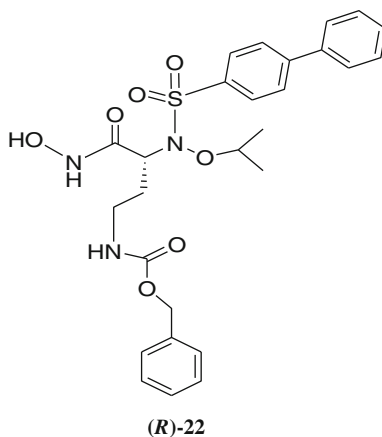
In continuation to this, Rossello et al. (2005b) further reported some twin hydroxamic acids ((**R,R**)-**23**) using some suitable linkers as 'a' and 'b'. Among the series, only compounds having hydroxyl and hydroxylamine substituents at R-position had shown activities against MMP-1, -2, -9, and -14, but were found to be poorly active as compared to the monomeric compound (**R**)-**22**. The hydroxamic acid moiety was found to be essential as proven by the loss of activity of carboxylic analog toward MMP-2 and -9 and it was not evaluated against MMP-1 and -14.
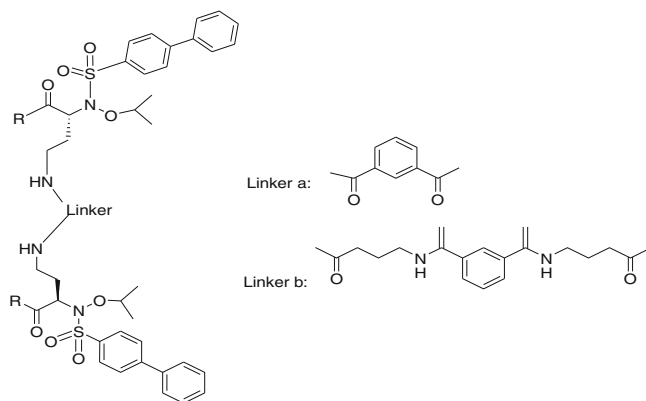
(**R,R**)-23

In a series of tetrahydroisoquinoline-based sulfonamide hydroxamates (**24**) studied by Ma et al. (2004), most compounds were found to display potent inhibition activity for some selected MMPs and it was observed that

- The variation of substituents at the 6- and 7-positions and arylsulfonyl group showed marked differences in potency and selectivity and also imparted some subtle isozyme selectivity. Thus these positions plays some role toward activity as seen by alteration of activity due to 6-hydroxyl/benzoxyl and 7-methoxy substituents.
- Among the 6-hydroxy analogs, the 4′-Me substituted derivative was found to be more potent than 4′-H or 4′-OMe substituted, however, the latter was found to be the most favored for MMP-15 inhibition.
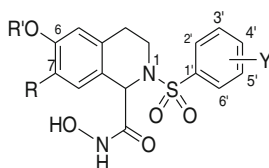

24

Yang et al. (2008) reported a few promising series of β-N-biaryl ether sulfonamide hydroxamates (**25–30**) as novel gelatinase (MMP-2 and -9) inhibitors, in which analogs of **28** were observed to have great selectivity for MMP-9/MMP-2 over MMP-1. Here the group attached to the sulfonamide nitrogen is referred as P1′. Some preliminary SAR conclusions were derived which demonstrated the advantage and potential of a β-N-biaryl ether sulfonamide moiety in the design of MMP inhibitors.

- The pairing of methanesulfonyl group with biaryl ether type P1′ moiety affords single-digit nanomolar activity against MMP-9.

- A β-N-biaryl ether sulfonamide with a methyl substituent at P1$'$ (**28**; R = H; IC$_{50}$ = 6.6 nM) was found to be about 5-fold more potent than an α-N-biaryl ether sulfonamide (**25**; R^2 = Me; IC$_{50}$ = 31 nM) against MMP-9.
- The introduction of small α-substituents (such as OMe/OH/Me at R-position) in **28**, **29,** and **30** and the chirality of the α-position (*R vs. S*) in **26** and **28** had marginal influence on the IC$_{50}$ and potency.
- Various substituents on the sulfonamide had the rank order for potency against MMP-2 and -9 as: methyl > ethyl > *n*-propyl > *iso*-propyl > NMe$_2$ > phenyl.
- The potency was restored to double-digit nanomolar range against MMP-9 on replacing the phenyl with a benzyl group at R^1-position.
- The preference shown by analogs having *para*-substituted phenyl moiety at R^1-position in **29** for MMP-2 over MMP-9 enzyme could be attributed to the tunnel-like S1$'$ subsite of MMP-2, which shows better tolerance of the longer P1$'$ moiety than the S1$'$ pocket of MMP-9.
- In **29**, R$_2$ = Cl or CH$_3$ was observed to be more important than any other R$_2$-substituent.
- Replacement of the phenyl ring with a heteroaryl moiety in **29** (Y = N) was found to reduce potency as the hydrophobic residues surrounding the S1$'$ pocket typically favor a more lipophilic P1$'$ moiety.
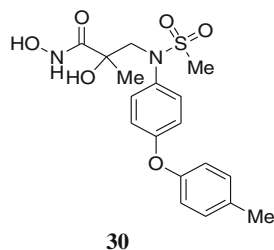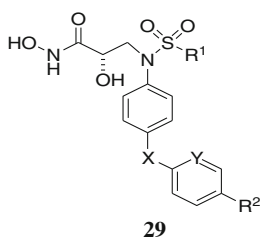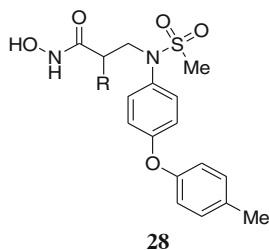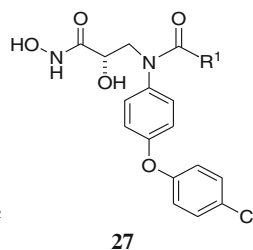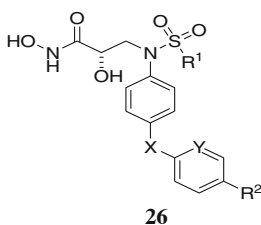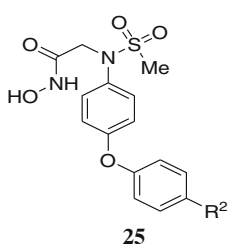

In a new series of arylsulfonamidic scaffold (**31**), selective for MMP-13 inhibition (Nuti et al. 2009), the following structure–activity relationships were observed.

31   32
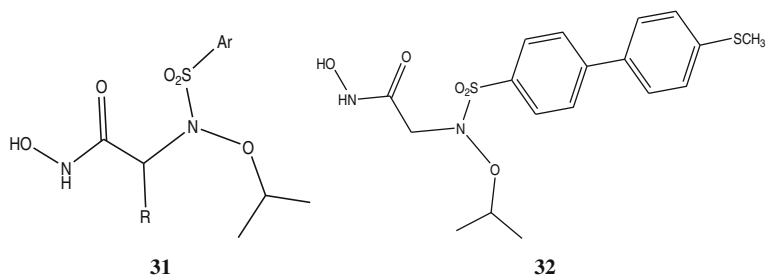
The 4-substituted biphenyl group at Ar was found contributing toward the inhibitory profile especially against MMP-2 as compared to the unsubstituted biphenyl for all tested enzymes without affecting the selectivity profile. Among the various substitutions on biphenyl moiety, the 4-methylthio (32) and 4-chlorobenzoxy substituents were found to be most significant for inhibition of MMP-13 (IC_{50} = 7.2 and 19 nM, respectively). It also exhibited a slight to good selectivity over MMP-1, -2, -3, -14, -16, and TACE. Compound with an isopropyl group as P1 substituent (R-substituent) was identified to be a promising slow-binding inhibitor of MMP-13 at nanomolar concentration, but with very high selectivity for it as compared to MMP-1, -14, and TACE.

In a series of 4-butylphenyl(ethynylthiophene)sulfonamido-based hydroxamates (33) studied by Nuti et al. (2011) for the inhibition of MMP-3, -8, -9, -14, and -25 and for the effective treatment of glioma, a compound having benzophenone substituent (R = –PhCOPh) was identified to have nanomolar potency against MMP-2, 9, and -25 but to be weaker against other members of MMP family. It was also observed that the MMP-2 inhibition activity of 33 was governed by its P1′ group, i.e., 4-butylphenylethynylthiophene, but its enzyme's selectivity profile by its P1 group (α-substituent). The elongated α-chain contributes toward selectivity. The compound with benzophenone moiety was indentified to have highest selectivity over MMP-1, -3, -8, and -14.

33
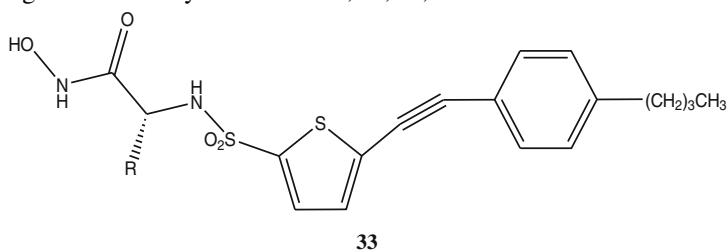
5.4 Sulfone-Based Hydroxamates

Some α- and β-piperidinesulfone hydroxamic acids (34–38) were studied by Becker et al. (2005) as potent inhibitors of MMP-2, -9, and -13. Among them, 35

with R = propargyl (SC-276) was selected for further development as it demonstrated excellent antitumor activity against MX-1 breast tumor in mice when dosed orally as monotherapy or in combination with paclitaxel. This work culminated in the discovery of a thioether sulfone hydroxamate (**36,** R = propargyl) having excellent efficacy in murine xenograft tumor models and antiangiogenesis assays and exhibited excellent potency for target enzymes and selectivity against MMP-1. The unsubstituted α-sulfone (**37**) maintained good inhibitory potency against MMP-13 (IC_{50} = 5 nM) and -2 (IC_{50} = 2.6 nM) and was selective against MMP-1 (IC_{50} = 6600 nM). It was, therefore, concluded that the α-sulfone hydroxamates could be developed as potent MMP inhibitors (Becker et al. 2001b; Barta et al. 2003). Consequently, Beckers et al. (2001a) prepared an α,α-dimethyl analog (**38**) that had nanomolar potency better that β-sulfones against MMP-13 and -2 (IC_{50} = 0.25 for MMP-13 and 0.1 for MMP-2).

34

35

36

37

38
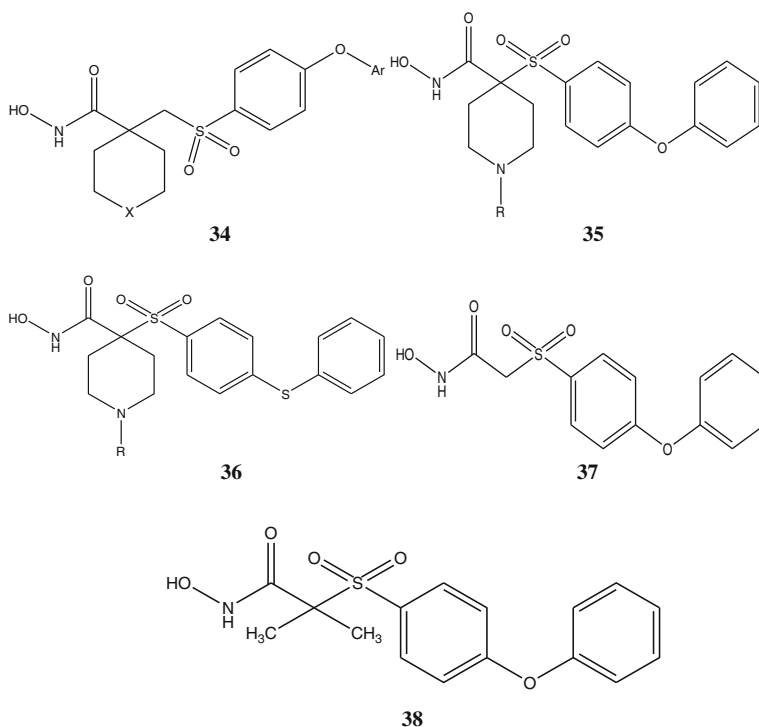
## 5.5 Sulfone N-Formylhydroxylamines (Retrohydroxamates)

An *N*-formylhydroxylamine (retrohydroxamate) **39** (ABT-770) was investigated by Curtin et al. (2001) to be a potent inhibitor with selectivity for inhibition of MMP-2 over MMP-1. It was moderately active against MMM-9. But in the next

communication, the same group of authors (Wada et al. 2002) reported that the replacement of the ether group of **39** by sulfone group led to a compound (**40**) which had substantially increased MMP-9 inhibition activity but with a loss of selectivity for inhibition of MMP-2 and -9 over MMP-1 and diminished oral exposure. Further, replacement of the biphenyl P1′ substituent in sulfone retro-hydroxamates with a phenoxyphenyl group provided compounds (**41**) that were highly selective for inhibition of MMP-2 and -9 over MMP-1. In this series, optimization of the substituent R adjacent to the retrohydroxamate center in this series led to a clinical candidate (**42**, ABT-518) which was found to be a highly potent, selective, and orally bioavailable MMP inhibitor that could significantly inhibit tumor growth in animal cancer models.


39   **40 (ABT-770)**

41   **42** (ABT-518)
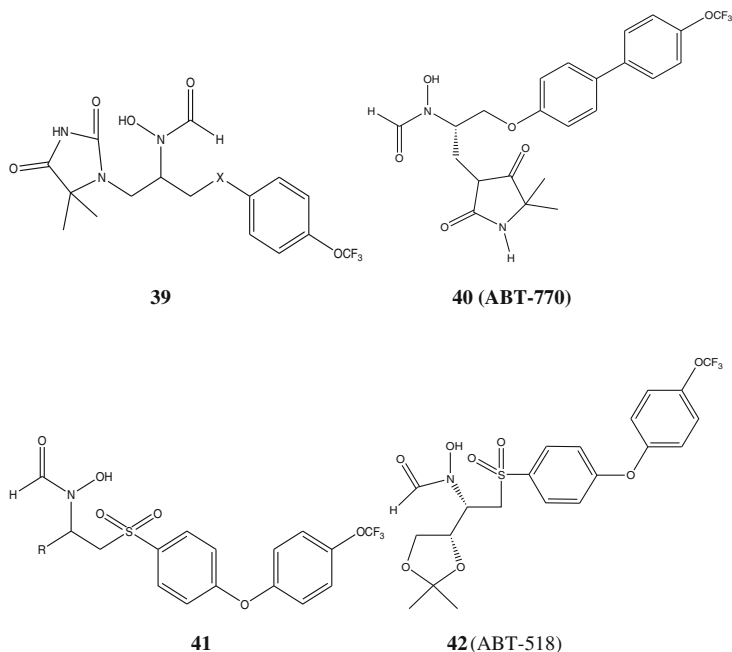
A small library of *N*-aryl piperazine α-sulfone hydroxamic acid derivatives was designed to explore the effect of substituent on the distal aryl rings of **43a** and **43b** (Kolodziej et al. 2010a). Compounds having *N*-aryl piperazine α-sulfone moiety failed to show any measurable potency for MMP-1 (IC$_{50}$ > 1000 nM) but had 1000 times MMP-13 selectivity over MMP-1. *N*-aryl piperazines (**44a** and **44b**) had nanomolar potency for MMP-13 and -2 but moderate selectivity for the former over the latter. Some of their derivatives were found equipotent. As compared to *ortho* and *meta* substituted derivatives of **46**, the *para*-substituted derivatives maintained high potency and selectivity for MMP-13.
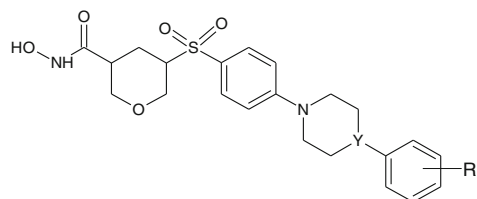
43a: Y = N;   **43b**: Y = CH
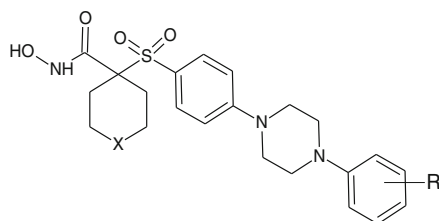
44a: X = O;   **44b**: X = N-*c*Pr

Kolodzeij et al. (2010b) derived another series of inhibitors (**45**) by varying the substituent at the aryl ring of **43b**. In order to boost the MMP-2 and -13 selectivity, they studied *para*-substituted analogs and found that the MMP-2 selectivity depended on the size of the substituent, with methoxy being optimal: H < Cl, OH < CH_3, CF_3 < OMe, OEt, and 4-F-C_6H_4. The decrease in affinity for MMP-13 was attributed to steric effects. The additional substituents like 2,3-(CH=CH)naphthyl, methyl, and methoxy showed increased MMP-2 potency and the *para*-substituted *N*-aryl piperazines showed superior MMP-13 potency.
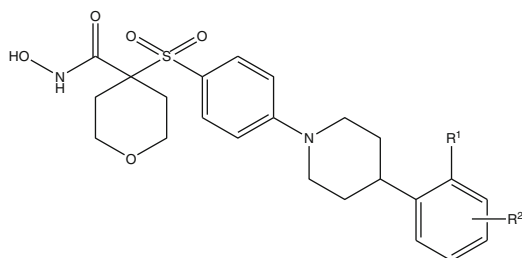

45

Some orally active and MMP-1 sparing α-tetrahydropyranyl (α-THP) sulfone hydroxamates, such as **46**, and several α-piperidine sulfone hydroxamates (**47**) were synthesized and found to be potent inhibitors of MMP-2, -9, and -13 by Becker et al. (2010) with oral efficacy in inhibiting tumor growth in mice and left-ventricular hypertrophy in rats and in the bovine cartilage degradation explant system. In most cases, the α-piperidines exhibited greater exposure than the α-THP analogs. An analog of **47** (R = methoxyethyl; SC-78080/SD-2590) was selected for development toward the initial indication of cancer, while its another analog

(R = cyclopropyl; SC-77964) and **46** (SC-77774) were identified as backup compounds.

46   **47**
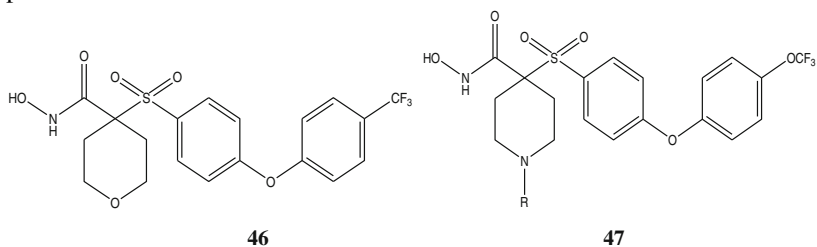
In *N*-arylsulfonyl-based MMPIs, the poor bioavailability is the major drawback for the development of this family of molecules. To enhance the water solubility, Attolino et al. (2010) applied a structure-based approach and performed structural analysis of **48** (NNGH) with MMP-12 to find that the *sec*-butyl residue was not directly involved in the binding with MMP. A new series of compounds (**49**) was then studied, where *sec*-butyl residue was replaced with hydroxamic acid moiety, to get water soluble potent inhibitors.

**48** (NNGH)   **49**
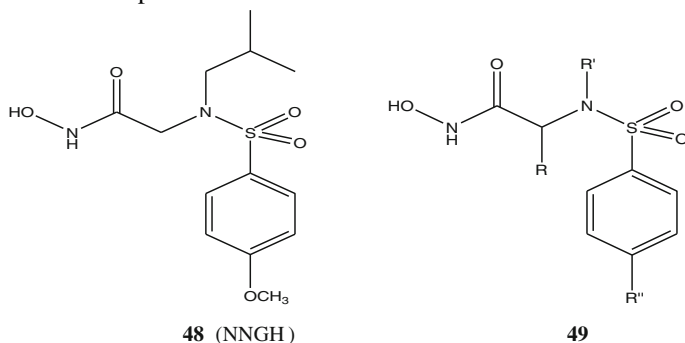
All the newly prepared analogs of **49** were evaluated, using NNGH as reference, against MMP-1, -7, -8, -9 -12, and -13 to find that all of them had low nanomolar K_i values for the MMPs tested except for MMP-1 and -7.

Analogs of **49** prepared with fluorine and biphenyl substituents instead of methoxy group to compliment the characteristic shape of the S1′ binding pocket were not found beneficial. The lack of favorable interactions of Arg214 with fluorine contributed toward the low affinity of the inhibitors and micromolar *Ki* value for MMP-1. A decrease in hydrophilicity of the compounds was found and thus the necessity of at least one hydroxyl group was felt.

5.6 N-Benzoyl Aminobutyric Acid Hydroxamates

Nakatani et al. (2006) studied a series of *N*-benzoyl 4-aminobutyric acid hydroxamate analogs (**50–54**) as inhibitors of MMP-1, -2, -3, and -9. Most of the compounds, like *N*-[4-(benzofuran-2-yl)benzoyl]-4-amino-4*S*-hydroxymethyl butyric acid hydroxamates, were found to be highly potent inhibitors of the gelatinases (MMP-2 and -9) as compared to the corresponding 2*S*- or 3*S*-hydroxy analogs.


50   **51**

52   **53**

54
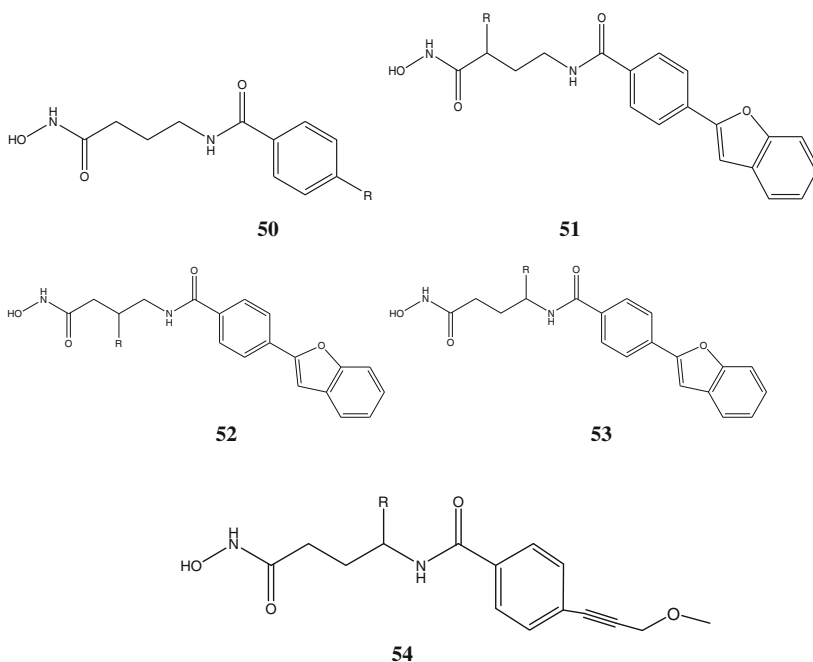
Ikura et al. (2006) performed chemical modification of the *N*-benzoyl residue of *N*-benzoyl γ-aminobutyric hydroxamic acids (**55**, **56**) by introducing electron-rich *para*-substituents and found it to be effective to increase the inhibitory activity of this class of MMPIs. Analogs having relatively more planar *N*-acyl residues demonstrated more potency. The three-dimensional arrangement of the two pharmacophores, hydroxamic acid and *N*-acyl residues, was optimized by chemical modifications of the γ-aminobutyric hydroxamic acid moiety (**50**) and this moiety was found as best spacer. All the compounds were evaluated for their inhibitory activity against MMP-1, -2, -3, and -9 and the *N*-benzoyl γ-aminobutyric hydroxamic acid was identified as a new chemical lead for MMP-2 and -9 inhibitions. Further chemical modification was focused on the 4-*N*-(4-methyl)benzoyl moiety, and a series of *N*-benzoyl γ-aminobutyric hydroxamic acids was prepared. As compared to 4-(*para*-alkylphenyl)benzoyl analogs, the 4-(*para*-substituted phenyl)benzoyl analogs were found to be stronger inhibitors. Introduction of electron-rich substituents (benzofuran-2-yl and *para*-chlorocinnamyl) at *para*-position of the *N*-benzoyl moiety was assumed to be

essential for strong activity. A secondary amide was found as a superior linkage compared to the ether or *N*-methyl amide with respect to the formation of hydrogen bonds with amino acid residues Pro238 and Leu181 in the S1′ pocket.

55   56
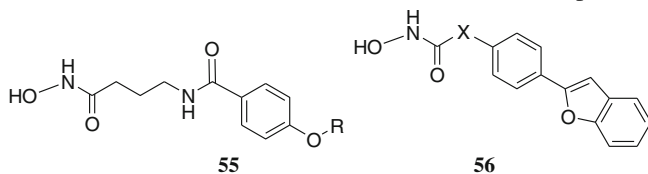
5.7 Aminoproline-Based Hydroxamates

A few series of hydroxamates (**57–60**) were reported as MMP inhibitors from an aminoproline scaffold by Natchus et al. (2000) where analogs of **57** were identified to have broad-spectrum activity with sub-nanomolar potency for some enzymes. Further modifications at the P1′ portion of this molecule with longer-chain aliphatic and aromatic substituents were found to affect both potency and selectivity within the MMP family. All compounds were assayed for the inhibition of MMP-1, -2, -3, -7, and -13.


57   58

59   60
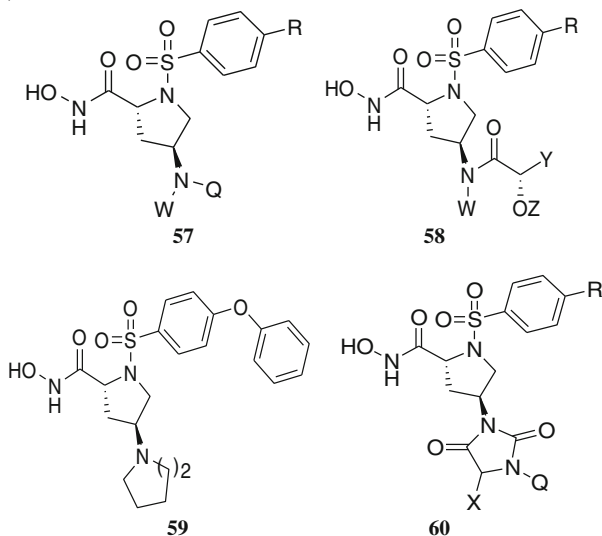
5.8 Aminopyrrolidine-Based Hydroxamates

A diverse family of aminopyrrolidine-based hydroxamate inhibitors were found to act as very potent inhibitors of MMP family with the exception of MMP-1 and -7 by Natchus et al. (2000). At the 4-position of the aromatic sulfonamides, long-

chain aliphatic groups were incorporated to enhance the selectivity against the shallow S1′ pocket of enzymes. The X-ray crystallography data of stromelysin-complex was used to explain the binding of aromatic sulfonamide structure into the S1′ pocket and the selectivity profile.

5.9 Phosphinamide/Phosphonamide-Based Hydroxamates

Pikul et al. (1999) studied some phosphinamide-based hydroxamates (**61**) where compounds having *R*-configuration at phosphorous were found to be potent inhibitors of MMP-1 and -3. The *S*-configuration was found inactive. A compound with $R_1 = CH_2CHMe_2$, $R_2 = CH_2Ph$, $R_3 = Me$, and $R_4 = Ph$ was found to be active against MMP-1 ($IC_{50} = 20.5$ nM) and MMP-3 ($IC_{50} = 24.4$ nM) where R_4-substituent could play key role in binding with S1′ pocket of the enzymes. The analysis of binding interactions indicated the involvement of Leu164, Ala165, Glu202, and Val163 residues of the enzymes.


61
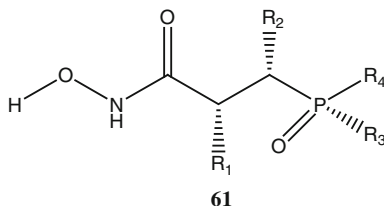
Some cyclophosphinamide- and cyclophosphonamide-based hydroxamates (**62**) were designed by altering the phosphorous substituent interacting with S1′ pocket and evaluated as potent MMPIs (Sorensen et al. 2003). The SAR conclusions were in accordance with those of Pikul et al. (1999) confirming the essential requirement of *R*-configuration of phosphorous atom and α-carbon. The 7-membered cyclophosphonamide and unsaturated 6-membered cyclophosphinamide hydroxamates were among the most potent inhibitors of MMP-1, -3, and -9. The proposed binding mode at MMP-3 has suggested interactions with Ala165, Leu164, Asn162, and Val163 as well as affinity of R_2-substituent toward S1′ pocket.


62
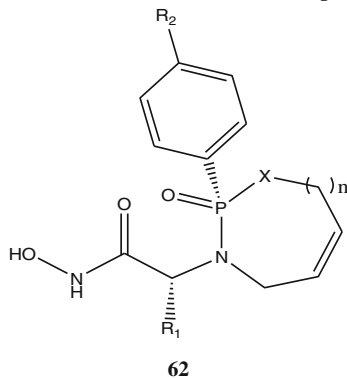
5.10 Non-Peptidyl Hydroxamates

A novel class of non-peptidyl hydroxamates, i.e., derivatives of *N*-aryl-iminodiacetic acid (IDA) (**63–65**) has been recently reported by Marques et al. (2006). To further improve the potency and selectivity versus MMP-2 and -13, some structural modifications were carried out to get new MMP-1/MMP-14-sparing hydroxamates inhibitors (Santos et al. 2006). As the specificity of MMP inhibition is correlated with the interactions at the S1′ pocket of the enzyme, the alkylaryl/ sulfonylaryl substituents were added at the nitrogen and the carboxylic moiety was replaced by an amide chain.

63   **64**
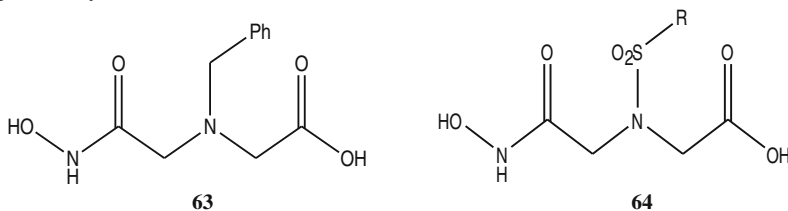
Among the sulfonamide analogs (**64**), the *para*-methoxybenzene, biphenyl, and *para*-phenoxybenzene showed good inhibitory potency against MMP-2, -7, -8, -9, -13, and -14. The *para*-phenoxybenzene analog was observed as most potent (IC$_{50}$ = 1–30 nM) and the order of activity was as: MMP-2 > MMP-13 > MMP-9 > MMP-8 > MMP-16 > MMP-14. The authors concluded that the lipophilic, electrostatic, and steric properties are liable toward MMPI potency and selectivity. Also the sulfonyl group at the nitrogen is important which permits its oxygen to form H–bonds with Leu164 and Ala165 (MMP-2) and directs the lipophilic groups in the S1′ pocket.

65
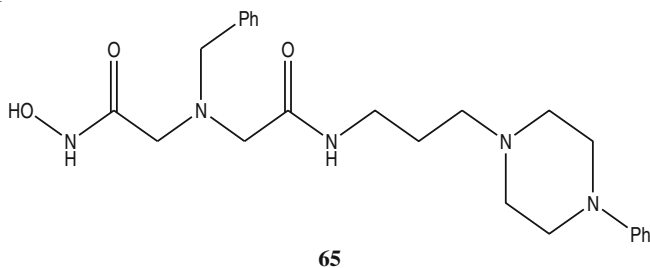
6 Conclusion

In conclusion, these SAR studies have indicated the following:

(1) The greatest potency with the MMP inhibitors can be associated with their ability to interact with S1, S1′, and S2′ subsites.

(2) S1′ differs most among the MMPs and a certain degree of specificity can be achieved by varying the P1′ residue of the inhibitors.

(3) Introduction of larger P1′ substituents generally gives greater specificity for MMP-2 and MMP-9.

(4) The P1′ substituent should preferably be a long side chain for the binding with MMP-2, MMP-3, and MMP-9.

In a recent article, Gupta and Patil (2012) have pointed out that the main subsites in MMPs for substrate recognition are the specificity pocket S1′ and, to a lesser extent, S2. The specificity pocket S1′ originates immediately to the right of catalytic Zn^{2+} ion and considerably differs in size and shape among the various MMPs. Due to this variation in size and shape, S1′ pocket offers selective inhibition of MMPs. The rough classification of S1′ specificity pockets according to the shape and size and the flexibility can aid in the development of selective MMP inhibitors. Because of the variation in the structure of S1′ pocket, modification of the P1′ can be used to introduce substrate specificity. The P1′–S1′ interaction is the main determinant for the affinity of inhibitors and the cleavage position of peptide substrates.

Several quantitative SARs (QSARs) on MMP inhibitors have been carried out. In a recent comprehensive review on QSAR studies on zinc-containing metalloproteinase inhibitors, Gupta (2007) concluded that in addition to binding with the catalytic Zn^{2+}, the MMP inhibitors may also have hydrophobic, steric, and electrostatic interactions with the enzymes that may provide them better potency. Verma and Hansch (2007) also came to the same conclusion from their QSAR studies on some series of hydroxamic acids acting as MMP inhibitors. Some molecular modeling studies have visualized these interactions (Matter et al. 1999; Matter and Schwab 1999; Tsai and Lin 2004). The SAR studies presented here also indicated these types of interactions between the inhibitors and various MMPs.

References

Andrews KL, Betsuyaku T, Rogers S, Shipley JM, Senior RM, Miner JH (2000) Gelatinase B (MMP-9) is not essential in the normal kidney and does not influence progression of renal disease in a mouse model of Alport syndrome. Am J Pathol 157:303–311

Aranapakam V, Davis JM, Grosu GT, Baker JL, Ellingboe J, Zask A, Levin JI, Sandanayaka VP, Du M, Skotnicki JS, Di Joseph JF, Sung A, Zhao W, McDevitt J, Xu ZB (2003a) Synthesis and structure-activity relationship of N-substituted 4-arylsulfonylpiperidine-4-hydroxamic acids as novel, orally active matrix metalloproteinase inhibitors for the treatment of osteoarthritis. J Med Chem 46:2376–2396

Aranapakam V, Grosu GT, Davis JM, Hu B, Ellingboe J, Baker JL, Skotnicki JS, Zask A, Di Joseph JF, Sung A, Sharr MA, Killar LM, Walter T, Jin G, Cowling R (2003b) Synthesis and structure-activity relationship of a-sulfonylhydroxamic acids as novel, orally active matrix metalloproteinase inhibitors for the treatment of osteoarthritis. J Med Chem 46:2361–2375

Attolino E, Calderone V, Dragoni E, Fragai M, Richichi B, Luchinat C, Nativi C (2010) Structure-based approach to nanomolar, water soluble matrix metalloproteinases inhibitors (MMPIs). Eur J Med Chem 45:5919–5925

Babine RE, Bender SL (1997) Molecular recognition of protein-ligand complexes: applications to drug design. Chem Rev 97:1359–1472

Barta TE, Becker DP, Boehm TL, DeCrescenzo GA, Villamil CI, McDonald JJ, Freskos JN, Getman DP (2003) Preparation of arylsulfonyl heterocyclyl hydroxamic acids and related compounds as matrix metalloproteases inhibitors. U.S. Patent 6, 541, 489, 2003. PCT Int. Appl. WO 9925687 A1 990527 CAN 131:18929; AN 1999:350651

Becker DP, Barta TE, Bedell L, DeCrescenzo G, Freskos J, Getman DP, Hockerman SL, Li M, Mehta P, Mischke B, Munie GE, Swearingen C, Villamil CI (2001a) α-amino-β-sulphone hydroxamates as potent MMP-13 inhibitors that spare MMP-1. Bioorg Med Chem Lett 11:2719–2722

Becker DP, Barta TE, Bedell LJ, Boehm TL, Bond BR, Carroll J, Carron CP, DeCrescenzo GA, Easton AM, Freskos JN, Funckes-Shippy CL, Heron M, Hockerman S, Howard CP, Kiefer JR, Li MH, Mathis KJ, McDonald JJ, Mehta PP, Munie GE, Sunyer T, Swearingen CA, Villamil CI, Welsch D, Williams JM, Yu Y, Yao J (2010) Orally active MMP-1 sparing α-tetrahydropyranyl and α–piperidinyl sulfone matrix metalloproteinase (MMP) inhibitors with efficacy in cancer, arthritis and cardiovascular disease. J Med Chem 53:6653–6680

Becker DP, DeCrescenzo G, Freskos J, Getman DP, Hockerman SL, Li M, Mehta P, Munie GE, Swearingen C (2001b) α-alkyl-α-amino-β-sulphone hydroxamates as potent MMP inhibitors that spare MMP-1. Bioorg Med Chem Lett 11:2723–2725

Becker DP, Villamil CI, Barta TE, Bedell LJ, Boehm TL, DeCrescenzo GA, Freskos JN, Getman DP, Hockerman S, Heintz R, Howard SC, Li MH, McDonald JJ, Carron CP, Funckes-Shippy CL, Mehta PP, Munie GE, Swearingen CA (2005) Synthesis and structure-activity relationships of β- and α-piperidine sulfone hydroxamic acid matrix metalloproteinase inhibitors with oral antitumor efficacy. J Med Chem 48:6713–6730

Bottomley KM, Johnson WH, Walter DS (1998) Matrix metalloproteinase inhibitors in arthritis. J Enzyme Inhib 13:79–101

Brown DA, Cuffe LP, Fitzpatrick NJ, Ryan AT (2004a) A DFT study of model complexes of zinc hydrolases and their inhibition by hydroxamic acids. Inorg Chem 43:297–302

Brown DA, Glass WK, Fitzpatrick NJ, Kemp TJ, Errington GJ, Haase W, Karsten F, Mahdy AH (2004b) Structural variations in dinuclear model hydrolases and hydroxamate inhibitor models: synthetic, spectroscopic and structural studies. Inorg Chim Acta 357:1411–1436

Chen D, Hackbarth C, Ni ZJ, Wu C, Wang W, Jain R, He Y, Bracken K, Weidmann B, Patel DV, Trias J, White RJ, Yuan Z (2004) Peptide deformylase inhibitors as antibacterial agents: identification of VRC3375, a proline-3-alkylsuccinyl hydroxamate derivative, by using an integrated combinatorial and medicinal chemistry approach. Antimicrob Agents Chemother 48:250–261

Cheng M, De B, Pikul S, Almstead NG, Natchus MG, Anastasio MV, McPhail SJ, Snider CE, Taiwo YO, Chen L, Dunaway CM, Gu F, Dowty ME, Mieling GE, Janusz MJ, Wang-Weigand S (2000) Design and synthesis of piperazine-based matrix metalloproteinase inhibitors. J Med Chem 43:369–380

Connolly PJ, Wetter SK, Beers KN, Hamel SC, Chen RH, Wachter MP, Ansell J, Singer MM, Steber M, Ritchie DM, Argentieri DC (1999) N-hydroxyurea and hydroxamic acid inhibitors of cyclooxygenase and 5-lipoxygenase. Bioorg Med Chem 9:979–984

Curtin ML, Florjancic AS, Heyman HR, Michaelides MR, Garland RB, Holms JH, Steinman DH, Dellaria JF, Gong J, Wada CK, Guo Y, Elmore IB, Tapang P, Albert DH, Magoc TJ, Marcotte PA, Bouska JJ, Goodfellow CL, Bauch JL, Marsh KC, Margon DW, Davidsen SK (2001) Discovery and characterization of the potent, selective and orally bioavailable MMP inhibitor ABT-770. Bioorg Med Chem Lett 11:1557–1560

Domingo JL (1998) Developmental toxicity of metal chelating agents. Reprod Toxicol 12:499–510

Dooley CM, Devocelle M, Mcloughlin B, Nolan KB, Fitzgerald DJ, Sharkey CT (2003) A novel family of hydroxamate-based acylating inhibitors of cyclooxygenase. Mol Pharmacol 63:450–455

El Yazal J, Pang Y-P (2000) Proton dissociation energies of zinc-coordinated hydroxamic acids and their relative affinities for zinc: insight into design of inhibitors of zinc-containing proteinases. J Phys Chem B 104:6499–6504

Fray MJ, Burslem MF, Dickinson RP (2001) Selectivity of inhibitors of matrix metalloproteinases MMP-3 and MMP-2 by succinyl hydroxamates and their carboxylic acid analogues is dependent on P3′ group chirality. Bioorg Med Chem Lett 11:567–570

Fray MJ, Dickinson RP (2001) Discovery of potent and selective succinyl hydroxamates inhibitors of matrix metalloproteinase-3 (stromelysin-1). Biorg Med Chem Lett 11:571–574

Gupta SP (2007) Quantitative structure-activity relationship studies on zinc-containing metalloproteinase inhibitors. Chem Rev 107:3042–3087

Gupta SP, Patil VM (2012) Specificity of binding with matrix metalloproteinases. In: Gupta SP (ed) Matrix metalloproteinase inhibitors: specificity of binding and structure-activity relationships. Springer, Basel, pp 35–56

Hannessian S, Bouzbouz S, Boudon A, Tucker GC, Peyroulan D (1999) Picking the S_1, S_1' and S_2' pockets of matrix metalloproteinases: a niche for potent acyclic sulfonamide inhibitors. Bioorg Med Chem Lett 9:1691–1696

Heath EI, Grochow LB (2000) Clinical potential of matrix metalloproteinase inhibitors in cancer therapy. Drugs 59:1043–1055

Hidalgo M, Eckhardt SG (2001) Matrix metalloproteinase inhibitors: how can we optimize their development? J Natl Cancer Inst 93:178–193

Igeta K, Tobetto K, Saiki I, Odake S, Fujisawa T, Matsuo T, Oku T (2000) PCT Int Appl, WO 00 03,703

Ikura M, Nakatani S, Yamamoto S, Habashita H, Sugiura T, Takahashi K, Ogawa K, Ohno H, Nakai H, Toda M (2006) Discovery of a new chemical lead for a matrix metalloproteinase inhibitor. Bioorg Med Chem 14:4241–4252

Jeng AY, Chou M, Parker DT (1998) Sulfonamide-based hydroxamic acids as potent inhibitors of mouse macrophage metalloelastase. Bioorg Med Chem Lett 8:897–902

Jeng AY, De Lombaert S (1997) Endothelin converting enzyme inhibitors. Curr Pharm Des 3:597–614

Johnson WH, Roberts NA, Borkakoti N (1987) Collagenase inhibitors: their design and potential therapeutic use. J Enzyme Inhib 2:1–22

Johnstone RW (2002) Histone-deacetylase inhibitors: novel drugs for the treatment of cancer. Nat Rev Drug Discov 1:287–299

Jung M (2001) Inhibitors of histone deacetylase as new anticancer agents. Curr Med Chem 8:1505–1511

Kelly WK, O'Connor OA, Marks PA (2002) Histone deacetylase inhibitors: from target to clinical trials. Expert Opin Investig Drugs 11:1695–1713

Kimura T, Tamakl K, Miyazaki S, Kurakata S, Fujiwara K (2001) PCT Int. Appl. WO 0123363, 5th Apr, 2001

Kolodziej SA, Hockerman SL, Boehm TL, Carroll JN, DeCrescenzo GA, McDonald JJ, Mischke DA, Munie GE, Fletcher TR, Rico JG, Stehle NW, Swearingen C, Becker DP (2010a) Orally bioavailable dual MMP-1/MMP-14 sparing, MMP-13 selective α-sulfone hydroxamates. Bioorg Med Chem Lett 20:3557–3560

Kolodziej SA, Hockerman SL, DeCrescenzo GA, McDonald JJ, Mischke DA, Munie GE, Fletcher TR, Stehle N, Swearingen C, Becker DP (2010b) MMP-13 selective isonipecotamide α-sulfone hydroxamates. Bioorg Med Chem Lett 20:3561–3564

Kontogiorgis CA, Papaioannou P, Hadjipavlou-Litina DJ (2005) Matrix metalloproteinase inhibitors: a review on pharmacophore mapping and (Q)SARs results. Curr Med Chem 12:339–355

Krumme D, Wenzel H, Tschesche H (1998) Hydroxamate derivatives of substrate-analogous peptides containing aminomalonic acid are potent inhibitors of matrix metalloproteinases. FEBS Lett 436:209–212

Leung D, Abbanate G, Fairlie DP (2000) Protease inhibitors: current status and future prospects. J Med Chem 43:305–341

Levin JI, Du MT, Di Joseph JF, Killar LM, Sung A, Walter T, Sharr MA, Roth CE, Moy FJ, Powers R, Jin G, Cowling R, Skotnicki JS (2001) The discovery of anthranilic acid-based MMP inhibitors. Part 1: SAR of the 3-position. Bioorg Med Chem Lett 11:235–238

Levin JI, Nelson FC, Delos SE, Du MT, MacEwan G, Chen JM, Ayral-Kaloustian S, Xu J, Jin G, Cummons T, Barone D (2004) Benzodiazeine inhibitors of the MMPs and TACE. Part 2. Bioorg Med Chem Lett 14:4147–4151

Lipczynska-Kochany E (1988) In some new aspects of hydroxamic acid chemistry. Pr Nauk-Politech Warsz Chem 46:3–98

Ma D, Wu W, Yang G, Li J, Ye Q (2004) Tetrahydroisoquinoline based sulfonamide hydroxamates as potent matrix metalloproteinase inhibitors. Bioorg Med Chem Lett 14:47–50

Marks PA, Richon VM, Rifkind RA (2000) Histone deacetylase inhibitors: inducers of differentiation or apoptosis of transformed cells. J Natl Cancer Inst 92:1210–1216

Marques SM, Chaves S, Rossello A, Tuccinardi T, Santos MA (2006) Metal ions in biology and medicine, vol 9. John Libbey Eurotext, Paris, pp 117–121

Matter H, Schwab W (1999) Affinity and selectivity of matrix metalloproteinase inhibitors: a chemometrical study from the perspective of ligands and proteins. J Med Chem 42:4506–4523

Matter H, Schwab W, Barbier D et al (1999) Quantitative structure-activity relationship of human neutrophil collagenase (MMP-8) inhibitors using comparative molecular field analysis and X-ray structure analysis. J Med Chem 42:1908–1920

Miller MJ (1989) Syntheses and therapeutic potential of hydroxamic acid based siderophores and analogues. Chem Rev 89:1563–1579

Mishra H, Parrill AL, Williamsom JS (2002) Three-dimensional quantitative structure-activity relationship and comparative molecular field analysis of dipeptide hydroxamic acid Helicobacter pylori urease inhibitors. Antimicrob Agents Chemother 46:2613–2618

Moore WM, Spilburg CA (1986a) Peptide hydroxamic acids inhibit skin collagenase. Biochem Biophys Res Commun 136:390–399

Moore WM, Spilburg CA (1986b) Purification of human collagenase with a hydroxamic acid affinity column. Biochemistry 25:5189–5195

Muri EM, Nieto MJ, Sindelar RD, Williamson JS (2002) Hydroxamic acids as pharmacological agents. Curr Med Chem 9:1631–1653

Nakatani S, Ikura M, Yamamoto S, Nishita Y, Itadani S, Habashita H, Sugiura T, Ogawa K, Ohno H, Takahashi K, Nakai H, Toda M (2006) Design and synthesis of novel metalloproteinase inhibitors. Bioorg Med Chem 14:5402–5422

Natchus MG, Bookland RG, De B, Almstead NG, Pikul S, Janusz MJ, Heitmeyer SA, Hookfin EB, Hsies LC, Dowty ME, Dietsch CR, Patel VS, Garver SM, Gu F, Pokross ME, Mieling GE, Baker TR, Foltz DJ, Peng SX, Bornes DM, Strojnowski MJ, Taiwo YO (2000) Development of new hydroxamates matrix metalloproteinase inhibitors derived from functionalized 4-aminoprolines. J Med Chem 43:4948–4963

Nishino N, Powers JC (1978) Peptide hydroxamic acids as inhibitors of thermolysin. Biochemistry 17:2846–2850

Noe MC, Snow SL, Wolf-Gouveia LA, Mitchell PG, Lopresti-Morrow L, Reeves LM, Yocum SA, Liras JL, Vaughn M (2004) 3-hydroxy-4-arylsulfonyltetra hydrohydropyranyl-3-hydroxamic acids are novel inhibitors of MMP-13 and aggrecanase. Bioorg Med Chem Lett 14:4727–4730

Nuti E, Casalini F, Avramova SI, Santamaria S, Cercignani G, Marinelli L, Pietra VL, Novellino E, Orlandini E, Nencetti S, Tuccinardi T, Martinelli A, Lim NH, Visse R, Nagase H, Rossello A (2009) N-O-isopropyl sulfonamide-based hydroxamates: design, synthesis and biological evaluation of selective matrix metalloproteinase-13 inhibitors as potential therapeutic agents for osteoarthritis. J Med Chem 52:4757–4773

Nuti E, Casalini F, Santamaria S, Gabelloni P, Bendinelli S, Pozzo ED, Costa B, Marinelli L, Pietra VL, Novellino E, Bernardo MM, Fridman R, Settimo FD, Martini C, Rossello A (2011) Synthesis and biological evaluation of U87MG glioma cells of (ethynylthiophene) sulfon-amide-based hydroxamates as matrix metalloproteinase inhibitors. Eur J Med Chem 46:2617–2629

Parvathy S, Hussain I, Karran EH, Turner AJ, Hooper NM (1998) Alzheimer's amyloid precursor protein alpha-secretase is inhibited by hydroxamic acid-based zinc metalloprotease inhibitors: similarities to the angiotensin converting enzyme secretase. Biochemistry 37:1680–1685

Pikul S, McDow Dunham KL, Almstead NG, De B, Natchus MG, Anastasio MV, McPhail SJ, Snider CE, Taiwo YO, Chen L, Dunaway CM, Gu F, Mieling CE (1999) Desgin and synthesis of phosphinamide-based hydroxamic acids as inhibitors of matrix metalloproteinases. J Med Chem 42:87–94

Robinson RP, Laird ER, Blake JF, Bordner J, Donahue KM, Lopresti-Morrow LL, Mitchell PG, Reese MR, Reeve LM, Stam EJ, Yocum SA (2000) Structure-based design and synthesis of a potent matrix metalloproteinase-13 inhibitor based on a pyrrolidinone scaffold. J Med Chem 43:2293–2296

Robinson RP, Laird ER, Donahue KM, Lopresti-Morrow LL, Mitchell PG, Reese MR, Reeves LM, Rouch AI, Stam EJ, Yocum SA (2001) Design and synthesis of 2-oxoo-imidazolidine-4-carboxylic acid hydroxamides as potent matrix metalloproteinase-13 inhibitors. J Med Chem 119:1211–1213

Roedern GE, Brandstetter H, Engh RA, Bode W, Grams F, Moroder L (1998) Bis-substituted malonic acid hydroxamates derivatives as inhibitors of human neutrophil collagenase. J Med Chem 41:3041–3047

Rossello A, Nuti E, Carelli P, Orlandini E, Macchia M, Nencetti S, Zandomeneghi M, Balzano F, Uccello BG, Albini A, Benelli R, Cercignani G, Murphy G, Balsamo A (2005a) N-i-propoxy-N-biphenylsulfonyl aminobutylhydroxamic acids as potent and selective inhibitors of MMP-2 and MT1-MMP. Bioorg Med Chem Lett 15:1321–1326

Rossello A, Nuti E, Catalani MP, Carelli P, Orlandini E, Rapposelli S, Tuccinardi T, Atkinson SJ, Murphyb G, Balsamoa A (2005b) A new development of matrix metalloproteinase inhibitors: twin hydroxamic acids as potent inhibitors of MMPs. Bioorg Med Chem Lett 15:2311–2314

Rossello A, Nuti E, Orlandini E, Carelli P, Rapposelli S, Macchia M, Minutolo F, Carbonaro L, Albini A, Benelli R, Cercignani G, Murphy G, Balsamo A (2004) New N-arylsulfonyl-N-alkoxyaminoacetohydroxamic acids as selective inhibitors of gelatinase A (MMP-2). Bioorg Med Chem 12:2441–2450

Salvino JM, Mathew R, Kiesow T, Narensingh R, Mason HJ, Dodd A, Groneberg R, Burns CJ, McGeehan G, Kline J, Orton E, Tang SY, Morrisette M, Labaudininiere R (2000) Solid-phase synthesis of an arylsulfone hydroxamate library. Bioorg Med Chem Lett 10:1637–1640

Santos MA, Marques SM, Tuccinardi T, Carelli P, Panelli L, Rossello A (2006) Design, synthesis and molecular modeling study of iminodiacetyl monohydroxamic acid derivatives as MMP inhibitors. Bioorg Med Chem 14:7539–7550

Shingledecker K, Jiang S, Paulus H (2000) Reactivity of the cysteine residues in the protein splicing active center of the *Mycobacterium tuberculosis* RecA intein. Arch Biochem Biophys 375:138–144

Shuttleworth S (1998) An overview of combinatorial chemistry and its applications to the identification of matrix metalloproteinase inhibitors (MMPIs). In: Harvey AL (ed.) Advances in drug discovery techniques. Wiley, New York, p 115

Sorensen MD, Blaehr LKA, Christensen MK, Hoyer T, Latini S, Hjaranaa PJV, Bjoekling F (2003) Cyclic phosphinamides and phosphonamides, novel series of potent matrix metalloproteinase inhibitors with antitumor activity. Bioorg Med Chem 11:5461–5484

Supuran CT, Scozzafava A (2002) Matrix Metalloproteinase (MMPs). In: Smith HJ, Simons C (eds.) Proteinase and peptidase inhibition: recent potential targets for drug development. Taylor and Francis, London, pp 35-61

Szekeres T, Fritzer-Szekeres M, Elford HL (1997) The enzyme ribonucleotide reductase: target for antitumor and anti-HIV therapy. Critical Rev Clin Lab Sci 34:503–528

Torres G (1995) Hydroxyurea, a potential new anti-HIV agent. GMHC Treat Issues 9:7–9

Tsai KC, Lin TH (2004) A ligand-based molecular modeling study on some matrix metalloproteinase-1 inhibitors using several 3D QSAR techniques. J Chem Inf Comput Sci 44:1857–1871

Tsukamoto K, Itakura H, Sato K, Fukuyama K, Miura S, Takahashi S, Ikezawa H, Hosoya T (1999) Binding of salicylhydroxamic acid and several aromatic donor molecules to *Arthromyces ramosus* peroxidase, investigated by X-ray crystallography, optical difference spectroscopy, NMR relaxation, molecular dynamics, and kinetics. Biochemistry 38:12558–12568

Tu G, Xu W, Huang H, Li S (2008) Progress in the development of matrix metalloproteinase inhibitors. Curr Med Chem 15:1388–1395

Valapour M, Gou J, Schroeder JT, Keen J, Cianferoni A, Casolaro V, Georas SN (2002) Histone deacetylation nhibits IL4 gene expression in T cells. J Allergy Clin Immunol 109:238–245

Venkatesan AM, Davis JM, Grosu GT, Baker J, Zask A, Levin JI, Ellingboe J, Skotnicki JS, Di Joseph JF, Sung A, Jin G, Xu W, McCarthy DJ, Barone D (2004) Synthesis and structure-activity relationships of 4-alkynyloxy phenyl sulfanyl sulfinyl and sulfonyl alkyl hydroxamates as tumor necrosis factor-α converting enzyme and matrix metalloproteinase inhibitors. J Med Chem 47:6255–6269

Verma RP, Hansch C (2007) Matrix metalloproteinases (MMPs): chemical-biological functions and (Q)SARs. Biorg Med Chem 15:2223–2268

Wada CK, Holms JH, Curtin ML, Dai Y, Florjancic AS, Garland RB, Guo Y, Heyman HR, Stacey JR, Steinman DH, Albert DH, Bouska JJ, Elmore IN, Goodfellow CL, Marcotte PA, Tapang P, Morgan DW, Michaelides MR, Davidsen SK (2002) Phenoxyphenyl sulfone N-formylhydroxylamines (retrohydroxamates) as potent, selective, orally bioavailable matrix metalloproteinase inhibitors. J Med Chem 45:219–232

Weisburger JH, Weisburger EK (1973) Formation and pharmacological, toxicological, and pathological properties of hydroxylamines and hydroxamic acids. Pharmacol Rev 25:1–66

Whittakar M (1998) Discovery of protease inhibitors using targeted libraries. Curr Opin Chem Biol 2:386–396

Whittaker M, Floyd CD, Brown P, Gearing JH (1999) Design and therapeutic application of matrix metalloproteinase inhibitors. Chem Rev 99:2735–2776

Yang SM, Scannevin RH, Wang B, Burke SL, Wilson LJ, Karnachi P, Rhodes KJ, Lagu B, Murray WV (2008) β-N-biaryl ether sulfonamide hydroxamates as potent gelatinase inhibitors: Part 1. Design, synthesis, and lead identification. Bioorg Med Chem Lett 18:1135–1139

Yao W, Wasserman ZR, Chao M, Reddy G, Shi E, Liu RQ, Covington MB, Arner EC, Pratta MA, Tortorella M, Magolda RL, Newton R, Qian M, Ribadeneira MD, Christ D, Wexler RR, Decicco CP (2001) Design and synthesis of a series of (2R)-N(4)-hydroxy-2-(3-hydroxyben-zyl)-N(1)-[(1S,2R)-2-hydroxy-2,3-dihydro-1H-inden-1-yl] butanediamide derivatives as potent, selective, and orally bioavailable aggrecanase inhibitors. J Med Chem 44:3347–3350

Zhang X, Gonnella NC, Koehn J, Pathak N, Ganu V, Melton R, Parker D, Hu SI, Nam KY (2000) Solution structure of the catalytic domain of human collagenase-3 (MMP-13) complexed to a potent non-peptidic sulfonamide inhibitor: binding comparison with stromelysin-1 and collagenase-1. J Mol Biol 301:513–524

Zhang Y, Li D, Houtman JC, Witiak DT, Seltzer J, Bertics PJ, Lauhon CT (1999) Design, combinatorial chemical synthesis and in vitro characterization of novel urea based gelatinase inhibitors. Bioorg Med Chem Lett 9:2823–2826

Hydroxamic Acids as Histone Deacetylase Inhibitors

Florian Thaler, Vaishali M. Patil and Satya P. Gupta

Abstract HDAC inhibition has been, for over a decade (and continues to remain), a highly competitive area. Hydroxamic acids represent the largest class of HDAC inhibitors. One product, SAHA is already approved and more than ten different chemical entities are in various clinical stages. A detailed discussion about compounds from various classes like phenyloxopropenyl, amidopropenyl analogues, spiropiperidines, biphenyl/arylamide/styrenyl, tetrahydroisoquinoline-based hydroxamic acid derivatives and *N*-hydroxyphenylacrylamide derivatives has been included along with the computational studies. It also covers brief details about the HDAC imaging agents. These successes as well as the enormous amount of experiences gained in preclinical and clinical studies may be useful—beyond the HDAC field—to future drug discovery programmes studying hydroxamic acid derivatives.

Keywords Chromatin · Nucleosome · Histone deacetylases · HDAC inhibitors · Oral bioavailability · Isoform selectivity

Abbreviations

AUC	Area under curve
B16	Murine melanoma cell line
Caco-2	Human epithelial colorectal adenocarcinoma cells
COLO205	Human colon cancer cell line
CTCL	Cutaneous T cell lymphoma

F. Thaler (✉)
Drug Discovery Unit, European Institute of Oncology, Via Adamello 16, 20139 Milan, MI, Italy
e-mail: florian.thaler@ieo.eu

V. M. Patil
School of Pharmacy, Bharat Institute of Technology, Meerut 250103, Uttar Pradesh, India

S. P. Gupta
Meerut Institute of Engineering and Technology, Meerut 250005, Uttar Pradesh, India

F	Dose-corrected area under curve (AUC) non-intravenous divided by AUC intravenous
HAT	Histone acetyltransferase
HCT116	Human colon cancer cell line
HDAC	Histone deacetylase
HDLP	Histone deacetylase-like protein
ip	Intraperitoneal
iv	Intravenous
K562	Chronic myelogenous leukaemia cell line
MM	Multiple myeloma
qd	Every day
PK	Pharmacokinetic
$t_{1/2}$	Half-life
T/C	Ratio mean relative tumour volume of the treated tumours/mean relative volume of control group
V_{ss}	Steady-state volume of distribution

Contents

1 Introduction

1.1 Chromatin

The eukaryotic genome is packaged with histone proteins to form the chromatin, which allows condensing of over a metre of DNA into the small volume of the nucleus. The fundamental repeating unit of the chromatin that occurs generally after every 157–240 base pairs is the nucleosome. The nucleosome core itself is composed of a histone octamer consisting of two copies of H2A, H2B, H3 and H4 histones around which 147 base pairs of DNA are wrapped in 1.65 turns of a flat, left-handed superhelix. The stabilisation of the nucleosome occurs through a series of protein–protein interactions within the histone octamer and by electrostatic and hydrogen bonds between the proteins and the DNA. The core histones are composed of two distinct functional domains: the "histone-fold" motif sufficient for both histone–histone and histone–DNA contacts within the nucleosome, and N and C-terminal tail domains, which remain mostly unresolved in the crystal structures (Luger et al. 1997; Davey et al. 2002). These tails extend away from nucleosomal DNA and are mainly involved in interaction with other nucleosomes or with nuclear factors (Luger and Richmond 1998).

The chromatin itself condenses to more compact structures. Short-range nucleosome–nucleosome interactions result in folded chromatin fibres ("secondary chromatin structure"). Long-range interactions between individual nucleosomes result in fibre–fibre interactions and form tertiary chromatin structures. However, these arrangements are not highly defined structural states. Rather, the current view is to consider them as a continuum of various inter-convertible states at different levels of condensation (Horn and Peterson 2002; Luger et al. 2012).

These structural states of the nucleosomes have obviously a major impact on any process requiring access to genomic DNA, such as transcription, replication and DNA repair. Not surprisingly, a plethora of studies has shown that the chromatin structure plays a crucial role in the regulation of all of these processes. These states and their variation are determined by various factors. The DNA sequence of each nucleosome is unique; and this unique DNA sequence affects the nucleosome structure through its sequence-encoded susceptibility for being distorted into the tight superhelical conformation imposed by the histone octamer. Histones are among the most highly conserved proteins in terms of sequence and structure. However, histone variants have been identified for the histone subtypes, in particular for histone H2A and H3. These variants have an influence on the structures of the nucleosomes (Malik and Henikoff 2003; Henikoff et al. 2004; Brown 2001). Furthermore, several proteins have been found interacting with the chromatin. This adds further complexity in the structural regulations. Posttranslational modifications have been one of the most intensively studied aspects as regulatory factors for structural changes of nucleosomes. Posttranslational modifications are small chemical modifications to amino acid side chains of a protein after its translation. The histone tails which account for almost 30 % of the core

histone sequences are, as already mentioned above, unstructured. Thus, they can be the subject of several posttranslational modifications, including acetylation, methylation, phosphorylation, sumoylation or ubiquitination.

1.2 The Histone Acetylase and Deacetylase Machinery

Already in 1964, Allfrey et al. first reported the isolation of acetylated and methylated histones and speculated well ahead on their time about their possible role in the regulation of RNA synthesis (Allfrey and Mirsky 1964; Allfrey et al. 1964). The authors hypothesised that these modifications of the histone structure, particularly acetylation, have an influence of RNA synthesis. Some years later, Riggs et al. (1977) found that the exposure of cultured cells to sodium *n*-butyrate caused a reversible accumulation of highly acetylated histones. However, the picture became clearer only during the early 1990s, when the first histone deacetylase (HDAC) was cloned in 1996 (Taunton et al. 1996). One year earlier, Kleff et al. (1995) had identified a gene encoding a yeast H4 acetyltransferase (HAT). Currently, a series of HATs and HDACs have been identified to be responsible for the tight control of the acetylation state of histones. HATs are enzymes which transfer an acetyl group from acetyl coenzyme A (acetyl CoA) onto to the ε-amino group of one or more lysine residues contained within the *N*-terminal tails of the histone proteins. The neutralisation of the basic charge of the tails reduces the electrostatic interactions with the DNA sequence leading to a nucleosome unwrapping (Simon et al. 2011). This relaxation of the chromatin conformation allows the transcriptional factors to access the gene promoter regions and the process of gene expression is facilitated. HATs can be classified into two different classes based on their functional localisation: the nuclear type A HATs and the cytoplasmic type B HATs. The latter ones are involved in the modification of newly synthesised histones before the assembly. Type A HATs can be further divided into five different classes based on structural and functional differences: GNAT, CBP/p300, transcriptional factors such as ATF2, nuclear hormone related (for example SRC4) and the MYST family proteins (Selvi and Kundu 2009; Grant and Berger 1999).

The counteracting histone deacetylases re-establish the positive charge in the *N*-terminus of the histone tails. This causes a tighter histone–DNA interaction and blocks the binding sites on promoters and thus inhibits gene transcription. The HDAC enzymes can be grouped into two families: the classical HDACs and the silent information regulator (Sir)-related protein (sirtuin) families. HDAC class III proteins (also known as sirtuins, Sirt1–Sirt7) form a structurally and mechanistically distinct class and are defined by their dependency on NAD^+ as cofactor. They catalyse the removal of the acetyl group of the acetylated lysines by transferring it to the ribose moiety of NAD^+ yielding *O*-acetyl-ADP-ribose and nicotinamide, which acts as a physiological inhibitor of the sirtuins by means of negative feedback (Huber and Superti-Furga 2011).

Classical HDACs are metalloenzymes harbouring a catalytic pocket with a Zn^{2+} ion. In humans, classical HDACs are grouped based on the homology to yeast enzymes in four distinct classes that vary in size and function (Grozinger et al. 1999; Gray and Ekstrom 2001; Lin et al. 2006; Ficner 2009). Class I HDACs, which comprise HDACs 1, 2, 3, and 8, share a certain degree of homology to the yeast Rpd3. These enzymes are generally nuclear proteins and are ubiquitously expressed in many human cell lines and tissues. HDAC11 is the sole member of Class IV HDACs and is found to be present in the nucleus. Class II HDACs, which are homologues to yeast Hda1, can be divided into two further sub-classes: class IIa (HDACs 4, 5, 7, 9) and class IIb HDACs (HDACs 6 and 10) (Verdin et al. 2003; Yang and Gregoire 2005). Class IIa HDACs contain a highly conserved C-terminal deacetylase domain with around 420 amino acids, and are homologous to yeast Hda1. However, their N-terminal domain, which has regulatory functions, does not show any similarity to HDACs in other classes. Class IIb HDACs have an additional deacetylase domain, although this duplication is partial in the case of HDAC10. Class II HDACs exhibit nucleocytoplasmic shuffling, suggesting their involvement in the deacetylation of non-histone substrates. For example, deacetylation of acetyl-α-tubulin is mediated by the second deacetylase domain of HDAC6 (L'Hernault and Rosenbaum 1985a, b; Hubbert et al. 2002; Haggarty et al. 2003). Recently, it has become clear that HDACs and not only the class II enzymes are involved in the deacetylation of a series of non-histone proteins (Glozak et al. 2005; Yang and Seto 2008; Singh et al. 2010; Yao and Yang 2011). Proteomic studies allowed to identify a remarkable amount of acetylation sites: Kim et al. (2006) found 388 acetylation sites on 195 proteins in HeLa cells and mouse liver mitochondria by immunoaffinity purification using an anti-acetyl lysine antibody; high-resolution mass spectrometry experiments permitted to identify even more impressive number of 3,600 lysine acetylation sites on 1,750 proteins (Choudhary et al. 2009). These results propose that acetylation/deacetylation is a regulatory modification that rivals phosphorylation in number of substrates (Kouzarides 2000; Choudhary et al. 2009). Furthermore, these acetylation sites were found on proteins involved in diverse cellular processes, such as chromatin remodelling, cell cycle, splicing, nuclear transport, signal transduction and apoptosis.

Several of these proteins were found to be relevant for tumorigenesis and cancer cell proliferation (Buchwald et al. 2009; Yao and Yang 2011). On the other hand, acetylation of histones results in changes of chromatin structures and this has an impact on any process requiring access to genomic DNA. Thus, it is not surprising that abnormal activities of HDACs and HATs have been found involved in the development of several diseases. Indeed, HDACs expression and their activity showed to be altered in many cancers. For example, HDACs are associated with the function of oncogenic-translocation products, such as PML-RARα in acute promyelocytic leukaemia. PML-RAR associate with a corepressor complex containing HDAC activity. This complex is able to inhibit the transcription of genes involved in haematopoietic differentiation, and thus contributing to the differentiation block found in this form of leukaemia (Grignani et al. 1998; Lin

**Table 1** Classification of hydroxamic acid-based HDAC inhibitors

Cap structure	Hydroxamic acid class
Absent	Short-chain fatty hydroxamic acids
Relatively small hydrophobic group	TSA
	Hybrid polar compounds: SAHA, Pyroxamide
	Benzamide-based HA
	Arylketones
	Amino acid-contains, benzamide-based HA
	Indole amide-based HA
	Aroyl-heterocyclic-based HA
	Aroyl-pentadienoic HA
	Aroyl-urea-based HA
	Sulfonamide-based HA: Oxamflatin, PXD101
	(Bi-)aryl-(heterocyclic)-based HA
	SK-7041, NVP-LAQ824
	A-161906
	Aroyl-pyrrole HA
Cyclic peptides	Cyclic hydroxamic acid-containing peptides
	Cyclic hexapeptides
Macro- or monocyclic succinimide	Succinimide-based HA
N- and C-substituted cysteine	Cysteine-based HA
1,3-dioxane	1,3-dioxanes: Tubacin

et al. 1998; Richon and O'Brien 2002). Subsequently, it has been shown that inhibition of HDACs resulted in a cell-cycle arrest and differentiation through an increased expression of p21WAF1/CIP1. Inhibition also affected tumour survival by blocking angiogenesis through the increased acetylation of HIF-1α and protein degradation through the acetylation of Hsp90. These findings have made HDACs as attractive targets for cancer therapy (Federico and Bagella 2011; Mercurio et al. 2010). The diverse mechanisms through which HDAC inhibitors exert their cytotoxic activity include induction of apoptosis by both intrinsic and extrinsic pathways, selective expression of repressed genes, cell-cycle arrest, DNA damage and repair, inhibition of angiogenesis, cell death due to accumulation of reactive oxygen species (ROS), autophagy and immunomodulatory effects (Bolden et al. 2006).

During the last 20 years, a variety of HDAC inhibitors have been developed based on the structures of the naturally occurring inhibitors, or discovered randomly in HDAC screening assays. The currently available HDAC inhibitors can be classified according to the nature of the metal binding group into different categories, i.e. hydroxamic acid-based, carboxylic acid-based, disulfide-based, epoxide-based, and anilide-based inhibitors. The hydroxamic acid-based HDAC inhibitors can be sub-classified according to the nature of cap structure (Table 1) (Elaut et al. 2007) or broadly classified as small-capped and large-capped hydroxamic acid-based inhibitors.

2 Histone Deacetylase Inhibitors: From *n*-Butyrate to SAHA

The first example of HDAC inhibition was reported in 1977. Riggs et al. (1977) found an accumulation of acetylated histones in the presence of sodium *n*-butyrate (Fig. 1). It was then questioned, if the accumulation of highly acetylated histones caused by this carboxylic acid was really linked to the observed induced differentiation in tumoral HeLa and Friend erythroleukemia cells. It took some years until Yoshida et al. (1987) found that Trichostatin A (TSA) (Fig. 1), a hydroxamic acid derivative originally found as fungistatic antibiotic (Tsuji et al. 1976), caused induction of Friend leukaemia cell differentiation at low nanomolar concentration. Three years later, the same authors disclosed that the (*R*) isomer of TSA was able to cause an accumulation of highly acetylated histones in vivo and to inhibit the activity of the partially purified histone deacetylase in vitro. The (*S*) isomer as well as the trichostatic acid did not show inhibitory activity and had no effect on the induction of Friend cell differentiation and the inhibition of the cell-cycle progression (Yoshida et al. 1990a). Furthermore, (*R*)-TSA was found to exhibit a significant lower inhibitory activity in a tumour cell line containing mutated histone deacetylases. These important observations provided the first evidence that the effect of TSA on cell proliferation and differentiation was directly related to the inhibition of histone deacetylases (Yoshida et al. 1987, 1990b). After 16 years later, suberoylanilide hydroxamic acid (SAHA) (Fig. 1) gained approval by FDA as the first HDAC inhibitor to be used for the treatment of cutaneous T cell lymphoma (CTCL) (Marks 2007; Marks and Breslow 2007). SAHA, disclosed in 1993 (Breslow et al. 1993), was the result of two decades of research activities carried out at the Columbia University and the Memorial-Sloan Kettering Cancer Center. In the early 1970s, Friend et al. (1971) found that DMSO acted as differentiating agent—murine erythroleukemia cells (MELC) after being placed in
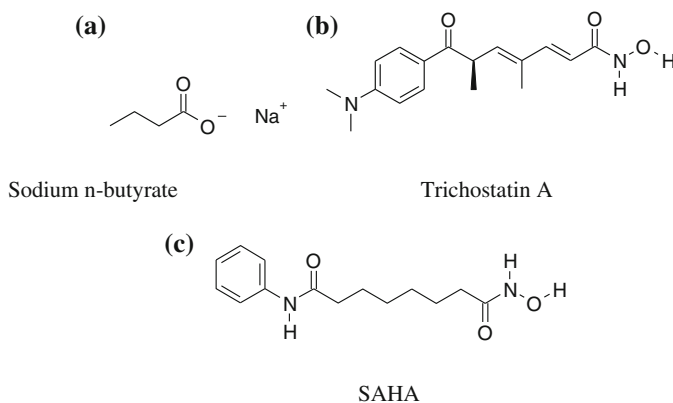
Fig. 1 Chemical structures of Sodium *n*-butyrate (**a**), Trichostatin A (**b**), and SAHA (**c**)

culture with dimethylsulfoxide turned red, suggesting the presence of haemoglobin. The search for new derivatives able to induce cytodifferentiation and growth arrest resulted in the discovery of polar solvent species, such as *N*-methylformamide or acetamide (Tanaka et al. 1975). While these compounds showed only a slight increase of activity compared to DMSO, dimeric amides proved to be much more potent. They were able to induce differentiation at low millimolar concentrations (Reuben et al. 1976, 1978). One example of this series, hexamethylene bisacetamide (HMBA), was selected for clinical studies. The trials showed that the compound was able to induce minor and partial remission in myelodysplastic syndrome and acute myelogenous leukaemia. However, the remission resulted to be transient and the doses required were not tolerated by cancer patients (Andreeff et al. 1992). Even though the biological target of these compounds was not identified, it was hypothesised that the dimeric amide structures may possibly act as chelating agents of metal ions. Exploration of new chemical entities led to the discovery of hydroxamic acids as well as bishydroxamates (Breslow et al. 1991; Richon et al. 1996). One example, SAHA, (but also other hydroxamic acid derivatives), was approximately 2,000-fold more potent than HMBA and was able to induce differentiation in MELC cells at low micromolar concentrations. Richon et al. (1998) confirmed that SAHA, like TSA, showed an HDAC inhibitory activity and caused accumulation of hyperacetylated histone H4 in cultured cells. One year later, the X-ray crystallographic structures of SAHA and TSA bound to the *Aquifex aeolicus* HDAC homologue histone deacetylase-like protein (HDLP) revealed that the hydroxamic acid moiety of both compounds is doubly coordinated to a zinc atom at the bottom of a cavity (Finnin et al. 1999). In 2000, SAHA entered clinical studies and, after intravenous and the oral administration, showed a good safety profile and antitumor activity in different malignancies, in particular haematological malignancies (Kelly et al. 2003, 2005). Finally, in October 2006, FDA approved the compound as first HDAC inhibitor for the treatment of CTCL, after that a significant response rate in prior therapy-resistant CTCL patients was observed (Mann et al. 2007).

3 Histone Deacetylase Inhibitors: Orally Available Hydroxamic Acid Derivatives

While SAHA showed a considerable efficacy in different haematological malignancies in clinical trials, patient response in other cancers remained much more uncertain and often rather limited (Graham et al. 2009; Mercurio et al. 2010). SAHA had demonstrated some activity in patients with advanced solid tumours in phase I trials. However, phase II studies in patients with breast, colorectal or non-small cell lung cancer showed a limited drug exposure, which did not allow a reliable efficacy analysis (Vansteenkiste et al. 2008). SAHA was well tolerated, but exhibited only medium potency (Marks and Breslow 2007) and was cleared

rapidly (Kelly et al. 2003). Short half-lives in vitro as well as in vivo are quite common to several first generation hydroxamic acid inhibitors (Elaut et al. 2007), and thus hydroxamates are often considered as poor drugs. They are frequently down prioritised in drug discovery programmes because of their poor physico-chemical and ADME properties, despite their good in vitro potency (Elaut et al. 2007; Flipo et al. 2009).

However, the overall impressive in vitro and in vivo data of the first drugs made HDACs and their inhibition an attractive target for several drug discovery pro-grammes. Research efforts were directed to highly potent compounds with a prolonged in vivo exposure and generally a better pharmacokinetic (PK) profile. In fact, we can find a significant number of research groups, both from industry and academia, involved in the exploration of novel chemical entities with HDAC inhibitory properties. Almost 400 PCT patent applications claiming new HDAC inhibiting agents is just one indicator of the impressive amount of efforts done in this field during the last decade. It is noticeable that more than 50 % of the applications are related to hydroxamic acid derivatives (Thaler 2012). Another sign is that the significant number of molecules have entered clinical studies. Around 20 chemical entities, either alone or in combination, have entered clinical studies for the treatment of several diseases, mainly tumours. Among them there is a considerable amount of hydroxamic acid derivatives e.g. LBH589 or panobi-nostat (Novartis) (Atadja 2009; Neri et al. 2012), and PXD101 or belinostat (Topotarget) (Steele et al. 2008) are currently in phase III studies, ITF-2357 or givinostat (Italfarmaco) (Rambaldi et al. 2012), PCI-24781 or abexinostat (Servier, Pharmacyclics) (Buggy et al. 2006), SB939 or pracinostat (S*BIO Pte Ltd) (Novotny-Diermayr et al. 2010; Wang et al. 2011), JNJ-26481585 or quisinostat (Johnson & Johnson) (Arts et al. 2009; Tong et al. 2010) and 4SC-201 or res-minostat (4SC) (Mandl-Weber et al. 2010; Brunetto et al. 2009) have reached clinical phase II (Fig. 2). Examples in phase I can be given as AR-42 or OSU-HDAC-42 (Arno Therapeutics) (Kulp et al. 2006; Lu et al. 2005), CG-200745 (CrystalGenomics Inc) (Hwang et al. 2012), CHR-3996 (Chroma Therapeutics) (Donald et al. 2010; Banerji et al. 2010), the HDAC6 selective ACY-1215 (Acetylon Pharmaceuticals Inc) (Santo et al. 2012) and the dual kinase and HDAC inhibitor CUDC-101 (Curis and Ligand Pharmaceuticals) (Cai et al. 2010; Lai et al. 2010; Shimizu et al. 2010) (Fig. 3).

In the following sections, the research efforts directed towards the development of hydroxamic acid derivatives with improved PK properties are discussed.

3.1 From SB639 to Pracinostat

Scientists from the Singaporean biotech company S*Bio Pte explored different fused heterocyclic rings such as benzimidazoles as new linkers for low molecular weight HDAC inhibiting agents. This research led to the discovery of the first lead compound, SB639 (Fig. 4) (Wang et al. 2009). The compound showed good
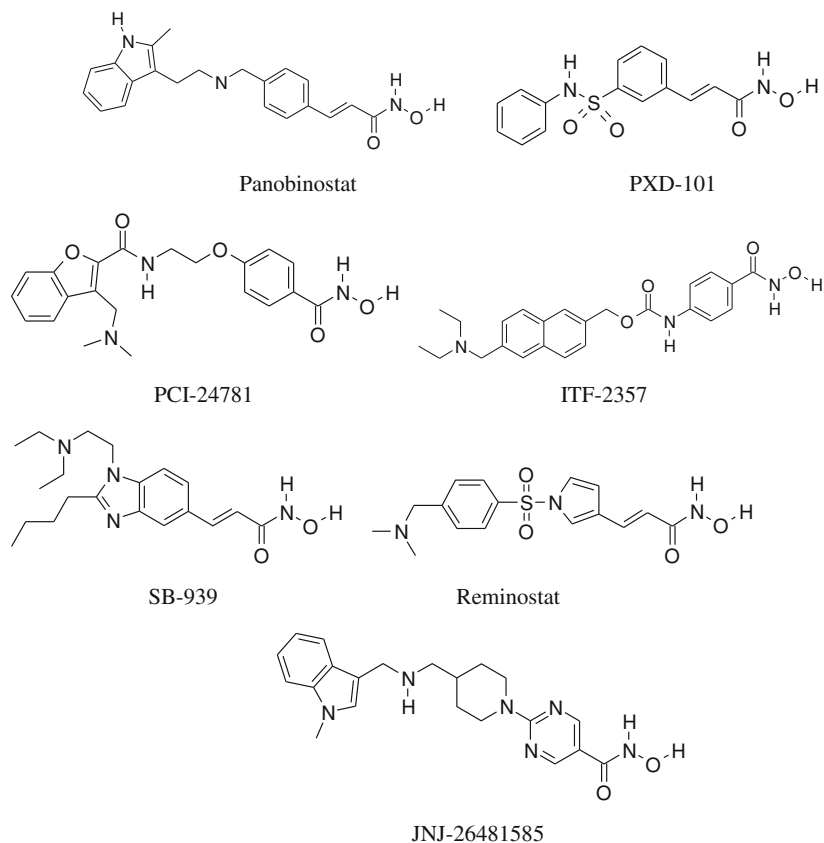
Fig. 2 HDAC inhibitors in phase II and Phase III clinical trials

in vitro potency with an IC$_{50}$ value of 0.035 ± 0.016 μM against HDAC1 and antiproliferative activity against the human colon cancer cell line COLO205 in the submicromolar range (IC$_{50}$ = 0.14 ± 0.05 μM). The compound was stable in human and dog liver microsomes with a half-life of around 1 h. However, the half-life dropped in rat and mouse microsomes to 6 and 3 min, respectively. The compound showed high clearance rates in mice (15.8 L/h/kg) and in rats (3.84 L/h/kg). The oral bioavailability was 13 % (mice) and 10.5 % (rats), respectively (Venkatesh et al. 2007). Nevertheless, the plasma concentration of the compound reached levels above the HDAC IC$_{50}$ value and the compound showed antitumor activity in HCT116 tumour-bearing nude mice after oral administration (Wang et al. 2009).

Metabolic profiling experiments in rat liver hepatocytes showed that the major metabolic paths of SB639 were the oxidation of the pyrrolidinylethyl group and the reduction of the hydroxamic acid to amide (Wang et al. 2011). Further development of this series was carried out considering particularly the metabolic stability of the compounds. This expansion resulted in several compounds. Among

ACY-1215

CUDC-101

(S)-Ar-42

CG200745

CHR-3996
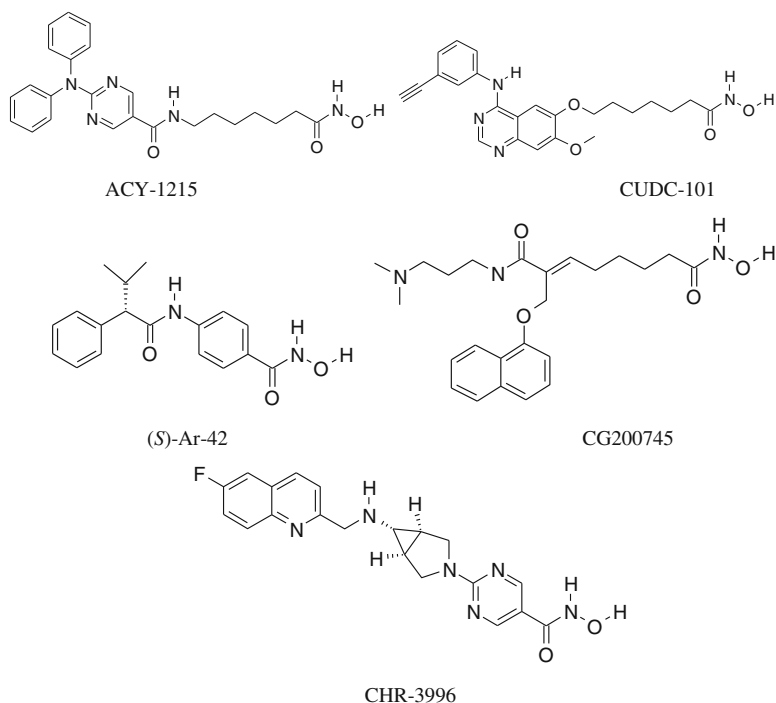
Fig. 3 HDAC inhibitors currently in phase I clinical trials

them, compound SB939 (Fig. 4) was found to be potent against HDAC1 with an IC_{50} value of 0.077 ± 0.014 µM and showed antiproliferative activity against a series of cancer cell lines in the submicromolar range. For example, the compound with an IC_{50} of 0.48 ± 0.27 µM was around six times more active than SAHA ($IC_{50} = 2.85 \pm 0.27$ µM) against HCT116 cells. An interesting observation was that the microsomal liability in human and mouse microsomes generally increased with higher lipophilicity of the molecules. SB939 as well as several other derivatives were relatively stable in human and dog microsomes. On the other hand, a major variability was found in rodents. Consistent with the in vitro microsomal data, SB939 exhibited an oral bioavailability of 65, 34 and 3.1 % in beagle dogs,

(a)

(b)
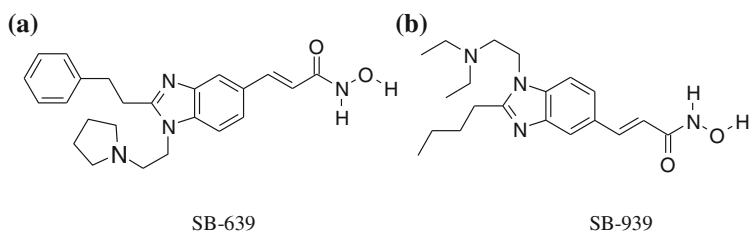
SB-639

SB-939

Fig. 4 Structures of **a** SB-639 and **b** SB-939

nude mice and Wistar rats, respectively. Furthermore, the compound had high
systemic clearance (relative to liver blood flow) of 1.5, 9.2 and 4.5 L/h/kg and high
volume of distribution at steady state of 4.2, 3.5 and 1.7 l/kg in dog, mouse and rat,
respectively (Jayaraman et al. 2011). The superior in vitro activities and PK
properties compared to SAHA translated into a higher antitumor efficacy in a
HCT116 tumour xenograft model. SB939 was approximately twice as efficacious
at the maximum tolerated dose as SAHA: the tumour growth inhibition for SAHA
was 48 % at 200 mg/kg compared to 94 % for SB939 at 100 mg/kg. In addition,
an accumulation of the compound was observed in tumour tissues (Novotny-
Diermayr et al. 2010). This was not found after administering the reference of
SAHA. In addition, SB939 has good aqueous solubility and high permeability in
human Caco-2 cells with low efflux. These characteristics are indicative of a high-
intestinal absorption in vivo (Jayaraman et al. 2011). In fact, phase I studies con-
ducted in patients with advanced solid malignancies showed that the pharmaco-
logically active concentrations were achieved already at the lowest dose of 10 mg
(Jayaraman et al. 2011). The drug was rapidly absorbed (t_{max} = 1–3 h). The mean
elimination half-life was around 7 h and oral clearance was 53 $\pm$ 8.5 L/h. C_{max} and
AUC were dose proportional between 10 and 60 mg doses. Furthermore, no
substantial accumulation of SB939 on day 15 following repeated dosing was found.
At the 60 mg dose high acetylation levels was found in all patients indicating
sustained target inhibition. Two patients experienced prolonged disease stabilisa-
tion (Yong et al. 2009). An interesting aspect is that the human PK was successfully
predicted based on the in vitro ADME data using an ADME simulator and
allometric scaling (Jayaraman et al. 2011).

3.2 CHR-3996

The HDAC project at the British biotech company, Chroma Therapeutics, was
focused on the synthesis of pyrimidine hydroxamate derivatives bound to bicyclic
hexahydropyrrolo[3,4-c]pyrrole and azabicyclo[3,1,0]hexane linkers (Moffat et al.
2010). The inhibitory activities of around 25 described azabicyclo[3,1,0]hexanes
varied only slightly and were in the low nanomolar range against HDACs from
nuclear HeLa extracts. This narrow range in activity despite substantial variations
of the linker structures is not uncommon; for example, as already described above,
a similar behaviour was experienced in house for several examples within the
amidopropenyl and the spiropiperidine series (cf. Sects. 3.4 and 3.5). The

Fig. 5 Structure of CHR-
3996
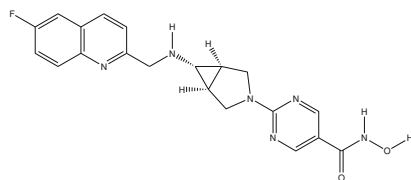
compounds showed good antiproliferative activity in tumoral HCT116 cells with GI_{50} values in the micro- or submicromolar range. In particular, it was found that diminishing the polar surface area was beneficial for the cell growth inhibition. PK studies using oral cassette dosing allowed identifying CHR-3996 as one lead compound (Fig. 5). The compound was potent against HDACs 1, 2 and 3 with IC_{50} values of 3, 4 and 7 nM, respectively. On the other hand, it was significantly less active against the class II members HDACs 5 and 6. CHR-3996 showed good oral bioavailability in rat and dog of 27 and 40 %, respectively. Furthermore, the compound exhibited high systemic clearance (relative to liver blood flow) of 4.2 (dog) and 8.0 L/h/kg (rat), respectively. In vivo HCT116 xenograft experiments showed that the compound had a significant antitumor activity: administration of 50 mg/kg once daily orally resulted in almost complete inhibition of the tumour. CHR-3996 advanced into clinical studies. Phase I clinical studies showed that the compound was rapidly absorbed, had a mean elimination plasma half-life of 3 h and mean AUC values exceeding the levels effective in xenograft studies at doses ≥40 mg. Five patients demonstrated stable disease for at least two cycles (Banerji et al. 2010, 2012).

3.3 Phenylhydroxamic Acid Derivatives (AR-42)

The phenylhydroxamic acid derivative AR-42 (known also as OSU-HDAC-42 or (*S*)-HDAC-42) (Fig. 6) was originated at the Ohio State University. The compound resulted from an exploration of new HDAC inhibitors composed of short-chain fatty acids linked to a hydroxamic acid group as Zn^{2+}-chelating motif (Lu et al. 2005). The compound showed good HDAC inhibitory potency with an IC_{50} value of 16 nM and was around five times more potent than its corresponding *R*-isomer. Antiproliferative activities in three myeloma cell lines, IM-9, RPMI-8226 and U266, were in the submicromolar range. The compound was around four to seven times more active than SAHA (Bai et al. 2011). This good potency, but even more its pharamacokinetic behaviour in rodents, has made the compound an attractive agent for further studies. Indeed, Ar-42 displayed a good oral bioavailability in rats (Cheng et al. 2006a) and in mice (Cheng et al. 2006b): the oral bioavailability was ∼ 100 % in rats and 27.4 % in mice. Total body clearance was 1.40 L/h/kg (rats) and 1.47 L/h/kg (mice). The good in vitro potency as well as the PK profile translated in good antitumor activity in different in vivo efficacy models. For example, the compound administered 25 mg/kg daily and 50 mg/kg

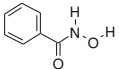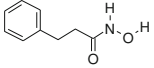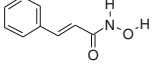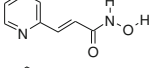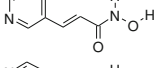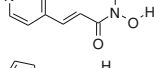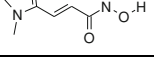**Fig. 6** Structure of (*S*)-Ar-42
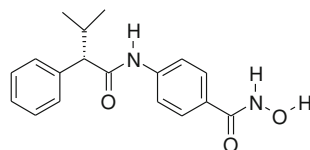
every other day significantly inhibited tumour growth in mouse PC-3 tumour xenografts by 52 and 67 %, respectively (Kulp et al. 2006). The compound was licensed to Arno Therapeutics, which is currently conducting phase I/IIa trials in adult patients with relapsed or recurrent haematological malignancies and solid tumours (http://clinicaltrials.gov/ct2/show/NCT01129193?term=AR-42&rank=1).

3.4 Phenyloxopropenyl and Amidopropenyl Analogues

The HDAC inhibitory programme in DAC was initiated in collaboration with Antonello Mai from the University of Rome, who had intensively studied aroyl-pyrrolyl hydroxyamides (APHAs) as histone deacetylase inhibitors (Massa et al. 2001; Mai et al. 2005a, b, 2006) and identified several class II selective compounds. It is noticeable that these research efforts have origins in programmes carried out by the same group in the late 1980s, when pyrrole-containing analogues of trichostatin were explored for their antifungal, antibacterial and antiviral activities (Massa et al. 1990) but ended with HDAC inhibitory (Massa et al. 2001) activity.

A small library of aryl- and heteroaryl-hydroxamic acid fragments was designed and subjected for biological characterisation (Thaler et al. 2010a). The HDAC inhibitory activity was performed using HeLa nuclear extract as enzyme source and the percentage of inhibition of the enzymes was assessed at 0.1, 1.0 and 10 μM concentration of the inhibitors. As shown in Table 2, the phenyl hydroxamate (**1**) was almost inactive under the experimental conditions, whereas **2**

Table 2 HDAC inhibitory activity of a fragment library

| Compounds	Structure	Percentage of inhibition at		
		0.1 (μM)	1 (μM)	10 (μM)
1		0	1	19
2		0	36	89
3		18	55	93
4		34	82	100
5		13	75	96
6		0	34	87
7		9	13	53

Table 3 HDAC enzyme, antiproliferative activity, and microsomal stability data of the phenyloxopropenyl series
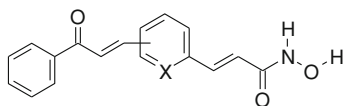
Compound	X	Position	Enzyme (μM)	K562 (μM)	Microsomes	
					Mouse (%)	Human (%)
8	CH	5	1.48	2.28	2	5
9	N	4	0.323	1.06	14	16
10	N	5	0.022	0.69	6	14
11	CH	6	0.085	3.21	6	9
12	N	6	0.020	0.51	11	38

was moderately active with 36 % enzyme inhibition at 1 μM. Introduction of an acrylic group (**3**) led to a further increase in activity. Within the pyridine-acryl-hydroxamic acid series, the pyridine-2-yl derivative (**4**) demonstrated to be the most potent compound and the activity decreased from the pyridine-2-yl to the pyridine-4-yl analogue (**6**). The electron-rich pyrrolyl derivative (**7**), present in the APHA series, was less potent than the other acryl hydroxamates.

The heteroaryl-hydroxamate **4** and the phenylacryl-hydroxamate **3** were selected for further expansion. In the first step, a scaffold with a phenyloxopropenyl moiety (Mai et al. 2005a) positioned in *meta* or *para* position with respect to the acrylhydroxamate substituent was prepared. The *meta* phenyl analogue **11** (Table 3), with an IC$_{50}$ value of 0.085 μM, was almost 20 times more potent than the corresponding *para* derivative **8** (IC$_{50}$ = 1.48 μM). A slightly different behaviour was found in the pyridinyl series: the 2,5 di-substituted derivative **10** and the 2,6 di-substituted analogue **12** exhibited similar IC$_{50}$ value ($\sim$0.02 μM) and were around 15 times more active than the 2,4-substituted derivative **9**. Further, the compounds and in particular the pyridinyl derivatives showed good antiproliferative effects in the chronic myelogenous leukaemia cell line K562. In specific, the cellular IC$_{50}$ values for **10**, **12** and **9** ranged between 0.5 and 1 μM. The phenylacrylates **8** and **11** exhibited IC$_{50}$ values of 2.3–3.2 μM, respectively.

The good biochemical and cellular inhibitory activity of this series, however, was compromised with an overall low metabolic stability in microsomes. It was observed that the compounds were almost completely degraded in mouse microsomes after 30 min incubation: the percentage of the recovery ranged from just 2 % (**8**) to 14 % (**9**) (Table 3). Similar data were obtained in human microsome preparations with the exception of compound **12**, which was more stable than the other examples. Metabolic profiling experiments of **8** in mouse microsomes showed that the major sites of metabolism were the hydroxamic acid moiety and the unsaturated ketone (Thaler et al. 2009). While the major metabolite of the hydroxamic acid moiety was the acrylic acid (**8a**), α,β-unsaturated ketone was either reduced to the corresponding alcohol (**8b**) or to the saturated ketone derivative (**8c**) (Fig. 7).
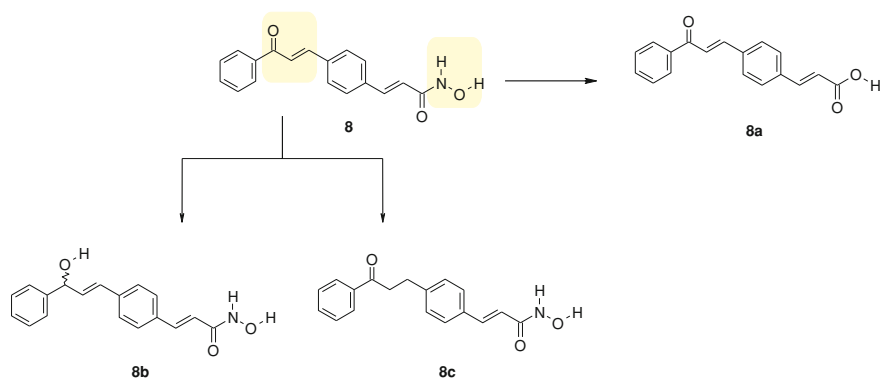
Fig. 7 Metabolic profiling of compound **8** in mouse microsomes

A similar outcome was found for the pyridine derivative **9**. Since the hy-droxamic acid was essential for the biological activity, research efforts were directed towards new chemical entities devoid of the metabolically unstable α,β-unsaturated ketone. One approach was the replacement of the phenyl by 4-phe-nylpiperazine group (Thaler et al. 2010b) (Fig. 8).

Similar to the phenyloxopropenyl series, 4-phenylpiperazinyl analogues of the following four linkers were prepared: phenylacrylate, *meta* and *para* substituted, and pyridin-2-ylacrylate, substituted in positions 5 or 6. As summarised in Table 4, replacement of the phenyl led to a minor decrease in the HDAC inhibitory activity. However, the trends within both series were quite comparable: the *meta* substituted phenylacrylate derivative **15** exhibited an IC$_{50}$ value of 0.354 μM, and was
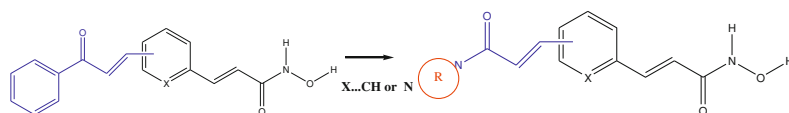
Fig. 8 From phenyloxopropenyl to amidopropenyl series

Table 4 SAR of 4-methyl- and 4-phenyl-piperazinyl analogues **13–16**
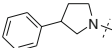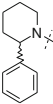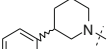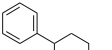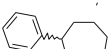
Compound	X		R	Enzyme (μM)	Cells (μM)		Microsomes (%)	
					K562	HCT116	Mouse	Human
13	CH	5	Ph	5.60	3.37	5.77	27	51
14	N	5	PPh	0.299	1.41	1.33	91	82
15	CH	6	PPh	0.354	0.980	0.780	72	60
16	N	6	PPh	0.069	1.13	1.07	74	77

about 15 times more potent than the corresponding *para* substituted (**13**). In the pyridinyl series, the differences between 2,5 and 2,6 di-substituted pyridin-2-yl-acrylates were smaller: compound **16** exhibited an IC_{50} value of 0.069 μM and was the most potent example in this series, around four times more than **14**. Comparison of the compounds containing a central phenyl ring with those with the pyridinyl ring showed the inhibitors with the pyridinyl ring were generally more potent. Compounds **14**, **15** and **16** exhibited comparable antiproliferative potency in leukemic K562 and human colon cancer HCT116 cells with IC_{50} values of around 1 μM. Hydroxamate **13**, in line with the lower enzymatic inhibition, had IC_{50} values in K562 and HCT116 cells of 3.77 and 5.77 μM, respectively.

The major difference between the phenyloxopropenyl and the 4-phenylpiper-azinyl series was their microsomal stability: all four amidopropenyl compounds were metabolised <50 % in the tested conditions and were remarkably more stable than the ketone analogues. The only exception was **13** with a recovery of just 27 % in mouse microsomal preparation. These results confirmed that the α,β-unsaturated ketone moiety was a major site of metabolic liability and replacement with an amide group resulted in stable compounds in microsomal preparations.

These encouraging data prompted to explore this series in a greater depth and the hydroxamic acid **16** was selected as starting point for this expansion. The synthetic efforts were concentrated on a series of cyclic amine derivatives substituted by phenyl. This selection was based on the fact that hydrophobic aromatic groups represent a common surface recognition domain in several HDAC inhibitors (Miller et al. 2003). As shown in Table 5, IC_{50} values ranged between

Table 5 SAR of phenyl-cycloamine analogues **17–21**

Compound	R	Enzyme (μM)	Cells (μM)		Microsomes (%)	
			K562	HCT116	Mouse	Human
17		0.294	1.220	1.300	66	66
18		0.269	0.616	0.432	52	90
19		0.025	0.445	0.294	74	86
20		0.146	1.730	1.470	75	98
21		0.286	0.568	0.581	29	46

Table 6 Pharmacokinetic profile for **15**, **16** and **19** (administered 5 mg/kg, i.v. and 15 mg/kg, orally)

Compound	**15**	**16**	**19**
AUC$iv_{0-\infty}$ (ngh/mL)	440	590	1191
$t_{1/2}$ (h)	1.22	0.27	0.67
Cl (L/h/kg)	11.37	8.47	4.19
V_{ss} (L/kg)	5.2	0.8	0.55
F (%)	10	2.9	3.1

0.025 μM (**19**) and 0.294 μM (**17**). These differences in activities are quite small compared to the substantial structural variations. These findings can be ascribed to the fact that the surface region of the HDAC enzyme is highly flexible and able to accommodate inhibitors with different capping groups (Somoza et al. 2004; Wang et al. 2005). The compounds exhibited comparable antiproliferative activities in K562 and HCT116 cells; compound **19** (IC$_{50}$ = 0.445 μM) was around four-fold more active than the least potent analogue **20** (IC$_{50}$ = 1.730 μM) in K562 cells. Furthermore, hydroxamic acid **19** was around five times more active than **20** (IC$_{50}$ = 1.470 μM) in HCT116 cells.

All compounds exhibited a good stability in mouse and human microsomes with <50 % of the inhibitors metabolised. The only outlier was compound **21**, with 29 and 46 % remaining in mouse and human microsomes, respectively.

However, the remarkable stability of the compounds in microsomes was not confirmed by in vivo PK experiments in mice. Three selected derivatives, the aryl-hydroxamate **15** and the two heteroaryl-hydroxamates **16** and **19**, displayed a low oral bioavailability with $F \leq 10$ % (Table 6). The compounds also showed very high clearance rates. In particular, inhibitors **15** and **16** showed clearance rates, which exceed the hepatic blood flow of 5.4 L/h/kg in mice (Davies and Morris 1993).

Further investigations revealed that the three representative compounds had high clearance rates in rat and human hepatocytes. These observations indicated a metabolic degradation of these hydroxamic acid derivatives catalysed preferentially by non-microsomal enzymes. Reduction of the hydroxamic acid group to its corresponding amide was identified for the three compounds as one relevant biotransformation pathway. The same outcome was found for SAHA, which was studied as reference compound. Similar results had been previously reported for TSA (Elaut et al. 2002). These observations suggest that this metabolic behaviour is likely to be common to further hydroxamic acids.

These results are in agreement with the observed in vivo PK behaviour in mice. They show that the metabolic stability of these hydroxamates in microsomes was neither found in hepatocytes nor in vivo. ADME experiments employing microsomes are widely used and they are often very suitable indicators for the in vivo PK behaviour. However, our experiences as well as other cases have shown that microsomes may not be sufficient for predicting in vivo clearances of structures containing hydroxamic acid moieties. Hepatocyte preparations, even though more expensive, demonstrated to be a more valid alternative for predicting the in vivo clearance behaviour of the studied hydroxamates.

3.5 Spiropiperidines

The phenyloxopropenyl and the amidopropenyl series resulted in the discovery of several compounds with good in vitro biochemical and antiproliferative activity. However, none of them exhibited an oral bioavailability superior to 20 % in mice (Thaler et al. 2010a, b). Therefore, various other scaffolds were evaluated. Major focus was particularly on privileged structures, which already had provided derivatives with good oral bioavailability. Privileged structures with their inherent affinity for diverse biological targets represent an ideal source of core scaffolds for the design of molecules able to target various receptors (DeSimone et al. 2004; Costantino and Barlocco 2006). One of them is the conformationally constraint 4-oxospiro[chroman-2,4′-piperidine] ring system, which is, for example, present in antiarrhythmic agents (Elliott et al. 1992).

Some 4-oxospirochromanes linked to an acrylhydroxamic acid group as zinc binding motif were prepared based on the results obtained during the exploration of different hydroxamic acid fragments (Fig. 9) (Thaler et al. 2010a; Varasi et al. 2011). In the first run, unsubstituted and the N-methyl, N-acetyl and N-benzyl substituted piperidine analogues (22–25, Table 7) were synthesised. As shown in Table 7, all compounds inhibited the HDAC activity in the submicromolar range. No major differences in potencies were found: the unsubstituted spiropiperidine (22) with an IC$_{50}$ value of 0.082 μM was around eight-fold more active than the least potent one within this series, the acetyl analogue (24). Compound 24 was also the least potent compound within this group against leukemic K562 and colon cancer HCT116 cells, while the other analogues showed good antiproliferative activity in the micromolar or submicromolar range. Next, synthetic efforts were focused on modifications of the central spirochromane core structure. Shift of the acrylamide moiety to position 7 and reduction of the chromane ring size to spirobenzofuran furnished compounds, which were generally less active (Varasi et al. 2011). Then, the importance of the ketone group was assessed. The hydroxy derivative 25a (Fig. 10) and the chromene 25b exhibited IC$_{50}$ values of 1.21 and 1.19 μM, respectively, and were around ten-fold less active than the 4-oxo-chromane 25. Also the chromane 25c (IC$_{50}$ = 9.0 μM) and the N-acetyl derivatives 25d (IC$_{50}$ = 5.15 μM) were significantly less active. In addition, these four compounds showed a lower antiproliferative activity in K562 and HCT116 cells

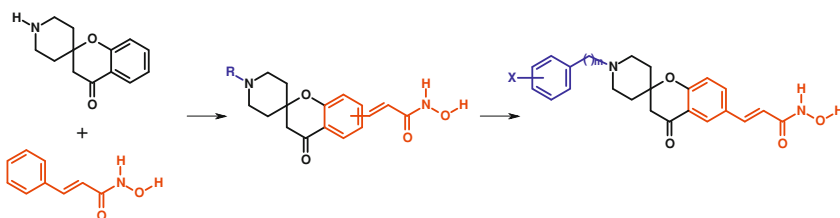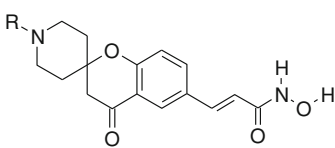Fig. 9 Spiropiperidines

Table 7 Spiro [chromane-2,4′-piperidine]-N-hydroxy-acrylamides and their activities

Compound	R	Enzyme	Cells (μM)		Microsomes (%)	
		(μM)	K562	HCT116	Mouse	Human
22	H	0.082	5.77	1.59	nd.	nd.
23	CH₃	0.288	0.806	0.266	nd.	nd.
24	Acetyl	0.641	9.37	5.66	nd.	nd.
25	Benzyl	0.121	0.399	0.477	32	35
26	Ph	0.410	0.913	1.261	23	4
27	Ph-CH₂-CH₂-	0.113	0.180	0.201	57	66
28	Ph-(CH₂)₃-	0.171	0.449	0.445	29	46
29	2-F-Bn	0.118	0.742	0.920	23	36
30	3-F-Bn	0.251	0.585	1.026	32	54
31	4-F-Bn	0.108	0.681	0.777	47	63
32	2-MeO-Bn	0.197	0.150	0.151	40	47
33	3-MeO-Bn	0.199	0.385	0.473	38	36
34	4-MeO-Bn	0.175	0.184	0.205	43	35
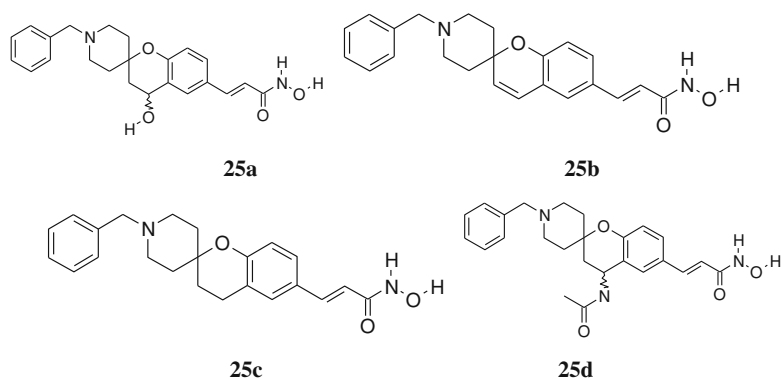
Fig. 10 Analogues of the 4-Oxospirochromane **25** (Table 1)

confirming the importance of the carbonyl group for the biochemical and cellular potency (Varasi et al. 2011).

These explorations consolidated the 4-oxospiro[chromane-2,4′-piperidine]-6-yl series as the most promising scaffold for a further expansion. For this purpose, different N-piperidine substituents and a number of compounds were made around the benzyl derivative **25** (Thaler et al. 2012). The few representatives **22–25**, prepared in the first run, showed no major differences in potencies. This indicated that variations on this site were likely well tolerated. But at that stage, one of the

major objectives was to obtain inhibitors with a good ADME profile with an acceptable activity.

Not surprisingly, no major differences in HDAC inhibitory activities were found. As shown in Table 7, the phenyl spiropiperidine (26) exhibited an IC_{50} value of 0.41 μM, whereas all other tested compounds had IC_{50} values in the range of 0.10–0.28 μM. All compounds showed good antiproliferative activities in K562 and HCT116 cells with IC_{50} values in the submicromolar to low micromolar range. The 2-phenylethyl analogue (27) was the most potent and the spirocycle (26) the least potent compound among the unsubstituted derivatives. Further elongation of the alkyl chain did not result in an increase of activity. Compound 32 with IC_{50} value of 0.15 μM was the most potent compound against K562 and HCT116 cells among the substituted benzyl analogues.

But as already mentioned earlier, the main selection criteria were set by the stability experiments. In fact, the tested compounds already showed different metabolic behaviours in microsomal preparations. In specific, the phenyl analogue (26) was rapidly metabolised both in mouse and human microsomes, with only 23 and 4 % of the product recovered unmodified after 30 min of incubation. The benzyl spirocycle (25) demonstrated a better stability with 32 % remaining in the mouse and 55 % in the human preparation. The 2-phenylethyl analogue (27) was even more stable with 57 % (mouse) and 66 % (human) remaining, respectively. However, this trend did not continue, when the alkyl chain was further increased: the 3-phenylpropyl spirocycle (28) had a microsomal stability similar or even lower than the benzyl derivative (25). The 4-fluorobenzyl derivative (31) emerged as the most stable derivative among the substituted benzyl analogues with 47 and 63 % of the compound recovered in mouse and human microsomes, respectively. Within the fluoro series, the 2-fluorobenzyl derivative (29) had the lowest stability compared to the 3- and 4-fluoro analogues (30) and (31) with 23 and 36 % remaining in mouse and human microsomes, respectively. On the other hand, no major differences were observed among the *ortho*, *meta* and *para* methoxybenzyl inhibitors (32–34).

Three representative examples 25, 27 and 31 displayed good oral bioavailability in mouse PK experiments with an oral bioavailability F of 31.5, 51.1 and 27.6 %, respectively (Table 8). Spirocycle 25 showed a high systemic plasma clearance with 5.88 mL/h/kg, similar to the hepatic flood flow of 5.4 mL/h/kg in mice (Davies and Morris 1993). The other two examples, 27 and 31, exhibited lower clearance rates with 4.79 and 3.35 mL/h/kg, respectively. This outcome is in line

**Table 8** Pharmacokinetic properties of 25, 27 and 31 in mice

Compound	25	27	31
$AUC_{iv0-\infty}$ (ngh/mL)	847	1042	1494
$t_{1/2}$ (h)	8.4	9.1	13
Cl (L/h/kg)	5.88	4.79	3.35
V_{ss} (L/kg)	8.9	8.6	5.9
F (%)	31.5	51.1	27.6

with their superior stability in human and mouse microsomes compared to **25**. Estimated elimination half-lives for the three examples ranged between 8 and 13 h. All three examples had very high estimated steady-state volume of distribution (V_{ss}), suggesting substantial distribution into tissues. The V_{ss} of **27** with 8.6 L/kg was in the same range of the compound **25** (8.9 L/kg). The 4-fluorobenzyl derivative (**31**) had a V_{ss} of 5.9 L/kg, lower than the other two spirocycles, **25** and **27**, but still ∼8 times the total body water in mice (Table 8) (Davies and Morris 1993).

The three spirocycles also showed good in vivo antitumor activity in an HCT116 xenograft model after oral administration. Consistent with the PK experiments, the 2-phenylethyl and the *para* fluorobenzyl analogues (**27** and **31**) were slightly more potent than **25**. In specific, the calculated T/C were 0.2 at 75 mg/kg for **31** and 0.2 and 0.34 at 150 mg/kg for **27** and **25,** respectively (Varasi et al. 2011; Thaler et al. 2012).
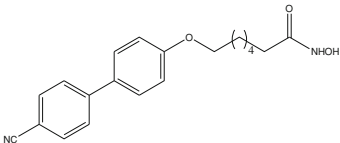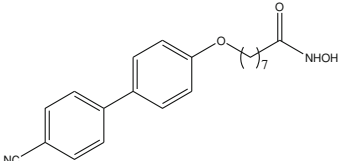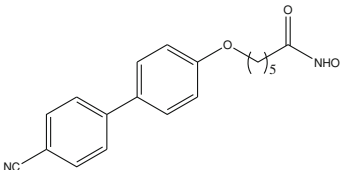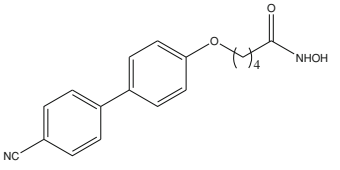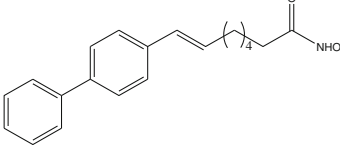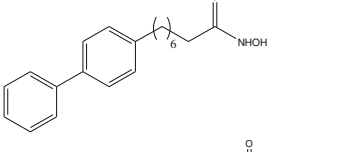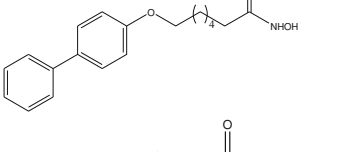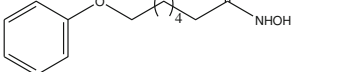
3.6 Biphenyl/Arylamide/Styrenyl Hydroxamic Acid Analogues

In mid 1999, the Abbott Medicinal Chemistry started to work on HDAC programme with the preparation and evaluation of several series of hydroxamic acids. Two HDAC inhibitors, the macrocyclic hydroxamate (**35**) and the α-ketoamide (**36**), were evaluated for their selectivity profile in comparison to SAHA and MS-275, but no selectivity was observed for a particular class of HDAC.
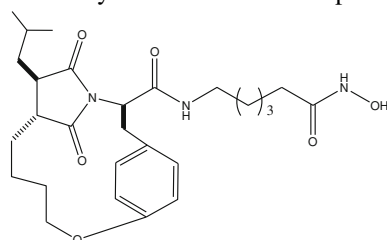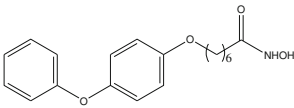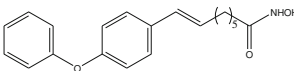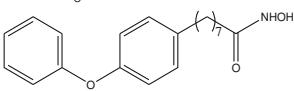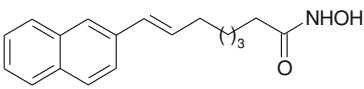

35
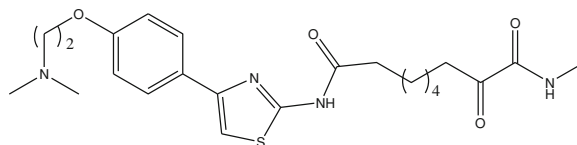
36

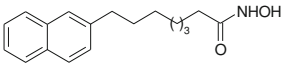The biphenyl ether series was among the first examined families leading to the identification of **37a** (Table 9) as a screening hit and having complimentary fit to the proposed general structure for HDAC inhibitors (Jung et al. 1999; Jung 2001). The SAR studies concluded that the 6-methylene linker was optimal and a longer/shorter tether showed loss of potency (**37a**, **37b–d**) (Table 9). Reduction of double

Table 9 A series of biphenyl hydroxamic acids

Compound	Structure	HDAC IC$_{50}$ (nM, K562 nuclear extract))
37a		9
37b		31
37c		76
37d		181
37e		5
37f		550
37g		17
37h		178

(continued)

Table 9 (continued)

Compound	Structure	HDAC IC$_{50}$ (nM, K562 nuclear extract))
37i		31
37j		6
37k		552
38a		6
38b		25

bond to saturated alkyl ether (**37f**) showed loss of inhibitory activity. Similar results were observed for compounds **38a–b** (Woo et al. 2002).

The nitrile group on the biphenyl was not important for activity (**37f** and **37g**), but replacement of the biphenyl moiety with phenyl resulted in a significant loss of potency (**37h**). Replacement of the tether ether of **37i** with alkenyl (**37j**) and alkyl (**37k**) showed similar trends as with compounds **37g**, **37e** and **37h**. All compounds had modest cellular potency (>1 μM) against HT1080 and MDA435 cell lines and were not considered for further studies.

The poor cellular activity profile of SAHA and the 'reverse-amide' series stimulated the evaluation of some biphenyl analogues (**39a–i,** Table 10). The 'SAHA-like' amides, the *para*-biphenyl and *meta*-biphenyl isomers (**39a** and **39b**) were found equipotent and had shown submicromolar cellular activity against both cell lines (Remiszewski et al. 2002). The series has shown beneficial effect by introducing a 4-phenylthiazol-2-yl moiety (**39c**) as compared to **39a** or **39b**. The *meta*-biphenyl analogue (**39e**) was more potent than the *para*-biphenyl isomer (**39d**); the reverse-amide 4-phenyl thiazole (**39f**) was equipotent with the *meta*-biphenyl analogue (**39e**), but exhibited a better cellular activity. Some of the favourable replacements include the 5-phenyl oxazol-2-yl (**39g**), 5-phenyl fur-2-yl (**39h**) and 5-phenylthiophen-2-yl (**39i**) (Curtin et al. 2002).
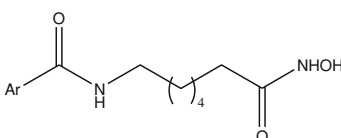
Some heteroaromatic phenyl replacements on the 'reverse-amide' template (**40a**) are shown in Table 11. The 2-pyridyl and 2-pyrrole substituents (**40b** and **40c**) had given equipotent inhibitors and the polycyclic heterocycles (**40d** and **40e**) had shown improved potency. *N*-substitution on the indole moiety of **40d** with phenyl (**40h**) or substituents on the indole phenyl ring (**40i**) led to an increase of potency, while the *N*-methyl analogue (**40g**) was less active (Wada et al. 2003).
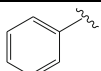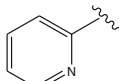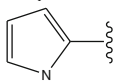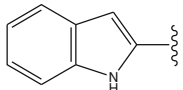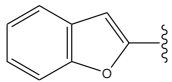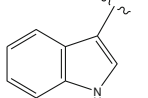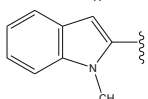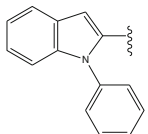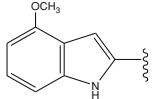
Examples of expected improvements of inhibitory activity by using a highly rigid, lipophilic tether like analogues are shown in Table 12. Submicromolar

Table 10 A series of arylamide hydroxamic acids along with cellular and enzymatic potency

Compound	Structure	HDAC IC$_{50}$ (nM)	HT1080 proliferation IC$_{50}$ (μM)	MDA435 proliferation IC$_{50}$ (μM)
SAHA	–	120	2.4	1.9
39a		6	0.47	0.38
39b		14	0.67	0.50
39c		0.7	0.13	0.04
39d		23	1.5	0.52
39e		3	2.3	9.1
39f		4	0.52	0.47
39g		22	0.34	0.31
39h		5	1.5	0.38
39i		4	0.40	0.20
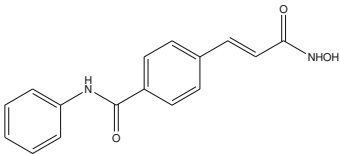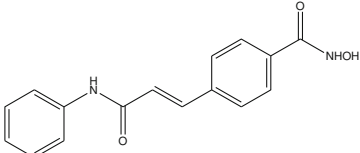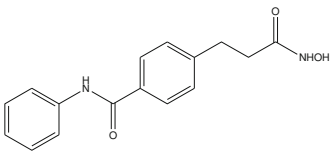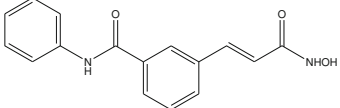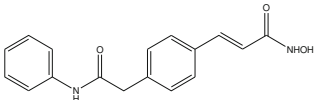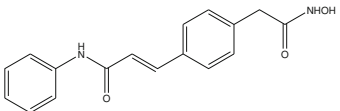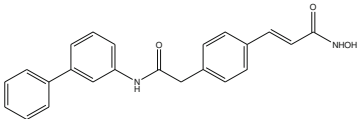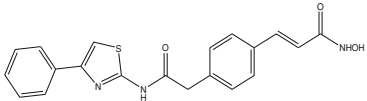
Table 11 Arylamide hydroxamic acids and their enzymatic and cellular potency

Compoundd	Ar	HDAC IC$_{50}$ (nM)	HT1080 proliferation IC$_{50}$ (μM)	MDA435 proliferation IC$_{50}$ (μM)
40a		1000	–	–
40b		1680	–	–
40c		524	–	–
40d		15	0.14	0.15
40e		30	0.76	0.49
40f		38	1.0	0.72
40g		56	0.78	0.39
40h		4	2.5	0.76
40i		3	0.12	0.13

activity was observed with the styrenyl tethers (**41a**, **41b**) and the potency was diminished with saturation of double bond (**41c**). The para substituted phenyl derivative **41a** resulted to be slightly more active than the corresponding 1,3-phenyl analogue (**41d**). The 2-anilino-2-oxo-ethyl analogue of **41a** resulted to be almost three times more active in the HDAC inhibitory assay and showed an

Table 12 Series of styrenyl hydroxamic acids and their enzymatic and cellular potency

Compound	Structure	HDAC IC$_{50}$ (nM)	HT1080 proliferation IC$_{50}$ (μM)	MDA435 proliferation IC$_{50}$ (μM)
41a		260	–	–
41b		640	–	–
41c		3200	–	–
41d		450	–	–
41e		97	0.58	0.37
41f		>5000	–	–
41g		15	0.88	0.63
41h		6	0.10	0.07

antiproliferative activity with IC$_{50}$ values in the submicromolar range. Further modifications of **41e** as in *meta*-biphenyl analogue (**41g**) and 4-phenylthiazol-2-yl-hydroxamate (**41h**) had shown excellent inhibitory and cellular activity (Curtin et al. 2002).

In a further study, the linking amide functionality in the arylamide **39c** was removed giving hydroxamates **42a** and **42b**. Both compounds showed a lower

HDAC inhibitory activity with IC_{50} values of 19 nM (**42a**) and 9 nM (**42b**), respectively, as well as a reduced cellular activity (Dai et al. 2003).

42a

42b
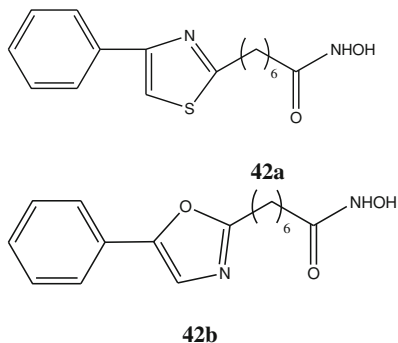
As illustrated in the previous examples, variations of the cap group are in general well tolerated. Even significant structural variation, e.g. by introducing a macrocyclic cap group resulted in derivatives with potent HDAC inhibitory activity (Sternson et al. 2001). For example, the hydroxamic acid (**43**) having a cyclic tetrapeptide terminal group has shown reversible HDAC inhibition (HDAC1 ($IC_{50} = 1.9$ nM) with a slight selectivity over HDAC6 ($IC_{50} = 19$ nM).

43
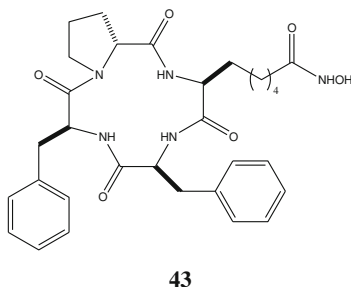
Modifications of the peptidic analogue **43** by replacing the cyclic tetrapeptide with the peptidomimetic core of Abbott's macrocyclic matrix metalloproteinase inhibitor (Steinman et al. 1998) resulted in derivatives, which had reduced HDAC inhibitory activity. For example, the macrocyclic hydroxamic acid inhibitors **44** and **45a** (Fig. 11) exhibited HDAC IC_{50} values of 2.1 μM and 38 nM, respectively (Curtin et al. 2002).

The studies concluded that the parent macrocycle succinimide **45a** had significant antiproliferative activity, but any further modifications did not make any significant improvement in the HDAC and cellular growth inhibitory activity (Table 13).

The nature of the amino acidic side chain was important for activity. Compound **45g**, devoid of benzyl moiety, resulted to be a weak HDAC inhibitor with no measureable antiproliferative potency at the tested conditions. Compound **45h**,
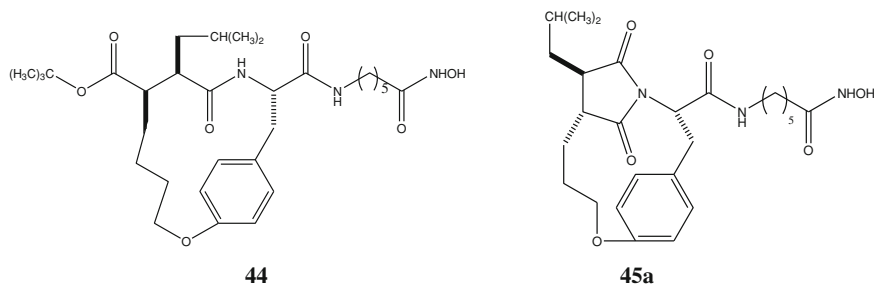
Fig. 11 Macrocyclic hydroxamic acid analogues
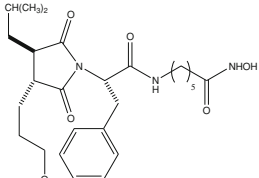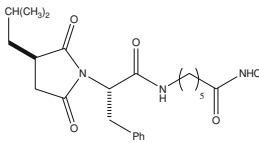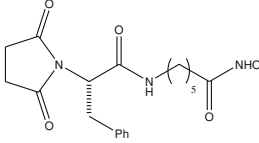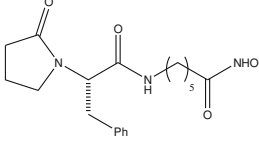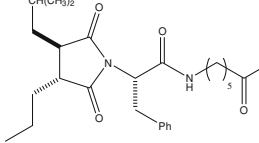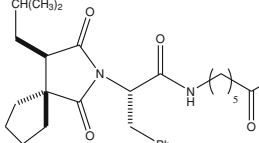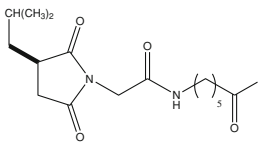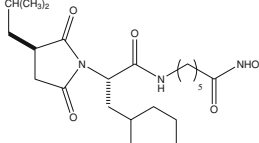
which comprises an L-cyclohexylalanine residue, regained the potency and the *para* methoxy-Ph analogue **45i** exhibited potencies similar to the macrocyclic inhibitor **45a**. The penta- and hexa-methylene tethered analogues of the disubstituted succinimide (**45e** and **45j**) had similar activity, while the tetra-methylene analogue (**45k**) was much less potent (Curtin et al. 2002; Curtin and Glaser 2003).

3.7 Tetrahydroisoquinoline-Based Hydroxamic Acid Derivatives

A novel class of tetrahydroisoquinoline-based hydroxamic acid analogues was evaluated in vitro and in vivo as potential anticancer and HDAC inhibitor agents at the Shandong University (Zhang et al. 2010, 2011a, b). The designing was based on the common pharmacophore having three parts, the Zn^{2+} binding group and a linker and the surface recognition domain (Miller et al. 2003). The 1,2,3,4-tetra-hydroisoquinoline-3-carboxylic acid having distinct geometrical conformation and biological activity (Klutchko et al. 1986) was used to design novel HDAC inhibitors (**46**, **47**, **48**, Table 14) (Zhang et al. 2010). Most of the target compounds showed an inhibitory activity against HDAC8 comparable to SAHA, some of them were more potent than the reference compound. Modifications of the R_1, both in the BOC series **46** and well as for the free amine analogues **47**, were well tolerated with IC_{50} values ranging from 1.06 (**47l**) to 8.21 μM (**47a**). Compounds with aromatic R_1 groups (**46a–m**, **47a–m**) were slightly more potent than the compounds bearing aliphatic R_1 groups (**46n–p**, **47n–p**).
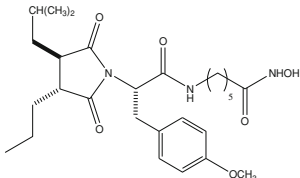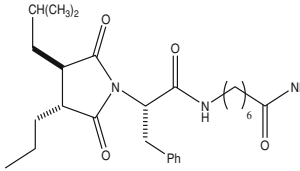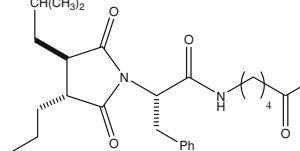
A further expansion led to compound **48a**, which resulted to be more potent than the derivatives in the **46** or **47** series, such as **46d**. On the other hand, the rigid compounds **48b** and **48c** were found almost inactive. These results indicated that variations of the substituents on the secondary amine influence the inhibitory activity more than the R_1 groups in the **46** or **47** series. Some of the compounds showed also better antiproliferative activity against HCT116, SKOV3 and HL60 cell lines.

Table 13 Structures of succinimide acids and their enzymatic and cellular potency

Compound	Structure	HDAC IC$_{50}$ (nM)	HT1080 proliferation IC$_{50}$ (μM)	MDA435 proliferation IC$_{50}$ (μM)
45a		38	0.25	0.15
45b		99	2.3	0.67
45c		660	14	10
45d		>5000	–	–
45e		51	0.40	0.57
45f		66	1.5	0.7
45g		5000	–	–
45h		640	–	–

(continued)

Table 13 (continued)

Compound	Structure	HDAC IC$_{50}$ (nM)	HT1080 proliferation IC$_{50}$ (μM)	MDA435 proliferation IC$_{50}$ (μM)
45i		38	0.53	0.18
45j		230	2.9	1.6
45k		1600	–	–

Table 14 Structures and HDAC8 inhibitory activities of compounds **46a–p** and **47a–p**

46a-p   **47a-p**
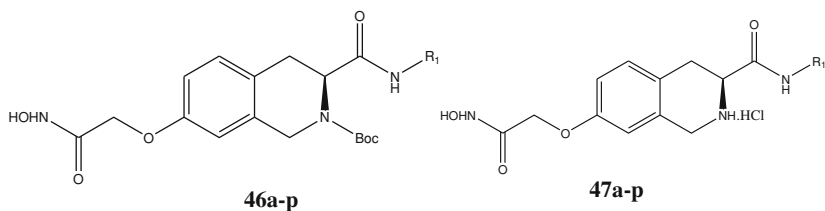
Compound	R$_1$	IC$_{50}$ (μM, HDAC8)
46a	-Ph	1.29
47a		8.21
46b	-CH$_2$-Ph	3.41
47b		5.10
46c	-(CH$_2$)$_2$-Ph	2.67
47c		4.07
46d	-(*p*-OCH$_3$)Ph	1.00
47d		5.57
46e	-(*p*-CH$_3$)Ph	1.65
47e		3.82

Table 14 (continued)
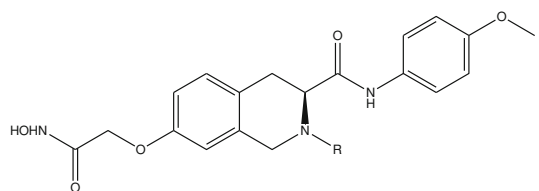
Compound	R_1	IC$_{50}$ (µM, HDAC8)
46f	-(*o*-CH$_3$)Ph	4.00
47f		4.13
46g	-(*m*-CH$_3$)Ph	1.77
47g		3.62
46h	-(*p*-F)Ph	2.56
47h		3.23
46i	-(*m*-Cl)Ph	1.17
47i		3.20
46j	-(*o,p*-diCH$_3$)Ph	3.78
47j		3.39
46k	-(*m*-Cl,*p*-F)Ph	1.55
47k		3.34
46l	-1-naphthyl	4.25
47l		1.06
46m	-(*p*-Ph)Ph	1.98
47m		2.21
46n	-(CH$_2$)$_4$CH$_3$	3.02
47n		3.54
46o	-(CH$_2$)$_5$CH$_3$	4.42
47o		5.77
46p	-C(CH$_3$)$_3$	4.58
47p		12.17
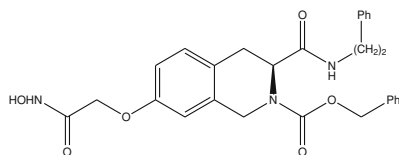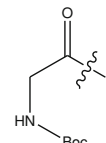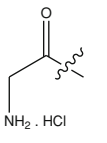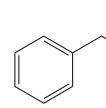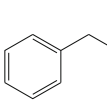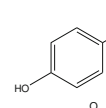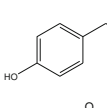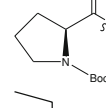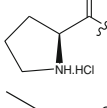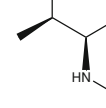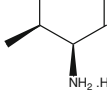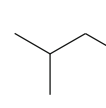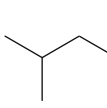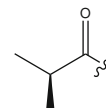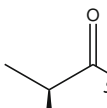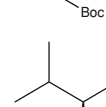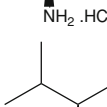
48a
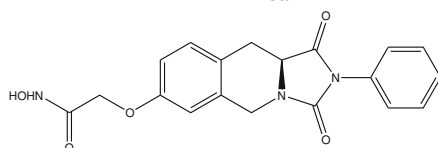
48b
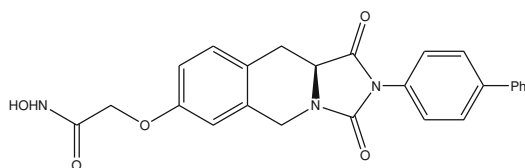
48c
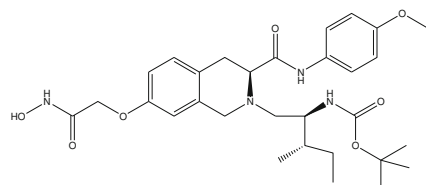
49a
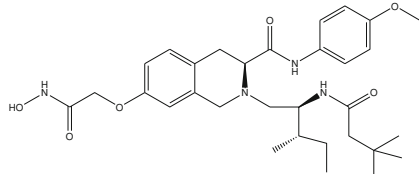
49b
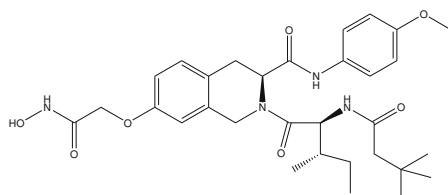
49c

Based on the lead structure **46d**, further extensive structure–activity relationship studies were performed in order to optimise anticancer activities of this series (Zhang et al. 2011b). For this purpose, the R_1 moiety (4-OCH$_3$–Ph) was kept fixed and the Boc group was replaced with other functional groups as shown in Table 15; the less polar BOC protected compounds (**50a–h**) were more potent than the corresponding deprotected analogues (**51a–h**). The reduction of the amide group to a tertiary amine group was found detrimental (**50l–n**). The antiproliferative activities of potent compounds were found similar to that of SAHA in A549 (lung cancer) and MDA-MB-231 (breast cancer) cell lines (Zhang et al. 2011b). Furthermore, compound **50e** showed in vivo antitumor activity comparable to SAHA.
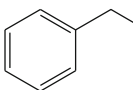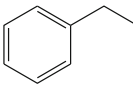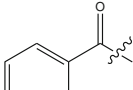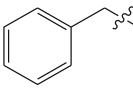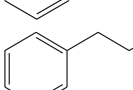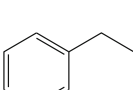
As further exploration, the synthetic efforts were directed towards compounds (examples **52a–c**) having the tertiary butyloxycarbonyl group and a better water solubility (Fig. 12), but the in vitro results were inferior to those of **50e**. A further exploration culminated in compounds **53a**, **b**, (Fig. 13) which exhibited mid-nMIC$_{50}$ values against HDAC8 and potent growth inhibition in multiple tumour cell lines. Compounds **50e** and **52a–c** were selected for in vivo activity experiments and showed good anticancer potencies comparable to SAHA in a human breast carcinoma (MDA-MB-231) xenograft model after ip administration.

Table 15 Structures and HDAC8 inhibitory activities of compounds **50a–n** and **51a–h**

Compound	R	IC$_{50}$(μM) HDAC8	Compound	R	IC$_{50}$ (μM) HDAC8
50a		0.51	**51a**		2.14
50b		0.103	**51b**		0.368
50c		0.175	**51c**		0.634
50d		0.212	**51d**		0.481
50e		0.139	**51e**		1.04
50f		0.163	**51f**		0.675
50g		0.182	**51g**		1.28
50h		0.104	**51h**		1.02

(continued)

Table 15 (continued)

Compound	R	IC$_{50}$(μM) HDAC8	Compound	R	IC$_{50}$ (μM) HDAC8
50i		0.141	**50m**		1.02
50j		0.164	**50n**		1.92
50k		0.114	**50l**		1.72

52a-c

52a (ZYJ-34a), R =

52b (ZYJ-34b), R =

52c (ZYJ-34c), R =
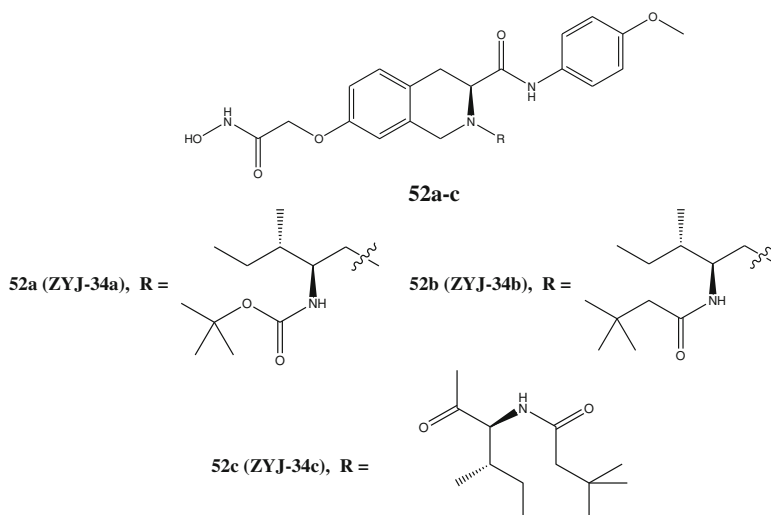
Fig. 12 Structures of hydroxamic acid based HDAC inhibitors having tertiary butyloxycarbonyl group

3.8 N-*Hydroxy Phenylacrylamide Derivatives*

Research activities at the Novartis Institutes for Biomedical Research resulted in a series of potent HDAC inhibitors, among them the clinical candidates LAQ824 and LBH589 in the early 2000 (Remiszewski et al. 2003). The development of second-generation HDAC inhibitors was aimed towards improving in vitro potency and in vivo efficacy of hydroxamate-based HDAC inhibitors and simultaneous elimination of interactions with cardiac ion channels linked to QT prolongation (Shultz et al. 2011). The *N*-hydroxy phenylacrymide pharmacophore

Fig. 13 Structures of
compounds **53a** and **53b**

53a-b

53a, R=   **53b, R=**
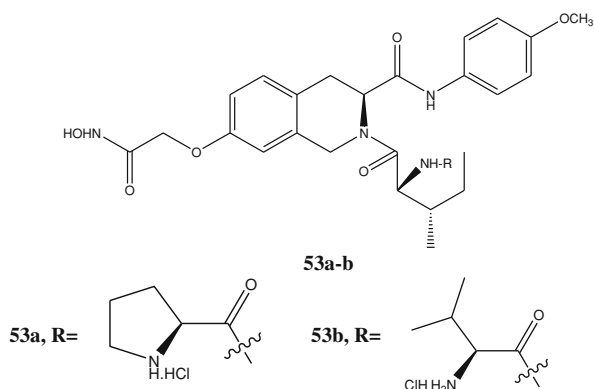
explored also in their first-generation HDAC inhibitors was modified using
structure-based drug design, physicochemical property modulation and a matched
molecular pair approaches and a series of data were prepared (Shultz et al. 2011,
see Table 16). The cardiac safety profile was measured using the *i*CSI (in vitro
cardiac safety index) parameter. Compounds **54a**, **54b** and **54c** were found to be
highly potent, efficacious, and having greater in vitro cardiac safety as compared to
several HDAC inhibitors in clinical trials. Steric effect and amphiphilicity were
identified as the contributing parameters for the activity (Table 16). Compounds
54a and **54c** showed significant in vivo antitumor activity in an HCT116 xenograft
model. The tumour growth regression in mice treated with 10 mg/kg of **54a**,
administrated iv, qd for eight total doses, or with **54c**, administered 50 mg/kg iv,
qd for 13 total doses, resulted to be 22 or 9 %, respectively.

Table 16 Azaindole analogues and their inhibitory activity and *i*CSI against HDAC1, HCT116
and hERG

Compound	R$_1$	R$_2$	IC$_{50}$ (nM)			iCSI
			HDAC-1	HCT116	hERG (%)	
54a		-CH(CH$_3$)$_2$	4	4	36	>7500
54b		-H	5	122	20	>256
54c		-H	3	4.5	31	>6667

4 Isoform Selective HDAC Inhibitors

Sodium *n*-butyrate, trichostatin and SAHA have in common that their biological targets were unknown at the time when their antitumor activity in different cell lines was assessed. Their activity against HDACs has been only ascertained afterwards. Most of HDAC inhibitors are natural products or derivatives, such as the cyclic tetrapeptide trapoxin, which contains an epoxide group capable of binding irreversibly with histone deacetylase enzymes (Itazaki et al. 1990; Kijima et al. 1993), and the thiol FK228. FK228 was the second HDAC inhibitor reaching the market after gaining approval by the FDA in November 2009 (Ueda et al. 1994; Nakajima et al. 1998; Bertino and Otterson 2011; Grant et al. 2010; Jain and Zain 2011). After the discovery of the above-mentioned inhibitors, the knowledge on HDACs and their biological functions has grown rapidly. New assays have been developed and crystal structures of several HDACs have been disclosed after the structure of *Aquifex aeolicus* HDAC homologue HDLP (Finnin et al. 1999). Thus, with the advances of the biological knowledge on HDACs, there is no surprise that the selectivity profile for TSA and SAHA was found to be typical for "pan-inhibitors". The compounds were able to inhibit all enzymes with similar potency, though this belief has been recently challenged (Bradner et al. 2010).

Currently, the more advanced compounds can be classified either as pan-HDAC inhibitors, such as the majority of the hydroxamic acids, or as class I selective inhibitors, such as the pyrimidinhydroxamates CHR-3996 or JNJ-26481585 (Arts et al. 2009) as well as some non-hydroxamic acid derivatives like aminoanilide MGCD0103 (Garcia-Manero et al. 2008; Younes et al. 2011). In addition, there are compounds, like the thiol FK228, which can be described as a potent class I inhibitor and a moderate class II inhibitor. The clinical studies of these HDAC inhibitors have shown a similar toxicity profile, which includes gastrointestinal disturbances, fatigue and in several cases cardiotoxicity (Marsoni et al. 2008; Hymes 2010; Lynch et al. 2012). Toxicities were similar in pan-HDAC inhibitors, class I selective inhibitors and FK228. Thus, the clinical outcome has left open the question, whether selective inhibitors of HDACs would be less toxic and overall more advantageous compared to the more advanced HDAC inhibitors as anti-cancer agents.

As mentioned above, the growing understanding of HDACs and their biological functions provided new tools or knowledge, which is crucial for the design of new selective HDAC inhibitors. Recombinant HDAC proteins as enzymes for the assays have become available. Furthermore, class IIa and IV specific substrates have been identified, which allow a precise profiling of compounds against bio-chemically active HDAC1-11 (Hauser and Jung 2009; Lahm et al. 2007; Bradner et al. 2010; Madsen and Olsen 2012). Interestingly, it has been recently found that HDAC3 showed in vitro decrotonylase activity (Madsen and Olsen 2012). Thus, the knowledge on HDACs continues to grow and it won't be surprising to find that these enzymes may be possibly involved in further activities in cellular environments. In this context, it should be remembered that HDACs are components of

multiprotein complexes (frequently having multiple enzymatic activities); and testing isolated recombinant HDACs in biochemical assays may not necessarily represent the best mode to reveal their cellular enzymatic functions. The crystal structures of human histone deacetylases HDAC2 (Cronin et al. 2009), HDAC3 (Watson et al. 2012), HDAC4 (Bottomley et al. 2008), HDAC7 (Schuetz et al. 2008) and HDAC8 (Somoza et al. 2004; Vannini et al. 2004) revealed the differences in the active enzymatic sites. These discoveries have provided new tools for the design of isoform selective compounds or compounds with a different selectivity profile than the older ones. These compounds may clarify if the toxicities seen in the more advanced HDAC inhibitors could be associated to one or more HDAC isoform(s).

At present, there are some examples, which exhibit isoform selectivity different from that of the above described HDAC inhibitors (Fig. 14). One example is the HDAC8 selective inhibitor PCI-34051 (Pharmacyclics) (Balasubramanian et al. 2009). PCI-34051 was found to be over 200-fold selective for HDAC8 compared to HDAC1-3, HDAC6 and HDAC10. The compound selectively induced apoptosis in cell lines derived from T cell lymphomas and leukaemias, but not in other haematopoietic or solid tumour cells. A further example is compound **55**, presented as A8B4 (Tang et al. 2011). The compound showed IC_{50} values of 0.023 μM against HDAC8, 3.6 μM against HDAC2, and 15 μM against HDAC3/ nCoR2. No further data are yet available. Other examples comprise some *ortho* substituted *N*-hydroxycinnamates, e.g., **56** (Huang et al. 2012). Compound **56** exhibited IC_{50} values of 27.2 ± 3.1 nM against HDAC8, 3 μM against HDACs 1 and 3 and ≥20 μM against HDACs 2, 4, 6, 10 and 11.

More examples can be found in the field of HDAC6 selective compounds (Fig. 15). The first example, tubacin, was already discovered in 2003, but its development was hampered by its poor drug properties (Haggarty et al. 2003). A

PCI-34051

55   **56**
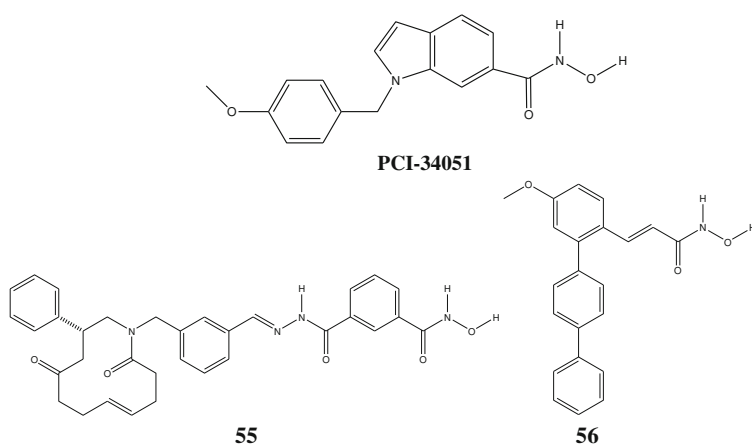
Fig. 14 HDAC8 selective compounds
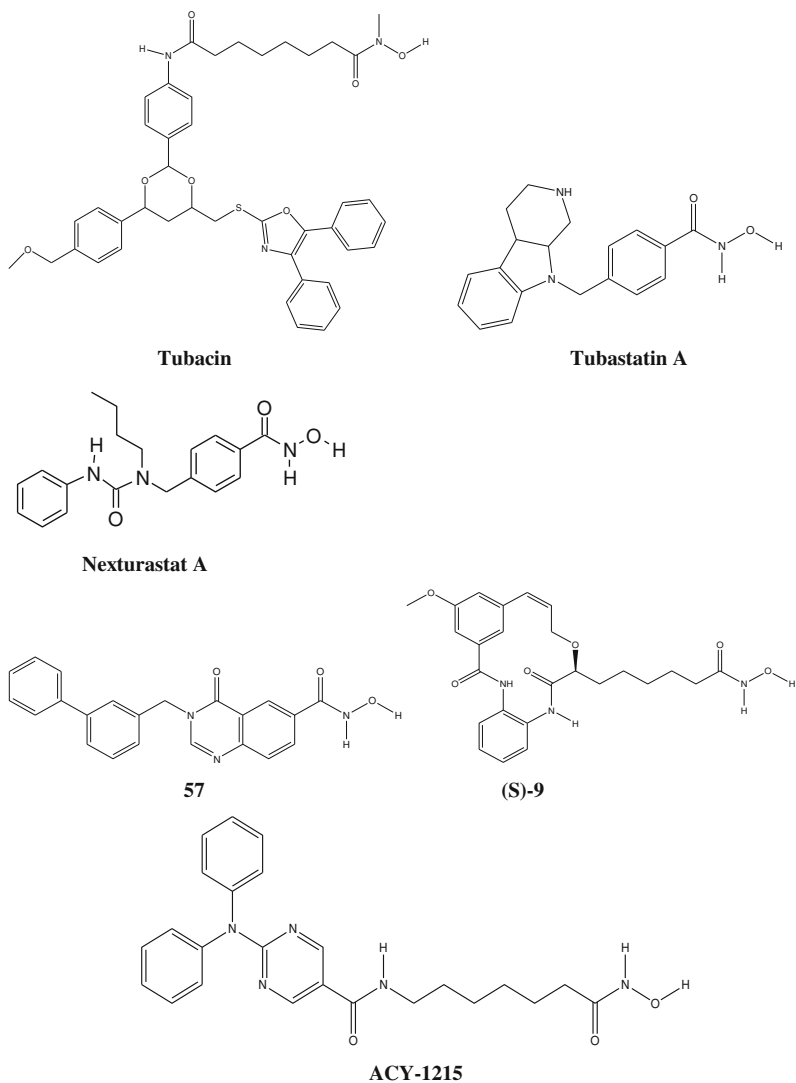
Fig. 15 HDAC6 selective compounds

homology model of HDAC6 revealed that the dimensions of the outer rim of the catalytic channel differ greatly between HDAC6 and HDAC1 (17.5 Å vs. 12.5 Å) (Butler et al. 2010). This structural diversity allowed designing compounds containing a cap moiety large and rigid enough to accommodate the rim region of HDAC6 but not of HDAC1. The resulting lead compound Tubastatin A was more than 1,000-fold selective versus all isoforms excluding HDAC8, where it had approximately 57-fold selectivity. The same laboratory disclosed recently the urea derivative Nexturastat A, which—compared to Tubastatin A—exhibited an

improved inhibition of HDAC6, while maintaining the selectivity of approximately 600-fold relative to the inhibition of HDAC1 (Bergmann et al. 2012). The compound showed also a superior antiproliferative activity against B16 melanoma cells (GI_{50} = 14.3 ± 1.15 μM) than Tubastatin (40.5 ± 1.21 μM), but lower than LBH589 (0.150 ± 0.001 μM).

Also the HDAC6 selectivity has been found by exploring different hydroxamic acids linked to a macrocyclic structure (Auzzas et al. 2010). Representative compound (**S**)-**9** inhibited HDAC6 with an IC_{50} value of 0.84 nM. The inhibitor was around 30 times more selective over HDAC1 and HDAC7 and even more over the other isoforms. HDAC6 selective inhibitors have been also described by scientists from Millennium Pharmaceuticals. For example, representative compound **57** (exemplified as I-126 in the in WO2012/054332) blocked HDAC6 activity by 95.6 % at 0.37 μM (England et al. 2012).

Currently, ACY-1215 has attracted great interest. The HDAC6 selective inhibitor initiated phase I/II clinical studies in July 2011 (www.clinicaltrials.gov/ct2/show/NCT01323751). The compound exhibited an IC_{50} value of 5 nM against HDAC6 and was around ten times less active against HDACs 1, 2 and 3. The activities against the class II enzymes HDAC 4, 5, 7 9 and against HDAC11 were in the micromolar range (Santo et al. 2012). Antiproliferative activities in Multiple Myeloma (MM) cell lines resulted with IC_{50} values ranging from 2 to 8 μM. A synergistic effect was found, when the compound was dosed in combination with bortezomib. These synergistic effects were seen both in vitro and in vivo in a human MM xenograft mouse model.

Inhibitors selective for other enzymes are even less explored. A series of diphenylmethylene hydroxamic acids as class IIa selective HDAC inhibitors have been described by scientists from Methylgene (Fig. 16) (Tessier et al. 2009). One of the described compounds, *N*-hydroxy-9*H*-xanthene-9-carboxamide (**58**), was somewhat more selective for HDAC7 with an IC_{50} of 0.05 μM. Other class II selective compounds have been disclosed in WO2012/103008 (CHDI Foundation Inc. 2012). Representative compound **59** had IC_{50} values of 0.02 μM against HDAC4 and 0.22 μM in human T cell lymphocyte Jurkat E6.1 cells. These structures are quite different from the hydroxamic acids described so far. In fact,

Fig. 16 Class IIa selective compounds

58 **59**
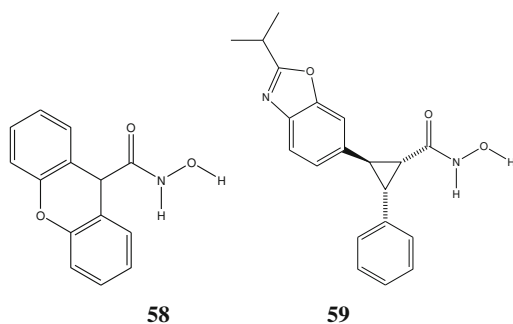
the X-ray structure of HDAC7 (Schuetz et al. 2008) revealed that the catalytic domain of class IIa HDACs is significantly different from that of the previously reported class I and class IIb-like HDACs. The presence of a hydrophobic pocket in the enlarged active site of HDAC7 is absent in class I and IIb and allows to accommodate compounds with bulky moieties adjacent to the hydroxamic acid as Zn^{2+}-chelating motif.

5 Computational Studies

In 1999, the histone deacetylase-like protein (HDLP) in complex with TSA and SAHA has been elucidated (Finnin et al. 1999). Later, various structure-based and ligand-based computational studies were carried out towards development of HDAC inhibitors (Wang 2009) and the results of various studies are as summarised below:

- Very few isoforms selective HDAC inhibitors have been studied and rarely any compound having high selectivity has been found.
- The zinc-binding groups are present in the majority of HDAC inhibitors. The ionisation states of the HDAC enzymes and the bound ligands need further study.
- Future consideration is required towards the flexibility of the HDAC8's pocket and surface mobility.
- For rapid virtual screening of libraries, a more effective scoring function with predictive power is required.

Very few QSAR studies on HDAC inhibitors have been reported until now. The first QSAR model was developed using TSA- and SAHA-like hydroxamic acids (Lan-Hargest et al. 2002) suggesting the importance of shape and area of the molecules for biological activity (Wang et al. 2004). Further, on a data set of 124 compounds, a QSAR study has been reported. The model has shown role of van der Waals surface area and hydrophobicity towards biological activity (Xie et al. 2004). A series of substituted biaryl hydroxamates and mercaptoacetamides as HDAC inhibitors against pancreatic cancer cell growth with nanomolar potency have been designed and synthesised (Kozikowski et al. 2008) and QSAR derived equations have shown significant correlations between different HDAC isoforms (Wang 2009).

The binding mode of indole amide analogues in human HDAC1 catalytic core has been explored by Guo et al. (2005). Further, 3D-QSAR model using CoMFA and CoMSIA has been established for 29 substituted hydroxamic-based HDAC inhibitors with an indole amide residue at the terminus. A comparison between both studies concluded good correlation between the two analyses. On the same set of compounds, a multiple regression analysis by Bajpai et al. (2013) revealed that the inhibition of the histone deacetylase by this series of compounds might involve the dispersion interaction with the receptor where charge transfer between pairs of atoms might greatly help to polarise the molecule. The results obtained by this

multiple regression analysis were in good agreement with those obtained by CoMFA and CoMSIA.

Juvale et al. (2006) performed CoMFA and CoMSIA studies on a data set of 40 hydroxamate analogues reported by Jung et al. (1999), Remiszewski et al. (2002) and Woo et al. (2002). The derived models have shown significance of steric and electronic fields along with lipophilicity as contributing parameters. A 3D-QSAR pharmacophore model has been developed using 30 known HDAC inhibitors (Chen et al. 2008). It concluded the essential ligand features, i.e. hydrogen-bond acceptor and hydrogen-bond donor features corresponding to the metal-binding function and coordination to the Zn(II) ion. Along with this, the hydrophobic/π-π stacking interactions between ligand and enzyme play a critical role for the inhibitory activity.

6 Development of HDAC Imaging Agents

As outlined above, a significant number of HDAC inhibitors have entered various clinical phases. In vivo imaging of HDACs and their inhibition is important and hence development of appropriate imaging agents has become a major challenge.

The conventional anatomic imaging modalities used to monitor clinical response can only help to identify tumour size or rudimentary physiologic changes and both of them occur relatively late after treatment onset. The ex vivo techniques can be utilised to analyse readily accessible tissue specimens. Thus, imaging probes are needed to investigate the efficiency of existing novel HDAC inhibitors with the hope that they may provide basic scientific insights which could lead to novel clinical applications.

Very few compounds for in vivo HDAC imaging have been reported. Some examples include 6-([^{18}F]fluoroacetamide)-1-hexanoicanilide (FAHA) (**60**) (Reid et al. 2009) and [^{11}C]MS-275, a carbon-11-labeled version of the benzamide class HDAC inhibitor MS-275 (entinostat) (**61**) for cerebral imaging (Hooker et al. 2010). These efforts were terminated because the short half-life of carbon-11- ($\sim$20 min) compared to fluorine-18 ($\sim$110 min) presents technical challenges and limits potential applications. Ronen and co-workers studied Boc-lysine trifluoroacetic acid 6 (BLT) as a substrate for HDACs using ^{19}F magnetic resonance spectroscopy (Sankaranarayanapillai et al. 2008). Hendricks et al. reported development of ^{18}F-suberoylanilide hydroxamic acid (^{18}F-SAHA) (**62**), a close analogue of the clinically relevant SAHA. This compound results to be one of the first ^{18}F-position emission tomography (PET) HDAC imaging agent (Hendricks et al. 2011).
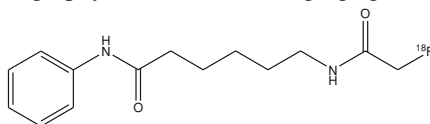
60
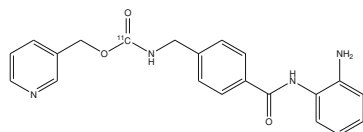
61
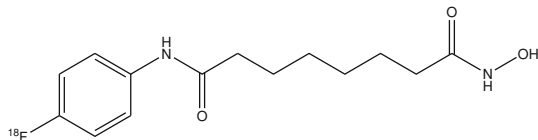
62

7 Conclusion

Hydroxamic acids demonstrated to be very potent inhibitors of several enzymes, such as matrix metalloproteinases, carbonic anhydrases, lipoxygenases, ureases and many others (Muri et al. 2002; Gupta and Sharma 2013). However, hydroxamic acid derivatives are often considered as poor drugs and are down prioritised in drug discovery programmes despite their good in vitro potency, the reasons being their poor physicochemical and ADME properties. Drug discovery programmes related to hydroxamic acids as HDAC inhibitors faced the same issues; nevertheless, the research efforts in this field have been appreciable and several successes achieved such as discovery of acetohydroxamic acid (Marwick 1983), adrafinil (Siwak et al. 2003) and SAHA (Grant et al. 2007). SAHA was considerably efficacious in different haematological malignancies, even though having just medium potency and being cleared rapidly (Kelly et al. 2003; Marks and Breslow 2007), while the clinical outcome in other cancers remained much more uncertain and often rather limited (Graham et al. 2009; Mercurio et al. 2010). However, the notable in vitro and in vivo data of these first inhibitors made HDACs an attractive target for drug discovery programmes. Intensive research efforts resulted in a remarkable number of clinical candidates—over ten hydroxamic acid derivatives—for tumours and some other diseases. This chapter presents a case history of the drug discovery for the treatment of cancers based on HDAC inhibition by hydroxamic acids with a particular attention for the PK properties of the drugs discovered. Extensive in vitro ADME assays, for example by studying the stability of the inhibitors in hepatocytes, or PK cassette experiments as well as computational tools for simulating the ADME properties have been proved fundamental for overcoming the poor drug properties.

The toxicity profile of SAHA and of other more "mature" HDAC inhibitors are not strictly related to the hydroxamic acid groups, but can also be related to 2-aminoanilides, such as MGCD0103, or to thiols such as FK228. To date, a major topic in the HDAC inhibitory field is the development of selective HDAC inhibitors

with a different selectivity profile than those already in advanced clinical studies. These compounds may clarify if the toxicities observed in the more advanced HDAC inhibitors might be associated with one or several HDACs. For future drug discovery programmes based on hydroxamic acid derivatives, the experiences gained from these preclinical and clinical studies may be of great value.

References

Allfrey VG, Faulkner R, Mirsky AE (1964) Acetylation and methylation of histones and their possible role in the regulation of RNA synthesis. Proc Natl Acad Sci U S A 51:786–794

Allfrey VG, Mirsky AE (1964) Structural modifications of histones and their possible role in the regulation of RNA synthesis. Science 144:559

Andreeff M, Stone R, Michaeli J, Young CW, Tong WP, Sogoloff H, Ervin T, Kufe D, Rifkind RA, Marks PA (1992) Hexamethylene bisacetamide in myelodysplastic syndrome and acute myelogenous leukemia: a phase II clinical trial with a differentiation-inducing agent. Blood 80:2604–2609

Arts J, King P, Marien A, Floren W, Belien A, Janssen L, Pilatte I, Roux B, Decrane L, Gilissen R, Hickson I, Vreys V, Cox E, Bol K, Talloen W, Goris I, Andries L, Du Jardin M, Janicot M, Page M, van Emelen K, Angibaud P (2009) JNJ-26481585, a novel "second-generation" oral histone deacetylase inhibitor, shows broad-spectrum preclinical antitumoral activity. Clin Cancer Res 15:6841–6851

Atadja P (2009) Development of the pan-DAC inhibitor panobinostat (LBH589): successes and challenges. Cancer Lett 280:233–241

Auzzas L, Larsson A, Matera R, Baraldi A, Deschenes-Simard B, Giannini G, Cabri W, Battistuzzi G, Gallo G, Ciacci A, Vesci L, Pisano C, Hanessian S (2010) Non-natural macrocyclic inhibitors of histone deacetylases: design, synthesis, and activity. J Med Chem 53:8387–8399

Bai LY, Omar HA, Chiu CF, Chi ZP, Hu JL, Weng JR (2011) Antitumor effects of (S)-HDAC42, a phenylbutyrate-derived histone deacetylase inhibitor, in multiple myeloma cells. Cancer Chemother Pharmacol 68:489–496

Bajpai A, Agarwal N, Srivastava V, Mishra A, Gupta SP (2013) A comparative 2D QSAR study on a series of hydroxamic acid-based histone deacetylase inhibitors vis-à-vis comparative molecular field analysis and comparative molecular similarity indices analysis. Personal Communication.

Balasubramanian S, Steggerda S, Sirisawad M, Schreeder M, Doiron L, Buggy JJ (2009) The histone deacetylase-8 (HDAC8) selective inhibitor PCI-34051 decreases interleukin-1 beta secretion in vitro and reduces inflammation in vivo. In: 50th ASH annual meeting and exposition, San Francisco, American society of Hematology, abstr 2581

Banerji U, van Doorn L, Papadatos-Pastos D, Debnam P, Tall M, Toal M, Hooftman L, Verweij J, Eskens F (2010) A phase I pharmacokinetic (PK) and pharmacodynamic (PD) study of CHR-3996, a class 1 selective histone deacetylase inhibitor (HDACi), in patients with advanced solid tumors. J Clin Oncol 28(Suppl):2552

Banerji U, van Doorn L, Papadatos-Pastos D, Kristeleit R, Debnam P, Tall M, Stewart A, Raynaud F, Garrett MD, Toal M, Hooftman L, De Bono JS, Verweij J, Eskens FA (2012) A phase I pharmacokinetic and pharmacodynamic study of CHR-3996, an oral class I selective histone deacetylase inhibitor in refractory solid tumors. Clin Cancer Res 18:2687–2694

Bergman JA, Woan K, Perez-Villarroel P, Villagra A, Sotomayor EM, Kozikowski AP (2012) Selective histone deacetylase 6 inhibitors bearing substituted urea linkers inhibit melanoma cell growth. J Med Chem 55:9891–9899

Bertino EM, Otterson GA (2011) Romidepsin: a novel histone deacetylase inhibitor for cancer. Expert Opin Investig Drugs 20:1151–1158

Bolden JE, Peart MJ, Johnstone RW (2006) Anticancer activities of histone deacetylase inhibitors. Nat Rev Drug Discov 5:769–784

Bottomley MJ, Lo Surdo P, Di Giovine P, Cirillo A, Scarpelli R, Ferrigno F, Jones P, Neddermann P, De Francesco R, Steinkuhler C, Gallinari P, Carfi A (2008) Structural and functional analysis of the human HDAC4 catalytic domain reveals a regulatory structural zinc-binding domain. J Biol Chem 283:26694–26704

Bradner JE, West N, Grachan ML, Greenberg EF, Haggarty SJ, Warnow T, Mazitschek R (2010) Chemical phylogenetics of histone deacetylases. Nat Chem Biol 6:238–243

Breslow R, Jursic B, Yan ZF, Friedman E, Leng L, Ngo L, Rifkind RA, Marks PA (1991) Potent cytodifferentiating agents related to hexamethylenebisacetamide. Proc Natl Acad Sci U S A 88:5542–5546

Breslow R, Marks PA, Rifkind RA, Jursic B (1993) Novel potent inducers of terminal differentiation and methods of use thereof. PTC Int Appl WO199307148

Brown DT (2001) Histone variants: are they functionally heterogeneous? Genome Biol 2: REVIEWS0006

Brunetto AT, Ang JE, Lal R, Olmos D, Frentzas S, Mais A, Hauns B, Mollenhauer M, Lahu G, de Bono JS (2009) A first-in-human phase I study of 4SC-201, an oral histone deacetylase (HDAC) inhibitor, in patients with advanced solid tumors. J Clin Oncol 27:15s (abstr 3530)

Buchwald M, Kramer OH, Heinzel T (2009) HDACi–targets beyond chromatin. Cancer Lett 280:160–167

Buggy JJ, Cao ZA, Bass KE, Verner E, Balasubramanian S, Liu L, Schultz BE, Young PR, Dalrymple SA (2006) CRA-024781: a novel synthetic inhibitor of histone deacetylase enzymes with antitumor activity in vitro and in vivo. Mol Cancer Ther 5:1309–1317

Butler KV, Kalin J, Brochier C, Vistoli G, Langley B, Kozikowski AP (2010) Rational design and simple chemistry yield a superior, neuroprotective HDAC6 inhibitor, tubastatin A. J Am Chem Soc 132:10842–10846

Cai X, Zhai HX, Wang J, Forrester J, Qu H, Yin L, Lai CJ, Bao R, Qian C (2010) Discovery of 7-(4-(3-ethynylphenylamino)-7-methoxyquinazolin-6-yloxy)-N-hydroxyheptanam ide (CUDc-101) as a potent multi-acting HDAC, EGFR, and HER2 inhibitor for the treatment of cancer. J Med Chem 53:2000–2009

Cheng H, Jones W, Wei X, Liu Z, Wang D, Kulp S, Chen C-S, Covey JKC (2006a) Preclinical pharmacokinetics studies of R- and S- enantiomers of the histone deacetylase inhibitor, HDAC-42 (NSC 731438), in the rat. Proc Am Assoc Cancer Res 47 (abstr 686)

Cheng H, Liu Z, Kulp SK, Chen C-S, Covey JM, Chan KK (2006b) Preclinical pharmacokinetic studies with s-HDAC-42 (NSC 736012), an inhibitor of histone deacetylase, by LC-MS/MS Proc Amer Assoc Cancer Res 47 (abstr 3091)

Chen YD, Jiang YJ, Zhou JW, Yu QS, You QD (2008) Identification of ligand features essential for HDACs inhibitors by pharmacophore modeling. J Mol Graph Model 26:1160–1168

Choudhary C, Kumar C, Gnad F, Nielsen ML, Rehman M, Walther TC, Olsen JV, Mann M (2009) Lysine acetylation targets protein complexes and co-regulates major cellular functions. Science 325:834–840

Costantino L, Barlocco D (2006) Privileged structures as leads in medicinal chemistry. Curr Med Chem 13:65–85

Cronin CN, Hilgers MT, Knuth MW, Navre ME, Sang C, Skene RJ, Tari LW, Wilson KP, Wittmer D, Zou H (2009) Crystallization of histone deacetylase 2. US Patent 7507522

Curtin ML, Garland RB, Heyman HR, Frey RR, Michaelides MR, Li J, Pease LJ, Glaser KB, Marcotte PA, Davidsen SK (2002) Succinimide hydroxamic acids as potent inhibitors of histone deacetylase (HDAC). Bioorg Med Chem Lett 12:2919–2923

Curtin M, Glaser K (2003) Histone deacetylase inhibitors: the abbott experience. Curr Med Chem 10:2373–2392

Dai Y, Guo Y, Curtin ML, Li J, Pease LJ, Guo J, Marcotte PA, Glaser KB, Davidsen SK, Michaelides MR (2003) A novel series of histone deacetylase inhibitors incorporating hetero aromatic ring systems as connection units. Bioorg Med Chem Lett 13:3817–3820

Davey CA, Sargent DF, Luger K, Maeder AW, Richmond TJ (2002) Solvent mediated interactions in the structure of the nucleosome core particle at 1.9 a resolution. J Mol Biol 319:1097–1113

Davies B, Morris T (1993) Physiological parameters in laboratory animals and humans. Pharm Res 10:1093–1095

DeSimone RW, Currie KS, Mitchell SA, Darrow JW, Pippin DA (2004) Privileged structures: applications in drug discovery. Comb Chem High Throughput Screen 7:473–494

Donald A, Belfield A, Day F, Patel S, Clark V, Needham L, Owen J, Bone E, Brotherton D, Bawden L, Rowlands M, Wibata J, Stimson L, Raynaud F, Aherne W, Moffat D (2010) The discovery and anti-tumor activity CHR-3996—a novel, orally available inhibitor of class 1 histone deacetylases. Paper presented at the EFMC-ISMC 2010 XXIst international symposium on medicinal chemistry, Brussels

Elaut G, Rogiers V, Vanhaecke T (2007) The pharmaceutical potential of histone deacetylase inhibitors. Curr Pharm Des 13:2584–2620

Elaut G, Torok G, Vinken M, Laus G, Papeleu P, Tourwe D, Rogiers V (2002) Major phase I biotransformation pathways of trichostatin a in rat hepatocytes and in rat and human liver microsomes. Drug Metab Dispos 30:1320–1328

Elliott JM, Selnick HG, Claremon DA, Baldwin JJ, Buhrow SA, Butcher JW, Habecker CN, King SW, Lynch JJ Jr, Phillips BT et al (1992) 4-Oxospiro[benzopyran-2,4′-piperidines] as class III antiarrhythmic agents. Pharmacological studies on 3,4-dihydro-1′-[2-(benzofurazan-5-yl)-ethyl]-6-methanesulfonamidospiro[(2H)-1-benzopyran-2,4′-piperidin]-4-one(L-691,121). J Med Chem 35:3973–3976

England D, Gigstad KM, Gould AE, Ma L, Xu H (2012) Substituted Hydroxamic Acids and Uses Therof. WO2012/054332

Federico M, Bagella L (2011) Histone deacetylase inhibitors in the treatment of hematological malignancies and solid tumors. J Biomed Biotechnol 2011:475–641

Ficner R (2009) Novel structural insights into class I and II histone deacetylases. Curr Top Med Chem 9:235–240

Finnin MS, Donigian JR, Cohen A, Richon VM, Rifkind RA, Marks PA, Breslow R, Pavletich NP (1999) Structures of a histone deacetylase homologue bound to the TSA and SAHA inhibitors. Nature 401:188–193

Flipo M, Charton J, Hocine A, Dassonneville S, Deprez B, Deprez-Poulain R (2009) Hydroxamates: relationships between structure and plasma stability. J Med Chem 52:6790–6802

Friend C, Scher W, Holland JG, Sato T (1971) Hemoglobin synthesis in murine virus-induced leukemic cells in vitro: stimulation of erythroid differentiation by dimethyl sulfoxide. Proc Natl Acad Sci U S A 68:378–382

Garcia-Manero G, Assouline S, Cortes J, Estrov Z, Kantarjian H, Yang H, Newsome WM, Miller WH Jr, Rousseau C, Kalita A, Bonfils C, Dubay M, Patterson TA, Li Z, Besterman JM, Reid G, Laille E, Martell RE, Minden M (2008) Phase 1 study of the oral isotype specific histone deacetylase inhibitor MGCD0103 in leukemia. Blood 112:981–989

Glozak MA, Sengupta N, Zhang X, Seto E (2005) Acetylation and deacetylation of non-histone proteins. Gene 363:15–23

Graham JS, Kaye SB, Brown R (2009) The promises and pitfalls of epigenetic therapies in solid tumours. Eur J Cancer 45:1129–1136

Grant C, Rahman F, Piekarz R, Peer C, Frye R, Robey RW, Gardner ER, Figg WD, Bates SE (2010) Romidepsin: a new therapy for cutaneous T-cell lymphoma and a potential therapy for solid tumors. Expert Rev Anticancer Ther 10:997–1008

Grant PA, Berger SL (1999) Histone acetyltransferase complexes. Semin Cell Dev Biol 10:169–177

Grant S, Easley C, Kirkpatrick P (2007) Vorinostat. Nat Rev Drug Discov 6:21–22

Gray SG, Ekstrom TJ (2001) The human histone deacetylase family. Exp Cell Res 262:75–83

Grignani F, De Matteis S, Nervi C, Tomassoni L, Gelmetti V, Cioce M, Fanelli M, Ruthardt M, Ferrara FF, Zamir I, Seiser C, Lazar MA, Minucci S, Pelicci PG (1998) Fusion proteins of the retinoic acid receptor-alpha recruit histone deacetylase in promyelocytic leukaemia. Nature 391:815–818

Grozinger CM, Hassig CA, Schreiber SL (1999) Three proteins define a class of human histone deacetylases related to yeast Hda1p. Proc Natl Acad Sci U S A 96:4868–4873

Guo Y, Xiao J, Guo Z, Chu F, Cheng Y, Wu S (2005) Exploration of a binding mode of indole amide analogues as potent histone deacetylase inhibitors and 3D-QSAR analyses. Bioorg Med Chem 13:5424–5434

Gupta SP, Sharma A (2013) Chemistry of hydroxamic acids (Chapter 1 of this book)

Haggarty SJ, Koeller KM, Wong JC, Grozinger CM, Schreiber SL (2003) Domain-selective small-molecule inhibitor of histone deacetylase 6 (HDAC6)-mediated tubulin deacetylation. Proc Natl Acad Sci U S A 100:4389–4394

Hauser AT, Jung M (2009) Assays for histone deacetylases. Curr Top Med Chem 9:227–234

Hendricks JA, Keliher EJ, Marinelli B, Reiner T, Weissleder R, Mazitschek R (2011) In vivo PET imaging of histone deacetylases by ^{18}F-Suberoylanilide hydroxamic Acid (^{18}F-SAHA). J Med Chem 54:5576–5582

Henikoff S, Furuyama T, Ahmad K (2004) Histone variants, nucleosome assembly and epigenetic inheritance. Trends Genet 20:320–326

Hooker JM, Kim SW, Alexoff D, Xu Y, Shea C, Reid A, Volkow N, Fowler JS (2010) Histone deacetylase inhibitor MS-275 exhibits poor brain penetration: pharmacokinetic studies of [^{11}C]MS-275 using positron emission tomography. ACS Chem Neurosci 1:65–73

Horn PJ, Peterson CL (2002) Molecular biology. Chromatin higher order folding—wrapping up transcription. Science 297:1824–1827

Huang WJ, Wang YC, Chao SW, Yang CY, Chen LC, Lin MH, Hou WC, Chen MY, Lee TL, Yang P, Chang CI (2012) Synthesis and biological evaluation of ortho-Aryl N-hydroxycinnamides as potent histone deacetylase (HDAC) 8 isoform-selective inhibitors. Chem Med Chem 7:1815–1824

Hubbert C, Guardiola A, Shao R, Kawaguchi Y, Ito A, Nixon A, Yoshida M, Wang XF, Yao TP (2002) HDAC6 is a microtubule-associated deacetylase. Nature 417:455–458

Huber K, Superti-Furga G (2011) After the grape rush: sirtuins as epigenetic drug targets in neurodegenerative disorders. Bioorg Med Chem 19:3616–3624

Hwang JJ, Kim YS, Kim T, Kim MJ, Jeong IG, Lee JH, Choi J, Jang S, Ro S, Kim CS (2012) A novel histone deacetylase inhibitor, CG200745, potentiates anticancer effect of docetaxel in prostate cancer via decreasing Mcl-1 and Bcl-(XL). Invest New Drugs 30:1434–1442

Hymes KB (2010) The role of histone deacetylase inhibitors in the treatment of patients with cutaneous T-cell lymphoma. Clin Lymphoma Myeloma Leuk 10:98–109

Itazaki H, Nagashima K, Sugita K, Yoshida H, Kawamura Y, Yasuda Y, Matsumoto K, Ishii K, Uotani N, Nakai H et al (1990) Isolation and structural elucidation of new cyclotetrapeptides, trapoxins A and B, having detransformation activities as antitumor agents. J Antibiot (Tokyo) 43:1524–1532

Jain S, Zain J (2011) Romidepsin in the treatment of cutaneous T-cell lymphoma. J Blood Med 2:37–47

Jayaraman R, Pilla Reddy V, Pasha MK, Wang H, Sangthongpitag K, Yeo P, Hu CY, Wu X, Xin L, Goh E, New LS, Ethirajulu K (2011) Preclinical metabolism and disposition of SB939 (Pracinostat), an orally active histone deacetylase inhibitor, and prediction of human pharmacokinetics. Drug Metab Dispos 39:2219–2232

Jung M, Brosch G, Kolle D, Scherf H, Gerhauser C, Loidl P (1999) Amide analogues of trichostatin a as inhibitors of histone deacetylase and inducers of terminal cell differentiation. J Med Chem 42:4669–4679

Jung M (2001) Inhibitors of histone deacetylase as new anticancer agents. Curr Med Chem 8:1501–1511

Juvale DC, Kulkarni VV, Deokar HS, Wagh NK, Padhye SB, Kulkarni VM (2006) 3D-QSAR of histone deacetylase inhibitors: hydroxamate analogues. Org Biomol Chem 15:2858–2868

Kelly WK, O'Connor OA, Krug LM, Chiao JH, Heaney M, Curley T, MacGregore-Cortelli B, Tong W, Secrist JP, Schwartz L, Richardson S, Chu E, Olgac S, Marks PA, Scher H, Richon VM (2005) Phase I study of an oral histone deacetylase inhibitor, suberoylanilide hydroxamic acid, in patients with advanced cancer. J Clin Oncol 23:3923–3931

Kelly WK, Richon VM, O'Connor O, Curley T, MacGregor-Curtelli B, Tong W, Klang M, Schwartz L, Richardson S, Rosa E, Drobnjak M, Cordon-Cordo C, Chiao JH, Rifkind R, Marks PA, Scher H (2003) Phase I clinical trial of histone deacetylase inhibitor: suberoylanilide hydroxamic acid administered intravenously. Clin Cancer Res 9:3578–3588

Kijima M, Yoshida M, Sugita K, Horinouchi S, Beppu T (1993) Trapoxin, an antitumor cyclic tetrapeptide, is an irreversible inhibitor of mammalian histone deacetylase. J Biol Chem 268:22429–22435

Kim SC, Sprung R, Chen Y, Xu Y, Ball H, Pei J, Cheng T, Kho Y, Xiao H, Xiao L, Grishin NV, White M, Yang XJ, Zhao Y (2006) Substrate and functional diversity of lysine acetylation revealed by a proteomics survey. Mol Cell 23:607–618

Kleff S, Andrulis ED, Anderson CW, Sternglanz R (1995) Identification of a gene encoding a yeast histone H4 acetyltransferase. J Biol Chem 270:24674–24677

Klutchko S, Blankley CJ, Fleming RW, Hinkley JM, Werner AE, Nordin I, Holmes A, Hoefle ML, Cohen DM, Essenburg AD, Kaplan HR (1986) Synthesis of novel angiotensin converting enzyme inhibitor quinapril and related compounds. A divergence of structure-activity relationships for non-sulfhydryl types. J Med Chem 29:1953–1961

Kouzarides T (2000) Acetylation: a regulatory modification to rival phosphorylation? EMBO J 19:1176–1179

Kozikowski AP, Chen Y, Gaysin AM, Savoy DN, Billadeau DD, Kim KH (2008) Chemistry, biology, and QSAR studies of substituted biaryl hydroxamates and mercaptoacetamides as HDAC inhibitors-nanomolar-potency inhibitors of pancreatic cancer cell growth. ChemMedChem 3:487–501

Kulp SK, Chen CS, Wang DS, Chen CY (2006) Antitumor effects of a novel phenylbutyrate-based histone deacetylase inhibitor, (S)-HDAC-42, in prostate cancer. Clin Cancer Res 12:5199–5206

L'Hernault SW, Rosenbaum JL (1985a) Chlamydomonas alpha-tubulin is posttranslationally modified by acetylation on the epsilon-amino group of a lysine. Biochemistry 24:473–488

L'Hernault SW, Rosenbaum JL (1985b) Reversal of the posttranslational modification on chlamydomonas flagellar alpha-tubulin occurs during flagellar resorption. J Cell Biol 100:457–462

Lahm A, Paolini C, Pallaoro M, Nardi MC, Jones P, Neddermann P, Sambucini S, Bottomley MJ, Lo Surdo P, Carfi A, Koch U, De Francesco R, Steinkuhler C, Gallinari P (2007) Unraveling the hidden catalytic activity of vertebrate class IIa histone deacetylases. Proc Natl Acad Sci U S A 104:17335–17340

Lai CJ, Bao R, Tao X, Wang J, Atoyan R, Qu H, Wang DG, Yin L, Samson M, Forrester J, Zifcak B, Xu GX, DellaRocca S, Zhai HX, Cai X, Munger WE, Keegan M, Pepicelli CV, Qian C (2010) CUDC-101, a multitargeted inhibitor of histone deacetylase, epidermal growth factor receptor, and human epidermal growth factor receptor 2, exerts potent anticancer activity. Cancer Res 70:3647–3656

Lan-Hargest H-Y, Kaufman RJ, Wiech NL (2002) US Patent Appl US2002143196

Lin HY, Chen CS, Lin SP, Weng JR (2006) Targeting histone deacetylase in cancer therapy. Med Res Rev 26:397–413

Lin RJ, Nagy L, Inoue S, Shao W, Miller WH Jr, Evans RM (1998) Role of the histone deacetylase complex in acute promyelocytic leukaemia. Nature 391:811–814

Lu Q, Wang DS, Chen CS, Hu YD (2005) Structure-based optimization of phenylbutyrate-derived histone deacetylase inhibitors. J Med Chem 48:5530–5535

Luger K, Dechassa ML, Tremethick DJ (2012) New insights into nucleosome and chromatin structure: an ordered state or a disordered affair? Nat Rev Mol Cell Biol 13:436–447

Luger K, Mader AW, Richmond RK, Sargent DF, Richmond TJ (1997) Crystal structure of the nucleosome core particle at 2.8 a resolution. Nature 389:251–260

Luger K, Richmond TJ (1998) The histone tails of the nucleosome. Curr Opin Genet Dev 8:140–146

Lynch DR Jr, Washam JB, Newby LK (2012) QT interval prolongation and torsades de pointes in a patient undergoing treatment with vorinostat: a case report and review of the literature. Cardiol J 19:434–438

Madsen AS, Olsen CA (2012) Profiling of substrates for zinc-dependent lysine deacylase enzymes: HDAC3 exhibits decrotonylase activity in vitro. Angew Chem Int Ed Engl 51:9083–9087

Mai A, Massa S, Pezzi R, Simeoni S, Rotili D, Nebbioso A, Scognamiglio A, Altucci L, Loidl P, Brosch G (2005a) Class II (IIa)-selective histone deacetylase inhibitors. 1. Synthesis and biological evaluation of novel (aryloxopropenyl)pyrrolyl hydroxyamides. J Med Chem 48:3344–3353

Mai A, Massa S, Rotili D, Cerbara I, Valente S, Pezzi R, Simeoni S, Ragno R (2005b) Histone deacetylation in epigenetics: an attractive target for anticancer therapy. Med Res Rev 25:261–309

Mai A, Massa S, Valente S, Simeoni S, Ragno R, Bottoni P, Scatena R, Brosch G (2006) Aroyl-pyrrolyl hydroxyamides: influence of pyrrole C4-phenylacetyl substitution on histone deacetylase inhibition. Chem Med Chem 1:225–237

Malik HS, Henikoff S (2003) Phylogenomics of the nucleosome. Nat Struct Biol 10:882–891

Mandl-Weber S, Meinel FG, Jankowsky R, Oduncu F, Schmidmaier R, Baumann P (2010) The novel inhibitor of histone deacetylase resminostat (RAS2410) inhibits proliferation and induces apoptosis in multiple myeloma (MM) cells. Br J Haematol 149:518–528

Mann BS, Johnson JR, Cohen MH, Justice R, Pazdur R (2007) FDA approval summary: vorinostat for treatment of advanced primary cutaneous T-cell lymphoma. Oncologist 12:1247–1252

Marks PA (2007) Discovery and development of SAHA as an anticancer agent. Oncogene 26:1351–1356

Marks PA, Breslow R (2007) Dimethyl sulfoxide to vorinostat: development of this histone deacetylase inhibitor as an anticancer drug. Nat Biotechnol 25:84–90

Marsoni S, Damia G, Camboni G (2008) A work in progress: the clinical development of histone deacetylase inhibitors. Epigenetics 3:164–171

Marwick C (1983) New drugs selectively inhibit kidney stone formation. JAMA 250:321–322

Massa S, Artico M, Corelli F, Mai A, Di Santo R, Cortes S, Marongiu ME, Pani A, La Colla P (1990) Synthesis and antimicrobial and cytotoxic activities of pyrrole-containing analogues of trichostatin A. J Med Chem 33:2845–2849

Massa S, Mai A, Sbardella G, Esposito M, Ragno R, Loidl P, Brosch G (2001) 3-(4-aroyl-1H-pyrrol-2-yl)-N-hydroxy-2-propenamides, a new class of synthetic histone deacetylase inhibitors. J Med Chem 44:2069–2072

Mercurio C, Minucci S, Pelicci PG (2010) Histone deacetylases and epigenetic therapies of hematological malignancies. Pharmacol Res 62:18–34

Miller TA, Witter DJ, Belvedere S (2003) Histone deacetylase inhibitors. J Med Chem 46:5097–5116

Moffat D, Patel S, Day F, Belfield A, Donald A, Rowlands M, Wibawa J, Brotherton D, Stimson L, Clark V, Owen J, Bawden L, Box G, Bone E, Mortenson P, Hardcastle A, van Meurs S, Eccles S, Raynaud F, Aherne W (2010) Discovery of 2-(6-{[(6-fluoroquinolin-2-yl)methyl]amino}bicyclo[3.1.0]hex-3-yl)-N-hydroxypyrim idine-5-carboxamide (CHR-3996), a class I selective orally active histone deacetylase inhibitor. J Med Chem 53:8663–8678

Muri EMF, Nieto MJ, Sindelar RD, Williamson JS (2002) Hydroxamic acids as pharmacological agents. Curr Med Chem 9:1631–1653

Nakajima H, Kim YB, Terano H, Yoshida M, Horinouchi S (1998) FR901228, a potent antitumor antibiotic, is a novel histone deacetylase inhibitor. Exp Cell Res 241:126–133

Neri P, Bahlis NJ, Lonial S (2012) Panobinostat for the treatment of multiple myeloma. Expert Opin Investig Drugs 21:733–747

Novotny-Diermayr V, Sangthongpitag K, Hu CY, Wu X, Sausgruber N, Yeo P, Greicius G, Pettersson S, Liang AL, Loh YK, Bonday Z, Goh KC, Hentze H, Hart S, Wang H, Ethirajulu K, Wood JM (2010) SB939, a novel potent and orally active histone deacetylase inhibitor with high tumor exposure and efficacy in mouse models of colorectal cancer. Mol Cancer Ther 9:642–652

Rambaldi A, Dellacasa CM, Finazzi G, Carobbio A, Ferrari ML, Guglielmelli P, Gattoni E, Salmoiraghi S, Finazzi MC, Di Tollo S, D'Urzo C, Vannucchi AM, Barosi G, Barbui T (2012) A pilot study of the histone-deacetylase inhibitor givinostat in patients with JAK2V617F positive chronic myeloproliferative neoplasms. Br J Haematol 150:446–455

Reid AE, Hooker J, Shumay E, Logan J, Shea C, Kim SW, Collins S, Xu Y, Volkow N, Fowler JS (2009) Evaluation of 6-([(^{18})F]fluoroacetamido)-1-hexanoicanilide for PET imaging of histone deacetylase in the baboon brain. Nucl Med Biol 36:247–258

Remiszewski S, Sambucetti L, Atadja P, Bair K, Cornell W, Green M, Howell K, Jung M, Kwon P, Trogani N, Walker H (2002) Inhibitors of human histone deacetylase: synthesis and enzyme and cellular activity of straight chain hydroxamates. J Med Chem 45:753–757

Remiszewski SW, Sambucetti LC, Bair KW, Bontempo J, Cesarz D, Chandramouli N, Chen R, Cheung M, Cornell-Kennon S, Dean K, Diamantidis G, France D, Green MA, Howell KL, Kashi R, Kwon P, Lassota P, Martin MS, Mou Y, Perez LB, Sharma S, Smith T, Sorensen E, Taplin F, Trogani N, Versace R, Walker H, Weltchek-Engler S, Wood A, Wu A, Atadja P (2003) N-hydroxy-3-phenyl-2-propenamides as novel inhibitors of human histone deacetylase with in vivo antitumor activity: discovery of (2E)-N-hydroxy-3-[4-[[(2-hydroxyethyl)[2-(1H-indol-3-yl)ethyl]amino]methyl]phenyl]-2-propenamide (NVP-LAQ824). J Med Chem 46:4609–4624

Reuben RC, Khanna PL, Gazitt Y, Breslow R, Rifkind RA, Marks PA (1978) Inducers of erythroleukemic differentiation. Relationship of structure to activity among planar-polar compounds. J Biol Chem 253:4214–4218

Reuben RC, Wife RL, Breslow R, Rifkind RA, Marks PA (1976) A new group of potent inducers of differentiation in murine erythroleukemia cells. Proc Natl Acad Sci U S A 73:862–866

Richon VM, Emiliani S, Verdin E, Webb Y, Breslow R, Rifkind RA, Marks PA (1998) A class of hybrid polar inducers of transformed cell differentiation inhibits histone deacetylases. Proc Natl Acad Sci U S A 95:3003–3007

Richon VM, O'Brien JP (2002) Histone deacetylase inhibitors: a new class of potential therapeutic agents for cancer treatment. Clin Cancer Res 8:662–624

Richon VM, Webb Y, Merger R, Sheppard T, Jursic B, Ngo L, Civoli F, Breslow R, Rifkind RA, Marks PA (1996) Second generation hybrid polar compounds are potent inducers of transformed cell differentiation. Proc Natl Acad Sci U S A 93:5705–5708

Riggs MG, Whittaker RG, Neumann JR, Ingram VM (1977) n-Butyrate causes histone modification in HeLa and Friend erythroleukaemia cells. Nature 268:462–464

Sankaranarayanapillai M, Tong WP, Yuan Q, Bankson JA, Dafni H, Bornmann WG, Soghomonyan S, Pal A, Ramirez MS, Webb D, Kaluarachchi K, Gelovani JG, Ronen SM (2008) Monitoring histone deacetylase inhibition in vivo: noninvasive magnetic resonance spectroscopy method. Mol Imaging 7:92–100

Santo L, Hideshima T, Kung AL, Tseng JC, Tamang D, Yang M, Jarpe M, van Duzer JH, Mazitschek R, Ogier WC, Cirstea D, Rodig S, Eda H, Scullen T, Canavese M, Bradner J, Anderson KC, Jones SS, Raje N (2012) Preclinical activity, pharmacodynamic, and pharmacokinetic properties of a selective HDAC6 inhibitor, ACY-1215, in combination with bortezomib in multiple myeloma. Blood 119:2579–2589

Schuetz A, Min J, Allali-Hassani A, Schapira M, Shuen M, Loppnau P, Mazitschek R, Kwiatkowski NP, Lewis TA, Maglathin RL, McLean TH, Bochkarev A, Plotnikov AN, Vedadi M, Arrowsmith CH (2008) Human HDAC7 harbors a class IIa histone deacetylase-specific zinc binding motif and cryptic deacetylase activity. J Biol Chem 283:11355–11363

Selvi RB, Kundu TK (2009) Reversible acetylation of chromatin: implication in regulation of gene expression, disease and therapeutics. Biotechnol J 4:375–390

Shimizu T, Tolcher AW, LoRusso P, Papadopoulos K, Patnaik A, Smith L, Keegan M (2010) 364 The first-in-human, first-in-class study of CUDC-101, a multi-targeted inhibitor of HDAC, EGFR, and HER2: A Phase I study in patients with advanced cancer. Eur J Cancer Suppl 8:115

Shultz MD, Cao X, Chen CH, Cho YS, Davis NR, Eckman J, Fan J, Fekete A, Firestone B, Flynn J, Green J, Growney JD, Holmqvist M, Hsu M, Jansson D, Jiang L, Kwon P, Liu G, Lombardo F, Lu Q, Majumdar D, Meta C, Perez L, Pu M, Ramsey T, Remiszewski S, Skolnik S, Traebert M, Urban L, Uttamsingh V, Wang P, Whitebread, Whitehead L, Yan-Neale Y, Yao YM, Zhou L, Atadja P (2011) Optimization of the in vitro cardiac safety of hydroxamate-based histone deacetylase inhibitors. J Med Chem 54:4752–4772

Simon M, North JA, Shimko JC, Forties RA, Ferdinand MB, Manohar M, Zhang M, Fishel R, Ottesen JJ, Poirier MG (2011) Histone fold modifications control nucleosome unwrapping and disassembly. Proc Natl Acad Sci U S A 108:12711–12716

Singh BN, Zhang G, Hwa YL, Li J, Dowdy SC, Jiang SW (2010) Nonhistone protein acetylation as cancer therapy targets. Expert Rev Anticancer Ther 10:935–954

Siwak CT, Tapp PD, Milgram NW (2003) Adrafinil disrupts performance on a delayed nonmatching-to-position task in aged beagle dogs. Pharmacol Biochem Behav 76:161–168

Somoza JR, Skene RJ, Katz BA, Mol C, Ho JD, Jennings AJ, Luong C, Arvai A, Buggy JJ, Chi E, Tang J, Sang BC, Verner E, Wynands R, Leahy EM, Dougan DR, Snell G, Navre M, Knuth MW, Swanson RV, McRee DE, Tari LW (2004) Structural snapshots of human HDAC8 provide insights into the class I histone deacetylases. Structure 12:1325–1334

Steele NL, Plumb JA, Vidal L, Tjornelund J, Knoblauch P, Rasmussen A, Ooi CE, Buhl-Jensen P, Brown R, Evans TR, DeBono JS (2008) A phase 1 pharmacokinetic and pharmacodynamic study of the histone deacetylase inhibitor belinostat in patients with advanced solid tumors. Clin Cancer Res 14:804–810

Steinman DH, Curtin ML, Garland RB, Davidsen SK, Heyman HR, Holms JH, Albert DH, Magoc TJ, Nagy IB, Marcotte PA, Li J, Morgan DW, Hutchins C, Summers JB (1998) The design, synthesis, and structure-activity relationships of a series of macrocyclic MMP inhibitors. Bioorg Med Chem Lett 8:2087–2092

Sternson SM, Wong JC, Grozinger CM, Schreiber SL (2001) Synthesis of 7200 small molecules based on a substructural analysis of the histone deacetylase inhibitors trichostatin and trapoxin. Org Lett 3:4239–4242

Tanaka M, Levy J, Terada M, Breslow R, Rifkind RA, Marks PA (1975) Induction of erythroid differentiation in murine virus infected eythroleukemia cells by highly polar compounds. Proc Natl Acad Sci U S A 72:1003–1036

Tang W, Luo T, Greenberg EF, Bradner JE, Schreiber SL (2011) Discovery of histone deacetylase 8 selective inhibitors. Bioorg Med Chem Lett 21:2601–2605

Taunton J, Hassig CA, Schreiber SL (1996) A mammalian histone deacetylase related to the yeast transcriptional regulator Rpd3p. Science 272:408–411

Tessier P, Smil DV, Wahhab A, Leit S, Rahil J, Li Z, Deziel R, Besterman JM (2009) Diphenylmethylene hydroxamic acids as selective class IIa histone deacetylase inhibitors. Bioorg Med Chem Lett 19:5684–5688

Thaler F (2012) Current trends in the development of histone deacetylase inhibitors: a review of recent patent applications. Pharm Pat Analyst 1:75–90

Thaler F, Colombo A, Mai A, Amici R, Bigogno C, Boggio R, Cappa A, Carrara S, Cataudella T, Fusar F, Gianti E, Joppolo di Ventimiglia S, Moroni M, Munari D, Pain G, Regalia N, Sartori L, Vultaggio S, Dondio G, Gagliardi S, Minucci S, Mercurio C, Varasi M (2010a) Synthesis and biological evaluation of N-hydroxyphenylacrylamides and N-hydroxypyridin-2-ylacrylamides as novel histone deacetylase inhibitors. J Med Chem 53:822–829

Thaler F, Colombo A, Mai A, Bigogno C, Boggio R, Carrara S, Joppolo di Ventimiglia S, Munari D, Regalia N, Dondio G, Gagliardi S, Minucci S, Mercurio C, Varasi M (2010b) Synthesis

and biological characterization of amidopropenyl-hydroxamates as HDAC inhibitors. ChemMedChem 5:1359–1372

Thaler F, Mai A, Colombo A, Bigogno C, Boggio R, Regalia N, Rozio MG, Vultaggio S, Gagliardi S, Minucci S, Mercurio C, Varasi M (2009) Synthesis and structure-activity relationships of phenyloxopropenyl- and amidopropenyl-hydroxamic acid derivatives as HDAC inhibitors. Paper presented at the abstract paper. XXIII Congresso Nazionale della Società Chimica Italiana, Sorrento

Thaler F, Varasi M, Carenzi G, Colombo A, Abate A, Bigogno C, Boggio R, Carrara S, Cataudella T, Dal Zuffo R, Reali V, Vultaggio S, Dondio G, Gagliardi S, Minucci S, Mercurio C (2012) Spiro[chromane-2,4′-piperidine]-based histone deacetylase inhibitors with improved in vivo activity. Chem Med Chem 7:709–721

Tong WG, Wei Y, Stevenson W, Kuang SQ, Fang Z, Zhang M, Arts J, Garcia-Manero G (2010) Preclinical antileukemia activity of JNJ-26481585, a potent second-generation histone deacetylase inhibitor. Leuk Res 34:221–228

Tsuji N, Kobayashi M, Nagashima K, Wakisaka Y, Koizumi K (1976) A new antifungal antibiotic, trichostatin. J Antibiot (Tokyo) 29:1–6

Ueda H, Nakajima H, Hori Y, Fujita T, Nishimura M, Goto T, Okuhara M (1994) FR901228, a novel antitumor bicyclic depsipeptide produced by chromobacterium violaceum No. 968. I. Taxonomy, fermentation, isolation, physico-chemical and biological properties, and antitumor activity. J Antibiot (Tokyo) 47:301–310

Vannini A, Volpari C, Filocamo G, Casavola EC, Brunetti M, Renzoni D, Chakravarty P, Paolini C, De Francesco R, Gallinari P, Steinkuhler C, Di Marco S (2004) Crystal structure of a eukaryotic zinc-dependent histone deacetylase, human HDAC8, complexed with a hydroxamic acid inhibitor. Proc Natl Acad Sci U S A 101:15064–15069

Vansteenkiste J, Van Cutsem E, Dumez H, Chen C, Ricker JL, Randolph SS, Schoffski P (2008) Early phase II trial of oral vorinostat in relapsed or refractory breast, colorectal, or non-small cell lung cancer. Invest New Drugs 26:483–488

Varasi M, Thaler F, Abate A, Bigogno C, Boggio R, Carenzi G, Cataudella T, Dal Zuffo R, Fulco MC, Rozio MG, Mai A, Dondio G, Minucci S, Mercurio C (2011) Discovery, synthesis, and pharmacological evaluation of spiropiperidine hydroxamic acid based derivatives as structurally novel histone deacetylase (HDAC) inhibitors. J Med Chem 54:3051–3064

Venkatesh PR, Goh E, Zeng P, New LS, Xin L, Pasha MK, Sangthongpitag K, Yeo P, Kantharaj E (2007) In vitro phase I cytochrome P450 metabolism, permeability and pharmacokinetics of SB639, a novel histone deacetylase inhibitor in preclinical species. Biol Pharm Bull 30:1021–1024

Verdin E, Dequiedt F, Kasler HG (2003) Class II histone deacetylases: versatile regulators. Trends Genet 19:286–293

Wada C, Frey R, Ji Z, Curtin M, Garland R, Li J, Pease L, Guo J, Glaser K, Marcotte P, Richardson P, Murphy S, Bouska J, Tapang P, Magoc T, Albert D, Davidsen S, Michaelides M (2003) Alpha-keto amides as inhibitors of histone deacetylase. Bioorg Med Chem Lett 13:3331–3335

Wang D (2009) Computational studies on the histone deacetylases and the design of selective histone deacetylase inhibitors. Curr Top Med Chem 9:241–256

Wang DF, Helquist P, Wiech NL, Wiest O (2005) Toward selective histone deacetylase inhibitor design: homology modeling, docking studies, and molecular dynamics simulations of human class I histone deacetylases. J Med Chem 48:6936–6947

Wang D-F, Wiest O, Helquist P, Lan-Hargestb H-Y, Wiech NL (2004) QSAR Studies of PC-3 cell line inhibition activity of TSA and SAHA-like hydroxamic acids. Bioorg Med Chem Lett 14:707–711

Wang H, Yu N, Chen D, Lee KC, Lye PL, Chang JW, Deng W, Ng MC, Lu T, Khoo ML, Poulsen A, Sangthongpitag K, Wu X, Hu C, Goh KC, Wang X, Fang L, Goh KL, Khng HH, Goh SK, Yeo P, Liu X, Bonday Z, Wood JM, Dymock BW, Kantharaj E, Sun ET (2011) Discovery of (2E)-3-{2-butyl-1-[2-(diethylamino)ethyl]-1H-benzimidazol-5-yl}-N-hydroxyacrylami   de

(SB939), an orally active histone deacetylase inhibitor with a superior preclinical profile. J Med Chem 54:4694–4720

Wang H, Yu N, Song H, Chen D, Zou Y, Deng W, Lye PL, Chang J, Ng M, Sun ET, Sangthongpitag K, Wang X, Wu X, Khng HH, Fang L, Goh SK, Ong WC, Bonday Z, Stunkel W, Poulsen A, Entzeroth M (2009) N-Hydroxy-1,2-disubstituted-1H-benzimidazol-5-yl acrylamides as novel histone deacetylase inhibitors: design, synthesis, SAR studies, and in vivo antitumor activity. Bioorg Med Chem Lett 19:1403–1408

Watson PJ, Fairall L, Santos GM, Schwabe JW (2012) Structure of HDAC3 bound to co-repressor and inositol tetraphosphate. Nature 481:335–340

Woo SH, Frechette S, Khalil EA, Bouchain G, Vaisburg A, Bernstein N, Moradei O, Leit S, Allan M, Fournel M, Trachy-Bourget M-C, Li Z, Besterman JM, Delorme D (2002) Structurally simple trichostatin A-like staight chain hydroxamates as potent histone deacetylase inhibitors. J Med Chem 45:2877–2885

Yang XJ, Gregoire S (2005) Class II histone deacetylases: from sequence to function, regulation, and clinical implication. Mol Cell Biol 25:2873–2884

Yang XJ, Seto E (2008) Lysine acetylation: codified crosstalk with other posttranslational modifications. Mol Cell 31:449–461

Yao YL, Yang WM (2011) Beyond histone and deacetylase: an overview of cytoplasmic histone deacetylases and their nonhistone substrates. J Biomed Biotechnol 2011:146493

Yong W, Goh B, Toh H, Soo R, Diermayr V, Goh A, Ethirajulu K, Lee S, Seah E, Zhu J (2009) Phase I study of SB939 three times weekly for 3 weeks every 4 weeks in patients with advanced solid malignancies. J Clin Oncol 27 (abstr 2560)

Yoshida M, Hoshikawa Y, Koseki K, Mori K, Beppu T (1990a) Structural specificity for biological activity of trichostatin A, a specific inhibitor of mammalian cell cycle with potent differentiation-inducing activity in Friend leukemia cells. J Antibiot (Tokyo) 43:1101–1106

Yoshida M, Kijima M, Akita M, Beppu T (1990b) Potent and specific inhibition of mammalian histone deacetylase both in vivo and in vitro by trichostatin A. J Biol Chem 265:17174–17179

Yoshida M, Nomura S, Beppu T (1987) Effects of trichostatins on differentiation of murine erythroleukemia cells. Cancer Res 47:3688–3691

Younes A, Oki Y, Bociek RG, Kuruvilla J, Fanale M, Neelapu S, Copeland A, Buglio D, Galal A, Besterman J, Li Z, Drouin M, Patterson T, Ward MR, Paulus JK, Ji Y, Medeiros LJ, Martell RE (2011) Mocetinostat for relapsed classical Hodgkin's lymphoma: an open-label, single-arm, phase 2 trial. Lancet Oncol 12:1222–1228

Xie A, Liao C, Li Z, Ning Z, Hu W, Lu X, Shi L, Zhou J (2004) Quantitative structure-activity relationship study of histone deacetylase inhibitors. Curr Med Chem Anticancer Agents 4:273–299

Zhang Y, Fang H, Feng J, Jia Y, Wang X, Xu W (2011a) Discovery of a tetrahydroisoquinoline-based hydroxamic acid derivative (ZYJ-34c) as histone deacetylase inhibitor with potent oral antitumor activities. J Med Chem 54:5532–5539

Zhang Y, Feng J, Liu C, Zhang L, Jiao J, Fang H, Su L, Zhang X, Zhang J, Li M, Wang B, Xu W (2010) Design, synthesis and preliminary activity assay of 1,2,3,4-tetrahydroisoquinoline-3-carboxylic acid derivatives as novel histone deacetylases (HDACs) inhibitors. Bioorg Med Chem 18:1761–1772

Zhang Y, Feng J, Jia Y, Wang X, Zhang L, Liu C, Fang H, Xu W (2011b) Development of tetrahydroisoquinoline-based hydroxamic acid serivatives: potent histone deacetylase inhibitors with marked in vitro and in vivo antitumor activities. J Med Chem 54:2823–2838

Hydroxamates as Ribonucleotide Reductase Inhibitors

Arijit Basu and Barij Nayan Sinha

Abstract This chapter presents the progress in the design and discovery of hydroxamic acids acting as ribonucleotide reductase (RR) inhibitors. The RR inhibitors act as anticancer agents. The initial sections present a background about hydroxamic acids, role of RR inhibitors as anticancer agents, and information on three-dimensional structure of RR. The remaining sections, discuss the mode of action of these compounds and their progress in computer-aided drug design. Finally, conclusive remarks and directives toward future research are discussed.

Keywords Hydroxamic acid · Ribonucleotide reductase · Radical scavengers · Di-iron center · Ion chelators · Drug designing

Abbreviations

BHA   Butylated hydroxyanisole
CoMFA   Comparative molecular field analysis
CoMSIA   Comparative molecular similarity index analysis
EPR   Electron paramagnetic resonance
HAG   N-hydroxy amino guanidine
HDAC   Histone deacetylase
HG   Hydroxyguanidines
hRRM2   Human ribonucleotide reductase M2 subunit
HSC   Hydroxysemicarbazones
HU   Hydroxyurea
LOX   Lipoxygenase
MD   Molecular dynamics

A. Basu (✉) · B. N. Sinha
Department of Pharmaceutical Sciences, Birla Institute of Technology, Mesra, Ranchi, Jharkhand 835215, India
e-mail: arijit4uin@gmail.com; abasu@bitmesra.ac.in

B. N. Sinha
e-mail: bnsinha@bitmesra.ac.in

MMP	Matrix metalloproteinases
PDF	Peptide deformylase
QM/MM	Quantum mechanics/molecular mechanics
RR	Ribonucleotide reductase
RRR2	Ribonucleotide reductase R2 subunit
VS	Virtual screening

Contents

1 Introduction

A hydroxamic acid is a class of chemical compounds sharing the same functional group in which a hydroxylamine is inserted into a carboxylic acid. Its general structure is R–CO–NH–OH, where R as is an organic residue, CO a carbonyl group, and NH–OH the hydroxyl amine moiety. Hydroxamates have been an interesting chemical scaffold for medicinal chemists and explored since long as an anticancer pharmacophore. They are also proven metal ion chelators and free radical scavengers. Many hydroxamates are in clinical use, a few are undergoing clinical trial, and some made it to the advanced stages of trials before they were withdrawn. They occupied a special place in anticancer drug discovery. It has been explored against a number of anticancer targets such as matrix metalloproteinases (MMP) (Yadav et al. 2011), histone deacetylase (HDAC), peptide deformylase (PDF) (Chen and Yuan 2005), lipoxygenase (LOX) (Pergola and Werz 2010), and ribonucleotide reductase (RR). In the current chapter, we focused only on those hydroxamates that have RR inhibitory property.

DNA is made up of deoxyribose subunits. During cell division a large pool of deoxyribose is essential for the replication process. Synthesis of deoxyribose has been identified as the rate-limiting step in the entire replication process. The

Fig. 1 Mechanism of action of hydroxamates and related compounds
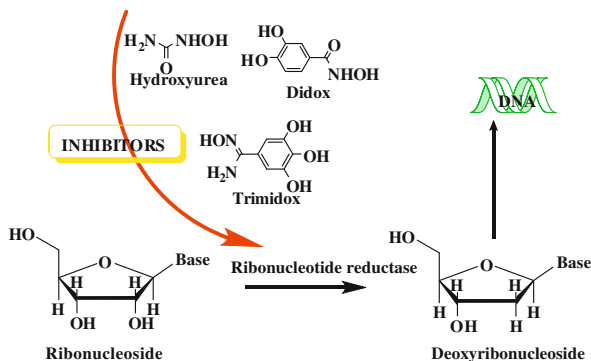
enzyme RR brings about the conversion of ribose to deoxyribose. Therefore, RR has been found to play an important role in DNA replication. It provides the much-needed pool of deoxyriboses during cell division. Cancer cells, unlike normal cells in our body, divide at a faster rate, and require more deoxyribose than normal. Inactivation of the enzyme RR starves the cells from the deoxyribonucleosides, which ceases DNA replication and cell division. RR is a validated anticancer drug target that has been explored extensively for many years. The mechanism of action of these analogs is given in Fig. 1. In the subsequent sections, we have compiled the information about those hydroxamates that have been reported as RR inhibitors.

2 Ribonucleotide Reductase and Its Inhibitors

The ribonucleotide reductase catalyzes the reduction of ribonucleotides to their corresponding deoxyribonucleotides, which are the building blocks for DNA in all living cells (Reichard and Ehrenberg 1983). There are three main classes (I, II, and III) of RR based on different metal cofactors. Class I enzymes are found in all eukaryotic organisms yeast, algae, plants, and mammals. It is also expressed in some prokaryotes and viruses. Class I is further divided into three subclasses (Ia, Ib, and Ic) based on polypeptide sequence homologies and their overall allosteric regulation behavior (Reichard 1993; Kolberg et al. 2004). Human RR belongs to Class Ia (Jordan and Reichard 1998). Reduction of ribonucleotides to deoxyribonucleotides is the rate-limiting step of DNA synthesis. Therefore, inactivation of RR ceases DNA synthesis and consequently inhibits cell proliferation.

Structurally, RR is made up of two subunits: large subunit called R1 (M1 for human enzyme), and the small one called R2 (M2 for human enzyme) (Shao et al. 2006). R1 is the actual substrate binding site that participates in the reduction of ribonucleotides. R2 subsite contains an oxygen-linked diferric (Fe^{2+}) center that generates a free radical (from Tyr-176 in human). Once this free radical is

generated, it is propagated by a relay mechanism to the active site in R1 separated by distance of 35 Å (Eklund et al. 2001; Shao et al. 2006). This free radical is essential for nucleotide reduction process taking place at the substrate binding site in R1 (Shao et al. 2006; Cerqueira et al. 2005; Nocentini 1996; Smith and Karp 2003; Reichard and Ehrenberg 1983; Jordan and Reichard 1998; Nordlund et al. 1990). RR is a validated and significantly explored anticancer target. Many inhibitors of RR have been reported, and some are even in clinical use.

RR inhibitors that act on the R2 subunit are classified as: (a) metal ion chelators and (b) free radical scavengers. Radical scavengers are a class of RR inhibitors that act by quenching the tyrosyl free radical in the R2 site. Numerous molecules like hydroxyurea (HU), didox, trimidox, hydroxyguanidines (HGs), hydroxamic acids, hydroxysemicarbazides (HSCs), and amidoximes were reported to quench the tyrosyl free radical, for inhibiting the enzyme RR (Cerqueira et al. 2005; Shao et al. 2006). These molecules are collectively called as radical scavengers (Fontecave 1998). Hydroxamic acids also interact with the di-iron center of RR. Iron chelation studies have shown that the hydroxamate ion complexes with iron(III) to form a five-membered ring (Monzyk and Crumbliss 1979). The chelation pattern may be different in the case of di-iron center of RR, but such iron complexation studies in the isolated system depicts the potential of hydroxamates to chelate with iron. Most of the hydroxamic acid derivatives act as both metal ion chelators and free radical scavengers. This feature makes them a unique scaffold for RR drug designing. Detailed description on the mode of inhibition has been included in the
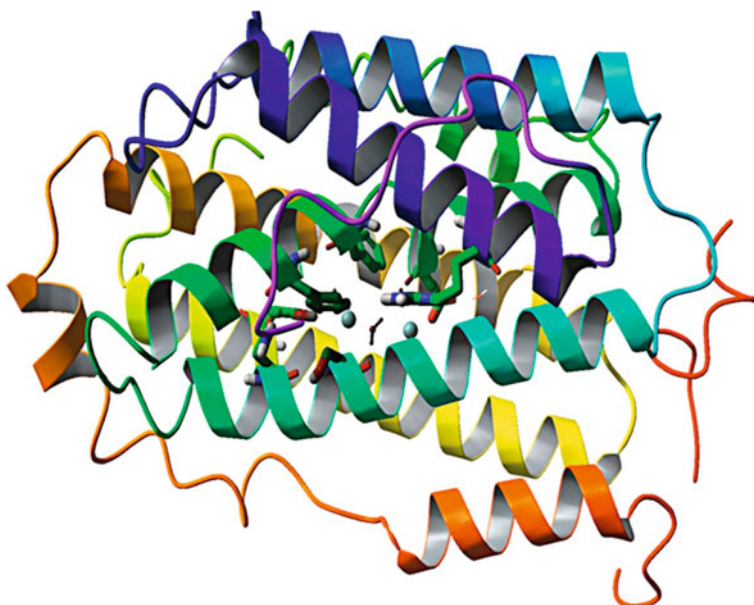
Fig. 2 Three dimensional structure of RR. The inset depicts the active site residues for hRRM2
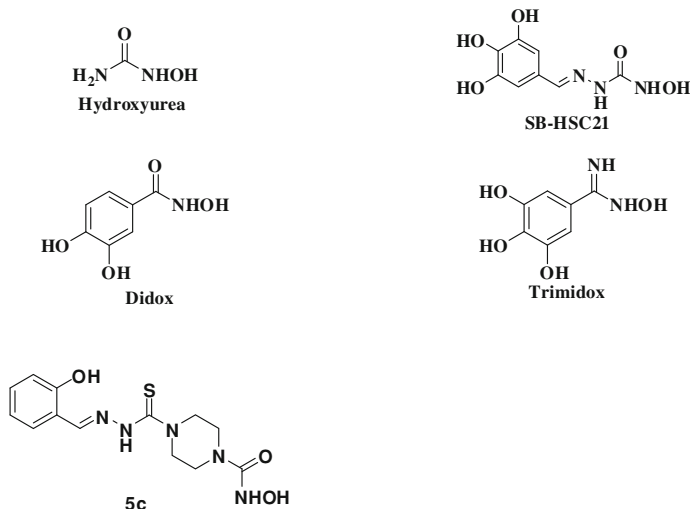
Fig. 3 Structures of a few established RRM2 inhibitors. Trimidox ($IC_{50} = 5$ μM, hRRM2), SB-HSC21($IC_{50} = 11$ μM, hRRM2), **5c**, HDAC8: $IC_{50} = 33.67$ μM, HL60: $IC_{50} = 0.6$ μM

later sections of this chapter. The architecture of the RRR2 active site is depicted in Fig. 2.

2.1 Hydroxamates as RR Inhibitors

Hydroxamic acids have been widely reported as anticancer agents, majority as HDAC inhibitors (Saban and Bujak 2009). However, their importance as RR inhibitors is also significant. We are discussing a few important hydroxamic acid derivatives, which were explored as RR inhibitors in the past (Fig. 3).

2.1.1 Discovery of Hydroxyurea

Hydroxyurea (HU) was discovered in 1963 (Stearns et al. 1963). Later it was found to specifically inhibit DNA synthesis (Young and Hodas 1964). The mode of action of HU was unclear at this stage, but its discovery initiated the exploration of similar kind of compounds. Later in 1968, (Krakoff et al. 1968) Krakoff et al. reported HU as an RR inhibitor. It was found to quench the tyrosyl free radical of R2 subunit of RR (Elford 1968; Adams and Lindsay 1967; Krakoff et al. 1968). HU belongs to the family of antimetabolites that was approved by Food and Drug Administration (FDA) for clinical use in 1967 (Donehower 1992). It has been used in the treatment of many neoplastic diseases such as myelocytic leukemia (Silver

et al. 1999; Goldman 1997; Hehlmann et al. 2003), ovary carcinoma, cervical carcinoma (Piver et al. 1983), melanoma, meningioma (Schrell et al. 1996, 1997). The main disadvantage of HU is the need for administration of large doses in order to maintain its effectiveness, as it is a relatively weak inhibitor of the enzyme in vitro (IC_{50} = 500 μM) (Elford 1968; Moore 1969).

HU is the first hydroxamic acid derivative established as RR inhibitor. It acts by interfering with the radical generation process, which takes place in the R2 subunit of the enzyme. However, the exact mode of inhibition is still unclear. A few studies reported that HU quenches the tyrosyl free radical. A few other reports suggested iron chelation as the mechanism of enzyme inhibition. We presume both free radical quenching and iron chelation may be occurring simultaneously. HU was a huge success; it initiated the exploration of different chemical moieties with similar pharmacophoric features, for example, HSCs, hydroxamic acids and amidoximes.

2.1.2 Discovery of Didox

Didox, is chemically 3,4-dihydroxy benzhydroxamic acid (Fig. 3) was discovered in 1979, by Van′t Riet et al. They reported the synthesis and antineoplastic evaluation of a series of hydroxy- and amino- substituted benzohydroxamic acids, and didox was one among them (Van′t Riet et al. 1979b). Later didox was found to be active in the NCI tumor panel, L1210 and P388 leukemia cell lines, B16 melanoma, Lewis lung carcinoma, Colo38, CDRF mammary tumor, and several human tumor xenografts, etc. (Elford and van′t Riet 1985). Didox was also found more effective than HU in in vivo screening. Its LD_{10} value was reported to be 643 mg/kg when given as a single dose.

Based on these preclinical studies, Phase 1 clinical trial for didox was carried out using 34 patients (Veale et al. 1988). Phase I studies demonstrated didox as safe and well tolerated, with few cases of hepatic and renal toxicity (Veale et al. 1988). Subsequent post phase 1 studies showed promise in combination therapy. These results prompted a phase II study, but didox was found less responsive in the treatment of advanced breast cancer patients and hence it was dropped from further trials. Didox had an appreciable safety profile in both the phases of clinical trials, but lacked therapeutic efficacy as a single chemotherapeutic agent. Didox had been a promising RR inhibitor with excellent in vitro and preclinical profile. Clinical studies for didox are still warranted at higher doses and combination therapy. Therefore, didox remained a promising molecule with more avenues yet to explore.

Didox have also been explored significantly post phase II clinical trial. It was proved to be an excellent radical scavenger (Tihan et al. 1991), 17 times more potent than HU. It has been explored widely alone or in combination for many types of cancers (Inayat et al. 2002; Fritzer-Szekeres et al. 1997; Raje et al. 2006).

2.1.3 Hydroxysemicarbazides

Hydroxamic acids have been widely reported as anticancer agents. However, most of the hydroxamic acid derivatives have been reported as HDAC inhibitors, and very few as RR inhibitors. These compounds were also found to inhibit the R2 subunit of the enzyme RR. Ren et al. (2002) studied the inhibitory activities of Schiff bases of HSC against eight human and murine tumor cell lines and one noncancer cell line using MTS/PES microculture tetrazolium and methylene blue assays. One compound was found to have IC_{50} of 2.8 and 6.5 μM against HU and gemcitabine resistant KB cells, respectively, but had no cross-resistance with HU or gemcitabine. Later Ren et al. (2002) synthesized 30 more Schiff's bases of HSC and screened them against L1210 murine leukemia cells. 17 out of 30 compounds showed higher inhibitory activity than HU (Ren et al. 2002). Later Shao et al. (Shao et al. 2005) reported the hRRM2 assay for a number of HSCs. Among them SB-HSC21 ($IC_{50} = 11$ μM) was found to be most promising. The development of hRRM2 specific assay has been the key to understand the mode of action of these analogs.

Hydroxamic acids and HSCs have shown promise as radical scavengers. They also have strong track record as HDAC inhibitors. Hydroxamates have the background as both HDAC and RR inhibitors. This background provided us the basis to explore its dual RR/HDAC inhibitory property. From our lab, we have reported a few piperazine linked hydroxamates as HDAC inhibitors such as **5c** (HDAC8, $IC_{50} = 33.67$ μM), which also showed additional RR inhibitory property (HL60, $IC_{50} = 0.6$ μM) (Chetan et al. 2010). This is a valid approach for designing anticancer drugs and can be explored in future.

2.2 Related Analogs with Similar Pharmacophoric Features

2.2.1 Amidoximes and Hydroxyguanidines

Anticancer activity of amidoxime analogues (Fig. 4) were reported for the first time by Flora et al. (1978). These authors have also reported the antitumor activity of a series of acyl and alkyl substituted amidoximes against murine leukemia cancer cell line (L1210). Formamidoxime, acetamidoxime, HG, and 2-
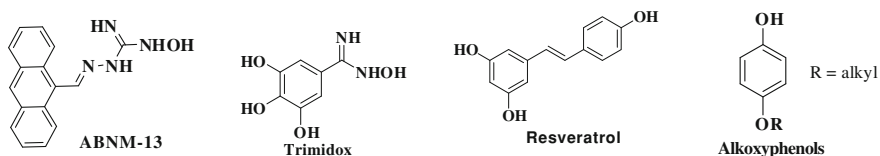
Fig. 4 Chemical structures of amidoximes, alkoxyphenols, etc

aminoacetamidoxime were found promising. Thereafter, many analogues of amidoximes and HGs have been reported for anticancer activity.

In fact, research on anticancer activity of amidoximes and related analogues got impetus after the discovery of trimidox in 1993–1994 (van't Riet et al. 1993; Elford 1994). It was initially patented for the treatment of hemoglobinopathies and later for leukemia. Structural analogs of trimidox have also been subsequently reported (Yang et al. 2010; Ziedan et al. 2010). Trimidox was later found to be an inhibitor of RRR2 (Szekeres et al. 1994b). Thereafter, it has been explored either as single therapy or in combination with other anticancer agents (Szekeres et al. 1994a; Rosenberger et al. 2000; Fritzer-Szekeres et al. 2000, 2002; Mayhew et al. 1997; Iyamu et al. 2000; Szekeres et al. 2009; Figul et al. 2003).

2.2.2 Phenolics

Alkoxyphenols and polyphenols have also been reported as RR inhibitors. Pötsch et al. reported a series of alkoxyphenols as RRR2 inhibitors (Pötsch et al. 1994). The EPR studies (using *E. coli* and mouse enzymes) proved that these molecules quench the tyrosyl radical. The para substituted alkoxy phenols were found to be most potent (IC_{50} in the range of 0.5–5 μM) (Pötsch et al. 1994; Lassmann and Pötsch 1995). Fontecave et al. proved resveratrol (3,5,4'-trihydroxystilbene, a naturally occuring polyphenolic compound found in grapes) as a potent inhibitor of RRR2 (Fontecave et al. 1998). The EPR studies further confirmed their ability to quench the tyrosyl radical (Fontecave et al. 1998). Later a few more analogs of resveratrol were reported with RR inhibitory property (Saiko et al. 2008; Handler et al. 2008; Saiko et al. 2007). Phenolics are an attractive scaffold to develop more promising radical scavengers and can be explored further in future.

3 Mechanism of Action of Hydroxamates

Hydroxamates have been proposed to act either by quenching the tyrosyl radical of the R2 subunit of RR or by chelating the iron responsible for generating the free radical. The in vitro antioxidant capacity of these compounds is similar to butylated hydroxyanisole (BHA) (Končić et al. 2011). A few other reports, based on enzyme assay or EPR-spectroscopic studies, supported the free radical quenching/iron chelation mechanism. However, the exact mode of binding/recognition process has not been reported. We are still waiting for the ligand bound crystal structure of hRRM2. The crystal structure will reveal significant information about the binding mode of hydroxamates. From our lab, we have recently reported a molecular dynamics study, which is the only available report on the molecular recognition of these kinds of inhibitors.

The M2 subunit of RR is responsible for generating the free radical that reduces ribonucleotides to their corresponding deoxyribonucleotides. This reduction
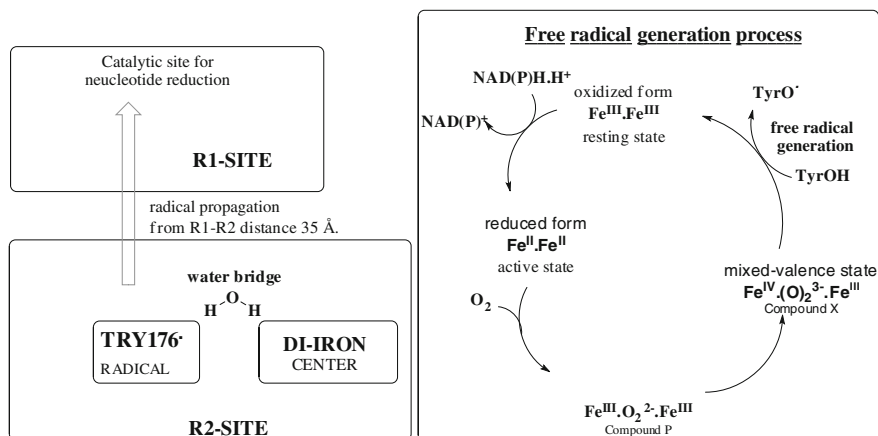
Fig. 5 Mechanism of reduction of ribonucleotides by the enzyme RR, showing the generation of free radical and activation cycle of the di-iron center

occurs via a single electron transfer from TYR176. The free radical on TYR176 is initiated by the radical-generating di-iron(III/IV) state via a single electron transfer, through a water molecule forming a bridge between the hydroxyl oxygen atom of TYR176 and the iron center (Stubbe et al. 2003; Himo and Siegbahn 2003; Torrent et al. 2002). The non-heme di-iron center of hRRM2 is unique; Torrent et al. (Torrent et al. 2002) have described the mechanism of activation of the di-iron center to generate the free radical. They have proposed an activation cycle which follows as: The active state $Fe^{II}.Fe^{II}$—formation of the μ-oxo bridge, by addition of oxygen $Fe^{III}.O_2^{2-}.Fe^{III}$ (Compound P)—mixed valence state $Fe^{IV}.O_2^{3-}.Fe^{III}$ (Compound X)—resting state $Fe^{III}.Fe^{III}$ via formation of the Tyrosyl radical (TYR-O$\cdot$). Yun and co-workers (Yun et al. 2007) later proved that addition of oxygen to the $Fe^{II}.Fe^{II}$ active state for the formation of compound P is the rate determining step in the entire process. Once this free radical is generated it is very quickly transferred by the relay mechanism to the catalytic active site in M1 subunit. It will be impossible to arrest the normal activity of the enzyme once this radical is generated. The mechanism is depicted in Fig. 5.

The di-iron-radical site is buried deep inside, shielded from the outside environment. The radical generation and propagation must be taking place in the core of the enzyme. We presume the catalytic activity should take place in a closed environment. Otherwise, the generated free radical may be immediately quenched by the cytosolic. We observed that the entry to the active site is guarded efficiently by residue ARG330 and by a water bridge between residues SER263 and GLU232 (Fig. 6). These two water molecules shield the 10 Å hydrophobic tunnel. Inhibitors binding to the RR active site should replace these water molecules to get access to the hydrophobic tunnel, lying underneath.
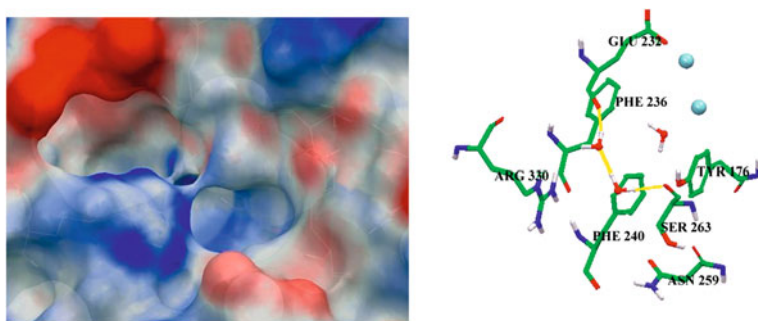
Fig. 6 Surface view to explain how this bridging guards the active site pocket. Bridging by the two water molecules (Ball and Stick) in between residues GLU232 and SER263. Adapted with permission from Basu and Sinha(2012). Copyright 2012 Springer Science+Business Media

3.1 The Structure of the Di-iron/Radical Site

We scrutinized a few previously reported holo protein structures for human (Smith et al. 2009), mouse (Strand et al. 2004; Logan et al. 1996), and *E. coli* (Nordlund et al. 1990; Nordlund and Eklund 1993). The following insights were obtained. Human and mouse R2 subunit shares an excellent sequence similarity of $\sim 80\,\%$ whereas for *E. coli* the sequence similarity is only $\sim 20\,\%$. Details of the mouse Tyrosyl radical environment were depicted in some of the reports (Logan et al. 1996; Strand et al. 2004). The crystal structure of human hRRM2 is available in protein data bank (pdb), but yet to be published as a journal paper. The homologous holo structure of hP53M2 (a homologous protein) was recently published (Smith et al. 2009). The tyrosyl radical is deeply buried in the interior of the protein forming a hydrophobic channel, reaching about 10 Å from the surface. The entrance to the radical site is about 15 Å wide. It is lined by mainly hydrophobic amino acids like; GLU233 (232), SER238 (237), ASN260 (259), and TYR324 (323) with their side-chain oxygen atoms turned away from the channel. The channel reaches all the way to SER267 (263), PHE241 (240), and SER264 (263) the residues lining the binding site (Fig. 6). These residue numbers correspond to the mouse pdb structure, corresponding human pdb residue numbers are given in bracket.

We have reported the working structure of the di-iron/radical site by using QM/MM. The active center has been generated under oxidizable conditions. The initial coordinates for the di-iron and the μ-oxo bridge were obtained from mouse pdb structure (pdb code 1w68). After a QM/MM optimization run, we observed the di-iron active center for human enzyme resembling with the earlier reported mouse enzyme structure. Computational (Torrent et al. 2002) and spectral studies (Lynch et al. 1989; Elgren et al. 1993) for the di-iron center of RRR2 described it as ferromagnetically coupled high-spin species. In accordance to these studies, we have chosen a total spin s = 4, resulting in multiplicity of 2s + 1 = 9, for the spin system. The hRRM2 iron site is buried in a four-helix bundle, which is coordinated
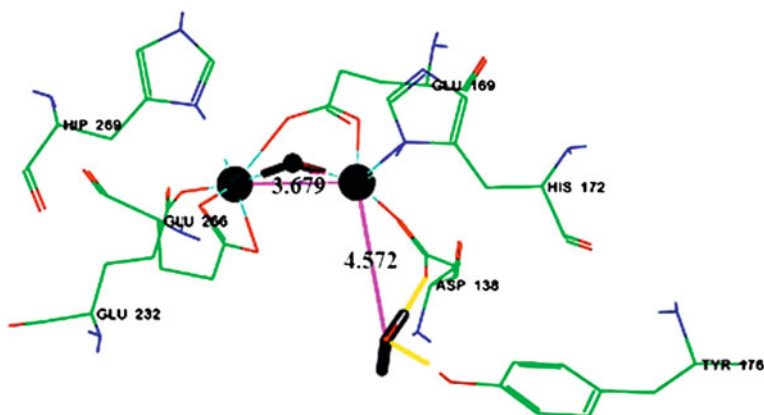
Fig. 7 Structure of human (hRRM2, pdb code 2uw2) di-iron center obtained after QM/MM optimization study. Adapted with permissionfrom Basu and Sinha (2012). Copyright 2012 Springer Science + Business Media

by the two histidines and the three glutamic acid carboxylate side chains. The Fe1, close to the TYR176, coordinates with ASP138 and HIS172. During minimization, we observed a bi-dented coordination of ASP138 carboxyl group with Fe1, but a single coordination was observed in the lowest energy conformation. The other iron atom, Fe2 is coordinated by GLU232, GLU266, and HIS269. Residue GLU169, coordinates with both the iron Fe1 and Fe2, and behaves as bidentate ligand. The optimal Fe1-Fe2 distance was found to be 3.68 Å, as compared to mouse 3.32 Å and *E. coli* 3.3 Å. The dihedral angle between Fe1–O–Fe2 was found to be 133 degrees. Hydrogen bonding was observed between TYR176 and a single water molecule, hypothesized to bridge between the di-iron and the radical center. The distance between the Fe1 and water molecule was found to be 4.57 Å, which is greater than 3.84 Å in mouse. Overall architecture of the di-iron center of mRRR2 resembled hRRM2, with minor differences observed in co-ordination patterns and distances (Fig. 7).

We are also required to use the correct tautomeric forms for the ligands during docking and MD studies. Amidoximes and HGs are present in two tautomeric forms; the amino oxime state, and imino hydroxylamine state (Bell et al. 1964). For SB-HSC21, hydroxamic acid tautomer will be favorable. We have generated all the possible tautomeric forms, which were then screened through tautomerizer, at target pH of 7.0 ± 2.0, and a tautomer probably cutoff threshold of 0.01. The tautomerizer program will assign a probability to each tautomeric form. Tautomers for the given input structure are produced in order of probability. We docked all the survived tautomers with hRRM2. Top ranking tautomer(s), after docking was considered as the most probable tautomeric state, and were used for further studies.

In addition to human and *E. coli* enzymes, QM/MM calculation has also been performed on mouse (pdb code1w68) enzyme. We observed that the di-iron center was extremely stable under the minimization conditions. The co-ordination pattern

also remained similar to that observed in the experimental structure (1w68). Modest deviations were observed in the water bridge between the TYR177 and the di-iron center. The distance between water molecule and the di-iron center was observed to be 3.03 Å, but in the crystal structure it was 3.87 Å.

4 Progress in Drug Design

Drug design or rational drug design is a process of finding new drug molecules based on the knowledge of the biological target (Ulf et al. 2002; Marshall and Beusen 1995). It involves design of small molecules that are complementary in shape and charge to the biomolecular target (Ekins et al. 2007). It is an important tool for medicinal chemists, which helps them to design a drug candidate. Readers may refer to many excellent reviews on this subject (Bohacek et al. 1996; Blundell 1996; Klebe 2000; Anderson 2003; Gane and Dean 2000; Hajduk and Greer 2007; Kitchen et al. 2004). Progress on drug designing for hydroxamates and related analogs are given as follows.

4.1 Ligand-Based Drug Design

This drug design technique relies on the knowledge of earlier reported molecules that bind to the same biological target of interest (Bacilieri and Moro 2006). A few ligand-based drug design studies for hydroxamates and related analogs have been reported, which can be mentioned as follows:

(a) Ren et al. (2002) reported the QSAR of a dataset of Schiff's bases of hydro-xysemicarbazones. They have pointed out that besides the essential pharma-cophore (-NHCONHOH), hydrophobicity, molecular size/molar refractivity, and the presence of an oxygen-containing group at the ortho position were important determinants for the antitumor activities (Ren et al. 2002).

(b) Raichurkar and Kulkarni (2003) performed the 3D-QSAR (CoMFA and CoMSIA) studies on same dataset of compounds (Raichurkar and Kulkarni 2003). The models were generated using 24 molecules as training set and four molecules as test set. The resulting significant QSAR model indicated that steric, electrostatic, hydrophobic, and hydrogen-bond donor fields were important. In addition to the standard fields in CoMFA and CoMSIA (Cramer III et al. 1988; Klebe et al. 1994), these authors also pointed out that hydro-phobicity also had significant effect on biological activity. These QSAR models predicted the activity of HU appropriately and indicated a similar mechanism of action.

(c) Kandemirli et al. (2006) also performed QSAR using the same dataset (Kandemirli et al. 2006). They used electronic, topological, and quantum chemical parameters for deriving a structure-activity relationship. Later, we have used combined datasets (Tai et al. 1984; Tang et al. 1985; Ren et al. 2002) and performed pharmacophore-based QSAR studies. These studies resulted in statistically robust model. We have further utilized this model for ligand-based virtual screening (Basu et al. 2011). This study resulted in identifying an anticancer lead molecule (ABNM13) (Basu et al. 2011; Saiko et al. 2011). ABNM13 (Fig. 4) is not a hydroxamic acid derivative, but it has been identified through a QSAR model, generated using hydroxamic acid derivatives.

4.2 Structure-Based Drug Design

This drug design technique relies on the knowledge of three-dimensional structure of the biological target obtained through X-ray crystallography or NMR spectroscopy (Oprea and Matter 2004). Structure-based drug design has been rare in case of hRRM2. A few reports have only come up during the past few years. Priya and Shanmughavel performed docking studies using AutoDock with two radical scavengers Flavin and Phenosafranine (Priya and Shanmughavel 2009). Natarajan and Mathews also reported a similar study by using the same ligands. Both the studies have proposed similar binding pocket of human ribonucleotide reductase M2 subunit (hRRM2). They proposed that these ligands may cleave the μ-oxo iron bridge during the radical transfer process, resulting in the arrest of radical generation (Natarajan and Mathews 2011). Luo and Gräslund (2011) employed a combination of molecular docking and dynamics to understand the mode of action of alkoxyphenols. They used a grid-based search method to locate the probable active site for R2. The site identification protocol resulted in identifying a site at the interface of A and B polypeptide chain. They proposed the alkoxy phenol moiety interferes with the electron transfer pathway during its transfer from the di-iron center to TRY176 to R1 site for actual catalysis.

Structure-based drug design using hydroxamates have been recently reported by our group. Binding mode analysis study of three hRRM2 inhibitors has been reported (Basu and Sinha 2012). We used molecular docking and dynamics simulation in this study. The working structure of hRRM2 has been generated by a QM/MM method. After defining the radical/di-iron active site, we performed the docking and MD studies to develop a valid structure-based model that may give us an idea about the binding mode of the established inhibitors.

Structure-based drug design of hRRM2 inhibitors has been hampered, due to various factors like unavailability of ligand-bound crystal structure, limited knowledge of mechanism of action (difficult to simulate), and possibility of induced-fit mechanism. More studies are required on drug designing of hRRM2, a few avenues for future drug designing on this target can be listed as follows:

1. Development and validation of VS protocol for radical scavengers (Good et al. 2004; Lyne 2002; Stahl and Rarey 2001).
2. Designing of decoy dataset for hRRM2 for setting up successful VS experiment (Huang et al. 2006).
3. Identifying appropriate docking and scoring protocols, which will work best for hRRM2.
4. Getting an appropriate crystallographic structure for ligand bound hRRM2.

We believe that the availability of ligand-bound crystal structure of R2 subunit would be the most crucial factor for drug development and design on this target. Currently we have few theoretical models, which have not been validated with the experimental structures.

Some examples in the progress of structure-based drug design for radical scavengers are mentioned as follows:

Docking and Molecular Dynamics

- Priya and Shanmughavel (2009) and Natarajan and Mathews (2011) performed docking studies using AutoDock on two radical scavengers, flavin, and phenosafranine, (Natarajan and Mathews 2011; Priya and Shanmughavel 2009).
- Luo and Gräslund (2011) employed a combination of molecular docking and dynamics to understand the binding mode of a series of alkoxyphenols. The results revealed that these molecules may bind to the R1-R2 interface of RR (Luo and Gräslund 2011).
- Popović-Bijelić et al. (2011) employed a combination of theoretical and experimental methodologies to study the inhibition of RR by a well-known metal ion chelator triapine.
- Basu and Sinha (2012) reported the a few ligand bound model of hRRM2 that can be used for structure-based drug designing. They have also proposed a possible molecular recognition process for radical scavengers.

5 Concluding Remarks and Future Prospective

Hydroxamic acids are an important class of anticancer drugs. They were mostly reported as HDAC inhibitors, but reports as RR inhibitors are also significant. The first reported hydroxamate-based RR inhibitor is HU. Later, didox and other hydroxamic acid analogs were reported. Since then lot of research on hydroxamic acid has been carried out, but didox remains the last hydroxamate that has undergone clinical trial. Didox showed lot of promise in the preclinical studies, but failed in the clinical trial due to lack of effectiveness in patients. It showed relatively high tolerance and less toxicity in the patients. The desired toxicity profile of didox prompted further research on hydroxamates (didox analogs). Many related molecules like HSC, amidoximes, etc., were explored for their RR inhibitory property.

RR is a promising and widely explored target that warrants more research. We believe that the elucidation of crystal structure of ligand bound hRRM2 may open a wide field to work on hydroxamic acids as RR inhibitors. In context to drug discovery research focusing on R2 subunit of RR, the following key milestones have been reached:

1. Discovery of HU in 1963 (Stearns et al. 1963).
2. Discovery of didox in 1979 (van′t Riet et al. 1979a).
3. Development of subunit specific assay for hRRM2 (Shao et al. 2005).
4. X-ray crystal structure of holo enzymes for mRRM2 (Strand et al. 2004; Kauppi et al. 1996) and hP53RRM2 (Smith et al. 2009).
5. Discovery of trimidox (van′t Riet et al. 1993).
6. Elucidation of radical generation and propagation pathway (Torrent et al. 2002; Per 2002; Mulliez and Fontecave 1999).

References

Adams RLP, Lindsay J (1967) Hydroxyurea. J Biol Chem 242(6):1314–1317

Anderson AC (2003) The process of structure-based drug design. Chem Biol 10(9):787–797

Bacilieri M, Moro S (2006) Ligand-based drug design methodologies in drug discov process: an overview. Curr Drug Disc Technol 3(3):155–165

Basu A, Sinha B (2012) Understanding the molecular interactions of different radical scavengers with ribonucleotide reductase M2 (hRRM2) domain: opening the gates and gaining access. J Comput Aided Mol Des 26(7):865–881

Basu A, Sinha BN, Saiko P, Graser G, Szekeres T (2011) N-Hydroxy-N′-aminoguanidines as anti-cancer lead molecule: QSAR, synthesis and biological evaluation. Bioorg Med Chem Lett 21(11):3324–3328

Bell CL, Nambury C, Bauer L (1964) The structure of amidoximes. J Org Chem 29(10): 2873–2877

Blundell TL (1996) Structure-based drug design. Nature 384(6604 Suppl):23

Bohacek RS, McMartin C, Guida WC (1996) The art and practice of structure-based drug design: a molecular modeling perspective. Med Res Rev 16(1):3–50

Cerqueira NM, Pereira S, Fernandes PA, Ramos MJ (2005) Overview of ribonucleotide reductase inhibitors: an appealing target in anti-tumour therapy. Curr Med Chem 12(11):1283–1294

Chen D, Yuan Z (2005) Therap potential of pept deformylase inhibitors J 14(9):1107–1116

Chetan B, Bunha M, Jagrat M, Sinha BN, Saiko P, Graser G, Szekeres T, Raman G, Rajendran P, Moorthy D (2010) Design, synthesis and anticancer activity of piperazine hydroxamates and their histone deacetylase (HDAC) inhibitory activity. Bioorg Med Chem Lett 20(13):3906–3910

Cramer RD III, Patterson DE, Bunce JD (1988) Comparative molecular field analysis (CoMFA). 1. Effect of shape on binding of steroids to carrier proteins. J Am Chem Soc 110(18): 5959–5967

Donehower RC (1992) An overview of the clinical experience with hydroxyurea. Semin Oncol 19(3 Suppl 9):11–19

Ekins S, Mestres J, Testa B (2007) In silico pharmacology for drug discov: methods for virtual ligand screening and profiling. Br J Pharmacol 152(1):9–20

Eklund H, Uhlin U, Färnegårdh M, Logan DT, Nordlund P (2001) Structure and function of the radical enzyme ribonucleotide reductase. Prog Biophys Mol Biol 77(3):177–268

Elford HL (1968) Effect of hydroxyurea on ribonucleotide reductase. Biochem Biophys Res Commun 33(1):129–135

Elford HL (1994) Method of treating hemoglobinopathies. US Patent 5366996

Elford HL, van′t Riet B (1985) Inhibition of nucleoside diphosphate reductase by hydroxybenzohydroxamic acid derivatives. Pharmacol Ther 29(2):239–254

Elgren TE, Hendrich MP, Que L Jr (1993) Azide binding to the diferrous clusters of the R2 protein of ribonucleotide reductase from Escherichia coli. J Am Chem Soc 115(20):9291–9292

Figul M, Söling A, Dong H, Chou TC, Rainov N (2003) Combined effects of temozolomide and the ribonucleotide reductase inhibitors didox and trimidox in malignant brain tumor cells. Cancer Chemother Pharmacol 52(1):41–46

Flora KP, van′t Riet B, Wampler GL (1978) Antitumor activity of amidoximes (hydroxyurea analogs) in murine tumor systems. Cancer Res 38(5):1291–1295

Fontecave M (1998) Ribonucleotide reductases and radical reactions. Cell Mol Life Sci 54(7):684–695

Fontecave M, Lepoivre M, Elleingand E, Gerez C, Guittet O (1998) Resveratrol, a remarkable inhibitor of ribonucleotide reductase. FEBS Lett 421(3):277–279

Fritzer-Szekeres M, Grusch M, Luxbacher C, Horvath S, Krupitza G, Elford HL, Szekeres T (2000) Trimidox, an inhibitor of ribonucleotide reductase, induces apoptosis and activates caspases in HL-60 promyelocytic leukemia cells. Exp Hematol 28(8):924–930

Fritzer-Szekeres M, Novotny L, Vachalkova A, Findenig G, Elford HL, Szekeres T (1997) Iron binding capacity of didox (3, 4-dihydroxybenzohydroxamic acid) and amidox (3, 4-dihydroxybenzamidoxime) new inhibitors of the enzyme ribonucleotide reductase. Life Sci 61(22):2231–2237

Fritzer-Szekeres M, Salamon A, Grusch M, Horvath Z, Höchtl T, Steinbrugger R, Jäger W, Krupitza G, Elford HL, Szekeres T (2002) Trimidox, an inhibitor of ribonucleotide reductase, synergistically enhances the inhibition of colony formation by Ara-C in HL-60 human promyelocytic leukemia cells. Biochem Pharmacol 64(3):481–485

Gane PJ, Dean PM (2000) Recent advances in structure-based rational drug design. Curr Opin Struct Biol 10(4):401–404

Goldman JM (1997) Optimizing treatment for chronic myeloid leukemia. New Engl J Med 337(4):270–271

Good AC, Hermsmeier MA, Hindle S (2004) Measuring CAMD technique performance: a virtual screening case study in the design of validation experiments. J Comput Aided Mol Des 18(7):529–536

Hajduk PJ, Greer J (2007) A decade of fragment-based drug design: strategic advances and lessons learned. Nat Rev Drug Discov 6(3):211–219

Handler N, Saiko P, Jaeger W, Szekeres T, Wacheck V, Berner H, Leisser K, Erker T (2008) Synthesis and cytotoxic activity of resveratrol-based compounds. Monatshefte für Chemie/Chemical Monthly 139(5):575–578

Hehlmann R, Berger U, Pfirrmann M, Hochhaus A, Metzgeroth G, Maywald O, Hasford J, Reiter A, Hossfeld D, Kolb H (2003) Randomized comparison of interferon α and hydroxyurea with hydroxyurea monotherapy in chronic myeloid leukemia (CML-Study II): prolongation of survival by the combination of interferon α and hydroxyurea. Leukemia 17(8):1529–1537

Himo F, Siegbahn PEM (2003) Quantum chemical studies of radical-containing enzymes. Chem Rev 103(6):2421–2456

Huang N, Shoichet BK, Irwin JJ (2006) Benchmarking Sets for Molecular Docking. J Med Chem 49(23):6789–6801

Inayat MS, Chendil D, Mohiuddin M, Elford HL, Gallicchio VS, Ahmed MM (2002) Didox (a novel ribonucleotide reductase inhibitor) overcomes Bcl-2 mediated radiation resistance in prostate cancer cell line PC-3. Cancer Biol Ther 1(5):539

Iyamu W, Adunyah S, Fasold H, Horiuchi K, Elford H, Asakura T, Turner E (2000) Enhancement of hemoglobin and F-cell production by targeting growth inhibition and differentiation of K562 cells with ribonucleotide reductase inhibitors (didox and trimidox) in combination with streptozotocin. Am J Hematol 63(4):176–183

Jordan A, Reichard P (1998) Ribonucleotide reductases. Annu Rev Biochem 67(1):71–98

Kandemirli F, Shvets N, Kovalishyn V, Dimoglo A (2006) Combined electronic-topological and neural networks study of some hydroxysemicarbazides as potential antitumor agents. J Mol Graphics Model 25(1):30–36

Kauppi B, Nielsen BB, Ramaswamy S, Kjøller Larsen I, Thelander M, Thelander L, Eklund H (1996) The three-dimensional structure of mammalian ribonucleotide reductase protein R2 reveals a more-accessible iron-radical site than escherichia coliR2. J Mol Biol 262(5):706–720

Kitchen DB, Decornez H, Furr JR, Bajorath J (2004) Docking and scoring in virtual screening for drug discov: methods and applications. Nat Rev Drug Discov 3(11):935–949

Klebe G (2000) Recent developments in structure-based drug design. J Mol Med 78(5):269–281

Klebe G, Abraham U, Mietzner T (1994) Molecular similarity indices in a comparative analysis (CoMSIA) of drug molecules to correlate and predict their biological activity. J Med Chem 37(24):4130–4146

Kolberg M, Strand KR, Graff P, Kristoffer Andersson K (2004) Structure, function, and mechanism of ribonucleotide reductases. Biochim Biophys Acta (BBA)-Proteins & Proteomics 1699(1):1–34

Končić MZ, Barbarić M, Perković I, Zorc B (2011) Antiradical, chelating and antioxidant activities of hydroxamic acids and hydroxyureas. Molecules 16(8):6232–6242

Krakoff IH, Brown NC, Reichard P (1968) Inhibition of ribonucleoside diphosphate reductase by hydroxyurea. Cancer Res 28(8):1559–1565

Lassmann G, Pötsch S (1995) Structure of transient radicals from cytostatic-active p-alkoxyphenols by continuous-flow EPR. Free Radical Biol Med 19(5):533–539

Logan DT, Su XD, Åberg A, Regnström K, Hajdu J, Eklund H, Nordlund P (1996) Crystal structure of reduced protein R2 of ribonucleotide reductase: the structural basis for oxygen activation at a dinuclear iron site. Structure 4(9):1053–1064

Luo J, Gräslund A (2011) Ribonucleotide reductase inhibition by p-alkoxyphenols studied by molecular docking and molecular dynamics simulations. Arch Biochem Biophys 516(1):29–34

Lynch J, Juarez-Garcia C, Münck E, Que Jr L (1989) Mössbauer and EPR studies of the binuclear iron center in ribonucleotide reductase from *Escherichia coli*. A new iron-to-protein stoichiometry. J Biol Chem 264(14):8091–8096

Lyne PD (2002) Structure-based virtual screening: an overview. Drug Discov Today 7(20):1047–1055

Marshall GR, Beusen DD (1995) Molecular modeling in drug design. In: Abraham DJ (ed) Burger's Medicinal Chemistry, Drug discov and development, vol 1, 6th edn. John Wiley and Sons, Inc., p 77–155

Mayhew C, Oakley O, Piper J, Hughes N, Phillips J, Birch N, Elford H, Gallicchio V (1997) Effective use of ribonucleotide reductase inhibitors (didox and trimidox) alone or in combination with didanosine (ddI) to suppress disease progression and increase survival in murine acquired immunodeficiency syndrome (MAIDS). Cellular and molecular biology (Noisy-le-Grand, France) 43(7):1019

Monzyk B, Crumbliss AL (1979) Mechanism of ligand substitution on high-spin iron(III) by hydroxamic acid chelators. Thermodynamic and kinetic studies on the formation and dissociation of a series of monohydroxamatoiron(III) complexes. J Am Chem Soc 101(21):6203–6213

Moore EC (1969) The effects of ferrous ion and dithioerythritol on inhibition by hydroxyurea of ribonucleotide reductase. Cancer Res 29(2):291

Mulliez E, Fontecave M (1999) Ribonucleotide reductases: metal and free radical interplay. Coord Chem Rev 185–186:775–793

Natarajan S, Mathews R (2011) Modeling and proposed mechanism of two radical scavengers through docking to curtail the action of ribonucleotide reductase. J Biophy Struc Biol 3(2):38–48

Nocentini G (1996) Ribonucleotide reductase inhibitors: new strategies for cancer chemotherapy. Crit Rev Oncol Hematol 22(2):89–126

Nordlund P, Eklund H (1993) Structure and function of the Escherichia coli ribonucleotide reductase protein R2. J Mol Biol 232(1):123–164

Nordlund P, Sjöberg BM, Eklund H (1990) Three-dimensional structure of the free radical protein of ribonucleotide reductase. Nature 345:593–598

Oprea TI, Matter H (2004) Integrating virtual screening in lead discov. Curr Opin Chem Biol 8(4):349–358

Per EMS (2002) A comparison of dioxygen bond-cleavage in ribonucleotide reductase (RNR) and methane monooxygenase (MMO). Chem Phys Lett 351(3–4):311–318

Pergola C, Werz O (2010) 5-Lipoxygenase inhibitors: a review of recent developments and patents. Expert Opin Ther Pat 20(3):355–375

Piver M, Barlow J, Vongtama V, Blumenson L (1983) Hydroxyurea: a radiation potentiator in carcinoma of the uterine cervix. A randomized double-blind study. Am J Obstet Gynecol 147(7):803

Popović-Bijelić A, Kowol CR, Lind MES, Luo J, Himo F, Enyedy ÉA, Arion VB, Gräslund A (2011) Ribonucleotide reductase inhibition by metal complexes of Triapine (3-aminopyridine-2-carboxaldehyde thiosemicarbazone): a combined experimental and theoretical study. J Inorg Biochem 105(11):1422–1431

Pötsch S, Drechsler H, Liermann B, Gräslund A, Lassmann G (1994) p-Alkoxyphenols, a new class of inhibitors of mammalian R2 ribonucleotide reductase: possible candidates for antimelanotic drugs. Mol Pharmacol 45(4):792–796

Priya PL, Shanmughavel P (2009) A docking model of human ribonucleotide reductase with flavin and phenosafranine. Bioinformation 4(3):123–126

Raichurkar AV, Kulkarni VM (2003) Understanding the antitumor activity of novel hydroxyse-micarbazide derivatives as ribonucleotide reductase inhibitors using CoMFA and CoMSIA. J Med Chem 46(21):4419–4427

Raje N, Kumar S, Hideshima T, Ishitsuka K, Yasui H, Chhetri S, Vallet S, Vonescu E, Shiraishi N, Kiziltepe T (2006) Didox, a ribonucleotide reductase inhibitor, induces apoptosis and inhibits DNA repair in multiple myeloma cells. Br J Haematol 135(1):52–61

Reichard P (1993) From RNA to DNA, why so many ribonucleotide reductases? Science 260(5115):1773–1777

Reichard P, Ehrenberg A (1983) Ribonucleotide reductase–a radical enzyme. Science 221:514–519

Ren S, Wang R, Komatsu K, Bonaz-Krause P, Zyrianov Y, McKenna C, Csipke C, Tokes Z, Lien E (2002) Synthesis, biological evaluation, and quantitative structure-activity relationship analysis of new schiff bases of hydroxysemicarbazide as potential antitumor agents†. J Med Chem 45(2):410–419

Rosenberger G, Fuhrmann G, Grusch M, Fassl S, Elford HL, Smid K, Peters GJ, Szekeres T, Krupitza G (2000) The ribonucleotide reductase inhibitor trimidox induces c-myc and apoptosis of human ovarian carcinoma cells. Life Sci 67(26):3131–3142

Saban N, Bujak M (2009) Hydroxyurea and hydroxamic acid derivatives as antitumor drugs. Cancer Chemother Pharmacol 64(2):213–221

Saiko P, Graser G, Giessrigl B, Lackner A, Grusch M, Krupitza G, Basu A, Sinha BN, Jayaprakash V, Jaeger W (2011) A novel N-hydroxy-N′-aminoguanidine derivative inhibits ribonucleotide reductase activity: effects in human HL-60 promyelocytic leukemia cells and synergism with arabinofuranosylcytosine (Ara-C). Biochem Pharmacol 81(1):50–59

Saiko P, Ozsvar-Kozma M, Bernhaus A, Jaschke M, Graser G, Lackner A, Grusch M, Horvath Z, Madlener S, Krupitza G (2007) N-hydroxy-N'-(3, 4, 5-trimethoxyphenyl)-3, 4, 5-trimethoxy-benzamidine, a novel resveratrol analog, inhibits ribonucleotide reductase in HL-60 human promyelocytic leukemia cells: synergistic antitumor activity with arabinofuranosylcytosine. Int J Oncol 31(5):1261

Saiko P, Pemberger M, Horvath Z, Savinc I, Grusch M, Handler N, Erker T, Jaeger W, Fritzer-Szekeres M, Szekeres T (2008) Novel resveratrol analogs induce apoptosis and cause cell cycle arrest in HT29 human colon cancer cells: inhibition of ribonucleotide reductase activity. Oncol Rep 19(6):1621–1626

Schrell UMH, Rittig MG, Anders M, Kiesewetter F, Marschalek R, Koch UH, Fahlbusch R (1997) Hydroxyurea for treatment of unresectable and recurrent meningiomas. I. Inhibition of primary human meningioma cells in culture and in meningioma transplants by induction of the apoptotic pathway. J Neurosurg 86(5):845–852

Schrell UMH, Rittig MG, Koch U, Marschalek R, Anders M (1996) Hydroxyurea for treatment of unresectable meningiomas. The Lancet 348(9031):888–889

Shao J, Zhou B, Chu B, Yen Y (2006) Ribonucleotide reductase inhibitors and future drug design. Curr Cancer Drug Targets 6(5):409–431

Shao J, Zhou B, Zhu L, Bilio AJ, Su L, Yuan YC, Ren S, Lien EJ, Shih J, Yen Y (2005) Determination of the potency and subunit-selectivity of ribonucleotide reductase inhibitors with a recombinant-holoenzyme-based in vitro assay. Biochem Pharmacol 69(4):627–634

Silver RT, Woolf SH, Hehlmann R, Appelbaum FR, Anderson J, Bennett C, Goldman JM, Guilhot F, Kantarjian HM, Lichtin AE (1999) An evidence-based analysis of the effect of busulfan, hydroxyurea, interferon, and allogeneic bone marrow transplantation in treating the chronic phase of chronic myeloid leukemia: developed for the American Society of Hematology. Blood 94(5):1517–1536

Smith BD, Karp JE (2003) Ribonucleotide reductase: an old target with new potential. Leukemia Res 27(12):1075–1076

Smith P, Zhou B, Ho N, Yuan YC, Su L, Tsai SC, Yen Y (2009) 2.6 Å X-ray crystal structure of human p53R2, a p53-inducible ribonucleotide reductase. Biochemistry 48(46):11134–11141

Stahl M, Rarey M (2001) Detailed analysis of scoring functions for virtual screening. J Med Chem 44(7):1035–1042

Stearns B, Losee KA, Bernstein J (1963) Hydroxyurea. A new type of potential antitumor agent1. J Med Chem 6(2):201–201

Strand KR, Karlsen S, Kolberg M, Røhr ÅK, Görbitz CH, Andersson KK (2004) Crystal structural studies of changes in the native dinuclear iron center of ribonucleotide reductase protein R2 from mouse. J Biol Chem 279(45):46794–46801

Stubbe JA, Nocera DG, Yee CS, Chang MCY (2003) Radical initiation in the class I ribonucleotide reductase: long-range proton-coupled electron transfer? Chem Rev 103(6):2167–2202

Szekeres T, Fritzer M, Strobl H, Gharehbaghi K, Findenig G, Elford HL, Lhotka C, Schoen H, Jayaram H (1994a) Synergistic growth inhibitory and differentiating effects of trimidox and tiazofurin in human promyelocytic leukemia HL-60 cells. Blood 84(12):4316–4321

Szekeres T, Gharehbaghi K, Fritzer M, Woody M, Srivastava A, Riet B, Jayaram HN, Elford HL (1994b) Biochemical and antitumor activity of trimidox, a new inhibitor of ribonucleotide reductase. Cancer Chemother Pharmacol 34(1):63–66

Szekeres T, Vielnascher E, Novotny L, Vachalkova A, Fritzer M, Findenig G, Göbl R, Elford HL, Goldenberg H (2009) Iron binding capacity of trimidox (3, 4, 5-trihydroxybenzamidoxime), a new inhibitor of the enzyme ribonucleotide reductase. Clin Chem Lab Med 33(11):785–790

Tai AW, Lien EJ, Lai MM, Khwaja TA (1984) Novel N-hydroxyguanidine derivatives as anticancer and antiviral agents. J Med Chem 27(2):236–238

Tang A, Lien EJ, Lai MM (1985) Optimization of the Schiff bases of N-hydroxy-N'-aminoguanidine as anticancer and antiviral agents. J Med Chem 28(8):1103–1106

Tihan T, Elford HL, Cory JG (1991) Studies on the mechanisms of inhibition of L1210 cell growth by 3, 4-dihydroxybenzohydroxamic acid and 3, 4-dihydroxybenzamidoxime. Adv Enzyme Regul 31:71–83

Torrent M, Musaev DG, Basch H, Morokuma K (2002) Computational studies of reaction mechanisms of methane monooxygenase and ribonucleotide reductase. J Comput Chem 23(1):59–76

Ulf M, Krogsgaard-Larsen P, Liljefors T (2002) Textbook of drug design and discov. In., 3 edn. Washington, DC: Taylor & Francis, p 1–37

van't Riet B, Elford HL, Wampler GL (1993) Polyhydroxybenzoic acid derivatives US patent 5183828

van't Riet B, Wampler GL, Elford HL (1979a) Synthesis of hydroxy- and amino-substituted benzohydroxamic acids: inhibition of ribonucleotide reductase and antitumor activity. J Med Chem 22(5):589–592

Van't Riet B, Wampler GL, Elford HL (1979b) Synthesis of hydroxy-and amino-substituted benzohydroxamic acids: inhibition of ribonucleotide reductase and antitumor activity. J Med Chem 22(5):589–592

Veale D, Carmichael J, Cantwell B, Elford H, Blackie R, Kerr D, Kaye S, Harris A (1988) A phase 1 and pharmacokinetic study of didox: a ribonucleotide reductase inhibitor. Br J Cancer 58(1):70

Yadav R, Gupta S, Sharma P, Patil V (2011) Recent advances in studies on hydroxamates as matrix metalloproteinase inhibitors: a review. Curr Med Chem 18(11):1704–1722

Yang X, Liu G, Li H, Zhang Y, Song D, Li C, Wang R, Liu B, Liang W, Jing Y, Zhao G (2010) Novel oxadiazole analogues derived from ethacrynic acid: design, synthesis, and structure–activity relationships in inhibiting the activity of glutathione S-transferase P1–1 and cancer cell proliferation. J Med Chem 53(3):1015–1022

Young CW, Hodas S (1964) Hydroxyurea: inhibitory effect on DNA metabolism. Science 146(3648):1172–1174

Yun D, Saleh L, García-Serres R, Chicalese BM, An YH, Huynh BH, Bollinger Jr JM (2007) Addition of oxygen to the diiron (II/II) cluster is the slowest step in formation of the tyrosyl radical in the W103Y variant of ribonucleotide reductase protein R2 from mouse. Biochemistry 46(45):13067–13073

Ziedan NI, Stefanelli F, Fogli S, Westwell AD (2010) Design, synthesis and pro-apoptotic antitumour properties of indole-based 3,5-disubstituted oxadiazoles. Eur J Med Chem 45(10):4523–4530

Hydroxamic Acid Derivatives as Potential Anticancer Agents

Manish K. Gupta, Gagandip Singh and Swati Gupta

Abstract Hydroxamic acid containing organic molecules display strong metal ion chelating property, and therefore used as metalloenzyme inhibitors. They display strong affinity toward histone deacetylase, matrix metalloproteinases, human epidermal growth factor receptor-2, and tumor necrosis factor alpha converting enzyme. These enzymes play crucial roles in the pathogenesis of cancer and are attractive targets for the development of new anticancer agents. Various molecules bearing free hydroxamic acid at one terminal have been synthesized and evaluated for their activities. This article will focus on the development of various classes of hydroxamic acid-based metalloenzyme inhibitors and anticancer agents.

Abbreviations

ADAM	A disintegrin and metalloproteinase
ALCAM	Activated leukocyte cell adhesion molecule
CA	Carbonic anhydrase
ECD	Extracellular domain
EGFR/HER2	Human epidermal growth factor receptor-2
HA	Hydroxamic acid
HAT	Histone acetyltransferase
HDAC	Histone deacetylase
IMPDH	Inosine-5′-monophosphate dehydrogenase
MCG	Metal chelating group
MMP	Matrix metalloproteinase
MPA	Mycophenolic acid

M. K. Gupta (✉) · G. Singh · S. Gupta
ISF College of Pharmacy, Moga, Punjab, India
e-mail: mkgupta5@gmail.com

MSS	Musculoskeletal syndrome
MTX	Methotrexate
NAHA	N-alkylated amino acid-derived hydroxamate
NSCLC	Non small cell lung cancer
RAMBA	Retinoic acid metabolism blocking agent
SAHA	Suberoyl anilide hydroxamic acid
TACE	Tumor necrosis factor alpha converting enzyme
TNF-α	Tumor necrosis factor alpha
TSA	Trichostatin A
WBA	White blood assay

Contents

1 Introduction

Hydroxamic acids are class of compounds characterized by the presence of a terminal –CONHOH functional group. The –CONHOH group functions as a strong metal ion chelator, and hence it has been used as a crucial metal binding group to develop various metalloenzyme inhibitors. The –CONHOH functional group has shown strong affinity for iron (III) (Miller 1989); therefore, various hydroxamic acid-based siderophores (low molecular weight, ferric ion specific chelators) and their analogs have been developed which make complex with iron (III) and show profound biological activities. These compounds also showed antibacterial and antifungal activities (Neilands 1995).

The metal chelating property of hydroxamic acids has been used extensively to develop inhibitors for metal containing enzymes and proteins such as histone deacetylase (HDAC) (Codd et al. 2009; Zhang et al. 2010a), matrix metalloproteins (MMPs) (Nuti et al. 2007; Yadav et al. 2011), tumor necrosis factor alpha converting enzyme (TACE) (Zhang et al. 2009), etc. The –CONHOH functional group bearing molecules has been evaluated specifically for their efficacy against cancer (Saban and Bujak 2009; Kovacic and Edwards 2011), rheumatoid arthritis (Vojinovic and Damjanov 2011; Li et al. 2012), and other autoimmune disorders. Most of the metalloproteinase (MMP) contains Zn^{++} or Mg^{++} at the catalytic side. The chelation of Zn^{++} or Mg^{++} ion is one of the major reasons for the inhibition of enzyme activity. The coordinated bond between Zn^{++} and –CONHOH greatly increases the drug–receptor interaction energy which is sufficient to block the activity of enzyme. The C=O and –OH functional group of metal chelating group are also involved in electrostatic attractions with Zn^{++}. Therefore, the hydroxamic acid-based inhibitors have been found very effective in the inhibition of MMPs. The various classes of compounds bearing terminal –CONHOH group have been evaluated for their activity against HDAC, epidermal growth factor receptor-2 (EGFR/HER2), MMPs, TACE, and IMP-dehydrogenase (IMPDH). These enzymes are involved in many cancer-related processes, and hence are attractive targets for the development of new and novel anticancer agents. This article will describe the design and development of various hydroxamic acid-based inhibitors to target the cancer.

2 Target Specific Hydroxamic Acid Derivatives

2.1 Histone Deacetylases Inhibitors

The various classes of hydroxamic acid-based histone deacetylases (HDACs) inhibitors (HDACi) have been developed and evaluated for their efficacy in in vitro and in vivo model of cancer (Codd et al. 2009; Zhang et al. 2010a). Nucleosomal histones comprise the structural component of chromatin and are involved in modulation of chromatin function and regulation of gene expression. The functional role of histones is firmly regulated by acetylation and deacetylation of its N-terminal serine residue. The histone acetyltransferases (HATs) and HDACs are two distinct classes of enzymes which tightly control the equilibrium of histone acetylation and hence its activity. An imbalance in the equilibrium of histone acetylation causes the aberrant regulation of gene expression which led to carcinogenesis and cancer progression (Ouaissi and Ouaissi 2006; Gallinari et al. 2007). HDACs have an important function in regulating DNA packaging in chromatin, thereby affecting the transcription of genes. These are overexpressed in cancer and aberrantly recruited by oncoproteins (Minucci and Pelicci 2006). The numerous studies proved that the inhibition of HDAC led to the modulation of transcription

Fig. 1 General structural features of hydroxamic acid-based HDAC inhibitors, ZCG (Zinc chelating group)
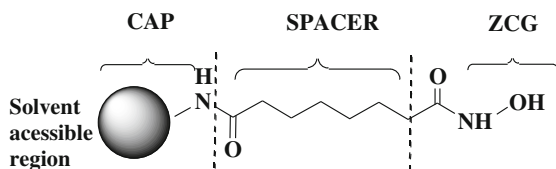
in eukaryotic cells, and therefore HDAC inhibitors have been developed as novel anticancer agents. Trichostatin A (TSA, **1**), a natural product, was among the first HDACi showed promising anticancer activity and demonstrated the therapeutic potential of HDAC inhibition in cancer (Yoshida et al. 1990). This generated much interest in the search of novel HDAC inhibitor and anticancer agents. Vorinostat, a HDAC inhibitor (suberoylanilide hydroxamic acid, SAHA) was the first US-FDA approved drug for the treatment of the cutaneous manifestations in patients with advanced and refractory cutaneous T-cell lymphoma (Howman and Prince 2011). Almost all HDAC inhibitors consist of three structural features: (i) a zinc chelating functional group (ZCG); (ii) a hydrophobic intermediate chain; and (iii) an aromatic group (CAP region) (Finnin et al. 1999; Marks et al. 2000) (Fig. 1).
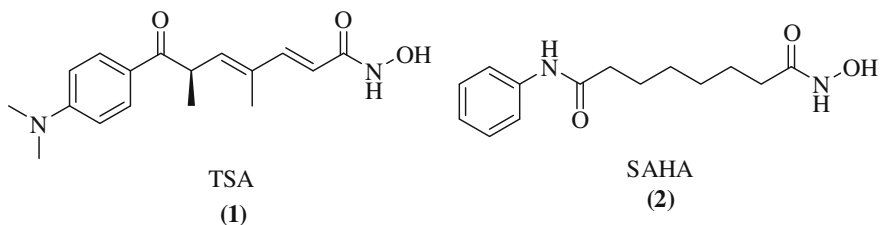
The 3D X-ray structure of HDAC8 (PDB entry 1T69) in complexed with SAHA (2) showed that Zn^{2+} is coordinated with –CONHOH of SAHA, two aspartic acids (Asp178 and Asp267), and one histidine residue (Fig. 2). The spacer is covered with hydrophobic residues Phe152, Phe208, and Pro273. The CAP region showed electrostatic interactions with Tyr100, Asp101, and Met274.

The molecular modeling studies on hydroxamic acid-based inhibitors also revealed that the metal binding group resides deep in the binding cavity and complexed with metal ion. The spacer (linker) remains surrounded by a tunnel of hydrophobic residues and the capping group gets positioned toward the solvent exposed area and interacts with the residues present at the entrance of the binding cavity (Charrier et al. 2009). Therefore, various hydroxamic acid-based HDAC inhibitors have been developed with structure variation in these regions.
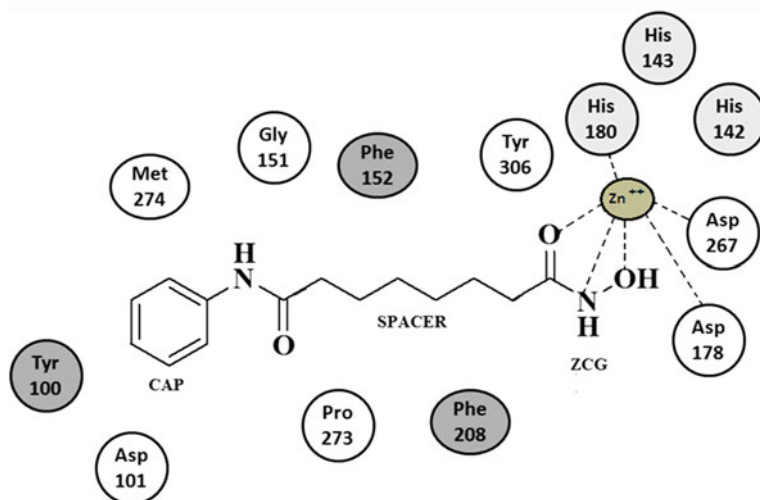
Fig. 2 2D depiction of binding site residues of HDAC8 complexed with SAHA

2.1.1 Hydroxamic Acids with Modified CAP Group

The TSA (**1**) and the cyclic tetrapeptides trapoxin B (**3**) are naturally occurring highly potent HDAC inhibitors (Kijima et al. 1993). These natural HDAC inhibitors and their close analogs possess potent differentiating properties on cancer cells in vitro, but they are cytotoxic to both normal and cancer cells. They displayed poor in vivo activity due to low bioavailability and rapid metabolism. To overcome the problems associated with natural HDAC inhibitors, Glenn et al. (2004) designed a series of compounds (**4**) composed of a simple cysteine scaffold fused at the C-terminus to benzylamine, at the S-terminus to 4-butanoylhydroxamate, and at the N-terminus to a small library of carboxylic acids, display structural and pharmacophoric features characteristic of known HDAC inhibitors such as TSA (**1**) and trapoxin (**3**). Some of the compounds (**5–8**) displayed excellent cytotoxic activity against MM96L melanoma cell lines and reasonable selectivity for cancer cells over normal cells. A retinoic acid metabolism blocking agents (RAMBAs, **9**) possess anticancer activity against LNCaP prostate carcinoma cells. The dose–response curves of **9** and SAHA (**2**) showed that SAHA (IC$_{50}$ = 1.0 μM) was a more potent antiproliferative agent than 4 (IC$_{50}$ = 5.5 μM) against LNCaP prostate carcinoma cells. Gediya et al. (2005) evaluated the additive/synergistic effect of **9** and SAHA (**2**) on the growth of LNCaP cells and observed that the inhibition of cell growth by this combination was additive i.e., the effect was equal to the sum of the effects of the **9** and SAHA (**2**), separately.

Trapoxin B
(3)

(4)

	R	IC$_{50}$(µg/ml)
5		0.14
6		0.2
7		0.13
8		0.2

(9)
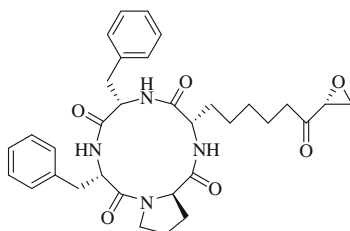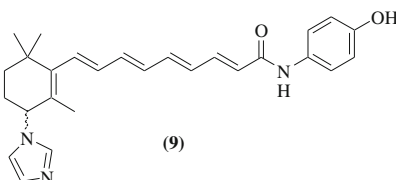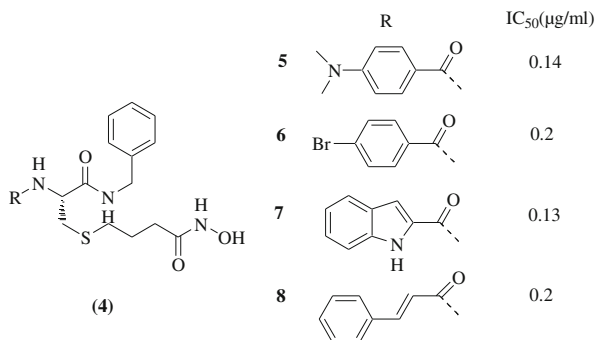
Jose et al. (2004) synthesized cyclic tetrapeptide (**10**) and hexapeptide (**11**) hydroxamic acids as HDAC6 inhibitors. **10** showed excellent HDAC6 inhibitory activity at IC$_{50}$ of 190 nM, but **11** failed to give activity even at the IC$_{50}$ of 100 µM. It was suggested that loss of activity may be due to the steric hindrance by the bulky CAP region of **11** compared to **10**.

(10)   (11)
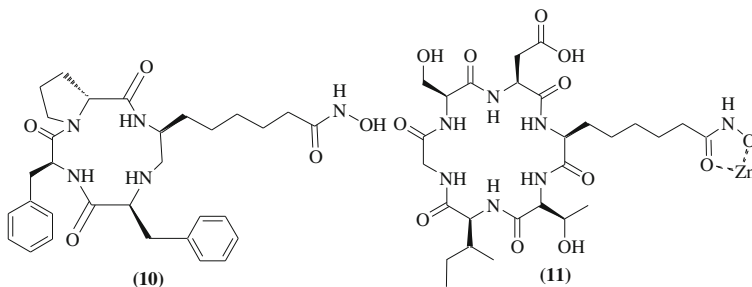
Chen et al. (2008) reported triazolylphenyl-based hydroxamic acids as HDAC1 and HDAC6 inhibitors. These compounds were designed by modification of CAP region with N-substituted triazolylphenyls in order to establish a rationale for their selectivity toward HDAC6 over HDAC1. The nature and position of substitutions on triazole ring play important role for their selectivity for HDAC6. The **12a** was identified as the most selective inhibitor of HDAC6 and showed 51-fold activity over HDAC1. In continuation of this work, He et al. (2010) reported **12d**, **12e**, and **12f** as HDAC1 and HDAC6 inhibitors, which showed antiproliferative activity (IC_{50}= 0.02–0.8 μM) in various pancreatic cancer cell lines.

	HDAC-1 IC50 nM	HDAC-6 IC50 nM	SI
12a	97.8	1.9	51
12b	52.4	7.3	7
12c	25.9	3.8	7
12d	18.0	9.6	2
12e	5.1	3.8	1.2
12f	4.6	3.1	1.3
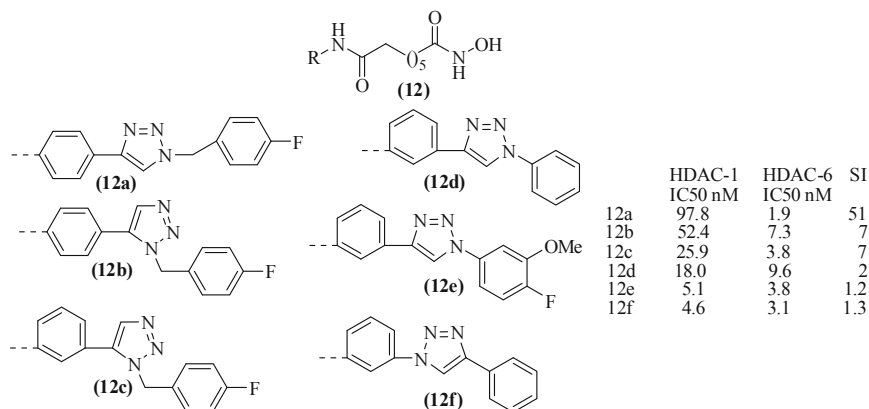
Kozikowski et al. (2008) reported novel biaryl hydroxamate (**13**) which showed in vitro inhibition of HDAC1 and HDAC2 at IC_{50} of 4 and 27 nM, respectively. **13** also possesses anticancer activity in nanomolar potency against various pancreatic cancer lines. Wang et al. (2010) reported **14**, a close analog to SAHA (**2**), as HDAC1 inhibitor and anticancer agent. **14** exhibited good HDAC1 inhibitory activity (IC_{50} = 53 nM) and demonstrated good antitumor efficacy in PC3 and HCT116 xenograft models. Salmi-Smail et al. (2010) modified the CAP region of SAHA with substituted phenyl and high molecular weight substituents in order to improve hydrophobicity of the new analogs. These analogs (**15**) have shown 10-fold higher antileukemic activity with respect to SAHA (**2**) in several human cancer cell lines. Their antiproliferative activity profile was observed in concentrations varying from 0.12 to >100 μM. The docking study suggested that the aromatic moiety of **15** was involved in noncovalent interactions with the tyrosine (Y306) residue of HDAC.

(13)

(14)

(15)
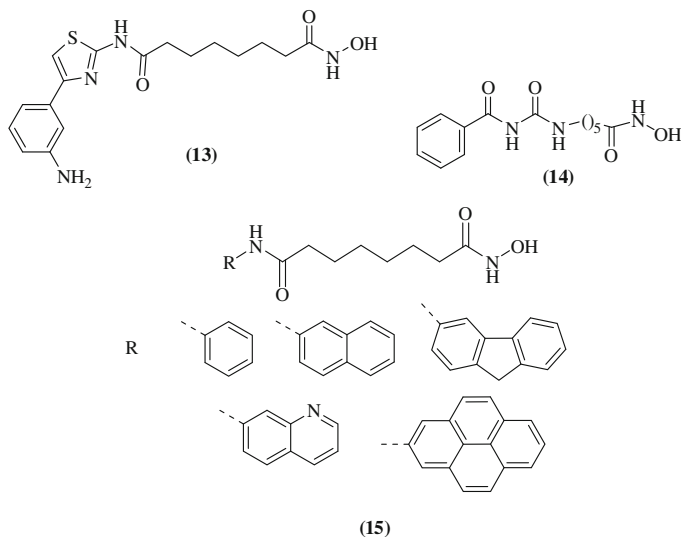
Huang et al. (2011) presented a series of osthole derivatives (osthole: a Chinese herbal compound) fused with the aliphatic-hydroxamate core of SAHA and evaluated for HDACs inhibitory activities. The **16**, most active compound of this series, showed significant HDAC inhibitory activity against HDAC1, 6, and 8 (IC_{50} = 32.3, 15.2, and 553.4 nM, respectively). **16** also showed potent antiproliferative activity on several human cancer cell lines. **17** is a unique class of HDAC inhibitor in which a 1,4-dithia-7-azaspiro head group attached with hydroxamic acid end with a linear linker. It showed HDAC8 inhibitory (IC_{50} = 0.6 μM) and antiproliferative activity against various cancer cell lines (Zhang et al. 2011c). Rossi et al. (2011) synthesized N-substituted 4-alkylpiperazine and 4-alkylpiperdine hydroxamic acids and evaluated for HDAC activity (**18**, **19**). The compounds were evaluated for antiproliferative activity on HCT-116 colon carcinoma cells. The **18** and **19** were showed HDAC inhibitory activity at the IC_{50} of 0.1 and 0.09 μM, respectively. Their antiproliferative activity (IC_{50}) on HCT-116 colon carcinoma cells was reported as 0.7 and 0.3 μM, respectively (SAHA IC_{50} = 0.6 μM). Oanh et al. (2011) reported two series of benzothiazole-containing analogs of SAHA (**1**) with linker length of four and six carbons, respectively (**20** and **21**). The several compounds with 6C-bridge between benzothiazole moiety and hydroxamic functional groups showed good inhibition of HDAC3 and HDAC4 (IC_{50} ∼ 1 μg/ml) compared to the 4C-bridge. They also exhibited potent cytotoxicity against five cancer cell lines with average IC_{50} of 0.81 μg/ml.

(16)　　　　　　　　　　　　　　**(17)**

(18)　　　　　　　　　　　　　　**(19)**

	R	IC$_{50}$(μg/ml)
20a	-H	9.8
20b	-CH3	7.9
20c	-OCH3	15.12
21a	-H	5.49
21b	-CH3	0.81
21c	-OCH3	1.28

20　n=1
21　n=3
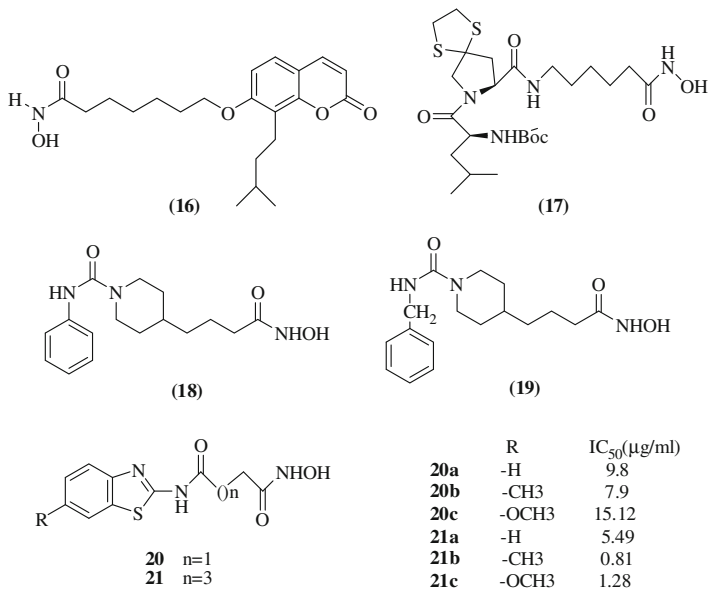
2.1.2 Hydroxamic Acids with Modified Linker and CAP Region

The length of spacer between CAP and ZCG is crucial for the optimum HDAC inhibitory activity (Oanh et al. 2011). Therefore, HA-based HDAC inhibitors with variation in linker size and structure have been reported. Jung et al. (1999) had synthesized some HDAC inhibitors to study the effect of length of spacer (linker between CAP and NHOH function) on the activity (**22**). The spacer length of five to six carbons was found to be the optimum for the maximum efficacy (**22a–c**). Bouchain et al. (2003) reported sulphonamide-hydroxamic acids as HDAC1 inhibitors (**23**). The synthesized compounds were evaluated for their activity on HDAC1 and induction of histone acetylation in human bladder T24 cancer cells. The substitution on the aryl ring of **23** by *p*-Me, *p-t*Bu, and an electron-donating group improves the activity compared to the unsubstituted compounds. Replacement of the phenyl ring with a biphenyl group showed comparable HDAC1 inhibitory activity. The activity appears to be similar for sulfonamide or "reverse" sulfonamide while the replacement of sulphonamide function with the urea was found detrimental for activity (**23**).

	n	IC_{50}
22a	3	>40μM
22b	5	100nM
22c	7	300nM

Ar = Ph, *p*-MeOPh, *p*-*t*BuPh

X--Y	HDAC-1 IC_{50} nM	H4-Ac EC μM
SO_2NH	0.01-0.5	1-25
$NHSO_2$	0.01-0.5	1-25
NHCONH	>25	
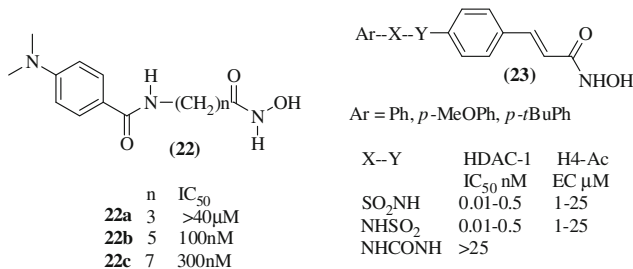
Zhang et al. (2010b) developed novel HDAC8 inhibitors by using rigid 1,2,3,4-tetrahydroisoquinoline-3-carboxylic acid fragment as a linker between CAP and NHOH group. In activity evaluation, compounds **24** (IC_{50} = 1.0 μM) showed better HDAC8 inhibitory activity than SAHA (**2**) (IC_{50} = 1.48 μM). Further development in this series led to the identification of **25a–c** which exhibited excellent HDAC8 inhibitory activity and in vivo anticancer activities in a human breast carcinoma xenograft model (MDA-MB-231; IC_{50} = 0.79, 2.20, and 2.54 μM, respectively) (Zhang et al. 2011a). The **25a** was further modified to **25d**, which showed improved HDAC8 inhibitory and anticancer profile (IC_{50} = 0.58 μM) (Zhang et al. 2011b).

(**24**)
IC_{50} = 1.0μM

(**25**)

(**25a**)
IC_{50} = 0.139μM

(**25b**)
IC_{50} = 0.263μM

(**25c**)
IC_{50} = 0.333μM

(**25d**)
IC_{50} = 0.146μM
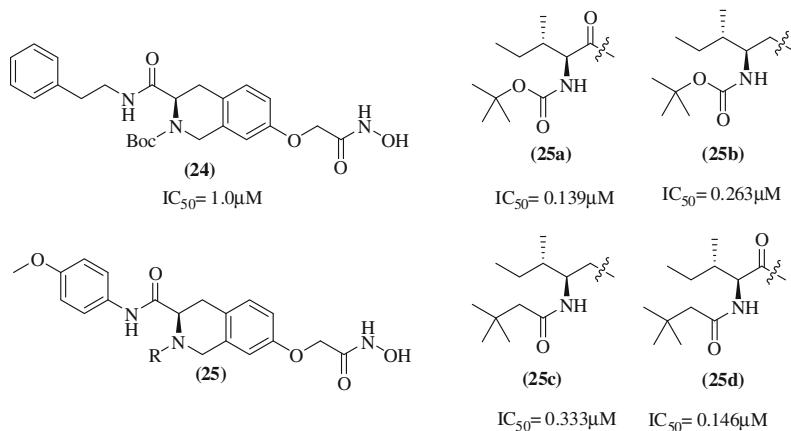
Catley et al. (2003) reported a novel hydroxamic acid derivative NVP-LAQ824 (**26**) as HDAC inhibitor and anticancer agent. The NVP-LAQ824 induces apoptosis in multiple myeloma (MM) cell lines resistant to conventional therapies without any toxicity to normal marrow or peripheral blood (IC_{50} = 100 nM) (Atadja et al. 2004). LBH-589 (**27**) is a hydroxamic acid-based HDAC inhibitor with a structure similar to vorinostat. It was approved for phase I clinical trials for the treatment of cutaneous T-cell lymphoma and as an oral anticancer agent. It possesses longer half-life than vorinostat (Giles et al. 2006; Scuto et al. 2008).

PXD101 (**28**) is under the phase II clinical trial for the treatment of advanced malignant pleural mesothelioma (Ramalingam et al. 2009). It showed HDAC inhibitory activity in HeLa cell extracts with an IC_{50} of 27 nM (Plumb et al. 2003). It induces a concentration-dependent (0.2–5 μM) rise in acetylation of histone H4 in tumor cell lines. The treatment of nude mice bearing human ovarian and colon tumor xenografts with PXD101 (10–40 mg/kg/day i.p.) daily for 7 days produced a notable dose-dependent growth delay without any toxicity to the mice (Plumb et al. 2002). The oxamflatin (**29**) is a potent HDAC inhibitor ($IC_{50} = 15.7$ nM) and antitumor agent. It is phenyl-sulfonamide-phenyl bearing hydroxamic acid analog. The oxamflatin possesses excellent antiproliferative activity against a panel of human cancer cell lines in range of 0.02–1. 4 μg/ml. The study has shown that the oxamflatin causes the accumulation of acetylated histone species in tumor cells, and thus histone hyperacetylation is responsible for its antitumor activity. It also induces an elongated cell shape with flamentous protrusions and arrest of the cell cycle at the G1 phase (Sonoda et al. 1996; Kim et al. 1999). The BL1521 (**30**) is a hydroxamic acid-based HDAC inhibitor and suggested as an attractive target for selective chemotherapy in neuroblastoma. It showed more than 85% inhibition of HDAC activity in a panel of neuroblastoma cell lines. The study has shown that the proliferation as well as the metabolic activity of neuroblastoma cells decreased significantly in response to treatment with BL1521 (de Ruijter et al. 2004; Ouwehand et al. 2005).

NVP-LAQ824 (Dacinostat)
(26)

LBH589 (Panobinostat)
(27)

PXD101 (Belinostat)
(28)

Oxamflatin
(29)

BL1521
(30)
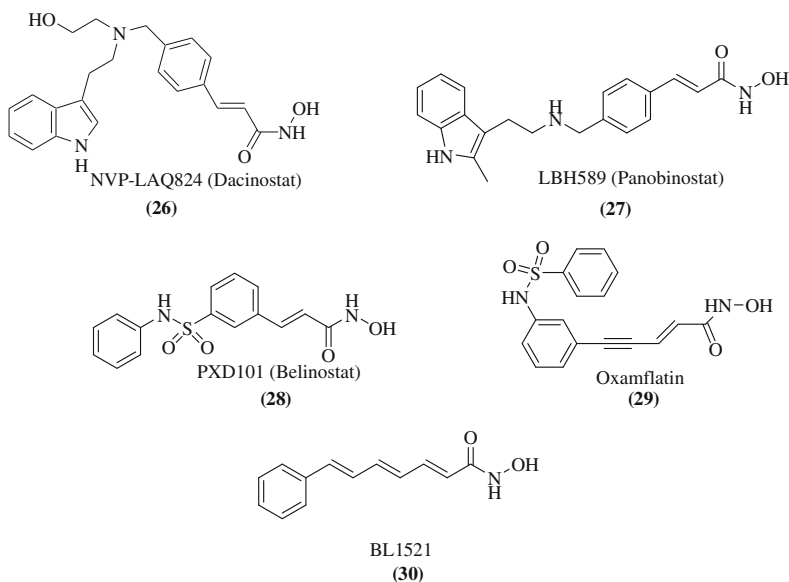
Dear et al. (2006) reported **31** and **32** as conformational analogs of oxamflatin. These compounds possess significant HDAC inhibitory activity and marked reduction in cell growth and proliferation in leukemia cells. Kim et al. (2006)

synthesized δ-lactam-based hydroxamic acids by ring closure metathesis of key diene intermediates followed by conversion to hydroxamic acid analogs. The HDAC inhibitory activity of synthesized compounds was evaluated against partly purified HDAC enzyme obtained from HeLa cell lysate. Among the synthesized compounds, **33a**, **b** and **34** showed good HDAC inhibitory activity (IC_{50} = 0.67, 0.35, and 0.5 μM, respectively). Compound **33b** and **34** exhibited growth inhibitory activity against a panel of five cancer cell lines with the GI_{50} between 1.62 and 9.58 μM, but **33a** failed to give anticancer activity (GI_{50} > 10 μM). **35**, reported by Su et al. (2008), is a furyl hydroxamic acid derivative possess moderate activity against HDAC1 (IC_{50} = 13.20 μM) and HDAC4 (IC_{50} = 1.10 μM), but showed significant effect in inducing apoptosis and antiproliferative activity in HCT119 cell line.
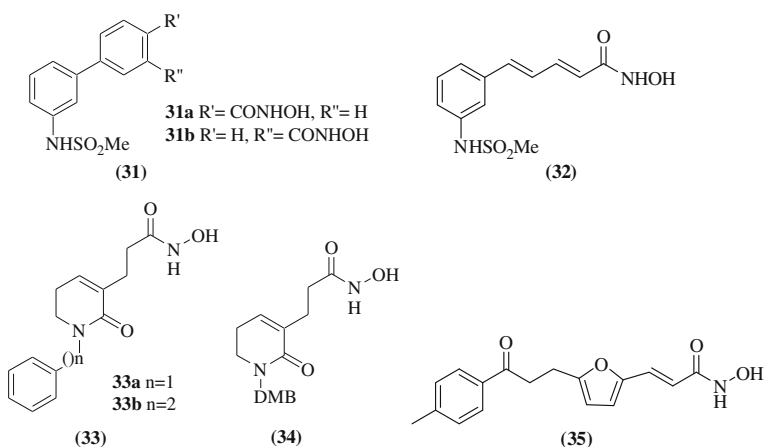
The compound **36**, reported by (Mahboobi et al. 2009) showed good HDAC1 and HDAC6 inhibitory activity (IC_{50} = 0.077 and 0.036 μM), respectively and cytotoxicity for HeLa (IC_{50} = 2.65 μM) and K562 (IC_{50} = 0.74 μM) cancer cell lines. Wang et al. (2009) synthesized N-hydroxy-1,2-disubstituted-1H-benzimdazol-5-yl acrylamides (**37**) as novel HDAC inhibitors. The representative compound **37a** exhibited excellent HDAC1 inhibitory activity (HDAC1 IC_{50} = 0.035 μM) and antitumor efficacy in a colon cancer xenograft model (IC_{50} = 0.14 μM). Angibaud et al. (2010) reported a series of substituted 2-piperazinyl-5-pyrimidylhydroxamic acids and evaluated for HDAC inhibiting properties and with tumor cell proliferation inhibition (**38**). These compounds possess excellent HDAC inhibitory activity at nanomolar range (IC_{50} = 1.5–7.0 nM) and good cell antiproliferative activity against A2780 ovarian carcinoma cancer cell lines (IC_{50} = 20–392 nM).

(36)

(37)

R_1/R_2: aliphatic, aromatic heterocyclic

(37a)

(38)

R = -CH$_3$, -CH$_2$OH, -CH$_2$OCH$_3$, -CH$_2$-1-morpholino
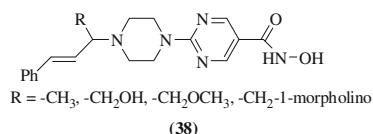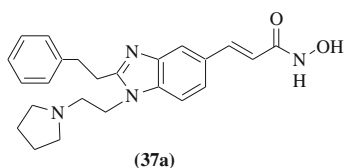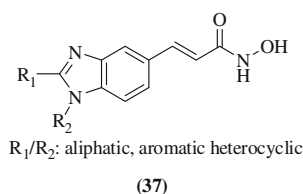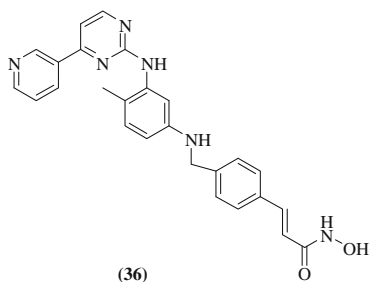
Charrier et al. (2009) synthesized hydroxamic acid containing benzofuranone derivatives and evaluated for their activity on HDAC6 and lung cancer cells (NCI-H661). These compounds were designed by replacement of methylene group of **39** by an isosteric oxygen atom to give a new family of HDAC inhibitors and anti-proliferative agents. Antiproliferative activities against NCI-H661 nonsmall cell lung cancer (NSCLC) cells showed that **39b** is more potent (IC$_{50}$ = 45 nM) than **39a** (IC$_{50}$ = 1 μM). The molecular modeling study of **39b** revealed several hydrophobic contacts of the dihydrofuran ring at the opening of the active site and electrostatic interactions of the dimethylamino moiety with the polar surface of the protein.

(39)

X= O/CH$_2$
39a = H
39b = N(Me)$_2$
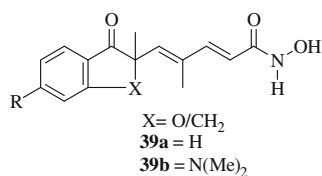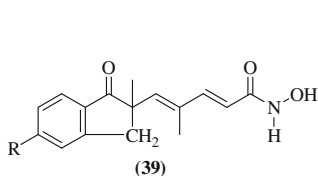
Lai et al. had identified 1-arylsulfonyl-5-(N-hydroxyacrylamide) indoles as a new class of HDAC inhibitors (**40**). The SAR revealed that the N-hydroxy-acrylamide group at the C-5 position of indole ring displayed the best activity compared to other positions like C-3, -4, -6, and -7. Compounds **40a–e** possess stronger antiproliferative activity than SAHA (**2**). Compound **40a** showed remarkable HDAC 1, 2, and 6 isoenzymes inhibitory activities with IC$_{50}$ of 12.3, 4.0, and 1.0 nM, respectively, which are comparable to SAHA (IC$_{50}$ = 8.9, 1.7, and 5.0 nM, respectively). Dallavalle et al. (2009) reported novel biphenyl-4-yl-

acrylohydroxamic acid derivatives (**41**) as HDAC inhibitors and antitumor agents. These compounds showed HDAC2 inhibitory activity in range of 0.22–1.7 μM (SAHA: $IC_{50} = 0.82$ μM) and exhibited significant antitumor activity.
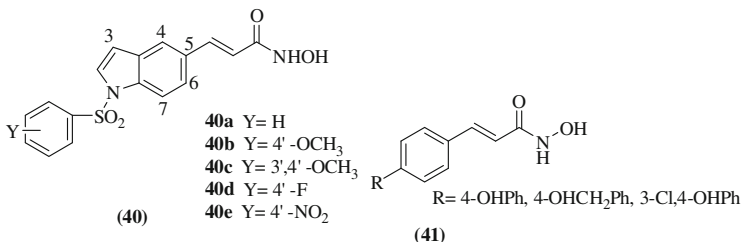
Kozikowski et al. (2008) reported a series of HDAC inhibitors containing an isoxazole moiety adjacent to hydroxamic acid group (**42**). The antiproliferative activity was observed against five pancreatic cancer cell lines. The compound **42a** was identified as the most active HDAC inhibitor ($IC_{50} = 30$–430 nM) of this series. It inhibited all tested cancer cell lines. Its IC_{50} values were similar to those of SAHA (**2**), while its amine analog (**42b**) moderately inhibits the cell lines.
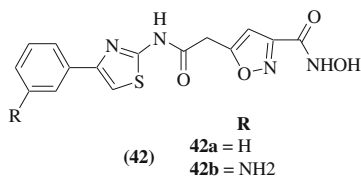
2.2 Human Epidermal Growth Factor Receptor-2 Inhibitors

The human EGFR/HER2 is a member of tyrosine kinase receptor family. Its activation, either by homo- and hetero-dimerization with other member of HER family-1 or by proteolytic cleavage (shedding) of extracellular domain (ECD) initiates intracellular signal transduction pathways which play important role in cell proliferation, differentiation, motility, adhesion, and survival (Arribas and Borroto 2002; Marmor et al. 2004). The overexpression and elevated plasma level of HER2 have been observed in various form of cancer which eventually decreases the effectiveness of cancer treatment (Mass 2004). The human epidermal growth factor receptor (EGFR, HER1) inhibitor erlotinib (**43**) and the dual EGFR/HER2 inhibitor lapatinib (**44**) are FDA-approved anticancer drugs for the treatment of multiple solid tumor cancers (Press and Lenz 2007). Both drugs are derived from the quinazoline scaffold which is an essential pharmacophore for interactions with
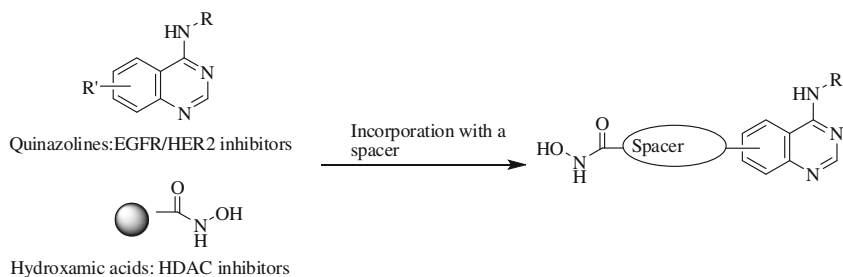
Fig. 3 Design of EGFR/HER2/HDAC inhibitors. (Reproduced with permission from Cai et al. (2010). Copyright American Chemical Society, 2010)

EGFR/HER2. On the other hand, the hydroxamic acid class of compounds is well-known HDAC inhibitors and anticancer agents (**1**, **2**). In this background, Cai et al. (2010) designed a series of multitargeted EGFR/HER2/HDAC inhibitors by combining hydroxamic acid and quinazoline with a linker (**45**) (Fig. 3). In this study, **46** was identified as the most active compound which displayed potent in vitro inhibitory activity against, EGFR, HER2, and HDAC with an IC_{50} of 2.4, 15.7, and 4.4 nM, respectively. Compound **46** also exhibited excellent antiproliferative activity ($IC_{50} = 0.04$–0.8 μM) in selected human cancer cell lines with better efficacy than vorinostat, erlotinib, lapatinib, and combinations of vorinostat/erlotinib and vorinostat/lapatinib. The pharmacological studies showed that **46** promotes tumor regression or inhibition in various cancer xenograft models including NSCLC, colon, breast, liver, pancreatic, head, and neck cancers. At present, **46** is in clinical development.
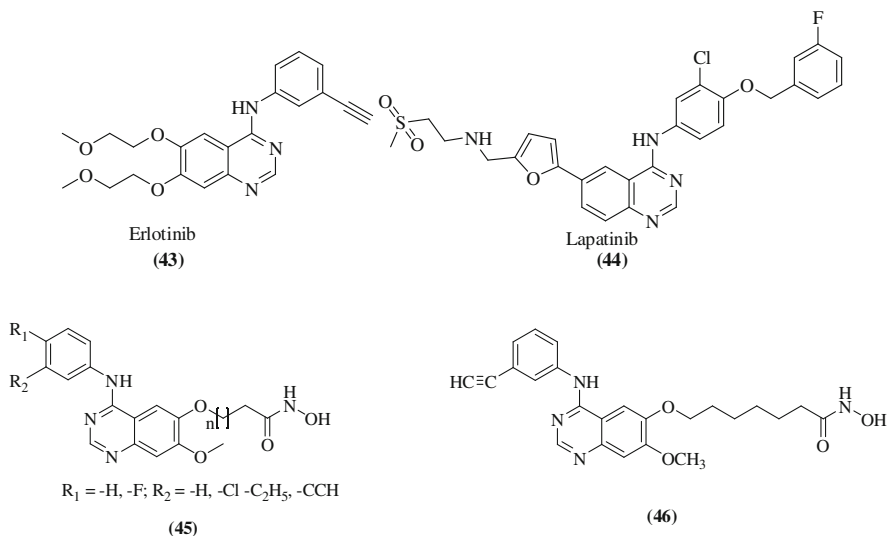
Yao et al. (2007) developed a novel class of conformationally restricted aza-spiro-hydroxamic acids as selective inhibitors of HER2 sheddase (**47**). The compound **47a–c** with IC_{50} of 18, 13, and 68 nM, respectively for HER2 were shown to decrease tumor growth, cleaved plasma level of HER2 ECD, and potentiate the effects of the humanized anti-HER2 monoclonal antibody (trastuzumab) in vivo in a HER2 overexpressing cancer murine xenograft model. Zuo et al. (2012) synthesized a series of N-aryl salicylamides with a hydroxamic acid moiety as novel HDAC–EGFR dual inhibitors (**48**, **49**). **48** and **49** have been identified as most potent inhibitor of HDAC and EGFR, respectively. These compounds also possess excellent antiproliferative activity against A431 and A549 and HL-60 human cancer cell lines.
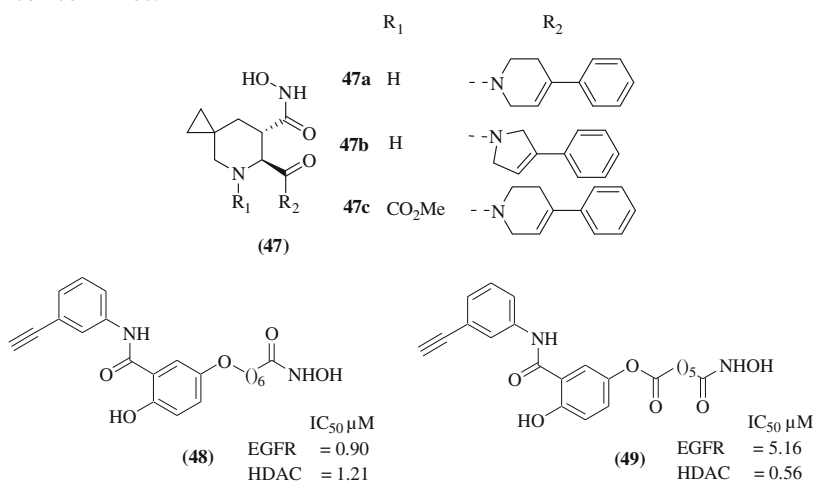
2.3 Matrix Metalloproteinase Inhibitors

MMPs comprise a family of extracellular matrix degrading proteins. The MMPs have been extensively investigated for their role in development and progression of cancer. It has been observed that MMPs, especially MMP2 and MMP9 play key role in cancer-related process like tumor growth, angiogenesis, and metastasis (Curran and Murray 2000; Egeblad and Werb 2002). The MMPs contain a zinc ion in coordination with a cysteine, glutamic acid, and three histidine residues and required for catalytic activity. The MMPs cause the modeling and degradation of extracellular matrix and plasminogen, and thus are implicated in invasion and metastasis during cancer progression. They also release and cause activation of growth factors. All these effect collectively, facilitates the angiogenesis, tumor growth, and metastasis (McCawley and Matrisian 2000). It has been observed that the MMPs inhibitors potentially reduce the angiogenesis and metastasis (Nelson et al. 2000). The hydroxamic acid-based MMPs inhibitors preferentially bind to the zinc ion at the active site of MMPs, and hence inhibit the MMPs induced extracellular matrix degradation, angiogenesis, tumor growth, and metastasis.

The search for MMPs inhibitor led to the identification of marimastat (**50**) which showed good absorption after oral administration. It possesses broad spectrum MMPs inhibition profile as evident by IC_{50} of 5, 6, 3, 16, 230, and 5 nM against MMP1, MMP2, MMP9, MMP7, MMP3, and MMP12, respectively (Steward and Thomas 2000; Millar et al. 1998). Marimastat showed broad spectrum anticancer activity but was withdrawn from the clinical trials due to its poor therapeutic response (Sparano et al. 2004). The batimastat (**51**) was developed as potent MMP2 and MMP9 inhibitor and antineoplastic agent. Under physiological conditions, batimastat inhibits MMP2 and MMP9 with IC_{50} of 9 and 10 nM, respectively. It showed broad spectrum anticancer activity but suffer from poor oral bioavailability (Botos et al. 1996; Low et al. 1996). The prinomastat (**52**) is a potent MMP inhibitor with picomolar affinities for inhibiting MMP2, MMP9, MMP13, and MMP14 in various tumor models. It was developed for the front-line combination chemotherapy for the patients with advanced malignancies of the lung and prostate (Shalinsky et al. 1999). The prinomastat (**52**) was also withdrawn from the Phase III clinical trials due to the lack of effectiveness in patients with late-stage disease (Bissett et al. 2005).

It was observed that broad spectrum inhibition of MMPs led to the stiffening of the joints in rats and development of musculoskeletal syndrome (MSS) (Renkiewicz et al. 2003). The inhibition of MMP1 specifically causes the MSS. Therefore, the MMP inhibitors (MMP2, 9, and 13) devoid of MMP1 inhibitory activity have been developed by Becker et al. (2005). **53**, a piperidine sulfone hydroxamate, showed good inhibitory activity and selectivity for MMP2, MMP9, and MMP13 (Ki = 0.33, 1.5, and 0.4 nM, respectively) over MMP1 (Ki = 8,660 nM). **53** also showed excellent efficacy in murine xenograft tumor models and antiangiogenesis assays (Becker et al. 2005).

Marimastat
(**50**)

Batimastat
(**51**)

Prinomastat
(**52**)

(**53**)
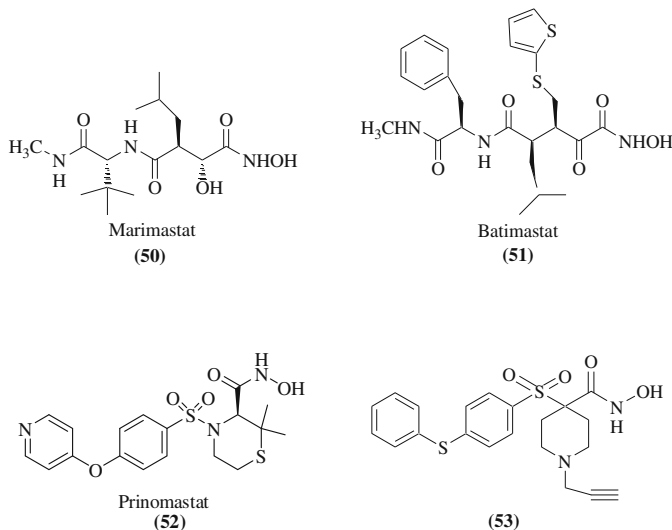
Santos et al. (2007) reported methotrexate (**54**) and folic acid (**55**) derivatives of hydroxamic acid as MMPs inhibitors. Both classes of compounds have shown moderate to good MMPs inhibitory activities. In in vitro, anticancer activity evaluation against NSCLC and prostate cancer cell lines, the MTX derivatives **54a–c** showed many fold superior activity profile (IC$_{50}$ = 1.8–7.5 μM) than folic acid derivatives (IC$_{50}$ = 80–150 μM). Scozzafava and Supuran (2000) reported sulfonylated amino acid hydroxamates (**56**) and N-hydroxysulfonamides (**57**) as human carbonic anhydrase (hCA) and MMPs dual inhibitors. The sulfonylated amino acid hydroxamates showed better inhibitory activity for MMPs, while N-hydroxysulfonamides (**57**) showed selectivity for hCA.

	a	**b**	**c**
X	-OH	-NHOH	

% inhibition at 100μM

	MMP2	MMP7	MMP9	MMP14
54b	67	100	61	48
54c	56	43	61	47
55b	66	53	55	42
55c	58	54	30	100

Ki (nM)

	MMP1	MMP2	MMP8	MMP9	hCAII	HCA IV
56	3	0.7	0.1	0.6	107	130
57	80	90	120	100	0.9	1.2
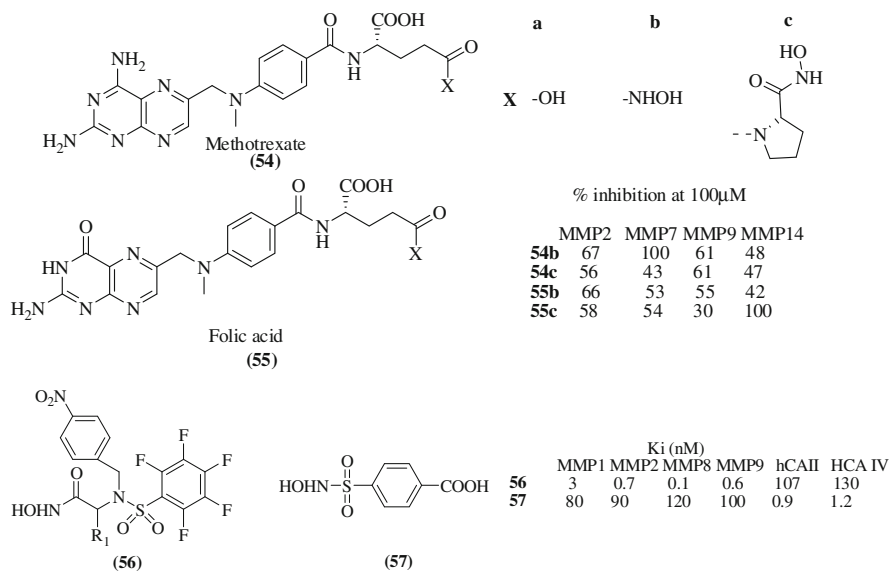
2.4 Tumor Necrosis Factor-α Converting Enzyme Inhibitors

Tumor Necrosis Factor alpha (TNF-α) is a member of cytokine family. It is primarily produced by activated macrophages and other immune cells. TNF-α is involved in autoimmunity, homeostasis, and acute as well as chronic inflammation, and hence proposed as a viable target for rheumatoid arthritis (Alonso-Ruiz et al. 2008). It has been observed that the TNF-α is involved in cancer-related processes but its role in pathogenesis and treatment of cancer remains less understood (Keystone 2011). The TNF-α mediated cell signaling pathway regulates the cell proliferation and apoptosis. It is reported that TNF-α in tumor cells induces the stimulation of growth factors and angiogenesis which results in tumor

growth. The high level of TNF-α has been detected in wide range of tumor cells which can be correlated with the tumor progression and pathogenesis. TNF-α convertase enzyme (TACE) is a metalloprotein, closely related to MMPs. TACE is responsible for the processing of pro-TNF-α to TNF-α. The recent reviews suggested that the TACE inhibitors may be valuable drug candidates for cancer (Kenny 2007; Dasgupta et al. 2009). Several MMP inhibitors, such as marimastat (**50**) and AG3340 (**58**) possess good TACE inhibitory activity but displayed poor pharmacokinetics properties (Barlaam et al. 1999).

	nM		
	TACE	MMP1	MMP8
50	3.8	5	7
58	5.5	8.2	16.6
59a	0.57	-	-
60	0.6	1.1	
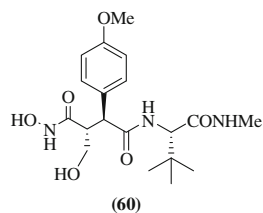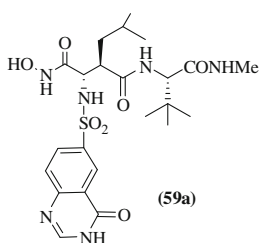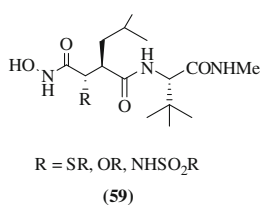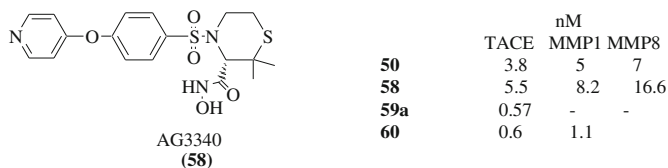
In an attempt to find potent TACE inhibitors with acceptable pharmacokinetic profile, Barlaam et al. (1999) investigated bulky ethers, thioether, and sulfonamides containing hydroxamic acids (**59**). The bulky substituents were selected in order to prevent action of metabolizing enzymes. In this study, the sulfonamide series exhibited improved potency both against TACE and in whole blood assay (WBA) compared with marimastat, while thioether or ether showed poor activity. Optimization of sulfonamide series led to the identification of heterocyclic bicyclic sulfonamides **59a** (TACE IC$_{50}$ = 0.57 nM; WBA IC$_{50}$ = 0.28 μM). The **60**, reported by Kottirsch et al. (2002) is a dual inhibitor of MMP and TACE at nanomolar potencies. It also inhibits the release of TNF-α from cells with an IC$_{50}$ of 48 nM. Ott et al. (2008a) reported α,β-cyclic-β-benzamido hydroxamic acid derivatives as a new class of TACE inhibitors (**61a, b**). The **61a** and **61b** showed good in vitro TACE inhibitory activity at IC$_{50}$ of 0.14 and 1.0 nM, respectively. Ott et al. (2008b) also reported novel oxaspiro[4,4]nonane b-benzamido hydroxamic acids (**62**, **63**, and **64**) which showed excellent TACE inhibitory activity at IC$_{50}$ of 1 nM and selectivity over a wide range of MMPs.
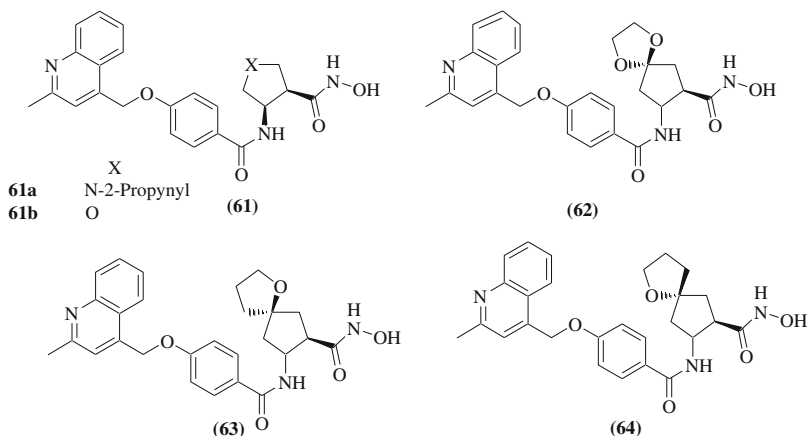
Lu et al. (2008) reported benzofuran, imidazopyridine, and pyrazolopyridine containing benzamido hydroxamic acid derivatives as selective TACE inhibitors (**65**). The **65a** has been identified as a potent TACE inhibitor (IC$_{50}$ = 2.2 nM in pTACE and 52 nM in WBA) with good oral bioavailability.
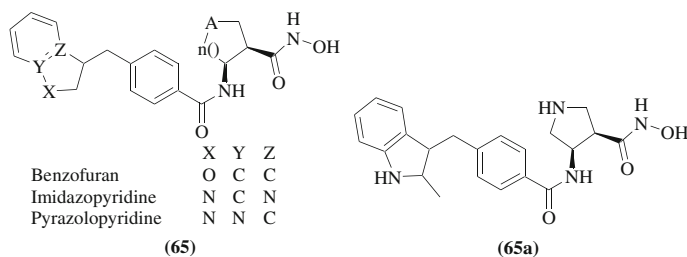
Gilmore et al. (2006) synthesized three series of aminohydroxamic acid analogs i.e., α,β-cyclic-β-aminohydroxamic acid; α,α -cyclic-β-aminohydroxamic acid; and β,β-cyclic-β-aminohydroxamic acid series (Fig. 4) and evaluated for their efficacy for TACE in in vitro and WBA. In this study, the most active compounds were found in β,β-cyclic-β-aminohydroxamic acid series (**66**). The compound (**66**) showed TACE inhibitory activity (Ki) at 0.35 nM in pTACE assays and (IC$_{50}$) 150 nM in WBA. The compound **67**, reported by Duan et al. (2008), is also a β,β-cyclic-β-benzamido hydroxamic acid derivative. **67** showed excellent TACE inhibitory activity (Ki = 0.15 nM) and oral bioavailability. Holms et al. (2001) reported macrocyclicamide hydroxamic acid analog and evaluated for TACE and MMP inhibitory activity. The **68** was identified with good TACE inhibitory activity (IC$_{50}$ = 140 nM) but showed poor selectivity over MMPs (IC$_{50}$ = 0.79–6.8 nM) (Fig. 4).
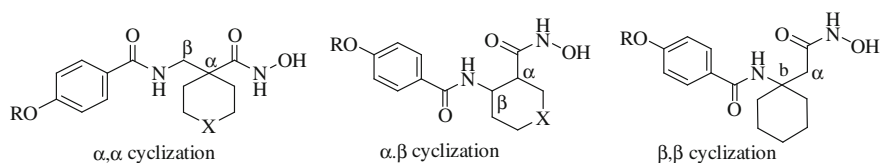
Fig. 4 Development of cyclic-β-aminohydroxamic acids
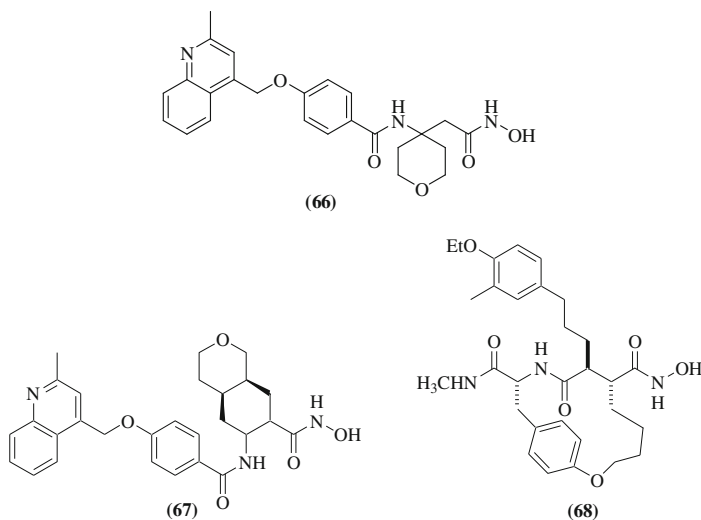
2.5 IMP-Dehydrogenase Inhibitors

IMP-dehydrogenase (IMPDH) inhibitors possess significant ability to induce differentiation and apoptosis (Inai et al. 1998, 2000). Mycophenolic acid (MPA, **69**) is a potent inhibitor of human IMPDH (Ki = 10 nM). Floryk et al. (2004, 2006) studied the MPA-assisted differentiation of human prostate cancer PC-3 cells and DU145 cells. Chong et al. (2006) reported that MPA potentially inhibits endothelial cell proliferation in vitro and block tumor-induced angiogenesis in vivo. Chen et al. (2007) reported synthesis of a series of dual inhibitors of IMPDH and HDACs by modification in CAP region of MPA and isosteric replacement of –COOH group of MPA by –CONHOH (**70**). In this study, mycophenolic hydroxamic acid (**70a**, MAHA) was identified as the most potent IMPDH (Ki = 30 nM) and HDAC inhibitor (IC$_{50}$ = 5.0 μM). The CAP region of SAHA (**2**) was also modified to give compound **70b** by introducing the CAP region of

MPA. **70b** was found to inhibit IMPDH and HDAC at IC_{50} of 1.7 and 0.06 μM, respectively. Both MAHA (**70a**, IC_{50} = 4.8 μM) and **70b** (IC_{50} = 0.29 μM) were found more potent antiproliferative agents than MAP (IC_{50} = 7.7 μM) and SAHA (**2**, IC_{50} = 0.75 μM), respectively.

MPA
(69)

n = 1, 2; R = H/Me
(70)

MAHA
(70a)

(70b)
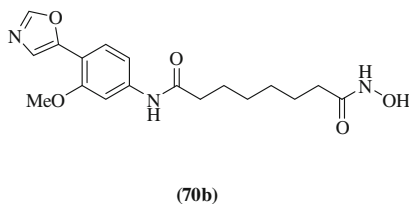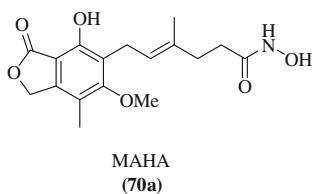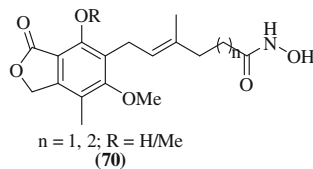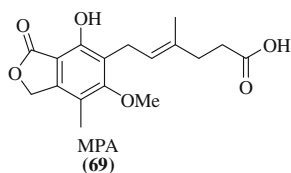
2.6 Ribonucleotide Reductase Inhibitors

van't Riet et al. (1979) reported benzohydroxamic acids (BHA) as inhibitors of mammalian ribonucleotide reductase. **71** and **72** were showed mammalian ribonucleotide reductase inhibition at the ID_{50} of 3.5 and 30 μM, respectively. The **71** and **72** also showed antineoplastic activity on L1210 leukemic mice.

(71)

(72)
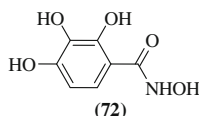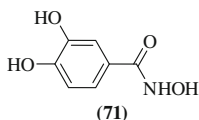
3 Nonspecific Hydroxamic Acid Derivatives

3.1 Benzodiazepines-Hydroxamic Acid Analogs

Some benzodiazepines like BMS-214662 (**73**) (Hunt et al. 2000) and BZ-423 (**74**) (Sundberg et al. 2006) possess strong antiproliferative activity against wide range of cancer cell lines. Tardibono and Miller (2009) reported a new series of 1,4-benzodiazepines, bearing hydroxamic acid as a part of diazepine ring and their

anticancer activities. The representative compound **75** showed 100 and 96 % inhibition of MCF-7 and PC-3 tumor cell lines at the concentration of 20 μM.

BMS-214662 **(73)**   BZ-423 **(74)**   **(75)**
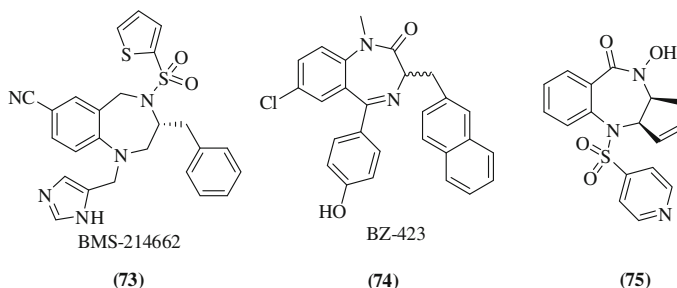
3.2 α-Aminosuberic-Hydroxamic Acid Analogs

Kahnberg et al. (2006) reported a series of hydroxamic acid-based anticancer agents derived from parallel synthesis from α-aminosuberic acid. The compound **76** was identified as the most potent anticancer agent. It showed good anticancer activity ($IC_{50} < 100$ nM) against MM329, MM470, MM604, Mel RM, SK-Mel-28, D17, and A2058 melanoma cells. **76** showed excellent activity (90 nM) against the cervical carcinoma HeLa cells and found moderately selective (SI 9.7) over normal NFF cells.

(76)
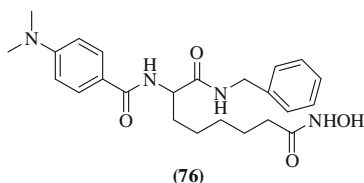
3.3 Arylsulfonamide-Hydroxamic Acid Analogs

A disintegrin and MMPs (ADAMs, zinc endopeptidases) play important role in the cleavage and release of substrates that are involved in cancer cell proliferation and progression (Mochizuki and Okada 2007). On the other hand, the activated leukocyte cell adhesion molecule (ALCAM) involved in homeostasis and cellular architecture by cell–cell and cell–matrix interactions. The studies have shown that ALCAM is involved in tumor biology and development (Swart et al. 2005). This

has been observed that the ALCAM is expressed at the surface of epithelial ovarian cancer (EOC) cells and is released in a soluble form (sALCAM) by ADAM-17 mediated shedding (Piazza 2005). Nuti et al. (2010) reported arylsulfonamide-based hydroxamic acid inhibitors of ADAM-17 and ALCAM. **77a** and **77b** are representatives of this class of compounds showing ADAM-17 inhibitory activity (IC_{50} = 1.6 and 0.7 nM), respectively. These compounds also inhibit the release of sALCAM at IC_{50} of 11 and 15 nM, respectively, from A2774 (human EOC cells) cell lines.
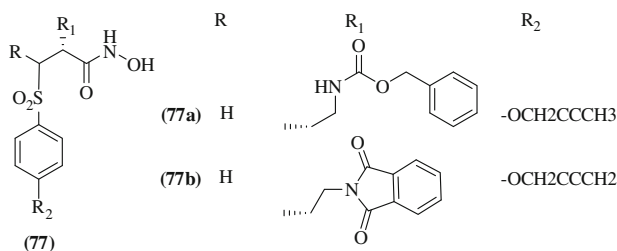
3.4 N-Alkylated Amino Acid-Derived Hydroxamate

Stanger et al. (2006) reported novel N-alkylated amino acid-derived hydroxamate, 2-[Benzyl-(2-nitrobenzenesulfonyl)-amino]-N-hydroxy-3-methyl-N-propyl-butyramide (NAHA, **78**) as antiproliferative agent. Jiang et al. (2012) reported the anticancer profile of NAHA against human breast cancer cells MDA-MB-231 in vitro and in vivo. The NAHA (**78**), inhibited the growth of human breast cancer cells at IC_{50} of 30 μM. It was found very active against highly invasive human breast cancer cells MDA-MB-231. It showed 84% suppression in proliferation of MDA-MB-231 at 50 μM. The suggested underline mechanism of the suppression of MDA-MB-231 includes the inhibition of mitotic figures, induction of apoptosis, and the reduction of CD31 and VEGF positive cells in tumors.

NAHA

(78)
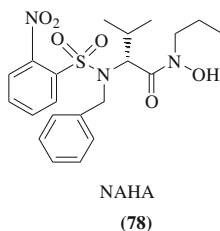
3.5 Retrohydroxamates

Amamistatins A and B (**79**, linear lipopeptides) are natural products from actinomycete *Nocardia asteroids* (Kokubo et al. 2000). Both, Amamistatins A and B possess antiproliferative activity against MCF-7, A549, and MKN45 human tumor cell lines ($IC_{50} = 0.24$–0.56 μM). Compound **80**, an amamistatin-based retrohydroxamate exhibited 73% inhibition of HDAC activity at the 10 μM concentration and 65% growth inhibition of MCF-7 cell lines (breast cancer) at 20 μM concentration (Fennell and Miller 2007).

	X
Amamistatin A	-OMe
Amamistatin B	-H

(79) **(80)**
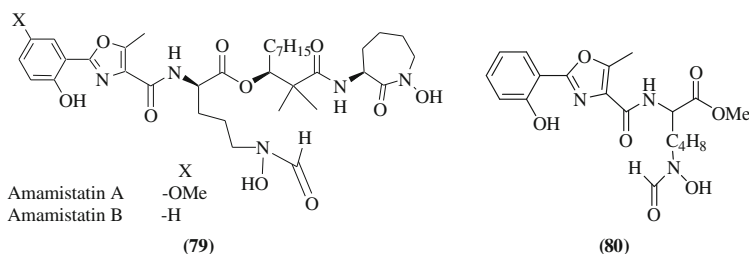
4 Future Prospects and Concluding Remarks

The metalloenzymes, i.e., HDAC, MMPs and TACE, and kinases, i.e., human EGFR/HER2 are attractive targets for the development of anticancer agents. The various classes on hydroxamic acid derivatives have been studied for their relative affinities toward these anticancer drug targets. Batimastat (**51**) and prinomastat (**52**) (MMPs inhibitors); marimastat (TACE/MMPs inhibitors) etc., have been identified as a potential anticancer agents, but these drug molecules have been withdrawn from the clinical trials due to either poor pharmacological response in cancer patient or due to insufficient bioavailability. The hydroxamic acid derivatives are also suffered from poor selectivity for cancer cells over normal cells. However, efforts have been made by judicious and careful selection of scaffold to overcome these problems but therapeutically acceptable hydroxamic acid-based anticancer agent is still not available. The new scaffolds like N-substituted 4-alkylpiperazine and 4-alkylpiperdine hydroxamic acids (**18**, **19**), osthole derivatives (**16**), 1,2,3,4-tetrahydroisoquinoline-3-carboxylic acids (**24** and **45**), N-alkylated amino acid-derived hydroxamate (**78**) rise a hope to develop potential anticancer agents.

References

Alonso-Ruiz A, Pijoan JI, Ansuategui E, Urkaregi A, Calabozo M, Quintana A (2008) Tumor necrosis factor alpha drugs in rheumatoid arthritis: systematic review and metaanalysis of efficacy and safety. BMC Musculoskelet Disord 9:52

Angibaud P, Van Emelen K, Decrane L, van Brandt S, Ten Holte P, Pilatte I, Roux B et al (2010) Identification of a series of substituted 2-piperazinyl-5-pyrimidylhydroxamic acids as potent histone deacetylase inhibitors. Bioorg Med Chem Lett 20:294–298

Arribas J, Borroto A (2002) Protein ectodomain shedding. Chem Rev 102:4627–4638

Atadja P, Gao L, Kwon P, Trogani N, Walker H, Hsu M, Yeleswarapu L, Chandramouli N, Perez L, Versace R, Wu A, Sambucetti L, Lassota P, Cohen D, Bair K, Wood A, Remiszewski S (2004) Selective growth inhibition of tumor cells by a novel histone deacetylase inhibitor, NVP-LAQ824. Cancer Res 64:689–695

Barlaam B, Bird TG, Lambert-Van Der Brempt C, Campbell D, Foster SJ, Maciewicz R (1999) New alpha-substituted succinate-based hydroxamic acids as TNFalpha convertase inhibitors. J Med Chem 42:4890–4908

Becker DP, Villamil CI, Barta TE, Bedell LJ, Boehm TL, Decrescenzo GA, Freskos JN, Getman DP, Hockerman S, Heintz R, Howard SC, Li MH, McDonald JJ, Carron CP, Funckes-Shippy CL, Mehta PP, Munie GE, Swearingen CA (2005) Synthesis and structure-activity relationships of beta- and alpha-piperidine sulfone hydroxamic acid matrix metalloproteinase inhibitors with oral antitumor efficacy. J Med Chem 48:6713–6730

Bissett D, O'Byrne KJ, von Pawel J, Gatzemeier U, Price A, Nicolson M, Mercier R, Mazabel E, Penning C, Zhang MH, Collier MA, Shepherd FA (2005) Phase III study of matrix metalloproteinase inhibitor prinomastat in non-small-cell lung cancer. J Clin Oncol 23:842–849

Botos I, Scapozza L, Zhang D, Liotta LA, Meyer EF (1996) Batimastat, a potent matrix mealloproteinase inhibitor, exhibits an unexpected mode of binding. Proc Natl Acad Sci U S A 93:2749–2754

Bouchain G, Leit S, Frechette S, Khalil EA, Lavoie R, Moradei O, Woo SH, Fournel M, Yan PT, Kalita A, Trachy-Bourget MC, Beaulieu C, Li Z, Robert MF, MacLeod AR, Besterman JM, Delorme D (2003) Development of potential antitumor agents. Synthesis and biological evaluation of a new set of sulfonamide derivatives as histone deacetylase inhibitors. J Med Chem 46:820–830

Cai X, Zhai HX, Wang J, Forrester J, Qu H, Yin L, Lai CJ, Bao R, Qian C (2010) Discovery of 7-(4-(3-ethynylphenylamino)-7-methoxyquinazolin-6-yloxy)-N-hydroxyheptanamide (CUDc-101) as a potent multi-acting HDAC, EGFR, and HER2 inhibitor for the treatment of cancer. J Med Chem 53:2000–2009

Catley L, Weisberg E, Tai YT, Atadja P, Remiszewski S, Hideshima T, Mitsiades N, Shringarpure R, LeBlanc R, Chauhan D, Munshi NC, Schlossman R, Richardson P, Griffin J, Anderson KC (2003) NVP-LAQ824 is a potent novel histone deacetylase inhibitor with significant activity against multiple myeloma. Blood 102:2615–2622

Charrier C, Clarhaut J, Gesson JP, Estiu G, Wiest O, Roche J, Bertrand P (2009) Synthesis and modeling of new benzofuranone histone deacetylase inhibitors that stimulate tumor suppressor gene expression. J Med Chem 52:3112–3115

Chen L, Wilson D, Jayaram HN, Pankiewicz KW (2007) Dual inhibitors of inosine monophosphate dehydrogenase and histone deacetylases for cancer treatment. J Med Chem 50:6685–6691

Chen Y, Lopez-Sanchez M, Savoy DN, Billadeau DD, Dow GS, Kozikowski AP (2008) A series of potent and selective, triazolylphenyl-based histone deacetylases inhibitors with activity against pancreatic cancer cells and *Plasmodium falciparum*. J Med Chem 51:3437–3448

Chong CR, Qian DZ, Pan F, Wei Y, Pili R, Sullivan DJ Jr, Liu JO (2006) Identification of type 1 inosine monophosphate dehydrogenase as an antiangiogenic drug target. J Med Chem 49:2677–2680

Codd R, Braich N, Liu J, Soe CZ, Pakchung AA (2009) Zn(II)-dependent histone deacetylase
    inhibitors: suberoylanilidehydroxamic acid and trichostatin A. Int J Biochem Cell Biol
    41:736–739
Curran S, Murray GI (2000) Matrix metalloproteinases: molecular aspects of their roles in tumour
    invasion and metastasis. Eur J Cancer 36:1621–1630
Dallavalle S, Cincinelli R, Nannei R, Merlini L, Morini G, Penco S, Pisano C, Vesci L, Barbarino
    M, Zuco V, De Cesare M, Zunino F (2009) Design, synthesis, and evaluation of biphenyl-4-
    yl-acrylohydroxamic acid derivatives as histone deacetylase (HDAC) inhibitors. Eur J Med
    Chem 44:1900–1912
DasGupta S, Murumkar PR, Giridhar R, Yadav MR (2009) Current perspective of TACE
    inhibitors: a review. Bioorg Med Chem 17:444–459
de Ruijter AJ, Kemp S, Kramer G, Meinsma RJ, Kaufmann JO, Caron HN, van Kuilenburg AB
    (2004) The novel histone deacetylase inhibitor BL1521 inhibits proliferation and induces
    apoptosis in neuroblastoma cells. Biochem Pharmacol 68:1279–1288
Dear AE, Liu HB, Mayes PA, Perlmutter P (2006) Conformational analogues of Oxamflatin as
    histone deacetylase inhibitors. Org Biomol Chem 4:3778–3784
Duan JJ, Chen L, Lu Z, Xue CB, Liu RQ, Covington MB, Qian M, Wasserman ZR, Vaddi K,
    Christ DD, Trzaskos JM, Newton RC, Decicco CP (2008) Discovery of beta-benzamidohydr-
    oxamic acids as potent, selective, and orally bioavailable TACE inhibitors. Bioorg Med Chem
    Lett 18:241–246
Egeblad M, Werb Z (2002) New functions for the matrix metalloproteinases in cancer
    progression. Nat Rev Cancer 2:161–174
Fennell KA, Miller MJ (2007) Syntheses of amamistatin fragments and determination of their
    HDAC and antitumor activity. Org Lett 9:1683–1685
Finnin MS, Donigian JR, Cohen A, Richon VM, Rifkind RA, Marks PA, Breslow R, Pavletich
    NP (1999) Structures of a histone deacetylase homologue bound to the TSA and SAHA
    inhibitors. Nature 401:188–193
Floryk D, Huberman E (2006) Mycophenolic acid-induced replication arrest, differentiation
    markers and cell death of androgen-independent prostate cancer cells DU145. Cancer Lett
    231:20–29
Floryk D, Tollaksen SL, Giometti CS, Huberman E (2004) Differentiation of human prostate
    cancer PC-3 cells induced by inhibitors of inosine 5'-monophosphate dehydrogenase. Cancer
    Res 64:9049–9056
Gallinari P, Di Marco S, Jones P, Pallaoro M, Steinkuhler C (2007) HDACs, histone
    deacetylation and gene transcription: from molecular biology to cancer therapeutics. Cell Res
    17:195–211
Gediya LK, Chopra P, Purushottamachar P, Maheshwari N, Njar VC (2005) A new simple and
    high-yield synthesis of suberoylanilide hydroxamic acid and its inhibitory effect alone or in
    combination with retinoids on proliferation of human prostate cancer cells. J Med Chem
    48:5047–5051
Giles F, Fischer T, Cortes J, Garcia-Manero G, Beck J, Ravandi F, Masson E, Rae P, Laird G,
    Sharma S, Kantarjian H, Dugan M, Albitar M, Bhalla K (2006) A phase I study of intravenous
    LBH589, a novel cinnamic hydroxamic acid analogue histone deacetylase inhibitor, in
    patients with refractory hematologic malignancies. Clin Cancer Res 12:4628–4635
Gilmore JL, King BW, Harris C, Maduskuie T, Mercer SE, Liu RQ, Covington MB, Qian M,
    Ribadeneria MD, Vaddi K, Trzaskos JM, Newton RC, Decicco CP, Duan JJ (2006) Synthesis
    and structure-activity relationship of a novel, achiral series of TNF-alpha converting enzyme
    inhibitors. Bioorg Med Chem Lett 16:2699–2704
Glenn MP, Kahnberg P, Boyle GM, Hansford KA, Hans D, Martyn AC, Parsons PG, Fairlie DP
    (2004) Antiproliferative and phenotype-transforming antitumor agents derived from cysteine.
    J Med Chem 47:2984–2994
He R, Chen Y, Chen Y, Ougolkov AV, Zhang JS, Savoy DN, Billadeau DD, Kozikowski AP
    (2010) Synthesis and biological evaluation of triazol-4-ylphenyl-bearing histone deacetylase
    inhibitors as anticancer agents. J Med Chem 53:1347–1356

Holms J, Mast K, Marcotte P, Elmore I, Li J, Pease L, Glaser K, Morgan D, Michaelides M, Davidsen S (2001) Discovery of selective hydroxamic acid inhibitors of tumor necrosis factor-alpha converting enzyme. Bioorg Med Chem Lett 11:2907–2910

Howman RA, Prince HM (2011) New drug therapies in peripheral T-cell lymphoma. Expert Rev Anticancer Ther 11:457–472

Huang WJ, Chen CC, Chao SW, Yu CC, Yang CY, Guh JH, Lin YC, Kuo CI, Yang P, Chang CI (2011) Synthesis and evaluation of aliphatic-chain hydroxamates capped with osthole derivatives as histone deacetylase inhibitors. Eur J Med Chem 46:4042–4049

Hunt JT, Ding CZ, Batorsky R, Bednarz M, Bhide R, Cho Y, Chong S, Chao S, Gullo-Brown J, Guo P, Kim SH, Lee FY, Leftheris K, Miller A, Mitt T, Patel M, Penhallow BA, Ricca C, Rose WC, Schmidt R, Slusarchyk WA, Vite G, Manne V (2000) Discovery of (R)-7-cyano-2,3,4, 5-tetrahydro-1-(1H-imidazol-4-ylmethyl)-3-(phenylmethyl)-4-(2-thienylsulfonyl)-1H-1,4-benzodiazepine (BMS-214662), a farnesyltransferase inhibitor with potent preclinical antitumor activity. J Med Chem 43:3587–3595

Inai K, Tsutani H, Yamauchi T, Nakamura T, Ueda T (1998) Differentiation and reduction of intracellular GTP levels in HL-60 and U937 cells upon treatment with IMP dehydrogenase inhibitors. Adv Exp Med Biol 431:549–553

Inai K, Tsutani H, Yamauchi T, Fukushima T, Iwasaki H, Imamura S, Wano Y, Nemoto Y, Naiki H, Ueda T (2000) Differentiation induction in non-lymphocytic leukemia cells upon treatment with mycophenolate mofetil. Leuk Res 24:761–768

Jiang J, Thyagarajan-Sahu A, Krchnak V, Jedinak A, Sandusky GE, Sliva D (2012) NAHA, a novel hydroxamic acid-derivative, inhibits growth and angiogenesis of breast cancer in vitro and in vivo. PLoS One 7:e34283

Jose B, Okamura S, Kato T, Nishino N, Sumida Y, Yoshida M (2004) Toward an HDAC6 inhibitor: synthesis and conformational analysis of cyclic hexapeptide hydroxamic acid designed from alpha-tubulin sequence. Bioorg Med Chem 12:1351–1356

Jung M, Brosch G, Kolle D, Scherf H, Gerhauser C, Loidl P (1999) Amide analogues of trichostatin A as inhibitors of histone deacetylase and inducers of terminal cell differentiation. J Med Chem 42:4669–4679

Kahnberg P, Lucke AJ, Glenn MP, Boyle GM, Tyndall JD, Parsons PG, Fairlie DP (2006) Design, synthesis, potency, and cytoselectivity of anticancer agents derived by parallel synthesis from alpha-aminosuberic acid. J Med Chem 49:7611–7622

Kenny PA (2007) TACE: a new target in epidermal growth factor receptor dependent tumors. Differentiation 75:800–808

Keystone EC (2011) Does anti-tumor necrosis factor-alpha therapy affect risk of serious infection and cancer in patients with rheumatoid arthritis? A review of longterm data. J Rheumatol 38:1552–1562

Kijima M, Yoshida M, Sugita K, Horinouchi S, Beppu T (1993) Trapoxin, an antitumor cyclic tetrapeptide, is an irreversible inhibitor of mammalian histone deacetylase. J Biol Chem 268:22429–22435

Kim YB, Lee KH, Sugita K, Yoshida M, Horinouchi S (1999) Oxamflatin is a novel antitumor compound that inhibits mammalian histone deacetylase. Oncogene 18:2461–2470

Kim HM, Lee K, Park BW, Ryu DK, Kim K, Lee CW, Park SK, Han JW, Lee HY, Lee HY, Han G (2006) Synthesis, enzymatic inhibition, and cancer cell growth inhibition of novel delta-lactam-based histone deacetylase (HDAC) inhibitors. Bioorg Med Chem Lett 16:4068–4070

Kokubo SS K, Shinohara C, Tsuji T, Uemura D (2000) Structures of amamistatins A and B, novel growth inhibitors of human tumor cell lines from nocardia asteroides. Tetrahedron 56:5

Kottirsch G, Koch G, Feifel R, Neumann U (2002) Beta-aryl-succinic acid hydroxamates as dual inhibitors of matrix metalloproteinases and tumor necrosis factor alpha converting enzyme. J Med Chem 45:2289–2293

Kovacic P, Edwards CL (2011) Hydroxamic acids (therapeutics and mechanism): chemistry, acyl nitroso, nitroxyl, reactive oxygen species, and cell signaling. J Recept Signal Transduct Res 31:10–19

Kozikowski AP, Chen Y, Gaysin AM, Savoy DN, Billadeau DD, Kim KH (2008) Chemistry, biology, and QSAR studies of substituted biaryl hydroxamates and mercaptoacetamides as HDAC inhibitors-nanomolar-potency inhibitors of pancreatic cancer cell growth. Chem Med Chem 3:487–501

Li NG, Shi ZH, Tang YP, Wei L, Lian Y, Duan JA (2012) Discovery of selective small molecular TACE inhibitors for the treatment of rheumatoid arthritis. Curr Med Chem 19:2924–2956

Low JA, Johnson MD, Bone EA, Dickson RB (1996) The matrix metalloproteinase inhibitor batimastat (BB-94) retards human breast cancer solid tumor growth but not ascites formation in nude mice. Clin Cancer Res 2:1207–1214

Lu Z, Ott GR, Anand R, Liu RQ, Covington MB, Vaddi K, Qian M, Newton RC, Christ DD, Trzaskos J, Duan JJ (2008) Potent, selective, orally bioavailable inhibitors of tumor necrosis factor-alpha converting enzyme (TACE): discovery of indole, benzofuran, imidazopyridine and pyrazolopyridine P1′ substituents. Bioorg Med Chem Lett 18:1958–1962

Mahboobi S, Dove S, Sellmer A, Winkler M, Eichhorn E, Pongratz H, Ciossek T, Baer T, Maier T, Beckers T (2009) Design of chimeric histone deacetylase- and tyrosine kinase-inhibitors: a series of imatinib hybrides as potent inhibitors of wild-type and mutant BCR-ABL, PDGF-Rbeta, and histone deacetylases. J Med Chem 52:2265–2279

Marks PA, Richon VM, Rifkind RA (2000) Histone deacetylase inhibitors: inducers of differentiation or apoptosis of transformed cells. J Natl Cancer Inst 92:1210–1216

Marmor MD, Skaria KB, Yarden Y (2004) Signal transduction and oncogenesis by ErbB/HER receptors. Int J Radiat Oncol Biol Phys 58:903–913

Mass RD (2004) The HER receptor family: a rich target for therapeutic development. Int J Radiat Oncol Biol Phys 58:932–940

McCawley LJ, Matrisian LM (2000) Matrix metalloproteinases: multifunctional contributors to tumor progression. Mol Med Today 6:149–156

Millar AW, Brown PD, Moore J, Galloway WA, Cornish AG, Lenehan TJ, Lynch KP (1998) Results of single and repeat dose studies of the oral matrix metalloproteinase inhibitor marimastat in healthy male volunteers. Br J Clin Pharmacol 45:21–26

Miller MJ (1989) Synthesis and therapeutic potential of hydroxamic acid-based siderophores and analogues. Chem Rev 89:1563–1579

Minucci S, Pelicci PG (2006) Histone deacetylase inhibitors and the promise of epigenetic (and more) treatments for cancer. Nat Rev Cancer 6:38–51

Mochizuki S, Okada Y (2007) ADAMs in cancer cell proliferation and progression. Cancer Sci 98:621–628

Neilands JB (1995) Siderophores: structure and function of microbial iron transport compounds. J Biol Chem 270:26723–26726

Nelson AR, Fingleton B, Rothenberg ML, Matrisian LM (2000) Matrix metalloproteinases: biologic activity and clinical implications. J Clin Oncol 18:1135–1149

Nuti E, Tuccinardi T, Rossello A (2007) Matrix metalloproteinase inhibitors: new challenges in the era of post broad-spectrum inhibitors. Curr Pharm Des 13:2087–2100

Nuti E, Casalini F, Avramova SI, Santamaria S, Fabbi M, Ferrini S, Marinelli L, LaPietra V, Limongelli V, Novellino E, Cercignani G, Orlandini E, Nencetti S, Rossello A (2010) Potent arylsulfonamide inhibitors of tumor necrosis factor-alpha converting enzyme able to reduce activated leukocyte cell adhesion molecule shedding in cancer cell models. J Med Chem 53:2622–2635

Oanh DT, Hai HV, Park SH, Kim HJ, Han BW, Kim HS, Hong JT, Han SB, Hue VT, Nam NH (2011) Benzothiazole-containing hydroxamic acids as histone deacetylase inhibitors and antitumor agents. Bioorg Med Chem Lett 21:7509–7512

Ott GR, Asakawa N, Lu Z, Liu RQ, Covington MB, Vaddi K, Qian M, Newton RC, Christ DD, Traskos JM, Decicco CP, Duan JJ (2008a) Alpha, beta-cyclic-beta-benzamido hydroxamic acids: novel templates for the design, synthesis, and evaluation of selective inhibitors of TNF-alpha converting enzyme (TACE). Bioorg Med Chem Lett 18:694–699

Ott GR, Asakawa N, Liu RQ, Covington MB, Qian M, Vaddi K, Newton RC, Trzaskos JM, Christ DD, Galya L, Scholz T, Marshall W, Duan JJ (2008b) Alpha, beta-cyclic-beta-

benzamido hydroxamic acids: novel oxaspiro[4.4]nonane templates for the discovery of potent, selective, orally bioavailable inhibitors of tumor necrosis factor-alpha converting enzyme (TACE). Bioorg Med Chem Lett 18:1288–1292

Ouaissi M, Ouaissi A (2006) Histone deacetylase enzymes as potential drug targets in cancer and parasitic diseases. J Biomed Biotechnol 2006:13474

Ouwehand K, de Ruijter AJ, van Bree C, Caron HN, van Kuilenburg AB (2005) Histone deacetylase inhibitor BL1521 induces a G1-phase arrest in neuroblastoma cells through altered expression of cell cycle proteins. FEBS Lett 579:1523–1528

Piazza T, Cha E, Bongarzone I, Canevari S, Bolognesi A, Polito L, Bargellesi A, Sassi F, Ferrini S, Fabbi M (2005) Internalization and recycling of ALCAM/CD166 detected by a fully human single-chain recombinant antibody. J Cell Sci 118:1515–1525

Plumb JA, Williams RJ, Finn PW, Bandara MJ, Romero MR, Watkins CJ, La Thangue NB, Brown R (2002) Inhibition of tumour cell growth in vitro and in vivo by the histone deacetylase inhibitor PXD101. Proc Am Assoc Cancer Res 43:333–334

Plumb JA, Finn PW, Williams RJ, Bandara MJ, Romero MR, Watkins CJ, La Thangue NB, Brown R (2003) Pharmacodynamic response and inhibition of growth of human tumor xenografts by the novel histone deacetylase inhibitor PXD101. Mol Cancer Ther 2:721–728

Press MF, Lenz HJ (2007) EGFR, HER2 and VEGF pathways: validated targets for cancer treatment. Drugs 67:2045–2075

Ramalingam SS, Belani CP, Ruel C, Frankel P, Gitlitz B, Koczywas M, Espinoza-Delgado I, Gandara D (2009) Phase II study of belinostat (PXD101), a histone deacetylase inhibitor, for second line therapy of advanced malignant pleural mesothelioma. J Thorac Oncol 4:97–101

Renkiewicz R, Qiu L, Lesch C, Sun X, Devalaraja R, Cody T, Kaldjian E, Welgus H, Baragi V (2003) Broad-spectrum matrix metalloproteinase inhibitor marimastat induced musculoskeletal side effects in rats. Arthritis Rheum 48:1742–1749

Rossi C, Porcelloni M, D'Andrea P, Fincham CI, Ettorre A, Mauro S, Squarcia A, Bigioni M, Parlani M, Nardelli F, Binaschi M, Maggi CA, Fattori D (2011) Alkyl piperidine and piperazine hydroxamic acids as HDAC inhibitors. Bioorg Med Chem Lett 21:2305–2308

Saban N, Bujak M (2009) Hydroxyurea and hydroxamic acid derivatives as antitumor drugs. Cancer Chemother Pharmacol 64:213–221

Salmi-Smail C, Fabre A, Dequiedt F, Restouin A, Castellano R, Garbit S, Roche P, Morelli X, Brunel JM, Collette Y (2010) Modified cap group suberoylanilide hydroxamic acid histone deacetylase inhibitor derivatives reveal improved selective antileukemic activity. J Med Chem 53:3038–3047

Santos MA, Enyedy EA, Nuti E, Rossello A, Krupenko NI, Krupenko SA (2007) Methotrexate gamma-hydroxamate derivatives as potential dual target antitumor drugs. Bioorg Med Chem 15:1266–1274

Scozzafava A, Supuran CT (2000) Carbonic anhydrase and matrix metalloproteinase inhibitors: sulfonylated amino acid hydroxamates with MMP inhibitory properties act as efficient inhibitors of CA isozymes I, II, and IV, and N-hydroxysulfonamides inhibit both these zinc enzymes. J Med Chem 43:3677–3687

Scuto A, Kirschbaum M, Kowolik C, Kretzner L, Juhasz A, Atadja P, Pullarkat V, Bhatia R, Forman S, Yen Y, Jove R (2008) The novel histone deacetylase inhibitor, LBH589, induces expression of DNA damage response genes and apoptosis in Ph-acute lymphoblastic leukemia cells. Blood 111:5093–5100

Shalinsky DR, Brekken J, Zou H, McDermott CD, Forsyth P, Edwards D, Margosiak S, Bender S, Truitt G, Wood A, Varki NM, Appelt K (1999) Broad antitumor and antiangiogenic activities of AG3340, a potent and selective MMP inhibitor undergoing advanced oncology clinical trials. Ann N Y Acad Sci 878:236–270

Sonoda H, Nishida K, Yoshioka T, Ohtani M, Sugita K (1996) Oxamflatin: a novel compound which reverses malignant phenotype to normal one via induction of JunD. Oncogene 1321:143–149

Sparano JA, Bernardo P, Stephenson P, Gradishar WJ, Ingle JN, Zucker S, Davidson NE (2004) Randomized phase III trial of marimastat versus placebo in patients with metastatic breast

cancer who have responding or stable disease after first-line chemotherapy: Eastern Cooperative Oncology Group trial E2196. J Clin Oncol 22:4683–4690

Stanger KJ, Sliva D, Jiang J, Krchnak V (2006) Synthesis and screening of N-alkyl hydroxamates for inhibition of cancer cell proliferation. Comb Chem High Throughput Screen 9:651–661

Steward WP, Thomas AL (2000) Marimastat: the clinical development of a matrix metalloproteinase inhibitor. Expert Opin Investig Drugs 9:2913–2922

Su H, Nebbioso A, Carafa V, Chen Y, Yang B, Altucci L, You Q (2008) Design, synthesis and biological evaluation of novel compounds with conjugated structure as anti-tumor agents. Bioorg Med Chem 16:7992–8002

Sundberg TB, Ney GM, Subramanian C, Opipari AW Jr, Glick GD (2006) The immunomodulatory benzodiazepine Bz-423 inhibits B-cell proliferation by targeting c-myc protein for rapid and specific degradation. Cancer Res 66:1775–1782

Swart GW, Lunter PC, Kilsdonk JW, Kempen LC (2005) Activated leukocyte cell adhesion molecule (ALCAM/CD166): signaling at the divide of melanoma cell clustering and cell migration? Cancer Metastasis Rev 24:223–236

Tardibono LP, Miller MJ (2009) Synthesis and anticancer activity of new hydroxamic acid containing 1,4-benzodiazepines. Org Lett 11:1575–1578

van't Riet B, Wampler GL, Elford HL (1979) Synthesis of hydroxy- and amino-substituted benzohydroxamic acids: inhibition of ribonucleotide reductase and antitumor activity. J Med Chem 22:589–592

Vojinovic J, Damjanov N (2011) HDAC inhibition in rheumatoid arthritis and juvenile idiopathic arthritis. Mol Med 17:397–403

Wang H, Yu N, Song H, Chen D, Zou Y, Deng W, Lye PL, Chang J, Ng M, Sun ET, Sangthongpitag K, Wang X, Wu X, Khng HH, Fang L, Goh SK, Ong WC, Bonday Z, Stunkel W, Poulsen A, Entzeroth M (2009) N-Hydroxy-1,2-disubstituted-1H-benzimidazol-5-yl acrylamides as novel histone deacetylase inhibitors: design, synthesis, SAR studies, and in vivo antitumor activity. Bioorg Med Chem Lett 19:1403–1408

Wang H, Lim ZY, Zhou Y, Ng M, Lu T, Lee K, Sangthongpitag K, Goh KC, Wang X, Wu X, Khng HH, Goh SK, Ong WC, Bonday Z, Sun ET (2010) Acylurea connected straight chain hydroxamates as novel histone deacetylase inhibitors: synthesis, SAR, and in vivo antitumor activity. Bioorg Med Chem Lett 20:3314–3321

Yadav RK, Gupta SP, Sharma PK, Patil VM (2011) Recent advances in studies on hydroxamates as matrix metalloproteinase inhibitors: a review. Curr Med Chem 18:1704–1722

Yao W, Zhuo J, Burns DM, Xu M, Zhang C, Li YL, Qian DQ et al (2007) Discovery of a potent, selective, and orally active human epidermal growth factor receptor-2 sheddase inhibitor for the treatment of cancer. J Med Chem 50:603–606

Yoshida M, Kijima M, Akita M, Beppu T (1990) Potent and specific inhibition of mammalian histone deacetylase both in vivo and in vitro by trichostatin A. J Biol Chem 265:17174–17179

Zhang C, Lovering F, Behnke M, Zask A, Sandanayaka V, Sun L, Zhu Y, Xu W, Zhang Y, Levin JI (2009) Synthesis and activity of quinolinylmethyl P1′ alpha-sulfone piperidine hydroxamate inhibitors of TACE. Bioorg Med ChemLett 19:3445–3448

Zhang L, Fang H, Xu W (2010a) Strategies in developing promising histone deacetylase inhibitors. Med Res Rev 30:585–602

Zhang Y, Feng J, Liu C, Zhang L, Jiao J, Fang H, Su L, Zhang X, Zhang J, Li M, Wang B, Xu W (2010b) Design, synthesis and preliminary activity assay of 1,2,3,4-tetrahydroisoquinoline-3-carboxylic acid derivatives as novel Histone deacetylases (HDACs) inhibitors. Bioorg Med Chem 18:1761–1772

Zhang Y, Feng J, Jia Y, Wang X, Zhang L, Liu C, Fang H, Xu W (2011a) Development of tetrahydroisoquinoline-based hydroxamic acid derivatives: potent histone deacetylase inhibitors with marked in vitro and in vivo antitumor activities. J Med Chem 54:2823–2838

Zhang Y, Fang H, Feng J, Jia Y, Wang X, Xu W (2011b) Discovery of a tetrahydroisoquinoline-based hydroxamic acid derivative (ZYJ-34c) as histone deacetylase inhibitor with potent oral antitumor activities. J Med Chem 54:5532–5539

Zhang Y, Feng J, Jia Y, Xu Y, Liu C, Fang H, Xu W (2011c) Design, synthesis and primary activity assay of tripeptidomimetics as histone deacetylase inhibitors with linear linker and branched cap group. Eur J Med Chem 46:5387–5397

Zuo M, Zheng YW, Lu SM, Li Y, Zhang SQ (2012) Synthesis and biological evaluation of N-aryl salicylamides with a hydroxamic acid moiety at 5-position as novel HDAC-EGFR dual inhibitors. Bioorg Med Chem 20:4405–4412

Quantitative Structure–Activity Relationship Studies on Hydroxamic Acids Acting as Histone Deacetylase Inhibitors

Dimitra Hadjipavlou-Litina and Eleni Pontiki

Abstract Hydroxamic acids have been found to react with both proteins and nucleic acids attracting increasing attention for their potential as highly efficacious in combating various biological targets, free radicals, and biological disorders among them cancer and inflammation. The reactivity of hydroxamic acids toward sulfhydryl groups and metal ions of proteins has been suggested to be the reason for their inhibitory effect on various enzymes. The ability of the hydroxamic acid functionality to form chelates with metals in the enzyme's active site is considered to be an important functional feature for a metalloenzyme inhibition. Many approaches in developing hydroxamic drugs, such as trichostatin and vorinostat, that interfere with (metallo) enzymes and act as anticancer drugs have been pursued over the past few decades. We present here a brief review of the QSAR and molecular modeling studies performed on hydroxamic acid derivatives acting as histone deacetylase inhibitors that have been studied as anticancer agents. These studies have shown that the anticancer activity of these compounds is basically controlled by their hydrophobic and steric properties.

Keywords Hydroxamic acids · Anticancer compounds · Quantitative structure-activity relationships · Comparative molecular field analysis · Comparative molecular similarity indices analysis · Histone deacetylase inhibitors

Abbreviations

ACxDN	Index of cohesive interactions in solids
B_1	Sterimol parameter of Verloop for the smallest width of substituent
BMLR	Best multilinear regression method
Clog P	Overall calculated lipophilicity
CMR	Molar refractivity of the whole molecule
CoMFA	Comparative molecular field analysis

D. Hadjipavlou-Litina (✉) · E. Pontiki
Department of Pharmaceutical Chemistry, School of Pharmacy, Aristotle University of Thessaloniki, 54124 Thessaloniki, Greece
e-mail: hadjipav@pharm.auth.gr

CoMSIA   Comparative molecular similarity indices analysis
DPL   Dipole
ES-SWR   Elimination selection-stepwise regression method
FISA   Hydrophilic component of the solvent-accessible surface area
GFA   Genetic function approximation
Glob   Globularity of the compounds
HAT   Histone acetyl-transferase
HDAC   Histone deacetylase
HOMO   Highest occupied molecular orbital
L   Verloop parameter for the length of the first atom of the substituent
LFER   Linear free energy related
LSSVM   Least squares support vector machine
MgVol   MacGovan volume
MLR   Multiple linear regression
MMPs   Matrix metalloproteinases
MR_{-R} Molar refractivity of the substituent
MSA   Molecular shape analysis
MW   Molecular weight
PCA   Principal component analysis
PLS   Partial least squares
PMIX   Principal moment of inertia along X-axis
QSAR   Quantitative structure-activity relationships
QTMS   Quantum topological molecular similarity
r   Radius
SAR   Structure-activity relationships
SASA   Solvent-accessible surface area
ShpC   Shape coefficient
TopoJ   Balaban topological index
TSAR   Tool for structure-activity relationships
WLS   Weighted least square
WPSA   Weak polar component of the solvent-accessible surface area

Contents

1 Introduction

Hydroxamic acids constitute a chemical class sharing the same functional group in which a hydroxylamine is inserted into a carboxylic acid. Their general structure is R–CO–NH–OH, with a CO carbonyl group, and a hydroxylamine residue NH_2–OH. Since Lossen discovered the first of these acids more than 100 years ago, an extraordinary amount of work has been published (Murri et al. 2002; Lipczynska-Kochany 1988). In recent years, hydroxamic acid and derivatives have attracted increasing attention for their potential as highly efficacious in combating various biological targets. The chemistry and biochemistry of hydroxamic acids and their derivatives have attracted considerable attention, due to their pharmacological, toxicological, and pathological properties. Hydroxamic acids have been found to react with both proteins and nucleic acids (Niemeyer et al. 1989). The reactivity of hydroxamic acids toward sulfhydryl groups of proteins has been suggested to be the reason for their inhibitory effect on various enzymes. They are capable of the inhibition of a variety of enzymes. In terms of structure-activity relationships, hydroxamic acids moieties have been used in the design of therapeutic agents targeting cancer (Steward and Thomas 2000; Munster et al. 2001), cardiovascular diseases (Muri et al. 2002), Alzheimer's (Parvathy et al. 1998; El Yazal and Pang 2000), metal poisoning (Domingo 1998), iron-overload (Turcot et al. 2000), and as antioxidants (Green et al. 1993; Taira et al. 2002). The following is an attempt to describe in terms of (Q)SAR the role of hydroxamates as anticancer agents.

2 Hydroxamic Acids as Histone Deacetylase Inhibitors

For the last four decades, a number of potential targets have been proposed for the treatment of cancer. One of the recent targets is histone deacetylase (HDAC). Modification of histone acetylation level, promoted by histone acetyl-transferase (HAT) and HDAC enzymes, has been recognized to play an important role in the epigenetic modulation of gene expression. Histone acetyltransferases (HATs) and histone deacetylases (HDACs) are two opposing classes of enzymes, which tightly control the equilibrium of histone acetylation. Nucleosomal histone acetylation and deacetylation play an important role in the modulation of chromatin structure, chromatin function, and in the regulation of gene expression. An imbalance in the equilibrium of histone acetylation has been associated with carcinogenesis and cancer progression from rare leukemias and lymphomas to breast, prostate and ovarian cancers. The enzymatic inhibition of histone deacetylases (HDACs) has come out as a novel and efficient means for the treatment of these cancers. Inhibition of HDACs induces cell differentiation, apoptosis, and cell-cycle arrest in several cancer cell lines and in vivo preclinical models and thus HDAC inhibitors present a promising class of anticancer agents. More than 80 clinical trials are underway, testing different HDAC inhibitors in several kinds of malignant

diseases. HDAC inhibitors are able to activate differentiation, to arrest the cell cycle in G1 and/or G2, and to induce apoptosis in transformed or cancer cells. So far, a number of structurally distinct classes of compounds have been identified as HDAC inhibitors including the short-chain fatty acids, hydroxamates, cyclic tetrapeptides, and benzamides. These compounds lead to an accumulation of acetylated histone proteins both in tumor cells and in normal tissues. Several clinical trials have shown that HDAC inhibitors in well-tolerated doses have significant antitumoral activities. Half of the HDAC inhibitors under trial have the hydroxamic acid moiety, a typical zinc-binding group. One of them, SAHA, is the first HADC inhibitor that has been approved by FDA for the second line treatment of cutaneous T cell lymphoma.

Quantitative structure-activity relationships (QSAR) studies have been reported on HDAC inhibitors in order to identify the structural determinants for anticancer activity.

2.1 Quantitative Structure-Activity Relationships

The quantitative structure-activity relationship (QSAR) studies have been of great importance in the drug design. They try to explain the observed variations in biological activities of a group of congeners in terms of molecular variations caused by a change in the substituents. Thus, they also throw the light on the mechanism of drug-receptor interactions. Among the various approaches applied to QSAR studies, the most historical and fundamental has been the parametric method developed by Hansch, which correlates the biological activity of molecules with their physicochemical, electronic, and steric properties. This parametric method by Hansch has been called as Hansch Analysis. However, it is also called the *extra thermodynamic method* or *linear free energy-related approach* as all the molecular descriptors used in this method as well as biological activity terms are linear free energy-related terms derived from rate or equilibrium constants. Besides linear free energy-related terms, this method also uses several mathematical descriptors, i.e., topological indices, such as Wienerr index, Hosoya index, Randic's molecular connectivity index, and many more defined by various authors and initially used in quantitative structure-property relationship (QSPR) studies.

Apart from the Hansch approach, there have been a few more approaches, e.g., Free-Wilson, or Fujita-Ban approach, discriminated analysis, and pattern recognition technique (Gupta 2011) that have been successfully applied to QSAR studies. Additionally, there have been some manual stepwise methods, such as Topliss operation scheme, Craig plots, Fibonacci search method, and sequential simplex strategy (Siverman 2004); but these approaches have been of limited use.

All the above-mentioned QSAR approaches are related to 2-D structures of the molecules. With the advent of computer technologies came the era of 3D-QSAR studies which led to the development of methods such as distance geometry approach, comparative molecular field analysis (COMFA), comparative molecular

similarity indices analysis (COMSIA), hypothetical active site lattice (HASL) technique, *de novo* ligand design, docking (Gupta 2011), etc.

The QSAR studies on HDAC inhibitors that we are going to describe here have mostly used the 2-D Hansch approach or 3-D COMSIA or COMFA. The CoMFA calculates the steric and electrostatic interaction energies for a molecule binding with the receptor and CoMSIA is simply a modified version of CoMFA which not only calculates the steric and electrostatic interaction energies but also the hydrophobic and hydrogen-bond energies. In both the methods, the different interaction energies calculated for a series of molecules at different grid points are correlated with the biological activity using partial least square (PLS) method, also known as *projection to latent structures* technique, and are represented as 3-D contour maps in which contours of various colors represent locations on the molecular structure where low or high steric, electrostatic, hydrophobic, hydrogen-bond donor, and/or hydrogen-bond acceptor interactions would take place. A detailed discussion of these methods can be found in (Gupta 2011).

The PLS regression analysis is an alternative approach to the linear multiple regression analysis. It is used when the number of independent variables (descriptors) is relatively high compared to the number of data points (number of compounds in a given series) and several of the independent variables are mutually correlated. In such a situation, the PLS analysis generates latent variables from the linear combinations of the descriptors. These latent variables, which are orthogonal to each other, are then used to correlate the dependent variables. The quality of a PLS model can be assessed graphically by plotting the values of the dependent variable predicted by the model against the measured ones and its predictive ability is judged by calculating the cross-validated r^2 (r^2_{cv} or Q^2) (Gupta 2011).

2.2 Results and Discussion

A QSAR study was reported by Xie et al. (2004) for 124 compounds collected from various sources. A highly predictive QSAR model with $r^2 = 0.76$ and leave-one-out cross-validated $r^2 = 0.73$ was obtained. The overall rate of cross-validated correct prediction of the classification model was around 92 %. The QSAR and the classification models provided direct guidance to the internal programs for identifying and optimizing HDAC inhibitors. Limitations of the models were also discussed by the investigators.

Wang et al. (2004) developed QSAR models for a series of new trichostatin A (TSA)-like hydroxamic acids (Fig. 1) for the inhibition of cell proliferation of standard PC-3 cell line using molecular descriptors from Quikprop and electronic parameters.

The predictive ability of the proposed model was investigated using a cross-validation method. The descriptors used were: molecular weight (MW), the total solvent accessible surface area (SASA), the hydrophilic component of the solvent-accessible surface area (FISA), the weak polar component of the solvent-accessible
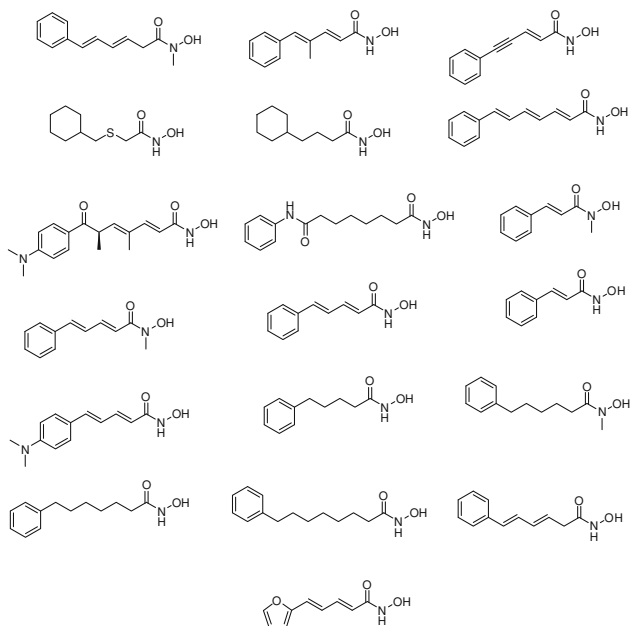
Fig. 1 Trichostatin A (TSA)-like hydroxamic acids

surface area (WPSA), an index of cohesive interactions in solids (ACxDN), the globularity of the compound (Glob) ($4\pi r^2$/SASA, whereas r is the radius of a sphere with a volume equal to the molecular volume), calculated octanol/water partition coefficient (LogP), and the PM3 atomic charge on the carbon atom of the CONHOH moiety (Qco). The derived QSAR models (Eqs. 1 and 2) reflected a PC3 cellular response driven by a net contribution of a mixture of the different HDAC enzyme in the cell as well as a contribution from the transport properties of the compounds.

$$pIC_{50}(\mu M) = 1.96 + 14.08Qco - 15.73Glob + 0.05FISA$$
$$R = 0.96, R^2 = 0.92, N = 19, F = 59.25 \tag{1}$$
$$t\text{-value}: 4.33(Qco), -4.02(Glob), 9.70(FISA)$$

$$pIC_{50}(\mu M) = 0.44 + 422.85ACxDN - 10.03Glob + 1.26\log P$$
$$R^2 = 0.90, N = 19, F = 46.63 \tag{2}$$
$$t\text{-value}: 8.377(ACxDN), -1.551(Glob), 3.844(\log P)$$

Equations 1 and 2 showed good linear relationship having a squared correlation coefficient R^2 of 0.96 and 0.90. Collinearity and multicollinearity tests were performed. Both models passed the colinearity test, while the second equation failed the multicollinearity test.

Park and Lee (2004) applied a computational protocol sequentially involving homology modeling, docking experiments, molecular dynamics simulation, and
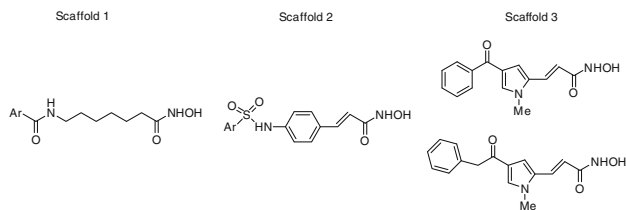
Fig. 2 Hydroxamate inhibitor scaffolds of the 12 derivatives investgated

free energy perturbation calculations in order to find the structural features of HDACIs that can increase their activity. With the newly developed force field parameters for the coordination environment of the catalytic zinc ion, FEP calculations could successfully predict the rank orders for 12 derivatives of three hydroxamate-based inhibitor scaffolds with indole amide, pyrrole, and sulfonamide moieties (Fig. 2).

The free energy of an inhibitor in aqueous solution proved to be an important factor in determining the binding free energy, showing that the increased stabilization in solution due to structural modifications must be overcome by the enzyme-inhibitor interaction. Introduction of a hydrogen-bond donor at the hydrophobic head is found to increase the inhibitory activity due to the formation of a hydrogen bond with the side chain of Asp99. Further optimization of the inhibitory potency can be achieved by elongating or enlarging the hydrophobic head so that hydrophobic interactions with Pro29 and His28, components of the flexible loop at the top of the active site, can be facilitated.

Docking simulations and 3-D quantitative structure-activity relationship (3D-QSAR) analysis were conducted by Guo et al. (2005) on a series of 29 substituted hydroxamic acid-based HDAC inhibitors with an indole amide residue at the terminus (Fig. 3) (Dai et al. 2003).

3D-QSAR models were developed using comparative molecular field analysis (CoMFA) and comparative molecular similarity indices analysis (CoMSIA). This study included two parts. The first demonstrated the common binding mode of indole amide hydroxamic acid inhibitors with HDAC, and the other derived QSAR models to find the main intermolecular interactions between inhibitors and HDAC and to predict accurately activities of newly designed inhibitors. These models could also offer valuable information about structural modification for designing new inhibitors with higher potency against HDAC.

Selected ligands were docked into the active site of human HDAC1 using the FlexX program interfaced with SYBYL 6.9. Based on the docking results, a novel
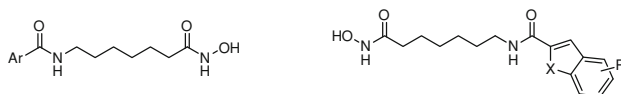
Fig. 3 Series of indole amide analogues used to obtain the models

binding mode of indole amide analogues in the human HDAC1 catalytic core was presented, and enzyme/inhibitor interactions were discussed. The indole amide group was located in the open pocket and anchored to the protein through a pair of hydrogen bonds with Asp99 O-atom and amide NH group on ligand. Based on the binding mode, predictive 3D-QSAR models were established, which had the values of conventional r^2 and cross-validated r^2 (r^2_{cv}) as 0.982 and 0.601 for CoMFA and 0.954 and 0.598 for CoMSIA, respectively.

The five similarity indices in CoMSIA (steric, electrostatic, hydrophobic, H-bond donor, and H-bond acceptor descriptors) were calculated using a C^{1+} probe atom with a radius of 1.0 Å placed at regular grid spacing of 2 Å. The derived CoMFA and CoMSIA descriptors above were used as explanatory variables, and pIC50 values were used as the target variable in PLS analysis to derive 3D-QSAR models using the implementation in the SYBYL package. The conventional correlation coefficient, r^2, and its standard error, S, were also computed for the final PLS models. CoMFA and CoMSIA coefficient maps were generated by interpolation of the pairwise products between the PLS coefficients and the standard deviations of the corresponding CoMFA or CoMSIA descriptor values.

Both CoMFA and CoMSIA models showed similar predictive capabilities. A comparison of the 3D-QSAR field contributions with the structural features of the binding site showed good correlation between the two analyses. The results of 3D-QSAR and docking studies validated each other and provided insight into the structural requirements for activity of this class of molecules as HDAC inhibitors. The CoMFA and CoMSIA PLS contour maps and MOLCAD-generated active site electrostatic, lipophilicity, and hydrogen-bonding potential surface maps, as well as the docking studies, provided good insights into inhibitor–HDAC interactions at the molecular level.

Lu et al. (2005) provided a novel strategy of tethering short-chain fatty acids (valproate, butyrate, phenylacetate, and phenylbutyrate) with Zn^{2+}-chelating motifs through different aromatic amino acid linkers to develop a novel class of HDAC inhibitors. N-hydroxy-4-(4-phenylbutyryl-amino)benzamide (HTPB), a hydroxamate-tethered phenylbutyrate derivative proved to be the optimal HDACI. In this study, a structure-based optimization of HTPB was carried out using the framework generated by the crystal structure of histone deacetylase-like protein HDLP-TSA complexes.

Comparison of the HTPB docking versus TSA into the HDLP binding domain revealed unique structural features responsible for the activity. For both molecules, hydrophobic and/or π–π interactions of its scaffold with the Phe-141/Phe-198 and Tyr-91/Glu-92 subdomains play an important role in anchoring the ligand to allow optimal access of the hydroxamate group to the zinc cation. Docking studies suggested that the hydrophobic microenvironment encompassed by Phe-198 and Phe-200 could be exploited for designing more active derivatives. This premise was corroborated by the greater potency of (S)-(+)-N-hydroxy-4-(3-methyl-2-phenylbutyrylamino)-benzamide (IC$_{50}$ for HDAC inhibition = 16 nM) (Fig. 4), of which the isopropyl moiety was favorable for interacting with this hydrophobic

Fig. 4 (*S*)-(+)-*N*-hydroxy-
4-(3-methyl-2-
phenylbutyrylamino)-
benzamide
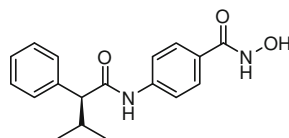
Fig. 5 Sulfonamide
hydroxamic acids
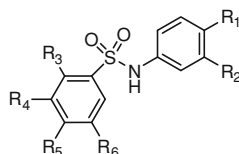
motif. For the (*S*)-derivative, a high degree of flexibility was found in the active-
site pocket to allow for the design of novel inhibitors with distinct stereo electronic
properties.

Liu et al. (2005) obtained a CoMFA model for a series of sulfonamide hy-
droxamic acids HDACIs (Fig. 5). The derived model presented a good cross-
validated correlation ($q^2 = 0.704$). The non-cross-validated partial least squares
(PLS) model was also well built and analyzed by the prediction of the activity data
by CoMFA steric, and electrostatic contours. The results showed that steric field
(0.697) played a better role than the electrostatic field (0.303). Additionally, larger
groups at R_5-position and smaller groups at the R_1-position were found to favor the
activity.

Docking simulation and 3-D quantitative structure-activity relationships (3D-
QSARs) analysis were conducted by Ragno et al. (2006) on a large series of
compounds, including TSA, SAHA, belonging to the four different series of hy-
droxamic acids: TSA amide analogues (TAAs) (Jung et al. 1999), SAHA phen-
ylalanine containing analogues (SPACAs) (Wittich et al. 2002), aroyl-pyrrolyl-
hydroxy-amides (APHA1), and APHA2 (Mai et al. 2002, 2003a, b, 2004; Massa
et al. 2001) (Fig. 6). The studies were performed using the GRID/GOLPE com-
bination and led to twelve 3-D QSAR models (Tables 1 and 2) which all displayed
high statistical coefficient values.

Compared to previous studies on similar inhibitors, the present 3-D QSAR
investigation proved to be of higher statistical value. From the 3-D QSAR model
interpretation, using the structure of a virtual HDAC 1, it was possible to depict the
areas around the training set (ligand-based approach) and enzyme residues
(structure-based approach), in order to have a potent HDAC inhibitor. A com-
parison of the 3-D QSAR maps with the structural features of the binding site
showed good correlation.

In order to gain further insight into the structural requirements of HDAC
inhibitors, Juvale et al. (2006) performed a 3D-QSAR study using comparative
molecular field analysis (CoMFA) and comparative molecular similarity indices
analysis (CoMSIA). The data set consisted of 57 hydroxamic acid analogues taken
from the literature (Jung et al. 1999; Remiszewski et al. 2002; Woo et al. 2002).
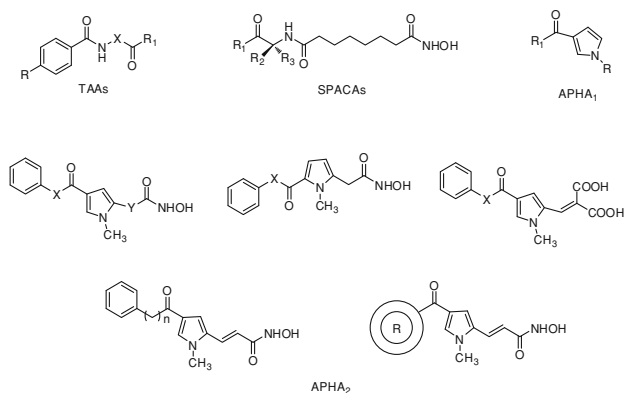
Fig. 6 HDAC inhibitors used in 3D-QSAR analysis (*TAAs* TSA amide analogues, *SPACAs* SAHA phenylalanine containing analogues, and *APHA1* and *APHA2* aroyl-pyrrolyl-hydroxy-amides)

Table 1 Statistical results of the 3-D QSAR models 1–8

Model	Series	Alignement	N^a	Vars[b]	PC[c]	r^2	q^2	SDEP$_{CV}$
1	TAAs	TSA-based	26	622	2	0.98	0.85	0.62
2	TAAs	SAHA-based	26	930	2	0.96	0.73	0.85
3	SPACAs	TSA-based	21	780	3	0.98	0.72	0.29
4	SPACAs	SAHA-based	21	805	3	0.99	0.66	0.32
5	APHA1	TSA-based	31	609	3	0.98	0.78	0.57
6	APHA1	SAHA-based	31	885	3	0.98	0.78	0.57
7	APHA2	TSA-based	31	745	3	0.97	0.76	0.62
8	APHA2	SAHA-based	31	753	2	0.95	0.78	0.62

[a] Number of compounds used in the model
[b] Number of selected variables
[c] Number of principal components which showed the maximum q^2 value

Table 2 Statistical results of the 3-D QSAR models 9–12

Model	Series	Alignement	N^a	Vars[b]	PC[c]	r^2	q^2	SDEP$_{CV}$	SDEP$_{test\ set-1}$	SDEP$_{test\ set-2}$
9	United	TSA-based	103	726	3	0.90	0.75	0.69	1.20	1.46
10	United	SAHA-based	103	829	2	0.83	0.71	0.74	1.00	1.39
11	United OA[d]	TSA-based	71	659	3	0.94	0.83	0.41	1.30	1.06
12	United OA[d]	SAHA-based	71	770	3	0.91	0.75	0.51	0.96	0.99

[a] Number of compounds used in the model
[b] Number of selected variables
[c] Number of principal components which showed the maximum q^2 value
[d] *OA* only active compounds were used in the training set

QSAR models were derived from a training set of 40 molecules. A test set consisting of 17 molecules was used to check the external predictive ability of the CoMFA and CoMSIA models. For the superposition of the molecules on the template structure/molecule (the most active molecule) three different techniques were applied, namely RMS alignment (atom-based), multifit alignment (flexible fitting), and the SYBYL QSAR rigid body field alignment. The statistical quality of the QSAR models was assessed using the parameters r^2_{conv}, r^2_{cv} and r^2_{pred}. In addition to the steric and electronic fields, Clog P (calculated using ClogP/CMR application within Sybyl 6.9.1.) was also taken as a descriptor to account for lipophilicity. It has been proved that ClogP as an additional descriptor increased the statistical significance of the model, indicating that lipophilicity enhances the HDAC inhibitory activity.

By comparing the results of the different alignments, the atom-based alignment with the hydroxamic acid functional group gave a better result than other atom-based alignment, highlighting the importance of the interaction of hydroxamic acids with the enzyme residues. Of all these alignments, the field fit alignment (along with ClogP) resulted the best in CoMFA model. The same alignment was also considered for CoMSIA where all five fields were considered in different combinations. The resulting models had good values of conventional r^2_{conv} and cross-validated r^2_{cv} –0.910 and 0.502 for CoMFA and 0.987 and 0.534 for CoMSIA, respectively.

Jaiswal et al. (2006) performed a QSAR analysis on a set of sulfonamide derivatives (Fig. 7) studied for their HDAC inhibition activity by Bouchain et al. (2003). The compounds were subjected to energy minimization and the lowest energy structure of each was used to calculate physicochemical parameters related to the thermodynamic, steric, and electronic properties of all the molecules. The best correlation revealed by a multiple regression was as shown by Eq. 3, which suggests an important role for the energy of highest occupied molecular orbital (HOMO) and torsion energy (TOE).

$$pIC_{50} = -8.377(\pm 3.635) - 1.668(\pm 0.409)HOMO - 0.0263(\pm 0.0186)TOE$$
$$n = 24, R = 0.881, \%EV = 77.6, \text{variance} = 0.138, Std = 0.372431,$$
$$F_{(3,20)} = 36.369, \text{Chance} < 0.01, SPRESS = 0.422, SDEP = 0.395,$$
$$q^2_{LOO} = 0.711 \tag{3}$$

The HOMO descriptor bears a negative coefficient in the model, indicating that electron-withdrawing substituents will increase the affinity of sulfonamide derivatives toward histone deacetylase. Similarly, the negative coefficient of TOE

Fig. 7 General structure of sulfonamide analogues
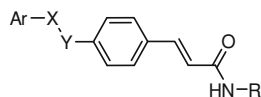
suggests that bulky substituents are not tolerable for HDAC inhibitory activity of these compounds.

The model has a good correlation coefficient of 0.881 with 77.6 % explained variance in the HDAC inhibitory activity. F statistics indicated statistical significance at 99 %. Its explained variance in the activity is 77.6 % with low standard deviation value (0.37) and it has good predictive ability with $q^2_{LOO} = 0.711$ obtained by leave-one-out (LOO) method.

Wagh et al. (2006) reported a 3-D quantitative structure-activity relationship (3D-QSAR) study for a series of hydroxamic acid analogues using genetic function approximation (GFA). QSAR models were generated using a training set of 39 molecules and the predictive ability of final model was assessed using a test set of 17 molecules. The obtained QSAR model presented internal consistency of 0.712 and good external predictivity of 0.585. The results of the present QSAR study indicated that molecular shape analysis (MSA) and thermodynamic and structural descriptors are important for HDAC inhibition.

Dawson et al. (2007) conducted a QSAR analysis on the apoptotic and anti-proliferative activities of small heterodimer partner (SHP) nuclear receptor ligand, (E)-4-[3′-(1-adamantyl)-4′A-hydroxyphenyl]-3-chlorocinnamic acid (3-Cl-AHPC), which was derived from 6-[3′-(1-adamantyl)-4′-hydroxyphenyl]-2-naphthalene-carboxylic acid (AHPN), and several carboxyl isosteric or hydrogen-bond accepting analogues. 3-Cl-AHPC continued to be the most effective apoptotic agent, whereas tetrazole, thiazolidine-2,4-dione, methyldinitrile, hydroxamic acid, boronic acid, 2-oxoaldehyde, and ethyl phosphonic acid hydrogen-bond acceptor analogues were inactive or less efficient inducers of KG-1 acute myeloid leukemia and MDA-MB-231 breast, H292 lung, and DU-145 prostate cancer cell apoptosis. Similarly, 3-Cl-AHPC was the most potent inhibitor of cell proliferation.

A fragment-based QSAR study was conducted to identify the core recognition elements of 55 analogues of AHPN and AHPC (Fig. 8) in apoptosis (MDA-MB-231). The 'overlap rule' was used to align the training set in SYBYL QSAR; and for the comparative molecular similarity index analysis (CoMSIA), electrostatic, hydrophobic, and steric fields were computed on a grid surrounding the overlapped ligands. The resulting CoMSIA analysis for apoptosis induction in MDA-MB-231 breast cancer cells resulted in a predictive R^2 of 0.78 and an un-cross-validated R^2 of 0.95 with a standard error of 0.45. It is a 3-D seven-point descriptive model with the following components: components 1 and 2, hydrogen-bond acceptor; 3, hydrogen-bond donor/acceptor; 4, hydrophobic ring; 5, hydrophobic group; 6, sterically accessible hydrophobic region; and 7, sterically accessible polar-permissible region. Key polar points include two adjacent hydrogen-bond acceptor groups and a hydrogen-bond donor/acceptor group. According to the resulting model the dimensions of the elements and their minima in computed electrostatic potential on the van der Waals surface of the fragments was found to play a major role in determining growth inhibitory activity.

Katritzky et al. (2007) tried to compare 2D- and 3D-QSAR approaches in order to correlate the inhibitory activity of a series of indole amide hydroxamic acids.
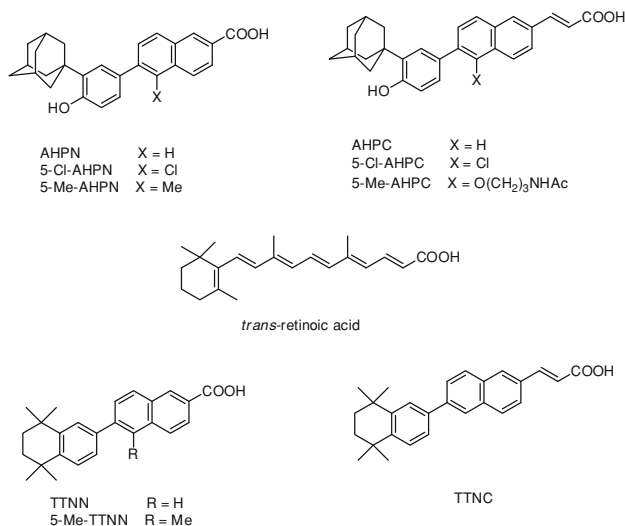
Fig. 8 Structures of some AHPN and AHPC analogues

The molecules (Fig. 9) and the biological data for the study were obtained from the work of Dai et al. (2003). The study involved two alternative treatments of the activity data for the inhibition of HDACs: (i) a QSAR modeling, by multilinear regression performed by the CODESSA-PRO software which calculated about 800 different constitutional, geometrical, topological, electrostatic, quantum chemical, and thermodynamic molecular descriptors and (ii) a 3D-QSAR analysis using CoMFA method as implemented in the Chem-X software combined with a Weighted Least Squares method (WLS) for important regional mapping and docking analysis. A Partial Least Squares (PLS) procedure generated the principal components needed to build a 3D-QSAR model. All descriptors used in 2D-QSAR were derived solely from molecular structure.

A Best Multilinear Regression Method (BMLR) applied for 2D-QSR revealed the following correlation.

$$\log \text{IC}_{50} = -25.31(\pm 3.20)\text{ABOC} - 9.40 \times 10^{-3}(\pm 9.98 \times 10^{-4})\text{TMSA}$$
$$+ 34.59(\pm 3.67)$$
$$N = 36, \ R^2 = 0.778, \ R^2_{\text{CVOO}} = 0.721, \ R^2_{\text{CVMO}} = 0.721,$$
$$F = 57.71, \ \text{s} = 0.328$$

$$(4)$$

In the above equation, ABOC is the average bond order for atom C and TMSA is the total molecular surface area. Molecular size and shape affect almost all

Fig. 9 General structure of amide hydroxamic acids
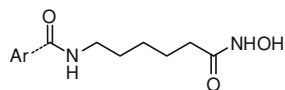
chemical processes. The TMSA descriptor is based on a calculation of van der Waals radii of the atoms and mainly reflects steric interactions. The ABOC descriptor defines the degree of unsaturation/aromaticity of the structure and its flexibility, which is related to the transport properties and the surface recognition profile of the molecules.

In 3D-QSAR analysis, the PLS model that used principal components exhibited the steric interactions with the following statistical parameters: $R^2 = 0.881$, predictive $R^2 = 0.708$, $Q^2 = 0.540$, predictive ERROR = 0.389. When four outliers were excluded, statistical parameters were as $R^2 = 0.937$, predictive $R^2 = 0.811$, $Q^2 = 0.624$, predictive ERROR = 0.322. The correlation coefficient of this prediction was $R^2_{ext} = 0.715$. By using the Weighted Least Square (WLS) method, R^2 maps for the steric and electrostatic fields were generated separately. The initial PLS model based on electrostatic fields had the following statistical parameters: $R^2 = 0.789$, predictive $R^2 = 0.642$, $Q^2 = 0.280$, predictive ERROR = 0.431 and after the removal of four outliers $R^2 = 0.931$, predictive $R^2 = 0.847$, $Q^2 = 0.434$, predictive ERROR = 0.295. The external predictive power of this model was evaluated and the correlation coefficient of this prediction R^2_{ext} was as 0.552. It suggests that the steric effect made a higher contribution to the biological activity than the electrostatic interaction.

Using HDAC inhibition data of Moradei et al. (2006) on some aminophenyl-benzamide and acrylamide derivatives (Fig. 10), Dessalew (2007) carried out a 2-D, 2D-QSAR study that had revealed Eq. (5), where L refers to Verloop's length parameter and B_2 and B_3 Verloop's width parameters of substituents orthogonal to length opposite to each other. This equation suggests that only the width of one side of substituents would be advantageous and the other two steric parameters will be detrimental to the activity.

$$pIC_{50} = -0.214845L + 0.452952875B_2 - 0.2152599B_3 + 2.5249031$$
$$r^2 = 0.725, \; r^2_{cv} = .594, \; r^2_{pred} = 0.577 \tag{5}$$

Ragno et al. (2008) performed molecular modeling and 3-D QSAR studies on a set of 25 aryloxopropenyl-pyrrolyl hydroxamates (Fig. 11) studied by Mai et al. (2005a, b) to gain insight into their activity and selectivity against maize HD1-B and HD1-A, the two enzymes homologous to mammalian class I and class II HDACs, respectively. The studies had been accomplished by calculating

Fig. 10 Structures of some aminophenyl-benzamides and acrylamides
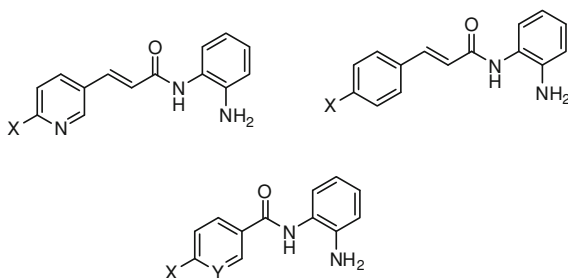
Fig. 11 Aryloxopropenyl-pyrrolyl hydroxamides
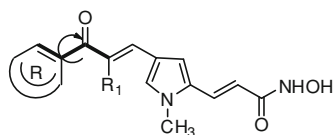
alignment-independent descriptors (GRIND descriptors) using the ALMOND software. Highly descriptive and predictive 3-D QSAR models were obtained. Comparison of the two PLS coefficient plots revealed some similarities and differences between the models. Both plots showed the distance between an H-acceptor bond group (C=O) and an aromatic portion of the cap to be the most important variable. In general, a bent molecular shape was a prerequisite for HD1-A-selective inhibitory activity, while straight shape molecular skeleton was observed to be selective to HD1-B. The reported 3-D QSAR models helped the interpretation of the selectivity issue for the class I and II HDAC inhibitors.

Chen et al. (2008a, b) built quantitative pharmacophore models from a training set of 30 diverse hydroxamic acid derivatives active as inhibitors of the HDAC1 enzyme. All pharmacophore models were generated using the Catalyst 4.10 software (Accelrys Inc., San Diego, CA) on Silicon Graphic O_2 workstation. The best pharmacophore hypothesis consisted of five pharmacophore features, including a hydrogen-bond donor, a hydrogen-bond acceptor, and three hydrophobic features. It is characterized by the highest cost difference, lower errors, lowest root mean square (rms) divergence, and best correlation coefficient of 0.924 ($r = 0.924$).

The type and spatial location of the chemical feature agree perfectly with the pattern of enzyme-inhibitor interactions (MS-275 and HDAC) identified from crystallography.

In order to investigate the potential for isoform selectivity in the inhibition of HDACs, Kozikowski et al. (2008) designed and synthesized a small series of ligands (Fig. 12) bearing the 2,4'-diaminobiphenyl scaffold in which the para-amino group bears an appendage containing either a hydroxamate or a mercaptoacetamide group coupled to an amino acid residue at the ortho-amino group. For comparison, a smaller series of substituted phenylthiazoles was also investigated by replacing the biphenyl group with a phenylthiazole containing a substituent at the 2-position or 3-position of the phenyl ring. This modification was explored based on the realization that connectivity through the five-membered thiazole ring will situate the phenyl ring substituent closer to the HDAC protein surface.

To examine the SAR of these compounds quantitatively, some QSAR equations (Eqs. 6–11) were developed against HDAC-1,2,6,8,10, where mostly two indicator variables, $I_{-\mathrm{NHCOCH_2SH}}$ and $I_{-\mathrm{Thiazole}}$, were found

$$\mathrm{pIC_{50}(HDAC-1)} = -1.844(\pm 0.248)I_{-\mathrm{NHCOCH_2SH}} + 0.983(\pm 0.149)I_{-\mathrm{Thiazole}}$$
$$+ 7.299(\pm 0.114)$$
$$n = 23, \ r^2 = 0.920, \mathrm{RMSE} = 0.322, p < 0.0001 \tag{6}$$
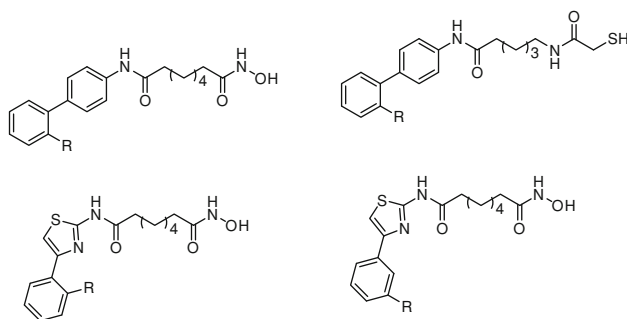
Fig. 12 General structures of biphenyl-bearing hydroxamates, mercaptoacetamides and phenyl-thiazole-bearing hydroxamates

$$\text{pIC}_{50}(\text{HDAC-2}) = -1.963(\pm 0.258)I_{-\text{NHCOCH}_2\text{SH}} + 0.606(\pm 0.155)I_{-\text{Thiazole}}$$
$$+ 6.813(\pm 0.115)$$
$$n = 20, \, r^2 = 0.860, \, \text{RMSE} = 0.326, \, p < 0.0001 \tag{7}$$

$$\text{pIC}_{50}(\text{HDAC-2}) = -2.127(\pm 0.195)I_{-\text{NHCOCH}_2\text{SH}}$$
$$+ 0.606(\pm 0.151)I_{-\text{Thiazole}} + 6.813(\pm 0.112) \tag{8}$$
$$n = 22, \, r^2 = 0.918, \text{RMSE} = 0.318, \, p < 0.0001$$

$$\text{pIC}_{50}(\text{HDAC-6}) = -1.429(\pm 0.246)I_{-\text{NHCOCH}_2\text{SH}} + 0.711(\pm 0.184)I_{-\text{Thiazole}}$$
$$+ 0.046(\pm 0.023)(\text{Clog}P)^2 + 7.799(\pm 0.163) \tag{9}$$
$$n = 23, r^2 = 0.861, \text{RMSE} = 0.384, \, p < 0.0001$$

$$\text{pIC}_{50}(\text{HDAC8}) = -0.461(\pm 0.097)I_{-\text{NHCOCH}_2\text{SH}} + 5.668(\pm 0.040)$$
$$n = 23, \, r^2 = 0.518, \text{RMSE} = 0.176, \, p < 0.0001 \tag{10}$$

$$\text{pIC}_{50}(\text{HDAC-10}) = -2.029(\pm 0.222)I_{-\text{NHCOCH}_2\text{SH}}$$
$$+ 1.007(\pm 0.153)I_{-\text{Thiazole}} + 7.192(\pm 0.116) \tag{11}$$
$$n = 22, \, r^2 = 0.916, \text{RMSE} = 0.328, \, p < 0.0001$$

to dominate. The indicator variable $I_{-\text{NHCOCH}_2\text{SH}}$. takes the value of 1.0 for the mercaptoacetamides and 0.0 for all others. The indicator variable $I_{-\text{Thiazole}}$ takes the value of 1.0 for the phenylthiazoles and 0.0 for all others. In almost all the cases mercaptoacetamides seem to be inferior to thiazoles.

Vadivelan et al. (2008) used Medichem database in order to identify HDAC inhibitors (Fig. 13). The aim of this study was: (a) to generate pharmacophore models as powerful search tools to be used as a 3-D query to identify lead molecules as HDAC inhibitors and (b) to utilize the pharmacophore model as a predictive tool for estimating biological activity of virtual molecules or molecules
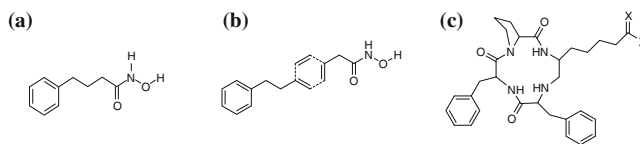
Fig. 13 Scaffolds **a**, **b,** and **c** represent three class of compounds, namely, hydroxamic acids/ short-chain fatty acids, sulfa/benzamides, and cyclic tetrapeptide or epoxides, respectively

designed on the basis of structure-activity relationship analysis. A total of 20 well-defined inhibitors representing three different chemotypes were used to generate pharmacophore models using HypoGen module of catalyst. The best quantitative HypoGen model consisted of four pharmacophore features: a hydrogen-bond acceptor, a hydrophobic aliphatic feature, and two ring aromatic features, which were further validated for 378 known HDAC inhibitors with a correlation coefficient of 0.897 ($r = 0.897$). This model was further used to retrieve molecules from NCI database with 238,819 molecules. 4,638 molecules were identified as hits that satisfied the 3-D query. Among them 297 presented high, 1,433 medium, and 2,988 low activity.

A series of hydroxamic acids with the general formula R′-C(=O)NROH have been designed, synthesized, and tested in vitro for their HDAC inhibition activity by Rajwade et al. (2008). Multivariate analytical tool, projection to latent structures was used to develop a suitably predictive model for the purpose of optimizing and identifying better HDACIs. The cross-validated Q^2_{cum} values for two optimal PLS models of hydroxamic acids were above 0.690 (remarkably higher 0.500), indicating good predictive abilities for $\log(1/IC_{50})$ values of hydroxamic acids. By partial least square regression, two QSAR models obtained revealed that, besides the essential pharmacophore –NOHC = O moiety, retention capacity factor (logk'), polar surface area (PSA), dipole moment (Dm), total number of hydrogen-bond donor and acceptor atoms, H, and chlorine atoms attached in upper or/and lower phenyl rings, were also important determinants for the inhibitory potency.

Continuing their research on N-aryl-substituted hydroxamic acids (Fig. 14), Rajwade et al. (2009) derived a 2D-QSAR model (Eq. 12) using principal component analysis (PCA) and partial least squares (PLS) regression.

$$\log(1/IC_{50}) = 4.870 \times 10^{-1} \log k_w + 3.764 \times 10^{-1} I_H + 1.966 \times 10^{-1} \omega$$
$$- 1.646 \times 10^{-1} E_{\text{LUMO}} + 1.515 \times 10^{-1} NVE + 17.9901$$
$$n = 14, \text{A} = 1, R^2_{x(\text{adj})(\text{cum})} = 0.334, R^2_{y(\text{adj})(\text{cum})} \quad (12)$$
$$= 0.732, Q^2_{(\text{cum})} = 0.638, \text{RMSEE} = 0.1153,$$

RMSEP = 0.2954, outliers 5

Fig. 14 *N*-aryl-substituted hydroxamic acids

R$_1$—N—OH
R$_2$—C=O
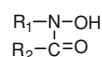
The model indicated that increase in lipophilicity ($\log k_w$), presence of H atom (I_H), global electrophilicity index (ω), total number of valance electrons (NVE), and decrease in energy of lowest unoccupied orbital (E_{LUMO}) value would increase the activity. The cross-validated $Q^2_{(cum)}$ values for optimal PLS model of hydroxamic acids is 0.638 (remarkably higher than 0.50), indicating good predictive ability for $\log(1/IC_{50})$ values of hydroxamic acids.

For the above case, the k-nearest neighbor molecular field analysis (kNN-MFA) was also performed. Statistically stepwise variable selection k-nearest neighbor molecular field analysis (SW-kNN-MFA) model was found comparatively better as compared to other methods. The developed SW-kNN-MFA model field plot indicated that the positive steric and electric potential were favorable for the increase in the activity and thus more bulky substituent at the 5-position of phenyl ring connected at amide group and less electronegative substituent at 3-position of phenyl ring connected to carboxyl group were postulated to be favorable for the increase in the potency of the molecules.

The biological data obtained by Price et al. (2007a, b) on a series of thienyl-based hydroxamic acids (Fig. 15) were analyzed by three groups of workers, Zhang et al. (2009), Pontiki and Hadjipavlou-Litina (2012), Melagraki et al. (2009). In order to rationalize the observed variance in inhibitory activity of these compounds, to propose a possible mechanism of antitumor activity and to guide the synthesis of additional compounds, Zhang et al. applied CoMFA and CoMSIA techniques. Models obtained by both the techniques exhibited the importance of steric, hydrophobic, and H-bond donor fields in the activity of the compounds.

Melagraki et al. (2009) performed a simple multiple regression analysis on a set of 58 compounds of the same series. For a training set of 45 compounds they obtained Eq. 13, in which DPL refers to the dipole moment of the compound, PMIX the principal moment of inertia along X-axis, ShpC the shape coefficient, TopoJ Balaban topological index, and ChiInf0 the Randic information index of zero order. This equation suggests that only Balaban topological index would have the favorable effect and other variables would have negative effect.

$$\begin{aligned}
\log(1/IC_{50}) = {} & 5.69 - 0.0762 \text{ DPL} - 0.000441 \text{ PMIX} - 2.11 \text{ ShpC} \\
& + 3.87 \text{ TopoJ} - 4.35 \text{ ChiInf0} \\
& n = 45,\ S = 0.34,\ R^2 = 0.78,\ \text{RMS} = 0.34, R^2_{adj} \\
& = 0.75,\ Q^2 = 0.68,\ \text{PRESS} = 6.59,\ F = 26.870
\end{aligned} \tag{13}$$

For a set of 34 compounds of the same series, Pontiki and Hadjipavlou-Litina (2012) derived the following 2D-model, exhibiting the importance of the molecular size of the compound in their HDAC inhibition activity.

Fig. 15 Structures of thienyl-based hydroxamic acids
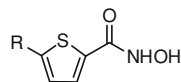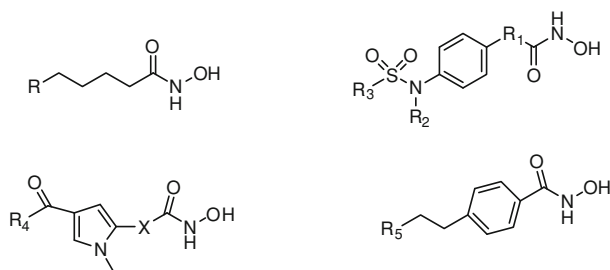
Fig. 16 Structures of hydroxamate-based HDAC inhibitors used by Chen et al

$$\log(1/\text{IC}_{50}) = 0.012(\pm 0.002)\text{MgVol} + 3.467(\pm 0.738)$$
$$n = 34,\ r = 0.893,\ r^2 = 0.797,$$
$$q^2 = 0.767,\ s = 0.368,\ Q = 2.426,\ F_{1,32} = 125.847,\ \alpha = 0.01$$
(14)

$$\text{Clog}\,P\,vs\,\text{MgVol}\,0.400$$

For a series of hydroxamate-based HDAC inhibitors (Fig. 16) collected from the studies of Remiszewski et al. (2002), Woo et al. (2002), Lavoie et al. (2001), Massa et al. (2001), and Delorme et al. (2001), two highly predictive and statistically significant models were derived by Chen et al. (2009) from CoMFA and CoMSIA based on pharmacophore alignment. With steric and electrostatic fields, the CoMFA model had $q^2 = 0.726$ and $r^2 = 0.998$ and with steric, electrostatic, hydrophobic, hydrogen-bond donor and acceptor fields the CoMSIA model had $q^2 = 0.610$ and $r^2 = 0.995$. Both the models were validated by an external test set, which gave a satisfactory predictive r^2 value of 0.800 and 0.732, respectively. The CoMSIA steric and electrostatic contour maps were in accordance with field distribution of CoMFA contour maps and consistent with structure-activity relationships. 3D-QSAR models seemed to agree with the active sites of HDAC as the amino acid residues interact with the three fragments of HDAC inhibitors with steric, electrostatic, hydrophobic, hydrogen bond fields around them.

Pontiki et al. (2009) tested a series of aryl-acetic and hydroxamic acids (Fig. 17) for their anticancer activity using different cancer cell lines. The activity data were subjected by us to a 2D-QSAR analysis which revealed the following correlations for different cell lines, where Eqs. 15 and 17

Human colon cancer cell lines (*HT-29*)

$$\log(1/\text{IC}_{50})(\text{HT} - 29) = 0.041(\pm 0.018)\text{Esp} - \min$$
$$+ 0.093(\pm 0.039)\text{Dm} + 5.543(\pm 0.728)$$
$$n = 13,\ r = 0.872,\ r^2 = 0.760,\ q^2 = 0.573,$$
$$s = 0.078,\ F_{2,10} = 15.737,\ \alpha = 0.01$$
(15)

Fig. 17 Substituted aryl-
acetic and hydroxamic acids
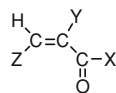
Lung cancer cells (A-549)

$$\log(1/\mathrm{IC}_{50})(A-549) = -0.002(\pm 0.001)\mathrm{MgVol}$$
$$+ 0.031(\pm 0.017)\mathrm{Esp-min} + 5.802(\pm 0.989)$$
$$n = 12,\ r = 0.826,\ r^2 = 0.683,\ q^2 = 0.426,$$
$$s = 0.083,\ F_{2,9} = 9.653,\ \alpha = 0.01$$

(16)

Ovary cancer cell lines (OAW-42)

$$\log(1/\mathrm{IC}_{50})(\mathrm{OAW}-42) = 0.062(\pm 0.028)\mathrm{Esp-min}$$
$$+ 0.084(\pm 0.065)\mathrm{Dm} + 6.447(\pm 1.142)$$
$$n = 12,\ r = 0.862,\ r^2 = 0.743,\ q^2 = 0.602,$$
$$s = 0.128,\ F_{2,9} = 13.038,\ \alpha = 0.01$$

(17)

suggest that minimum electrostatic potential (Esp-min) and dipole moment (Dm) of the compounds would be crucial for their activity against colon and ovary cancer cell and lines. For lung cancer cell line, Eq. 16 however suggests that while minimum electrostatic potential may be beneficial to the activity, the molar volume may be detrimental.

The QSAR analyses did not indicate any role for lipophilicity. Electrostatic potential, dipole moments, and the bulk primarily affected the biological response.

Like above, Pontiki and Hadjipavlou-Litina (2012) reported 2-D QSAR results in a recent review on several series of hydroxamic acids acting as HDAC inhibitors as described below.

Amide Analogues of Trichostatin (Fig. 18) (Jung et al. 1999)

Lipophilicity was found to be the most significant parameter (Pontiki and Hadjipavlou 2012).

$$\log(1/\mathrm{IC}_{50}) = 3.716(\pm 1.742)\mathrm{Clog}\,P - 2.471(\pm 1.347)(\mathrm{Clog}\,P)^2$$
$$+ 5.702(\pm 0.404)$$
$$n = 9,\ r = 0.925,\ r^2 = 0.856,\ q^2 = 0.713,$$
$$s = 0.196,\ Q = 4.719,\ F_{2,6} = 17.792,$$
$$\alpha = 0.01,\ \mathrm{Clog}\,P_{\mathrm{o}} = 0.752(\pm 0.129)\ \text{from } 0.674 \text{ to } 0.931$$

(18)

Sulfonamide hydroxamic acids (Lavoie et al. 2001) (Fig. 19)

Fig. 18 Hydroxamates
synthesized by Jung et al.
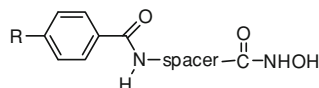
Fig. 19 Sulfonamide
synthesized by Lavoie et al.

a.
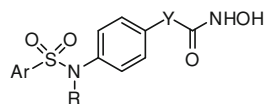
$$\log(1/IC_{50})(\text{recombinant human HDAC} - 1) = -0.240(\pm0.189)\text{CMR}$$
$$+ 1.444(\pm0.463)I_{-\text{CH}=\text{CH}}$$
$$- 1.059(\pm0.658)\sigma_P + 7.727(\pm1.629)$$
$$n = 18, \ r = 0.882, \ r^2 = 0.779,$$
$$q^2 = 0.666, \ s = 0.331, \ Q = 2.665,$$
$$F_{3,14} = 16.421, \ \alpha = 0.01,$$
$$\text{Clog} \, P \ vs \ \text{CMR} = 0.579$$

$$(19)$$

CMR represents the molar refractivity of the molecules. Its negative sign brings out a steric effect. The presence of a double bond seems to be favorable for the inhibitory activity. The role of σ_p (Hammet) term of p-substituents of R was found to be important.

b. The in vitro antiproliferative activity at human colon cancer HCT 116 cells

$$\log(1/EC_{50}) = -0.282(\pm0.164)\text{CMR} + 1.406(\pm0.388)I_{-\text{CH}=\text{CH}}$$
$$- 1.247(\pm0.627)\sigma_P + 7.397(\pm1.44)$$
$$n = 17, \ r = 0.916, \ r^2 = 0.840, \ q^2 = 0.747, \ s = 0.290, \ Q = 3.159,$$
$$F_{3,13} = 22.733, \ \alpha = 0.01, \text{Clog} \, P \ vs \ \text{CMR} = 0.571 \qquad (20)$$

CMR, $I_{\text{-CH}=\text{CH}}$ and σ_P were found to be conducive in this case also

c. *T24 cancer cells*

$$\log(1/EC_{50}) = -0.356(\pm0.220)\text{Clog} \, P$$
$$+ 0.428(\pm0.178)L_4 + 4.723(\pm0.479)$$
$$n = 11, \ r = 0.893, \ r^2 = 0.797, \ q^2 = 0.725, \qquad (21)$$
$$s = 0.199, \ Q = 4.487,$$
$$F_{2,8} = 15.697, \ \alpha = 0.01, \ \text{Clog} \, P \ vs \ L_4 = 0.207$$

Fig. 20 Succinimide
hydroxamic acids synthesized
by Curtin et al.
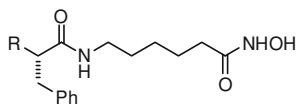
Hydrophilicity with a negative sign of Clog P seemed to be important followed by the Verloop parameter (L_4) for the length of the first atom of the substituent at the 4-position of the phenyl ring.

Succinimide Hydroxamic acids (Curtin et al. 2002) (Fig. 20)
For the antiproliferative activity in human HT1080 fibrosarcoma cells of these compounds the equation obtained was as

$$\log(1/\text{IC}_{50}) = 0.379(\pm0.316)\text{MR}_R + 4.070(\pm1.500)$$
$$n = 5,\ r = 0.911,\ r^2 = 0.829,\ q^2 = 0.567,\ s = 0.293,\ Q = 3.109,$$
$$F_{1,3} = 14.568,\ \alpha = 0.01,\ \text{Clog}\,P\ vs\ \text{MR}_{-R} = 0.436 \tag{22}$$

Simple Trichostatin A-Like Straight Chain Hydroxamates (Woo et al. 2002) (Fig. 21)

$$\log(1/\text{IC}_{50}) = 2.099(\pm1.027)\text{CMR} - 0.094(\pm0.059)\text{CMR}^2 - 3.238(\pm4.420)$$
$$n = 23,\ r = 0.909,\ r^2 = 0.826,\ q^2 = 0.777,\ s = 0.332,$$
$$Q = 2.738,\ F_{2,20} = 47.435,\ \alpha = 0.01,$$
$$\text{CMR}_o = 11.157(\pm2.576)\ \text{from}\ 10.122\ \text{to}\ 15.274 \tag{23}$$

Molar refractivity of the whole molecule is found to be the most important variable. CMR in a parabolic model explains 82.6 % of the variance.

Phenylalanine Containing Inhibitors of Histone Deacetylase (Wittich et al. 2002) (Fig. 22)
a. Maize HD inhibition

$$\log(1/\text{IC}_{50}) = 0.359(\pm0.154)\text{Clog}\,P + 0.141(\pm0.089)\text{MR}_{R'} + 5.953(\pm0.267)$$
$$n = 16,\ r = 0.892,\ r^2 = 0.796,\ q^2 = 0.713,\ s = 0.236,\ Q = 3.780,$$
$$F_{2,13} = 25.356,\ \alpha = 0.01,\ \text{Clog}\,P\ vs\ \text{MR}_{-R''}0.080 \tag{24}$$

Fig. 21 TSA like straight
chain hydroxamate analogues
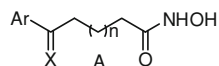
Fig. 22 Phenylalanine containing inhibitors of histone deacetylase
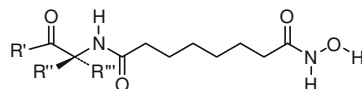
b. Proliferation of the Friend leukemic cells

$$\log(1/IC_{50}) = 0.543(\pm 0.197)\text{Clog}\,P - 0.413(\pm 0.125)\text{MR}_{R'} + 5.010(\pm 0.225)$$

$$n = 15,\ r = 0.905,\ r^2 = 0.818,\ q^2 = 0.739,\ s = 0.251,\ Q = 3.606,$$

$$F_{2,12} = 27.044,\ \alpha = 0.01,\ \text{Clog}\,P\ vs\ \text{MR}_{-R'}\ 0.470 \tag{25}$$

In both the above cases the hydrophobicity of the molecule is found to have a positive effect, while the molar refractivity of R″-substituent has the positive effect for maize HD-2 inhibition and that of R′-substituent a negative effect in proliferation of the Friend leukemic cells.

Indole Amide Hydroxamic Acids (Dai et al. 2003) (Fig. 23)
a. HDAC-1 and HDAC-2 Inhibition

$$\log(1/IC_{50}) = 0.167(\pm 0.108)\text{MR}_{\text{Ar}} + 1.892(\pm 0.481)I_{\text{IND}}$$

$$+ 0.507(\pm 0.227)I_2 + 4.894(\pm 0.619)$$

$$n = 32,\ r = 0.881,\ r^2 = 0.776,\ q^2 = 0.709,\ s = 0.303,\ Q = 2.908,$$

$$F_{3,28} = 32.257,\ \alpha = 0.01,\ C\log P\ vs\ \text{MR}_{\text{AR}}\,0.784 \tag{26}$$

This equation suggests a favorable role for molar refractivity of aromatic group Ar and an additional positive effect if Ar is an indolyl group since an indicator parameter I_{IND} used for it is positive. I_2 is an additional indicator variable used for a substituent at the 2-position of Ar group. The positive coefficient of it suggests a positive effect of such a substituent.

b. Antiproliferative activity against human HT1080 fibrosarcoma cell line

$$\log(1/IC_{50}) = -0.007(\pm 0.004)\text{MgVol} + 0.654(\pm 0.491)\text{MR}_4 + 8.699(\pm 1.415)$$

$$n = 12,\ r = 0.852,\ r^2 = 0.725,\ q^2 = 0.575,\ s = 0.192,\ Q = 4.438,$$

$$F_{2,9} = 11.89,\ \alpha = 0.01,\ \text{MR}_{-4}\ vs\ C\log P\,0.107 \tag{27}$$

MgVol (molar volume) with a negative sign is shown to have an unfavorable steric effect, but the MR_4, the molar refractivity of the substituent at the 4-position of aryl moiety, is shown to have the positive effect.

Fig. 23 Indole amide hydroxamic acids
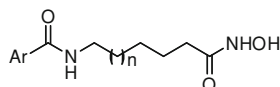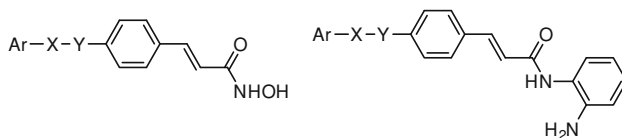
Fig. 24 Sulfonamide analogues

Sulfonamide Derivatives (Bouchain et al. 2003) (Fig. 24).

The inhibitory activity of these compounds on partially purified recombinant human HDAC-1 was shown to be with molar refractivity as shown by Eq. 28, where the molar refractivity of the whole molecule was shown detrimental to the activity but that of only aromatic group to be favorable. The whole molecule may create the steric problem but the aromatic group might be involved in a dispersion interaction with some site of the receptor.

$$\begin{aligned}
\log(1/IC_{50}) = &-0.455(\pm 0.104)CMR \\
&+ 0.506(\pm 0.190)MR_{Ar} + 9.537(\pm 1.022) \\
&n = 27,\ r = 0.879,\ r^2 = 0.772,\ q^2 = 0.708, \\
&s = 0.374,\ Q = 2.350,\ F_{2,24} = 40.716,\ \alpha = 0.01
\end{aligned} \tag{28}$$

N-Hydroxy-3-phenyl-2-propenamides (Remiszewski et al. 2003) (Fig. 25).

The activity of these compounds against HCT116 human colon carcinoma cells was found to be correlated with molar refractivity as shown by Eq. 29, where MR_{R_1} refers to the molar refractivity of only R_1-substituent. This equation suggests that only the molecular size of the R_1-substituent is important for the activity but a larger size ($MR_{R_1} > 4.714$) will be detrimental to the activity, which may be probably due to steric effect.

$$\begin{aligned}
\log(1/IC_{50}) = &\ 27.613(\pm 25.161)MR_{R_1} \\
&- 2.929(\pm 2.826)(MR_{R_1})^2 - 57.237(\pm 55.740) \\
&n = 10,\ r = 0.862,\ r^2 = 0.744, \\
&q^2 = 0.566,\ s = 0.430,\ Q = 2.005, \\
&F_{2,7} = 10.151,\ \alpha = 0.01,\ (MR_{R_1})_o = 4.714(\pm 3.797)\ \text{from } 4.530 \text{ to } 12.124
\end{aligned} \tag{29}$$

(Aryloxopropenyl)pyrrolyl Hydroxyamides (Mai et al. 2003a) (Fig. 26).

The activity of this series of compounds tested against the HD1-A was also shown to correlate with molecular refractivity as shown by Eq. 30. However, this

Fig. 25 *N*-Hydroxy-3-phenyl-2-propenamides
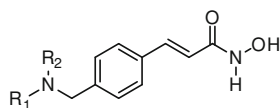
Fig. 26 (Aryloxopropenyl) pyrrolyl hydroxyamides
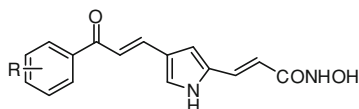
Fig. 27 3-(4-Substituted-phenyl)-*N*-hydroxy-2-propenamides
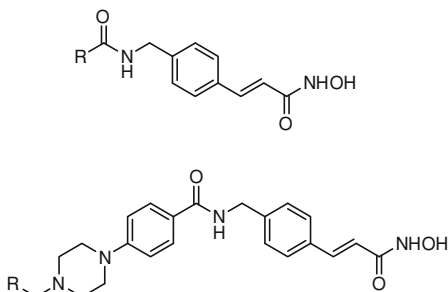
equation exhibited that the molecular refractivity of only R-substituent at 2-position of the phenyl ring was effective.

$$\log(1/IC_{50}) = 1.534(\pm 0.890)MR_{R2} + 6.366(\pm 0.309)$$
$$n = 6,\ r = 0.923,\ r^2 = 0.851, \tag{30}$$
$$q^2 = 0.735,\ s = 0.178,\ Q = 5.185,\ F_{1,4} = 23.484,\ \alpha = 0.01$$

3-(4-Substituted-phenyl)-N-hydroxy-2-propenamides (Kim et al. 2003) (Fig. 27).

For this series of compounds, their antiproliferative activity was reported against human lung cancer-A549 cell lines as well as human cell lines of breast cancer (SK-BR-3). Both the activities were shown to be significantly correlated with ClogP as exhibited by Eqs. 31 and 32, respectively, suggesting that hydrophilicity of these compounds was the major controlling factor of their activity

$$\log(1/IC_{50}) = 0.755(\pm 0.265)\mathrm{Clog}\,P + 4.984(\pm 0.338)$$
$$n = 6,\ r = 0.970,\ r^2 = 0.940,\ q^2 = 0.892, \tag{31}$$
$$s = 0.112,\ Q = 8.661,\ F_{1,4} = 62.560,\ \alpha = 0.01$$

$$\log(1/IC_{50}) = 1.058(\pm 0.514)\mathrm{Clog}\,P + 4.909(\pm 0.657)$$
$$n = 6,\ r = 0.944,\ r^2 = 0.891,\ q^2 = 0.778, \tag{32}$$
$$s = 0.217,\ Q = 4.350,\ F_{1,4} = 32.638,\ \alpha = 0.01$$

3-(4-Aroyl-1-methyl-1H-2-pyrrolyl)-N-hydroxy-2-propenamides (Mai et al. 2004) (Fig. 28).

For the inhibitory data of these compounds on maize histone deacetylase HD-2, a bilinear model, as shown by shown by Eq. 33, was reported.

Fig. 28 3-(4-Aroyl-1-methyl-1*H*-2-pyrrolyl)-*N*-hydroxy-2-propenamides
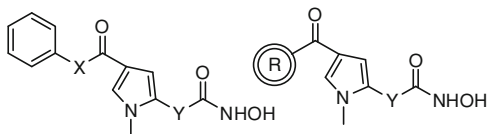
$$\log(1/IC_{50}) = 1.804(\pm 0.707)CMR - 2.193(\pm 0.957)\log(\beta \cdot 10^{CMR} + 1)$$
$$+ 1.074(\pm 0.353)I_{CH=CH} - 8.583(\pm 5.442)$$
$$n = 22, \ r = 0.931, \ r^2 = 0.868, \ q^2 = 0.773, \ s = 0.358, \ Q = 2.601,$$
$$F_{4,17} = 27.856, \ \alpha = 0.01, \ (CMR)_0 = 8.953, \log\beta : -8.286$$
$$\text{Clog}\,P \ vs \ CMR = 0.835 \tag{33}$$

This equation suggests that instead of a parabola, the correlation had a Λ-shaped curve. Whatsoever, the correlation indicated a positive role of molar refractivity of the compound till CMR attains an optimum value equal to 8.953. Indicator variable $I_{CH=CH}$ was used for analogues where X or Y bridge could be –CH=CH–. Its positive coefficient indicates that these compounds might be more active.

Pthalimide-type HDACIs (Shinji et al. 2005) (Fig. 29).

For this series of compounds also, the molar refractivity was found to play an important role as shown by Eq. 34. As is obvious, this equation suggests that while molar refractivity of R-substituent may be detrimental to the activity that of R_1 group would be conducive. The R-substituent might produce the steric effect, while R_1 group may participate in dispersion interaction with the receptor.

$$\log(1/EC_{50}) = -0.337(\pm 0.153)MR_R$$
$$+ 1.376(\pm 0.589)MR_{R_1} + 4.871(\pm 1.129)$$
$$n = 13, \ r = 0.892, \ r^2 = 0.795, \ q^2 = 0.638,$$
$$s = 0.318, \ Q = 2.805, \ F_{2,10} = 19.405, \ \alpha = 0.01 \tag{34}$$

Cyclic amide/imide-bearing hydroxamic acid derivatives (Shinji et al. 2006) (Fig. 30).

For this series of compounds the HDAC-6 inhibitory activity was found to correlate with ClogP and Taft's steric factor as shown by Eq.35, which suggests that not the hydrophobic but the hydrophilic property of the molecule would be

Fig. 29 Pthalimide-type HDACIs
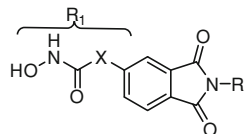
Fig. 30 Cyclic amide/imide-bearing hydroxamic acid derivatives
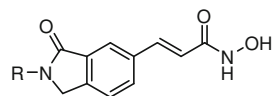
conducive and some steric interaction of 3-substituent in R-moiety may also be beneficial.

$$\log(1/\text{IC}_{50}) = -0.199(\pm 0.086)\text{Clog}\,P - 0.101(\pm 0.093)\text{E}_{S-3} \\ + 6.775(\pm 0.196)$$
$$n = 16,\ r = 0.835,\ r^2 = 0.698,\ q^2 = 0.571,\ s = 0.115,\ Q = 7.261,$$
$$F_{2,13} = 15.053,\ \alpha = 0.01,\ \text{C}\log P\,vs\,E_{S-3}\,0.000 \tag{35}$$

Novel uracil-based hydroxamates (Mai et al. 2005a, b) (Fig. 31).

The synthesized compounds were tested in different forms of HDAC.

For uracil-based hydroxamates reported by Mai et al. (Mai et al. 2005a, b) (Fig. 31), their maize HDAC class II (HD1-A) inhibition activity was found to be correlated as shown by Eq. 36 and maize HDAC class I (HD1-B) inhibition activity as shown by Eq. 37. Both the equations are parallel and suggest that both the activities would depend on the molar refractivity of Y moiety of the compounds with almost an equal optimum value of MR_Y around 4.5. This Y moiety may be assumed to have dispersion interaction with the receptor.

$$\log(1/\text{IC}_{50}) = 8.498(\pm 4.610)\text{MR}_Y - 0.934(\pm 0.578)(\text{MR}_Y)^2 - 11.843(\pm 9.090)$$
$$n = 11,\ r = 0.919,\ r^2 = 0.844,\ q^2 = 0.781,$$
$$s = 0.389,\ Q = 2.362,\ F_{2,8} = 21.704,\ \alpha = 0.01,$$
$$(\text{MR}_Y)_o = 4.548(\pm 0.662)\ \text{from } 4.246 \text{ to } 5.571 \tag{36}$$

$$\log(1/\text{IC}_{50}) = 8.621(\pm 4.124)\text{MR}_Y - 0.998(\pm 0.517)(\text{MR}_Y)^2 \\ - 11.268(\pm 8.122)$$
$$n = 10,\ r = 0.917,\ r^2 = 0.842,\ q^2 = 0.668, \tag{37}$$
$$s = 0.332,\ Q = 2.762,\ F_{2,7} = 18.588,\ \alpha = 0.01,\ (\text{MR}_Y)_o$$
$$= 4.317(\pm 0.340)\ \text{from } 4.104 \text{ to } 4.784$$

Pyrimidyl-5-Hydroxamic Acids (Angibaud et al. 2005) (Fig. 32).

Fig. 31 Novel uracil-based hydroxamates
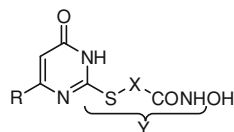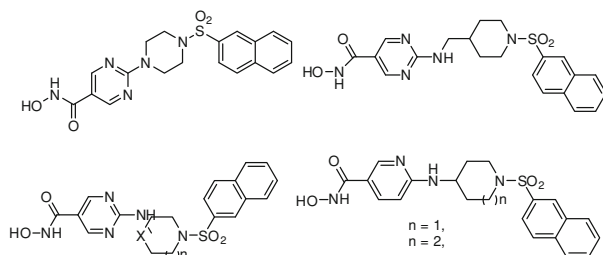
Fig. 32 Pyrimidyl-5-hydroxamic acids

The above compounds were tested on HeLa cell nuclear extracts as a source of HDAC enzyme. For these data the following 2D-QSAR model was formulated suggesting that bulky molecule will not be favorable to the activity.

$$\log(1/IC_{50}) = -0.030(\pm 0.014)MgVol + 20.759(\pm 6.169)$$
$$n = 8,\ r = 0.908,\ r^2 = 0.824,\ q^2 = 0.718,\ s = 0.161,\ Q = 5.640,$$
$$F_{1,6} = 27.646,\ \alpha = 0.01 \tag{38}$$

(Aryloxopropenyl)pyrrolyl Hydroxamides (Mai et al. 2005a) (Fig. 33).

These compounds were tested against maize HDACs (HD1-B and HD1-A).

For maize HD-1-A inhibition activity of this series of compounds the correlation obtained was as

$$\log(1/IC_{50}) = -0.025(\pm 0.008)MgVol + 1.813(\pm 0.826)B_{1-2}$$
$$+ 12.524(\pm 2.688)$$
$$n = 18,\ r = 0.893,\ r^2 = 0.798,\ q^2 = 0.693,\ s = 0.418,\ Q = 2.136,$$
$$F_{2,15} = 59.114,\ \alpha = 0.01,\ MgVol\ vs\ B_{1-2} = 0.020 \tag{39}$$

which revealed the role of steric effects. This coincides with the molecular modeling results of Mai et al. (2005b) which had pointed out that a bent molecular shape structure was a prerequisite for HD1-A-selective inhibitory activity. Mac-Gowan volume (MgVol) with negative sign implies steric hindrance. B_{1-2} is the sterimol parameter of Verloop for the smallest width of substituent at the 2-position of the phenyl ring at R. It seems that as the smallest width of substituent increases, the inhibitory activity also increases.

Fig. 33 (Aryloxopropenyl) pyrrolyl hydroxamides
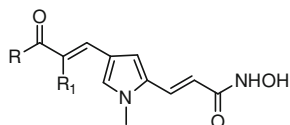
For the maize HD1-B inhibitory activity of these compounds the correlation obtained was as

$$\log(1/\text{IC}_{50}) = -1.747(\pm 0.933)\text{Clog}\,P + 0.889(\pm 0.491)\text{L}_{-2} + 6.275(\pm 2.091)$$
$$n = 18,\ r = 0.836,\ r^2 = 0.699,\ q^2 = 0.560,$$
$$s = 0.631,\ Q = 1.325,\ F_{2,15} = 17.365,$$
$$\alpha = 0.01,\ \text{Clog}\,P\,\text{vs}\,\text{L}_{-2} = 0.013 \qquad (40)$$

where negative Clog P term indicates that hydrophilic molecules would present better inhibitory activity. L_{-2}, the sterimol parameter for the length of the substituent at the 2-position of the aryl ring R would influence the activity positively.

Rigid Trichostatin A analogues (Charrier et al. 2006) (Fig. 34).

These trichostatin analogues were tested for their antiproliferative activity against non-small cell lung cancer H661 cells and their activity was found to be significantly correlated with hydrophobicity as

$$\log(1/\text{IC}_{50}) = -0.343(\pm 0.242)\text{C}\log P + 6.382\,(\pm 0.627)$$
$$n = 6,\ r = 0.891,\ r^2 = 0.795,\ q^2 = 0.567,\ s = 0.134,\ Q = 6.649,$$
$$F_{1,4} = 15.389,\ \alpha = 0.05 \qquad (41)$$

which suggest that not the hydrophobicity but hydrophilicity of the compounds would be important for their activity.

Hydrophilic Hydroxamates and 2-aminobenzamide-containing derivatives (Nagaoka et al. 2006) (Fig. 35).

These compounds were tested for their HDAC inhibitory activity and HCT116 colon carcinoma cell antiproliferative activity. For both these activities the correlations obtained were as shown by Eqs. 42 and 43, which suggests that both the activities will be primarily governed by hydrophobic property of the molecule. Thus the whole molecule in both the cases might be involved in hydrophobic interaction with the receptors. In Eq. 42, the presence of an indicator variable used for R=OH, however, indicates that HDAC inhibition activity may have an additional advantage of the presence of an OH moiety at R, and this may be due to the participation of OH in hydrogen bonding with some site of the receptor.

Fig. 34 TSA analogues

R = H, F, Me$_2$N
X = OH, 2-NH$_2$Ph
n = 1,2
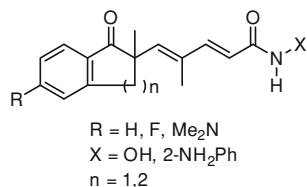
Fig. 35 Hydrophilic
Hydroxamates and 2-
aminobenzamide-
containing derivatives
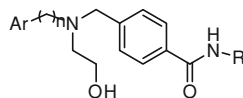
$$\log(1/\text{IC}_{50}) = 0.387(\pm 0.358)\text{Clog}\,P$$
$$+ 1.873(\pm 0.668)I_{\text{OH}} + 4.626(\pm 0.908)$$
$$n = 10,\ r = 0.933,\ r^2 = 0.871,\ q^2 = 0.761, \quad (42)$$
$$s = 0.355,\ Q = 2.628,\ F_{2,7} = 23.683,$$
$$\alpha = 0.01,\ \text{Clog}P\,vs\,I_{\text{OH}} = 0.243$$

$$\log(1/\text{IC}_{50}) = 0.434(\pm 0.175)\text{Clog}\,P + 4.207(\pm 0.357)$$
$$n = 9,\ r = 0.911,\ r^2 = 0.831,\ q^2 = 0.737,\ s = 0.217,\ Q = 4.198,$$
$$F_{1,7} = 34.427,\ \alpha = 0.01 \quad (43)$$

SAHA analogues functionalized adjacent to the hydroxamic acid (Bieliauskas et al. 2007) (Fig. 36).

For a small series of SAHA analogues, the correlation obtained was as

$$\log(1/\text{IC}_{50}) = 0.389(\pm 0.283)B_{5-R} + 2.316(\pm 1.099)$$
$$n = 6,\ r = 0.886,\ r^2 = 0.784,\ q^2 = 0.505,\ s = 0.149,\ Q = 5.946,$$
$$F_{1,4} = 14.651,\ \alpha = 0.05 \quad (44)$$

where B_{5-R} is the Sterimol parameter of Verloop for the largest width of R-substituent. The positive coefficient of B_{5-R} suggests that this subtstitent might be involved in some dispersion interaction with the receptor.

Aminosuberoyl hydroxamic acids (Belvedere et al. 2007) (Fig. 37).

The aminosuberoyl hydroxamic acids were tested for their activity against HDAC-1 for which the correlation obtained was as

$$\log(1/\text{IC}_{50}) = -12.545(\pm 4.636)\text{MR}_{R_1} + 1.934(\pm 0.686)(\text{MR}_{R_1})^2$$
$$+ 27.415(\pm 7.566)$$
$$n = 14,\ r = 0.924,\ r^2 = 0.854,\ q^2 = 0.778, \quad (45)$$
$$s = 0.236,\ Q = 3.915,\ F_{2,11} = 32.184,$$
$$\alpha = 0.01,\ (\text{MR}_{R_1})_{\text{o}} = 3.244(\pm 0.080)\ \text{from } 3.145 \text{ to } 3.305$$

Fig. 36 SAHA analogues
functionalized adjacent to the
hydroxamic acid
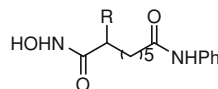
Fig. 37 Aminosuberoyl hydroxamic acids
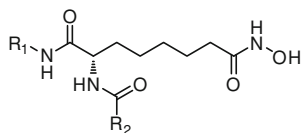
which suggests that the molar refractivity of R_1-substituent would govern the activity but would have the positive effect only after MR_{R_1} attains an optimum value of 3.244. An R_1-substituent of larger size might be involved in dispersion interaction.

δ-Lactam-Based Histone Deacetylase Inhibitors 9 (Fig. 38) (Kim et al. 2007).

For the HDAC inhibitory enzyme activities of these compounds obtained from HeLa cell lysate the following model was derived by Pontiki and Hadjipavlou (2012) to suggest that lipophilicity is the most important parameter describing the activity of these compounds.

$$\log(1/IC_{50}) = 0.556(\pm0.360)\text{Clog}\,P + 5.870\,(\pm0.389)$$
$$\log(1/IC_{50}) = 0.556(\pm0.360)\text{Clog}\,P + 5.870\,(\pm0.389)$$
$$n = 6,\ r = 0.906,\ r^2 = 0.821,\ q^2 = 0.506,\ s = 0.243,\ Q = 3.728,$$
$$F_{1,4} = 18.295,\ \alpha = 0.05 \tag{46}$$

2-Aroyloindoles and 2-Aroylbenzofurans with N-Hydroxyacrylamide Substructures (Mahboobi et al. 2007) (Fig. 39).

E-N-hydroxy-(2-aroylindole)acrylamides and *E-N*-hydroxy-(2-aroylbenzofuran)acrylamides were profiled using nuclear extra HDAC and recombinant HDAC-1. For HDAC inhibitory activity the correlation obtained was as shown by Eq. 47 and HDAC-1 inhibitory activity the correlation obtained was as shown by Eq. 48. As is obvious, while the molar refractivity of R_2-substituent at the 3-position of the phenyl ring will favor the HDAC inhibitory after it attains an optimum value equal to 0.707, the molar refractivity of R_2-substituent at the 4-position of the phenyl ring and that of R_3 group would be detrimental to HDAC-1 inhibitory activity.

$$\log(1/IC_{50}) = -0.875(\pm0.677)MR_{R2-3} + 0.618(\pm0.307)(MR_{R2-3})^2$$
$$+ 6.528(\pm0.196)$$
$$n = 13,\ r = 0.936,\ r^2 = 0.876,\ q^2 = 0.784, \tag{47}$$
$$s = 0.184,\ Q = 5.086,\ F_{2,13} = 35.294,$$
$$\alpha = 0.01,\ (MR_{R2-3})_o = 0.707(\pm0.287)\ \text{from}\ 0.308\ \text{to}\ 0.864$$

Fig. 38 δ-Lactam-based histone deacetylase inhibitors
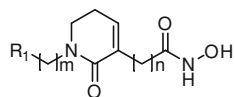
Fig. 39 2-Aroyloindoles and
2-aroylbenzofurans with
N-hydroxyacrylamide
substructures
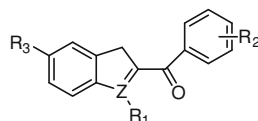
Fig. 40 Triazolylphenyl
derivatives

$$\log(1/\mathrm{IC}_{50}) = -0.418(\pm 0.162)\mathrm{MR}_{R3} - 0.514(\pm 0.172)\mathrm{MR}_{R2-4}$$
$$+ 7.388(\pm 0.295)$$
$$n = 13,\ r = 0.916,\ r^2 = 0.839,\ q^2 = 0.737,\ s = 0.215,\ Q = 4.260,$$
$$F_{2,13} = 25.995,\ \alpha = 0.01 \tag{48}$$

Triazolylphenyl-Based Histone Deacetylases Inhibitors (Chen et al. 2008b)
(Fig. 40).

For this series of compounds, their activity against HDAC-1 and HDAC-3 was
found to correlate with MR_{-3PH}, the molar refractivity of substitution at 3-position
of the phenyl group (X), and ClogP as shown by Eqs. 49 and 50, respectively. The
hydrophobicity is shown to have the effect only on HDAC-1 inhibitory activity and
not on that of HDAC-3.

$$\log(1/\mathrm{IC}_{50}) = 0.157(\pm 0.153)\,\mathrm{Clog}\,P + 0.137(\pm 0.031)\mathrm{MR}_{-3Ph}$$
$$+ 6.741(\pm 0.381)$$
$$n = 15,\ r = 0.949,\ r^2 = 0.900,\ q^2 = 0.839, \tag{49}$$
$$s = 0.108,\ Q = 8.787,\ F_{2,12} = 54.170,$$
$$\alpha = 0.01,\ \ \mathrm{Clog}\,P\ vs\ \mathrm{MR}_{-3Ph} = 0.286$$

$$\log(1/\mathrm{IC}_{50}) = 0.135(\pm 0.033)\,\mathrm{MR}_{-3Ph} + 7.051(\pm 0.116)$$
$$n = 15,\ r = 0.924,\ r^2 = 0.855,\ q^2 = 0.805,\ s = 0.141,\ Q = 6.553,$$
$$F_{1,13} = 76.488,\ \alpha = 0.01 \tag{50}$$

3 Conclusion

All the above QSAR studies on hydroxamic acids acting as HDAC inhibitors have
shown the importance of basically two properties of the compounds, the hydro-
phobicity and molar refractivity, where in the majority of cases the latter has been
more dominant. They basically indicate the involvement of dispersion, or say,

essentially the electrostatic interaction with the receptor. In a few cases, there can be, however, the hydrophobic interaction, too. In a few cases, the negative coefficient of MR also suggests the steric effect of bulky substituent or of the whole molecule. All the three kinds of interactions, i.e., electrostatic, hydrophobic, and steric have also been demonstrated by CoMFA and CoMSIA studies performed on several cases. Thus all the studies have provided the guidelines for designing better, more potent HDAC inhibitors in the class of hydroxamic acids.

References

Angibaud P, Arts J, Van Emelen K et al (2005) Discovery of pyrimidyl-5-hydroxamic acids as new potent histone deacetylase inhibitors. Eur J Med Chem 40:597–606

Belvedere S, Witter DJ, Yan J et al (2007) Aminosuberoyl hydroxamic acids (ASHAs): a potent new class of HDAC inhibitors. Bioorg Med Chem Let 17:3969–3971

Bieliauskas AV, Weerasinghe SVW, Pflum MKH (2007) Structural requirements of HDAC inhibitors: SAHA analogs functionalized adjacent to the hydroxamic acid. Bioorg Med Chem Let 17:2216–2219

Bouchain G, Leit S, Frechette S et al (2003) Development of potential antitumor agents. Synthesis and biological evaluation of a new set of sulfonamide derivatives as histone deacetylase inhibitors. J Med Chem 46:820–830

Charrier C, Bertrand P, Gesson JP et al (2006) Synthesis of rigid trichostatin A analogs as HDAC inhibitors. Bioorg Med Chem Lett 16:5339–5344

Chen Y, Jiang YJ, Zhou JW et al (2008a) Identification of ligand features essential for HDACs inhibitors by pharmacophore modeling. J Mol Graph Model 26:1160–1168

Chen Y, Li H, Tang W et al (2009) 3D-QSAR studies of HDACs inhibitors using pharmacophore-based alignment. Eur J Med Chem 44:2868–2876

Chen Y, Lopez-Sanchez M, Savoy DN et al (2008b) A series of potent and selective, triazolylphenyl-based histone deacetylases inhibitors with activity against pancreatic cancer cells and Plasmodium falciparum. J Med Chem 51:3437–3448

Curtin ML, Garland RB, Heyman HR et al (2002) Succinimide hydroxamic acids as potent inhibitors of histone deacetylase (HDAC). Bioorg Med Chem Lett 12:2919–2923

Dai Y, Guo Y, Guo J et al (2003) Indole amide hydroxamic acids as potent inhibitors of histone deacetylases. Bioorg Med Chem Lett 13:1897–1901

Dawson M, Xia Z, Liu G et al (2007) An adamantyl-substituted retinoid-derived molecule that inhibits cancer cell growth and angiogenesis by inducing apoptosis and binds to small heterodimer partner nuclear receptor: effects of modifying its carboxylate group on apoptosis, proliferation, and protein-tyrosine phosphatase activity. J Med Chem 50:2622–2639

Delorme D, Ruel R, Lavoie R et al (2001) Inhibitors of histone deacetylase, methylgene, Inc Int Patent Appl WO 01/38322

Dessalew N (2007) QSAR study on aminophenylbenzamides and acrylamides as histone deacetylase inhibitors: an insight into the structural basis of antiproliferative activity. Med Chem Res 16:449–460

Domingo JL (1998) Developmental toxicity of metal chelating agents. Reprod Toxicol 12:499–510

El Yazal J, Pang YP (2000) Proton dissociation energies of zinc-coordinated hydroxamic acids and their relative affinities for zinc: insight into design of inhibitors of zinc-containing proteinases. J Phys Chem B 104:6499–6504

Green ES, Evans H, Rice-Evans P et al (1993) The efficacy of monohydroxamates as free radical scavenging agents compared with di- and trihydroxamates. Biochem Pharmacol 45:357–366

Guo Y, Xiao J, Guo Z et al (2005) Exploration of a binding mode of indole amide analogues as potent histone deacetylase inhibitors and 3D-QSAR analyses. Bioorg Med Chem Let 13:5424–5434

Gupta SP (2011) QSAR and molecular modeling. Anamaya, New Delhi

Jaiswal D, Karthikeyan C, Shrivastava SK et al (2006) QSAR modeling of sulfonamide inhibitors of histone deacetylase. Int Electr J Mol Des 5:345–354

Jung M, Brosch G, Kolle D et al (1999) Amide analogues of trichostatin A as inhibitors of histone deacetylase and inducers of terminal cell differentiation. J Med Chem 42:4669–4679

Juvale DC, Kulkarni VV, Deokar HH et al (2006) 3D-QSAR of histone deacetylase inhibitors: hydroxamate analogues. Org Biomol Chem 4:2858–2868

Katritzky AR, Slavov SH, Dobchev DA et al (2007) Comparison between 2D and 3D-QSAR approaches to correlate inhibitor activity for a series of indole amide hydroxamic acids. QSAR Comb Sci 3:333–345

Kim DK, Lee JY, Kim JS et al (2003) Synthesis and biological evaluation of 3-(4-substituted-phenyl)-N-hydroxy-2-propenamides, a new class of histone deacetylase inhibitors. J Med Chem 46:5745–5751

Kim HM, Ryu DK, Choi Y et al (2007) Structure-activity relationship studies of a series of novel delta-lactam-based histone deacetylase inhibitors. J Med Chem 50:2737–2741

Kozikowski AP, Chen Y, Gaysin AM et al (2008) Chemistry, biology, and QSAR studies of substituted biaryl hydroxamates and mercaptoacetamides as HDAC inhibitors-nanomolar-potency inhibitors of pancreatic cancer cell growth. Chem Med Chem 3:487–501

Lavoie R, Bouchain G, Frechette S et al (2001) Design and synthesis of a novel class of histone deacetylase inhibitors. Bioorg Med Chem Lett 11:2847–2850

Lipczynska-Kochany E (1988) In: Some new aspects of hydroxamic acid chemistry. E. Pr Nauk Politech Warsz Chem 46:3–98

Liu B, Lu AJ, Liao CZ et al (2005) 3D-QSAR of sulfonamide hydroxamic acid HDAC inhibitors. Acta Phys Chim Sin 21:333–337

Lu Q, Wang DS, Chen CS et al (2005) Structure-based optimization of phenylbutyrate-derived histone deacetylase inhibitors. J Med Chem 48:5530–5535

Mahboobi S, Sellmer A, Höcher H et al (2007) 2-aroylindoles and 2-aroylbenzofurans with N-hydroxyacrylamide substructures as a novel series of rationally designed histone deacetylase inhibitors. J Med Chem 50:4405–4418

Mai A, Massa S, Cerbara I et al (2004) 3-(4-Aroyl-1-methyl-1H-2-pyrrolyl)- N-hydroxy-2-propenamides as a new class of synthetic histone deacetylase inhibitors. 2. Effect of pyrrole-C2 and/or -C4 substitutions on biological activity. J Med Chem 47:1098–1109

Mai A, Massa S, Pezzi R et al (2003a) Discovery of (aryloxopropenyl)pyrrolyl hydroxyamides as selective inhibitors of class IIa histone deacetylase homologue HD1-A. J Med Chem 46:4826–4829

Mai A, Massa S, Pezzi R et al (2005a) Class II (IIa)-selective histone deacetylase inhibitors. 1. Synthesis and biological evaluation of novel (aryloxopropenyl)pyrrolyl hydroxyamides. J Med Chem 48:3344–3353

Mai A, Massa S, Ragno R et al (2002) Binding mode analysis of 3-(4-benzoyl-1-methyl-1H-2-pyrrolyl)-N-hydroxy-2-propenamide: a new synthetic histone deacetylase inhibitor inducing histone hyperacetylation, growth inhibition, and terminal cell differentiation. J Med Chem 45:1778–1784

Mai A, Massa S, Ragno R et al (2003b) 3-(4 Aroyl-1-methyl-1H-2-pyrrolyl)-N-hydroxy-2-alkylamides as a new class of synthetic histone deacetylase inhibitors. 1. Design, synthesis, biological evaluation, and binding mode studies performed through three different docking procedures. J Med Chem 46:512–524

Mai A, Massa S, Rotili D et al (2005b) Exploring the connection unit in the HDAC inhibitor pharmacophore model: novel uracil-based hydroxamates. Bioorg Med Chem Lett 15:4656–4561

Massa S, Mai A, Sbardella G et al (2001) 3-(4-aroyl-1H-pyrrol-2-yl)-N-hydroxy-2-propenamides, a new class of synthetic histone deacetylase inhibitors. J Med Chem 44:2069–2072

Melagraki G, Afantitis A, Sarimveis H et al (2009) Predictive QSAR workflow for the in silico identification and screening of novel HDAC inhibitors. Mol Divers 13:301–311

Moradei O, Leit S, Zhou N et al (2006) Substituted N-(2-aminophenyl)-benzamides, (E)-N-(2-aminophenyl)-acrylamides and their analogues: novel classes of histone deacetylase inhibitors. Bioorg Med Chem Lett 16:4048–4052

Munster PN, Troso-Sandoval T, Rosen N et al (2001) The histone deacetylase inhibitor suberoylanilide hydroxamic acid induces differentiation of human breast cancer cells. Cancer Res 61:8492–8497

Muri EMF, Nieto MJ, Sindelar RD et al (2002) Hydroxamic acids as pharmacological agents. Cur Med Chem 9:1631–1653

Nagaoka Y, Maeda T, Kawai Y et al (2006) Synthesis and cancer antiproliferative activity of new histone deacetylase inhibitors: hydrophilic hydroxamates and 2-aminobenzamide containing derivatives. Eur J Med Chem 41:697–708

Niemeyer HM, Pesel E, Copaja SV et al (1989) Changes in hydroxamic acid levels of wheat plants induced by aphid feeding. Phytochem 28:447–449

Park H, Lee S (2004) Homology modeling, force field design, and free energy simulation studies to optimize the activities of histone deacetylase inhibitors. J Comp-Aid Mol Des 18:375–388

Parvathy S, Hussain I, Karran EH et al (1998) Alzheimer's amyloid precursor protein alpha-secretase is inhibited by hydroxamic acid-based zinc metalloprotease inhibitors: similarities to the angiotensin converting enzyme secretase. Biochem 37:1680–1685

Pontiki E, Hadjipavlou- Litina D, Geromichalos G et al (2009) Anticancer activity and quantitative–structure activity relationship (QSAR) studies of a series of antioxidant/anti-inflammatory aryl-Acetic and hydroxamic Acids. Chem Biol Drug Des 74:266–275

Pontiki E, Hadjipavlou-Litina D (2012) Histone deacetylase inhibitors (HDACIs). Structure-activity relationships: history and new QSAR perspectives. Med Res Rev 32:1–165

Price S, Bordogma W, Braganza R et al (2007a) Identification and optimisation of a series of substituted 5-pyridin-2-yl-thiophene-2-hydroxamic acids as potent histone deacetylase (HDAC) inhibitors. Bioorg Med Chem Lett 17:363–369

Price S, Bordogna W, Bull RJ et al (2007b) Identification and optimisation of a series of substituted 5-(1H-pyrazol-3-yl) thiophene-2-hydroxamic acids as potent histone deacetylase (HDAC) inhibitors. Bioorg Med Chem Lett 17:370–375

Ragno R, Simeoni S, Rotili D et al (2008) Class II-selective histone deacetylase inhibitors. Part 2: alignment-independent GRIND 3-D QSAR, homology and docking studies. Eur J Med Chem 43:621–632

Ragno R, Simeoni S, Valente S et al (2006) 3-D QSAR studies on histone deacetylase inhibitors. A GOLPE/GRID approach on different series of compounds. J Chem Inf Model 46:1420–1430

Rajwade RP, Pande R, Mishra KP et al (2009) Hydroxamic acids analogous against breast cancer cells: 2D-QSAR and 3D-QSAR studies. QSAR Comb Sci 28:1500–1508

Rajwade RP, Pande R, Mishra KP et al (2008) Quantitative structure—activity relationship (QSAR) of N-arylsubstituted hydroxamic acids as inhibitors of human adenocarinoma cells A431. Med Chem 4:237–243

Remiszewski SW, Sambucetti LC, Atadja P et al (2002) Inhibitors of human histone deacetylase: synthesis and enzyme and cellular activity of straight chain hydroxamates. J Med Chem 45:753–757

Remiszewski SW, Sambucetti LC, Bair KW et al (2003) N-hydroxy-3-phenyl-2-propenamides as novel inhibitors of human histone deacetylase with in vivo antitumor activity: discovery of (2E)-N-hydroxy-3-[4-[[(2-hydroxyethyl) [2-(1H-indol-3-yl) ethyl] amino] methyl]phenyl]-2 propenamide (NVP-LAQ824). J Med Chem 46:4609–4624

Shinji C, Maeda S, Imai K et al (2006) Design, synthesis, and evaluation of cyclic amide/imide-bearing hydroxamic acid derivatives as class-selective histone deacetylase (HDAC) inhibitors. Bioorg Med Chem 14:7625–7651

Shinji C, Nakamura T, Maeda S et al (2005) Design and synthesis of phthalimide-type histone deacetylase inhibitors. Bioorg Med Chem Lett 15:4427–4431

Siverman RB (2004) The organic chemistry of drug design and drug action. Academic Press, USA

Steward WP, Thomas AL (2000) Marimastat: the clinical development of a matrix metalloproteinase inhibitor. Expert Opin Invest Drugs 9:2913–2922

Taira J, Chika M, Aniya Y (2002) Dimerumic acid as an antioxidant from the mold, Monascus anka: the inhibition mechanisms against lipid peroxidation and hemeprotein-mediated oxidation. Biochem Pharmacol 63:1019–1026

Turcot I, Stintzi A, Xu J et al (2000) Fast biological iron chelators: kinetics of iron removal from human differic transferring by multidentate hydroxypyridonates. Biol Inorg Chem 5:634–641

Vadivelan S, Sinha BN, Rambabu G et al (2008) Pharmacophore modeling and virtual screening studies to design some potential histone deacetylase inhibitors as new leads. J Mol Graph Model 26:935–946

Wagh NK, Deokar HS, Juvale DC et al (2006) 3D-QSAR of histone deacetylase inhibitors as anticancer agents by genetic function approximation. Ind J Biochem Biophys 43:360–371

Wang DF, Wiest O, Helquist P et al (2004) QSAR studies of PC-3 cell line inhibition activity of TSA and SAHA-like hydroxamic acids. Bioorg Med Chem Let 14:707–711

Wittich S, Scherf H, Xie C et al (2002) Structure-activity relationships on phenylalanine-containing inhibitors of histone deacetylase: in vitro enzyme inhibition, induction of differentiation, and inhibition of proliferation in Friend leukemic cells. J Med Chem 45:3296–3309

Woo SH, Frechette S, Abou Khalil E et al (2002) Structurally simple trichostatin A-like straight chain hydroxamates as potent histone deacetylase inhibitors. J Med Chem 45:2877–2885

Xie A, Liao C, Li Z et al (2004) Quantitative structure-activity relationship study of histone deacetylase inhibitors. Curr Med Chem Anticancer Agents 4:273–299

Zhang L, Fang H, Zhu HW et al (2009) QSAR studies of histone deacetylase (HDAC) inhibitors by CoMFA, CoMSIA, and molecular docking. Drug Discov Ther 3:41–48

Hydroxamic Acids as Inhibitors of Urease in the Treatment of *Helicobacter pylori* Infections

E. M. F. Muri and T. G. Barros

Abstract *Helicobacter pylori* (*H. pylori*) is a microaerophilic spiral bacterium and infection by it in the human stomach causes gastritis and is considered to be involved in the pathogenesis of peptic ulcer and in the development of gastric carcinoma. It produces a nickel-dependent enzyme called urease which catalyzes the hydrolysis of urea to produce ammonia and carbamate. This ammonia produced by urease elevates the level of pH in the stomach, breaks gastric mucus, inhibits the consumption of oxygen, and reduces the production of ATP in gastric mucus cells or in mitochondria. In order to stop the pathogenesis of these disorders in the body, it is therefore essential that potent inhibitors of *H. pylori* urease be developed. The present chapter discusses the role of hydroxamic acids as inhibitors of this enzyme.

Keywords Hydroxamic acids · *Helicobacter pylori* · Urease · Enzyme inhibition · Gastric disorders

Abbreviations

AHA	Acetohydroxamic acid
CAB	Cellulose acetate butyrate
CoMFA	Comparative molecular field analysis
CoMSIA	Comparative molecular similarity indices analysis
HA	Hydroxamic acid
HP	*Helicobacter pylori*
JB	Jack bean
PPI	Proton pump inhibitor

E. M. F. Muri (✉) · T. G. Barros
Faculdade de Farmácia, Universidade Federal Fluminense, Rua Mario Viana 523,
Santa Rosa, Niterói, RJ 24241-000, Brazil
e-mail: estelamuri@yahoo.com.br

Contents

1 Introduction

The bacterium *Helicobacter pylori* (*H. pylori*) was discovered in 1982 by Marshall and Warren (1984). These researchers were jointly awarded the Nobel Prize in Physiology and Medicine in 2005 for their discovery of "the bacterium *H. pylori* and its role in gastritis and peptic ulcer disease".

Helicobacter pylori is a spiral-shaped gram-negative bacterium that colonizes the stomach or duodenum in about 50 % of all humans and causes more than 90 % of duodenal ulcers and up to 80 % of gastric ulcers (Dunn et al. 1997). However, although *H. pylori* is definitely responsible for these diseases, only less than 10 % of people colonized with *H. pylori* portray disease symptoms. This suggests that specific *H. pylori* strains may be responsible for virulence in different hosts (Ahmed and Sechi 2005).

Various drug regimens have been proposed for the initial treatment of *H. pylori* infection. The most recommended therapy for the eradication of *H. pylori* is the so called standard or proton pump inhibitor (PPI)-based, triple therapy, which combines two antibiotics—clarithromycin plus amoxicillin or metronidazole—with a PPI for at least 7 days (Chey and Wong 2007; McLoughlin et al. 2004). An alternative to standard triple therapy is sequential treatment, which involves a simple dual regimen including a PPI plus amoxicillin for the first 5 days followed by a triple regimen including a PPI, clarithromycin, and tinidazole for the following 5 days. It is not clear if the sequential approach, which may be more complicated, can offer specific advantages (Gisbert and Calvet 2012; Gisbert et al. 2010; Moayyedi 2007). Despite the progress, the eradication of *H. pylori* remains elusive because of the *H. pylori* resistance is still increasing. So, it is clear that alternative treatment regimens are urgently needed.

2 The Urease Enzyme

Helicobacter pylori produces an nickel-dependent enzyme called urease which catalyzes the hydrolysis of urea to produce ammonia and carbamate. The carbamate hydrolyzes to form carbonic acid and a second molecule of ammonia
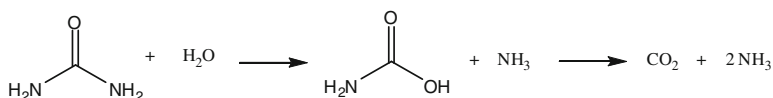
Scheme 1 Hydrolysis of urea by urease

(Scheme 1) (Kosikowska and Berlicki 2011). This production of ammonia by the microorganism helps to counteract the harsh environment of the stomach. So, inhibition of this urea to ammonia catalysis should be beneficial by stopping this neutralization mechanism (Mobley 1996; Mobley and Hausinger 1989; Mobley et al. 1995; Jabri et al. 1995).

The two nickel centers in the urease active site coordinate by residues of histidine, bridged with a carbamoyl lysine group, and one of the two nickel forms a bond with aspartate residue (Mobley et al. 1995). The *H. pylori* (HP) urease enzyme consists of two monomers, a α- and β-subunit exhibiting 26.5 and 61.7 kDa, respectively, as shown in its crystal structure (Fig. 1) (Kosikowska and Berlicki 2011; Ha et al. 2001).

According to their binding mode, compounds acting as inhibitors of urease activity are divided in two classes: (i) Substrate-like or active site-directed inhibitors, which include the urea derivatives, chemotypes and analogs, phosphazenes and the hydroxamic acids (HAs), (ii) Non-substrate-like or mechanism-based inhibitors, e.g., phosphorodiamidate and imidazoles (Amtul et al. 2002). Many urease inhibitors have been described in the last decades, such as, phosphoramidates, urea derivatives, quinones, heterocyclic compounds, and HAs, in

Fig. 1 Crystal structure of *Helicobacter pylori* urease (PDB id 1E9Z) (Kosikowska and Berlicki 2011; Ha et al. 2001)
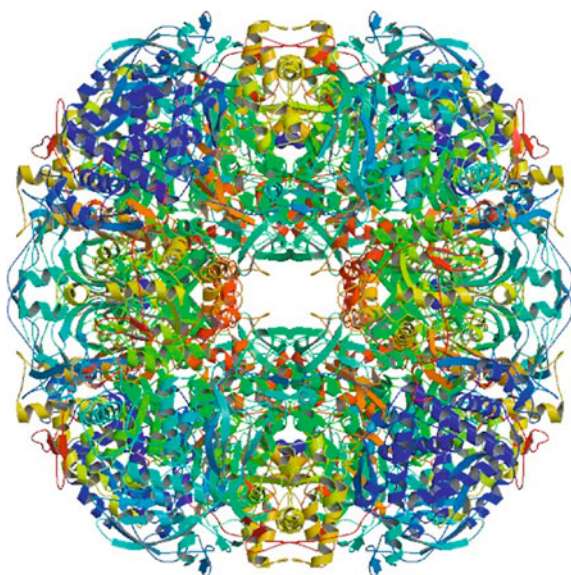
which the hydroxamic acids have been well recognized. Unfortunately, most of HAs acting as urease inhibitors have been rejected due to their instability or toxicity (Kosikowska and Berlicki 2011; Muri et al. 2003; Amtul et al. 2002; Nujumi et al. 1991; Huang et al. 2011). Therefore, studies on novel *H. pylori* urease inhibitors have become essential and an urgent need for the development of a therapy for bacterial infections. In this chapter, we therefore have focused on the design and development of new HAs acting as *H. pylori* urease inhibitors and new technologies in drug delivery systems. Till to date there is only one hydroxamic acid to be used clinically for the treatment of urinary tract infections by urease inhibition, and that is acetohydroxamic acid (Kosikowska and Berlicki 2011; Nujumi et al. 1991).

3 Hydroxamic Acids as Urease Inhibitors

Hydroxamic Acids are among the most well-studied compounds due to their significance in so many different applications, for example, as inhibitors of a variety of enzymes such as ureases (Muri et al. 2003, 2004a, b; Barros et al. 2009; Amtul et al. 2002), peroxidases (Tsukamoto et al. 1999), and matrix metalloproteinases (Leung et al. 2000). The coordination chemistry of HAs can explain their ability to inhibit different classes of enzymes, since they can coordinate with metal ions in the Ni(II)- and Zn(II)-containing metalloenzymes. These observations can explain their ability to inhibit ureases which contains in their active sites two nickel(II) atoms linked by a carbamate bridge (Jabri et al. 1995; Benini et al. 2000). The HAs are also capable of competing as siderophores for iron-(III) (Codd 2008; Benini et al. 2000; Puerta and Cohen 2002; Brown et al. 2004; Jedner et al. 2002; Arnold et al. 1998). The current use of the mesylate salt of DFOB (Desferal®) in the treatment of iron-overload disease in humans shows a significant use of HAs in medicine (Chaston and Richardson 2003). In the context of pharmacological potentials of HAs, which has been recently reviewed, we present here their utility HP urease inhibitors (Codd 2008; Muri et al. 2002; Muri et al. 2004a, b).

Since the first determination of X-ray structure of acetohydroxamic acid-enzyme complex by Stemmler et al. (1995), a few different interaction models of HAs in the active site of urease have been presented—Zerner model (Blakeley et al. 1969; Dixon et al. 1980), Stemmler model (Stemmler et al. 1995), and Wedekind and Zhang Model (Wedekind et al. 1994; Zhang et al. 1994) . The HAs were initially described as potent and specific inhibitors of urease from plants and bacterial origins more than 30 years ago by Kobashi and co-workers (Kobashi et al. 1962; Kobashi 1992; Park et al. 1995). For the last few decades, researchers have started the search for aliphatic, aromatic, amino acids, and dipeptidyl HA derivatives that could be able to inhibit the urease mainly of Jack bean (JB) and *Proteus mirabilis* with low IC_{50} values (e.g., Structures 1–6, Fig. 2). Hydroxamic Acids as inhibitors of urease can be very interesting to treat *H. pylori* and urinal tract infections. Therefore, *N*-aroyl-glycino-hydroxamic acid series was obtained
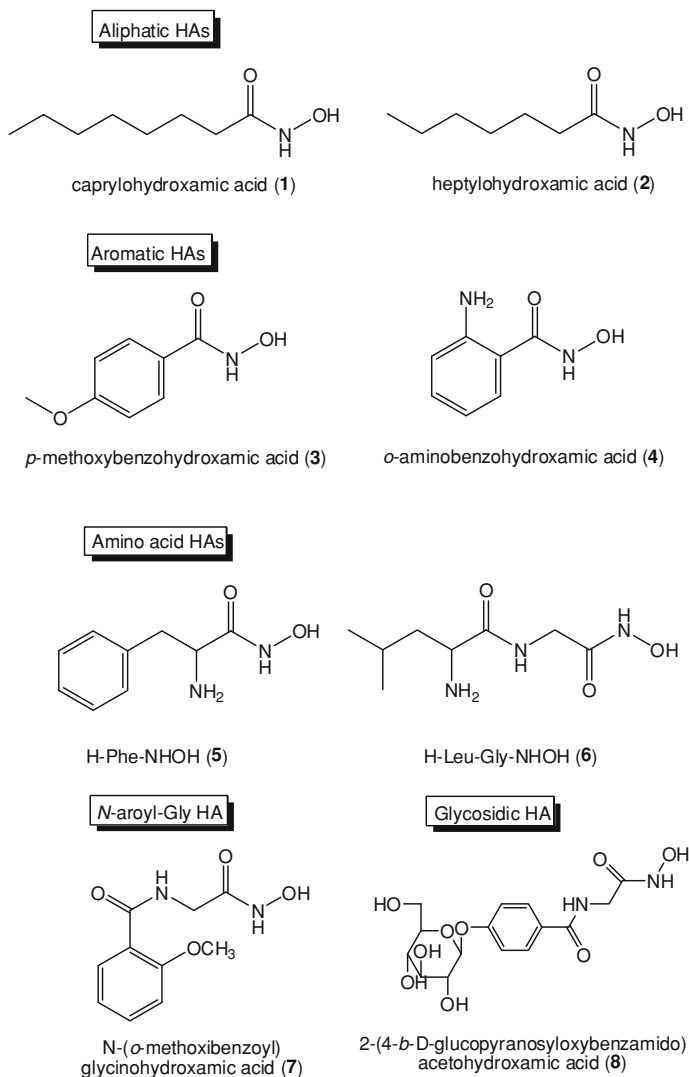
Fig. 2 Structures of the most active HA analogs studied by Kobashi group (Kobashi et al. 1971; Odake et al. 1992, 1994; Ito et al. 1994)

and well studied, resulting in active compounds with IC_{50} values in the range of 0.5–2.0 μM (e.g., Structure 7, Fig. 2) and useful for treating urolithiasis and pyelonephritis, but most of them were mutagenic (Munakata et al. 1980; Esai Co. Ltd. 1978).
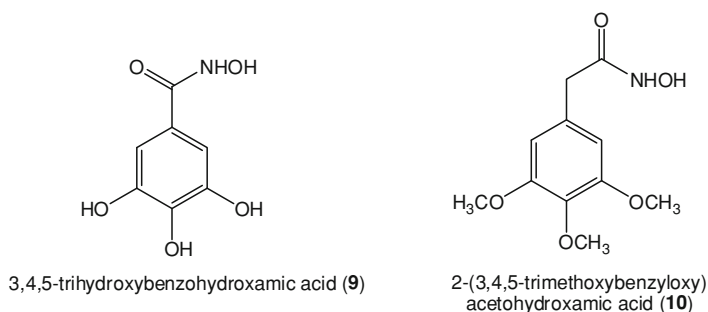
In the early studies on the synthesis and structure-activity relationship (SAR) on HAs, an absolute importance of their –CONHOH group in the urease inhibition was pointed out (Kobashi et al. 1966, 1971; Kumaki et al. 1972; Odake et al. 1992;

Chyioda et al. 1998; Satoh et al. 1991; Fishbein and Carbone 1965; Blakeley et al. 1969). Later, Kobashi et al. investigated the inhibitory effects of HAs on urease of HP and compared their inhibitory activities with the urease obtained from JB and *P. mirabilis* (Odake et al. 1994). Also, some authors (Ito et al. 1994) made a study on HA derivatives obtained from glycoside with hexose residues, such as glucose, galactose, glucuronic acid or galacturonic acid and Park et al. (1995) found that a glycoside derivative (Structure 8, Fig. 2) inhibited rat feces-derived urease by 80 % after 60-min incubation in vitro. The most active compounds investigated are shown in Fig. 2.

In 1983, the acetohydroxamic acid (AHA) ($CH_3CONHOH$) was approved by FDA and is used to treat chronic urea-splitting urinary infections and hyperammonemia associated with liver cirrhosis in Europe and USA (Griffith et al. 1978; Griffith and Musher 1975). Until now, AHA is the most studied and considered a prototype for the HA class of compounds. It is a highly potent urease inhibitor with a K_i value of 5 μM (Fishbein and Carbone 1965; Kumaki et al. 1972).

In 1990s, some authors (Ramadan and Megahed 1994; Abou-Sier et al. 1995) described the synthesis and bacterial urease inhibiting activity of hydroxy benzohydroxamic acid derivatives, where the 3,4,5-trihydroxybenzohydroxamic acid and 2-(3,4,5-trimethoxybenzyloxy)acetohydroxamic acid (Fig. 3) exhibited high potency. Activities of these compounds were compared with those of some non-HA compounds as hydrazone derivatives.

In order to achieve a better knowledge of the urease inhibition mechanism by HAs, several molecular modeling and model dinuclear complexes studies were performed (Stemmler et al. 1995; Arnold et al. 1998; Brown et al. 2004, 2005). Manunza et al. (1997) made a molecular dynamics study on the formation of HA–urease complexes and concluded that the oxime oxygen of HA acts as a bidentate ligand and bridges two nickel atoms forming a chelate with the first nickel by the carbonyl oxygen. In a 3D-QSAR study on 35 HAs, comparative molecular field analysis (CoMFA) and comparative molecular similarity indices analysis (CoMSIA) contour maps were obtained which provided important information on

3,4,5-trihydroxybenzohydroxamic acid (**9**)

2-(3,4,5-trimethoxybenzyloxy) acetohydroxamic acid (**10**)

Fig. 3 Structures of some potent trihydroxy-HA derivatives studied by Abou-Sier et al. (1995) and Ramadan and Megahed (1994)

the factors required for the activity and possible modification on HA structures for improved activity (Zaheer-ul-Haq et al. 2009).

Mishra et al. (2002) developed a 3D-QSAR model in order to explain the biological activity of HAs inhibitors of HP urease and correlated with a homology model by using the urease crystal structure from *Klebsiella aerogenes* as template. They confirmed the importance of HA moiety and the requirement of an ionizable NH$_2$ group and identified a hydrophobic region, providing significant advantage in the design of new inhibitors. On the basis of these 3D-QSAR results, several heterocyclic HA derivatives as mimics of the dipeptide inhibitors were designed and synthesized, via transamination of heterocyclic esters, to have compounds with increased biological stability and inhibitory activity (Muri et al. 2003, 2004a, b; Barros et al. 2009) (Fig. 4).

Although the literature on HAs is extensive, little information is available on polymers containing HAs and acting as urease inhibitors (Johnson and Andersen 1972; Kobashi and Shimizu 1977; Domb et al. 1988). Domb et al. (1988), however, attempted to synthesize polymers that may have biological activity, with a predominance of HA groups and a low percentage of carboxylic acid groups. For this, they allowed primary amide polymers to react with hydroxylamine under mild conditions to give products useful as an ion exchanger and in biomedical applications. In a urease inhibition test, the poly(hydroxamic acid), synthesized from poly(acrylamide), showed activity similar to that of acetohydroxamic acid used as standard.
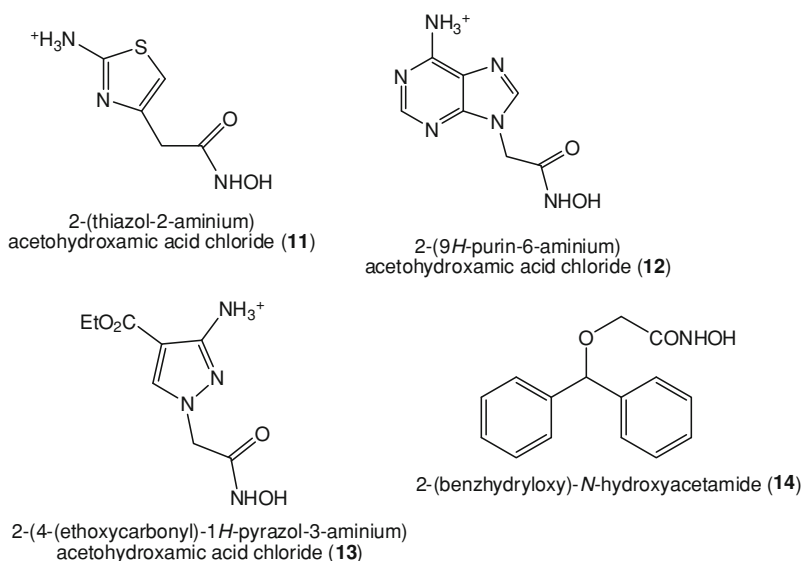
Fig. 4 Structures of some heterocyclic HA derivatives as reported by Muri et al. (2003, 2004a, b) and Barros et al. (2009)

4 Acetohydroxamic Acid: New Technologies for Delivery

The effectiveness of treatment regimens frequently recommended for therapy against *H. Pylori* infection has been increasingly compromised with increased bacterial resistance (De Francesco et al. 2012; Rimbara et al. 2011; Chuah et al. 2011; Malfertheiner et al. 2006), making the establishment of a scheme of re-treatment difficult (Nallasamy and Ramanathan 2012; Mégraud and Doermann 1998).

Clinicians should prescribe therapeutic regimens that have eradication rate ≥90 % or the most effective therapeutic regimen available. However, for several treatment regimens reported in the literature, this eradication rate has declined to below 80 %, the minimum recommended by Maastricht III Consensus (Rimbara et al. 2011; Chuah et al. 2011; Malfertheiner et al. 2006).

Despite the adversities related to the oral route, it is preferred for drug delivery, primarily by patient compliance. In order to improve therapy against *H. pylori* infection and overcome several physiological adversities, attempts are being made to find the drug administration forms from which the drug can be retained in the stomach for extended period of time. For this propose, gastroretentive drug delivery technology is showing promise to enhancing the bioavailability and controlled release of drugs (Pahwa et al. 2010). Here we highlight several works related to the gastroretentive drug delivery technology.

Drug delivery carriers and gastroretentive drug delivery systems are two site-specific techniques that could be used synergistically for the improvement of *H. pylori* therapy (Umamaheswari et al. 2002). Bioadhesive (plugging and sealing effect) and floating microspheres (gastroretentive formulations) are joined in floating-bioadhesive microspheres containing AHA by novel quasi-emulsion solvent diffusion method, in which the floating microspheres can be distributed widely throughout the stomach and may provide longer lasting and more reliable release of drugs (Kawashima et al. 1991; Pahwa et al. 2010).

The device is a polymeric microsphere with a spherical cavity that was termed "microballon" because of its characteristic internal hollow structure and excellent floatability in vitro. The preparation of AHA microballons consisted of co-dissolution of the drug (AHA) and an acrylic polymer (Eudragit E) in ethanol/dichloromethane mixture. This phase was poured into a stirred aqueous medium containing polyvinyl alcohol (PVA) and dispersed into discrete droplets, forming an oil–water (o/w) emulsion. Bioadhesive microspheres were prepared by coating the Eudragit E microballons with polycarbophil. As a result, the drug release rate could be controlled by the polymer concentration. Furthermore, it was reported that almost 90 % of microballons remained floating on the surface of the test solution even after 12 h of testing, because of their low densities (because the gas phase remained inside the microballons). So, the microballons with the higher concentration of polymer were more floatable than those with lower concentrations of polymer. The fact that there was no swelling or gelation of the microballons during the floating test suggested that they were dispersed individually in the

stomach after administration, leading to decreased variability of drug action among patients compared with that occurring in the case of the single unit dosage form. For bioadhesive microspheres, with bioadhesive coating, the rate of the drug release decreased. With an increase in polymer concentration, the adhesive property of the microspheres is also increased. These studies suggest that the spherical matrix can interact with mucosubstrate on the surface of the stomach, leading to prolonged stay in the stomach (Umamaheswari et al. 2002).

In 2003, Umamaheshwari and co-workers prepared cellulose acetate butyrate (CAB)-coated cholestyramine microcapsules as intragastric floating drug delivery system endowed with floating ability due to the carbon dioxide generation when exposed to the gastric fluid and with mucoadhesive property. Ion-exchange resin particles could be loaded with bicarbonate followed by AHA and coated with CAB by emulsion solvent evaporation method. According to the report, the drug release rate was higher in simulated gastric fluid than in simulated intestinal fluid. Cholestyramine microcapsules were distributed throughout the stomach that exhibited prolonged gastric residence via mucoadhesion. These results suggested that CAB-coated microcapsules could be a floating as well as a mucoadhesive drug delivery system. Thus, it can be a promising treatment for *H. pylori* infections (Umamaheshwari et al. 2003). Later, the researchers showed a receptor-mediated targeting of lipobeads, bearing AHA for eradication of *H. pylori*. The final formation of lipobeads was accomplished by combining acylated PVA beads with a phosphatidyl ethanolamine (PE) liposome suspension. In this study, pretreatment of *H. pylori* with lipobeads was found to completely inhibit the adhesion of *H. pylori* to both human stomach cells and in KATO-III cells. These assays could serve as in vitro models for the study of binding efficacy of lipobeads with *H. pylori* surface receptors. This proposed site-specific drug delivery system targets the *H. pylori* more effectively and could serve to optimize antibiotic monotherapy of *H. pylori* based infections (Umamaheshwari and Jain 2004).

In 2007, Rajinikanth and Mishra used gellan gum as a matrix polymer for the preparation of AHA beads in the formulation. This gum is a bacterial anionic deacetylated polysaccharide secreted by *Pseudomonas elodea* and it has characteristic property of temperature-dependent and cation-induced gelation. So, these authors developed an anti-*H. pylori* agent (anti-urease), AHA-loaded gellan floating beads coated with chitosan, for stomach-specific drug delivery by the ionotropic gellation method. The chitosan coating increased encapsulation efficiency of the beads and reduced the initial burst release of the drug from the beads. The prepared gellan beads of AHA floated in simulated gastric fluid for a prolonged period of time and sustained drug release from the beads over a period of at least 8 h. In vivo results indicated that the prepared floating beads of AHA remained buoyant for at least 6 h in rabbit's stomach and that they had good floatability. With these results, the gellan-based floating beads containing AHA have a promising potential for delivering AHA at the stomach site (Rajinikanth and Mishra 2007).

5 Conclusion

In conclusion, the article emphasizes the need for the development of new drugs for the treatment of *H. pylori* infections, to minimize the side effects of the triple therapy and overcoming the resistance against the bacterium. The chapter describes the search for HA derivatives that can be further developed for *H. pylori* infection treatment, since there is no HA drugs commercially available for this propose so far. The chapter also presents some new technologies in drug delivery systems for the acetohydroxamic acid, the only HA used clinically for the treatment of urinary tract infections. Among them, the floating-bioadhesive microspheres appear to be the most interesting, as in them the floating microspheres can be distributed widely throughout the stomach and may provide long lasting and more reliable release of drugs.

References

Abou-Sier AH, Essawi MYH, Khalifa M et al (1995) Synthesis and bacterial urease inhibition activity of 3,4,5-trihydroxy/methoxybenzohydroxamic acid and related derivatives. Bull Fac Pharm Cairo Univ 33:19–23

Ahmed N, Sechi LA (2005) *Helicobacter pylori* and gastroduodenal pathology: new threats of the old friend. Ann Clin Microbiol 4:1–10

Amtul Z, Atta-ur-Rahman Siddiqui RA et al (2002) Chemistry and mechanism of urease inhibition. Curr Med Chem 9:1323–1348

Arnold M, Brown DA, Deeg O et al (1998) Hydroxamate-bridged dinuclear nickel complexes as models for urease inhibition. Inorg Chem 37:2920–2925

Barros TG, Williamson JS, Antunes OAC et al (2009) Hydroxamic acids designed as inhibitors of urease. Lett Drug Des Discov 6:182–192

Benini S, Rypniewski WR, Wilson KS et al (2000) The complex of *Bacillus pasteurii* urease with acetohydroxamate anion from X-ray data at 1.55 Å resolution. J Biol Inorg Chem 5:110–118

Blakeley RL, Hinds JA, Kunze HE et al (1969) Jack bean urease (EC3.5.1.5). Demonstration of a carbamoyl transfer reaction and inhibition by hydroxamic acids. Biochemistry 8:1991–2000

Brown DA, Glass WK, Fitzpatrick NJ et al (2004) Structural variations in dinuclear model hydrolases and hydroxamate inhibitor models: synthetic, spectroscopic and structural studies. Inorg Chim Acta 357:1411–1436

Brown DA, Glass WK, Fitzpatrick NJ et al (2005) Mononuclear and dinuclear model hydrolases of nickel and cobalt. Inorg Chim Acta 358:2755–2762

Chaston TB, Richardson DR (2003) Iron chelators for the treatment of iron overload disease: Relationship between structure, redox activity, and toxicity. Am J Hematol 73:200–210

Chuah S-K, Tsay F-W, Hsu P-I et al (2011) A new look at anti-*Helicobacter pylori* therapy. World J Gastroenterol 17(35):3971–3975

Codd R (2008) Traversing the coordination chemistry and chemical biology of hydroxamic acids. Coord Chem Rev 252:1387–1408

Chey WD, Wong BC (2007) American college of gastroenterology guideline on the management of *Helicobacter pylori* infection. Am J Gastroenterol 102:1808–1825

Chiyoda T, Iida K, Takatori K et al (1998) Screening system for urease inhibitors using ^{13}C-NMR. Chem Pharm Bull 46:718–720

De Francesco V, Ierardi E, Hassan C et al (2012) *Helicobacter pylori* therapy: present and future. World J Gastrointest Pharmacol Ther 3(4):68–73

Dixon NE, Hinds JA, Fihelly AK et al (1980) Jack bean urease (EC 3.5.1.5). IV. The molecular size and the mechanism of inhibition by hydroxamic acids. Spectrophotometric titration of enzymes with reversible inhibitors. Can J Biochem 58:1323–1334

Domb, AJ, Langer RS, Cravalho EG et al (1988) Preparation and uses of hydroxamic acid polymers from primary amide polymers. WO 8806602 A1 19880907

Dunn BE, Cohen H, Blaser MJ (1997) *Helicobacter pylori*. Clin Microbiol Rev 10:720–741

Eisai Co. Ltd. (1978) Novel hydroxamic acid derivatives and medicaments for treatment of urolithiasis and pyelonephrosis comprising such derivatives. US4083996

Fishbein WN, Carbone PP (1965) Urease catalysis: II. Inhibition of the enzyme by hydroxyurea, hydroxylamine, and acetohydroxamic acid. J Biol Chem 240:2407–2414

Gisbert JP, Calvet X (2012) Update on non-bismuth quadruple (concomitant) therapy for eradication of *Helicobacter pylori*. Clin Exp Gastroenterol 5:23–34

Gisbert JP, Calvet X, O'Connor A et al (2010) Sequential therapy for *Helicobacter pylori* eradication: a critical review. J Clin Gastroenterol 44:313–325

Griffith DP, Gibson JR, Clinton CW et al (1978) Acetohydroxamic acid: clinical studies of a urease inhibitor in patients with staghorn renal calculi. J Urol 119:9–15

Griffith DP, Musher DM (1975) Acetohydroxamic acid. Potential use in urinary infection caused by urea-splitting bacteria. Urology 5:299–302

Ha N-C, Oh S-T, Sung J-Y et al (2001) Supramolecular assembly and acid resistance of *Helicobacter pylori* urease. Nat Struct Biol 8:505–509

Huang X-S, Liu K, Yin Y et al (2011) The synthesis, structure and activity evaluation of secnidazole derivatives as *Helicobacter pylori* urease inhibitors. Curr Bioact Compd 7:268–280

Ito H, Myazaki T, Nakamura T et al (1994) Preparation of hydroxamic acid derivatives of hexoses as urease inhibitors. JP 06256375 A 19940913

Jabri E, Carr MB, Hausinger RP et al (1995) The crystal structure of urease from *Klebsiella aerogenes*. Science 268:998–1004

Jedner SB, Schwoppe H, Nimir H et al (2002) Ni(II) complexes as models for inhibited urease. Inorg Chim Acta 340:181–186

Johnson RN, Andersen JA (1972) Urease inhibiting benzamidoacetohydroxamic acids. Ger Offen DE 2223857 A 19721207

Kawashima Y, Niwa T, Jakouchi H et al (1991) Preparation of multiple unit hollow microspheres (microballons) with acrylic resin containing tranilast and their drug release characteristics (in vitro) and floating behavior (in vivo). J Controlled Release 16:279–290

Kobashi K (1992) Urease activity of *Helicobacter pylori*. J Clin Pathol 45:367–368

Kobashi K, Hase J, Komai T (1966) Evidence for the formation of an inactive urease-hydroxamic acid complex. Biochem Biophys Res Commun 23:34–38

Kobashi K, Hase J, Uehaka K (1962) Specific inhibition of urease by hydroxamic acids. Biochim Biophys Acta 65:380–383

Kobashi K, Kumaki K, Hase J (1971) Effect of acyl residues of hydroxamic acids on urease inhibition. Biochim Biophys Acta 227:429–441

Kobashi K, Shimizu T (1977) Inhibitor urease. JP 52117485 A 19771001

Kosikowska P, Berlicki L (2011) Urease inhibitors as potential drugs for gastric and urinary tract infections: a patent review. Exp Opin Ther 21:945–957

Kumaki K, Tomioka K, Kobashi K et al (1972) Structure-activity correlations between hydroxamic acids and their inhibitory powers on urease activity. I. Quantitative approach to the effect of hydrophobic character of acyl residue. Chem Pharm Bull 20:1599–1606

Leung D, Abbenante G, Fairlie DP (2000) Protease inhibitors: current status and future prospects. J Med Chem 43:305–341

Malfertheiner P, Megraud F, O'Morain C et al (2006) The European Helicobacter study group (EHSG). Current concepts in the management of *Helicobacter pylori* infection: the Maastricht III Consensus report. Gut 56(6):772–781

Manunza B, Deiana S, Pintore M et al (1997) A molecular modeling study of the urease active site. J Mol Struct Theochem 419:33–36

Marshall BJ, Warren RM (1984) Unidentified curved bacilli in the stomach of patients with gastritis and peptic ulceration. Lancet 16:1311–1315

McLoughlin R, Racz I, Buckley M et al (2004) Therapy of *Helicobacter pylori*. Helicobacter 9(Suppl. 1):42–48

Mégraud F, Doermann HP (1998) Clinical relevance of resistant strains of *Helicobacter pylori*: a review of current data. Gut 43(suppl 1):S61–S65

Mishra H, Parrill A, Williamson JS (2002) Three-dimensional quantitative structure-activity relationship: comparative molecular field analysis of dipeptide hydroxamic acid as *Helicobacter pylori* urease inhibitors. Antimicrob Agents Chemother 46:2613–2618

Moayyedi P (2007) Sequential regimens for *Helicobacter pylori* eradication. Lancet 370(9592):1010–1012

Mobley HLT (1996) The role of *Helicobacter pylori* urease in the pathogenesis of gastritis and peptic ulceration. Aliment Pharmacol Ther 10:57–64

Mobley HLT, Hausinger RP (1989) Microbial ureases: significance regulation and molecular characterization. Microbiol Rev 53:85–108

Mobley HLT, Island MD, Hausinger RP (1995) Molecular biology of microbial ureases. Microbiol Rev 59:451–480

Munakata K, Tanaka S, Toyoshima S (1980) Theraphy for urolithiasis with hydroxamic acids. I. Synthesis of new N-(aroyl)glycino hydroxamic acid derivatives and related compounds. Chem Pharm Bull 28:2045–2051

Muri EMF, Nieto MJ, Sindelar RD et al (2002) Hydroxamic acids as pharmacological agents. Curr Med Chem 9:1631–1653

Muri EMF, Mishra H, Avery MA et al (2003) Design and synthesis of heterocyclic hydroxamic acid derivatives as inhibitors of *Helicobacter pylori* urease. Synth Commun 33:1977–1995

Muri EMF, Mishra H, Stein SM et al (2004a) Molecular modeling, synthesis and biological evaluation of heterocyclic hydroxamic acids designed as *Helicobacter Pylori* urease inhibitors. Lett Drug Des Discov 1:1–51

Muri EMF, Nieto MJ, Williamson JS (2004b) Hydroxamic acids as pharmacological agents: an update. Med Chem Rev Online 1:385–394

Nallasamy V, Ramanathan S (2012) Role of novel drug delivery systems in stomach specific anti-*Helicobacter Pylori* therapy. J Pharm Res 5(2):1165–1168

Nujumi AMEl, Dorrian CA, Chittajallu RS et al (1991) Effect of inhibition of *Helicobacter pylori* urease activity by acetohydroxamic acid on serum gastrin in duodenal ulcer subjects. Gut 31:866–870

Odake S, Morikawa T, Tsuchiya M et al (1994) Inhibition of *Helicobacter pylori* urease activity by hydroxamic acid derivatives. Biol Pharm Bull 17:1329–1332

Odake S, Nakahashi K, Morikawa T et al (1992) Inhibition of urease activity by dipeptidyl hydroxamic acids. Chem Pharm Bull 40:2764–2768

Pahwa R, Neeta Bhagwan S et al (2010) Floating microspheres: an innovative approach for gastric retention. Der Pharm Lettre 2(4):461–475

Park JB, Imamura L, Kobashi K, Itoh H, Miyazaki T, Horisaki T (1995) Inhibitory effect of beta-glucosyl-phenolic hydroxamic acid against urease in the presence of microfloral beta-glucosidase. Biol Pharm Bull 18:208–213

Puerta DT, Cohen SM (2002) Elucidating drug-metalloprotein interactions with Tris(pyrazolyl)borate model complexes. Inorg Chem 41:5075–5082

Rajinikanth PS, Mishra B (2007) Preparation and in vitro characterization of gellan based floating beads of acetohydroxamic acid for eradication of H. pylori. Acta Pharm 57:413–427

Ramadan MA, Megahed SA (1994) In vitro inhibition of bacterial urease by hydroxamic and non-hydroxamic acid and related compounds. Al-Azhar J Microbiol 26:93–98

Rimbara E, Fischbach LA, Graham DY (2011) Optimal therapy for *Helicobacter pylori* infections. Nat Rev Gastroenterol Hepatol 8(2):79–88

Satoh M, Munakata K, Takeuchi H, Yoshida O, Takebe S, Kobashi K (1991) Evaluation of effects of novel urease inhibitor, N-(pivaloyl)glycinohydroxamic acid on the formation of an infection bladder stone using a newly designed urolithiasis model in rats. Chem Pharm Bull 39:894–896

Stemmler AJ, Kampf JW, Kirk ML et al (1995) A model for the inhibition of urease by hydroxamates. J Am Chem Soc 117:6368–6369

Tsukamoto K, Itakura H, Sato K et al (1999) Binding of salicylhydroxamic acid and several aromatic donor molecules to *Arthromyces ramosus* peroxidase, investigated by X-ray crystallography, optical difference spectroscopy, NMR relaxation, molecular dynamics, and kinetics. Biochemistry 38:12558–12568

Umamaheswari RB, Jain S, Tripathi PK et al (2002) Floating-bioadhesive microspheres containing acetohydroxamic acid for clearance of *Helicobacter Pylori*. Drug Delivery 9:223–231

Umamaheshwari RB, Jain S, Jain NK (2003) A new approach in gastroretentive drug delivery system using cholestyramine. Drug Delivery 10:151–160

Umamaheshwari RB, Jain NK (2004) Receptor-mediated targeting of lipobeads bearing acetohydroxamic acid for eradication of *Helicobacter pylori*. J Controlled Release 99:27–40

Wedekind JE, Poyner RR, Reed GH et al (1994) Chelation of serine 39 to Mg2+ latches a gate at the active site of enolase: structure of the bis(Mg2+) complex of yeast enolase and the intermediate analog phosphonoacetohydroxamate at 2.1-A resolution. Biochemistry 33:9333–9342

Zahee-ul-Haq Z, Wood A, Uddin R (2009) CoMFA and CoMSIA 3D-QSAR analysis on hydroxamic acid derivatives as urease inhibitors. J Enzyme Inhib Med Chem 24:272–278

Zhang E, Hatada M, Brewer JM et al (1994) Catalytic Metal Ion Binding in Enolase: The Crystal Structure of Enolase-Mn2+-Phosphonoacetohydroxamate Complex at 2.4 Å Resolution. Biochemistry 33:6295–6300

Therapeutic Potential of Hydroxamic Acids for Microbial Diseases

Giseli Capaci Rodrigues, Flavia Alexandra Gomes de Souza, Whei Oh Lin and Alane Beatriz Vermelho

Abstract Hydroxamic acid derivatives have recently been recommended for therapeutic treatment of several diseases, such as hypertension, cancer, as well as inflammations and infectious diseases due to their ability to chelate metals, especially in metalloenzymes. This chapter will focus on the role of metallopeptidases and their homologs in microbial diseases and the potential use of hydroxamates and their derivates for the treatment and control of such diseases. A general overview of the structure, synthesis, and inhibition mechanisms of hydroxamates as well as their potential use, including the advantages and relative problems, for medicinal chemistry will be discussed.

Keywords Hydroxamic acid · Metalloenzyme inhibitors · Zinc metalloproteinases · LpxC inhibitors · HDAC inhibitors

Abbreviations

AAT	Aminoglycoside acetyltransferases
AIDS	Acquired immunodeficiency syndrome
ANTs	Aminoglycoside nucleotidyltransferases
APH(3')s	Aminoglycoside 3′-phosphotransferases
BNZ	Benznidazole
cART	Combination antiretroviral therapy

G. C. Rodrigues · A. B. Vermelho
Department of General Microbiology, Institute of Microbiology Paulo de Góes, Federal University of Rio de Janeiro, Rio de Janeiro, Brazil

G. C. Rodrigues · F. A. G. de Souza · W. O. Lin
Department of Science and Technology, Universidade do Grande Rio (UNIGRANRIO), Duque de Caxias, Rio de Janeiro, RJ, Brazil

A. B. Vermelho (✉)
Biocatalysis, Bioproducts and Bioenergy Unit, Biotechnology Center-BIOINOVAR, Federal University of Rio de Janeiro, Rio de Janeiro, Brazil
e-mail: abvermelho@micro.ufrj.br

DC	Dendritic cells
ECM	Extracellular matrix
Glu	Glutamate
HDACs	Histone deacetylases
HDACi	Histone deacetylase inhibitors
HIV	Human immunodeficiency virus
*Lma*CP1	*Leishmania major* carboxypeptidase
LpxC	UDP-3-O-(R-3-hydroxymyristol)-*N*-acetylglucosamine deacetylase
LPS	Lipopolysaccharide
MCPs	Metallocarboxypeptidases
MMPs	Matrix metalloproteinases
MRSA	Gram-positive methicillin-resistant *Staphylococcus aureus*
MVEC	macrovascular endothelial cells
NFX	Nifurtimox
6-PGDH	6-Phosphogluconate dehydrogenase
*Tc*MCP-*t*	*Trypanosoma cruzi* metallocarboxypeptidase-*type*
	Ex. *Trypanosoma cruzi* metallocarboxypeptidase-1
TIMPs	Tissue inhibitors of metalloproteinases
TNF-α	Tumor necrosis factor-alpha
WHO	World Health Organization
ZBG	Zinc-binding group

Contents

1 Introduction

The involvement of matrix metallopeptidases (MMPs) and their homologs in microbial disease pathogenesis has been extensively investigated in recent years. Several studies demonstrated the multiple functions of these enzymes in viral,

protozoan, and bacterial infections. These findings point to the metallopeptidases as being a potential target for the treatment and control of these infections. Many researcher groups are involved in the search for new therapeutic agents focused on metallopeptidases. Based on such works, the hydroxamic acids and their derivatives have been highlighted as a new, effective class of compounds for the inhibition of the metallopeptidases (Hoekstra et al. 2001; Hou et al. 2012; Pepeljnjak et al. 2005).

Several articles in the literature report the involvement of these peptidases with the pathogenesis of microbial diseases including those caused by viruses, protozoa, fungi, and bacteria (Lindsey and Zamilpa 2012; Marson et al. 2012).

The dengue virus has been shown to infect dendritic cells (DC) and macrovascular endothelial cells (MVEC) with different effects. In dendritic cells, the infection increases the MMP-9 production triggering vascular leakage. In MVEC, the virus infection causes an overproduction of MMP-2 leading to an enhanced endothelial permeability (Luplertlop and Missé 2008).

Metallopeptidases have been described in a number of parasites. An increased production of tumor necrosis factor-alpha (TNF-α) by monocytes, macrophages, or lymphocytes is involved in symptoms of severe malaria such as hypoglycemia, hyperthermia and neurological manifestations, dyserythropoiesis, and immunodepression. Phagocytosed hemozoin (malarial pigment) stimulated the production of TNF-α and other proinflammatory cytokines in human monocytes and displayed increased gelatinaseB (MMP-9) activity showing higher matrix invasion ability (Prato et al. 2011). Studies using a mouse model for study of the *Plasmodium berghei* ANKA cerebral malaria infection showed an increase of MMP-9 expression in positive cells and CD11b^{+}cells in the brain (Van den Steen et al. 2006).

Toxoplasma gondii, an obligate intracellular protozoan that can be found worldwide, is the etiologic agent of toxoplasmosis, a zoonotic infection of humans and animals. Following oral infection, *T. gondii* crosses the intestinal epithelium, disseminates into the deep tissues and crosses many biological barriers such as the blood–brain barrier and placenta. However, the molecular mechanisms involved in migration of *T. gondii* remain poorly characterized. The study of Buache et al. (2007) demonstrated that the *T. gondii* RH strain invasion of THP-1 cells induced a decrease in latent gelatinase A (proMMP-2) and latent gelatinase B (proMMP-9) secretion and the author postulated that *T. gondii* may mediate its effects on gelatinase expression through the modulation of the NF-κB (nuclear factor kappa-light-chain-enhancer of activated B cells) activation pathway. Toxoplasmic encephalitis is a marked astrocyte reaction to sites of inflammation and parasite replication. Using astroglia infected with the TS-4 strain of *T.gondii* tachyzoites, MMP-2, and MMP-9 increased significantly until 12 h post-infection in the cell homogenates, and they increased until 48 h post-infection in the cell-cultured supernatants. The author suggested that MMP-2 and MMP-9 cleave fibronectin and may contribute to the astroglial reaction and leukocyte migration to the sites of *T. gondii* replication during toxoplasmic encephalitis (Lu and Lai 2012).

In *Trypanosoma cruzi*, metallopeptidases, belonging to the MMP-9 family, were revealed after Western blotting as an 85 kDa polypeptide in both cellular and secreted parasite extracts. The surface location of homologs of MMP-9 in *T. cruzi* was also evidenced by means of flow cytometry analysis (Nogueira de Melo et al. 2010). Furthermore, in hepatocyte culture infected with *T. cruzi*, the active (85 kDa) and latent (100 kDa) forms of MMP-9 were detected using Western blotting and immunocytochemistry. MMP-9-like activity was detected in the cytoplasm of *T. cruzi* during in vitro infection of hepatocyte cells (Nogueira de Melo et al. 2010). Gutierrez et al. (2008) suggested an important role for MMPs in the induction of *T. cruzi*-induced acute myocarditis, since mice treated with an MMP inhibitor showed a significant decrease in heart inflammation, delayed peak in parasitemia, and improved survival rates compared with the control group.

On the other hand, studies have suggested a great important role for gp63 (63-kDa glycoprotein) in the pathogenesis of leishmaniasis. gp63 is a zinc-dependent metalloprotease found on the surface of the parasite whose expression enhances capacity of the parasite migration through extracellular matrix (McGwire et al. 2003). Other studies demonstrated the presence of metallopeptidases during the leishmanicidal activity in infected macrophages (Costa et al. 2008). An increase in TGF-β production in *Leishmania chagasi*-hepatocyte-macrophage co-culture supernatants was observed during the highest leishmanicidal activity by macrophages, coinciding with higher MMP-9 activity. The high levels of TGF-β can be related to the synthesis of metallopeptidases and the conversion of the latent form to the active form (Costa et al. 2008).

MMPs have also been studied in bacteria. In group A *streptococcus* (GAS), *Streptococcus pyogenes* causes a wide range of human diseases, including bacterial arthritis. Bacterial septic arthritis occurs by bacterial invasion into the joint cavities through blood circulation. Bacterial infection and IL-1 activate different signaling pathways and transcription factors involved in the expression of MMP-13. GAS infection induces MMP-13 expression in chondrocytes through the activation of the c-Jun *N*-terminal kinase (JNK) and the AP-1 transcription factor. MMP-13 plays an important role in the destruction of infected joints during the development of septic arthritis (Sakurai et al. 2008).

In keratomycosis, an experimental murine (BALB/c mice) model, the transcriptional and translational levels of MMP-8, -9, -13, and TIMP-1 increase during the early stages of *Candida albicans* keratitis indicating a possible role of these enzymes in the pathogenesis of the infection (Yuan et al. 2009).

The role of the metallopeptidases in the microbial infections cited above is an example of the participation of this class of peptidase in the pathogenesis process of microorganisms. This chapter discusses the current understanding of the role of metallopeptidases in microbial diseases and their inhibition by hydroxamates and derivates. The following section will be discussed in more detail about this potential target of hydroxamic acids.

2 Metalloenzymes

2.1 Peptidases

Peptidases are hydrolases that hydrolyze peptide bonds in proteins and peptides. They are classified using three criteria: the chemical mechanism of catalysis, the catalytic reaction and, the molecular structure and homology. The former classification is based on the presence of catalytic amino acids, any metal ion or any unknown catalytic thing at their active site. The amino acid may be Aspartic acid (A), Cysteine (C), Glutamic acid (G), Asparagine (N), Serine (S), and Threonine (T). The catalytic reaction depends on the selectivity for the bonds that the peptidases will hydrolyze. The molecular structure and homology is the next approach. The amino acid sequences and three-dimensional structures of the peptidases are analyzed and compared in order to classify and evaluate relationships. The MEROPS database integrated the three systems of peptidase classification and grouped them into protein species, which are in turn grouped into families, and then into clans (release 9.8). Metallopeptidases are currently grouped in 67 families in the MEROPS database (Rawlings et al. 2012).

2.2 Metallopeptidases: Endopeptidases

Metallopeptidases are produced by all species of plants, animals, and microorganisms. In mammals they are called matrix metallopeptidases (Rawlings et al. 2012). Based on the work of Schechter and Berger (1967), Gomis-Rüth et al. (2012) suggested a "standard orientation" for the overall description of MMPs as shown in Fig. 1. In the interaction mode, the active site of the enzyme have subsites named S1, S2, S3, etc., interacting with the side chains of the residues flanking the scissile bond. The substrate side chains on the non-primed side away from the scissile bond are termed P1, P2, P3, and their cognate enzyme subsites (S1, S2, S3) (Gomis-Rüth et al. 2012).

Metallopeptidases contain one or two metal ions in their active site. Most metallopeptidases contain Zn^{2+}, while a few contain Mg^{2+}, Ni^{2+}, or Cu^{2+}. The role of the catalytic metal ions in metallopeptidases is to activate a water molecule, which serves as a nucleophile in catalysis. Many metallopeptidase inhibitors developed against these enzymes included pseudopeptides, mimicking their substrates, as well as small molecules that bind with the catalytic zinc ion. Small non-peptidic molecules are mostly hydroxamate derivatives (Whittaker et al. 1999).

Some metallopeptidases function within the cell or on the membrane (Wu and Chen 2011). Other bacterial metallopeptidases are secreted to the periplasm or outside the cell and are called extracellular metallopeptidases. Microorganisms secrete peptidases in order to degrade environmental proteins for nutrition. However, in recent years due to their role in pathogenicity, metallopeptidases have
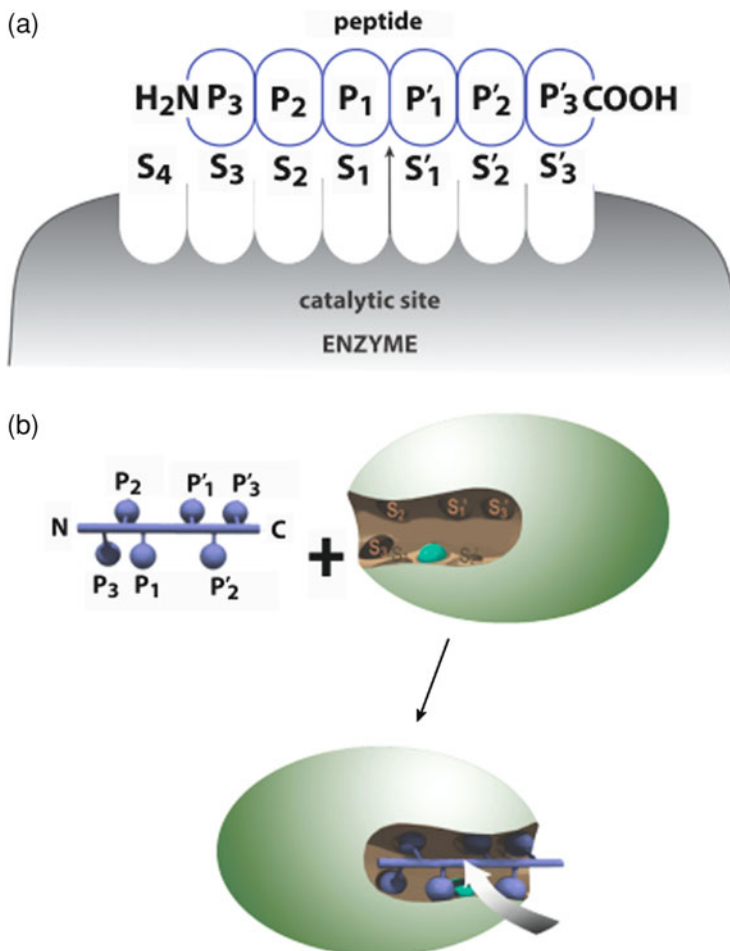
Fig. 1 a Model of enzyme-substrate interaction according to Schechter and Berger nomenclature (Schechter and Berger 1967) showing the active site of the peptidase (papain) with subsites (S) and the peptide substrate (P). **b** Three-dimensional model of a metallopeptidase. The metal ion in the active site is shown by *green* and the *arrow* points to the cleavage point. Diagram based on Gomis-Rüth et al. (2012)

been exploited as a target for drug development (Klemba and Goldberg 2002; McKerrow et al. 2008, Vermelho et al. 2010; Wu and Chen 2011).

An important subset of MMPs comprises a short zinc-binding consensus sequence, HEXXH—first reported by McKerrow et al. (1987) which includes two metal-binding histidines and the general-base/acid glutamate for catalysis. The most studied metallopeptidases are the MMPs or matrixins. MMPs represent an important family of metal-dependent endopeptidases that are responsible for the degradation of extracellular matrix (ECM) components. These enzymes can degrade all of the components of the extracellular matrix, including fibrillar and

Fig. 2 MMPs groups
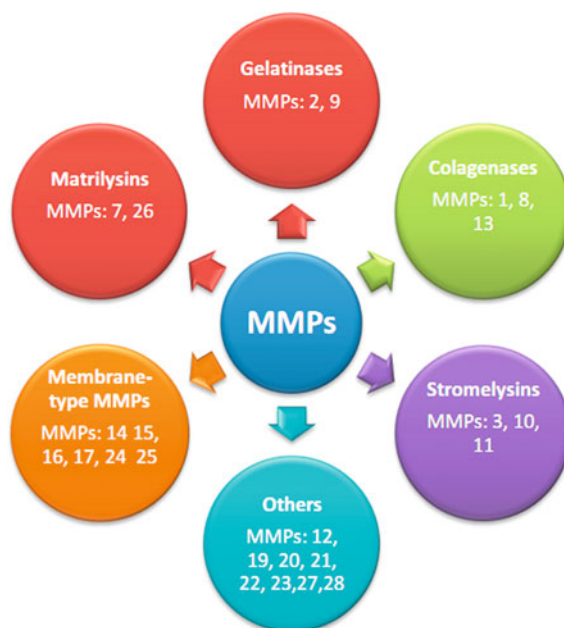
non-fibrillar collagens, fibronectin, laminin, and basement membrane glycoproteins. Since the discovery of MMPs in 1962 (Gross and Lapiere 1962), the MMP family has grown to include six groups (Fig. 2) and at least 28 members. Table 1 shows the members of each group.

MMPs are secreted in a latent, proenzyme form and require activation by a proteolytic cleavage of a propeptide domain at the *N*-terminus of the MMP molecule (Wojtowicz-Praga et al. 1997). They are regulated at multiple levels including gene transcription and by oxidative stress (Castro et al. 2009). Under physiological conditions the proteins are selectively regulated by inhibitors called tissue inhibitors of metalloproteinases (TIMPS) (Murphy 2011). MMP activity has been related to a number of important diseases such as rheumatoid arthritis, osteoarthritis, abdominal aortic aneurysm, acute myocardial infarction, end-stage kidney disease, and cancer. Although MMPs are crucial for a normal inflammatory response, uncontrolled activity of these enzymes after infection could lead to tissue damage, microbial dissemination, and immunopathology in the host that might lead to death. Besides inducing MMP secretion by host cells, pathogens themselves may also produce MMPs which are required for virulence (Geurts 2012; Vargová et al. 2012).

2.3 Metallocarboxypeptidases: Exopeptidases

Another class of metallopeptidases includes the metallocarboxypeptidases (MCPs). They are exopeptidases that catalyze the hydrolysis of peptide bonds at

Table 1 Members of MMPs

MMPs	Enzyme
MMP-2	Gelatinase A
MMP-9	Gelatinase B
MMP–3	Stromelysin–1
MMP-10	(Progelatinase)
MMP-11	Stromelysin–2
	Stromelysin–3
MMP-1	Collagenase–1
MMP-8	Neutrophil collagenase;
MMP-13	Collagenase–3
MMP-7	Matrilysin–1
MMP-26	Matrilysin–2
MMP-14	MT1–MMP
MMP-15	MT2–MMP
MMP-16	MT3–MMP
Mmp-24	MT5–MMP
MMP-25	MT6–MMP
MMP-12	Macrophage elastase
MMP-19	RASI–1
MMP-20	Enamelysin
MMP-21	XMMP (Xenopus)/Cy–MMP
MMP-22	Femalysin
MMP-23	CA–MMP
MMP-27	CMMP (Gallus)
MMP-28	Epilysin

the C-terminus of peptides and proteins. These enzymes possess a tightly bound Zn^{2+} ion directly involved in catalysis (Vendrell et al. 2000). The most studied MCPs are those that belong to the family M14 which contains four subfamilies. The M14 family includes enzymes which participate in diverse processes such as blood coagulation and fibrinolysis, inflammation, innate immunity response, food digestion and pro-hormone, and neuropeptide processing. The family M32 with the *carboxypeptidase Taq* (*Thermus aquaticus*) as the enzyme type has also been subject of study. This group contains two zinc-binding histidines and a catalytic glutamate in an HEXXH zinc-binding motif. The peptidases and homologs of this family include peptidases from trypanosomatids, such as the *Tc*MCP1 and *Tc*MCP2 (*T. cruzi* carboxypeptidase 1 and 2) and *Leishmania major* carboxypeptidase 1 (*Lma*CP1), and recently a M32 metallocarboxypeptidase of *Trypanosoma brucei* was described (Frasch et al. 2012). Peptidase members of M32 family have been detected in several bacteria, archaea, plants, and animals.

The following section describes the recent studies on structure–activity relationship, synthesis, inhibition mechanisms, and clinical trials of hydroxamic acids developed against microbial diseases.

3 Hydroxamic Acids

Hydroxamic acids were discovered by Lossen more than 100 years ago. Since then these acids have been extensively studied due to their multiple uses. Hydroxamic acid derivatives have shown numerous applications from insecticides to the treatment of many diseases, such as cancer, cardiovascular diseases, HIV, Alzheimer's, malaria, allergic diseases, tuberculosis, and antimicrobials. It is mainly because of their ability to coordinate with metal ions in metal-containing enzymes such as metalloproteins, urease, MMPs, carbonic anhydrase, and many others (Codd 2008; Muri et al. 2002).

The most frequent and economical methodology employed to obtain hydroxamic acids (**1**, Fig. 3) is from the reaction between a carboxylic acid derivative and hydroxylamine. Usually the carboxylic acid is converted to the ester and sequentially undergoes a reaction with the hydroxylamine (Codd 2008).

Other methodologies for the synthesis of hydroxamic acids have been reported that include the use of carboxylic acids and *N*-protected amino acids with cyanuric chloride (Giacomelli 2003) and the treatment of *N*-acyloxazolidinones with hydroxylamines using samarium triflate as a Lewis acid (Sibi 2002). In addition, the solid-phase synthesis of hydroxamic acids has been widely described which is becoming an important method for obtaining this acid (Floyd 1996; Grigg 1999; Nandurkar 2011; Zhai 2012).

An important strategy for the design of these drugs is predicting how they will reach their site of action in a concentration which produces a pharmacological effect. Their absorption through a membrane into solution in the blood is affected by physical–chemical factors. For drugs which are weak acids or bases, their dissociation constant (pKa) and the pH of the gastrointestinal tract fluid and blood stream will control their solubility. Ionized drugs will not be able to get through the lipid membrane. However, they can do so in the non-ionized form when they have increased lipid solubility (Fazary 2005).

Hydroxamic acids are basically acids but also behave as weak bases because of the NC=O moiety. In aqueous solvents, they have their pKa values in the range of 8.5–9.4. Studies have shown that their dissociation constant is a function of temperature, and usually, it has a minimum pKa value near room temperature, which it could be decreased as the temperature is raised (Fazary 2005). In addition, their acidity has received particular attention since two structures of the anion are possible. This equilibrium depends on both the structure of the hydroxamic acid and the reaction conditions. *N*-deprotonation yields the hydroxamate anion (**3**, Fig. 4) and it could be generated in the gas phase. In non-protic solvents, it is strengthened by an electron attracting substituent. In this case, the generated anion

Fig. 3 Conventional synthesis of hydroxamic acids
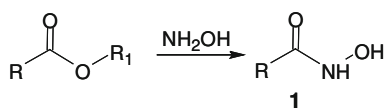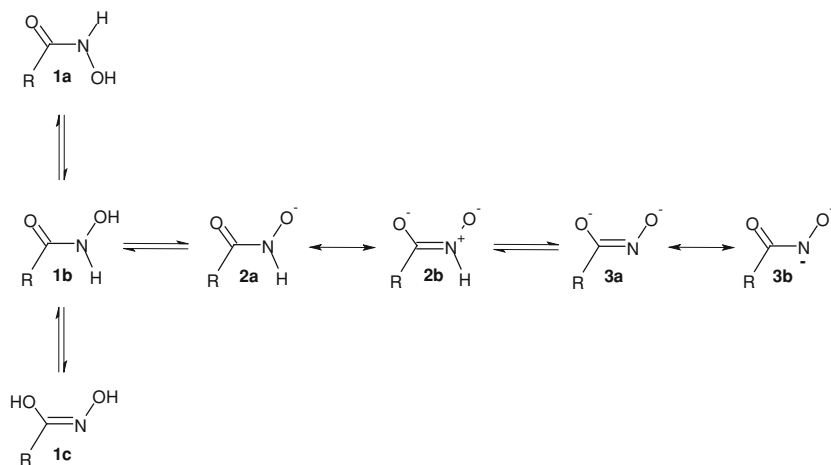
Fig. 4 Structures of hydroxamic acids (**1**), hydroxamates (**2**) and hydroximates (**3**) (based on Codd 2008)

may be stabilized by resonance. In water, the *O*-deprotonation yields the hydroxamate anion (**2**, Fig. 4) and it may be found in a comparable amount or even prevailing. Nevertheless, some studies have suggested that the acidity of hydroxamic acids is due to the destabilizing inductive effect of the hydroxyl group in the acid molecule and not due to any effect of the anion (Böhma 2003). The proven anions have some resonance contributing structures. On the other hand, hydroxamic acids may also be present in the tautomeric form (Fig. 41b, c).

In addition, in consequent to the free rotation about the C–N bond, hydroxamic acid and, the hydroxamate and hydroxamate groups can exhibit cis/trans (or Z, E) isomerism (Fig. 41a, b). Among other factors, the preferential configuration could be related to the steric effects of the N- and C-substituents since studies have shown that for *N*-methyl-substituted hydroxamic acids, the Z/E ratio increases with the bulk of the C-substituent in DMSO-*d*6, CDCl$_3$, or C$_6$D$_6$.

However, for the metal ion coordination, a change to the cis-geometry must occur. Studies have shown that increasing the negative charge on the coordinating oxygen atom with the electron donation to C or N atoms form more stable metal-hydroxamato/imato complexes. The coordination compounds of hydroxamic acids have been intensively studied (Riedel and Kaupp 2009). This is because negatively charged species, such as hydroxamates (Fig. 42a, 3a), act as good ligands with positively charged metal ions present in metalloenzymes (Goyer 2004).

The hydroxamic acids are one of the most important families of organic bi-oligands, as they constitute as one of the major classes of naturally occurring metal complexing agents and have been thoroughly studied as ligands. Complexes of metals or metalloids with hydroxamic acids are spread widely throughout and are well characterized by X-ray crystallography (Farkas et al. 2000).

The formation of complex of the hydroxamate group with metals can occur in different ways but the most common mode of binding is bidentate coordination. Coordination is through the deprotonated hydroxamate oxygen and carbonyl oxygen forming a very stable five-membered ring. Monodentate binding through the deprotonated nitrogen or oxygen atoms have also been reported but this requires specially designed coordination environments to provide additional stabilization (Farkas et al. 2000).

The formation of simple complexes with primary hydroxamic acid ligands in aqueous solution depends on the pH. The hydroxamato (charge -1) type mode arises from the first deprotonation step and involves the coordination of the NHO$^-$ moiety (**4**, Fig. 5). The hydroximato form (charge -2) of the ligand is produced by further metal-induced deprotonation of NHO$^-$ (**5**, Fig. 5) (Farkas et al. 2000).

Mononuclear homoleptic complexes with bidentate *O,O*-hydroxamato/imato coordination from monohydroxamic acids have been characterized with Fe(III), Cr(III), Co(III), Ga(III), In(III), Si(IV) or Ge(IV) (octahedral geometry), Cu(II) (square planar geometry), B(III) (tetrahedral geometry), or Hf(IV) or Th(IV) (distorted dodecahedral geometry). Mononuclear heteroleptic complexes with bidentate *O,O*-hydroxamato/imato coordination from monohydroxamic acids have been characterized with Si(IV), V(V), Co(II), Co(III), Ni(II), Zn(II), Mo(VI), Ru(III), Rh(III), Sn(IV), W(VI), Os(III), Pt(II), and U(IV) (Codd 2008).

Zinc is the second most prominent trace metal in the human body after iron. In the adult human there are 2–3 g of zinc, as compared to 4–6 g of iron and only 25 mg of copper. Zinc deficiency may cause growth defects, although unlike copper and iron, few harmful effects due to an excess of zinc have been observed. Zinc is known to have an important role in a wide range of cellular processes, including cell proliferation, reproduction, immune function, and the defense against free radicals. The biochemical functions of zinc can be classified as catalytic, structural, and regulatory. At neutral pH, all acid–base catalyzes by metal ions in biological systems are catalyzed by Zn^{2+}. At acid pH, manganese and iron adopt the role. Zn^{2+}, a d^{10} electron system, is a good Lewis acid which is unable to undergo redox reactions. In acidic media, Zn^{2+} complexes are unstable; therefore, Zn^{2+} is a good Lewis acid only under neutral or basic pH conditions. Zn^{2+} as a catalyst in metallobiomolecules is in low symmetry sites bound to amino acid side chains containing N, S, or O donor ligands. In addition, H_2O/OH^- is an excellent ligand in biological systems (Goyer 2004).

Metal has an essential role in metalloenzymes. For example, all known matrix MMPs use a zinc ion during hydrolysis of the substrate. This catalytic mechanism is described in Fig. 6. The active site zinc (II) ion is generally bound by three protein ligands and a water molecule suggestive of an open coordination site which
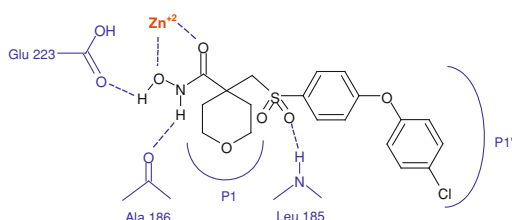
Fig. 5 Deprotonation of hydroxamic acid (based on Farkas et al. 2000)
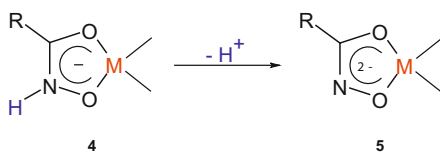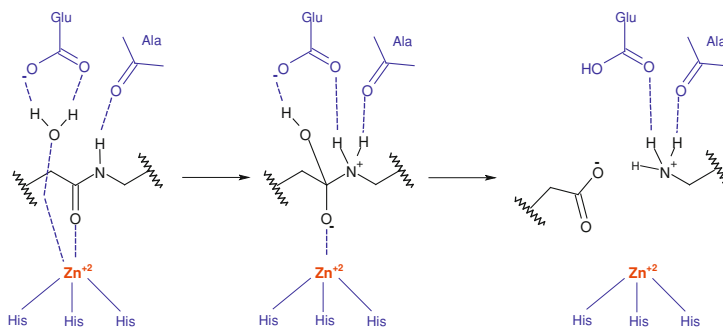
Fig. 6 Role of zinc ion in metalloproteins: reaction mechanism for MMPs (based on: Muri et al. 2002)

Fig. 7 Inhibition mechanism of hydroxamic acid derivative (RS 130830) in MMP (based on Zhang et al. 2000)

is considered essential for the function of zinc during catalysis. Thereby, the substrate amide carbonyl group also coordinates to zinc. This carbonyl group undergoes nucleophilic attack by a water molecule that are both hydrogen bonded to a conserved glutamic acid and coordinated to the zinc ion.

The water donates a proton to the active site glutamate (Glu) residue which transfers it to the nitrogen of the amide group. Transferring the proton from the Glu to the amide nitrogen is followed by the breaking of the N–C amide between Glu and the free amine of the cleaved substrate (Muri et al. 2002).

The molecular design of effective MMPs inhibitors has as a prerequisite to insert a group capable of chelating the zinc ion. The hydroxamic acid derivatives are, so far, the most extensively studied class of MMP inhibitors. This is due to the ability of the hydroxamate group to efficiently combine with the catalytic zinc ion besides its ability to form hydrogen bonds to glutamic acid and alanine residue MMPs (Fig. 7).

4 Bacterial Diseases

Bacterial resistance to multiple antibiotics is a global public health problem, especially for seriously ill, hospitalized patients. Frequently, these infections fail to respond to usual treatment and this results in prolonged illness and greater risk of

death (WHO 2012a−d). Unfortunately, while resistance to recent therapies continues to increase, there are inadequate numbers of new clinical drugs to treat these infections (Brown et al. 2012).

A strategy to combat multiresistant bacteria could be to focus on new targets involved in the biochemical processes that are essential for bacterial growth and thus develop new antibacterial agents. Highlighted among the multiresistant pathogens could be the Gram-positive methicillin-resistant *Staphylococcus aureus* (MRSA) (Gould et al. 2012) and the Gram-negative bacteria resistant to multiple antibiotics that are responsible for several difficult-to-treat infections in humans, such as *Escherichia coli* and *Pseudomonas aeruginosa* (Elhani et al. 2012).

The most frequent resistance mechanism used by bacteria is to modify their structural enzymes so that they are able to make the antibacterial agents inactive. Some families of resistant enzymes are well-known, such as those in aminoglycoside antibiotics. In this case, specifically three enzymes - aminoglycoside 3′-phosphotransferases [APH(3′)s], aminoglycoside nucleotidyltransferases (ANTs), and aminoglycoside acetyltransferases (AAT) have been extensively studied and among these, APH(3′) is most studied. Their mechanism of resistance is based on the enzyme's ability to transfer the α-phosphoryl group of ATP to the 3′-hydroxyl of aminoglycosides, such as kanamycin A (**6**, Fig. 8), thus making them inactive and clinically obsolete (**7**, Fig. 8) (Haddad et al. 1999).

Infectious diseases caused by Gram-negative bacteria are clinically relevant mainly as nosocomial pathogens. In these infections, there is an increased risk due to their endotoxin that may become a complicating factor in many serious diseases. The syndromes most frequently associated with bacterial endotoxin are systemic complications such as septicemias. Systemic infections or septicemias caused by invasive Gram-negative bacteria are a well-known effect of endotoxin exposure and *E. coli* is the most frequently isolated Gram-negative organism. Approximately 600,000 cases of septicemia are diagnosed annually in the US, leading to about 100,000 deaths per year (Shin et al. 2007).

Gram-negative bacteria septicemia results from the systemic response to infection, generally in the overexpression of cytokines and inflammatory mediators in response to macrophage activation by lipopolysaccharide (LPS). LPS, the primary component of the outer monolayer of the outer membrane of Gram-negative bacteria, and an essential protective barrier against such agents as detergents and
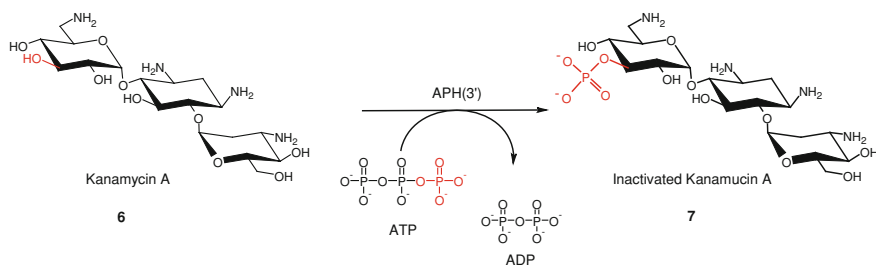
**Fig. 8** Kanamycin A inactivation by APH(3′) (based on Haddad et al. 1999)
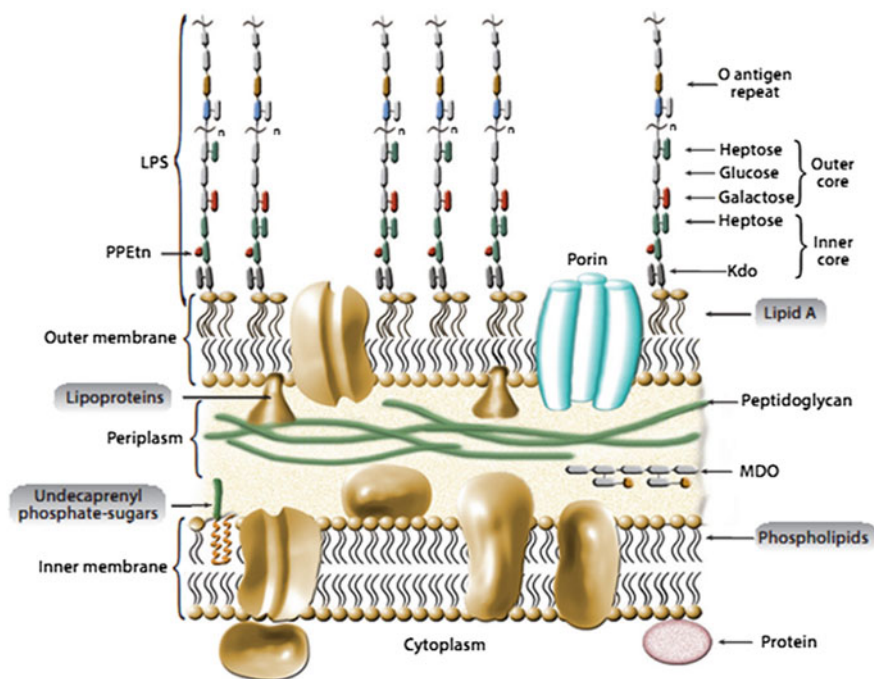
Fig. 9 Model of the inner and outer membranes of *E. coli* (based on Raetz and Whitfield 2002)

antibiotics, is anchored to a hydrophobic domain known as lipid A (Fig. 9) (Brown et al. 2012).

The hexaacylated disaccharide lipid A, also known as endotoxin, is a glucosamine-based phospholipid required for bacterial growth (Raetz and Whitfield 2002; Shin et al. 2007) and it is estimated that there are 10^6 lipid A residues and 10^7 glycerophospholipids in a single cell of *E. coli* (Raetz and Whitfield 2002). When there is a lack of lipid A, the bacteria either become not viable or increase their susceptibility to anti-bacterial agents (Brown et al. 2012).

Lipid A biosynthesis is catalyzed by nine enzymes, however, the UDP-3-O-(R-3-hydroxymyristol)-*N*-acetylglucosamine deacetylase (LpxC) has been widely studied due to the lack of homology to mammalian metalloamidases. Therefore, LpxC has been considered an attractive chemotherapy target for the treatment of the gram-negative bacteria infections. LpxC is a cytosolic zinc-metalloamidase enzyme that uses a Zn^{2+} ion as cofactor, which is essential for cell viability. This enzyme is present in all Gram-negative bacteria and plays a crucial role in the pathway leading to the construction of Lipid A (**11**, Fig. 10) which specifically participates in the first biosynthetic step (Brown et al. 2012). In this step the metal-dependent deacetylase, LpxC, hydrolyzes UDP-3-O-(R-3-hydroxymyristoyl)-*N*-acetylglucosamine (**8**, Fig. 10) to form acetate and UDP-3-O-(R-3-hydroxymyristoyl) glucosamine (**9**, Fig. 10) (Gennadios et al. 2006).
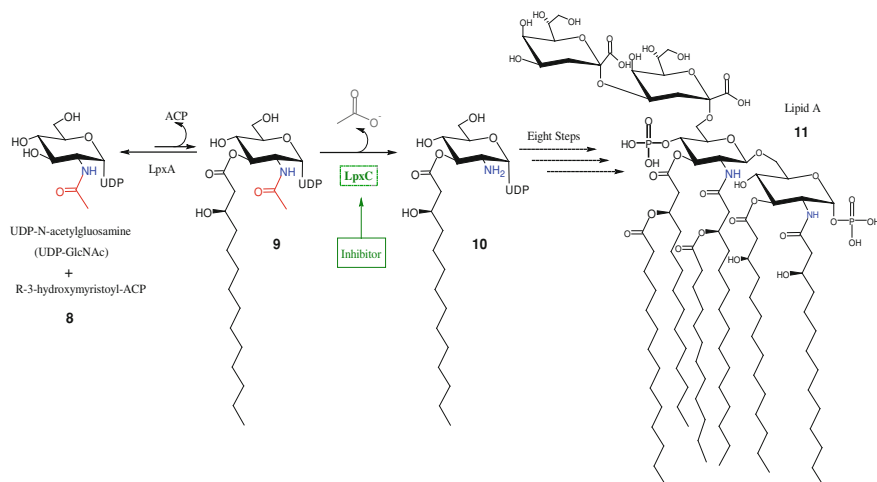
Fig. 10 Lipid A biosynthesis (based on Barb et al. 2007 and Zhang et al. 2012)

Studies have shown that the inhibition of enzymes in the lipid A biosynthetic pathway kills Gram-negative bacteria and reduces toxic lipid A concentrations shed by dying bacteria. Specific studies with LpxC have proven that the LpxC gene inactivation was able to suppress bacterial growth (Mdluli et al. 2006). Consequently, this is considered an attractive target for the development of a new class of antibiotics. Thus the research for novel chemical substances with potential inhibitory action of LpxC has been stimulated (Shin et al. 2007). Since the discovery of this enzyme target, several LpxC inhibitors have been reported, especially those focused on the hydroxamate class (Warmus et al. 2012). However, none of these inhibitors have as yet effectively advanced through clinical trials (Brown 2012).

The first hydroxamic acid-based potent LpxC inhibitor discovered was L-161,240 (**12**, Fig. 11) (Onishi et al. 1996). This compound contains an aryloxazoline moiety. Thus, the discovery of this compound opened up a new pathway in the design and development of novel aryloxazoline-based hydroxamate LpxC inhibitors. However, this oxazoline derivative does not have a broad spectrum against gram-negative bacteria; it has been found to be potent particularly against *E. coli* but weak against *Pseudomonas aeruginosa* (Warmus et al. 2012; Zhang et al. 2012).

In order to search for potent LpxC inhibitors against broad spectrum gram-negative bacteria the substrate-based hydroxamates, such as TU-517, were designed (**13**, Fig. 11). In these new structures, the hydroxamate group was introduced into the tetrahydropyran ring of the natural LpxC substrate and appended at the position analogous to the location of the *N*-acetyl group. However, these compounds, although demonstrated a considerable potency against the wild-type strain of the *E. coli* LpxC, were not able to inhibit the growth of a mutant
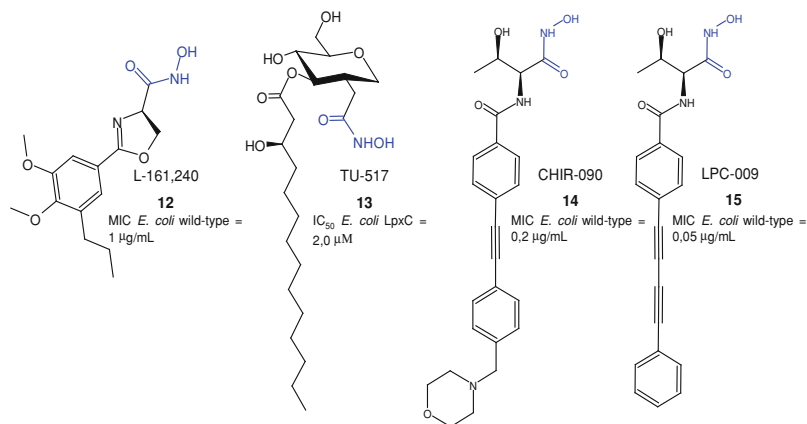
Fig. 11 LpxC inhibitors (based on Warmus et al. 2012)

strain of the *E.coli* (Jackman et al. 2000; Zhang et al. 2012). Afterward, in an attempt to obtain the effective interaction with the hydrophobic tunnel in the active site of LpxC, the CHIR-090 (**14**, Fig. 11), which is based on the diphenyl-acety-lene scaffold, was developed.

Thus CHIR-090 is the first reported compound that in fact kills both *E. coli* and *Pseudomonas aeruginosa* in bacterial disk diffusion assays (Liang et al. 2011). Nonetheless, CHIR-090 was about 600-fold less effective against LpxC orthologs from the Rhizobiaceae family than against *E. coli* LpxC. In this way, studies have shown that the removal of morpholine ring (LPC-009, **15**, Fig. 11), based on a chemical scaffold of reduced radius, was able to increase affinity by 20-fold for LpxC enzymes from the Rhizobiaceae family of bacteria and enhance the antibiotic activity against *E. coli* and *P. aeruginosa* by 2–4 fold over CHIR-090 (**14**, Fig. 11).
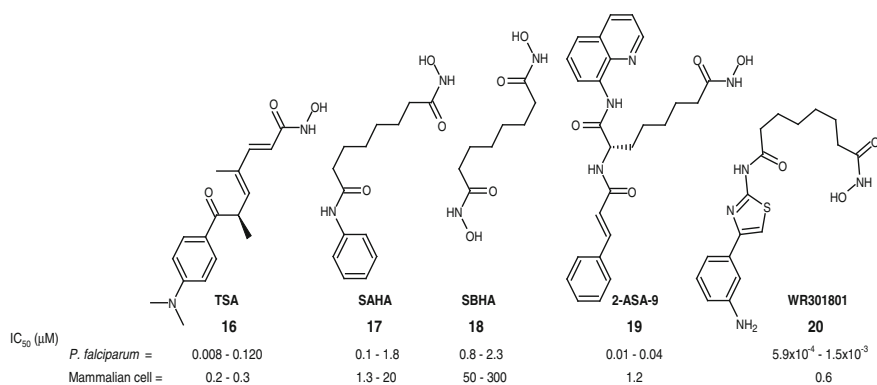
5 Protozoal Diseases

Today, more than a billion people, around one-sixth of the world population, are infected with one or more of the neglected tropical diseases (NTDs). However, since these diseases do not cause sudden outbreaks and are mainly in countries with limited resources for investment in public health, they do not attract the necessary attention of the competent authorities, and thus become neglected dis-eases (WHO 2012a−d). Prominent among the existing NTDs could be leish-maniasis, sleeping sickness, Chagas disease, and malaria, which together account for nearly 50 % of all deaths caused by NTDs every year (WHO 2012a−d). Such NTDs are caused by protozoa, which are among the most prevalent pathogens throughout the world.

More than 225 million individuals are infected with malaria alone and this NTD causes about 700 thousand deaths each year. This disease is caused by the Plasmodium species, of which there are four main types able to infect humans: *Plasmodium vivax*, *Plasmodium ovale*, *Plasmodium malariae*, and *Plasmodium falciparum* (Andrews et al. 2009). However, *P. falciparum* is the most common causative agent. Nowadays, some strains of *P. falciparum* have been showing resistance against chloroquine, the most accessible antimalarial drug available. The most recent antimalarial treatment is artemisinin-based combination therapy (Andrews et al. 2012; Aguiar et al. 2012). However, due to treatment failure and growing parasite resistance to current antimalarial drugs new research has been focusing on novel therapeutic targets and new classes of chemical substances. A better understanding of the biology of these parasites is contributing to the discovery and development of novel drugs and vaccines (Aguiar et al. 2012).

In this context, histone deacetylases (HDACs) have been identified as an important chemotherapeutic target since they play essential roles in regulating gene transcription in both eukaryotes and prokaryotes. HDACs regulate chromatin status and gene expression, and their inhibition is of significant therapeutic interest. This enzyme affects the post-translational modification of proteins by altering the acetylation state of the lysine residues. Thus, the acetylated form induces the gene expression while the deacetylated form silences genes. Consequently, this enzyme has also been considered a potential target for the treatment of several diseases, such as cancer, neurodegeneration, metabolic, inflammatory and autoimmune disorders, as well as infectious and cardiovascular diseases (Carafa et al. 2013). The HDACs have also been investigated as novel prospective drug targets for malaria. HDACs are grouped into two families, Class I and II, which differ significantly in size and structural organization, but share a similar catalytic core that uses zinc as the essential co-factor for deacetylase activity (Andrews et al. 2012).

There are several HDAC inhibitors under development and most of them are hydroxamate-based inhibitors such as Trichostatin A (TSA, **16**, Fig. 12),

IC$_{50}$ (µM)	TSA **16**	SAHA **17**	SBHA **18**	2-ASA-9 **19**	WR301801 **20**
P. falciparum =	0.008 - 0.120	0.1 - 1.8	0.8 - 2.3	0.01 - 0.04	5.9×10^{-4} - 1.5×10^{-3}
Mammalian cell =	0.2 - 0.3	1.3 - 20	50 - 300	1.2	0.6

Fig. 12 Histone deacetylase inhibitors (based on Andrews et al. 2012)

suberoylanilide hydroxamic acid (SAHA or Vorinostat®, **17**, Fig. 12), suberic bishydroxamate (SBHA, **18**, Fig. 12), 2-aminosuberic acid-based hydroxamate (2-ASA-9, **19**, Fig. 12), and WR301801 (**20**, Fig. 12) (Andrews et al. 2012).

Recently, hydroxamic acid-based compounds, selective for *P. falciparum* have been described. The selectivity has been identified by screening compounds with variations in the basic structure of HDAC inhibitors. This includes a small zinc-binding group (ZBG) that accesses the active zinc ion site, a linker region capable of fitting the narrow, hydrophobic, tubular cavity emanating from the ZBG to the HDAC surface, and a capping group that blocks the entrance to the active site cavity (Andrews et al. 2012).

Other neglected tropical diseases such as Leishmaniasis, caused by the parasitic protozoa of the genus Leishmania, are fatal if not treated, and the majority of deaths go unrecognized, even with access to treatment. According to World Health Organizations (WHO) there are four main forms of leishmaniasis: the cutaneous, diffused cutaneous, mucocutaneous, and visceral forms, which affect approximately 12 million people worldwide. Furthermore, there are 350 million people in 88 countries at risk of contracting it (WHO 2012a−d). Vaccination remains the best hope for control of all forms of this disease. Despite great advances in research, no vaccine is yet available (Palatnik-de-Sousa 2012).

Studies of new drugs for the treatment of this parasitic disease have shown that iron deficiency induced by an iron chelator such as desferrioxamine (**21**, Fig. 13), which is a hydroxamic acid derivative, could favor the host in Leishmaniosis. This is because metal chelating groups form complexes with iron in hemoglobin, and thus with no iron available to the parasite its multiplication would be reduced and infection attenuated (Malafaia et al. 2011).

The most important diseases caused by protozoan parasites of the genus *Trypanosoma* are African trypanosomiasis or sleeping sickness and the American disease or Chagas disease. According to the World Health Organization (WHO), African trypanosomiasis affects at least 70,000 people per year and there are about 500,000 people infected with this disease. Furthermore, 60 million people in 36 countries are at risk of contracting it (WHO 2012a−d; Lopes et al. 2010). The treatment available for the advanced stage of disease is the nifurtimox-eflornithine combination therapy (NECT). It consists of a simplified co-administration of nifurtimox, which is given orally, and eflornithine, which is given intravenously (DNDi 2012).

Fig. 13 Desferrioxamine

Desferrioxamine

21
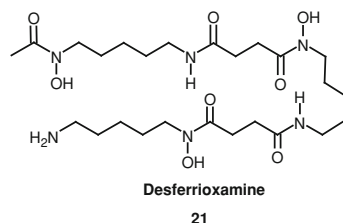
Researchers have identified a hydroxamic acid derivative as a potential therapeutic agent for the treatment of the disease. This is because studies have shown the importance of 6-phosphogluconate dehydrogenase (6-PGDH), the third enzyme of the pentose phosphate pathway, for the parasite survival, especially in *Trypanosoma brucei*. 6-PGDH of the *Trypanosoma brucei* has been shown to be inhibited by 2,3-O-Isopropylidene-4-erythrono hydroxamate. However, this compound has reduced membrane permeability and it does not have trypanocidal activity. Therefore, the attempt is being made to improve the antiparasitic activity of this inhibitor by converting the phosphate group into a lower charged phosphate prodrug. Based on this new compound, a small library of phosphoramidates was synthesized, where some of the compounds showed high trypanocidal activity (Ruda et al. 2010).

In Chagas disease, there are about 10,000 deaths per year caused by *Trypanosoma cruzi*, and it is estimated that 10 million people are infected worldwide, mostly in Latin America, and that 75–90 million are exposed to infection. There is an urgent need for safer and more efficient drugs against Chagas disease given that there are only two compounds in clinical use, which were introduced in the 1960s and 1970s. They are Benznidazole (BNZ) {*N*-benzyl-2-nitroimidazole-1-acetamide} (Rochagan®, Roche) and Nifurtimox (NFX) {4[(5-nitrofurfuryl-idene)amino]-3-methylthio-morpholine-1,1-dioxide} (Lampit®, Bayer) (Capaci-Rodrigues et al. 2010). Several studies have been made and new chemical substances and new therapeutic targets investigated. However, none of the chemicals investigated are in the advanced stage of clinical trials.

Studies of MMPs in *T. cruzi* infections have shown that the expression and activity of two of them, MMP-2 and MMP-9, were up regulated in cardiac tissue during the acute phase of the disease. This study detected an association with inflammatory cells infiltrating the myocardium. Additionally, in order to establish the role of MMPs in vivo, *T. cruzi*-infected mice were treated with doxycycline, a potent inhibitor of MMP activity. It was found that mice treated with doxycycline, a member of the tetracycline antibiotic group able to chelate the zinc metallo-peptidases, showed a significantly decreased inflammation of the heart, delayed peak in parasitemia, and improved survival rates, compared with the control group. These results suggest an important role of MMPs in *T. cruzi*-induced acute myocarditis (Gutierrez et al. 2008).

Metallopeptidase activities have been expressed at high density at the surface of Leishmania promastigotes such as gp63 and in multiple isoforms in *T. cruzi*. An MMP-9-like activity was detected in the cytoplasm of the *T.cruzi* during in vitro infection of embryonic hepatocyte cells (Nogueira de Melo et al. 2004). Subsequent studies have also demonstrated the presence of MMP-9 homologs in *T. cruzi* cells and spent culture medium (Nogueira de Melo et al. 2010). There are no efficient non-toxic inhibitors developed for these potential targets, since this proteolytic activity could possibly contribute to an ECM protein degradation, facilitating invasion of host cells, an activity that is probably highly relevant in vivo during the navigation of interstitial tissue spaces by trypomastigote forms.

Peptidase-dependent ECM remodeling is one of the key events for the regulation of *T. cruzi* infection and pathogenesis of Chagas disease (Capaci-Rodrigues et al. 2010).

6 Viral Disease

The human immunodeficiency virus (HIV) affects 34 million people worldwide, of which 16.7 million are women, 14 million men, and 3.3 million children below 15. Only in 2011, 2.5 million individuals became infected with the virus. HIV is a retrovirus that infects cells of the immune system, destroying or impairing their function. As the infection progresses, the immune system becomes weaker, and the person becomes more susceptible to infections. The most advanced stage of HIV infection is acquired immunodeficiency syndrome (AIDS). It can take 10–15 years for an HIV-infected person to develop AIDS; antiretroviral drugs can slow down the process even further (WHO 2012a−d).

Now 25 years on, HIV therapy, previously focused on developing and optimizing drugs based on inhibiting active HIV replication, is about to enter a new phase. Recently, researchers have demonstrated the need for new therapeutic strategies able to present an effective cure for latent HIV. This is because the therapeutic strategy adopted at the moment has limitations since HIV persists even when viral replication is suppressed. HIV persists during effective therapy, in part because its genome becomes stably integrated in certain white blood cells known as resting memory CD4$^+$ T cells. In this way, these infected cells remain invisible to the immune system as they do not express viral proteins. Supposedly, drugs that reverse latency might lead consecutively to HIV RNA synthesis, viral protein production, and release of HIV particles. It could lead to the death of the infected cell and to the elimination of the viral reservoir by the virus or by the patient's immune system. Histone deacetylase (HDAC) plays an important role in latency related to the removal of acetyl groups from the DNA-bound histone proteins and, in so doing, affects gene expression. Thereby, it could reverse latency (Deeks 2012).

Some histone deacetylase inhibitors (HDACIs) have been tested. Vorinostat$^®$ or SAHA (**17**, Fig. 12) that is licensed for the treatment of cutaneous T cell lymphoma, has been tested in vitro and was able to activate HIV production in latently infected cell lines from 0.25 to 100 mm. Thus, this drug was shown to be a potent inducer to activate HIV production of latently infected monocytic cell lines (U1), T cell lines (J89 and ACH2), primary CD4$^+$ T cells and of CD4$^+$ T cells from HIV-infected patients on suppressive combination antiretroviral therapy (cART). In view of these results, several other HDACIs have been tested which can also activate HIV production from latently infected cells such as givinostat, belinostat, entinostat, and panobinostat (Wightman et al. 2012).

On the other hand, although HDACIs present an exciting new approach to activate HIV production from latently infected cells and so possibly enhance

elimination of these cells and achieve a cure, there are no answers for some questions such as how much of the viral reservoir might be eliminated by HDAC inhibition. Thus, there is a need for new studies to evaluate the toxicity of this treatment (Deeks 2012; Wightman et al. 2012).

7 Conclusion

Hydroxamic acids involve a simple synthesis and possess a substantial versatile pharmacological usefulness. Innumerous new hydroxamic acid-based compounds have been developed for the treatment of various diseases. This is mainly due to their ability to form complexes with various metals, particularly iron, zinc and calcium, which are most abundant in the human body. In this chapter, the importance of the formation of this complex with enzymes of microorganisms has been discussed. In this context, the metallopeptidases were shown to be extremely significant since they have been discovered in several pathogens with a key role in their survival. Also other metalloenzymes of microorganisms that are inhibited by hydroxamate derivatives are shown to act as potential therapeutic targets.

References

Aguiar AC, Rocha EM, Souza NB, França TC, Krettli AU (2012) New approaches in antimalarial drug discovery and development: a review. Mem Inst Oswaldo Cruz 107:831–845

Andrews KT, Tran TN, Wheatley NC, Fairlie DP (2009) Targeting histone deacetylase inhibitors for anti-malarial therapy. Curr Top Med Chem 9:292–308

Andrews KT, Tran TN, Fairlie DP (2012) Towards histone deacetylase inhibitors as new antimalarial drugs. Curr Pharm Des 18:3467–3479

Barb AW, Jiang L, Raetz CR, Zhou P (2007) Structure of the deacetylase LpxC bound to the antibiotic CHIR-090: Time-dependent inhibition and specificity in ligand binding. Proc Natl Acad Sci U S A 104:18433–18438

Böhma S, Exner O (2003) Acidity of hydroxamic acids and amides. Org Biomol Chem 1:1176–1180

Brown MF, Reilly U, Abramite JA, Arcari JT, Oliver R, Barham RA, Che Y, Chen JM, Collantes EM, Chung SW, Desbonnet C, Doty J, Doroski M, Engtrakul JJ, Harris TM, Huband M, Knafels JD, Leach KL, Liu S, Marfat A, Marra A, McElroy E, Melnick M, Menard CA, Montgomery JI, Mullins L, Noe MC, O'Donnell J, Penzien J, Plummer MS, Price LM, Shanmugasundaram V, Thoma C, Uccello DP, Warmus JS, Wishka DG (2012) Potent inhibitors of LpxC for the treatment of Gram-negative infections. J Med Chem 55:914–923

Buache E, Garnotel R, Aubert D, Gillery P, Villena I (2007) Reduced secretion and expression of gelatinase profile in Toxoplasma gondii-infected human monocytic cells. Biochem Biophys Res Commun 359:298–303

Capaci-Rodrigues G, Aguair AP, Vianez-Júnior JLSG, Macrae A, Nogueira de Melo AC, Vermelho AB (2010) Peptidase Inhibitors as a possible therapeutic strategy for chagas disease. Curr Enz Inhib 6:183–194

Carafa V, Miceli M, Altucci L, Nebbioso A (2013) Histone deacetylase inhibitors: a patent review (2009–2011). Expert Opin Ther Pat 23:1–17

Castro MM, Rizzi E, Rodrigues GJ, Ceron CS, Bendhack LM, Gerlach RF, Tanus-Santos JE (2009) Antioxidant treatment reduces matrix metalloproteinase-2-induced vascular changes in renovascular hypertension. Free Radic Biol Med. 46:1298–1307

Codd R (2008) Traversing the coordination chemistry and chemical biology of hydroxamic acids. Coord Chem Rev 252:1387–1408

Costa JD, Nogueira de Melo AC, Vermelho AB, Meirelles Mde N, Porrozzi R (2008) In vitro evidence for metallopeptidase participation in hepatocyte damage induced by *Leishmania chagasi*-infected macrophages. Acta Trop 106:175–183

Deeks SG (2012) HIV: Shock and kill. Nature 487:439–440

Drugs for Neglected Diseases initiative (DNDi) - http://www.dndi.org/treatments/nect-c-treatments.html. Accessed in 29.11.2012***

Elhani D, Elhani I, Aouni M (2012) Resistance in gram negative bacteria: what is the current situation? Tunis Med 90:680–685

Farkas E, Enyedy EA, Micera G, Garribba E (2000) Coordination modes of hydroxamic acids in copper(II), nickel(II) and zinc(II) mixed-ligand complexes in aqueous solution. Polyhedron 19:1727–1736

Fazary AE (2005) Thermodynamic studies on the protonation equilibria of some hydroxamic acids in $NaNO_3$ solutions in water and in mixtures of water and dioxane. J Chem Eng. 50:888–895

Floyd CD, Lewis CN, Patel SR, Whittaker M (1996) A method for the synthesis of hydroxamic acids on solid phase. Tetrahedron Lett 37:8045–8048

Frasch AP, Carmona AK, Juliano L, Cazzulo JJ, Niemirowicz GT (2012) Characterization of the M32 metallocarboxypeptidase of Trypanosoma brucei: differences and similarities with its orthologue in *Trypanosoma cruzi*. Mol Biochem Parasitol 184:63–70

Gennadios HA, Whittington DA, Li X, Fierke CA, Christianson DW (2006) Mechanistic inferences from the binding of ligands to LpxC, a metal-dependent deacetylase. Biochemistry 45:7940–7948

Geurts N, Opdenakker G, Van den Steen PE (2012) Matrix metalloproteinases as therapeutic targets in protozoan parasitic infections. Pharmacol Ther 133(3):257–279

Giacomelli G, Porcheddu A, Salaris M (2003) Simple one-flask method for the preparation of hydroxamic acids. Org Lett 5:2715–2717

Gomis-Rüth FX, Botelho TO, Bode W (2012) A standard orientation for metallopeptidases. Biochim Biophys Acta 1824:157–163

Gould IM, David MZ, Esposito S, Garau J, Lina G, Mazzei T, Peters G (2012) New insights into meticillin-resistant *Staphylococcus aureus* (MRSA) pathogenesis, treatment and resistance. Int J Antimicrob Agents 39:96–104

Goyer R, Golub M, Choudhury H, Hughes M, Kenyon E, Stifelman M (2004) U.S. Environmental Protection Agency. Issue paper on the human health effects of metals. pp 1–22

Grigg R, Major JP, Martin FM, Whittaker M (1999) Solution and solid-phase synthesis of hydroxamic acids via palladium catalysed cascade reactions Original Research Article. Tetrahedron Lett 40:7709–7711

Gross J, Lapiere CM (1962) Collagenolytic activity in amphibian tissues: a tissue culture assay. Proc Natl Acad Sci U S A 48:1014–1022

Gutierrez FR, Lalu MM, Mariano FS, Milanezi CM, Cena J, Gerlach RF, Santos JE, Torres-Dueñas D, Cunha FQ, Schulz R, Silva JS (2008) Increased activities of cardiac matrix metalloproteinases matrix metalloproteinase (MMP)-2 and MMP-9 are associated with mortality during the acute phase of experimental *Trypanosoma cruzi* infection. J Infect Dis 197:1468–1476

Haddad J, Vakulenko S, Mobashery S (1999) An antibiotic cloaked by its own resistance enzyme. J Am Chem Soc 121:11922–11923

Hoekstra R, Eskens FA, Verweij J (2001) Matrix metalloproteinase inhibitors: current developments and future perspectives. Oncologist 6:415–427

Hou T, Zhang W, Xu X (2012) Molecular docking studies of a group of hydroxamate inhibitors with gelatinase-A by molecular dynamics. J Comput Aided Mol Des 16:27–41

Jackman JE, Fierke CA, Tumey LN, Pirrung M, Uchiyama T, Tahir SH, Hindsgaul O, Raetz CR (2000) Antibacterial agents that target lipid A biosynthesis in gram-negative bacteria. Inhibition of diverse UDP-3-O-(r-3-hydroxymyristoyl)-n-acetylglucosamine deacetylases by substrate analogs containing zinc binding motifs. J Biol Chem 275:11002–11009

Klemba M, Goldberg DE (2002) Biological roles of proteases in parasitic protozoa. Annu Rev Biochem 71:275–305

Liang X, Lee CJ, Chen X, Chung HS, Zeng D, Raetz CR, Li Y, Zhou P, Toone EJ (2011) Syntheses, structures and antibiotic activities of LpxC inhibitors based on the diacetylene scaffold. Bioorg Med Chem 19:852–860

Lindsey ML, Zamilpa R (2012) Temporal and spatial expression of matrix metalloproteinases and tissue inhibitors of metalloproteinases following myocardial infarction. Cardiovasc Ther 30:31–41

Lopes AH, Souto-Padrón T, Dias FA, Gomes MT, Capaci-Rodrigues G, Zimmermann LT, Silva TLA, Vermelho AB (2010) Trypanosomatids: odd organisms, devastating diseases. Open Parasit J 4:30–59

Lu CY, Lai SC. (2012) Matrix metalloproteinase-2 and -9 lead to fibronectin degradation in astroglia infected with *Toxoplasma gondii*. Acta Trop (in Press)

Luplertlop N, Missé D (2008) MMP cellular responses to dengue virus infection-induced vascular leakage. Jpn J Infect Dis 61:298–301

Malafaia G, Marcon LN, Pereira LF, Pedrosa ML, Rezende AS (2011) *Leishmania chagasi*: effect of the iron deficiency on the infection in BALB/c mice. Exp Parasitol 127:719–723

Marson BP, Poli de Figueiredo CE, Tanus-Santos JE (2012) Imbalanced matrix metalloproteinases in cardiovascular complications of end-stage kidney disease: a potential pharmacological target. Basic Clin Pharmacol Toxicol 110:409–415

McGwire BS, Chang KP, Engman DM (2003) Migration through the extracellular matrix by the parasitic protozoan Leishmania is enhanced by surface metalloprotease gp63. Infect Immun 71:1008–1010

McKerrow JH (1987) Human fibroblast collagenase contains an amino acid sequence homologous to the zinc-binding site of Serratia protease. J Biol Chem 262:5943

McKerrow JH, Rosenthal PJ, Swenerton R, Doyle P (2008) Development of protease inhibitors for protozoan infections. Curr Opin Infect Dis 21:668–672

Mdluli KE, Witte PR, Kline T, Barb AW, Erwin AL, Mansfield BE, McClerren AL, Pirrung MC, Tumey LN, Warrener P, Raetz CR, Stover CK (2006) Molecular validation of LpxC as an antibacterial drug target in *Pseudomonas aeruginosa*. Antimicrob Agents Chemother 50:2178–2184

Muri EM, Nieto MJ, Sindelar RD, Williamson JS (2002) Hydroxamic acids as pharmacological agents. Curr Med Chem 9:1631–1653

Murphy G (2011) Tissue inhibitors of metalloproteinases. Genome Biol 12:233

Nandurkar NS, Petersen R, Qvortrup K, Komnatnyy VV, Taveras KM, Le Quement ST, Frauenlob R, Givskov M, Nielsen TE (2011) A convenient procedure for the solid-phase synthesis of hydroxamic acids on PEGA resins. Tetrahedron Lett 52:7121–7124

Nogueira de Melo AC, Meirelles MNL, Porrozzi R, Costa JD, Branquinha MH, Vermelho AB (2004) Reduced activity of matrix metalloproteinase-9 in *Trypanosoma cruzi*-infected mouse embryo hepatocyte cell. Hepatol Res 28:49–56

Nogueira de Melo AC, de Souza EP, Elias CG, dos Santos AL, Branquinha MH, d'Avila-Levy CM, dos Reis FC, Costa TF, Lima AP, de Souza Pereira MC, Meirelles MN, Vermelho AB (2010) Detection of matrix metallopeptidase-9-like proteins in *Trypanosoma cruzi*. Exp Parasitol 125:256–263

Onishi HR, Pelak BA, Gerckens LS, Silver LL, Kahan FM, Chen MH, Patchett AA, Galloway SM, Hyland SA, Anderson MS, Raetz CRH (1996) Antibacterial agents that inhibit Lipid A biosynthesis. Science 274:980–982

Palatnik-de-Sousa CB (2012) Vaccines for canine leishmaniasis. Front Immunol 3:69

Pepeljnjak S, Zorc B, Butula I (2005) Antimicrobial activity of some hydroxamic acids. Acta Pharm 55:401–408

Prato M, Giribaldi G (2011) Matrix Metalloproteinase-9 and Haemozoin: Wedding Rings for Human Host and *Plasmodium falciparum* Parasite in Complicated Malaria. J Trop Med 2011:628435

Raetz CR, Whitfield C (2002) Lipopolysaccharide endotoxins. Annu Rev Biochem 71:635–700

Rawlings ND, Barrett AJ, Bateman A (2012) MEROPS: the database of proteolytic enzymes, their substrates and inhibitors. Nucleic Acids Res 40:D343–D350

Riedel S, Kaupp M (2009) The highest oxidation states of the transition metal elements. Coord Chem Rev 253:606–624

Ruda GF, Wong PE, Alibu VP, Norval S, Read KD, Barrett MP, Gilbert IH (2010) Aryl phosphoramidates of 5-phospho erythronohydroxamic acid, a new class of potent trypanocidal compounds. J Med Chem 53:6071–6078

Sakurai A, Okahashi N, Maruyama F, Ooshima T, Hamada S, Nakagawa I (2008) *Streptococcus pyogenes* degrades extracellular matrix in chondrocytes via MMP-13. Biochem Biophys Res Commun 373:450–454

Schechter I, Berger A (1967) On the size of the active site in proteases. I. Papain. Biochem Biophys Res Commun 27:157–162

Shin H, Gennadios HA, Whittington DA, Christianson DW (2007) Amphipathic benzoic acid derivatives: synthesis and binding in the hydrophobic tunnel of the zinc deacetylase LpxC. Bioorg Med Chem 15:2617–2623

Sibi MP, Hasegawa H, Ghorpade SR (2002) A convenient method for the conversion of *N*-acyloxazolidinones to hydroxamic acids. Org Lett 4:3343–3346

Van den Steen PE, Van Aelst I, Starckx S, Maskos K, Opdenakker G, Pagenstecher A (2006) Matrix metalloproteinases, tissue inhibitors of MMPs and TACE in experimental cerebral malaria. Lab Invest 86:873–888

Vargová V, Pytliak M, Mechírová V (2012) Matrix metalloproteinases. EXS 103:1–33

Vendrell J, Querol E, Avilés FX (2000) Metallocarboxypeptidases and their protein inhibitors. Structure, function and biomedical properties. Biochim Biophys Acta 1477:284–298

Vermelho AB, Branquinha MH, d'Ávila-Levy CM, Santos ALS, Dias EPS, Noguera de Melo AM (2010) Biological roles of peptidases in trypanosomatids. The Open Parasitol J 4:5–23

Warmus JS, Quinn CL, Taylor C, Murphy ST, Johnson TA, Limberakis C, Ortwine D, Bronstein J, Pagano P, Knafels JD, Lightle S, Mochalkin I, Brideau R, Podoll T (2012) Structure based design of an in vivo active hydroxamic acid inhibitor of *P. aeruginosa* LpxC. Bioorg Med Chem Lett 22:2536–2543

Whittaker M, Floyd CD, Brown P, Gearing AJ (1999) Design and therapeutic application of matrix metalloproteinase inhibitors. Chem Rev 99:2735–2776

Wightman F, Ellenberg P, Churchill M, Lewin SR (2012) HDAC inhibitors in HIV. Immunol Cell Biol 90:47–54

Wojtowicz-Praga SM, Dickson RB, Hawkins MJ (1997) Matrix metalloproteinase inhibitors. Invest New Drugs 15:61–75

World Health Organization–WHO (2012a) http://www.who.int/hiv/data/2012_epi_core_en.png. Accessed 29 Nov 2012

World Health Organization–WHO (2012b) http://www.who.int/leishmaniasis/resources/leishmaniasis_epidemiology_access_to_medicine/en/index.html. Accessed 29 Nov 2012

World Health Organization–WHO (2012c) http://www.who.int/neglected_diseases/diseases/chagas/en/index.html. Accessed in 30.11.2012

World Health Organization–WHO (2012d) http://www.who.int/tdr/research/ntd/en/ Accessed 29 Nov 2012

Wu JW, Chen XL (2011) Extracellular metalloproteases from bacteria. Appl Microbiol Biotechnol 92:253–262

Yuan X, Mitchell BM, Wilhelmus KR (2009) Expression of matrix metalloproteinases during experimental *Candida albicans* keratitis. Invest Ophthalmol Vis Sci 50:737–742

Zhai W, Gerritz SW, Sofia MJ (2012) Solid phase synthesis of 1,5-disubstituted pyrazole-4-hydroxamic acids and pyrazole-4-carboxamides via direct amidation of β-ketoesters. Tetrahedron Lett 53:267–270

Zhang X, Gonnella NC, Koehn J, Pathak N, Ganu V, Melton R, Parker D, Hu SI, Nam KY (2000) Solution structure of the catalytic domain of human collagenase-3 (MMP-13) complexed to a potent non-peptidic sulfonamide inhibitor: binding comparison with stromelysin-1 and collagenase-1. J Mol Biol 301:513–524

Zhang J, Zhang L, Li X, Xu W (2012) UDP-3-O-(R-3-hydroxymyristoyl)-N-acetylglucosamine deacetylase (LpxC) inhibitors: a new class of antibacterial agents. Curr Med Chem 19:2038–2050

Hydroxamic Acids as Chelating Mineral Collectors

Ramanathan Natarajan

Abstract Owing to the ability to form coordination complexes with several metal ions, hydroxamic acids have application in different fields such as analytical chemistry, chelation therapy, nuclear fuel reprocessing, solvent extraction, ion exchange and mineral processing. Application of hydroxamic acids as chelating mineral collectors for ore beneficiation is a unique area of their use and has attracted the attention of limited readers working in the relevant area. A review of the use of alkyl and aryl hydroxamic acids in mineral processing is presented. Some basic information on mineral flotation chemistry is provided for the sake of common readers. Adsorption of hydroxamates on several minerals is compared because mostly the mineral flotation studies are preceded with adsorption studies. Usually, hydroxamic acids take the *trans* conformation about the carbonyl carbon and amine nitrogen bond. However, crystal structures of two aryl hydroxamic acids with *cis* conformation are furnished. Extension of QSAR approach and molecular modelling, hitherto known in drug design, is also covered to present them as scientific tools for design of mineral collectors that are more selective.

Keywords Hydroxamic acids · Froth flotation · Mineral collectors · Ore beneficiation

Abbreviations

CMC	Carboxy methyl cellulose
DCS	Dissimilar cluster selection
HCNPHA	*N*-Hydrocinnamoyl-*N*-phenylhydroxylamine
IR	Infrared
MDS	Maximum dissimilarity-based selection
NAnFPHA	*N*-4-Anisoyl-*N*-(4-flurophenyl)hydroxylamine
NAnPHA	*N*-4-Anisoyl-*N*-phenylhydroxylamine

R. Natarajan (✉)
V.K.A. Polymers Private Limited, 3A Coimbatore Road, Karur, Tamil Nadu 639002, India
e-mail: rnataraj@lakeheadu.ca; rn@vkapolymers.com

NBNXHA	N-Benzoyl-N-(2, 6-dimethylphenyl)hydroxylamine
NBuXHA	N-Butanoyl-N-(2, 6-dimethylphenyl)hydroxylamine
NMR	Nuclear magnetic resonance
PANEPHA	N-Phenylacetyl-N-(4-ethylphenyl)hydroxylamine
PANXPHA	N-Phenylacetyl-N-(2,6-dimethylphenyl)hydroxylamine
PC	Principal component
PCA	Principal component analysis
PCS	Principal component score
QSAR	Quantitative structure-activity relationship
SCS	Simple cluster-based selection
TBP	Tributylphosphate
tBuAPHA	N-t-Butylacetyl-N-phenylhydroxylamine
TI	Topological index
TMAPHA	N-Trimethylacetyl-N-phenylhydroxylamine
TMEPHA	N-Trimethylacetyl-N-(4-ethylphenyl)hydroxylamine

Contents

1 Introduction

Hydroxamic acids are N-acyl derivatives of hydroxylamine (NH_2OH) and act as bi-dentate ligands to complex with several metal ions (Fig. 1). Their ability to form stable complexes with transition, lanthanide and actinide metal ions extends their application in different areas such as analytical chemistry, spectral-colorimetric analyses, solvent extraction, ion exchange, and several other fields. A large number of articles including two early reviews in Chemical Reviews published on

Fig. 1 Generic structures of hydroxamic acids and their metal chelates
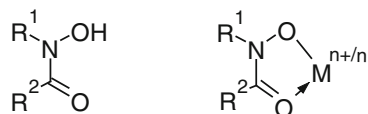
the chemistry of hydroxamic acids and their metal chelates highlight the versatility of applications of hydroxamic acids in several fields (Agrawal 1973, 1977, 1979; Agrawal and Tandon 1974; Agrawal and Kapoor 1977; Barocas et al. 1966; Baroncelli and Grossi 1965; Chatterjee 1978; Inoue et al. 2000; Lutwick and Ryan 1954; Natarajan and Nirdosh 2006; Pradip and Fuerstenau 1983, 1985; Shendrikar 1960; Yale 1943; Lipczynska-Kochany 1991; Raymond et al. 1984; Anderegg et al. 1963; Cheng et al. 1982; Majumdar 1972; Verma et al. 1977).

Application of hydroxamic acids extends to fields such as enzyme inhibitors, soil enhancers, fungicides, mutagens, carcinogens, DNA cleavage, artificial metallonucleases, drug delivery systems, malarial research (Ghosh 1997), and analytical chemistry (Brandt 1960). Octyl hydroxamic acid and its salts have also been used in solvent extraction of metals (Vernon and Khorassani 1978; Vernon 1982), and to prevent corrosion of copper (Notoya and Ishikawa 1980). Some naturally occurring hydroxamic acids are involved in microbial iron transport (Neilands 1974), and in the transport and deposition of heavy metals in aquatic metals in aquatic systems (Vuceta and Morgan 1978). Hydroxamate functionalities are also utilised by natural siderophores for the sequestration of iron by fungi in the environment (Raymond et al. 1984; Renshaw et al. 2002a).

Hydroxamic acids form stable coloured complexes with transition metal ions, which form the basis for their usefulness as photometric analytical reagents for the determination of trace metals (Sandell and Onishi 1978). The deep purple or red colour of iron (III) hydroxamate complexes and the violet coloured vanadium (V) complex have been used for the detection of microgram amounts of hydroxamic acids (Agarwal 1973).

Study of interactions of hydroxamic acids with actinides does not just limit it to stability constant measurements of actinide-hydroxamate complexes (Anderegg et al. 1963; Barocas et al. 1966; Baroncelli and Grossi 1965; Maggio et al. 1966; Sinkov and Choppin 2002) but extends its application towards the extraction of metal ions of nuclear interest, such as zirconium, plutonium and other fission products. Furia et al. (1983) explained the role of hydroxamic acid in the retention of fission products, especially ^{95}Zr, by radiolytically degraded tributyl phosphate in dodecane. Dissolution of αFeO(OH), $ThO_2.2H_2O$ and γ-UO3 by hydroxamate and carboxylate ligands was reported by Renshaw et al. (2002b) while solublisation of actinides by hydroxamic acid-based microbial sideraphores was reported by Brainard et al. (1992). Microbial uptake of uranium and plutonium hydroxamates (John et al. 2001; Renshaw et al. 2003), their solvent extraction (Dasaradhi et al. 1997) and actinide sequestration agents (Durbin et al. 1989) are examples of actinide hydroxamate interactions in radiation chemistry. A mixture of branched chain isomers of 13-carbon atoms, neo-tridecano-hydroxamic acid, had been

reported as extractants in nuclear fuel processing (Cao et al. 1973, 1974; Grossi 1970; Mannone et al. 1977). Hydroxamic acids have higher coordinating ability with tetravalent actinides such as Np^{4+}, Pu^{4+} than with hexavalent uranium (Taylor et al. 1998). Hence, hydroxamic acids were tested for the stripping of actinides in Purex flowsheets for Advanced Fuel Cycles (Fox et al. 2006; Birkett et al. 2005, 2007; Zilberman et al. 2002; Todd and Wigelund 2006). Formo- and aceto-hydroxamic acids were also found to be redox-active and therefore can be oxidised by metal ions such as Np(VI) (Colston et al. 2000; Chung and Lee 2006). The redox behaviour exhibited by hydroxamic acids had been utilised in controlling Np and Pu in Purex reprocessing systems both by coordination stripping of tetravalent ions from the TBP solvent phase and by selective reduction of Np(VI) to inextractable Np(V) (Birkett et al. 2005). It was also found that at the acidities used in the process, U(VI) ions were not affected by hydroxamic acids and remain solvated in the TBP phase (May et al. 1998). Carrott et al. (2007) reported the distribution coefficients of Pu(IV) in the presence of hydroxamic acids in order to understand the behaviour of hydroxamate complexes of Pu(IV) under Purex process condition. Saha et al. (2002) tested the use of an aryl hydroxamic acid in the solvent extraction of uranium from acid solution with pH > 3.

One of the most interesting fields that utilises the ability of hydroxamic acids to form stable coordination compounds with several metal ions is mineral processing. Hydroxamic acids have been tested as mineral collectors in ore beneficiation by froth flotation. This chapter presents the review of studies on testing hydroxamic acids as mineral collectors. A brief outline of froth-flotation process is given below for the benefit of readers and also certain fundamental concepts of froth flotation process are outlined in some other sections. Though this may appear to be trivial for experts it is deemed necessary for general readers.

2 Mineral Concentration by Flotation

Materials mined from ore deposits within the earth's crust are usually a highly heterogeneous mixture of solidified phases. Crushing and grinding operations are used to free the individual phases from their neighbours, that is, to liberate the mineral species and, occasionally, to reduce their size to a range suitable for the intended separation technique. Once mineral species are liberated, an economic recovery of the valuable components contained in the original mixture depends greatly on the application of the most appropriate separation or concentration process (Leja 1982).

The ultimate goal of ore beneficiation is mineral concentration. This is a separation process that is achieved by techniques exploiting physical and physico-chemical characteristics such as specific gravity, shape and size, electrical charge, magnetic susceptibility, radioactivity and surface properties (Leja 1982). Separation processes that exploit the possibility of varying the surface characteristics of minerals make such processes more versatile and universal. Froth flotation is one

such process that exploits surface properties of minerals and emerged as the most dominant pre-concentration process in mineral processing.

Though it was initially developed to concentrate sulphides of base metals, it has now been expanded to float oxides and oxidised minerals and non-metallic minerals such as phosphates, fluorites and fine coal. When air is passed through aqueous slurry, hydrophobic mineral particles adhere to the air bubbles. The mineralised air bubbles rise to the surface of the slurry. To prevent the mineral falling back into the slurry, a frother is added to the dispersion. The hydrophobised mineral transferred to the froth phase collects on the surface of the slurry as the concentrate and is periodically removed. All valuable minerals are not naturally hydrophobic. However, hydrophobicity can be imparted to minerals by adding suitable surfactants, called collectors, to the mineral suspension. In addition to collectors and frothers, other auxiliary chemicals are also added to modify the pH or the surface properties of the mineral to effect selective separation (Fuerstenau et al. 1985). Thus, mineral concentration by froth flotation is based on the different affinity for water exhibited by mineral surfaces.

Collectors are organic substances whose molecules may accumulate at the mineral–water interface or react with the mineral surface. Collector molecule has polar group (hydrophilic group) and a nonpolar hydrocarbon back bone. At the mineral water interface the polar part of the molecule faces the mineral surface while the non-polar group (the hydrocarbon part) faces the solution. While collectors are added to make specific minerals hydrophobic, other chemicals are also introduced in the system to keep selected components water-wetted. These "modifying agents" are called depressants. Other modifying agents called activators are added to reinforce the action of the given collector. Though, froth flotation is a multiphase heterogeneous system and is very complex involving several variables the solid/liquid interface and the reaction at the interface plays the most important and primary role (Raghavan and Fuerstenau 1976).

2.1 Measurement of Flotation Behaviour

Flotation is a complex process which is further complicated in the case of ore flotation by the presence of a mixture of minerals. In order to elucidate the complex phenomena involved in flotation, flotation behaviour of individual minerals has to be understood. Flotation studies involving pure samples of minerals can only be accomplished with a laboratory flotation device wherein the physical and chemical variables can be closely controlled. The Hallimond tube is the most extensively used laboratory flotation device that fulfilled the purpose. The device was originally designed by Hallimond (1944), modified by Evans and Ewers (1952), and later by Fuerstneau et al. (1957). Hallimond tube allows only a few milligrams of ores to be tested, hence laboratory bench scale flotation devices that use up to 1 kg of ore are available and scaling up results obtained using such systems are more reliable (Wills 1997).

In flotation research, one of the main objectives is to investigate the surface chemistry of minerals and how the adsorption of surface-active agents affects hydrophobicity. Hence, preliminary investigations are usually carried out by studying adsorption of collectors on pure minerals and their flotation using Hallimond tube followed by bench scale flotation using real complex ores.

2.2 Chelating Agents as Mineral Collectors

Chelating agents attach themselves to a mineral surface by chelate formation. The chelating tendency of the compounds is higher for transition metals which are rendered hydrophobic in preference to alkali and alkaline earth metals. The valuable minerals are normally compounds of transition and inner transition metals while the gangue and clay minerals are that of silica, calcium and aluminium. This makes chelating agents to perform better than conventional collectors and has therefore attracted attention as mineral collectors in flotation research. Chelating collectors suffer from two main defects: (i) absence of long hydrocarbon chain in their molecules and (ii) prohibitively high cost. Marabini et al. (1988) and Natarajan and Nirdosh (2006) had demonstrated that the first defect could be overcome by new synthesis methodologies. Once it is established, a particular chelating agent enjoys good selectivity and has promise to be used, its production in bulk would be potentially economic.

2.2.1 Selection of Chelating Mineral Collectors

The molecule of a chelating collector has two parts, viz., the chelating group (hydrophilic part) and the hydrocarbon backbone (hydrophobic part). Though the chelating group can be decided from literature and experiments done in solvent extraction (liquid–liquid extraction) of metals from process and waste solutions, and also from solution chemistry of metal ions and their interaction with various chelating agents, one has to bear in mind that the metal ion under consideration in a mineral being floated is not present as a completely free metal ion. Rather, it is present on the surface of the mineral as a unionised entity with only some of its valencies liberated during grinding. Therefore, a chelating agent, which is a selective extractant for a *free* metal ion, may not be a selective collector for the mineral of the same metal. For example thenoyltrifluoroacetone, a good extractant for uranium ion, was not found to function as a good collector for uranium minerals (Muthusamy et al. 1983, 1985) and the same is true for tributylphosphate (TBP). Marabini (1993) had laid down a guideline to choose the chelating group based on conditional constants. Conditional constants are nothing but modified form of thermodynamic stability constants where concentrations of hydroxylated metal ion and protonated-ligand are used instead of the concentrations of free metal ion and ligand:

$$\text{Stability constant} \log K = [\text{ML}]/[\text{M}][\text{L}] \tag{1}$$

Table 1 Effect of pH on hydroxamate adsorption and flotation recovery

Mineral	pH, maximum adsorption	pH optimum flotation recovery	Reference
Haematite	8.5	8.0–9.0	Fuerstenau et al. (1970); Ragavan and Fuerstenau (1975a, b)
γ-MnO$_2$	9.0	9.0	Natarajan and Fuerstenau (1983)
Rhodonite(Mn, Fe, Cu) Sio$_3$	–	9.0	Palmer, Gutierrez, Fuerstneau (1973)
Chrysocolla CuSio$_3$·2H$_2$O	–	6.0	Palmer et al. (1973), Fuersenau and Pradip (1984)
Malachite CuCO$_3$,Cu(OH)$_2$	9.0 also adsorption below 5	Plateau 6 – 10; 9.5 at 10^{-4} M	Lenormand et al. (1979)
Barite	9.0	9.5	Pradip (1987), Fuerstenau et al.(1983)
Calcite	9.5 also below 8	9.5 also below 8	Pradip (1987), Fuerstenau et al. (1982), Pradip and Fuerstenau (1983)
Bastnaesite(Ce, La)FCO$_3$	Plateau adsorption decreases above 8.5	Plateau 5–9	Pradip (1987), Fuerstenau et al. (1982), Pradip and Fuerstenau (1983)
Hubnerite	9.0	9.0	Bodanov et al. (1974)
Fluorite	8.5	8.5	Bodanov et al. (1974)
Pyrochlore	–	6.0	Bodanov et al. (1974)
Cassiterite	6.2	6.2–9.0	Sreenivas and Padmanabhan (2002)
Sphalerite	9.0	9.0	Natarajan et al. (2010)
Galena	9.0	9.0	Natarajan et al. (2010)
Pyrite	9.0	9.0	Natarajan et al. (2010)
Chalcopyrite	9.0	9.0	Natarajan et al. (2010)

$$\text{Conditional constant } \log K^1 = [\text{ML}]\big/\big[\text{M}^1\big]\big[\text{L}^1\big] \tag{2}$$

where [M], [L] and [ML] are concentrations of metal ion *M*, ligand *L* and complex *ML*, respectively, while [M^1] and [L^1] are that of hydroxylated metal ion protonated ligands, respectively.

For a ligand *L* to act as a collector for a mineral that contains the cation *M$_1$* and forms the complex *M$_1$L* the conditional constant

$$\log K^1_{\text{M1L}} \geq 6 \tag{3}$$

For the same ligand to act as a selective collector for M1 against the cation M2 in another mineral in a poly mineral dispersion, the difference between the conditional constants for the complexes *M$_1$L* and *M$_2$L* must be

$$\log K^1_{\text{M1L}} - \log K^1_{\text{M2L}} \geq 5 \tag{4}$$

The first criterion characterises the absolute chelating power towards a cation and the second one defines the relative chelating power of the ligand between two cations.

Once the head group is decided on the basis of the above two criteria, the molecular architecture needs to be designed. Among the congeners (the compounds with the same chelating group), the collector efficiency varies according to the peculiarities of the hydrocarbon part and the substituents in it.

3 Adsorption of Hydroxamates on Mineral/Water Interface

Mineral flotation involves adsorption of collector molecules at the mineral/water interface and the understanding of adsorption of a collector on minerals is necessary before testing the flotation response of minerals towards a particular collector. Adsorption studies on hydroxamates, therefore, precede flotation studies. Hydroxamates adsorb at the mineral surface through electrical double layer interaction and the adsorption peaks around pH 9.0 which is close to the pK$_a$ of several hydroxamic acids and at this pH hydroxamic acids are in the completely dissociated form, i.e. the highly negatively charged form. Flotation recovery of several minerals by hydroxamic acid collectors is maximum around pH 9.0 (Table 1). Pradip (1987) characterised the adsorption isotherms of alkyl hdyroxamates at mineral/water interface with five distinct regions.

1. Chemisorption occurring in horizontal configuration.
2. Saturation adsorption density corresponding to a horizontal monolayer.
3. Chemisorption leading to a vertical monolayer.
4. Saturation adsorption density corresponding to a vertical monolayer.
5. Multilayer adsorption through chain-chain interaction, hydrogen bonding, surface participation and bulk chelation.

The free energies of adsorption $\Delta G^\circ_{\text{ads}}$ can be computed using the well-known Stern–Grahame equation:

Table 2 Standard free energies of adsorption for mineral-hydroxamate systems

Mineral	Constituent cations	Adsorption energies		
		ΔG°_{ads} kcal/mole	ΔH°_{ads} kcal/mole	ΔS°_{ads} Cal/mole° K
Bastnaesite	Ce^{3+}, La^{3+}	−13.6	42.3	190
Pyrolusite	Mn^{2+}, Mn^{4+}	−8.5	4.4	44
Haematite	Fe^{3+}, Fe^{2+}	−7.4	15.0	76
Calcite	Ca^{2+}	−6.4	7.8	48
Barite	Ba^{2+}	−5.7	7.8	46
Cassiterite	Sn^{4+}	−25.0	−36.8	–

$$\frac{\phi}{1-\phi} = \frac{C}{55.5} \exp\left(\frac{\Delta G^{\circ}_{ads}}{RT}\right) \tag{5}$$

Where ϕ is the fraction of stern plane sites covered with hydroxamate, C is the equilibrium concentration of collector in solution, R is the universal gas constant and T the temperature in Kelvin. Standard free energies of adsorption for different mineral-hydroxamate systems are given in Table 2.

Natarajan et al. (2010) studied the adsorption of an N-aryl hydroxamic acid on several minerals and the adsorption isotherms are fitted very well with Langmuir model (Giles et al. 1960) and this confirmed the formation of monolayer, whereas the adsorption of alkyl hydroxamates followed multilayer mechanism. Pradip and Fuerstenau (1983, 1985) proposed that adsorption of hydroxamates on semi soluble minerals such as bastnaesite, barite and calcite occurs via the formation of hydrolyzable cationic species. The metal ions from mineral surface hydrolyse in bulk solution and hydroxycomplexes formed then re-adsorb at the interface assisting adsorption. The surface reaction and bulk precipitation which lead to the formation of multilayers in the case of alkyl hydroxamates appeared to be least probable during the adsorption of aryl hydroxamates on minerals. In the case of alkyl hydroxamates, the hydrocarbon backbone is linear and has much more conformational flexibility to allow multilayer adsorption. The specific adsorption of the aryl hydroxamic acid studied was lower at pH 10.0 than at pH 9.0 and this might be due to hydroxylation of mineral sites at higher OH^- ion concentration. Iron-containing ores were found to have very high specific adsorption and this is due to the high affinity between the iron and hydroxamates. The adsorption on quartz was nearly one-tenth of that on sphalerite and galena which indicated that aryl hydroxamic acids will not float silica minerals. Comparison of specific adsorption of octyl hydroxamates and aryl hydroxamates is given in Table 3.

4 Hydroxamic Acids as Mineral Collectors

The first application of hydroxamic acids in mineral processing appears to have been proposed in 1940, when Popperle (1940) obtained a patent in Germany for the use of hydroxamic acids or their salts as collectors in the flotation of ores.

Table 3 Comparison of specific adsorption of octyl hydroxamate and *N*-phenylcinnamohydroxamate

Adsorbent	Adsorbate	PH	Conc. (mmol/L)	µmol/g	Reference
Haematite (0.5 m^2/g)	Octylhydroxamate	7.5	1.0	5	Raghavan et al. (1975a), Fuerstenau et al. (1970)
Malachite (<3 µm)	Octylhydroxamate	6.6	0.11	113	Lenormand et al. (1979)
Chrysocolla (<75 µm)	Octylhydroxamate	9.0	0.17 1.13	415.0 685.0	(Urbina 1985)
Calcite (2.15 m^2/g)	Octylhydroxamate	9.0	0.6	1.7 (µmol/ m^2)	Pradip and Fuerstenau (1983)
Barite (2.4 m^2/g)	Octylhydroxamate	9.0	1.0	1.3 (µmol/ m^2)	Pradip and Fuerstenau (1983)
Sphalerite (<75 µm)	HCNPHA	9 10	0.24 0.25	30.5 10.0	Natarajan et al. (2010)
Galena (<75 µm)	HCNPHA	9 10	0.24 0.27	26.9 8.8	
Pyrite (<75 µm)	HCNPHA	9 10	0.54 1.45	145.4 119.5	
Chalcopyrite (<75 µm)	HCNPHA	9 10	0.22 0.22	112.3 90.4	
Quartz (<75 µm)	HCNPHA	9 10	0.20 0.24	2.9 0.7	

However, Peterson et al. (1965) reported the use of potassium octyl hydroxamate as a collector for chrysocolla only after 25 years. Since then, numerous investigations on alkylhydroxamate flotation of minerals have been reported.

Promising flotation results were obtained in the laboratory with minerals such as chrysocolla (Fuerstenau and Pradip 1984; Peterson et al. 1965; Barbaro et al. 1997), malachite (Lenormand et al. 1979), haematite (Fuerstenau et al. 1967, 1970; Ragavan and Fuerstenau 1975a), pyrolusite (Natarajan and Fuerstenau 1983), rhodonite (Palmer et al. 1973), bastnaesite (Pradip 1987) copper oxide (Rule 1982), copper-cobalt oxide ores (Evard and De Cuyper 1975) and oxidised zinc lead ores (Kierscznicki 1981). Hallimond tube microflotation test using alkyl hydroxamic collectors showed that the flotation response of different minerals towards these collectors increase in the order spheen > ilmanite > pyrochlore > pyrolucite > bastnaesite > malachite > calcite > cassiterite > barite. As mentioned in the previous section, maximum flotation recoveries occur at pH 8.0–9.0.

The reagent IM-50 (a mixture of alkyl hydroxamic acids and their salts containing 7–9 carbon atoms) was developed in the Soviet Union and has shown to effectively float wolframite, cassiterite and pyrochlore (Bogdanov et al. 1973), as well as quartz in the presence of iron salts (Koltunova et al. 1978). This reagent

was also used for processing tin and rare metal ores (Bogdanov et al. 1977). Hydroxamate collectors with 6–9 carbon atoms are also being used in China for the flotation of copper oxide ores.

Fuerstenau et al. (1970) developed octyl hydroxamate-based collector for the beneficiation of iron ores and showed that the new collectors performed better than the conventional tall oil fatty acids. Pradip and Fuerstenau (1989) tested hydroxamate collectors for the beneficiation of rare earth ores. Hydroxamates were found to be more selective than fatty acids for the separation of bastnaesite, a serium lanthanum fluoro carbonate. This ore from California had calcite, barite and celestite as gangue minerals and was successfully suppressed by using ammonium lignin sulphonate and washing soda. A rare earth ore from China that could not be beneficiated using fatty acids was successfully beneficiated using a hydroxamate reagent scheme (Ref. 26 in Pradip 1987).

Many sulphide minerals of copper have oxidised copper minerals, such as malachite, associated with them. The oxidised copper minerals such as malachite, azurite, cuprite, tenorite and chrysocolla do not respond to the traditional xanthate collectors used to float sulphide minerals of copper and require alternative flotation methods. Generally, the oxide minerals are treated by sulphidisation using reagents such as sodium hydrogen sulphide and then floated with conventional collectors. Hydroxamate collectors were found to float the oxidised copper minerals (Peterson et al. 1965) without sulphidisation. Ausmelt Ltd developed a hydroxamate-based flotation reagent AM 28 for the recovery of copper and gold from sulphide ore bodies that contain oxidised copper ore. Several mines are currently using Ausmelt hydroxamate collectors for the flotation of copper oxide deposits. Hydroxamates are also used in conjunction with xanthate collectors for improved copper recovery (Lee et al. 2009). A copper cobalt oxide ore which failed to float even after sulphidisation was successfully beneficiated using laurohydroxamate collector.

Bogdanov et al. (1973) concentrated wolframite, cassiterite and pyrochlore using IM-50, a hydroxamate-based collector developed in previous USSR. In the flotation of the tungsten minerals higher flotation recoveries were obtained at low acidic pH. A niobium-tantalum ore was preconcentrated by flotation using hydroxamic acids in combination with transformer oil (Ref. 26 in Pradip 1987), Sreenivas and Padmanabhan (2002) studied the surface chemistry and flotation of cassiterite using alkylhydroxamic acid of carbon chain length 8, 10 and 14. Unlike several other studies, octyl hydroxamate adsorption was found to be in an acidic pH indicating the involvement of undissociated hydroxamic acids. Similar phenomenon was reported in the alkyl hydroxamate-ferric oxide-manganese dioxide systems by Raghavan and Fuerstenau (1975b) and Natarajan and Fuerstenau (1983).

Carboxylic acids were conventionally used to remove coloured impurities (TiO$_2$) from kaolin clay. Yoon and Hilderbrand (1986) developed a hydroxamate-based process for clay flotation and patented the technology. The hydroxamate collector has many advantages over the conventional fatty acids flotation. The amount of hydroxamate collector required is far less than the carboxylic acid (tall oil) and moreover, no frother is needed owing to the frothing properties of hydroxamic acid (Willis et al. 1999). Cytec industry developed a new hydroxamate-

based commercial collector under the name S-6493 Promotor and this is currently used by several kaolin industries. Hydroxamates were found to yield higher kaolin recoveries with better grade in reverse flotation of kaolin clay (Yoon et al. 1992; Clifford 1998); Yordan et al. (1993) and Yoon et al. (1992) showed that direct flotation of anatase using hydroxamates gave higher yields with faster flotation kinetics. The clay product obtained using hydroxamates were better in quality and the hydroxamate-based process could be extended to different kinds of kaolin clays. Cytec's S-6493 has been shown to recover oxide copper minerals.

4.1 Arylhydroxamic Acids as Mineral Collectors

Natarajan and Nirdosh (2001a) preferred to synthesise and test N-aryl hydroxamic acids with wide structural variations that might affect electronic and steric parameters. Sphalerite (ZnS) is associated with galena (PbS) and in the conventional xanthate flotation of scheme galena is floated first by suppressing sphalerite using NaCN. Suppressed sphalerite is activated by copper sulphate and then floated with potassium amyl xanthate (PAX). Amount of copper sulphate required for activation depends on the grade of the ore and it varies from 500 g to 1 kg per tonne of ore. Copper sulphate is corrosive and expensive. Natarajan and Nirdosh (2006) synthesised several arylhydroxamic acids (Table 4) and tested for the flotation of sphalerite without copper sulphate activation. Though they successfully floated sphalerite without copper sulphate activation, concomitant flotation of iron minerals, pyrite and pryrrhotite, owing to the strong affinity of hydroxamic acids towards iron, the reduced grade of zinc concentrate was obtained. Hamilton et al. (2009) went on to improve the zinc grade by suppressing pyrrhotite using carboxy methyl cellulose (CMC).

4.2 Flotation Kinetics Using Arylhydroxamic Acids

It is generally accepted that froth flotation follows first order kinetics (Wills 1997), and the rate expression therefore leads to

$$\ln \frac{Co}{C_t} = kt \tag{6}$$

On rearrangement, this gives

$$C_0 - C_t = C_0(1 - e^{-kt}) \tag{7}$$

C_0 in the above equation is the initial concentration of the mineral in the ore at time zero, i.e. the *maximum theoretically flotable amount* or the *theoretically maximum possible recovery* of the mineral. However, the complete recovery of the entire mineral present in the ore feed is never achievable because some mineral

Table 4 Structures of hydroxamic acids synthesised and tested with abbreviated names

$$R^1 \underset{}{\overset{OH}{\underset{R^2}{\bigcirc - N - C}}} $$

No.	R^1	R^2	Name	Abbreviation
1	H	$n\text{-}C_3H7$	*N*-Butanoyl-*N*-phenylhydroxylamine	NBuPHA
2	$4\text{-}C_2H_5$	$n\text{-}C_3H7$	*N*-Butanoyl-*N*-(4-ethylphenyl)hydroxylamine	NBuEPHA
3	H	$C(CH_3)_3$	*N*-Trimethylacetyl-*N*-phenylhydroxylamine	TMAPHA
4	H	$CH_2C(CH_3)_3$	*N*-t-butylacetyl-*N*-phenylhydroxylamine	tBuAPHA
5	$2,6\text{-diCH}_3$	$n\text{-}C_3H7$	*N*-Butanoyl-*N*-(2,6-dimethylphenyl)hydroxylamine	NBuXHA
6	$2,6\text{-diCH}_3$	$C(CH_3)_3$	*N*-Trimethylacetyl- *N*-(2,6-dimethylphenyl)hydroxylamine	TMAXHA
7	$2,6\text{-diCH}_3$	$CH_2C(CH_3)$	*N*-t-Butylacetyl-*N*-(2,6-dimethylphenyl)hydroxylamine	tBuAXHA
8	$4\text{-}C_2H_5$	$C(CH_3)_3$	*N*-Trimethylacetyl- *N*-(4-ethylphenyl)hydroxylamine	TMAEPHA
9	H	$n\text{-}C_5H11$	*N*-Hexanoyl-*N*-phenylhydroxylamine	NHexPHA
10	4-Br	$n\text{-}C_3H7$	*N*-Butanoyl-*N*-(4-bromophenyl) hydroxylamine	NBuBPHA
11	H	C_6H_5	*N*-Benzoyl-*N*-phenylhydroxylamine	NBPHA
12	H	$4\text{-}CH_3O\text{-}C_6H_4$	*N*-4-Anisoyl-*N*-phenylhydroxylamine	NAnPHA
13	H	$4NO_2\text{-}C_6H_4$	*N*-(4-Nitrobenzoyl)-*N*-phenylhydroxylamine	NNBPHA
14	4-F	C_6H_5	*N*-Benzoyl-*N*-4-(fluorophenyl)hydroxylamine	NBFPHA
15	2-OCH$_3$	C_6H_5	*N*-Benzoyl-*N*-(2-methoxyphenyl)hydroxylamine	NBoMPHA
16	4-F	$4\text{-}CH_3O\text{-}C_6H_4$	*N*-4-Anisoyl-*N*-phenylhydroxylamine	NAnFPHA
17	$4\text{-}C_2H_5$	C_6H_5	*N*-Benzoyl-N-(4-ethylphenyl)hydroxylamine	NBEPHA
18	$2,6\text{ -diCH}_3$	C_6H_5	*N*-Benzoyl-*N*-(2,6-dimethylphenyl)hydroxylamine	NBXHA
19	$4\text{-}n\text{-}C_3H_7$	C_6H_5	*N*-Benzoyl-*N*-(4-propylphenyl)hydroxylamine	NBPPHA
20	$4\text{-}i\text{-}C2H_7$	C_6H_5	*N*-Benzoyl-*N*-(4-i-propylphenyl)hydroxylamine	NBiPPHA
21	$4\text{-}t\text{-}C_4H_9$	C_6H_5	*N*-Benzoyl-N-(4-t-butylphenyl)hydroxylamine	NBtBuPHA
22	H	$C_6H_5CH_2$	*N*-Phenylacetyl-*N*-phenylhydroxylamine	PANPHA
23	H	$C_6H_5CH_2CH_2$	*N*-Hydrocinnamoyl-*N*-phenylhydroxylamine	HCNPHA

(continued)
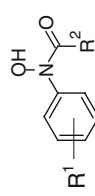
Table 4 (continued)

No.	R^1	R^2	Name	Abbreviation
24	4-C_2H_5	$C_6H_5CH_2$	N-Phenylacetyl-N-(4-ethylphenyl)hydroxylamine	PANEPHA
25	4-C_2H_5	$C_6H_5CH_2CH_2$	N-Hydrocinnamoyl-N-(4-ethylphenyl)hydroxylamine	HCNEPHA
26	2,6-diCH_3	$C_6H_5CH_2$	N-Phenylacetyl-N-(2,6-dimethylphenyl)hydroxylamine	PANXHA
27	2,6-diCH_3	$C_6H_5CH_2CH_2$	N-Hydrocinnamoyl-N-(2,6-dimethylphenyl)hydroxylamine	HCNXHA
28	H	CH_2–C(= O)	N,N-Diphenylmalanodihyroamic acid	MALDHA
29	H	$(CH_2)_2$–C(= O)	N,N-Diphenylsuccinonodihyroamic acid	SUCDHA
30	H	$(CH_2)_3$–C(= O)	N,N-Diphenylglutarodihyroamic acid	GLUDHA
31	H	$(CH_2)_4$–C(= O)	N,N-Diphenyladipodihyroamic acid	ADIDHA

particles will remain inaccessible due to their being locked inside other matrices such as quartz or in very coarse particles. Hence, C_0 on the right hand side of Eq. (7) is replaced by the term R_∞, where R_∞ is the *maximum recovery achievable* or the *cumulative recovery at infinite time*. Noting that C_t is the concentration of the mineral at time t during flotation, $C_0 - C_t$ is therefore equal to the cumulative recovery, R_t, at time t. Thus, Eq. (7) can be rewritten as:

$$R_t = R_\infty(1 - e^{-kt}) \tag{8}$$

A plot of cumulative recovery *versus* time is an asymptotic curve and the cumulative recovery corresponding to the asymptotic portion is the maximum recovery achieved, R_∞. Agar (1985) introduced a time correction factor φ in Eq. (8) for the first order flotation kinetics. The modified rate equation is:

$$R_t = R_\infty(1 - e^{-k(t+\phi)}) \tag{9a}$$

The changes in flotation variables such as airflow rate and collector dosage alter the numerical values of R_∞ and/or k. The effect of an operating variable on flotation characteristics is usually interpreted from the trend observed in the change in the values of these parameters. However, in a batch flotation test, a change in one flotation variable may have opposing effects on the parameters. Since selectivity of a collector for a certain mineral over others depends on the value of R_∞ and k, it becomes difficult to interpret the change in selectivity between a valuable mineral and a gangue mineral. In order to overcome this, Xu (1998) suggested a modified rate constant, K_m, which is a combination of R_∞ and k and is given by the equation:

$$K_m = R_\infty \times k \tag{9b}$$

It is known that for a first order kinetics,

$$\text{rate} = C_t \times k \tag{10}$$

when time $t = 0$, $C = C_0$ (but $C_0 \approx R_\infty$), therefore

$$\text{rate} = R_\infty \times k \tag{11}$$

Hence, the modified rate constant, K_m, is the rate of the reaction at time $t = 0$.

The modified rate constants were used by Xu (1998) to define a new quantity, viz., the *selectivity index* (SI) or the relative rate constant of one mineral (M_1) over that of the other mineral (M_2). The selectivity index therefore may be given by the following expression:

$$\text{SI}_{(M_1/M_2)} = \frac{K_m \text{of } M_1}{K_m \text{of } M_2} \tag{12}$$

Thus, the selectivity index between a valuable mineral M and a gangue mineral G may be calculated by the equation:

$$SI_{(M/G)} = \frac{K_{m_M}}{K_{m_G}} \tag{13}$$

Selectivity index (SI) is the quantification of the selectivity of a collector for a particular mineral over another mineral under the given set of process variables. It is therefore helpful to identify the factors that have positive effects on SI in order to maximise the separation between the two minerals. Effect of substituents on the kinetics of flotation of a copper–nickel ore from Canada by N-arylhydroxamic acids was studied. Seven N-arylhydroxamic acids were synthesised and tested to float a nickel ore containing pentlandite (4–5 %), chalcopyrite (4–5 %) and pyrrhotite (30–35 %). N-phenylacetyl-N-(2,6-dimethylphenyl)hydroxylamine (PANXPHA) was found to have highest first order rate constant for the kinetics of flotation of pentlandite and this was higher than that for potassium amyl xanthate, the conventional collector for sphalerite. Amongst the seven N-arylhydroxamic acids, PANXHA was also found to have the highest selectivity index for pentlandite. Modified rate constants were linearly related to calculated dissociation constants (pK_a) of the N-arylhydroxamic acids used in the study. It may be interesting to note that the compound found to have the highest first order rate constant and the highest selectivity is the one detected to have the cis (E) conformation even in the solid state.

5 Crystal Structure of Hydroxamic Acids

The hydroxamate group has to be in the $cis(Z)$ conformation to form the chelate ring with metal ions. However, in free hydroxamic acid the C(=O)NHOH group is usually in the trans conformation and this had been confirmed in the case of several aryl-hydroxamic acids by X-ray crystal structure determination (Raman et al. 1984; Bryde and Kjoeller 1993; Andreas et al. 1990; Jaroslav 2000; Urbina 2003; Fuerstenau et al. 2000; David et al. 1996). Brown et al. (1996) studied the conformational behaviour of hydroxamate group using ab initio calculation, NMR and IR spectroscopy, and X-ray crystal structure determination. IR and NMR studies showed the presence E and Z isomers in chloroform while the Z form was found to be the predominate isomer in DMSO. The ab initio calculations indicated the stabilisation of the $cis(Z)$ conformation in water by hydrogen bonding with water molecules. On the other hand, the X-ray crystal structure of p-CH$_3$C$_6$H$_4$N(CH$_3$)OH confirmed the trans conformation of the molecules in the solid state. In spite of being crystallised from the same solvent mixture, two unique hydroxamic acids were identified to have the $cis(E)$ form even in the solid state among the six arylhydroxamic acids investigated using single crystal X-ray crystallography. This was a very rare instance where the $cis(E)$ form was detected even in the solid state. The two N-aryhydroxamic acids (NBNXHA and PAN-XHA) in the cis form were found to have 2,6-dimethylphenyl group attached to the nitrogen atom. This group on nitrogen appeared to be bulky enough to restrict the

N-hydrocinnamoyl-N-phenylhydroxylamine (HCNPHA)

N-tert-butylacetyl-N-2,6-dimethylphenylhydroxylamine (tBuNXHA)

N-Benzoyl-N-2,6dimethylphenylhydroxylamine (NBNXHA)

N-Trimethylacetyl-N-phenylhydroxylamine (TMANPHA)

N-Phenylacetyl-N-2,6-dimethylphenylhydroxylamine (PANXHA)

N-Trimethylacetyl-N-2,6-dimethylphenylhydroxylamine (TMANXA)
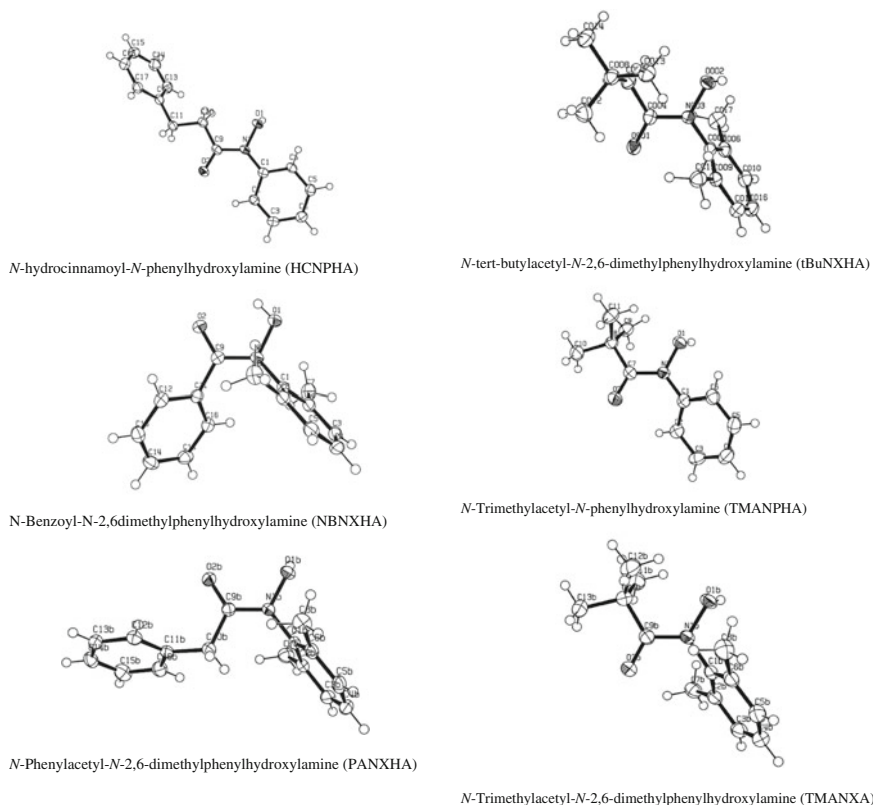
Fig. 2 Crystal structures of *N*-aryl hydroxamic acids. PANXHA and NBNXHA in unusual *cis* form

free rotation around the C–N bond provided a sterically bulky group or an anchoring group such as phenyl (C_6H_5-) or benzyl ($C_6H_5CH_2$-) is attached to the carbonyl carbon. The *trans* conformation of TMAXHA clearly indicated that bulky substituents should be present on both the nitrogen and the carbonyl carbon of the hydroxamate group to restrict free rotation and lock the conformation in the *cis* form (Fig. 2).

6 QSAR Approach for the Selection of Hydroxamic Acid Collectors

Though the dependence of efficiency of chelating collectors on their molecular structures had been studied (Nagaraj 1987; Marabini et al. 1988; Marabini 1993; Das et al. 1995; Fuerstenau et al. 1967; Ackerman et al. 1984, 1987, 1999; Nirdosh

Fig. 3 Quadratic fit of separation efficiency against logKoc (data points 1, 3 and 16 are not included in curve fitting)
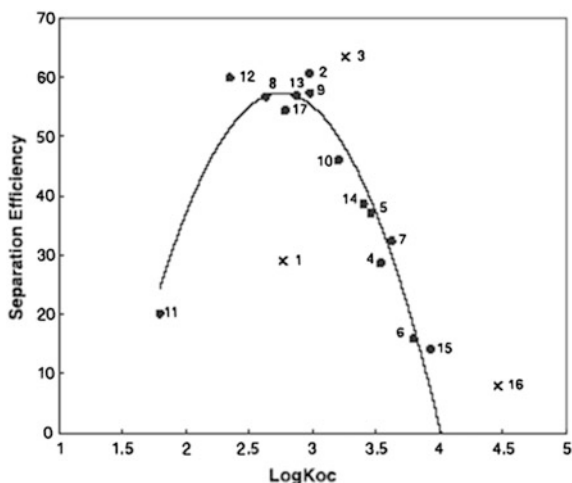
et al. 1994; Natarajan and Nirdosh 2001a, 2006), no quantitative treatment had been reported. There is implicit dependence of efficiency of a chelating agent (organic compound) as flotation collector on the molecular architecture, and QSAR is the approach that quantifies this intuitiveness. Natarajan et al. (1999; 2002a, b; 2003) extended the QSAR approach to model the efficiency of chelating collectors. They successfully showed that the separation efficiencies of chelating collectors are amenable to QSAR modelling and topological indices (Natarajan et al. 2001b). Separation efficiencies of aryhydroxamic acids used to float a Canadian zinc ore was modelled (Natarajan and Nirdosh 2003) using electronic parameters, physicochemical properties such as octanol–water partition coefficient ($\log P$) and soil–water partition coefficient ($\log K_{oc}$), and geometrical parameters that describe the molecular surface area and volume. Several of the computed parameters were found to fit in a second-order polynomial regression with the separation efficiencies (SE) of the collectors (Fig. 3). Soil–water partition coefficient, $\log K_{oc}$ and Connolly solvent-excluded volume gave good correlation for the complete data set. The quadratic fit showed that the collector performance peaks at particular structural feature optimum to give the best flotation response.

6.1 Selection of Hydroxamic Acid Collectors by Molecular Similarity Method

The success in the extension of QSAR modelling approach to flotation chemistry indicated that efficiency of chelating collectors for a given mineral is a function of molecular structure assuming the other conditions (variables) such as pH, particle size, air-flow rate, etc., are constant. Hence, it may be concluded that compounds with similar structure have comparable flotation efficiency for a mineral. In the

case of a chelating collector, the molecule can be visualised to consist of two parts, namely the chelating group (polar group) and the hydrocarbon backbone. The polar group can be decided using the difference in stability constants discussed in Sect. 2.2.1 (Marabini 1993). Once the molecular skeleton with a polar group is decided, the combinatorial library of possible structures can be explored for the selection of a small number of compounds for synthesis and testing.

6.1.1 Molecular Dissimilarity/Similarity Clustering

Johnson and Maggiora (1990) showed that molecular similarity clustering was an efficient method in the selection of compounds and prediction of biological and physicochemical properties, and Lajiness (1990) found this method useful for the selection of a small number of compounds from a virtual library (a database of compounds that contain all possible structures) in the process of identification of new therapeutic agents. To create a similarity space for the selection of compounds, an appropriate measure of molecular similarity is needed. Physicochemical properties, topological indices and substructures, called atom-pairs, had been used in constructing structure spaces for selections. Use of experimental data has a very restricted application due to the limitation in their availability for all the chemicals under consideration. Computable properties are always preferred for the purpose.

Let us consider that t numbers of topological indices are calculated for the given set of m structures. The data set is very large, hence the ($t \times m$) data matrix is subjected to data reduction by principal component analysis (PCA). Principal components with Eigenvalues ≥ 1 are extracted. Before performing PCA, the calculated topological indices are transformed into $\log_e(TI + 1)$. This is necessary because the magnitudes of some topological indices are several times greater than those of the others. Principal Components (PCs) derived from Topological Indices (TIs) are efficient in clustering structurally similar compounds. The similarity space is an n-dimensional space, where n is the number of PCs extracted from TIs and the compounds are clustered based on their structural similarities encoded by the PCs. The principle component scores of the extracted factors are standardised. The standardised scores are used to form similarity spaces by a nonhierarchical cluster analysis. Thus, the m chemicals in the virtual database are classified into a few clusters of related compounds. The clusters are formed around a centre point, the centroid, and have a set radius based on the molecular density around the centroid. The number of clusters to which the chemicals are to be grouped is decided on the basis of the selection method. One or more compounds are selected from the clusters based on the distance from the cluster centre. There are three methods for the selection of chemicals by cluster analysis. They are:

1. Simple cluster-based selection (SCS)
2. Maximum dissimilarity-based selection (MDS)
3. Dissimilar cluster selection (DCS)

In the SCS method, the cluster analysis based on the similarity measures is performed to generate a given number of clusters. One compound can then be chosen from each cluster either randomly or on the basis of the distance from the centroid. In the MDS method, compounds are chosen such that they are maximally different from the compounds already chosen or tested. This can be achieved by ordering the set of compounds in the selection list. In the DCS method, cluster analysis is performed on the dataset to generate $D + S$ clusters where D is the number of compounds decided for testing and S is the number of compounds already tested or selected. Clusters containing screened compounds are then eliminated and one compound from each of the remaining clusters is chosen. The DCS method was found to be superior to the other two methods (Lajiness 1990).

A library of 3,800 N-arylhydroxamic acids was created, this being a virtual library of compounds because most of the chemicals were not even synthesised while preparing the database. Ninety-four topological indices were calculated for these 3,800 compounds. Data reduction was performed using Principal Component Analysis (PCA) extracted seven principal components (PCs) and they explained 95 % of the variance. Thus, the 600 compounds were clustered in a seven-dimensaional space. The ten N-arylhydroxamic acids selected were synthesised and tested as mineral collectors for two different types of ores. Results of flotation tests indicated that out of the ten aryl hydroxamates tested in the zinc-rougher stage, same four collectors namely HCNPHA, PANEPHA, TMEPHA, tBuAPHA were found to be the top performers for both the ores. The collectors NAnPHA, NAnFPHA,

NBuXHA and TMAPHA did not show any promise in the flotation of sphalerite. Hence, other compounds in the clusters to which each of the four chemicals was a member were not pursued further in testing. HCNPHA was found to give the best results in both the cases and in addition its synthesis was found to give the best percentage yield. Results of the study indicated that molecular similarity-based selection could be used to select a desired number of compounds for synthesis and testing as mineral collectors from a large database. This offers a scientific tool for the selection of compounds and avoids the trial-and-error method and saves considerable amount of laboratory testing as one explores a large structural database by testing a few compounds.

7 Molecular Modelling Approach for Mineral Collector Design

Molecular modelling and docking ligands onto protein molecules are very common tool in drug design. Pradip et al. (2002) extended this approach for the design of mineral collectors. In the molecular modelling approach the geometry of the collector molecule is optimised using quantum chemical calculation. The optimised geometry is docked on to the cluster model of mineral surface generated to

represent the cleavage plane of the mineral under consideration. The mineral collector interaction energies are calculated to simulate adsorption of the collector on to the mineral surface. (Pradip et al. 2002) studied octyl hydroxamate-calcium minerals interactions. The theoretical predictions were compared with the results of the laboratory microflotation tests. There was excellent correlation between theoretical prediction and experimental results.

The success of molecular modelling approach in designing mineral collectors and the molecular similarity-based selection of compounds for synthesis and testing offer scientific tools for the designing mineral collectors. A combination of both these computational approaches is expected to make the significant contribution in the design of tailor-made mineral collectors that are better selective than commercially available ones. With the depletion of easy to handle high grade ores it is necessary to find new collector molecules that are selective to effectively separate valuable minerals from low grade ores from complex ore deposits.

8 Conclusion

Xanthate reagent scheme is widely used in the mineral processing industry and is the most studied system over a few decades. Hydroxamate-based reagent schemes are relatively new and most of the research is still to attract the attention of the industry and at present appears to be simple laboratory tests. As more and more of the high grade easy-to-process mineral resources are depleting and complex low grade ores need to be processed, new reagents such as hydroxamate reagents are expected to find more application. Moreover, xanthates are cheaper than hydroxamates and several of the hydroxamic acids are not ready to be used as commercial chemicals. They are specialised reagents and are apparently expensive in the absence of a demand to manufacture in large quantities. Chemical industries such as Cytec started bringing in reagents based on hydroxamates to process oxidised ores either alone or in combination with xanthates. It appears as lot more research has to be carried out to develop hydroxamate-based reagent scheme that includes proper combination of frother, suppressant, activator and other modifiers.

References

Ackerman PK, Harris GH, Klimpel RR, Aplan FF (1984) Effect of alkyl substituents' performance on the thionocarbamate as copper sulphides and pyrite collectors. In: Jones MJ, Oblatt R (eds) Reagents in mineral industry. The Institution of Mining and Metallurgy, London, pp 69–78

Ackerman PK, Harris GH, Klimpel RR, Aplan FF (1987) Evaluation of flotation collectors for copper sulphides and pyrite. III. Effect of xanthate chain length and branching. Int J Miner Process 21:141–156

Ackerman PK, Harris GH, Klimpel RR, Aplan FF (1999) Use of chelating agents as collectors in the flotation of copper sulphides and pyrite. Miner Metall Process 16:27–35

Agar GE (1985) The optimization of flotation circuit design from laboratory rate data. In: Proceedings of the XVth International Mineral Processing Congress, vol 2. Cannes, pp. 100-108

Agarwal YK (1973) Method for the detection of microgram amounts of hydroxamic acids. Analyst 98:147–148

Agrawal YK (1977) Thermodynamics of proton dissociation in mixed aqueous media I pKa ΔH and ΔS values for proton-ligand stability constants of several N-m-tolyl-p-substituted benzohydroxamic acids. Thermochim Acta 18:250–254

Agrawal YK (1979) Hydroxamic acids and their metal complexes. Russ Chem Rev 48:948–963

Agrawal YK, Kapoor HL (1977) Stability constants of rare earths with hydroxamic acids. J Inorg Nucl Chem 39:479–482

Agrawal YK, Tandon SG (1974) Metal-ligand stability constants of hydroxamic acids. J Inorg Nucl Chem 36:869–873

Anderegg G, L'Eplattenier F, Schwarzenbach G (1963) Hydroxamatkomplexe II Die Anwendung der pH-methode. Helv Chim Acta 46:1400–1408

Andreas D, Douglas PR, Eng-Wilmot DL, Hossain MB, Helm D (1990) Structures of two isomeric hydroxamic acids: N-methil-p-toluohydroxamic acid (MTH) and N-(4-methulphe-nyl)acetohydroxamic acid(MPA). Acta Crystallogr Sect C: Cryst Struct Commun C46(5):816–821

Barbaro M, Herrera Urbina R, Cozza C, Fuerstenau D, Marabini A (1997) Flotation of oxidised minerals of copper using a new synthetic chelating reagent as collector. Int J Miner Process 50:275–287

Barocas A, Baroncelli F, Biondi GB, Grossi G (1966) The complexing power of hydroxamic acids and its effect on behaviour of organic extractants in the reprocessing of irradiated fuels—II: the complexes between benzohydroxamic acid and thorium uranium (IV) and plutonium (IV). J Inorg Nucl Chem 28:2961–2967

Baroncelli F, Grossi G (1965) The complexing power of hydroxamic acids and its effect on the behaviour of organic extractants in the reprocessing of irradiated fuels—I the complexes between benzohydroxamic acid and zirconium iron (III) and uranium (VI). J Inorg Nucl Chem 27:1085–1092

Bettina Bryde N, Ingrid Kjoeller L (1993) 345-Trihydroxybenzohydroxamic acid monohydrate a ribonucleotide reductase inhibitor. Acta Crystallogr Sect C: Cryst Struct Commun C49(4):810–813

Birkett JE, Carrott MJ, Fox OD, Jones CJ, Maher CJ, Roube CV, Taylor RJ, Woodhead DA (2005) Recent developments in the purex process for nuclear fuel reprocessing: Complexant based stripping for uranium—plutonium separation. Chimia 59:898–904

Birkett JE, Carrott MJ, Fox OD, Jones CJ, Maher CJ, Roube CV, Taylor RJ, Woodhead DA (2007) A progress report on the control of neptunium and plutonium within single cycle solvent extraction flowsheets for advanced fuel cycles. J Nucl Sci Tech 44:337–343

Bogdanov OS, Podnek AK, Rjaboy VI Janis NA (1977) Reagents chemisorptions on minerals as a process of formation of surface compounds with a coordination bond. In: Proceedings of the XXI international mineral processing congress, San Paulo Brazil 2: 280–303

Bogdanov OS, Yeropkin YI, Koltunova TE, Khobotova NP, Shtchukina NE (1973) Hydroxamic acids as collectors in the flotation of wolframate cassiterite and pyrochlore In: MJ Jones (ed) 10th international mineral processing congress, London pp. 553–564

Brainard JR, Strietelmeier BA, Smith PH, Langston-Unkefer PJ, Barr ME, Ryan RR (1992) Actinide binding and solubilization by microbial siderophores. Radiochim Acta 58(59):357–363

Brandt WW (1960) Analytical applications of hydroxamic acids. Record of Chemical Progress 21:159–177

Brown DA, Coogan RA, Fitzpatrick NJ, Glass WK,: Abukshima DE, Shiels L, Ahlgren M, Smolander K, Pakkanen TT, Pakkanen TA, Perakyla M (1996) Conformational behaviour of hydroxamic acids: ab initio and structural studies J Chem Soc Perkin Trans 2, 2673–2679

Cao S, Dworschak H, Hall A (1973) Experiences of the hot reprocessing campaign of irradiated MTR fuel elements with an amine flowsheet at the Eurex plant Saluggia Italy Comitato Nazionale Energia Nucleare RT/CHI(73):10

Carrott MJ, Fox OD, Maher CJ, Mason C, Sinkov SI, Choppin GR (2007) Solvent extraction behaviour of plutonium (IV) ions in the presence of simple hydroxamic acids. Solvent Extr Ion Exch 25:723–745

Chatterjee B (1978) Donor properties of hydroxamic acids. Coord Chem Rev 26:281–303

Cheng KL, Ueno K, Imamura T (eds) (1982) Handbook of organic analytical reagents. CRC Press, Boca Raton (in Press)

Chung DY, Lee EH (2006) The reduction of Np(VI) by acetohydroxamic acid in nitric acid solution. In: Alvarez R, Bryan ND, May I (eds) Recent advances in actinide. Science Royal Society of Chemistry, Cambridge, pp 587–589

Clifford D (1998) Flotation advances. Min Mag 179:235–244

Colston BJ, Choppin GR, Taylor RJ (2000) A preliminary study of the reduction of Np(VI) by formohydroxamic acid using stopped-flow near-infrared spectrophotometry. Radiochim Acta 88:329–334

Das K, Pradip, Suresh B (1995) Role of molecular architecture and chain length in the flotation separation of oxidized copper-lead-zinc minerals using salicyaldoxime. In: Proceedings of the XIX international mineral processing congress, San Francisco, SME-AIME, USA pp. 245–248

Dasaradhi L, Stark PC, Huber VJ, Smith PH, Jarvinen GD, Gopalan AS (1997) 4-tert-butylcalix [4] arene tetrahydroxamate chelators for the selective extraction of actinide ions: synthesis and preliminary metal ion extraction studies. J Chem Soc Perkin Trans 2:1187–1192

David AB, Raymond AG, Noel JF, William KG, Dau A, Loreto S, Markku A, Kimmo S, Tuula TP, Tapani AP, Mikael P (1996) Conformational behaviour of hydroxamic acids ab initio and structural studies. J Chem Soc Perkin Trans 2: Phy Orgc Chem 12:2673–2680

Durbin PW, Jeung N, Rodgers SJ, Turowski PN, Weitl FL, White DL, Raymond KN (1989) Removal of 238Pu(IV) from mice by polycatecholate -hydroxamate or -hydroxypyridinonate ligands. Radiat Prot Dosimetry 26:351–358

Evans LF, Ewers WE (1952) The process of bubble mineral attachment. In: Recent Developments in Mineral Dressing. Proceedings of the 1st international mineral processing congress, London, IMM, London 457–464

Evard L, De Cuyper J (1975) Flotation of copper–cobalt oxide ores with alkylhydroxamates. In: 10th international mineral processing congress, Cagliari, Italy 655–669

Fox OD, Jones CJ, Birkett JE, Carrott MJ, Maher CJ, Roube CV, Taylor RJ (2006) Advanced PUREX flowsheets for future Np and Pu fuel cycle demands. In: Lumetta GJ, Nash KL, Clark SB, Friese JI (eds) Separations for the nuclear fuel cycle in the 21st Century. ACS symposium Series 933, American Chemical Society, Washington DC pp. 89–102

Fuerstenau DW, Herrera-Urbina R, McGlashan DW (2000) Studies on the applicability of chelating agents as universal collectors for copper minerals. Int J Miner Process 58:15–33

Fuerstenau DW, Metzger PH, Steele GD (1957) Modified hallimond tube for flotation testing. Eng Min J 158:93–95

Fuersetnau DW, Pradip, Khan LA, Raghavan S (1982) An Alternate Reagent Scheme for the Flotation of Mountain Pass Rare-Earth Ore. Proceedings of the XIV International Mineral Processing Congress, Toronto, Canada IV6 1-12

Fuerstenau DW, Pradip C (1984) Mineral flotation with hydroxamate collectors. In: Jones MJ, Oblatt R (eds) Reagents in the minerals industry. The IMM, London, pp 161–168

Fuerstenau MC, Harper RW, Miller JD (1970) Hydroxamate vs fatty acid flotation of iron oxide. Trans SME/AIME 247:69–73

Fuerstenau MC, Miller JD, Gutierrez G (1967) Selective flotation of iron oxide. Trans SME/AIM 238:200–203

Fuerstenau MC, Miller JD, Kuhn MC (1985) Chemistry of flotation. Society of mining metallurgy p177

Furia FD, Modena G, Scrimin P, Gasparin GM, Grossi G (1982) The role of hyrdroxamic acids in the retention of fission products in TBP diluents. A quantitative study in a model system, Sepn Sci Tech 17:1451–1468

Ghosh KK (1997) Kinetic and mechanistic aspects of acid-catalysed hydrolysis of hydroxamic acids. Ind J Chem 36B:1089–1102

Giles CH, MacEwan TH, Nakhwa SN, Smith D (1960) Studies in adsorption Part XI A system of classification of solution adsorption isotherms and its use in diagnosis of adsorption mechanisms and in measurement of specific surface area of solids. J Chem Soc 3:3973–3993

Grossi G (1970) Solvent extraction with hydroxamic acids -.1 Comitato Nazionale Energia Nucleare RT/CHI(70):15

Hallimond AF (1944) Min mag 70:87

Hamilton D, Natarajan R, Nirdosh I (2009) Sphalerite flotation using an arylhydroxamic acid collector: improving grade while using reduced amount of copper sulphate for activation. Ind Eng Chem Res 48:5584–5589

Inoue S, Zhang Q, Uto M (2000) Distribution equilibrium of lanthanide(iii) complexes with N-benzoyl-N-phenylhydroxylamine in several inert solvent systems. Solvent Extr Ion Exch 18:441–450

Jaroslav P, Ivana C, Ludmila S, Jan S (2000) Molecular and crystal structure of benzohydroaxmic acid and its ring-substituted derivatives. Collect Czech Chem Commun 65(8):1273–1288

John SG, Ruggerio CE, Hersman LE, Tung C-S, Neu MP (2001) Siderophore mediated plutonium accumulation by microbacterium flavescens (JG-9). Environ Sci Technol 35:2942–2948

Johnson MA, Maggiora G (eds) (1990) Concepts and applications of molecular similarity. Wiley, New York

Kiersznicki T, Borkowski J, Majewski J (1981) Flotation enrichment of oxidized zinc-lead ores. Rudy Met Niezelaz 26(12):640–643

Koltunova TE, Bogdanov OS, Poroshina AN (1978) Effect of iron salts on the flotation of quartz by hydroxamic acids and their salts. Obogashch Rud 23(3):12–16

Lajiness M (1990) Molecular similarity-based methods for selecting compounds forscreening. In: Rouvary DH (ed) Computational chemical graph theory. Nova, New York, pp 299–316

Lee K, Archibald D, McLean J, Reuter MA (2009) Flotation of mixed copper oxide and sulphide minerals with xanthate and hydroxamate collectors. Miner Eng 22:395–401

Leja J (1982) Surface chemistry of froth flotation. Plenum Press, New York, p 758

Lenormand J, Salam T, Yoon RH (1979) Hydroxamate flotation of malachite. Can Metall Q 18:125–129

Lipczynska-Kochany E (1991) Photochmistry of hydroxamic acids and derivatives. Chem Rev 91:477–491

Lutwick G, Ryan DE (1954) Aromatichydroxylamines as organo analytical reagents. Canad J Chem 32:949–955

Maggio F, Romano V, Cefalu RA (1966) Study of the nature and stability of the system uranyl-benzohydroxamic acid in acid medium. J Inorg Nucl Chem 28:1979–1984

Majumdar AK (1972) N-Benzoylphenylhydroxylamine and its analogues. Pergamon Press, Oxford, p 221

Mannone F, Cecille L, Landat D (1977) Neo-tridecano-hydroxamic acid as an extractant of long-lived actinides from Purex-type HAW raffinates, Proceedings of international solvent extraction conference ISEC '77, Toronto, pp 661–668

Marabini AM (1993) Criteria for the design and synthesis of chelating reagents for flotation. In: Lakshmanan VI, Bautista RG, Somasundaran P (eds) Emerging separation technologies for metals and fuels. The mineral metals and materials society, Pennsylvania, pp 141–152

Marabini AM, Barbarao M, Allesse V (1988) New synthetic collectors for selective flotation of zinc and lead oxidised minerals. In: Forssberg E (ed) Proceedings of (XVI) international mineral processing 1988, Develop Miner Process, vol 10. pp 1197–1208

May I, Taylor RJ, Denniss IS, Brown G, Wallwork AL, Hill NJ, Rawson JM, Less R (1998) Neptunium(IV) and Uranium(VI) Complexation by hydroxamic acids. J Alloys Cpds 275–277:769–772

Muthuswami SV, Vijayan S, Woods DR (1985) Flotation of uranium from uranium ores in Canada: Part II- Cupferron adsorption on uranium oxide quartz illite and a uranium ore from Elliot lake. Canad J Chem Eng 63:650–661

Muthuswami SV, Vijayan S, Woods DR, Banerjee S (1983) Flotation of uranium from uranium ores in Canada: Part I- Flotation results with Eliot lake uranium ores using chelating agents as collectors. Canad J Chem Eng 61:7280–7744

Nagaraj DR (1987) Reagents in mineral technology. In: Somasundaran P, Moudgil BM (eds) Reagents in mineral technology. Marcel Dekker Inc, New York, pp 257–334

Natarajan R, Nirdosh I (2001a) N-Arylhydroxamic acids as mineral collectors for ore beneficiation. Can J Chem Eng 79:941–945

Natarajan R, Fuerstenau DW (1983) Adsorpiton and flotation behaviour of manganese dioxide in the presence of octylhydroxamate. Int J Min Process 11:139–153

Natarajan R, Kamalakannan P, Nirdosh I (2003) Applications of topological indices to structure–activity relationship modeling and selection of mineral collectors. Indian J Chem 42A:1330–1346

Natarajan R, Nirdosh I (2001b) QSAR modeling of flotation collectors part 1—application of valence connectivity indices to the flotation of a uranium ore using substituted-cupferrons. Indian J Chem 40A:130–134

Natarajan R, Nirdosh I (2003) Application of topochemical, topostructural, physicochemical and geometrical parameters to model the flotation efficiencies of N-arylhydroxamic acids. Int J Miner Process 71:113–129

Natarajan R, Nirdosh I (2006) New collectors for sphalerite flotation. Int J Miner Process 79:141–148

Natarajan R, Nirdosh I (2008) Quantitative structure-activity relationship (QSAR) approach for the selection of chelating mineral collectors. Min Eng 21:1038–1043

Natarajan R, Nirdosh I (2009) Effect of molecular structure on the kinetics of flotation of a Canadian nickel ore by N-arylhydroxamic acids. Int J Min Process 93:284–288

Natarajan R, Nirdosh I, Muthuswami SV (1999) Application of topological indices to froth-flotation of a uranium ore. Curr Sci 77:1170–1174

Natarajan R, Nirdosh I, Basak SC, Mills D (2002a) QSAR modeling of flotation collectors using principle components extracted from topological indices. J Chem Inform Comput Sci 42:1425–1430

Natarajan R, Nirdosh I, Venuvanalingam P, Ramalingam M (2002b) Quantitative property–property relationship (QPPR) approach in predicting flotation efficiency of chelating agents as mineral collectors. SAR QSAR Environ Res 13:499–508

Natarajan R, Sharma J, Nirdosh I (2010) Adsorption of N-hydrocinnamoyl-N-phenylhydroxyl-amine on pure minerals. Adsorption 16:541–548

Nirdosh I, Natarajan R, Muthuswami SV, Jeyaraman R (1994) Effect of substituent on the performance of cupferron as a collector for uranium. Develop Chem Eng Miner Process 4:202–217

Neilands JB (ed) (1974) Microbial iron metabolism. Academic Press, New York

Notoya T, Ishikawa T (1980) Corrosion inhibition of copper with potassium octylhydroxamate. Bull Fac of Eng Hokkaido Univ 98:13–19

Palmer BR, Gutierrez BG, Fuerstenau MC (1973) Mechanisms involved in the flotation of oxides and silicates with anionic collectors Part I. Trans AIME 258:257–260

Peterson HD, Feurstenau MC, Richard RS, Miller JD (1965) Chrysocolla flotation by the formation of insoluble surface chelates. Trans AIME 232:388–392

Popperle J (1940) German patent 700 735

Pradip C, Fuerstenau DW (1985) Adsorption of hydroxamate collectors on semisoluble minerals Part II: effect of temperature on adsorption. Colloids Surf 15:137–146

Pradip C (1987) Surface chemistry and applications of alkyl hydroxamate collectors in mineral flotation. Trans Indian Inst Metals 40:287–304

Pradip C, Fuerstenau DW (1983) The adsorption of hydroxamate on semi-soluble minerals Part I: adsorption on barite calcite and bastnaesite. Colloids Surf 8:103–119

Pradip C, Fuerstnau DW (1989) Alkyl hydroxamtes as collectors for the flotation of bastnaesite rare earth ores. In: Bautista RG, Wong MM (eds) RARE-EARTHE-extraction preparation and application. TMS-AIMETMS-AIME Publishers, Pennsylvania, USA, pp 55–70

Pradip C, Rai B, Rao TK, Krishnamurthy S, Vetrivel R, Mielczarski J, Cases JM (2002) Molecular modelling of interactions of alkyl hydroxamates with calcium minerals. J Colloid Interface Sci 256:106–113

Raghavan S, Fuerstenau DW (1976) Some aspects of the thermodynamics of flotation. In: Fuerstenau MC (ed) Flotation 1: Ch. 3, AIME, New York, 21–65

Raghavan S, Fuerstenau DW (1975a) On the wettability and flotation concentration of submicron hematite particles with octylhydroxamate as collector In: Somasundaran P, Grieves R B (eds) Advances in interfacial phenomena of particulate/solution/gas systems: applications to flotation research, AIChE Symp Ser 71(150):59-67

Raghavan S, Fuerstenau DW (1975b) The adsorption of aqueous octylhydroxamate on ferric oxide. J Colloid Interface Sci 50:319–330

Raman M, Douglas RP, Dick VH (1984) Structure of N-(3-cyanophenyl)acetohydroxamic acid hydrate $C_9H_8N_2O_{21}/3H_2O$. Acta Crystallgr Sect C: Cryst Struct Commun C40(8):1369–1371

Raymond KN, Freeman GE, Kappel MJ (1984) Actinide specific complexing agents: their structural and solution chemistry. Inorg Chim Acta 94:193–204

Renshaw JC, Halliday V, Robson GD, Trinci APJ, Wiebe MG, Livens FR, Collison D, Taylor RJ (2003) Development and application of anassay for uranyl complexation by fungal metabolites including siderophores. Appl Environ Microbiol 69:3600–3606

Renshaw JC, Livens FR, Collison D, Robson GD, Trinci APJ, Taylor RJ (2002a) Solubilization of a-FeO(OH) ThO22H2O and g-UO3 by hydroxamate and carboxylate ligands. J Nucl Sci Tech Supp 3:251–254

Renshaw JC, Robson GD, Trinci APJ, Wiebe MG, Livens FR, Collison D, Taylor RJ (2002b) Fungal siderophores: structures functions and applications. Mycol Res 106:1123–1142

Rule WT (1982) Recovery of copper from copper oxide minerals US Patent No 4: 324 654

Saha B, Venkatesan KA, Natarajan R, Antony MP, Vasudeva Rao PR (2002) Studies on the extraction of uranium by N-octanoyl-N-phenylhydroxamic acids. Radiochim Acta 90:455–459

Sandell EB, Onishi H (1978) Photometric determination of trace metals Part I, 4th edn, Chemical analysis, Vol 3. Wiley, New York, p 1085

Shendrikar AD (1960) Substituted hydroxylamines as analytical reagents. Talanta 16:51–63

Sinkov SI, Choppin GR (2002) Acetohydroxamic acid complexes with trivalent f-block metal cations. J Nucl Sci Tech Supp 3:359–362

Sreenivas T, Padmanabhan NPH (2002) Surface chemistry and flotation of cassiterite with alkyl hydroxamates. Colloids Surf A Physicochem Eng Asp 205:47–59

Taylor RJ, May I, Wallwork AL, Denniss IS, Hill NJ, Galkin BYa, Zilberman BYa, Fedorov YuS (1998) The applications of formo- and acetohydroxamic acids in nuclear fuel reprocessing. J Alloys Cpds 271–273:534–537

Todd TA, Wigelund RA (2006) Advanced separation technologies for processing spent nuclear fuel and the potential benefits to a geologic repository In: Lumetta GJ, Nash KL, Clark SB, Friese JI (eds) Separations for the Nuclear Fuel Cycle in the 21st Century, ACS Symposium Series 933, American Chemical Society, Washington DC pp 41–56

Urbina RH (1985) Surface properties and flotation behaviour of chrysocolla in the presence of potassium octyl hydroxamate Ph.D. thesis, University of California

Urbina RH (2003) Recent developments and advances in formulations and applications of chemical reagents used in froth flotation. Min Proc Extr Metall Rev 24:139–182

Verma PC, Khadikar PV, Agrawal YK (1977) Thermodynamic metal-ligand stability constants of hydroxamic acids with divalent metal ions. J Inorg Nucl Chem 39:1847–1848

Vernon F (1982) Chelating ion exchangers—the synthesis and uses of poly (hydroxamic acid) resins. Pure and Applied Chem 54:2151–2158

Vernon F, Khorassani JH (1978) Solvent extraction of metals with hydroxamic acids. Talanta 25:410–412

Vuceta J, Morgan JJ (1978) Chemical modeling of trace metals in fresh waters: role of complexation and adsorption. Environ Sci Technol 12:1302–1309

Willis MJ, Mathur S, Young RH (1999) Kaolin flotation: beyond the classical. In: Parekh BK, Miller JD (eds) Advances in flotation technology. SME, Littleton Colorado, pp 219–229

Wills BA (1997) Mineral processing technology, 6th edn. Butterworth-Heinemann, Burlington, MA

Xu MQ (1998) Modified flotation rate constant and selectivity index. Miner Eng 11:271–278

Yale HL (1943) The hydroxamic acids. Chem Rev 33:209–256

Yoon RH, Nagaraj DR, Wang SS, Hildebrand TM (1992) Benefication of kaolin clay by froth flotation using hydroxamate collectors. Miner Eng 5:457–467

Yoon RH, Hilderbrand TM (1986) Purification of kaolin clay by froth flotation using hydroxamate collectors. US Patent 4,629,556

Yordan JL, Yoon RH, Hilderbrand TM (1993) Hydroxamate vs. fatty acid flotation for the beneficiation of Georgia kaolin. In: Mulukutla PS (ed) Reagents for better metallurgy, SME, Littleton Coloroda pp 215–224

Zilberman BY, Fedorov YS, Mishin EN, Sytnik LV, Shmidt OV, Kukharev DN, Goletsky ND, Glekov RG, Palenik YuV, Sukhareva SY (2002) Superpurex as a TBP-compatible process for recovery and partitioning of long lived radionuclides from NPP spent fuel. In: Banba T, Tsubata Y (eds) Proceedings of the international symposium NUCEF 2001—Scientific basis for criticality safety separation process and waste disposal 189–196, JAERI-Conf 2002–004 Tokai-Mura 2002

Index